BENTHIC FORAMINIFERA OF THE SEA OF MARMARA: DISTRIBUTION, ECOLOGY AND SIGNIFICANCE AS BIOTIC INDICES

A THESIS SUBMITTED TO
THE GRADUATE SCHOOL OF NATURAL AND APPLIED SCIENCES
OF
MIDDLE EAST TECHNICAL UNIVERSITY

BY

GAMZE TANIK

IN PARTIAL FULFILLMENT OF THE REQUIREMENTS
FOR
THE DEGREE OF DOCTOR OF PHILOSOPHY
IN
GEOLOGICAL ENGINEERING

JANUARY 2025

Approval of the thesis:

BENTHIC FORAMINIFERA OF THE SEA OF MARMARA: DISTRIBUTION, ECOLOGY AND SIGNIFICANCE AS BIOTIC INDICES

submitted by **Gamze Tanık** in partial fulfillment of the requirements for the degree of **Doctor of Philosophy** i**n Geological Engineering, Middle East Technical University** by,

Prof. Dr. Naci Emre Altun
Dean, **Graduate School of Natural and Applied Sciences** _____

Prof. Dr. Erdin Bozkurt
Head of the Department, **Geological Engineering** _____

Prof. Dr. Sevinç Altıner
Supervisor, **Geological Engineering, METU** _____

Prof. Dr. Mustafa Yücel
Co-Supervisor, **Institute of Marine Sciences, METU** _____

Examining Committee Members:

Prof. Dr. F. Bora Rojay
Geological Engineering, METU _____

Prof. Dr. Sevinç Altıner
Geological Engineering, METU _____

Prof. Dr. Muhittin Görmüş
Geological Engineering, Ankara University _____

Assoc. Prof. Dr. Ayşe Özdemir
Geophysical Engineering, Van Yüzüncüyıl University _____

Assoc. Prof. Dr. Ulaş Avşar
Geological Engineering, METU _____

Date: 06.01.2025

I hereby declare that all information in this document has been obtained and presented in accordance with academic rules and ethical conduct. I also declare that, as required by these rules and conduct, I have fully cited and referenced all material and results that are not original to this work.

Name Last name : Gamze Tanık

Signature :

ABSTRACT

BENTHIC FORAMINIFERA OF THE SEA OF MARMARA: DISTRIBUTION, ECOLOGY AND SIGNIFICANCE AS BIOTIC INDICES

Tanık, Gamze
Doctor of Philosophy, Geological Engineering
Supervisor: Prof. Dr. Sevinç Altıner
Co-Supervisor: Prof. Dr. Mustafa Yücel

January 2025, 652 pages

Sea of Marmara (SoM), connecting the Black Sea and Mediterranean Sea, has a stratified water column with a strong pycnocline at ~25-40 m depth with limited mixing. As a result, the top layer is oxygenated, but in depth the dissolved oxygen values drop drastically and produce suboxic or anoxic conditions in bottom waters. This layered structure of the water column directly translates into the benthic foraminifera (BF) communities with *Ammonia* and *Elphidium* dominated shallow assemblages (<40 m), *Cassidulina laevigata* dominated deeper assemblages (40-150 m) and *Bolivina spathulata*, *Bolivina vadescens* and *Paracassidulina minuta* dominated deepest assemblages. This study quantitatively documented the BF assemblages from 18 stations (short sediment cores) from the SoM, presenting a comprehensive systematic taxonomy (of 172 identified taxa) and high-quality illustrations. With integration of the previously published quantitative BF data, this study generated the geographic distributions of BF assemblages and the relationship of BF communities with environmental variables. The changes in BF assemblages in the vertical dimension were investigated by the study of 15 sediment cores. Depositional history of the core from the Karamürsel Basin was documented in this

way, and the establishment of sulfidic bottom water in the basin was linked to the 1999 earthquake with the abundance of *Virgulinella fragilis*. The quantitative data set was applied to assess the utility and applicability of four quantitative foraminiferal biotic indices: %P*, morphotype classification, BFOI and Foram-AMBI. In conclusion, this study forms a basis for future monitoring and taxonomic studies by documenting the present configuration in the SoM.

Keywords: Benthic foraminifera, Sea of Marmara, quantitative analysis, biotic indices, Foram-AMBI.

ÖZ

MARMARA DENİZİ BENTİK FORAMİNİFERLERİ: DAĞILIM, EKOLOJİ VE BİYOTIK İNDİSLER OLARAK ÖNEMİ

Tanık, Gamze
Doktora, Jeoloji Mühendisliği
Tez Yöneticisi: Prof. Dr. Sevinç Altıner
Ortak Tez Yöneticisi: Prof. Dr. Mustafa Yücel

Ocak 2025, 652 sayfa

Karadeniz ve Akdeniz'i birbirine bağlayan Marmara Denizi (MD) ~25-40m derinlikteki piknoklin ile ayrılan, karışımın sınırlı olduğu bir tabakalı su kolonuna sahiptir. Sonuç olarak üst su tabakası oksijence zengin olmasına rağmen, alt su tabakasında oksijen bolluğu ciddi miktarda düşerek derin dip sularında suboksik veya anoksik ortamlar oluşturur. Su kolonunun bu tabakalı yapısı sayesinde sığ ortamlarda *Ammonia* ve *Elphidium* cinslerince zengin (<40 m), daha derinlerde *Cassidulina laevigata* türünce zengin (40-150 m), en derin ortamlarda ise *Bolivina spathulata, Bolivina vadescens* ve *Paracassidulina minuta* türlerince zengin olan bentik foraminifer (BF) toplulukları bulunur. Bu çalışma Marmara Denizinden alınmış 18 örnekteki (kısa sediman karotları) BF topluluklarını sayısal olarak belgelemekte, tanımlanmış 172 adet BF taksonu için kapsamlı bir sistematik taksonomi ve kaliteli görseller sunmaktadır. Daha önce Marmara Denizinden yayınlanmış sayısal BF verisi kullanılarak BF topluluklarının coğrafi dağılımları ve ortamsal değişkenlerle ilişkileri belirlenmiştir. 15 karotun çalışılması ile BF topluluklarının düşeydeki değişimleri de araştırılmıştır. Bu şekilde, Karamürsel

Havzasındaki karotun çökelim geçmişi belirlenmiş, *Virgulinella fragilis* türünün bolluğu ile karakterize olan sülfidik dip suyu ortamının oluşumunun 1999 depremi ile ilişkisi ortaya konmuştur. Oluşturulan sayısal veri seti ile dört sayısal foraminiferal biyotik indisin, %P*, morfotip sınıflandırması, BFOI ve ForamAMBI, kullanışlılığı ve uygulanabilirliği test edilmiştir. Sonuç olarak bu çalışma, güncel durumu ortaya koyarak gelecek izleme ve taksonomik çalışmalarına zemin oluşturmaktadır.

Anahtar Kelimeler: Bentik foraminifera, Marmara Denizi, sayısal analiz, biyotik indisler, Foram-AMBI.

To my grandmother,

The strongest person I knew

ACKNOWLEDGMENTS

I would like to express my gratitude to my thesis supervisor Prof. Dr. Sevinç Altıner and co-supervisor Prof. Dr. Mustafa Yücel whose guidance and trust had been invaluable. I would like to acknowledge the precious comments of and discussions with the thesis monitoring committee members Prof. Dr. F. Bora Rojay and Assoc. Dr. Ayşe Özdemir.

I would like to thank the METU IMS R/V Bilim 2 crew for their precious work on the cruises that supplied the material of this thesis. I also want to thank to the previous and current DEEPREDOX research group members, especially Dr. İsmail Akçay and Nimet Alımlı for their expertise. I would like to thank to Prof. Dr. Demir Altıner for being an inspiration, and to late Prof. Dr. Aral Okay for his sincerity and supportive curiosity. Dr. Serdar Görkem Atasoy also deserves a mention for fruitful discussions. I am grateful to Serkan Yılmaz for the SEM images of the foraminifera.

Hilal Işık is owed a huge thanks, for her friendship and help in the data visualization. For the help with maps, and maybe more so for the help with my sanity every other day during the writing of this thesis, Dr. Duygu Tüfekçi Enginar is greatly appreciated. I would like to thank to Zeynep Önal and Zeynep Bektaş for sedimentological, and to Ayça Aydoğan for statistical discussions.

I want to thank my brother, Nahit Doğan Tanık, for being a patient flat mate during this time. Ahmet Özkök, Bulut Çağdaş and Dr. Sanem Elidemir should be acknowledged for their friendship and support. I also would like to thank Erdem Kazak for his warmth, compassion, and understanding.

The material for this study was procured during the cruises of T.C. ÇŞİB MARMOD and TÜBİTAK BIDEB 2247 DEEPREDOX projects. This thesis was supported by METU, project number ÇDAP-309-2021-10691.

TABLE OF CONTENTS

ABSTRACT v

ÖZ vii

ACKNOWLEDGMENTS x

TABLE OF CONTENTS xi

LIST OF TABLES xviii

LIST OF FIGURES xxiv

LIST OF ABBREVIATIONS xxxv

CHAPTERS

1 INTRODUCTION 1

1.1 Purpose and scope 2

1.2 Geographic setting 2

1.3 Material and methods 4

1.3.1 Sampling 4

1.3.2 Chemical properties of water and sediment samples 8

1.3.3 Washing 8

1.3.4 Grain size 9

1.3.5 Micropaleontological identification, quantification and imaging 9

1.3.6 Statistical analysis 12

1.3.7 Diversity indices 12

1.3.8 Radiocarbon dating 15

1.4 Oceanographic setting 15

1.5 Geologic setting 17

1.6 Previous studies in the Sea of Marmara 19
1.6.1 Previous studies in planktonic nanno- and microbiota and palynomorphs 20
1.6.2 Previous studies in benthic microbiota 21
1.7 Outline of the thesis 25
2 SEDIMENT AND WATER CHARACTERISTICS 27
2.1 Water characteristics 27
2.1.1 Bottom water 27
2.1.2 Interface water 29
2.1.3 Pore water 30
2.1.4 Hydrogen sulfide in the Izmit-deep station 31
2.1.5 Correlation of variables 32
2.2 Sediment characteristics 35
2.2.1 Carbon and nitrogen content of 2019 stations 36
2.2.2 Grain size 38
3 LATERAL DISTRIBUTION OF BENTHIC FORAMINIFERA: ASSEMBLAGES AND RELATIONSHIPS WITH ENVIRONMENTAL VARIABLES 39
3.1 Total absolute abundance of foraminifera 39
3.1.1 Rose Bengal stained benthic foraminifera 45
3.2 Diversity indices 47
3.3 Geographic distributions and relative abundances of benthic foraminifera taxa 49
3.3.1 Taxa showing wide geographic distribution 50
3.3.2 Taxa showing limited geographic distribution 52

3.3.3 Taxa showing restricted geographic distribution 53
3.3.4 Taxa in only one station: singletons 53
3.4 Benthic foraminifera assemblages and similarities of sites 54
3.5 Relationship of benthic foraminifera relative abundances with environmental gradients 62
4 VERTICAL DISTRIBUTION OF BENTHIC FORAMINIFERA: CHANGES IN CORES 69
4.1 Total absolute abundance of foraminifera 69
4.2 Relative abundance changes in cores 77
4.2.1 Station 2 77
4.2.2 Station 4 77
4.2.3 Station 5 79
4.2.4 Station 6 81
4.2.5 Station 7-2 82
4.2.6 Station 8 83
4.2.7 Station 1 (2021) 84
4.2.8 Station 3 (2021) – Izmit Bay shelf – 195 m 85
4.2.9 45C-2 87
4.2.10 Izmit-deep 88
4.2.11 K40K46 91
4.2.12 K42K20 92
4.2.13 K49.5L04 94
4.2.14 K51.2K09 94
4.2.15 MM-50 95

5 BENTHIC FORAMINIFERA ASSEMBLAGES OF THE SEA OF MARMARA: A COMPILATION OF QUANTITAVE DATA 99
5.1 Selection of studies 99
5.2 Methodological and reporting differences between studies 104
5.3 Distribution of stations 109
5.4 Taxonomic remarks and homogenization 113
5.5 Absolute abundance and diversity in the surface samples 116
5.6 Relative abundances of taxa in the surface data set 125
5.7 Similarity of sites 133
5.7.1 Cluster 1 133
5.7.2 Cluster 2 133
5.7.3 Clusters 3, 4, 5 135
5.7.4 Clusters 6, 7, 8, 9 136
5.7.5 Cluster 10 138
5.7.6 Cluster 11 139
5.7.7 Cluster 12 139
5.7.8 Cluster 13 141
5.7.9 Clusters 14 and 15 143
6 FORAMINIFERA AS BIOTIC INDICES 145
6.1 Background 146
6.1.1 Planktonic foraminifera and water depth 146
6.1.2 Benthic foraminifera and organic carbon flux 149
6.1.3 Benthic foraminifera and dissolved oxygen: Benthic Foraminifera Oxygen Index 151

6.1.4 Benthic foraminifera and ecological quality: Foram-AMBI..... 153
6.2 Applications 158
6.2.1 Planktonic foraminifera ratio and water depth..... 159
6.2.2 Corliss's Morphotypes..... 166
6.2.3 Benthic Foraminifera Oxygen Index..... 172
6.2.4 Foram-AMBI 180
7 A FORAMINIFERAL EVIDENCE FOR THE ESTABLISHMENT OF SULFIDIC BOTTOM WATER CONDITIONS IN THE KARAMÜRSEL BASIN AFTER THE '99 EARTHQUAKE 187
7.1 Properties of the Karamürsel Basin and previous works 187
7.2 Turbidite-Homogenite Units (THUs) in the Karamürsel Basin 190
7.3 Properties of the Izmit-deep core 192
7.3.1 Sand content..... 193
7.3.2 Bottom and pore water chemistry (Alımlı, 2022)..... 194
7.3.3 Sedimentation rate 194
7.3.4 Benthic foraminifera absolute abundance..... 195
7.3.5 Planktonic foraminifera absolute abundance 196
7.3.6 Benthic foraminifera assemblage..... 197
7.3.7 Radiocarbon dating 200
7.4 Subdivisions of the Izmit-deep core..... 200
7.4.1 Interval A 201
7.4.2 Interval B 202
7.4.3 Interval C 202
7.4.4 Interval D 203

7.5 Depositional interpretation of the Izmit-deep core 204
7.5.1 Intervals A and B 204
7.5.2 Interval C 206
7.5.3 Interval D 207
7.6 Summary 208
8 SYSTEMATIC TAXONOMY 209
9 DISCUSSION AND CONCLUSION 443
9.1 Environmental preferences of selected taxa identified in this study 443
9.2 Changes in the vertical dimension for the studied cores 446
9.2.1 Station 8 446
9.2.2 45C-2 447
9.2.3 Izmit-deep 447
9.2.4 K40K46 448
9.2.5 K51.2K09 449
9.2.6 MM50 449
9.3 Need for taxonomic review and establishment of a solid framework 449
9.4 Applicability and utility of the quantitative foraminiferal indices 454
9.5 Conclusions 457
REFERENCES 461
APPENDICES 531
A. Taxa names and abbreviations 531
B. Raw count data 535
C. Relative abundances in the core-top samples 536
D. Numerical results for CCA 537

E. Data for Chapter 5 538
F. Data for Chapter 6 539
G. Systematic taxonomy: summary and plates 540
CURRICULUM VITAE 651

LIST OF TABLES

TABLES

Table 1.1 Water depths, coordinates (decimal degrees) and location tags of the stations sampled during Dekosim (2019; above dashed line) and Deepredox (2021; below dashed line) cruises. Note that stations 1 and 3 were sampled in both cruised, and two cores were taken from station 45C (during the same multicorer cast). 5
Table 1.2. Sampling scheme of cores (bold); numbers represent the bottom boundary of the sample (cm below surface). Samples used for micropaleontological analysis shaded blue. Rose Bengal added sample numbers colored pink. 7
Table 2.1. Bottom depth of stations (m), sampling depth (m) of the bottom water with Niskin bottles, temperature (°C), salinity (psu), pH of the bottom water. 28
Table 2.2 Total phosphorous (TP, µM), phosphate (PO_4, µM), nitrate and nitrite (NO_3+NO_2, µM), nitrite (NO_2, µM), silicon (Si, µM), ammonium (NH_4, µM), and dissolved oxygen (DO, µM) in bottom water samples (see sample depths in Table 2.1).....29
Table 2.3. Phosphate (PO_4, µM), nitrate and nitrite (NO_3+NO_2, µM), nitrite (NO_2, µM), silicon (Si, µM), ammonium (NH_4, µM) in interface water samples.....30
Table 2.4. Phosphate (PO_4, µM), nitrate and nitrite (NO_3+NO_2, µM), nitrite (NO2, µM), silicon (Si, µM), ammonium (NH_4, µM) in pore water samples (top 1 cm of the cores). 31
Table 2.5. Hydrogen sulfide (H_2S, µM) in Izmit-deep station; sample 0 cm stands for bottom water, rest comes from pore water. 32
Table 2.6. Total carbon (TC), total organic carbon (TOC), total nitrogen (TN), and TOC/TN and TC/TN ratios in top centimeters of cores. Units: * mg/g, ** mmol/g. 36

Table 2.7. Total organic carbon (TOC), total nitrogen (TN), and TOC/TN ratios in the core-top samples studied, as averages of values given in Table 2.6. Units: * mg/g, ** mmol/g. 37
Table 2.8. Sand content of the surface samples as weight percent. 38
Table 3.1 Initial volume (~: approximation), working split, numbers of benthic ($BF_{\#}$) and planktonic ($PF_{\#}$) foraminifera counted from the working split and benthic ($BF_{\#v}$) and planktonic ($PF_{\#v}$) foraminiferal number of the core-top samples normalized to 1 ml volume. Shades in normalized foraminiferal numbers darkens with increasing values. 40
Table 3.2. Initial weight, working split, numbers of benthic ($BF_{\#}$) and planktonic ($PF_{\#}$) foraminifera counted from the working split and benthic ($BF_{\#W}$) and planktonic ($PF_{\#W}$) foraminiferal number of the core-top samples of 2021 cruise normalized to 1 g of dry sediment. Shades in normalized foraminiferal numbers darkens with increasing values. 41
Table 3.3. Number of total ($BF_{\#}$), rose Bengal stained (rB $BF_{\#}$) benthic foraminifera picked from the working split of the core-top samples and the relative abundance of rB stained forms in total BF assemblage (Live %). 47
Table 3.4. Species richness (S) and counted benthic foraminifera number ($BF_{\#}$) in the working splits, and dominance (D), Shannon's diversity (H) and evenness (E) of the core-top samples. 48
Table 3.5. The widely distributed taxa, in how many core-top samples they occurred (Count), and their minimum, maximum and average relative abundances (%). Taxa abbreviations as in Supplementary Table A.1. 51
Table 3.6. The total relative abundance of the >2% taxa (SUM, percent), and the number of these taxa occurring (S) in the core-top samples. Station names colored according to the cluster they belong to (Figure 3.9). 54
Table 3.7. Environmental variables used in canonical correspondence analysis (see Section 2.1.5). Bottom depth in meters; dissolved oxygen (DO), nitrite (NO_2), ammonium (NH_4), and phosphate (PO_4) in micromolar (μM), total organic carbon

(TOC) as percent (weight); BW: bottom water; PW: pore water; TOC values from 1: Ergin et al. 1993, 2: Ergin and Yücel, 1990, 3: 2019 results. 63
Table 4.1. Number of benthic foraminifera ($BF_{\#}$) of the working split size (Split), approximate initial volume of samples (ml) and total absolute abundance of benthic foraminifera normalized to 1 ml of sediment ($BF_{\#V}$) in the studied sediment cores of 2019 cruise.....70
Table 4.2. Number of benthic foraminifera ($BF_{\#}$) of the working split size (Split), initial volume of samples (ml), total absolute abundance of benthic foraminifera normalized to 1 ml of sediment ($BF_{\#V}$), initial weight of samples (g), total absolute abundance of benthic foraminifera normalized to 1 g dry sediment ($BF_{\#W}$), and the ratio of $BF_{\#W}$ to $BF_{\#V}$ in the studied sediment cores of 2021 cruise. * for possible measurement error. 71
Table 4.3. Number of benthic foraminifera ($PF_{\#}$) of the working split size, total absolute abundance of planktonic foraminifera normalized to 1 ml of sediment ($PF_{\#V}$) (see Split and Initial volume in Table 4.1 and Table 4.2), relative abundance of planktonic foraminifera in total foraminifera assemblage (P%), weight-wise ratio of material coarser than 63 μm in the sediment (Sand%, for 2021 samples only)..74
Table 5.1. Counting and other method details of the quantitative benthic foraminifera studies of the Sea of Marmara. 100
Table 5.2. Type of sample, amount of stations, locations, water depths, studied assemblage type (Live / Dead / Undifferentiated) and size fraction (coarser than 63 or 125 μm) of the analyzed quantitative benthic foraminifera studies. 105
Table 5.3. For each location (alphabetically ordered), number of studies, number of stations, the code of the studies (see Table 5.2 for references) and station names/numbers. 111
Table 5.4. Total number of identified taxa (S_{TOT}), average species richness per sample ($S_{AV} = (\Sigma S_i)/k$, where S_i= species richness in ith sample, k= number of samples in the study) and number of average reported individuals per sample ($N_{AV}= (\Sigma N_i)/k$, where N_i= collected/reported number of individuals in ith sample) in the studied publications. See Table 5.2 for references.).....113

Table 5.5. Number of taxa in relative abundance ranges for the surface data set. 125
Table 5.6. Very dominant (>30%) taxa: their average (in stations they are present) and maximum abundances, the stations in which the taxa have their maximum abundance and the numbers of stations taxa are present in. 126
Table 5.7. Dominant (15-30%) taxa: their average (in stations they are present) and maximum abundances, the stations in which the taxa have their maximum abundance and the numbers of stations taxa are present in. 127
Table 6.1. Summary of four Foram-AMBI publications which made species assignments to ecological groups (EG). LBF: living benthic foraminifera, TBF: total (living+dead) benthic foraminifera, V: validation, C: calibration. #: number of. [1]: Alve et al. 2016 (Shelf to upper slope; below halocline), [2]: Jorissen et al. 2018, [3]: O'Malley et al. 2021, [4-]: [4-1]: Bouchet et al. 2021: English Channel/European Atlantic intertidal and Transitional Waters (TWs), [4-2]: Mediterranean Sea intertidal and TWs..... 156
Table 6.2. Ecological group assignments (in Arabic numerals) of species occurring in all five datasets. Agreeing assignments color matched. See Table 6.1 for references. 157
Table 6.3. The list of taxa occurring in more than one dataset with the same ecological group (EG) assignment. #: number of datasets. Ecological group assignments given in Arabic numerals. 158
Table 6.4. Epifaunal ($BF_{\#E}$) and total benthic foraminifera ($BF_{\#}$) and planktonic foraminifera ($PF_{\#}$) numbers counted from working splits, calculated planktonic foraminifera abundance in total foraminifera (P%), calculated planktonic foraminifera ratio (%P*, according to Van der Zwaan et al., omitting infaunal benthics), measured water depth (m) and estimated water depths (EWD, m) following Equation 6.1 [1], Equation 6.2 [2], Equation 6.3 [3] in the core-top samples. Colors according to sample clusters (Figure 3.9)..... 160
Table 6.5. Morphotype classification of the >2% taxa (see Section 3.4) in the core-top samples, except textularin and unidentified taxa. [1] Corliss and Chen, 1988; [2] Corliss and Fois, 1990; [3] Corliss, 1985; TS: this study. Morphotype classes

abbreviations as in Table 6.6. Taxon abbreviations as in Supplementary Table A.1. 167
Table 6.6. Morphotype classes and abbreviations, the microhabitat they belong to, number of taxa assigned to (#) and average relative abundance of (Average %) each morphotype class. 168
Table 6.7. Summed relative abundances of taxa assigned to different morphotype classes in core-top samples. Morphotype classes abbreviations as in Table 6.6. Colors according to sample clusters (Figure 3.9). 169
Table 6.8. Summed relative abundances of epifaunal (Tot EPIF = RT + PT + M + BT) and infaunal taxa (Tot INF = RP + TC + FT + S + FO), total relative abundances (Tot) of the taxa used in this analysis, epifaunal (E%) and infaunal (I%) ratios in core-top samples. Colors according to sample clusters (Figure 3.9). 170
Table 6.9. Assignments of the >2% taxa (see Section 3.4) in the core-top samples, except textularin and unidentified taxa, into oxic, suboxic and dysoxic indicator groups. [1] Kaiho, 1994; [2] Kaminski, 2012; TS: this study. O: Oxic, S-A, B, C: Suboxic A, B and C; D: Dysoxic. Taxa abbreviations as in Supplementary Table A.1. 172
Table 6.10. Summed relative abundances of taxa assigned to different groups in core-top samples: O: Oxic; S-A, B, C: Suboxic A, B and C; S: Suboxic total; D: Dysoxic; total relative abundances of the groups; ratios of the groups in all assigned population (%). Colors according to sample clusters (Figure 3.9). 176
Table 6.11. Results of BFOI calculations according to BFOI(O): Equation 6.4, BFOI(I): Equation 6.5, BFOI(S): Equation 6.6 and resulting bottom water oxygenation classes. Colors according to sample clusters (Figure 3.9). 177
Table 6.12. Bottom water oxygen conditions subdivisions in terms of dissolved oxygen (DO ml/l and μM) and corresponding BFOI ranges (Kaiho, 1999). 177
Table 6.13. Bottom depth, measured bottom water oxygen (DO ml/l and μM), corresponding oxygen conditions ([1] according to Kaiho, 1999, Table 6.12) and redox conditions ([2] Alımlı, 2022) and total organic carbon (TOC%). Colors according to sample clusters (Figure 3.9). 178

Table 6.14. Assignments of taxa to ecological groups (EG, in Arabic numerals) in this study [TS] and the reasoning (R) for those that differ from Jorissen et al. (2018, [2]) in name or assignment. M: mixed (for supraspecific assignments), *: see text for explanation. 181
Table 6.15. List of taxa assigned to ecological groups (EG, in Arabic numerals, color coded). Taxa abbreviations as in Supplementary Table A.1. 184
Table 6.16. Number of specimens (N, excluding unidentified and indeterminate taxa), ratio of not assigned taxa (NA%), calculated Foram-AMBI values for (1) using the total assemblage, and (2) using only the assigned taxa. 186
Table 7.1 Coordinates and water depth of cores from the Karamürsel Basin. 189
Table 7.2 Radiocarbon dating results as reported by the lab (TÜBİTAK-MAM).200
Table 7.3 Calibration results of ^{14}C dates of Izmit-deep samples by OxCal (posterior probability) and CALIB software. 201
Table 7.4 Uncalibrated (^{14}C BP), and calibrated (CALIB) ages for two bulk samples from the Izmit-deep core. Calibration curves and reservoir correction values as explained in the text. 201
Table 8.1. Five daughter taxa of *Sigmoilina* as listed by Schlumberger (1887), prominent changes in generic and specific attribution, and accepted names by WoRMS (2025). 422
Table 9.1. Co-occurrence table (symmetrical) for the taxa identified in the analyzed studies after homogenization of data (437 taxa). Number of identified taxa in the studies (after homogenization) given in the diagonal (purple). Maximum co-occurrence numbers (per column) are highlighted yellow. Study codes same as Table 5.2; 01: Fontanier et al. 2018; 02: Phipps et al. 2010, 03: Kırcı-Elmas, 2006; 06: Kırcı-Elmas, 2018; 07: Kırcı-Elmas, 2013; 08: Avşar, 2010; 09: Kırcı-Elmas et al., 2008; 11: Kaminski et al., 2002; 12: Avşar et al. 2006; 13: Alavi, 1988; TS: this study. 454

LIST OF FIGURES

FIGURES

Figure 1.1. Map of stations sampled during Dekosim (2019, blue) and Deepredox (2021, red) cruises. Note that stations 1 and 3 were sampled in both cruised, and two cores were taken from station 45C (during the same multicorer cast). 3
Figure 1.2. CTD and multicorer sampling schemes; positions showing bottom water, interface water and pore water samples; subsampling scheme of sediment cores. ... 4
Figure 1.3. Photographs from Dekosim (2019) and Deepredox (2021) cruises: A. CTD rosette with Niskin bottles (white arrow) and multicorer (green arrows showing the core tubes readied for sampling); B. sediment core tube before extraction from the sampling mechanism; C. sediment core tube after extraction from sampling mechanism; D. two sediment cores (yellow arrow shows undisturbed sediment-water interface); E. subsampling phase with extruder; F. sampling of the interface water with a syringe; G. extruder (blue arrow) and sediment core (orange arrow) readied for subsampling; H. subsampling phase with the extruder..... 6
Figure 1.4. Shaded elevation topography and bathymetry of the Marmara region: names of major bottom morphologic and geographic features as used in the text are indicated on map. Abbreviations and enumerated features: TS: Tekirdağ shelf, TB: Tekirdağ Basin, SiS: Silivri shelf, CeB: Central Basin, KuB: Kumburgaz Basin, IS: Istanbul shelf, CiB: Çınarcık Basin, PS: Prince Islands shelf, IB: Imralı basin; 1. Biga Stream, 2. Gönen Stream, 3. Çapraz (Kocaçay) Stream, 4. Dil Stream (Dilderesi), 5. Lake Küçükçekmece, 6. Lake Büyükçekmece, 7. Marmara Island, 8. Kapıdağ Peninsula, 9. Armutlu Peninsula. River network from EU-Hydro River Network Database (European Union's Copernicus Land Monitoring Service, https://doi.org/10.2909/393359a7-7ebd-4a52-80ac-1a18d5f3db9c), thick and enumerated ones stand for major rivers. Base map is extracted from GeoMapApp database (version 3.7.4) http://www.geomapapp.org (Ryan et al., 2009). 16

Figure 2.1. Correlation heatmap (ggcorrplot, Kassambara and Patil, 2023) for environmental variables, excluding stations Izmit-deep and K42K20, and bottom water total phosphorous. B: bottom water; P: pore water; I: interface water properties..... 34
Figure 2.2. Correlation heatmap (ggcorrplot, Kassambara and Patil, 2023) for environmental variables, excluding interface water variables. B: bottom water; P: pore water..... 35
Figure 2.3. Map of sand and mud content in the core-top samples of 2021 sampling. 38
Figure 3.1. Map of volume normalized total benthic foraminifera abundances ($BF_{\#V}$) in the core-top samples. Shades as in Table 3.1..... 42
Figure 3.2. Map of weight normalized total benthic foraminifera abundances ($BF_{\#w}$) in the core-top samples. Shades as in Table 3.2..... 42
Figure 3.3. Map of volume normalized total planktonic foraminifera abundances ($PF_{\#V}$) in the core-top samples. Shades as in Table 3.1. 43
Figure 3.4. Map of weight normalized total planktonic foraminifera abundances ($PF_{\#w}$) in the core-top samples. Shades as in Table 3.2. 44
Figure 3.5. Normalized foraminiferal abundance values plotted on log-log scale. Outlier (Izmit-deep) value marked..... 44
Figure 3.6. Rose Bengal stained and non-stained specimens. A. *Rectuvigerina phlegeri* Le Calvez, stained and non-stained individuals in Station 1 (21) 1 cm; B. *Bulimina elongata* d'Orbigny, stained and non-stained individuals in Station 1 (21) 1 cm; c. *Globobulimina* spp., stained and non-stained individuals in K51.2K09 1 cm; D. *Eilohedra vitrea* (Parker), one stained and three poorly colored individuals in Station 3 (21) 1 cm; E. *Bolivina spathulata* (Williamson), all poorly colored individuals in Station 3 (21) 1 cm; F. *Bolivina* cf. *vadescens* Cushman, two stained and one non-stained individuals in Station 3 (21) 1 cm; G. *Paracassidulina minuta* (Cushman), one stained (patchy staining) and seven poorly colored individuals in K49.5L04 1 cm. 46
Figure 3.7. Scatter plot of species richness (S) vs Shannon's diversity (H)..... 49

Figure 3.8. Scatter plot of dominance (D) vs evenness (E). 49
Figure 3.9. Two-way cluster (UPGMA, Bray-Curtis dissimilarity) diagram using relative abundances of taxa which are at least 2% abundant in at least one sample, across all core-top samples. Dendrogram across sites (samples) located horizontally, across taxa vertically; relative abundances of taxa summarized at the center, key to size of dots at top right corner. Taxa abbreviations as in Supplementary Table A.1. Graph colored to maximize readability, clusters (see text) labeled on the dendrogram across taxa (A-D) and across sites (I and II). 55
Figure 3.10. Relative abundances of taxa belonging to Cluster A. 56
Figure 3.11. Relative abundances of taxa of Cluster B. 57
Figure 3.12. Relative abundances of taxa of Clusters C and D (1 and 2). 58
Figure 3.13. Relative abundances of taxa of Subclusters D3a, D3b, D3c, D3d. 59
Figure 3.14. Pie charts showing the relative abundances of the five most abundant taxa in the core-top samples. Taxon abbreviations as in Supplementary Table A.1. 61
Figure 3.15. Geographic distribution of site clusters; cluster coloring as in Figure 3.9. Colors of station names as in Figure 1.1. 61
Figure 3.16. First two axes of canonical correspondence analysis done on environmental dataset given in Table 3.7 and the relative abundances of >2% taxa: station scores (colors as in Figure 3.9). 64
Figure 3.17. First two axes of canonical correspondence analysis done on environmental dataset given in Table 3.7 and the relative abundances of >2% taxa: taxa (abbreviations as in Supplementary Table A.1) and environmental gradient vectors (exaggerated 9 times for better visibility). 65
Figure 3.18. CCA biplot of first two axes, excluding the outliers and the unidentified taxa. Stations coloring according to Figure 3.9, environmental gradient vectors amplified 4 times. 68
Figure 4.1. Correlation of $BF_{\#V}$ and $BF_{\#W}$ values in 2021 samples, plotted on log-log scale for better visibility. 73

Figure 4.2. Total absolute benthic and planktonic foraminifera (volume normalized, $BF_{\#V}$ and $PF_{\#V}$), planktonic foraminifera ratio (P%), and sand content (Sand %, not present in stations 2, 4, 5, 6, 7, 8) in cores (ggplot2, Wickham, 2016). 76
Figure 4.3. Relative abundances of selected taxa in Station 2 sediment core. Panels from left to right: A: Bolivinitidae; B: Buliminoidea; C: Cassidulinoidea; D: Planorbulinoidea, Discorboidea, Rotaloidea; E: Nonionoidea, other Rotaliana, Spirillinida; F: Robertinida, Textulariana, Miliolida. Scales of x-axes of panels are the same. Y-axis not to scale. Taxa abbreviations as in Supplementary Table A.1. 78
Figure 4.4. Relative abundances of selected taxa in Station 4 sediment core. Panels from left to right: A: Bolivinitidae; B: Buliminoidea; C: Cassidulinoidea; D: Planorbulinoidea, Discorboidea, Rotaloidea; E: Nonionoidea, other Rotaliana, Spirillinida; F: Robertinida, Textulariana, Miliolida. Scales of x-axes of panels are the same. Y-axis not to scale. Taxa abbreviations as in Supplementary Table A.1. 79
Figure 4.5. Relative abundances of selected taxa in Station 5 sediment core. Panels from left to right: A: Bolivinitidae; B: Buliminoidea; C: Cassidulinoidea; D: Planorbulinoidea, Discorboidea, Rotaloidea; E: Nonionoidea, other Rotaliana, Spirillinida; F: Robertinida, Textulariana, Miliolida. Scales of x-axes of panels are the same. Y-axis not to scale. Taxa abbreviations as in Supplementary Table A.1. 80
Figure 4.6. Relative abundances of selected taxa in Station 6 sediment core. Panels from left to right: A: Bolivinitidae; B: Buliminoidea; C: Cassidulinoidea; D: Planorbulinoidea, Discorboidea, Rotaloidea; E: Nonionoidea, other Rotaliana, Spirillinida; F: Robertinida, Textulariana, Miliolida. Scales of x-axes of panels are the same. Y-axis not to scale. Taxa abbreviations as in Supplementary Table A.1. 82
Figure 4.7. Relative abundances of selected taxa in Station 7-2 sediment core. Panels from left to right: A: Bolivinitidae; B: Buliminoidea; C: Cassidulinoidea; D: Planorbulinoidea, Discorboidea, Rotaloidea; E: Nonionoidea, other Rotaliana,

Spirillinida; F: Robertinida, Textulariana, Miliolida. Scales of x-axes of panels are the same. Y-axis not to scale. Taxa abbreviations as in Supplementary Table A.1. 83
Figure 4.8. Relative abundances of selected taxa in Station 8 sediment core. Panels from left to right: A: Bolivinitidae; B: Buliminoidea; C: Cassidulinoidea; D: Planorbulinoidea, Discorboidea, Rotaloidea; E: Nonionoidea, other Rotaliana, Spirillinida; F: Robertinida, Textulariana, Miliolida. Scales of x-axes of panels are the same. Y-axis not to scale. Taxa abbreviations as in Supplementary Table A.1. 85
Figure 4.9. Relative abundances of selected taxa in Station 1 (21) sediment core. Panels from left to right: A: Bolivinitidae; B: Buliminoidea; C: Cassidulinoidea; D: Planorbulinoidea, Discorboidea, Rotaloidea; E: Nonionoidea, other Rotaliana, Spirillinida; F: Robertinida, Textulariana, Miliolida. Scales of x-axes of panels are the same. Y-axis not to scale. Taxa abbreviations as in Supplementary Table A.1. 86
Figure 4.10. Relative abundances of selected taxa in Station 3 (21) sediment core. Panels from left to right: A: Bolivinitidae; B: Buliminoidea; C: Cassidulinoidea; D: Planorbulinoidea, Discorboidea, Rotaloidea; E: Nonionoidea, other Rotaliana, Spirillinida; F: Robertinida, Textulariana, Miliolida. Scales of x-axes of panels are the same. Y-axis not to scale. Taxa abbreviations as in Supplementary Table A.1. 87
Figure 4.11. Relative abundances of selected taxa in 45C-2 sediment core. Panels from left to right: A: Bolivinitidae; B: Buliminoidea; C: Cassidulinoidea; D: Planorbulinoidea, Discorboidea, Rotaloidea; E: Nonionoidea, other Rotaliana, Spirillinida; F: Robertinida, Textulariana, Miliolida. Scales of x-axes of panels are the same. Y-axis not to scale. Taxa abbreviations as in Supplementary Table A.1. 89
Figure 4.12. Relative abundances of selected taxa in Izmit-deep sediment core. Panels from left to right: A: Bolivinitidae; B: Buliminoidea; C: Cassidulinoidea; D: Planorbulinoidea, Discorboidea, Rotaloidea; E: Nonionoidea, other Rotaliana,

Spirillinida; F: Robertinida, Textulariana, Miliolida. Scales of x-axes of panels are the same. Y-axis not to scale. Taxa abbreviations as in Supplementary Table A.1. 90
Figure 4.13. Relative abundances of selected taxa in K40K46 sediment core. Panels from left to right: A: Bolivinitidae; B: Buliminoidea; C: Cassidulinoidea; D: Planorbulinoidea, Discorboidea, Rotaloidea; E: Nonionoidea, other Rotaliana, Spirillinida; F: Robertinida, Textulariana, Miliolida. Scales of x-axes of panels are the same. Y-axis not to scale. Taxa abbreviations as in Supplementary Table A.1. 92
Figure 4.14. Relative abundances of selected taxa in K42K20 sediment core. Panels from left to right: A: Bolivinitidae; B: Buliminoidea; C: Cassidulinoidea; D: Planorbulinoidea, Discorboidea, Rotaloidea; E: Nonionoidea, other Rotaliana, Spirillinida; F: Robertinida, Textulariana, Miliolida. Scales of x-axes of panels are the same. Y-axis not to scale. Taxa abbreviations as in Supplementary Table A.1. 93
Figure 4.15. Relative abundances of selected taxa in K49.5L04 sediment core. Panels from left to right: A: Bolivinitidae; B: Buliminoidea; C: Cassidulinoidea; D: Planorbulinoidea, Discorboidea, Rotaloidea; E: Nonionoidea, other Rotaliana, Spirillinida; F: Robertinida, Textulariana, Miliolida. Scales of x-axes of panels are the same. Y-axis not to scale. Taxa abbreviations as in Supplementary Table A.1. 95
Figure 4.16. Relative abundances of selected taxa in K51.2K09 sediment core. Panels from left to right: A: Bolivinitidae; B: Buliminoidea; C: Cassidulinoidea; D: Planorbulinoidea, Discorboidea, Rotaloidea; E: Nonionoidea, other Rotaliana, Spirillinida; F: Robertinida, Textulariana, Miliolida. Scales of x-axes of panels are the same. Y-axis not to scale. Taxa abbreviations as in Supplementary Table A.1. 96
Figure 4.17. Relative abundances of selected taxa in MM50 sediment core. Panels from left to right: A: Bolivinitidae; B: Buliminoidea; C: Cassidulinoidea; D: Planorbulinoidea, Discorboidea, Rotaloidea; E: Nonionoidea, other Rotaliana,

Spirillinida; F: Robertinida, Textulariana, Miliolida. Scales of x-axes of panels are the same. Y-axis not to scale. Taxa abbreviations as in Supplementary Table A.1. 97
Figure 5.1. Location map of stations in analyzed studies (see Table 5.2 for references). Inset frames (A-G) show extents of maps A-G (continued on the text page). 106
Figure 5.2. Number of stations with respect to water depth: A. histogram for all studies included here, number of stations present in every water depth bin labelled above columns; B. stacked histogram showing stations belonging to different studies, number of studies present in every water depth bin labelled above columns. Data codes as in Table 5.2. 110
Figure 5.3. Relationship between number of counted individuals (N) and species richness (S) in the surface data set (see Supplementary Table E.3) excluding SoM_07. 117
Figure 5.4. Histogram showing the species richness distribution amongst stations for surface data set. 118
Figure 5.5. Relationship between dominance (D) and evenness (E) in the surface data set; different colors for different species richness intervals; trendlines (power) plotted and correlation coefficients indicated, except for 0-15 interval. Outlier and extreme stations labelled with data codes (Table 5.2) and station numbers. 119
Figure 5.6. Species richness (S), dominance (D), Shannon's diversity (H') and evenness (E) values plotted against water depth (x-axes, meters). 120
Figure 5.7. Box and Whisker plots for studies: species richness (S), dominance (D), Shannon's diversity (H') and evenness (E) values in the surface data set. Studied size fractions are noted in plot S. Table 5.2 for study references. 121
Figure 5.8. Box and Whisker plots for locations: species richness (S), dominance (D), Shannon's diversity (H') and evenness (E) values in the surface data set. Note Armutlu group includes both shelf and slope stations. Number of stations noted in plot S. Figure 1.4 for locations. 122

Figure 5.9. Box and Whisker plots for water depth ranges: species richness (S), dominance (D), Shannon's diversity (H') and evenness (E) values in the surface data set. 124
Figure 5.10. Dendrogram produced from the cluster analysis (hierarchical clustering, UPGMA, Bray-Curtis) of surface data set (384 taxa, 144 stations). A: Station numbers (shortened as "study code_station number", without using SoM prefix, and MAR prefix in SoM-11, MRS06: MRS-DV05-PC-06, MRS04: MRS-DV01-PC-04, TS_IzDeep: SoM_TS_Izmit-deep, other stations of this study shortened to first few characters only, see Table 5.2 for references) in clusters, colored according to location (see legend A); B: water depths the stations belong to (see legend B); C: dendrogram cut from about 32% similarity resulting in 15 separate clusters of stations, clusters and subclusters enumerated (as C#) starting from the root of the tree; station numbers colored according to studied size fraction (see legend C).. 134
Figure 5.11. Location map of stations belonging to clusters 1 and 2 (see Figure 5.10 and Figure 5.1 for station names). 135
Figure 5.12. Location map of stations belonging to clusters 3, 4 and 5 (see Figure 5.10 and Figure 5.1 for station names). 137
Figure 5.13. Location map of stations belonging to clusters 6, 7, 8 and 9 (see Figure 5.10 and Figure 5.1 for station names). 138
Figure 5.14. Location map of stations belonging to clusters 10 and 11 (see Figure 5.10 and Figure 5.1 for station names). 140
Figure 5.15. Location map of stations belonging to cluster 12 (see Figure 5.10 and Figure 5.1 for station names). 141
Figure 5.16. Location map of stations belonging to cluster 13 (see Figure 5.10 and Figure 5.1 for station names). 142
Figure 5.17. Location map of stations belonging to clusters 14 and 15 (see Figure 5.10 and Figure 5.1 for station names). 144
Figure 6.1. Plots of regression curves proposed by Van der Zwaan et al. (1990, Equation 6.1, with X = %P*) and De Rijk et al (1999, Equation 6.2 (east) and Equation 6.3 (west), with X = P%). 148

Figure 6.2. Foraminiferal morphotype classification scheme from Corliss and Chen (1988) and Corliss and Fois (1990). 150
Figure 6.3. Left: relative abundance distributions of the different ecological groups and right: examples of relative abundances of taxa belonging to the said groups (Jorissen et al. 2018). 155
Figure 6.4. Scatter plot of (A) P% (horizontal) and water depth (m, vertical) and (B) regression curves of De Rijk et al. (1999) for the western and eastern Mediterranean Sea. R^2 value is indicated on exponential trend-line. 161
Figure 6.5. Scatter plots of (A) unmodified (P%) and modified (%P*) planktonic foraminiferal ratios in the core-top samples; (B) difference between the two PF ratios and (C) relative abundance of infaunal foraminifera (I%) against P%. R^2 values are indicated on trend-lines. 162
Figure 6.6. Scatter plots of %P* (horizontal) and water depth (m, vertical) and regression curve of Van der Zwaan et al. (1999). R^2 values are indicated on exponential trend-lines. (A): regression for the whole data set; (B). regression for stations marked with purple triangles, which remain in between the error margins 1 and 2 (light blue dashed lines, see text). 163
Figure 6.7. Scatter plots of total organic carbon (TOC), dissolved oxygen in bottom water (DO) and bottom depth vs. infaunal (I%) and epifaunal (E%) ratios. 171
Figure 6.8. Maximum (O) and minimum (I) calculated BFOI values of the stations (Table 6.11) plotted against measured bottom water dissolved oxygen. Anoxic (A), dysoxic (D), suboxic (S) and low oxic (LO) ranges as given in Kaiho (1999) drawn on the plot. 180
Figure 6.9. Relative abundances of ecological groups (EGI-V) and not assigned (NA) taxa in the core-top samples: A. in total assemblage, B. only among assigned taxa. 185
Figure 6.10. Scatter plot for total organic carbon (TOC%, see Table 3.7) and Foram-AMBI values calculated for only assigned taxa (see Table 6.16). A linear trend-line added and its correlation coefficient noted. 186

Figure 7.1. A. Locations of the Darıca, Karamürsel and Gölcük basins (DB, KB, GB respectively), black rectangle shows the extent of the map in B; B. Locations of dated cores, from west to east: IZ33 (McHugh et al., 2006; Gasperini et al., 2018), IK2 (Arslan Kaya, 2023b); IZ115 and SW113 (Çağatay et al. 2012); and Izmit-deep (this study); and the Chirp profile line I-44 (Figure 7.2) on multibeam bathymetry of Karamürsel Basin (Cormier et al., 2006). 188
Figure 7.2. Line I-44 chirp profile: flat bottom of the central basin; note how beds become progressively tilted toward the North Anatolian Fault (Cormier et al., 2006). Positions of Izmit-deep (red arrow) and SW-113 (yellow arrow) cores projected onto the line of section are shown. 189
Figure 7.3. Cores from the Karamürsel Basin. Correlated historical earthquake dates in IZ-115 and 1954 AD (by ^{137}Cs isotope) in SW-113 are directly taken from Çağatay et al. (2012). Blue arrows show positions of dated material. Relative abundance of *V. fragilis* (V_frag%), hydrogen sulfide concentration (H_2S μM) and total benthic foraminiferal abundance (weight normalized: $BF_{\#V}$) given for Izmit-deep core. Red dashed lines for correlations made by original authors; red dash-dot lines with arrow heads and question marks added for visualization of probable continuations. Y-axis same throughout. See Figure 7.1and Table 7.1 for locations and references. 190
Figure 7.4. Sand content (% weight), calculated benthic foraminifera number in 10 ml of sediment, species richness, Shannon's diversity and evenness in the Izmit-deep core. 193
Figure 7.5. Pore water properties of the core Izmit-deep (Alımlı, 2022). 195
Figure 7.6. Absolute (number in gram dry sediment) and relative (%) abundances of *Virgulinella fragilis*, H_2S content of pore water (μM), absolute abundance of benthic foraminifera (x-axis log scale) and planktonic foraminifera (number in gram dry sediment). Y-axis not to scale. 197
Figure 7.7. Cluster analysis (UPGMA, Bray-Curtis) calculated from left: relative abundances of taxa, right: absolute abundances of taxa (number in gram dry sediment). 198

Figure 7.8. Cluster analysis (UPGMA, Bray-Curtis) calculated from relative abundances of taxa for the Izmit-deep core samples and surface samples from all stations. 199

LIST OF ABBREVIATIONS

AMBI: AZTI's Marine Biotic Index

BF: Benthic foraminifera

BFOI: Benthic Foraminifera Oxygen Index

CCA: Canonical Correspondence Analysis

DO: Dissolved oxygen

IMS: Institute of Marine Sciences

METU: Middle East Technical University

PF: Planktonic foraminifera

P%: Planktonic foraminifera ratio (as percent) in all foraminifera;

P% = PF/(PF+BF)*100

%P*: Planktonic foraminifera ratio (as percent) in all foraminifera except for stress indicators, Van der Zwaan et al. (1990); %P* = PF/(PF+BF-S)*100, where S indicates number of stress indicators (i.e., infaunal BF)

rB: rose Bengal

SEM: Scanning electron microscope

SoM: Sea of Marmara

TOC: Total organic carbon

CHAPTER 1

INTRODUCTION

Benthic foraminifera are diverse, some are very specialized, some are tolerant to variety of environmental conditions, abundantly present in many parts of the world's oceans and seas. In addition, their presence in the long geologic record and relatively fast evolution rate makes foraminifera ideal for both biostratigraphic and paleoenvironmental studies. Studies on recent foraminifera aim to grant a predictive power to foraminiferal taxa, assemblages, and shell chemistry in terms of environmental conditions. Increased understanding of foraminiferal habitat, ecology, distribution and the relationship of these with the special conditions in which they occur allow for higher resolution and accuracy in paleo- studies, environmental monitoring efforts, as well as future predictions.

Sea of Marmara, with its semi-enclosed nature, limited circulation, permanently stratified water column, suboxic to anoxic deep waters, and coastal waters with high eutrophication risk, offers a special case study for foraminiferal research. With the reality of climate change, increased pollution and risk of eutrophication, understanding of the responses of the foraminiferal assemblages in the Sea of Marmara becomes a worthy effort in terms of environmental monitoring.

As a contribution to the benthic foraminifera literature in the Sea of Marmara, this study reports a comprehensive systematic taxonomy and a quantitative account of the deep sea assemblages. The produced quantitative database becomes a baseline for future monitoring studies.

1.1 Purpose and scope

The main research question of this thesis was "can we use individual benthic foraminifera taxa or assemblages as indicative of some environmental conditions, did the assemblage changed over time (spanning the short sediment cores at hand), can we formulate the changes over time in assemblages into changes in environmental conditions". In order to answer this set of questions a study was conducted in the Sea of Marmara and aimed to:

- Construct a detailed and comprehensive taxonomy of the benthic foraminifera of the Sea of Marmara,
- Quantitatively document the benthic foraminiferal assemblages in the Sea of Marmara, focusing on the eastern part; develop the geographic distribution of the benthic foraminiferal taxa and assemblages,
- Explore relationships between benthic foraminiferal assemblages and environmental variables such as bottom water dissolved oxygen, total organic carbon, water depth,
- Compare the quantitative findings of deeper samples of the cores with the surface samples, investigate changes in assemblages in the vertical dimension,
- Compare the quantitative findings with previous works, investigate differences and similarities between different locations in the Sea of Marmara,
- Test the applicability of several quantitative benthic foraminiferal indices in this specialized environment.

1.2 Geographic setting

The Sea of Marmara where the study was conducted, is an inland sea connecting the Black Sea to the global ocean via the Mediterranean Sea (through the Aegean Sea). 18 short cores from 15 stations were taken from mainly the eastern part of the sea

including Izmit Bay, Çınarcık Basin, southern shelf (east of Bandırma), and deep Central Basin, taken during two cruises (Dekosim and Deepredox project cruises) in summer 2019 and summer 2021 (Figure 1.1, Table 1.1).

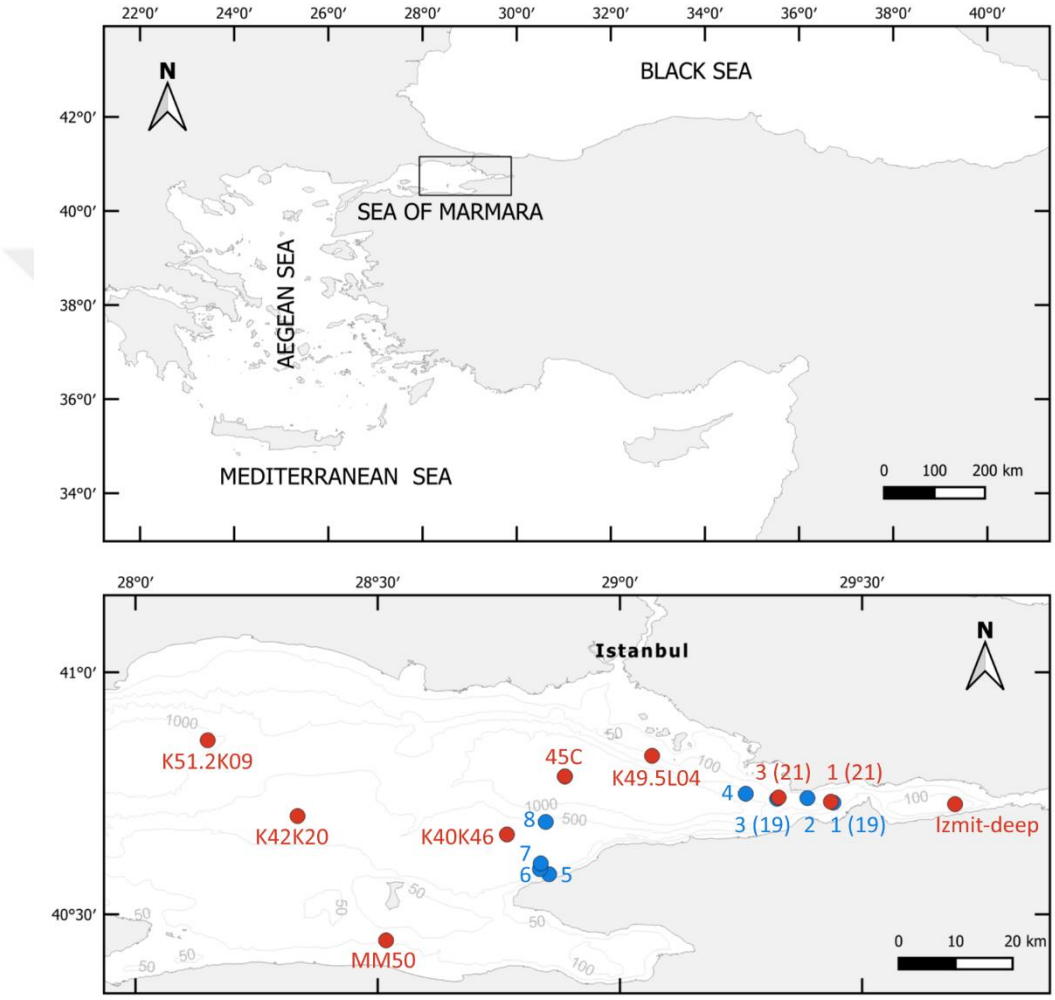


Figure 1.1. Map of stations sampled during Dekosim (2019, blue) and Deepredox (2021, red) cruises. Note that stations 1 and 3 were sampled in both cruised, and two cores were taken from station 45C (during the same multicorer cast).

1.3 Material and methods

1.3.1 Sampling

Samples were taken by a multicorer via the research vessel Bilim 2 of METU Institute of Marine Sciences in two cruises (Dekosim and Deepredox project cruises) in summer 2019 and summer 2021. In total 18 short (~40 cm) sediment cores (with intact sediment-water interface) were taken from total 15 stations in these two sampling phases (Figure 1.1, Table 1.1). The cores were subsampled on-board as slices by the use of an extruder (Figure 1.2, Figure 1.3). Slicing of the cores were done mostly as follows: 1 cm intervals for the first 4 centimeters, 2 cm intervals for following 6 centimeters, 5 cm intervals for the rest of the core (Figure 1.2; see sampling details for all cores in Table 1.2), and samples were named as the lower level of the sampling interval (e.g., 4 cm sample spans a 1 cm interval between the 3-4 cm of the core).

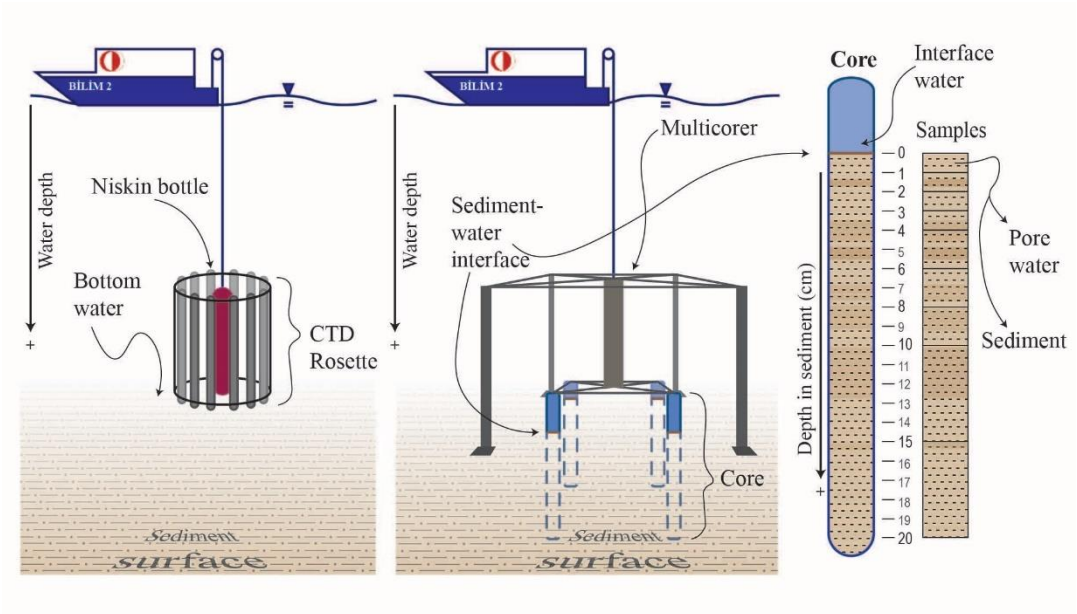


Figure 1.2. CTD and multicorer sampling schemes; positions showing bottom water, interface water and pore water samples; subsampling scheme of sediment cores.

Table 1.1 Water depths, coordinates (decimal degrees) and location tags of the stations sampled during Dekosim (2019; above dashed line) and Deepredox (2021; below dashed line) cruises. Note that stations 1 and 3 were sampled in both cruised, and two cores were taken from station 45C (during the same multicorer cast).

Station #	Bottom Depth (m)	Longitude	Latitude	Location
1	65	29.44111	40.73087	Izmit Bay Shelf
2	112	29.38750	40.74023	Izmit Bay Shelf
3	240	29.32482	40.73889	Izmit Bay Slope
4	435	29.26016	40.74921	Izmit Bay Slope
5	100	28.85404	40.58304	Armutlu Shelf
6	192	28.83508	40.59356	Armutlu Shelf
7	290	28.83676	40.60526	Armutlu Slope
8	414	28.84714	40.69099	Armutlu Slope
1	67	29.43593	40.73279	Izmit Bay Shelf
3	195	29.32812	40.74153	Izmit Bay Slope
45C	1214	28.88667	40.78500	Çınarcık Deep
Izmit-deep	206	29.69232	40.72777	Inner Izmit Bay
K40K46	318.5	28.76701	40.66507	Imralı Basin
K42K20	160	28.33465	40.70316	Southern Slope
K49.5L04	100	29.06667	40.82767	Prince Islands Outer Shelf
K51.2K09	1185	28.14906	40.85972	Central Deep
MM50	53.5	28.51746	40.44623	Southern Inner Shelf



Figure 1.3. Photographs from Dekosim (2019) and Deepredox (2021) cruises: A. CTD rosette with Niskin bottles (white arrow) and multicorer (green arrows showing the core tubes readied for sampling); B. sediment core tube before extraction from the sampling mechanism; C. sediment core tube after extraction from sampling mechanism; D. two sediment cores (yellow arrow shows undisturbed sediment-water interface); E. subsampling phase with extruder; F. sampling of the interface water with a syringe; G. extruder (blue arrow) and sediment core (orange arrow) readied for subsampling; H. subsampling phase with the extruder.

Table 1.2. Sampling scheme of cores (bold); numbers represent the bottom boundary of the sample (cm below surface). Samples used for micropaleontological analysis shaded blue. Rose Bengal added sample numbers colored pink.

1 (19)	**2**	**3 (19)**	**4**	**5**	**6**
1	1	1	1	1	1
2	2	2	2	2	2
3	5	3	3	3	3
4	10	4	4	4	4
6	15	6	6	6	6
8	20	8	8	8	8
10	25	10	10	10	10
15	27	15	15	15	15
20		20	20	20	20
25		25	25	25	25
30		30	30	30	30
32		35	35	35	35
			40	40	
			44		

7-2	**8**	**45C-1**	**45C-2**	**Izmit-deep**	**1 (21)**
1	1	1	1	1	1
2	2	2	2	2	2
3	3	3	3	3	3
4	4	4	4	4	4
6	6	6	6	6	6
8	8	8	8	8	8
10	10	10	10	10	10
15	15	15	15	15	15
20	20	20	20	20	
25	25	25	25	25	
30	30	30	30	30	
35	35	35	35	35	
40	40	40	40	40	
45		45	45	45	
		51	51	50	

3 (21)	**K49.5L04**	**K40K46**	**MM50**	**K51.2K09**	**K42K20**
1	1	1	1	1	2
2	2	2	2	2	4
3	3	3	3	3	6
4	4	4	4	4	8
6	6	6	6	6	10
8	8	8	8	8	15
10	10	10	10	10	
15	15	15	15	15	
		20	20	20	
		25	25	25	
		30	30	30	

Each slice was then divided for several different analyses. For micropaleontological analysis in 2019 cruise, samples were put into zip-lock bags (by combining top four slices, effectively producing one sample spanning 0-4 cm of the core, due to small

volume of sediment coming from each slice), and were kept frozen until washing (about 1.5 months). In 2021 cruise, samples were put into 50 ml falcon tubes and stored in the fridge (+4°C) until washing (3 months).

Rose Bengal method, a widely used method for identifying live foraminifera, was used for the 2021 cruise samples. Rose Bengal is a stain which binds to protein and stains the cytoplasm and test (inner lining) of live or recently dead foraminifera. For the samples coming from the approximately top 15 cm of the cores (Table 1.2), a rose Bengal solution was added to the samples equal to the sample volume (Schönfeld et al., 2012: 70% ethanol and 2 g/l rose Bengal), and gently shaken to disperse the solution.

1.3.2 Chemical properties of water and sediment samples

Before the multicorer casts in each station, a CTD (conductivity, temperature, and depth; Figure 1.2, Figure 1.3) cast was carried out to obtain data throughout the water column, and some water and sediment samples were taken for analysis to be carried out either onboard or later in METU-IMS facilities. Water samples were taken at specific water depths with Niskin bottles during the CTD cast, starting with the deepest point (bottom water) and going up; a water sample was taken from each core from the sediment-water interface (interface water). From these water samples dissolved oxygen (DO) and nutrients (P, N, Si) were measured. From each core slice, pore water was extracted (with centrifuge and filtering) and nutrients, hydrogen sulfide (H_2S) and dissolved iron (Fe) were measured. In addition, sediment samples were also analyzed in terms of carbon and nitrogen. The datils of the methods for chemical analysis and results can be found in Alımlı (2022) and Akçay (2022).

1.3.3 Washing

In preparation of micropaleontological analyses, washing of samples were done in METU-IMS Geology Lab. For the 2019 samples, approximately 50-100 ml of wet

sediment were soaked overnight, washed over 63 µm sieve, material coarser than 63 µm dried in an oven (~50°C) and packed into paper envelopes. For the 2021 samples the precise volumes were measured, samples were dried (~50°C) and weighed, then soaked in water overnight, a negligible volume was used in a laser diffraction grain size analyzer, then samples were washed over 63 µm sieve, material coarser than 63 µm dried in an oven (~50°C) weighed, and packed into paper envelopes. Material which is coarser than 2 mm were very little to non-existent in the samples, therefore sieving from that size was not deemed necessary for most samples.

1.3.4 Grain size

Grain size of the 2021 samples are here recorded as the weight ratio of the material coarser than 63 µm, as percent. This measure includes all sand and gravel sized material, and is referred as "sand content" as a short-hand since gravel size material is very little in the samples. Those stations with gravel size material are noted in the following chapter.

Grain size analysis was carried out for the 2021 samples by a laser diffraction grain size analyzer (Mastersizer 3000) in METU-IMS Geology Lab; however, the results differ from that of the gravimetric approach mentioned above. The difference is too high to be explained by any density differences between grains, or clumping of clay, or the presence of rose Bengal stain in the sample; therefore, the results of this analysis will not be shared.

1.3.5 Micropaleontological identification, quantification and imaging

Micropaleontology study was carried out in METU Department of Geological Engineering with a stereomicroscope. This study was carried out on material coarser than >63 µm.

For the identification of the individual foraminifera, previously published papers, books and catalogues were utilized. Main resources include the major taxonomic compilations (e.g., Loeblich and Tappan, 1988), comprehensive studies done in the Mediterranean Sea and the Sea of Marmara (e.g., Cimerman and Langer, 1991; Sgarrella and Moncharmont Zei, 1993; Sakınç, 2008), other works concerning the benthic foraminifera of the Sea of Marmara (e.g., Kaminski et al., 2002; Kırcı-Elmas, 2018), and original descriptions of taxa (Ellis and Messina catalogues and original publications where available).

For counting and picking of the foraminifera from the sediment samples a black, gridded counting tray and a wet, fine brush was used. Because the distribution of the sediment sample when transferred onto a counting tray cannot be homogeneous, and selection of foraminifera may become highly biased (e.g., towards larger specimens), counting of the whole volume of sample on the tray is advised (Schönfeld et al., 2012). The quantitative approach in foraminiferal studies require the identification and counting of foraminifera from a volume of sample which includes approximately 300 individuals (Buzas, 1990). When the original sample is too large to be processed (by picking, identifying, and storing all foraminifera in microslides), the sample can be split (by halving) as many times as needed by using a microsplitter to keep the homogeneity of the sample (Schönfeld et al., 2012) and then the whole split should be counted and picked.

Most of the samples examined in this study were fairly rich in benthic foraminifera so that they needed to be split before picking and counting can be done. For splitting samples, an aluminum dry microsplitter (Humboldt H-3971C) was used, and every spare split (e.g., 1/4, 1/8) was separately packed in paper envelopes (not merged into a single package) so that if the working split (e.g., 1/32) proves poorer than 250 individuals, next split (e.g., 1/32) can be added. The decided cut-off was 250 individuals: all samples were processed so that at least 250 benthic foraminifera were counted and picked. Only a few samples proved to be very poor, in that case the whole sample was counted and picked. The average of number of counted and picked benthic foraminifera individuals among all studied samples is approximately 500.

After picking of all benthic foraminifera from the tray, the rest of the sediment was packed into a paper envelope. All splits (counted and picked or untouched) are housed in METU Department of Geological Engineering Micropaleontology Lab under room temperature conditions.

For archiving purposes, identified, counted and picked foraminifera were fixed onto micropaleontologic slides (microslides: gridded carboard slides with black background, aluminum holder and glass cover) which were previously prepared with water soluble glue (tragacanth gum solution or commercial fixing glue for micropaleontological purposes). This counted material is housed in METU Department of Geological Engineering Micropaleontology Lab under room temperature conditions.

A new set of foraminifera individuals (about 1500 individuals: Imaging Specimens (IS) collection) were collected from various samples (other than counted splits) for imaging. For imaging of the specimens two methods were employed: stereomicrographs and scanning electron microscope (SEM) images. Stereomicrographs were taken in METU Department of Geological Engineering Active Tectonics Lab, via a Nikon SMZ25 stereomicroscope equipped with a camera (Nikon DS-Fi3) and NIS elements D 5.10 software. Almost all of the individuals in IS collection were photographed, for some individuals from various orientations. A subset of IS collection (609 individuals) was mounted onto a SEM stub (with carbon tape) for scanning electron microscopy. The stub was then coated with gold (HUMMLE VII Sputter Coating Device) and imaged with SEM (JSM-6400 Electron Microscope (JEOL), NORAN System 6 X-ray Microanalysis System & Semafore Digitizer) in METU Department of Metallurgical and Materials Engineering Scanning Electron Microscopy lab. All imaged materials are kept in METU Department of Geological Engineering Micropaleontology Lab under room temperature conditions.

1.3.6 Statistical analysis

Statistical analyses were carried out using Microsoft Excel, PAST (Hammer et al., 2001), and R. Statistical analyses used are mainly Canonical Correspondence Analysis and hierarchical clustering (UPGMA method and Bray-Curtis similarity index).

1.3.7 Diversity indices

The diversity in the assemblage can be used as a proxy for ecological health. Several indices are used to assess the diversity and evenness of a community (Magurran, 2004; Hammer and Harper, 2006). The most used indices are explained below:

1. Species richness (S): Number of species or species richness is the most straight forward of the diversity parameters. A count of species provides a numeric, comparable parameter. The idea behind is that the number of species (diversity) is higher for healthier ecosystems, but it decreases with increased stress factors such as euthrophy or deoxygenation as a smaller number of taxa are adapted to live in the extreme conditions (opportunistic taxa). However, this parameter is not very useful when comparing samples of different sample sizes (the more specimens examined the more species found, i.e., the rarest species), or samples of different dominance (i.e., the same number of species can be recorded in two samples one of which is dominated by only one species and the rest are very rare and the other one with all species occurring with about the same relative abundance). To compensate for these issues several other indices were proposed.
2. Menhinick's richness index (Menhinick, 1964, $S/\sqrt{n}$; S: species richness, n: sample size): This diversity index tries to compensate for the sample size by dividing the species richness by square root of sample size.

3. Margalef's richness index (Margalef, 1958, $(S - 1)/\ln n$; S: species richness, n: sample size): This diversity index tries an unbiased approach and compensates for the sample size by division by natural logarithm of sample size.

4. Chao1 (Chao, 1984): This is an estimate for the 'real' species richness. It is calculated by using the number of singleton (represented by one individual) and doubleton (represented by two individuals) species and sample size. This always results in a greater number than S, and may be a better fit for a study with low sample sizes.

5. Shannon's diversity index (Shannon & Weaver, 1949; Krebs, 1989, $H' = -\sum p_i * \ln(p_i)$; p_i: relative abundance of ith taxon): Shannon's diversity index (Shannon-Wiener or Shannon-Weaver index) is a measure of diversity which accounts for relative abundances of all recorded species. In the case of a single taxon H' becomes 0 (zero), and at maximum, i.e., all recorded species with the same relative abundance, $H' = \ln S$. Sometimes, instead of H', $e^{H'}$ is used since it is easier to be interpreted; it stands for the number of species the sample would constitute if all species had equal number of specimens (maximum evenness case).

6. Evenness (Buzas and Gibson, 1969, $e^{H'}/S$; S: species richness, H': Shannon's index): This index is a measure of evenness of the community, i.e., how "equally" taxa are distributed in the sample in terms of their relative abundances. In the case of maximum evenness, i.e., $H' = \ln S$, evenness ($e^{H'}/S$) becomes 1, and in the case of minimum evenness, i.e., one species very abundant and others very rare, evenness becomes 1/S.

7. Pielou's equitability (Pielou, 1966, $J = H'/H_{max}$; H': Shannon's index): This index measures evenness in the community. In the case of minimum evenness (i.e., S=1, H'=0), J becomes zero (0) and in the case of maximum evenness (i.e., $H' = \ln S$) it becomes 1. H_{max} stands for the hypothetical maximum diversity (i.e., $H_{max} = \ln S$).

8. Simpson index of diversity and dominance (Simpson, 1949, $1 - \lambda = 1 - \sum p_i^2$, $\lambda = \sum(p_i^2)$; p_i: relative abundance of ith taxon): Simpson's index (dominance: λ, sometimes D is used for notation) and its corresponding inverse (diversity: 1- λ) take into account the relative abundances of taxa. λ becomes close to 1 if one taxon is highly abundant, and if all taxa are equally abundant it takes the minimum value as $\lambda = 1/S$.

10. Fisher's α (Fisher et al., 1943, $S = \alpha \ln (1+ n/\alpha)$; S: species richness, n: sample size): this index assumes logarithmic abundance model for taxa and does not include relative abundances.

11. Berger-Parker (Berger and Parker, 1970): simply the number of individuals of the most common taxon divided by sample size.

The diversity indices were calculated via the program PAST (Hammer et al., 2001). Menhinick's and Margalef's richness indices are measures of species richness and used to diminish the sample size differences between sites, however do not take into account differences of abundances of taxa in a sample. Similarly, Fisher's α also do not include the relative abundances of taxa. Shannon's diversity provides a better alternative by considering the abundance differences between taxa, therefore is affected (controlled) by species richness and the abundance distribution between species. When used with species richness, Shannon's diversity directly, or as optimum number of species (e^H) gives more information than Menhinick's and Margalef's richness indices. Pielou's equitability is effectively equivalent to Evenness of Buzas and Gibson (1969). Lastly, Berger-Parker's index is a dominance measure and is the relative abundance of the most dominant taxon; since it does not consider the rest of the taxa in a sample, it is a limited measure. Simpson's dominance, similar to Berger-Parker index, measures the dominance in a sample, but uses relative abundances of all taxa therefore is a more robust index. Among these diversity indices, species richness, Shannon's diversity, dominance (Simpson's index) and Evenness are used as they are the most fitting for the type of data.

1.3.8 Radiocarbon dating

Two bulk sediment samples (sample 15 cm spanning between 10-15 cm and sample 45 cm spanning between 40-45 cm) from Izmit-deep station from the Karamürsel Basin (Izmit Bay) were air dried, packed in zip-lock bags, and sent to the laboratory for ^{14}C dating. TUBITAK-MAM (The Scientific and Technological Research Council of Türkiye – Marmara Research Center) radiocarbon laboratory carried out the analysis via the instrument National Electrostatics Corporation Model 3SDH-1 (UAMS) from total organic matter residue (after acid treatment) and reported conventional radiocarbon ages after $\delta^{13}C$ correction.

Calibration of conventional ^{14}C ages were done by using OxCal (v4.4.4; Bronk Ramsey, 1995, 2009, 2021) with marine calibration curve of Heaton et al. (2020; marine20.14c) and using marine reservoir correction value ($\Delta R = -63 \pm 40$) from the Sea of Marmara (Sinai et al. 2000: site number 28) as recalculated for use with Marine20 curve (Heaton et al. 2020) in the online marine reservoir correction database (map no 243; http://calib.org/marine/ accessed on April 1st, 2024; Reimer and Reimer, 2001). The calibration was also carried out by CALIB (rev8.2, Stuvier and Remier, 1993, 2020) with the same parameters. The two calibration programs resulted in slightly different results (2-5 years): this difference is very small with regard to the error margin of ^{14}C dating. The median probability ages given by CALIB program is used in this study.

1.4 Oceanographic setting

The Sea of Marmara is an inland sea, connecting the Black Sea to the north and the Mediterranean Sea to the southwest, the Bosphorus and the Dardanelles respectively, also called the Turkish Straits System (Ünlüata et al., 1990). It is bounded in the north by a narrow, in the south by a broad shelf (~100 m water depth maximum, Ünlüata et al., 1990). The Sea of Marmara is composed of three main deep basins (Figure 1.4): Tekirdağ (~1100 m), Central (~1200 m), and Çınarcık (~1200 m)

basins, separated by the Western (~440 m) and Central (~640 m) highs from west to east. A small subbasin in the north between the Central and Çınarcık basins is sometimes called Kumburgaz basin (~820 m). To the south of the Çınarcık Basin, to the north – northwest of Armutlu Peninsula, a relatively shallow depression (~400 m) is called Imralı Basin. At the most eastern end of the sea, Izmit Bay (~200 m) is situated.

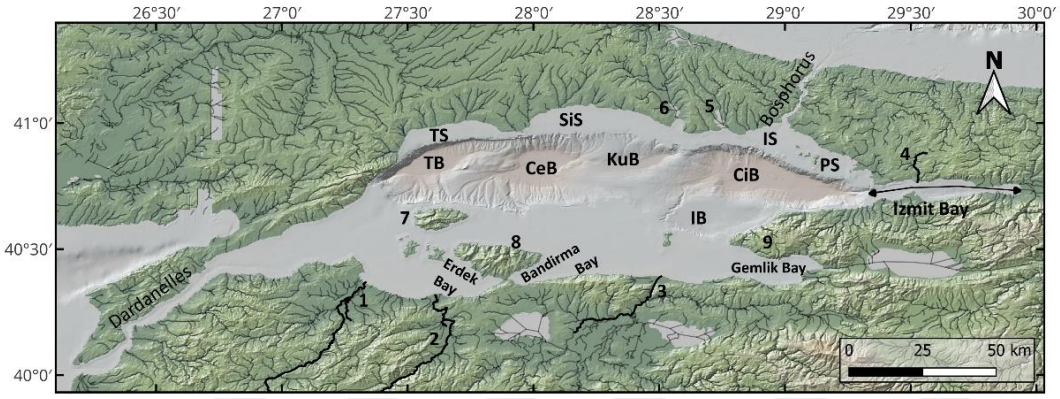


Figure 1.4. Shaded elevation topography and bathymetry of the Marmara region: names of major bottom morphologic and geographic features as used in the text are indicated on map. Abbreviations and enumerated features: TS: Tekirdağ shelf, TB: Tekirdağ Basin, SiS: Silivri shelf, CeB: Central Basin, KuB: Kumburgaz Basin, IS: Istanbul shelf, CiB: Çınarcık Basin, PS: Prince Islands shelf, IB: Imralı basin; 1. Biga Stream, 2. Gönen Stream, 3. Çapraz (Kocaçay) Stream, 4. Dil Stream (Dilderesi), 5. Lake Küçükçekmece, 6. Lake Büyükçekmece, 7. Marmara Island, 8. Kapıdağ Peninsula, 9. Armutlu Peninsula. River network from EU-Hydro River Network Database (European Union's Copernicus Land Monitoring Service, https://doi.org/10.2909/393359a7-7ebd-4a52-80ac-1a18d5f3db9c), thick and enumerated ones stand for major rivers. Base map is extracted from GeoMapApp database (version 3.7.4) http://www.geomapapp.org (Ryan et al., 2009).

The Sea of Marmara has a two layered water column with less dense, lower salinity waters supplied from the Black Sea on top, and denser, more saline waters supplied from the Mediterranean Sea at the bottom, separated by a strong halocline and pycnocline at about 25 m depth limiting the vertical mixing except for the winters

when strong winds allow for mixing to some extent (Beşiktepe et al., 1994). The dissolved oxygen in the top layer is higher (~6ml/l) compared to the bottom layer (~2ml/l), and dissolved oxygen decreases with depth, and in the bottom waters, it decreases from west to east (Beşiktepe et al., 1994). Circulation in the lower layer is limited due to the irregular bottom morphology, especially for the deep basins, and more so for the deep Çınarcık basin; therefore, the renewal of subhalocline waters is very slow and suboxic conditions in the bottom waters are permanent (Beşiktepe et al., 1994).

At the coasts of the Sea of Marmara, especially at the northeastern part, several highly populated cities, e.g., Istanbul and Kocaeli, and industrial settlements, e.g., Izmit, are situated. Hence, the organic influx to the sea from land is high especially in the eastern coasts (Tuğrul and Morkoç, 1989; Ediger et al., 2016; Yalçın et al., 2017). According to the Marmara Water Quality Bulletin [Deniz Kalitesi Bülteni: Marmara Denizi] (T.C. Çevre, Şehircilik ve İklim Değişikliği Bakanlığı [Ministry of Environment, Urbanization and Climate Change], 2022), except for the western regions which are under direct influence of Mediterranean waters coming in from the Dardanelles, the dissolved oxygen values are low (< 2 mg/l); in addition, water quality state is "poor" and "bad" and eutrophication risk is high especially in the eastern parts (Izmit Bay, Gemlik Bay, Bandırma, coasts of Istanbul and around Prince Islands, the discharge regions of Susurluk and Biga rivers; Beken, 2018; Marmara Water Quality Bulletin, 2022) Due to the high population and dense residential and industrial settlements, and despite the mitigation efforts (Bostan, 2018) the water quality decline is not eliminated (Beken, 2018).

1.5 Geologic setting

With the initiation of North Anatolian Shear Zone (NASZ, sensu Şengör et al., 2005) the SoM Basin started to develop in middle Miocene (Görür et al., 1997). As inferred from the lithostratigraphy from lands surrounding the SoM, the basin was a site of erosion and fluvio-lacustrine deposition for the most of the rest of the Miocene and

Pliocene except for short term connections with the Mediterranean Sea or the Paratethys, and became a waterway between the Mediterranean Sea and the Paratethys (later, Black Sea) during the late Pliocene (Görür et al., 1997). The connection and isolation of the sea with the Mediterranean Sea and the Black Sea were controlled by the NASZ (Şengör et al., 2005). During the Pleistocene the basin was connected to both the Mediterranean Sea and the Black Sea, yet, experienced isolation from the Mediterranean Sea during the glacial periods due to global sea level changes (Görür et al., 1997), and became a brackish lake intermittently (Çağatay et al., 2019). The last reconnection of the SoM and the Mediterranean Sea was established at 12 ka BP (Çağatay et al., 2000; McHugh et al., 2008). Several sapropelic layers were deposited in the SoM during the sea level rise and reconnection with the Mediterranean Sea, due to restricted circulation resulting from strong stratification in the water column (Çağatay et al., 2019).

The deep basins of the Sea of Marmara (Tekirdağ, Central and Çınarcık basins) and the Izmit Bay (Figure 1.4) are bounded and shaped as a part of North Anatolian Fault Zone (Görür et al., 1997; Okay et al., 2000; İmren et al., 2001; Yaltırak, 2002; Le Pichon et al., 2003; Şengör et al., 2005; Cormier et al., 2006; Okyar et al., 2008). The sea bottom morphology and sedimentary successions are modified and controlled by the active tectonism in terms of seismoturbidites, mass movements, gas/fluid release (Armijo et al., 2005; Kuşçu et al., 2005; Seeber et al., 2006; Sarı and Çağatay, 2006; Zitter et al., 2012; Eriş et al., 2012, Yakupoğlu et al., 2019). In conjunction with the tectonism, gas seepage (methane) occurs locally (Zitter et al., 2008; Gasperini et al., 2012; Ruffine et al., 2018).

The latest Quaternary sediments of the Sea of Marmara was divided into two main units (Unit 1 and Unit 2) in terms of their fossil content by Çağatay et al. (2000). The lower unit (Unit 2) is a lacustrine deposit, with a "Caspian" fresh water molluscan fauna on the shelves; Unit 1, on the other hand, is a marine deposit with abundant benthic and planktonic foraminifera (Çağatay et al., 2000).

The surficial sediments of the Sea of Marmara are mostly siliciclastic mud (<63 μm) and sandy mud, but locally sand and gravel are also present adjacent to river mouths (Ergin and Yörük, 1990; Bodur, 1991; Ergin et al., 1993; Ergin et al., 1997; Ergin and Bodur, 1999).

1.6 Previous studies in the Sea of Marmara

Studies concerned with the North Anatolian Fault Zone, its geologic history and risk of future seismic hazard in the Sea of Marmara include Ergün and Özel (1995), İmren et al. (2001), Armijo et al. (2002), Yaltırak and Alpar (2002), Le Pichon et al (2003), Polonia et al. (2004), Armijo et al. (2005), Cormier et al. (2006), McHugh et al. (2006), Oglesby and Mai (2012), Şengör et al. (2014), and Gasperini et al. (2021) among others, gaining special attention after the '99 earthquake.

The changes in the sea level, hence the changes in the depositional characteristics of the Sea of Marmara and its paleoceanography were mainly studied by Çağatay et al. (1999, 2000, 2019), Aksu et al. (2002), Yaltırak et al. (2002), Sarı and Çağatay (2006), Eriş et al. (2007), McHugh et al. (2008), Eriş et al. (2012), Artüz and Sakınç (2022).

The grain size of the surficial and core sediments was investigated by Ergin and Yörük (1990, Izmit Bay), Bodur (1991); Ergin et al. (1997, Southern shelf); Ergin et al. (1999, Southern shelf), Ergin and Bodur (1999), Ergin et al. (2012, entrance of Izmit Bay); the distribution of organic carbon in the surficial sediments were studied by Ergin et al. (1993). Organic carbon content was also evaluated in cores for detection of sapropelic sediments (e.g., Sarı and Çağatay, 2010; Çağatay et al. 1999, 2000, 2019).

Sediments of Sea of Marmara were evaluated for pollution by many researchers. These studies investigated the concentration of organic pollutants and heavy metals in the sediment (e.g., Yılmaz et al., 2019, Golden Horn, Izmit Bay; Akdemir and Dalgıç, 2021, Yalova; Kılıç et al., 2023, Golden Horn), trace elements and/or

radionuclides in surface sediments for ecological risk assessment (e.g., Pekey et al., 2004, Izmit Bay; Otansev et al., 2016, Bosphorus; Gözel et al., 2022, Golden Horn; Arslan Kaya et al., 2023a, Izmit Bay), the heavy metal concentrations and effects on foraminifera (e.g., Yümün and Nışancıoğlu, 2023, Southern shelf; Kam and Yümün, 2021, Istanbul shelf), and microplastics in the sediment (e.g., Belivermiş et al., 2021, Golden Horn; Olguner et al., 2023, Bosphorus).

The biogenic elements in much of the literature hold great importance in terms of paleoenvironmental, paleoclimatic, palaeoceanographic interpretations, as well as their modern distribution and tolerance/sensitivity towards environmental changes. Therefore, they are reviewed here with more detail under two main categories.

1.6.1 Previous studies in planktonic nanno- and microbiota and palynomorphs

Among planktonic organisms, planktonic foraminifera have lower abundance (compared to the Mediterranean assemblages, Alavi, 1988) and poor diversity (Kırcı-Elmas, 2006), as a result, were sparsely studied. The planktonic foraminiferal data given in the publications are usually as total planktonic foraminifera counts (or ratios) alongside the benthic foraminiferal abundance, for interpretation of change in water depth (e.g., McHugh et al., 2008) and primary productivity (e.g., Çağatay et al., 1999). Only in Kırcı-Elmas (2006) and Kırcı-Elmas et al. (2008) species of planktonic foraminifera were treated quantitatively. Planktonic foraminifera were also utilized in the analysis in oxygen isotopes ($\delta^{18}O$) for paleosalinity assessment (e.g., Sperling et al. 2003, Kırcı-Elmas et al., 2008).

Calcareous nannofossils were studied alongside foraminifera (Kırcı-Elmas et al., 2008; Meriç et al., 2020) and for biostratigraphic purposes (Yıldız and Toker, 2006).

Benthic diatoms were studied by Akçaalan et al. (2022), in terms of their environmental preferences and their potential for use in environmental monitoring. Planktic diatoms were studied in the water column by Uysal (1996), Taş and

Hernandez-Becerril (2017), Taş (2017) in terms of the diversity and distribution, as well as the relationships with environmental variables. Planktonic diatoms were also studied alongside other phytoplankton in terms of mucilage events (e.g., Tüfekçi et al., 2010; Tekdal et al., 2021). Balkıs and Taş (2016) provided a review and a checklist for the phytoplankton, including diatoms. Diatom studies from the sediments are limited to one: Kırcı-Elmas et al. (2021) reported diatom assemblage in addition to foraminiferal and calcareous nannofossil assemblage.

Palynomorphs were studied by Mudie et al. (2001, 2002, 2004, 2007, 2024), Caner and Algan (2002), Londeix et al. (2009), Balkıs et al. (2019), Leroy et al. (2023) for paleoenvironmental studies: paleosalinity, distinction of lacustrine and marine deposits, and paleoclimate; and in their relation to mucilage events.

1.6.2 Previous studies in benthic microbiota

Among the benthic fossilizable organisms, those with small body size and high abundance in the sediment, i.e., foraminifera and ostracoda were more frequently studied in terms of their geographic and temporal distribution, as well as for paleoenvironment and paleoclimate applications. Macrozoobenthos were studied in terms of biodiversity, and to some extent for their potential in environmental monitoring.

Ostracoda of the Sea of Marmara were studied by Tunoğlu (1996a, 1996b), Nazik (2001, Southern shelf and Dardanelles), Kubanç (2005, Southern shelf, Armutlu shelf, Izmit Bay), Kubanç et al. (2008, northern shelf), Mischke et al. (2012, Hersek Lagoon, Izmit Bay), Perçin-Paçal and Balkıs (2012 and 2015, Bandırma and Erdek bays), Perçin-Paçal et al. (2019, around Kapıdağ Peninsula) in terms of their geographic distribution and relationships with environmental conditions such as temperature and dissolved oxygen. Perçin-Paçal et al. (2016) provided a taxonomic checklist and references for each ostracoda species detected in the Sea of Marmara. Kırcı-Elmas et al. (2021) utilized ostracoda assemblage alongside with benthic

foraminifera and diatoms for the interpretation of salinity changes. Barut et al (2024, Dardanelles and Bosphorus) assessed ostracoda assemblages together with foraminifera assemblages in an investigation for radioactive pollutants.

Molluscan fauna, mainly including the pelecypoda and gastropoda, were studied by Demir (2003), Albayrak et al. (2004), Ritt et al. (2012, Tekirdağ and Central basins), Artüz et al. (2018), Çinar et al. (2020) mostly in terms of biodiversity and ecosystem documentation. Albayrak and Çağlar (2016) provided a checklist of 598 molluscan species. Molluscan fauna was also utilized for the detection of deposition under marine or lacustrine conditions in sediment cores (e.g., Çağatay et al., 2009).

Echinoderms were also studied in terms of biodiversity and their potential for use as indices in environmental monitoring (Acar et al., 2023; Çinar et al., 2024). Öztoprak et al. (2014) compiled a checklist for echinoderms of all coasts of Turkey, Özgür Özbek (2016) provided a recent checklist and distribution of echinoderms of Sea of Marmara.

1.6.2.1 Benthic foraminifera

Alavi (1988) was the first to study the benthic foraminifera from the Sea of Marmara. It is a quantitative study conducted on two cores from the deep Çınarcık Basin. Alavi reported that genus *Bolivina* dominated the assemblages, accompanied by buliminids and globobuliminids, *Chilostomella mediterranensis*, *Melonis pompilioides* and cassidulinids: an assemblage Alavi (1988) interpreted to occur under high productivity and low bottom oxygenation conditions.

Benthic foraminifera were utilized in Quaternary stratigraphy studies for detection of marine deposition as opposed to lacustrine; however, most studies did not report a quantitative account, or produced quantitative data only limited to genus or higher taxonomic level (e.g., Çağatay et al., 2000; McHugh et al., 2008).

Kaminski et al. (2002) quantitatively reported three sediment cores, two from the northern shelf: outside the Bosphorus and near Prince Islands, and one from the

southern part of Central High. With the sediment cores from the northern shelf, Kaminski et al (2002) documented the change from *Ammonia* and *Elphidium* dominated assemblages at the bottom to *Bolivina* dominated assemblages at the top, showing the transition from brackish but better oxygenated conditions to worse oxygenated conditions with the establishment of the two-way water exchange between the Black Sea and Sea of Marmara and the permanently stratified water column. Aksu et al. (2002) further analyzed benthic foraminifera for oxygen isotopes for paleo-salinity interpretations and the timing of connections between the Mediterranean Sea, Sea of Marmara and Black Sea.

Chendeş et al. (2004), Phipps et al. (2010), Kaminski (2012) and du Châtelet et al. (2013) studied samples coming from a depth transect at the most western part of the Sea of Marmara (west of Marmara Island). Chendeş et al. (2004) showed the presence of two distinct assemblages related with depth, an *Ammonia* and *Elphidium* dominated shallower assemblage (brackish assemblage, also present in the Black Sea shelves), and a dysoxic, saline, deeper assemblage (*Bolivina*, *Bulimina*, *Cassidulina*, *Gyroidina*, "Mediterranean species"). Chendeş et al. (2004) indicated that the change from shallow assemblage to deep assemble occurs around 25 m water depth. Phipps et al. (2010), using the sample set, distinguished three clusters of samples, one shallow cluster (< 50 m water depth), one intermediate (50-120 m), and one deep (>120 m) with distinct foraminiferal assemblages. Kaminski (2012) calculated and evaluated the Benthic Foraminifera Oxygen Index (Kaiho, 1994) from the same data set. Du Châtelet et al. (2013) investigated the agglutinant particles in textularin foraminifera and found that the test composition is independent from environmental conditions and controlled mainly by substrate and species preference.

Avşar et al. (2006) quantitatively studied surface samples from the Erdek Bay shallow shelf (28-57 m), reported that the assemblages were dominated by *Cassidulina carinata*, *Ammonia compacta*, *Discorbinella bertheloti*, *Cribroelphidium poeyanum* and *Elphidium crispum*, and showed that the foraminiferal assemblages in this region are quite homogeneous across the study site. Avşar (2010) conducted a similar study on the northern shelves (İstanbul, Silivri,

Tekirdağ; 13-111 m water depth), found assemblages dominated by *Brizalina spathulata*, *Cassidulina carinata*, *Elphidium crispum*, *Asterigerinata mamilla*, *Ammonia compacta* and *Ammonia parkinsoniana*, and showed the homogeneous nature of the foraminiferal assemblages.

Meriç et al. (2005) conducted a qualitative study on benthic foraminifera aiming to relate the morphological abnormalities to environmental stress. Meriç et al. (2014a) compiled an illustrated atlas for the benthic foraminifera of all three seas to which Türkiye has coasts, stating that the benthic foraminifera assemblages of the Sea of Marmara are less diverse than the Mediterranean (Aegean) but more diverse than the Black Sea. Kırcı-Elmas and Meriç (2016) compiled a benthic foraminiferal checklist and summarized the benthic foraminifera of the Sea of Marmara in seven different regions.

Sakınç (2008) compiled an illustrated account of the benthic foraminifera species of the Sea of Marmara, determined the biofacies belts on the shelves. According to Sakınç (2008), from shallower to deeper shelf, Rotalioidea (genera *Ammonia* and *Elphidium*), Planorbulinoidea (*Cibicides*, *Planorbulina*), and Bolivinitoidea (*Bolivina*) and Nonionoidea (*Nonionella*) dominated belts occur with Textulariina and Miliolina dominated belts locally present (Later, Sakınç and Artüz (2019) added to Sakınç's original work several other benthic foraminifera species.

Kırcı-Elmas (2006) studied six cores from Central and Çınarcık basins, two of which were published separately in Kırcı-Elmas et al. (2008). In these cores the benthic foraminifera were quantitatively analyzed, in addition planktonic foraminifera, nannoplankton and ostracoda were also studied. With these long cores (up to about 6.2 m) the changing environmental conditions from lacustrine to marine, from oxic to suboxic bottom conditions were determined according to micropaleontologic data.

Kırcı-Elmas (2013) quantitatively studied sediment surface samples distributed around the Sea of Marmara, including the Dardanelles, from 11-320 m water depth and showed that the distribution of the shallower assemblage (*Ammonia* and *Elphidium* dominated, 0-35 m) was linked to organic matter, the intermediate

assemblage (*Bulimina* and *Nonionella* dominated, 28-50 m) was present in the zone of seasonal vertical mixing, and the deep assemblage (*Cassidulina* and *Bolivina* dominated, 36-320 m) was with the highest density and diversity, and showed the stability of the lower water layer (Mediterranean supplied). Kırcı-Elmas et al. (2018) studied samples from shallow northern shelf (Tekirdağ and Silivri, 15-67 m water depth), reporting quantitative benthic foraminiferal data; showing that an assemblage change at about 40 m depth was present linked to the pycnocline, with a shallow assemblage of *Asterigerinata mamilla, Lobatula lobatula* and *Neoconorbina terquemi*, and a deeper assemblage of *Brizalina spathulata, Cassidulina carinata* and *Bulimina aculeata*. Kırcı-Elmas et al. (2021) showed the fluctuations of salinity during the Holocene due to the connections with the Mediterranean and the Black Seas at the entrance of Izmit Bay (north of Hersek Delta) by the changes in the foraminifera, Ostracoda and diatom assemblages.

1.7 Outline of the thesis

The following three chapters explain the results of this study under three different categories: chapter 2 is the sediment and water characteristics; chapter 3 explores the foraminiferal results from the core-top samples; and chapter 4 conveys the foraminiferal results from the cores, i.e., the vertical changes. The next following three chapters explain and discuss three different applications of these foraminiferal results: chapter 5 compares the results of this study with previously published quantitative foraminiferal studies and combines all for a full review of benthic foraminifera of the Sea of Marmara; chapter 6 explores several biotic indices, applies to the data of this study, and evaluates the results in terms of applicability and accuracy of these indices in such a specialized environment, i.e., the Sea of Marmara; and chapter 7 focuses on the Karamürsel Basin (Izmit Bay, Izmit-deep core), evaluating different sedimentological, oceanographic, and foraminiferal data together for a depositional hypothesis. Chapter 8 is composed of the systematic taxonomy part, arranged alphabetically in every rank; includes detailed taxonomic

and/or morphologic discussions of taxa and illustrated in 48 plates (in Appendix G); it is the backbone of this study. Lastly, chapter 9 gives a discussion and conclusion to the thesis.

CHAPTER 2

SEDIMENT AND WATER CHARACTERISTICS

The sampled stations were investigated in terms of water and sediment characteristics from the water column, interface and pore waters, and the sediments from taken cores. The results given in this chapter are utilized in Chapter 3 in terms of their relationship with the benthic foraminiferal assemblage, in Chapter 6 in terms of their relationship with the biotic indices, and in Chapter 7 for the characterization of the Izmit-deep core and evaluation of its depostiional history.

2.1 Water characteristics

For water characteristics, three sets of samples were analyzed by the personnel of METU-IMS, either onboard, or later in laboratories (Figure 1.2). Bottom water samples come from the bottommost part of the water column, sampled by Niskin bottles during CTD cast. Interface water samples were taken from top of the cores, just above the sediment-water interface. And pore water samples are extracted from slices of core. These samples were analyzed for several different variables, published in Alımlı (2022) and Akçay (2022); those related to and used in this study are given below.

2.1.1 Bottom water

In all station the bottom water temperature is 14-15 °C, salinity is between 38.7-38.8 psu, and pH is between 7.61-7.96 (Table 2.1).

Table 2.1. Bottom depth of stations (m), sampling depth (m) of the bottom water with Niskin bottles, temperature (°C), salinity (psu), pH of the bottom water.

Station	Bottom depth (m)	Sampling depth (m)	Temperature (C)	Salinity (psu)	pH
1 (19)	65	63	15.41	38.72	7.78
2	112	111	15.27	38.77	7.68
3 (19)	240	238	14.56	38.71	7.64
4	435	425	14.46	38.7	7.71
5	100	98	15.32	38.8	7.8
6	192	190	14.73	38.73	7.68
7	290	288	14.51	38.7	7.65
8	414	407	14.47	38.7	7.61
1 (21)	67	66	15.58	38.8	7.88
3 (21)	195	193	14.99	38.76	7.86
45C-1	1214	1213	14.65	38.7	7.72
45C-2	1214	1213	14.65	38.7	7.72
Izmit-deep	206	205	15.76	38.78	7.79
K40K46	318.5	318	14.57	38.71	7.83
K42K20	160	159	15.14	38.79	7.96
K49.5L04	100	96	15.37	38.8	7.84
K51.2K09	1185	1184	14.7	38.72	7.82
MM50	53.5	53	15.71	38.74	7.9

In Izmit-deep station, dissolved oxygen (DO) is not present in the bottom water, while ammonium (NH_4) and phosphorus (TP) are very abundant (Table 2.2). Stations 3, 7-2, 8 and K40K46 all have very low DO. Silica (Si) is richer in the deeper stations (45C, K51.2K09, 8, K40K46). Nitrite and nitrate (NO_3+NO_2 total) is variably present in all stations, almost diminished in Izmit-deep, fairly low in K49.5L04 and 45C.

Table 2.2 Total phosphorous (TP, µM), phosphate (PO_4, µM), nitrate and nitrite (NO_3+NO_2, µM), nitrite (NO_2, µM), silicon (Si, µM), ammonium (NH_4, µM), and dissolved oxygen (DO, µM) in bottom water samples (see sample depths in Table 2.1)

Station	TP (µM)	PO_4 (µM)	NO_3+NO_2 (µM)	NO_2 (µM)	Si (µM)	NH_4 (µM)	DO (µM)
1 (19)	1.15	1.06	9.45	0.06	21.39	0.54	45.71
2	1.76	1.03	10.32	0.18	23.08	0.43	35.92
3 (19)	1.52	1.04	7.66	0.07	33.34	0.4	7.68
4	1.28	0.85	5.42	0.05	26.12	0.28	10.26
5	0.95	0.85	9.06	0.06	20.79	0.22	57.4
6	NA	0.97	9.62	0.06	31.02	0.36	17.09
7	NA	1.06	8.32	0.02	35.69	0.17	7.25
8	NA	1.29	7	0.09	40.02	0.24	6.34
1 (21)	1.62	0.93	9.73	0.17	26.12	0.07	49.3
3 (21)	1.61	0.99	8.35	0.17	30.84	0.2	21.7
45C-1	1.66	1.03	4.35	0.06	49.8	0.15	4.6
45C-2	1.66	1.03	4.35	0.06	49.8	0.15	4.6
Izmit-deep	3.23	1.98	0.06	0.02	37.3	1.41	0
K40K46	1.89	1.05	5.82	0.15	39.48	0.05	5.5
K42K20	1.23	0.77	8.72	0.02	27.61	0.05	55.6
K49.5L04	1.48	0.43	3.4	0.03	28.07	0.19	38.4
K51.2K09	1.6	1.14	6.55	0.02	40.85	0.05	20.5
MM50	1.34	0.77	7.15	0.02	23	0.05	56.6

2.1.2 Interface water

For Izmit-deep and K42K20 stations, interface water data do not exist. Silica (Si) in the interface water is higher in deep basin stations (45C, K51.2K09). Phosphate (PO_4) is higher in the stations off Armutlu (stations 5-8) than stations of Izmit Bay transect (stations 1-4) in the 2019 sampling; however, in the 2021 sampling the PO_4 levels in stations 1 and 3 exceed that of the 2019 sampling (Table 2.3). K49.5L04 is the station where the lowest PO_4 amount was recorded.

Table 2.3. Phosphate (PO_4, µM), nitrate and nitrite (NO_3+NO_2, µM), nitrite (NO_2, µM), silicon (Si, µM), ammonium (NH_4, µM) in interface water samples.

Station	Bottom depth (m)	PO_4 (µM)	NO_3+NO_2 (µM)	NO_2 (µM)	Si (µM)	NH_4 (µM)
1 (19)	65	1.01	14.46	0.25	27.09	1.02
2	112	0.99	11.8	0.25	26.67	0.38
3 (19)	240	0.81	9.26	0.16	36.65	0.2
4	435	0.95	11.53	0.25	47.55	4.25
5	100	1.07	12.55	0.33	25.48	1.22
6	192	1.27	10.83	0.12	33.38	0.17
7	290	1.33	8.28	0.16	31.51	1.36
8	414	1.23	11.66	0.32	36.13	0.4
1 (21)	67	1.95	1.69	0.13	33.32	9.71
3 (21)	195	1.53	1.29	0.06	37	3.24
45C-1	1214	1.06	1.45	0.04	63.5	4.47
45C-2	1214	1.06	1.45	0.04	63.5	4.47
K40K46	318.5	1.24	1.21	0.07	35.37	5.21
K49.5L04	100	0.72	1.32	0.06	39.19	2.93
K51.2K09	1185	0.88	1.09	0.07	54.89	1.81
MM50	53.5	0.74	1.16	0.11	27.98	2.58

2.1.3 Pore water

Ammonium (NH_4) in the pore water is very high in Izmit-deep, fairly high 45C, K42K20, and station 3 (21). The Izmit bay samples (stations 1-4) are richer in NH_4 with respect to Armutlu samples (5-8) in the 2019 sampling. Nitrite and nitrate (NO_3+NO_2 total) is higher in 2019 stations than 2021 stations (Table 2.4).

Table 2.4. Phosphate (PO_4, µM), nitrate and nitrite (NO_3+NO_2, µM), nitrite (NO2, µM), silicon (Si, µM), ammonium (NH_4, µM) in pore water samples (top 1 cm of the cores).

Station	Bottom depth (m)	PO_4 (µM)	NO_3+NO_2 (µM)	NO_2 (µM)	Si (µM)	NH_4 (µM)
1 (19)	65	10.62	38.08	1.56	102.72	26.88
2	112	5.58	9.6	0.18	124.92	18.48
3 (19)	240	4.74	6.84	0.26	167.4	44.16
4	435	4.02	3.84	0.14	154.56	34.32
5	100	11.46	2.22	0.4	105	10.92
6	192	19.14	2.82	0.28	148.68	5.04
7	290	5.46	1.14	0.14	113.64	9.48
8	414	2.34	14.16	0.64	103.44	1.92
1 (21)	67	13.86	0.51	0.07	138.46	28.47
3 (21)	195	28.23	0.85	0.11	164.28	58.04
45C-1	1214	12.11	0.88	0.04	212.71	51.62
45C-2	1214	12.11	0.88	0.04	212.71	51.62
Izmit-deep	206	23.39	0.85	0.06	249.99	214.81
K40K46	318.5	7.48	0.59	0.08	160.9	81.3
K42K20	160	15.11	0.49	0.08	242.78	53.36
K49.5L04	100	20.18	0.81	0.1	181.09	28.07
K51.2K09	1185	1.28	0.65	0.12	96.43	10.56
MM50	53.5	2.69	0.37	0.06	67.24	9.45

2.1.4 Hydrogen sulfide in the Izmit-deep station

Hydrogen sulfide (H_2S) was measured for the Izmit-deep station in the bottom and pore water samples. It is present in the bottom water, increases in the pore water until 6 cm in the sediment, then decreases with depth (Table 2.5; Alımlı, 2022).

Table 2.5. Hydrogen sulfide (H_2S, µM) in Izmit-deep station; sample 0 cm stands for bottom water, rest comes from pore water.

Sample (cm)	H_2S (µM)
0	32.3
1	72.4
2	118.1
3	154.2
4	149.5
6	182.5
8	51.6
10	66.1
15	19.7
20	0.1
25	0.1
30	0.1
35	0.1
40	0.1
45	0.1
50	0.1

2.1.5 Correlation of variables

To see the relationships of these variables and to choose which of the variables to analyze with the micropaleontological data (see Section 3.5), the correlations between the variables were explored. Two correlation heatmaps are presented below: in both of them, total phosphorous (TP) is removed (missing data in stations 6, 7, 8), one heatmap is with Izmit-deep and K42K20 stations (due to missing interface water data) and hydrogen sulfide data (since it is only present in Izmit-deep) removed (Figure 2.1), and the other is with all interface water data removed but all stations used (Figure 2.2).

According to Figure 2.1 and Figure 2.2, silicon (Si) in bottom water and interface water are strongly correlated, but the pore water values are not as strongly correlated. Bottom water and interface water Si are also strongly corelated with bottom depth. Bottom water Si is also highly (negatively) correlated with bottom water dissolved

oxygen (DO), and interface water Si is highly (negatively) correlated with bottom water nitrate and nitrite (NO_3+NO_2 total). Moreover, porewater Si is highly correlated with porewater ammonium (NH_4). Therefore, bottom water and interface water Si are not used in the canonical correspondence analysis.

Bottom water DO, temperature, salinity and pH are all strongly or highly correlated with each other. They are mildly and negatively correlated with bottom water phosphate (PO_4), and bottom depth. Considering the very small variation in temperature, salinity and pH, and their high correlation with DO, they are removed from further analysis.

Bottom water PO_4 is strongly correlated with bottom water and pore water ammonium (NH_4), yet, a similar relationship is not present between pore water $PO_4$and bottom water or pore water NH_4 (Figure 2.2). NH_4 in the pore water and bottom water are highly correlated when all samples are considered (Figure 2.2), but this relationship is diminished when Izmit-deep and K42K20 are removed (Figure 2.1). Interface water NH_4 is highly (negatively) related with interface water NO_3+NO_2 total, and bottom water NH_4 (Figure 2.1). Pore water PO_4 and NH_4 are used in further analysis, but bottom water counterparts are eliminated.

The relationships of NO_3+NO_2, NO_2, and PO_4 with themselves from different datasets are very low to mild (Figure 2.1). NO_3+NO_2 of pore water is strongly correlated with NO_2 of pore water, however bottom water NO_3+NO_2 and NO_2 only have a mild correlation (Figure 2.2). Yet, bottom water NO_3+NO_2 is highly correlated with pore water NH_4 (Figure 2.2), therefore it is also removed from further analysis. Moreover, considering the missing interface water data in two stations, interface water variables are not used in further analysis.

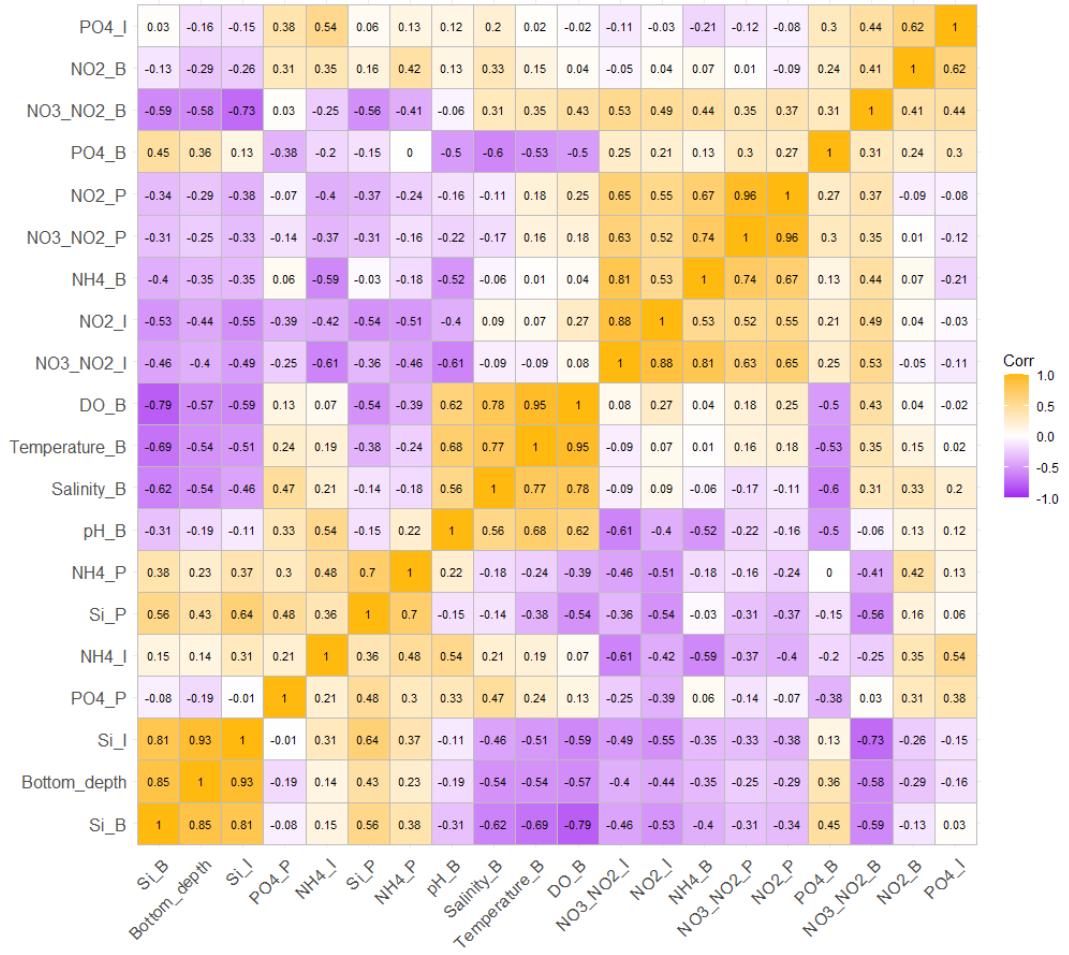


Figure 2.1. Correlation heatmap (ggcorrplot, Kassambara and Patil, 2023) for environmental variables, excluding stations Izmit-deep and K42K20, and bottom water total phosphorous. B: bottom water; P: pore water; I: interface water properties.

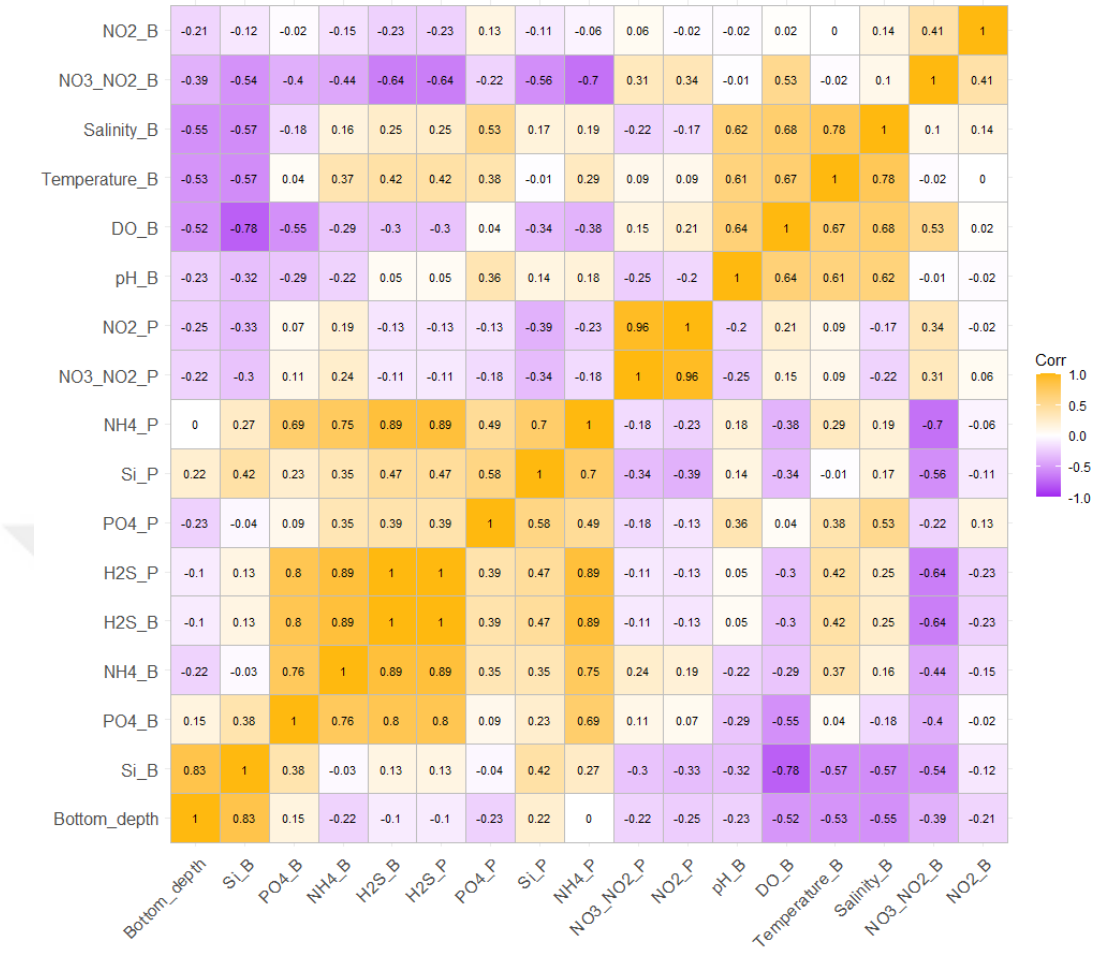


Figure 2.2. Correlation heatmap (ggcorrplot, Kassambara and Patil, 2023) for environmental variables, excluding interface water variables. B: bottom water; P: pore water

2.2 Sediment characteristics

Surface sediments of Sea of Marmara are dominantly fine grained (mud size, Ergin et al., 1993). Gravel size material (>2mm) is abundant in only Station 2, and present in only a few other stations (e.g., MM50). Due to their rarity, the gravel size material was not separately sieved and weighed. The fraction of sediment coarser than 63 μm, hereafter referred to as sand fraction, is composed of various ratios of lithogenic

elements (i.e., quartz, pyrite and other minerals, rock fragments, mica, mud clumps), and biogenic elements (i.e., benthic and planktonic foraminifera, plant debris, pollen casings, echinoid spines and test pieces, juvenile mollusks (pelecypods and gastropods), mollusk debris (shell pieces), ostracoda, sponge spicules, radiolaria). Coarse, coated grains are present in Station 2 (most likely manganese nodules). Pyrite is present in samples in the form of spherical framboidal grains and as infill (mostly in benthic foraminifera).

2.2.1 Carbon and nitrogen content of 2019 stations

Samples of 2019 stations were analyzed in terms of their carbon and nitrogen content (data published and analyzed in Akçay, 2022).

Table 2.6 gives the results from the first several slices of sediments cores. Because these sediment slices were lumped together for micropaleontologic sampling (Table 1.2) taking the average of these slices for use in further statistical analysis was deemed appropriate, these values are given in Table 2.7.

Table 2.6. Total carbon (TC), total organic carbon (TOC), total nitrogen (TN), and TOC/TN and TC/TN ratios in top centimeters of cores. Units: * mg/g, ** mmol/g.

Station	Depth (cm)	TC *	TC **	TOC *	TOC **	TN *	TN **	TOC/TN **	TC/TN **
1 (19)	1	28.41	2.37	13.37	1.11	1.66	0.12	9.41	20.01
	2	28.79	2.40	13.51	1.12	1.65	0.12	9.54	20.33
	3	28.37	2.36	13.57	1.13	1.55	0.11	10.20	21.32
	4	27.15	2.26	13.48	1.12	1.52	0.11	10.36	20.87
2	1	37.04	3.08	15.62	1.30	1.77	0.13	10.29	24.41
	2	33.51	2.79	12.11	1.01	1.37	0.10	10.29	28.49
3 (19)	1	30.28	2.52	16.57	1.38	1.80	0.13	10.72	19.60
	2	30.09	2.51	15.52	1.29	1.77	0.13	10.25	19.87
	3	28.71	2.39	15.71	1.31	1.67	0.12	10.95	20.01
	4	27.50	2.29	14.50	1.21	1.55	0.11	10.92	20.72

Table 2.6. Continued.

Station	Depth (cm)	TC *	TC **	TOC *	TOC **	TN *	TN **	TOC/TN **	TC/TN **
4	1	28.86	2.40	15.57	1.30	1.66	0.12	10.91	20.23
	2	23.88	1.99	12.75	1.06	1.45	0.10	10.23	19.16
	3	24.31	2.02	14.11	1.17	1.35	0.10	12.21	21.04
	4	26.42	2.20	13.46	1.12	1.55	0.11	10.11	19.84
5	1	32.82	2.73	11.80	0.98	1.46	0.10	9.44	26.25
	2	30.30	2.52	12.59	1.05	1.32	0.09	11.09	26.68
	3	29.10	2.42	10.98	0.91	1.28	0.09	10.04	26.60
	4	28.81	2.40	10.94	0.91	1.22	0.09	10.43	27.49
6	1	39.13	3.26	19.30	1.61	2.31	0.17	9.72	19.72
	2	36.59	3.05	16.51	1.37	1.96	0.14	9.82	21.76
	3	36.01	3.00	15.57	1.30	1.88	0.13	9.64	22.30
	4	34.67	2.89	16.06	1.34	1.74	0.12	10.76	23.23
7	1	34.01	2.83	17.51	1.46	1.89	0.14	10.77	20.94
	2	35.32	2.94	17.33	1.44	1.98	0.14	10.22	20.83
	3	34.64	2.88	16.45	1.37	1.96	0.14	9.77	20.58
	4	33.41	2.78	15.03	1.25	1.71	0.12	10.24	22.75
8	1	30.73	2.56	14.80	1.23	1.69	0.12	10.20	21.18
	2	30.80	2.56	14.64	1.22	1.71	0.12	9.99	21.01
	3	30.84	2.57	15.36	1.28	1.68	0.12	10.68	21.44
	4	29.07	2.42	14.63	1.22	1.62	0.12	10.52	20.91

Table 2.7. Total organic carbon (TOC), total nitrogen (TN), and TOC/TN ratios in the core-top samples studied, as averages of values given in Table 2.6. Units: * mg/g, ** mmol/g.

Station	TOC% * av.	TN% * av.	TOC/TN** av.	TOC/TN * av.
1 (19)	1.35	0.16	9.88	8.47
2	1.39	0.16	10.29	8.83
3 (19)	1.56	0.17	10.71	9.19
4	1.40	0.15	10.87	9.32
5	1.16	0.13	10.25	8.79
6	1.69	0.20	9.99	8.56
7	1.66	0.19	10.25	8.79
8	1.49	0.17	10.35	8.87

2.2.2 Grain size

For the 2021 sampling, sand contents (i.e., the material coarser than 63 μm collectively) were determined gravimetrically (Table 2.8). In stations K42K20, K49.5L04 and MM50 the sand content is about or higher than 10%, in rest of the stations sand content is significantly lower (Table 2.8, Figure 2.3).

Table 2.8. Sand content of the surface samples as weight percent.

Core	Sample (cm)	Sand (%W)
1 (21)	1	3.26
3 (21)	1	5.13
45C-1	1	0.37
45C-2	1	1.00
Izmit-deep	1	1.93
K40K46	1	0.64
K42K20	2	9.77
K49.5L04	1	12.24
K51.2K09	1	5.77
MM50	1	10.11

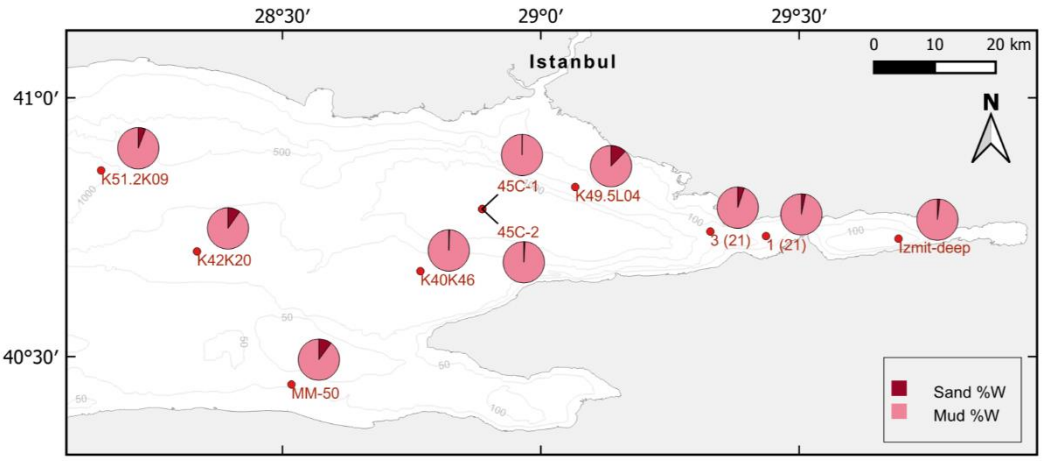


Figure 2.3. Map of sand and mud content in the core-top samples of 2021 sampling.

CHAPTER 3

LATERAL DISTRIBUTION OF BENTHIC FORAMINIFERA: ASSEMBLAGES AND RELATIONSHIPS WITH ENVIRONMENTAL VARIABLES

From the core-top samples (18 samples, Table 1.2) of all studied cores, the benthic foraminifera were identified and counted. Among these surface samples, 140 benthic foraminifera taxa were identified in total (see Appendix C). Using this data set, the total absolute abundances in the stations, diversity indices and relative abundances of individual taxa were calculated; cluster analysis on relative abundances of taxa was carried out to explore the similarities between stations and recognition of co-occuring taxa; and the relationship of the relative abundances of taxa to various environmental variables were investigated using Canonical Correspondence Analyses. The data presented here is further discussed in Chapter 5 for an overall compilation of benthic foraminiferal assemblages of the SoM, in Chapter 6 for applications of biotic indices and in Chapter 9 for environmental significance of several taxa.

3.1 Total absolute abundance of foraminifera

The total absolute abundances of benthic foraminifera in unit volume were calculated by multiplying the counted number in the working split size to reach the benthic foraminifera number in the whole sample, and normalizing to 1 ml of sediment (Table 3.1). Same procedure was also applied to planktonic foraminifera numbers. For the samples of 2021 cruise, numbers normalized to weight were also calculated (Table 3.2).

Initial volumes for the core-top samples were not noted for the 2019 cruise, however because they were lumped samples (of the first 4 cm of the core) the volumes were

quite high (around 100 ml) with respect to the 2021 samples (Table 3.1). Of the 2021 stations, initial volume of core-top sample of Izmit-deep station was also not noted, however it was taken in a 50 ml falcon tube with rB solution of at least the same volume of the sample, the initial sample volume for this sample is assumed to be around 15 ml.

Table 3.1 Initial volume (~: approximation), working split, numbers of benthic ($BF_{\#}$) and planktonic ($PF_{\#}$) foraminifera counted from the working split and benthic ($BF_{\#v}$) and planktonic ($PF_{\#v}$) foraminiferal number of the core-top samples normalized to 1 ml volume. Shades in normalized foraminiferal numbers darkens with increasing values.

Station & Sample	Initial volume (ml)	Split	$BF_{\#}$	$PF_{\#}$	$BF_{\#V}$	$PF_{\#V}$
1 (19) 4 cm	~100	1/256	1165	25	2982.4	64
2 2 cm	~30	1/128	380	6	1621.3	25.6
3 (19) 4 cm	~100	1/256	254	3	650.2	7.7
4 4 cm	~100	1/128	267	31	341.8	39.7
5 4 cm	~100	1/512	604	30	3092.5	153.6
6 4 cm	~100	1/512	500	49	4000.0	392
7-2 4 cm	~100	1/128	608	93	778.2	119
8 4 cm	~100	1/16	265	155	42.4	24.8
1 (21) 1 cm	16.25	1/64	405	7	1595.1	27.6
3 (21) 1 cm	16.25	1/32	282	4	555.3	7.9
45C-1 1 cm	18.75	1	136	116	7.3	6.9
45C-2 1 cm	12.5	1	505	155	40.4	12.4
Izmit-deep 1 cm	~15	1	96	6	6.4	0.4
K40K46 1 cm	16.25	1/4	328	836	80.7	205.8
K42K20 2 cm	13.75	1/128	944	500	8787.8	4654.5
K49.5L04 1 cm	16.5	1/256	931	1376	14444.6	2125.6
K51.2K09 1 cm	21.25	1/8	290	274	109.2	103.2
MM50 1 cm	17	1/16	421	9	396.2	8.5

The volume normalized total benthic foraminifera absolute abundances ($BF_{\#V}$) are given in Table 3.1 and Figure 3.1 (for comparison see weight normalized values in Table 3.2, Figure 3.2). The lowest absolute abundances of benthic foraminifera belong to the deepest and most extreme environments. Izmit-deep station is located

in the Karamürsel Basin, which has sulfidic bottom water conditions and very limited circulation; while 45C and K51.2K09 are the deepest sites of Çınarcık Basin and Central Basin respectively. K40K46 and Station 8 are both on the slope of the southern shelf, also with low absolute abundances; however, slope stations from the İzmit Bay (Stations 3 and 4) have higher absolute BF abundance than the other slope stations.

Table 3.2. Initial weight, working split, numbers of benthic ($BF_{\#}$) and planktonic ($PF_{\#}$) foraminifera counted from the working split and benthic ($BF_{\#W}$) and planktonic ($PF_{\#W}$) foraminiferal number of the core-top samples of 2021 cruise normalized to 1 g of dry sediment. Shades in normalized foraminiferal numbers darkens with increasing values.

Station & Sample	Initial weight (g)	Split	$BF_{\#}$	$PF_{\#}$	$BF_{\#W}$	$PF_{\#W}$
1 (21) 1cm	8.43	1/64	405	7	3075.10	53.15
3 (21) 1cm	6.12	1/32	282	4	1474.03	20.91
45C-1 1 cm	4.87	1	136	116	27.93	23.82
45C-2 1 cm	4.01	1/1	505	155	125.97	38.66
Izmit-deep 1 cm	1.40	1	96	6	68.67	4.29
K40K46 1 cm	7.91	1/4	328	836	165.80	422.60
K42K20 2 cm	6.07	1/128	944	500	19912.99	10547.13
K49.5L04 1 cm	5.94	1/256	931	137	40117.15	5903.38
K51.2K09 1 cm	6.75	1/8	290	274	343.91	324.93
MM50 1 cm	5.33	1/16	421	9	1264.03	27.02

Moderate absolute abundances are found on the southern inner shelf and outer Izmit Bay stations (Stations 1, 2, 5, 6, 7 and MM50). The two outer shelf samples K42K20 and K49.5L04 have the maximum recorded absolute abundance (Figure 3.1).

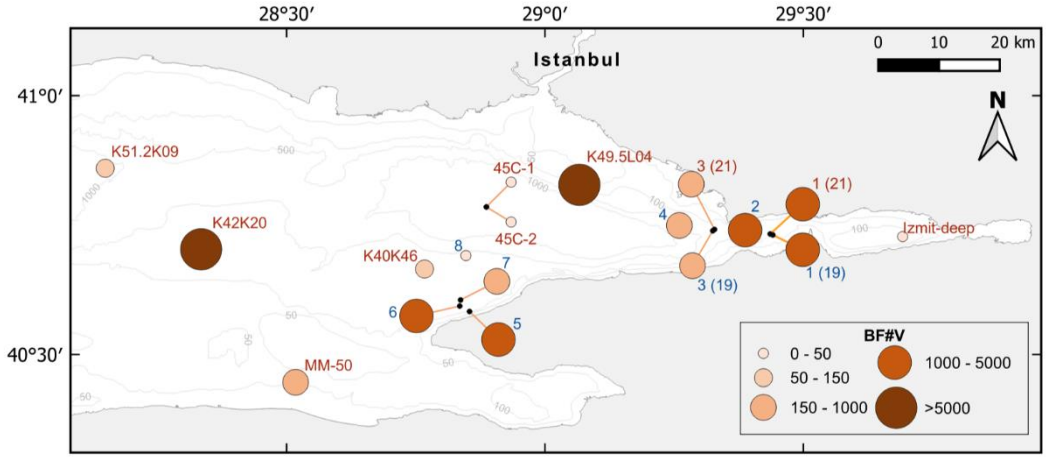


Figure 3.1. Map of volume normalized total benthic foraminifera abundances ($BF_{\#V}$) in the core-top samples. Shades as in Table 3.1.

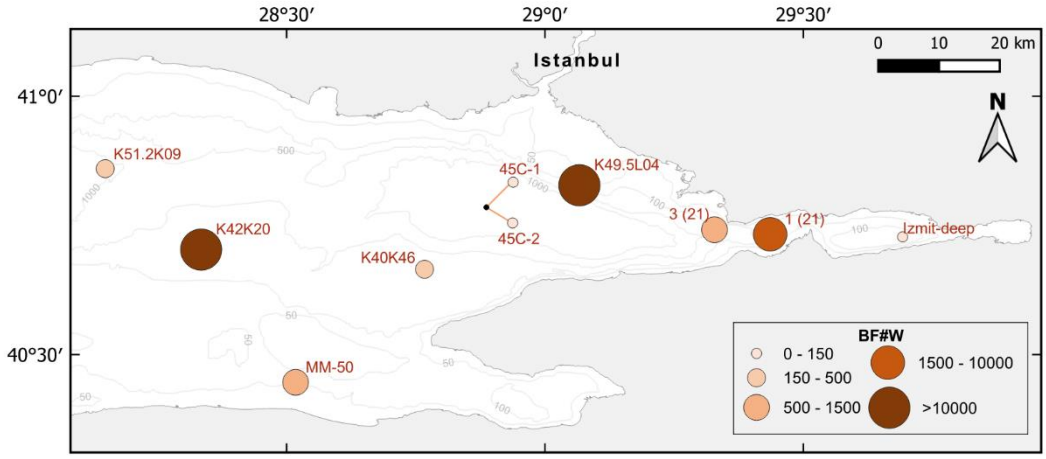


Figure 3.2. Map of weight normalized total benthic foraminifera abundances ($BF_{\#W}$) in the core-top samples. Shades as in Table 3.2.

Planktonic foraminiferal abundance is lowest in the Karamürsel Basin (Izmit-deep), followed by Station 3 (both 2019 and 2021), MM50, and 45C (Table 3.1, Figure 3.3, for comparison see weight normalized values in Table 3.2, Figure 3.4). Station 2, 8

and 1 (21), 4 and 1(21) also have low PF abundances. Rest of the core-top samples have PF abundances higher than 100 in 1 ml sediment. The highest numbers occur in K42K20 and K49.5L04 in which the BF abundances are highest as well.

As expected, the weight normalized abundances in the 2021 samples follow almost the same pattern in volumetric normalization, both in benthic and in planktonic foraminifera numbers (Table 3.2). The volume and weight normalizations are very well correlated for both benthic and planktonic foraminifera (R^2 values of 0.99; Figure 3.5). Izmit-deep values can be regarded as outliers, though, the differences from the other samples are very small.

Core-top samples of 45C-1 and 45C-2 are slightly different from each other in terms of both BF and PF absolute abundances (Table 3.1, Table 3.2), both are higher in 45C-2. Station 1 (19) and 1 (21) are also quite different, but Station 3 (19) and 3 (21) are relatively similar.

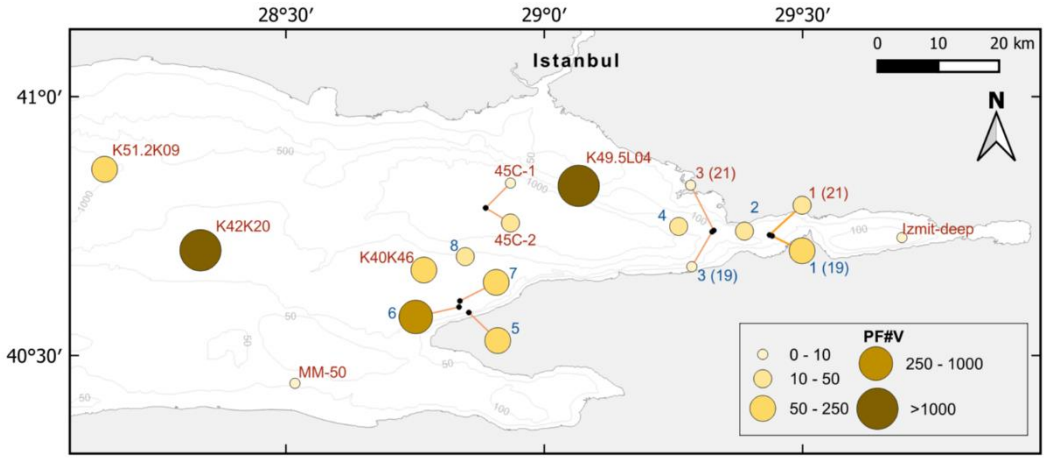


Figure 3.3. Map of volume normalized total planktonic foraminifera abundances ($PF_{\#V}$) in the core-top samples. Shades as in Table 3.1.

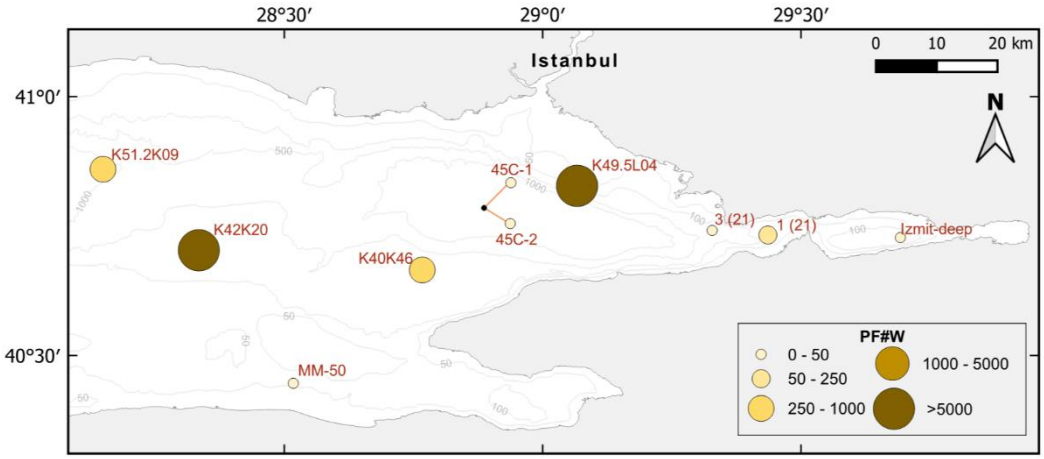


Figure 3.4. Map of weight normalized total planktonic foraminifera abundances ($PF_{\#w}$) in the core-top samples. Shades as in Table 3.2.

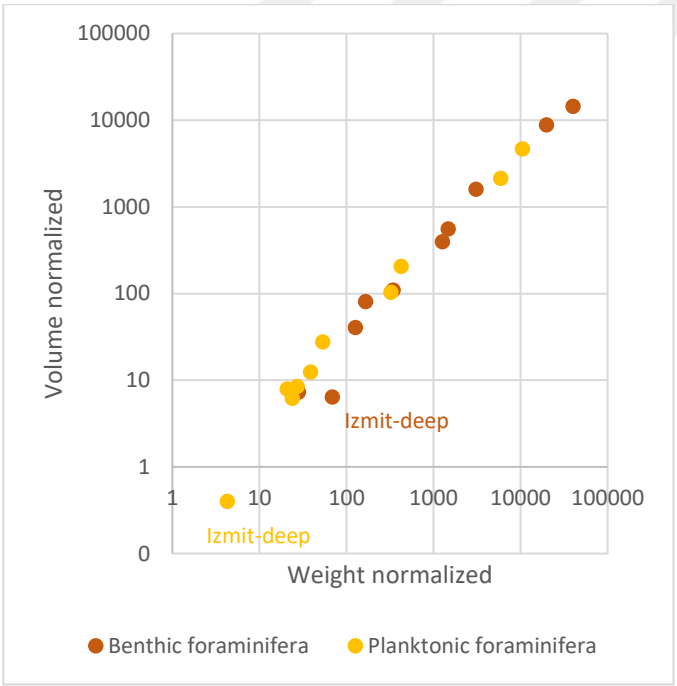


Figure 3.5. Normalized foraminiferal abundance values plotted on log-log scale. Outlier (Izmit-deep) value marked.

3.1.1 Rose Bengal stained benthic foraminifera

The foraminiferal assemblage of any given sample is composed of in-situ elements, which include not only the living assemblage (live at the time of sampling) and also the in-situ dead assemblage, and allochthonous elements, which include any translocated (vertically) material due to bioturbation and redeposited material from various other parts of the basin. The dead in-situ assemblage is further modified with winnowing, or transportation of tests vertically down in the sediment due to mixing. Therefore, any total (i.e., undifferentiated as live or dead) assemblage carries a large error margin. In order to minimize the possible error, in ecological studies, it is advised to carry out analyses on live benthic foraminifera counts. Using rose Bengal staining is the most commonly employed method for this purpose (Schönfeld et al. 2012).

In order to distinguish the live foraminifera, during the sampling of 2021, samples (usually down to 15 cm) were added a rose Bengal solution (Schönfeld et al., 2012). In the samples which were added the rB stain, the mud fraction, any organic material (e.g., plant debris, pollen casings), and some fraction of biogenic calcareous elements (Echinoid, Mollusca and Ostracoda debris and foraminifers) were colored various shades of pink. The most commonly used criteria for distinguishing the truly stained (assumed living at the time of sampling) individuals is that the whole test, except for the last chamber, should be stained vivid pink (e.g., Bernhard et al., 2006; Ishimura et al., 2012; Schönfeld et al., 2013; Guy-Haim et al., 2017; Barrientos et al., 2018). However, due to differences in test material (e.g., the staining of opaque miliolid tests usually cannot be determined from the outside, thicker or more porous test material may be less transparent) the intensity (brightness and vividness) of the staining may be different across taxa and size fractions of taxon, hence, for identification and selection of "live" foraminifera, Schönfeld et al. (2012) states that coloration intensity should be assessed for each taxon separately, and that the assessment should be done on wet individuals (either wet picking or wetting the dried

specimens). Figure 3.6 shows the variation in intensity of pink staining among taxa, as well as non-stained and poorly colored individuals.

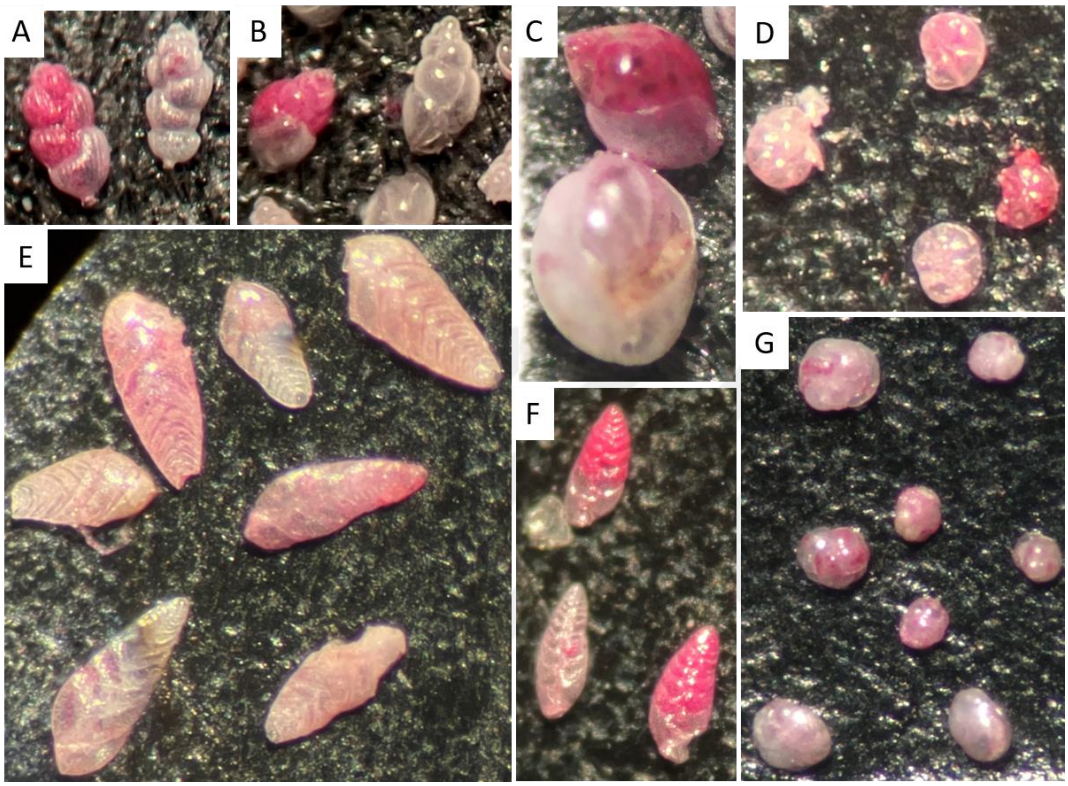


Figure 3.6. Rose Bengal stained and non-stained specimens. A. *Rectuvigerina phlegeri* Le Calvez, stained and non-stained individuals in Station 1 (21) 1 cm; B. *Bulimina elongata* d'Orbigny, stained and non-stained individuals in Station 1 (21) 1 cm; c. *Globobulimina* spp., stained and non-stained individuals in K51.2K09 1 cm; D. *Eilohedra vitrea* (Parker), one stained and three poorly colored individuals in Station 3 (21) 1 cm; E. *Bolivina spathulata* (Williamson), all poorly colored individuals in Station 3 (21) 1 cm; F. *Bolivina* cf. *vadescens* Cushman, two stained and one non-stained individuals in Station 3 (21) 1 cm; G. *Paracassidulina minuta* (Cushman), one stained (patchy staining) and seven poorly colored individuals in K49.5L04 1 cm.

During the picking and counting process, the number of rose Bengal (rB) stained specimens were noted. In Table 3.3, these numbers and the ratio of the rB stained

individuals to the total benthic foraminifera counts (Live %) are given for the core-top samples. The number of live foraminifera in the working splits of samples are very low (maximum of 50 in K49.5L04 sample 1 cm), and they constitute only a very small fraction of the total (live and dead together) assemblage (maximum of 10.3% in K51.2K09 sample 1 cm).

Although data on live foraminifera are more suited for ecological purposes, due to the scarcity, the picking and counting of rB stained foraminifera to reach statistically meaningful numbers (about 300) would be a highly time-consuming process. Therefore, any further analyses were carried on total assemblages only.

Table 3.3. Number of total ($BF_{\#}$), rose Bengal stained (rB $BF_{\#}$) benthic foraminifera picked from the working split of the core-top samples and the relative abundance of rB stained forms in total BF assemblage (Live %).

Station & Sample	$BF_{\#}$	rB $BF_{\#}$	Live %
1 (21) 1 cm	405	12	3.0
3 (21) 1 cm	282	10	3.5
45C-1 1 cm	136	2	1.5
45C-2 1 cm	505	4	0.8
Izmit-deep 1 cm	96	3	3.1
K40K46 1 cm	328	6	1.8
K42K20 2 cm	944	0	0.0
K49.5L04 1 cm	931	50	5.4
K51.2K09 1 cm	290	30	10.3
MM50 1 cm	421	20	4.8

3.2 Diversity indices

Calculated diversity indices are presented in Table 3.4 along with the number of benthic foraminifera counted ($BF_{\#}$) in the working splits. Species richness (S), i.e., the number of taxa among all counted specimens in the working split, changes between 27 and 84. The least richness is recorded in Izmit-deep station, while the

most richness is in Station 5 (shelf, off Armutlu Peninsula). Shannon's diversity (H, Shannon and Weaver, 1949) is highly similar, and somewhat correlated, to species richness (Figure 3.7) due to similar dominance and evenness values across samples (Table 3.4); changes between 2.451 (K49.5L04) and 3.464 (Station 2). Evenness (E, Buzas and Gibson, 1969) is inversely related to, and calculated from, Shannon's diversity; it changes between 0.237 (K49.5L04) and 0.658 (Izmit-deep). Dominance (D, Simpson, 1949) is inversely related, although not well correlated, to evenness (E); and changes between 0.055 (Station 2) and 0.184 (45C-2) (Figure 3.8).

Table 3.4. Species richness (S) and counted benthic foraminifera number ($BF_{\#}$) in the working splits, and dominance (D), Shannon's diversity (H) and evenness (E) of the core-top samples.

Station & Sample	S	$BF_{\#}$	D	H	E
1 (19) 4 cm	67	1165	0.093	3.059	0.318
2 2 cm	64	380	0.055	3.464	0.499
3 (19) 4 cm	43	254	0.095	2.929	0.435
4 4 cm	52	267	0.083	3.152	0.450
5 4 cm	84	604	0.095	3.307	0.325
6 4 cm	65	500	0.104	3.116	0.347
7-2 4 cm	68	608	0.099	3.081	0.320
8 4 cm	52	265	0.095	3.064	0.412
1 (21) 1 cm	42	405	0.105	2.782	0.385
3 (21) 1 cm	41	282	0.102	2.871	0.431
45C-1 1 cm	33	136	0.157	2.646	0.427
45C-2 1 cm	45	505	0.184	2.452	0.258
Izmit-deep 1 cm	27	96	0.079	2.877	0.658
K40K46 1 cm	35	328	0.086	2.82	0.479
K42K20 2 cm	54	944	0.133	2.609	0.252
K49.5L04 1 cm	49	931	0.170	2.451	0.237
K51.2K09 1 cm	41	290	0.087	2.965	0.473
MM50 1 cm	55	421	0.062	3.197	0.445

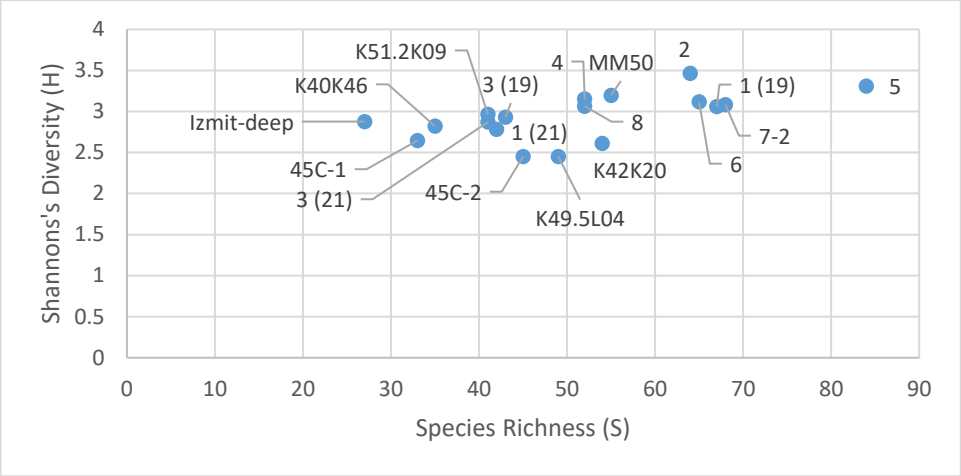


Figure 3.7. Scatter plot of species richness (S) vs Shannon's diversity (H).

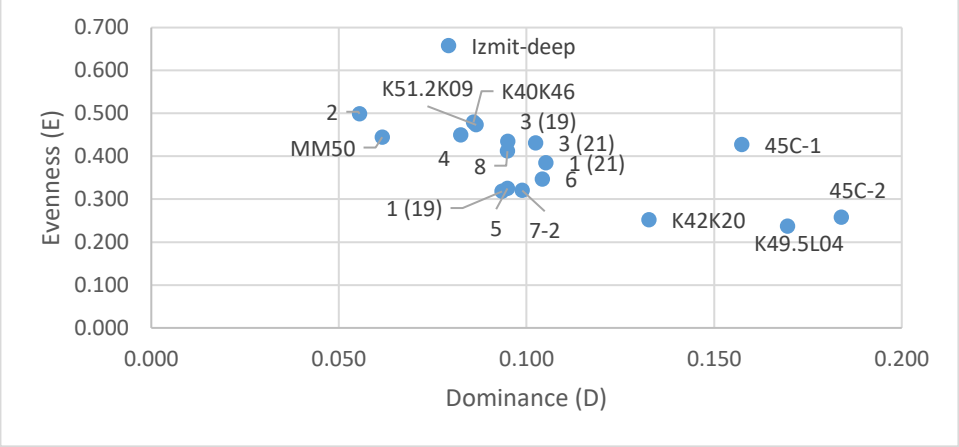


Figure 3.8. Scatter plot of dominance (D) vs evenness (E).

3.3 Geographic distributions and relative abundances of benthic foraminifera taxa

Benthic foraminifera taxa are arranged into classes with regards to i. the number of core-top samples they occur in as a measure for geographic distribution of taxa, and ii. the relative abundances (Supplementary Table C.1). The number of core-top

samples the taxa occur in and their maximum, minimum and average relative abundances relative abundances are given in Supplementary Table C.2. The relative abundances of the benthic foraminifera in the core-top samples are given Appendix C (Supplementary Table C.3). Below, under geographic distribution classes, the relative abundances of taxa are explained.

3.3.1 Taxa showing wide geographic distribution

16 taxa found in at least 15 of the 18 surface samples are classified as geographically widely distributed. Seven of these taxa occur in all samples, three in 17 samples, two in 16 samples and four in 15 samples (Table 3.5, Supplementary Table C.2).

Among the seven taxa occurring in all samples, *Paracassidulina minuta* (Cushman) in 14 samples, *Bolivina spathulata* (Williamson) in 11 samples, and *Bolivina* cf. *vadescens* Cushman in only one sample, are of dominant abundance (>15%). Among these 16 taxa which occur in at least 15 samples, no other ever reaches dominant abundance in any sample (i.e., are all <15%). These three taxa are the most abundant in the studied samples.

Bolivina dilatata Reuss is present in all samples except for two (Station 2 and MM50), and is abundantly present (5-15%) in four samples (Stations 6 and 7-2, K42K20 and K51.2K09).

Valvulineria bradyana (Fornasini) is present in 15 samples, abundantly so in two of them (Station 1 (21) and MM50).

Globocassidulina subglobosa Brady, *Bolivina striatula* (Cushman), *Cassidulina laevigata* d'Orbigny, *Bulimina marginata* d'Orbigny, *Bulimina aculeata* d'Orbigny occur abundantly (5-15%) in one sample each and in other samples they are of lower frequencies.

Eilohedra vitrea (Parker), *Gyroidina umbonata* (Silvestri), *Bolivina alata* (Seguenza) and *Discorbinella bertheloti* (d'Orbigny) are all widely distributed, occurring in almost all samples, but never abundances with higher than 5%.

Table 3.5. The widely distributed taxa, in how many core-top samples they occurred (Count), and their minimum, maximum and average relative abundances (%). Taxa abbreviations as in Supplementary Table A.1.

Taxa	Count	Min	Max	Average
B_acule	15	1.03	9.03	2.70
D_berthe	15	0.25	4.17	1.46
R_unid	15	0.20	3.68	1.12
V_brady	15	0.40	8.08	2.77
B_alata	16	0.32	4.88	1.80
B_dilat	16	0.25	10.49	3.59
B_margi	17	0.26	6.46	1.47
C_laevi	17	0.30	5.23	1.99
Elagen	17	0.24	1.51	0.82
B_spath	18	10.45	23.74	17.12
B_stria	18	0.17	10.67	1.89
B_vades	18	3.79	17.32	9.24
E_vitre	18	0.53	4.12	2.27
G_sglob	18	0.42	5.21	1.43
G_umbon	18	0.25	3.19	1.53
Pcas_mi	18	2.38	36.03	20.27

The other two widely occurring taxa are not identified in specific level, therefore require attention. First, Family Ellipsolagenidae is present in all samples except for K40K46. This group, overall, is highly diverse in the studied samples (16 species identified, see Chapter 8), and although were counted together (except for *Favulina hexagona* (Williamson)), are always in rare (1-2%) to very rare (<1%) abundances; therefore, individual species are all very rare, and also probably of limited or restricted distribution. Second, Unidentified Rotaliana are present in 15 samples in rare to frequent abundances, with maximum 3.68% abundance (Table 3.5). This group includes rotalid foraminifera specimens which are usually small (juvenile) and/or broken, prohibiting identification in lower taxonomic ranks. Therefore, the distribution and relative abundances of this taxon is meaningless.

3.3.2 Taxa showing limited geographic distribution

55 taxa which are present in 5-14 samples are categorized as having a limited distribution (Supplementary Table C.2). Among these only six of them are abundant in one or two samples. One of these, *Bulimina* spp., is of 8.33% abundance in Izmit-deep station, and includes small (juvenile) *Bulimina* specimens which were not definable down to species level. *Bulimina elongata* d'Orbigny is present in 13 samples with usually rare (1-2%) to frequent (2-5%) abundances, but is abundantly present (7.16%) in Station 1 (21) and MM50. *Bulimina costata* d'Orbigny is also present in 13 samples with usually rare to frequent abundances, but in K42K20 it is abundant with 6.14% abundance. *Rectuvigerina phlegeri* Le Calvez is abundant (9.74%) in MM50, but mostly very rare in all other samples (12 in total) it is found. *Melonis pompilioides* (Fichtel and Moll) is present in 11 samples with mostly very rare to rare frequencies, but in K51.2K09 it is abundant with 6.9%. *Haynesina depressula* (Walker and Jacob) is present in 9 samples and is usually very rare, while in Izmit-deep station it is slightly abundant (5.21%).

From the rest of the taxa with limited distribution, 19 occur in 10-14 samples, and usually are of very rare to rare abundances, occasionally reaching frequent

abundances. Among these taxa *Spiroplectinella wrighti* (Silvestri), *Ammonia* spp., *Eubuliminella* sp. and *Bolivina albatrossi* Cushman are higher than 4% in one sample each (Station 2, MM50, Station 3 (21), K40K46 respectively).

It appears the smaller the number of samples the taxon is found, smaller the abundances it has in the samples. An exception is *Bolivina variabilis* Williamson, which is found in 14 samples, however always with low abundances (maximum of 1.03%). Another exception is *Sigmoilinita tenuis* (Czjzek) which is found in 9 samples with very rare abundances, but is present in K40K46 with 3.05% abundance.

The rest of the 32 taxa found in 5-9 samples are all very rare to rare in abundance, occasionally being up to 4%.

3.3.3 Taxa showing restricted geographic distribution

46 taxa occur in 2-4 samples and usually have very rare to rare abundances. Three of these taxa have higher abundances. *Virgulinella fragilis* Grindell and Collen occurs in two samples, very rare in Station 1 (19), but abundant (7.29%) in Izmit-deep. *Sigmoilopsis* sp. 1 occurs in two samples, in K40K46 it is dominant (16.77%), and in K51.2K09 it is frequent (3.10%). And *Bulimina inflata* Seguenza is present in two samples, very rare in Station 8, but abundant (8.28%) in K51.2K09.

3.3.4 Taxa in only one station: singletons

There are 23 taxa which occur only in one sample, and all of these taxa are with very rare abundances. One exception is *Bigenerina nodosaria* d'Orbigny which is 1.38% (rare) in K51.2K09.

3.4 Benthic foraminifera assemblages and similarities of sites

Benthic foraminifera assemblages across most of the studied core-top samples are not drastically different from each other. A two-way cluster analysis visualizes the similarity of samples and the distributions of selected taxa across samples in Figure 3.9. As the contribution of taxa in the analysis are proportional to their relative abundance, the analysis was limited to the taxa with at least 2% relative abundance in at least one sample (>2% taxa hereafter). Rarer taxa were eliminated from the analysis since their contribution would be negligible. The relative abundances of these 45 taxa account for in average 89.9% of the total in these core-top samples (Table 3.6).

Table 3.6. The total relative abundance of the >2% taxa (SUM, percent), and the number of these taxa occurring (S) in the core-top samples. Station names colored according to the cluster they belong to (Figure 3.9).

Station	Sample	SUM	S
1 (19)	4	89.53	35
2	2	81.32	34
3	4	93.31	30
4	4	88.39	31
5	4	81.62	36
6	4	84.20	35
7	4	83.88	33
8	4	86.42	29
1 (21)	1	93.58	29
3 (21)	1	91.84	28
45C-1	1	94.85	26
45C-2	1	91.49	28
Izmit-deep	1	94.79	22
K40K46	1	96.04	26
K42K20	2	93.33	29
K49.5L04	1	94.84	31
K51.2K09	1	90.00	26
MM50	1	88.84	29

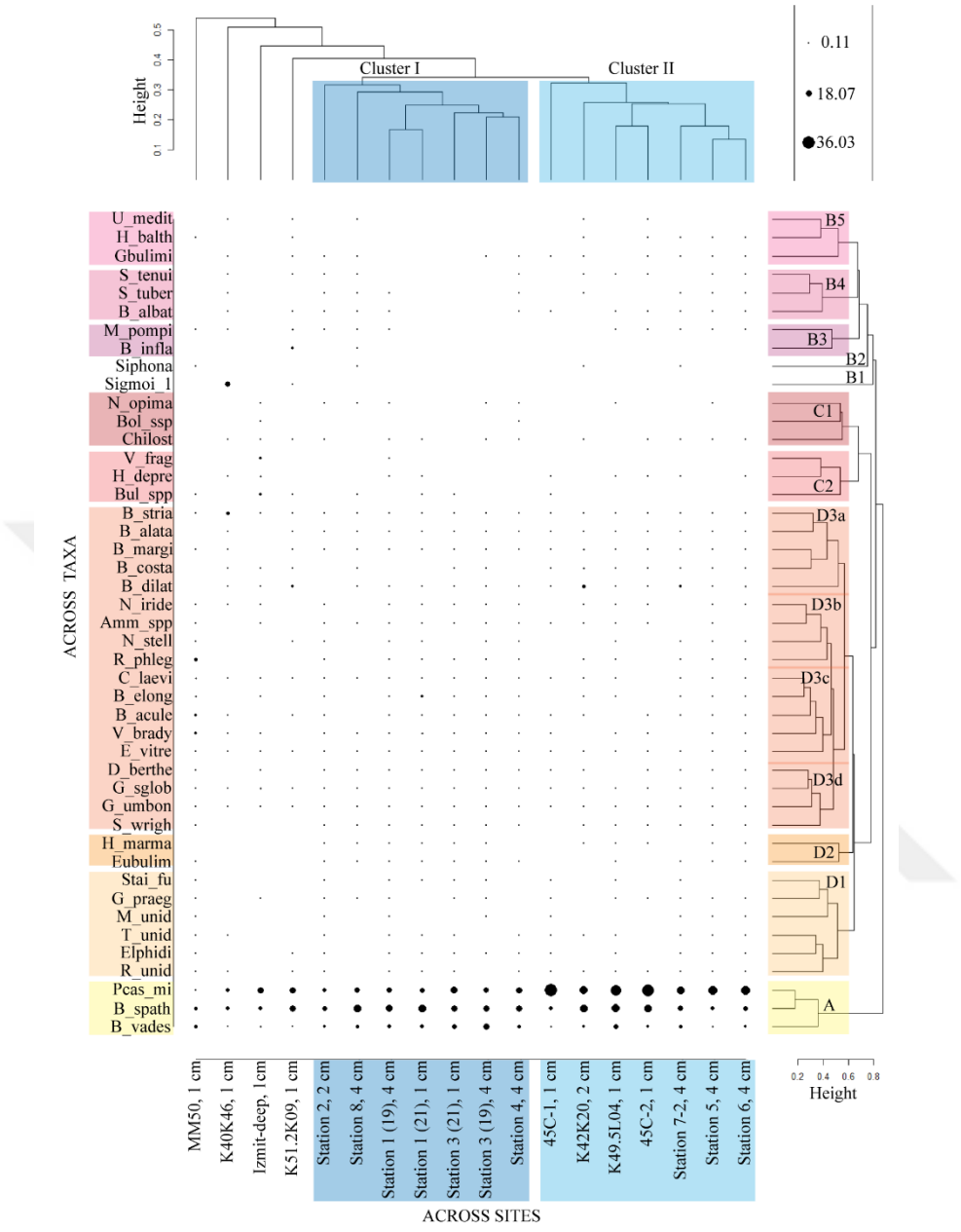


Figure 3.9. Two-way cluster (UPGMA, Bray-Curtis dissimilarity) diagram (Bapst, 2012; paleotree package version 3.4.7) using relative abundances of taxa which are at least 2% abundant in at least one sample, across all core-top samples. Dendrogram across sites (samples) located horizontally, across taxa vertically; relative abundances of taxa summarized at the center, key to size of dots at top right corner. Taxa abbreviations as in Supplementary Table A.1. Graph colored to maximize readability, clusters (see text) labeled on the dendrogram across taxa (A-D) and across sites (I and II).

The most dominant and widely distributed three taxa, namely *P. minuta*, *B.* cf. *vadescens* and *B. spathulata* group together in the cluster analysis (cluster A). Due to their very high abundance and presence in every sample, this group of taxa are different from all others. The distribution of the relative abundances of these three taxa are given in Figure 3.10, and are sometimes inversely, sometimes directly related.

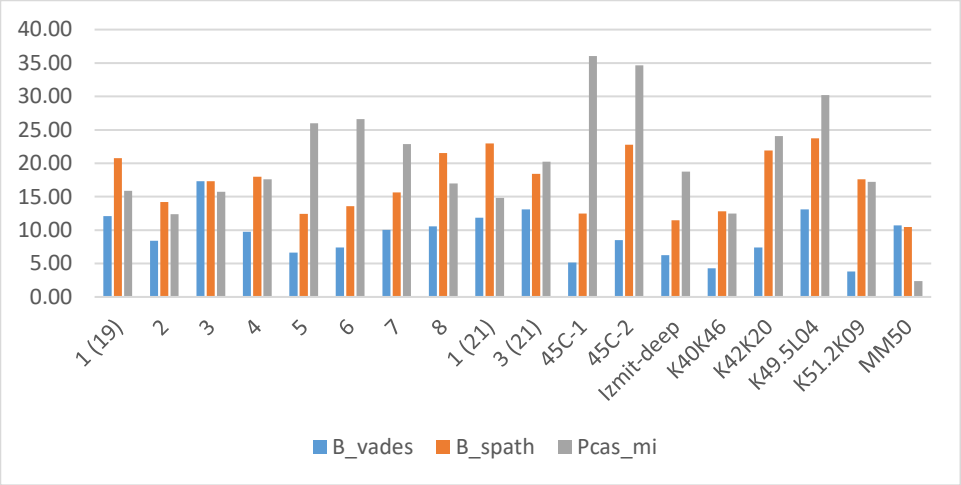


Figure 3.10. Relative abundances of taxa belonging to Cluster A.

Clusters B and C are composed of more sporadically present taxa (limited and restricted distributions). In Cluster B, the taxa with high relative abundances in K40K46, K42K20, and K51.2K09 stations are grouped together (Figure 3.11); while, in Cluster C, the taxa with high relative abundances in Izmit-deep station are present (Figure 3.12).

Cluster D is composed of taxa which are more regularly found in samples but with mostly less than 3% abundance (Figure 3.12,Figure 3.13).

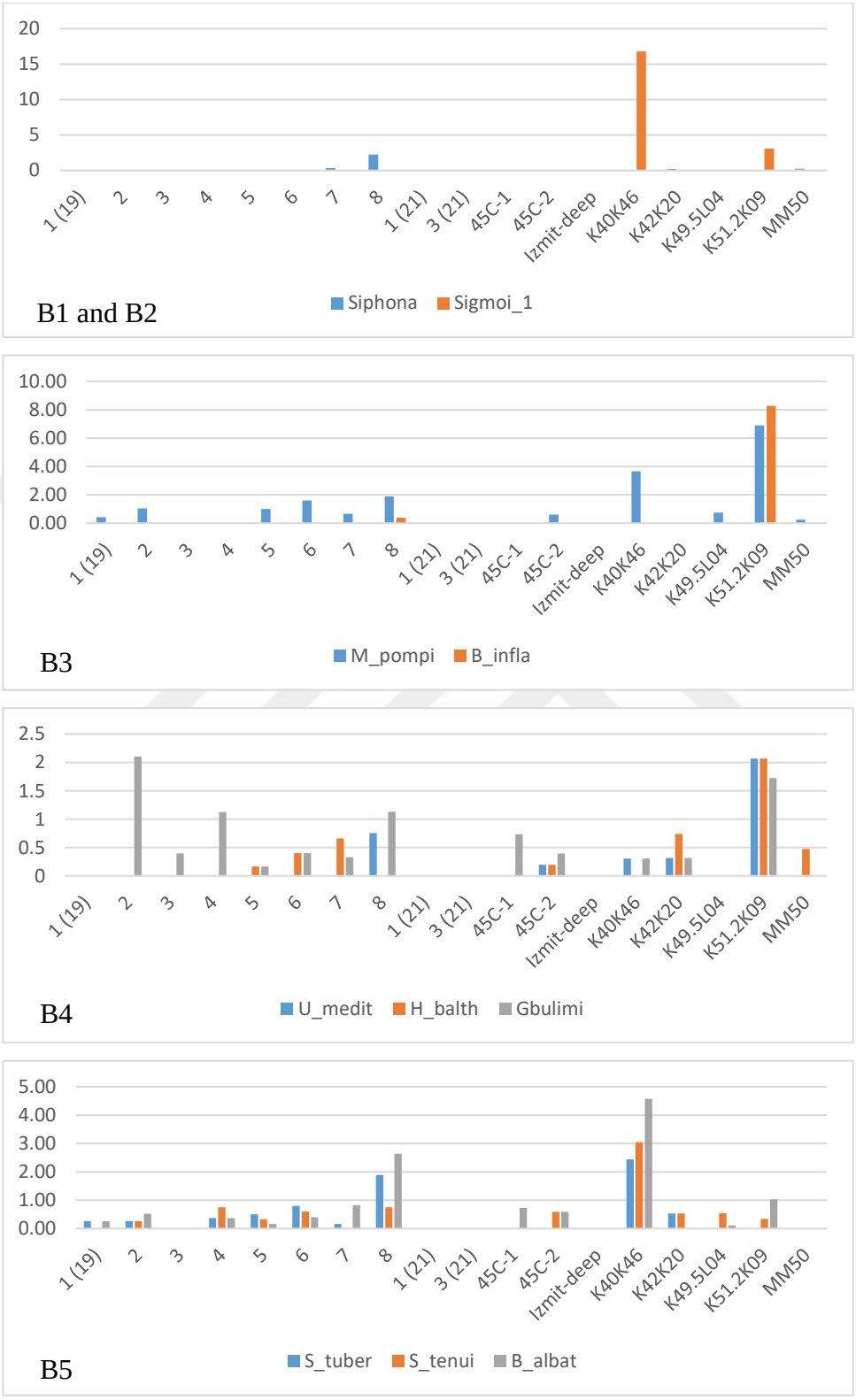


Figure 3.11. Relative abundances of taxa of Cluster B.

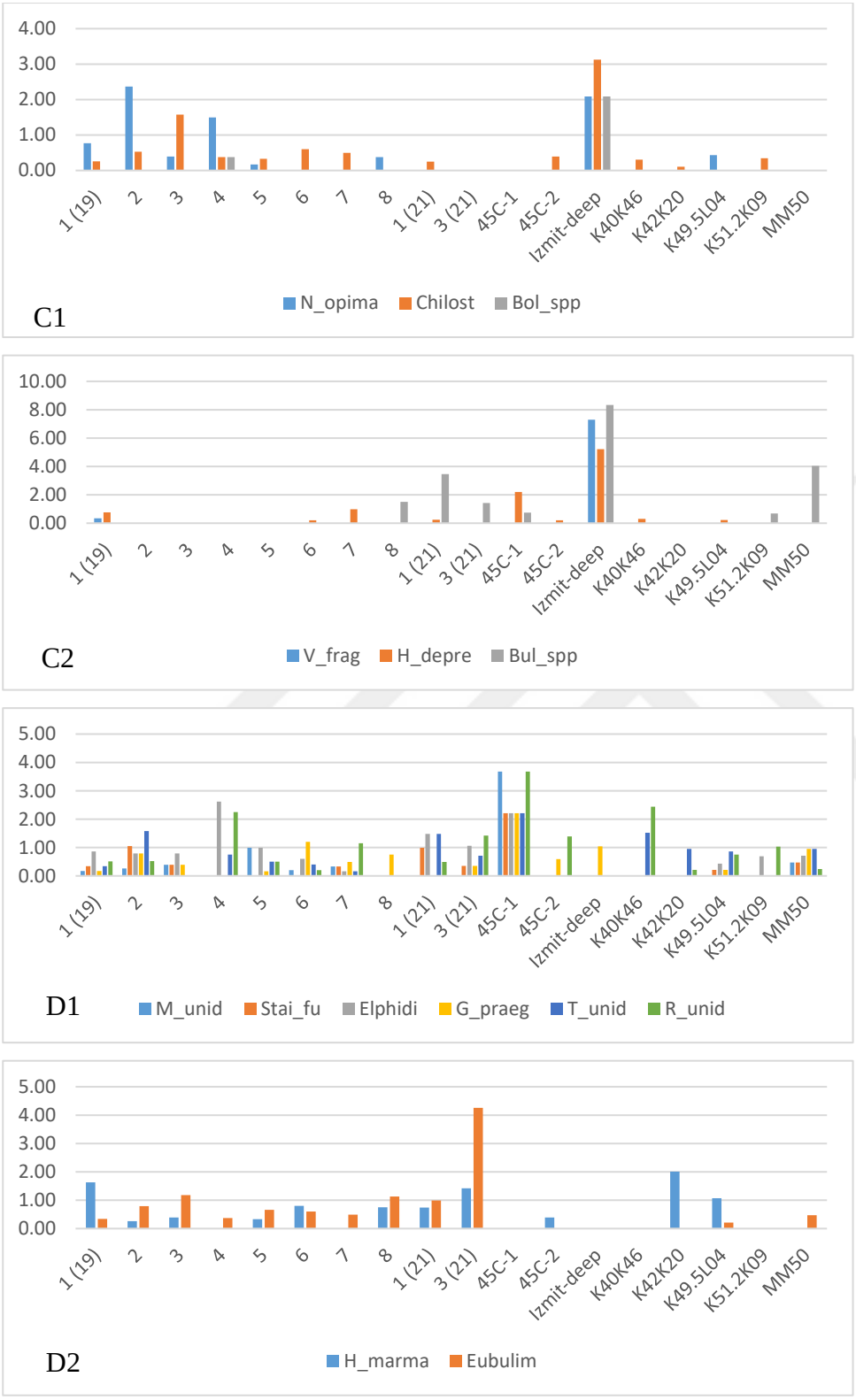


Figure 3.12. Relative abundances of taxa of Clusters C and D (1 and 2).



Figure 3.13. Relative abundances of taxa of Subclusters D3a, D3b, D3c, D3d.

Across the 18 core-top samples, MM50, K40K46, Izmit-deep and K51.2K09 are all different from each other and the rest of the samples (Figure 3.9, Figure 3.14). In these four samples the most dominant three taxa (Cluster A: *B. spathulata*, *B.* cf. *vadescens* and *P. minuta*) are of about average or lower abundances, while other taxa are more abundant in these samples compared to the rest of the samples. Subcluster D3c and *R. phlegeri* are the most abundant in MM50 while the cluster A taxa are the least abundant; Subcluster B4 and *Bolivina striatula* (Cushman) are the most abundant in K40K46, and *Sigmoilopsis* sp. 1 has dominant abundance (16.77%); Izmit-deep station is characterized by higher relative abundances of taxa belonging to Cluster C; and in K51.2K09 Subcluster B3 taxa has their highest abundance.

The rest of the samples are more similar to each other, and are grouped in two clusters (Figure 3.9, Figure 3.14, Figure 3.15). First includes samples 1 (19), 1 (21), 2, 3 (19), 3 (21), 4 and 8 (Cluster I) and in these samples, the abundance of *P. minuta* is lower than the abundance of *B. spathulata*. The opposite is true in the other group of samples which include samples 5, 6, 7-2, 45C-1, 45C-2, K42K20 and K49.5L04 (Cluster II). Moreover, Cluster II samples are richer in Subcluster D3a taxa than D3b; and Cluster I samples are richer in Subcluster D3c taxa compared to Cluster II samples.

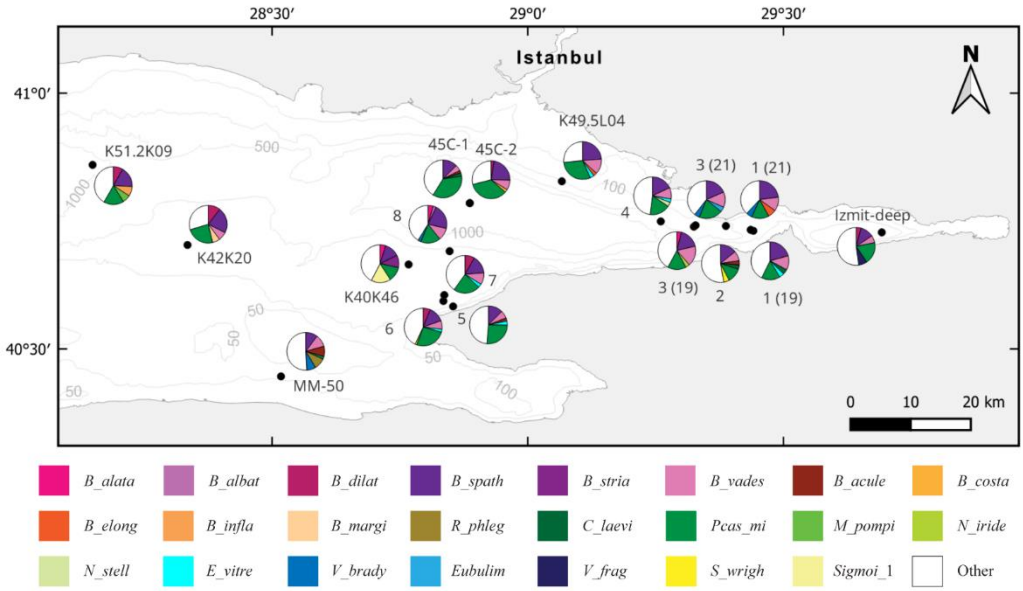


Figure 3.14. Pie charts showing the relative abundances of the five most abundant taxa in the core-top samples. Taxon abbreviations as in Supplementary Table A.1.

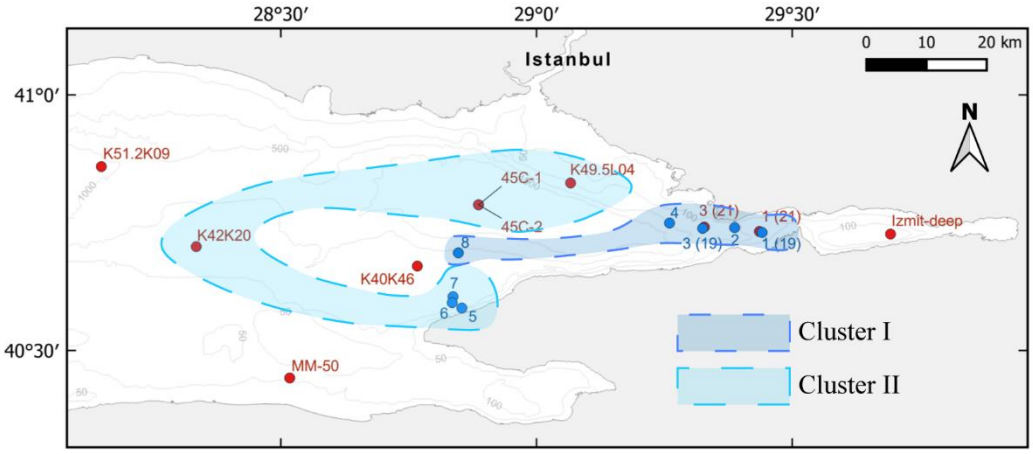


Figure 3.15. Geographic distribution of site clusters; cluster coloring as in Figure 3.9. Colors of station names as in Figure 1.1.

3.5 Relationship of benthic foraminifera relative abundances with environmental gradients

Canonical correspondence analysis (CCA) is an exploratory tool for investigating the relationships between the relative abundances of taxa and environmental variables: it assesses the variation in relative abundances of taxa across sites as best explained by the given environmental gradients (ter Braak, 1986).

CCA assumes Gaussian distribution of taxa (ter Braak, 1986), i.e., an 'optimum' range of a variable where the taxon is most abundant, and decreasing abundances towards the two extremes of the variable. In the case of multiple environmental vectors contributing to the abundances of taxa, choosing of the variables needs to achieve two goals: i. reducing noise by eliminating correlated variables, ii. increasing control on the full range of variation by including adequate number of independent variables. Since CCA treats environmental variables as if they are orthogonal to (independent of) each other, the correlations between the variables would create misguiding results. For this purpose, the variables in Table 3.7 (see Section 2.1.5) were chosen for the analysis despite the obvious inverse correlation between dissolved oxygen and bottom depth (Figure 2.1, Figure 2.2) because the evaluation of the relationship of taxa with both of these variables were desired.

To explore the distribution of benthic foraminiferal taxa along environmental gradients, chosen water and sediment variables (Table 3.7) were used with the relative abundance of benthic foraminifera in a canonical correspondence analysis. For the analysis, the >2% taxa (at least 2% relative abundance in at least one sample, see Section 3.4) were chosen. The environmental variables were normalized to between 0-1 to diminish the size effect and inherit only the directionality of the gradients, i.e., in order to eliminate the dominance of the variables with very high variation (e.g., bottom depth). The numerical results of the analysis (i.e., eigenvalues of axes and scores of taxa, stations and environmental variables) are given in Supplementary Table D.1 and Supplementary Table D.2.

Table 3.7. Environmental variables used in canonical correspondence analysis (see Section 2.1.5). Bottom depth in meters; dissolved oxygen (DO), nitrite (NO_2), ammonium (NH_4), and phosphate (PO_4) in micromolar (μM), total organic carbon (TOC) as percent (weight); BW: bottom water; PW: pore water; TOC values from 1: Ergin et al. 1993, 2: Ergin and Yücel, 1990, 3: 2019 results.

Station	Bottom depth	DO BW	NO_2 BW	NO_2 PW	NH_4 PW	PO_4 PW	TOC
1 (19)	65	45.71	0.06	1.56	26.88	10.62	1.35
2	112	35.92	0.18	0.18	18.48	5.58	1.39
3 (19)	240	7.68	0.07	0.26	44.16	4.74	1.56
4	435	10.26	0.05	0.14	34.32	4.02	1.4
5	100	57.4	0.06	0.4	10.92	11.46	1.16
6	192	17.09	0.06	0.28	5.04	19.14	1.69
7	290	7.25	0.02	0.14	9.48	5.46	1.66
8	414	6.34	0.09	0.64	1.92	2.34	1.49
1 (21)	67	49.3	0.17	0.07	28.47	13.86	1.35 [3]
3 (21)	195	21.7	0.17	0.11	58.04	28.23	1.56 [3]
45C-1	1214	4.6	0.06	0.04	51.62	12.11	1.25 [1]
45C-2	1214	4.6	0.06	0.04	51.62	12.11	1.25 [1]
Izmit-deep	206	0	0.02	0.06	214.81	23.39	1.4 [2]
K40K46	318.5	5.5	0.15	0.08	81.3	7.48	1.25 [1]
K42K20	160	55.6	0.02	0.08	53.36	15.11	1.25 [1]
K49.5L04	100	38.4	0.03	0.1	28.07	20.18	1.25 [1]
K51.2K09	1185	20.5	0.02	0.12	10.56	1.28	1.25 [1]
MM50	53.5	56.6	0.02	0.06	9.45	2.69	0.75 [1]

The CCA axes are formed in an n-dimensional space (n: the number of environmental variables), each axis being a linear combination of all n variables with different weights. In this analysis, the first two axes explain about 60% of the variance in the data (Supplementary Table D.1); while, 90% of the variance needs four axes to be explained. The scores of each environmental variable on the axes show the weight of that variable on that axis. For the first axis, ammonium has the most weight with ~0.9. Phosphate and dissolved oxygen both have ~0.4 weight, the former in the positive direction, the latter in the negative, and all other variables have very small contributions to this axis. The second axis is mostly influenced by bottom water nitrite (-0.48), then bottom depth and TOC (~0.4 both). Since the data used in

the analysis is normalized (to 0-1), the variables here can only be interpreted as non-numeric gradients.

Figure 3.16 and Figure 3.17are the plots of the first two axes of the CCA, separately shown for better visibility. Among stations, the variance across the first axis is quite narrow except for Izmit-deep station (Figure 3.16). Ammonium, the highest contributor to the first axis, is in all other stations in the range of ~2 to 60, while it is 214.81 μM in Izmit-deep, making it an outlier.

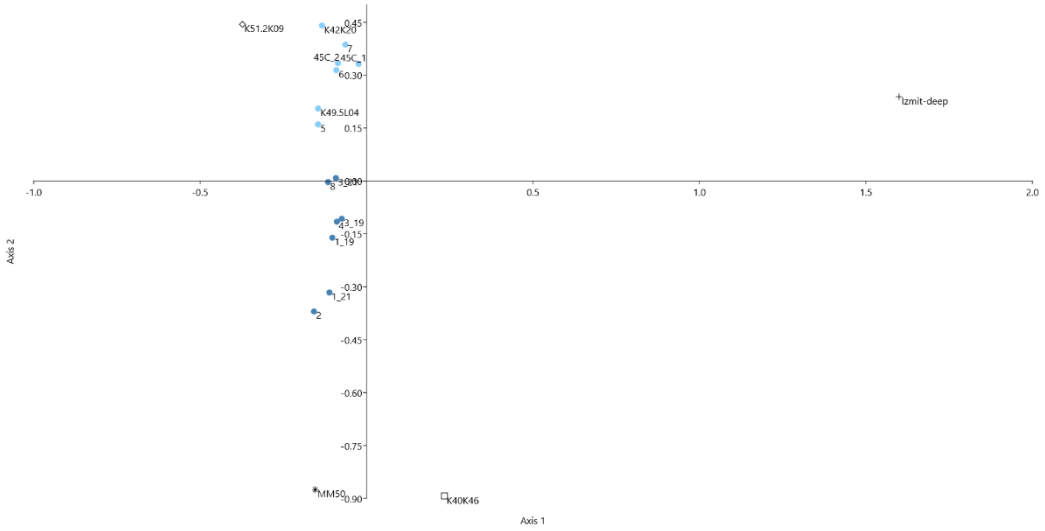


Figure 3.16. First two axes of canonical correspondence analysis done on environmental dataset given in Table 3.7 and the relative abundances of >2% taxa: station scores (colors as in Figure 3.9).

The stations belonging to the same cluster (Figure 3.9) plot on this graph close to each other as well (Figure 3.16). Cluster II samples plot on the positive side of the axis 2, while Cluster I samples plot on the negative side. Other outliers of the cluster analysis are on the fringes (most distant from the origin) in this graph.

Figure 3.17 shows the relationship of the taxa to the environmental variables. The taxa at the center (origin) of the plot are not distinguishing, i.e., do not show variation to differentiate between stations for the explained variation by the first two axis of the analysis. *Bolivina* cf. *vadescens* and *Bolivina spathulata* are two of these taxa. They are both abundant-dominant in all samples with low variation. *Paracassidulina minuta*, on the other hand, despite its presence in every station, is distinctly higher in relative abundance in Cluster II samples, and creates variation in the dataset, hence is located on the plot somewhat away from the origin. Contrary to *P. minuta*, *Gyroidina umbonata*, present in all samples, but the variation of its relative abundance across the dataset is very limited, therefore it is located near the center of the plot.

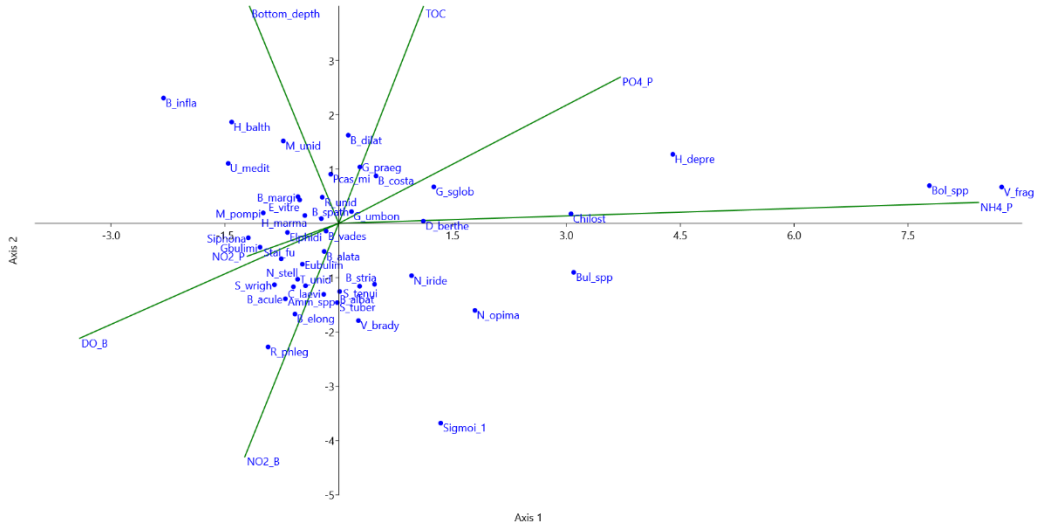


Figure 3.17. First two axes of canonical correspondence analysis done on environmental dataset given in Table 3.7 and the relative abundances of >2% taxa: taxa (abbreviations as in Supplementary Table A.1) and environmental gradient vectors (exaggerated 9 times for better visibility).

Taxa at the edges of the plot (Figure 3.17) are those that occur abundantly in only small number of samples. For example, *Virgulinella fragilis* is present in Izmit-deep station with ~7% abundance, and in station 1 (2019) with only 0.3% abundance, therefore is located at the very edge of the plot. Similarly, *Sigmoilopsis* sp. 1 is confined to two samples (K40K46: ~17% and K51.2K09: ~3%), and is located at the bottom edge of the plot. *Bulimina inflata* is only present in K51.2K09 abundantly (8.3%), while it is a very rare taxon in only one other station (Station 8, 0.4%). The very restricted distribution of these taxa creates the variation which separates those stations from others.

The taxa which are located midway between the origin and the periphery in the plot (Figure 3.17) are those that occur in high number of samples and are sources of variation in the data set. For example, *Bulimina elongata* and *Bulimina aculeata* are found in 13 and 15 stations, respectively, and usually together. These two taxa are located on the plot very close to each other due to their similarity in distribution. *Bulimina marginata* and *Eilohedra vitrea* are also plotted very close to each other, and they are present in 17 and 18 (all) stations respectively.

The directionality of the environmental vectors shows their contribution to the axes; and the angle between an environmental vector, and a line connecting a taxon to the origin of the plot represents the relationship of the taxon to the environmental variable. However, it should be noted that these two axes explain only the 60% of the variation in the data, and are a combination of all environmental variables. Yet, environmental vectors cannot be treated as direct gradients. For example, *Rectuvigerina phlegeri* is most abundant in MM50, and is highly related with bottom water nitrite according to the analysis (Figure 3.17); however, bottom water nitrite in station MM50 is very low (minimum of the data set). Other samples which are located at the same quadrant with MM50 are the Cluster I samples, which are ordered from origin towards the edge of the plot approximately in the order of increasing bottom water nitrite (Figure 3.16, Table 3.7), and in almost all of these samples, although in low abundances (0.7-2.6%), *Rectuvigerina phlegeri* is present. Despite the highest abundance of *R. phlegeri* in MM50 with the lowest nitrite, the placement

of both this station, and this taxon in this extreme edge of the plot is then justified: i.e., the environmental vector is formed by more contribution from Cluster I samples. On the other hand, axis 4, which is most influenced by bottom water nitrite (score -0.45) and TOC (-0.54), locates both MM50 and *R. phlegeri* on the far negative side of these environmental vectors (see scores in Supplementary Table D.2).

Removing the outliers (MM50, K40K46, Izmit-deep and K51.2K09, Figure 3.9) and the unidentified and rare (<2% in the remaining data set) taxa results in a slightly different configuration (Supplementary Table D.3, Supplementary Table D.4). With this analysis, the first two axes explain about ~65% of the variation in the data set (Supplementary Table D.3, Figure 3.18). With the exclusion of these outliers the effects of ammonium and TOC are substantially decreased in the first two CCA axes, while the effects of bottom depth and bottom water nitrite increased. In addition, although they do not have a linear relationship (Figure 2.1, Figure 2.2), bottom water and pore water nitrite are strongly related with each other (Figure 3.18). The samples of the two clusters plot on the opposite sides on the first axis.

This analysis (Figure 3.18) shows strong relationships between pore water phosphate and the taxa *B. marginata*, *B. costata* and *B. dilatata* which occur more abundantly in samples with higher pore water phosphate. In addition, *H. depressula*, is strongly related with water depth and inversely related with dissolved oxygen, while the opposite is true for *H. marmarica*. *B. aculeata*, *Ammonia* spp., *V. bradyana* and *N. opima* are strongly related to nitrite, with their optima occurring with increasing values of nitrite.

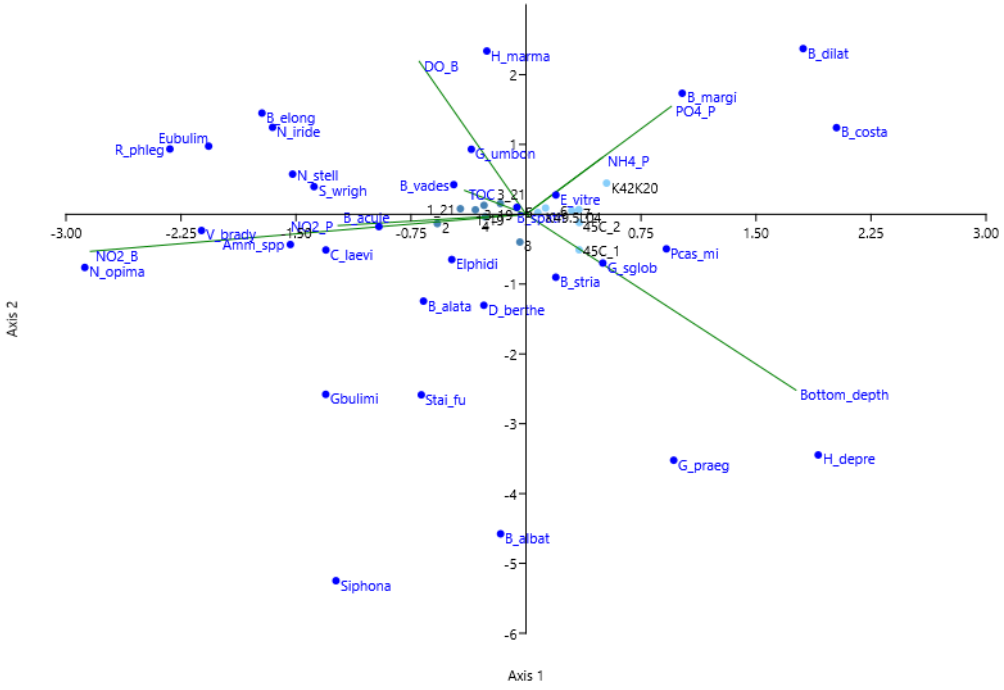


Figure 3.18. CCA biplot of first two axes, excluding the outliers and the unidentified taxa. Stations coloring according to Figure 3.9, environmental gradient vectors amplified 4 times.

CHAPTER 4

VERTICAL DISTRIBUTION OF BENTHIC FORAMINIFERA: CHANGES IN CORES

Selected samples (down-core samples) from 15 (out of 18 total; Table 1.2) sediment cores were examined (quantified) in order to evaluate the changes in benthic foraminiferal assemblages down-core. Stations 1 and 3 were sampled in both cruises (2019 and 2021) and the 2021 sediment cores were selected for this investigation. In station 45C, two sediment cores were taken during the same cast, and the core-top samples showed some difference between the cores in terms of foraminiferal assemblage and abundance: out of the two cores 45C-2 was chosen for this investigation due to higher total foraminiferal absolute abundance in the core-top sample. The vertical changes in the assemblage is very little for most of the cores, while in several cores some shifts are observed. These results are furhter discussed in Chapter 9 in terms of possible environmental or depositional shifts in stations, and the result for the Izmit-deep core is further utilized in Chapter 7 for evaluation of the depositional history of the core.

4.1 Total absolute abundance of foraminifera

The absolute abundances of benthic and planktonic foraminifera in down-core samples normalized to 1 ml sediment and 1 g dry sediment were calculated same as in core-top samples (Section 3.1). The initial volumes of samples of the 2019 cruise were not measured, but only noted approximately. Effectively, making the calculated volume normalized absolute abundance values not very precise. However, 2021 samples were measured in terms of both volume and weight. Table 4.1 includes the studied sediment cores of the 2019 cruise, and Table 4.2 includes those of the 2021 cruise.

Table 4.1. Number of benthic foraminifera ($BF_{\#}$) of the working split size (Split), approximate initial volume of samples (ml) and total absolute abundance of benthic foraminifera normalized to 1 ml of sediment ($BF_{\#V}$) in the studied sediment cores of 2019 cruise.

Station	Sample (cm)	$BF_{\#}$	Split	Initial volume (ml ~)	$BF_{\#V}$
2	2	380	1/128	30	1621.33
	5	537	1/128	40	1718.40
	10	272	1/256	50	1392.64
	15	517	1/256	50	2647.04
	20	482	1/256	50	2467.84
	25	761	1/256	50	3896.32
	27	655	1/256	30	5589.33
4	4	267	1/128	100	341.76
	8	572	1/64	100	366.08
	15	1087	1/16	50	347.84
	30	643	1/32	50	411.52
5	4	604	1/512	100	3092.48
	8	1982	1/256	50	10147.84
	10	692	1/256	50	3543.04
	15	335	1/512	50	3430.40
	20	899	1/512	50	9205.76
	30	419	1/1024	50	8581.12
	40	375	1/1024	50	7680.00
6	4	500	1/512	100	2560.00
	8	696	1/512	100	3563.52
	15	983	1/256	50	5032.96
	30	1032	1/512	50	10567.68
7-2	4	608	1/128	100	778.24
	8	735	1/256	100	1881.60
	15	1240	1/256	50	6348.80
	30	890	1/256	50	4556.80
8	4	265	1/16	100	42.40
	8	560	1/32	100	179.20
	15	313	1/32	50	200.32
	30	395	1/32	50	252.80

The volumetric normalization of benthic foraminiferal abundance is dependent to the actual abundance and the differences in density between samples; i.e., due to compaction, the volume of a sample coming from a deeper level of the core will be

smaller than a sample with same dry weight coming from the surface of the core. Therefore, comparison of volume normalized values in a core can produce errors. Nonetheless, the volume and weight normalized benthic foraminifera abundances in 2021 samples (Table 4.2) correlate linearly very well (R^2= 0.95, Figure 4.1). In addition, since weight measurements of 2019 samples do not exist, the volume normalized abundance values were used for further analysis and unless otherwise indicated. Hence, benthic foraminifera absolute abundance means volume normalized for the rest of this chapter.

Table 4.2. Number of benthic foraminifera ($BF_{\#}$) of the working split size (Split), initial volume of samples (ml), total absolute abundance of benthic foraminifera normalized to 1 ml of sediment ($BF_{\#V}$), initial weight of samples (g), total absolute abundance of benthic foraminifera normalized to 1 g dry sediment ($BF_{\#W}$), and the ratio of $BF_{\#W}$ to $BF_{\#V}$ in the studied sediment cores of 2021 cruise. * for possible measurement error.

Station	Sample (cm)	$BF_{\#}$	Split	Initial volume (ml)	$BF_{\#V}$	Initial weight (g)	$BF_{\#W}$	$BF_{\#W}$ / $BF_{\#V}$
1 (21)	1	405	1/64	16.25	1595.08	8.43	3075.10	1.93
	4	1122	1/32	20	1795.20	10.12	3548.53	1.98
	8	1492	1/32	15	3182.93	7.51	6354.85	2.00
	15	652	1/32	15	1390.93	11.61	1796.92	1.29
3 (21)	1	282	1/32	16.25	555.32	6.12	1474.03	2.65
	4	471	1/32	20	753.60	11.28	1336.64	1.77
	8	1265	1/16	16.25	1245.54	9.77	2072.50	1.66
	15	1510	1/32	27.5	1757.09	15.56	3105.80	1.77
45C-2	1	505	1/1	12.5	40.40	4.01	125.97	3.12
	4	845	1/1	11.25	75.11	4.35	194.34	2.59
	8	354	1/2	12.5	56.64	7.82	90.53	1.60
	15	736	1/8	12.5	471.04	11.50	512.04	1.09
45C-2	20	260	1/2	12.5	41.60	6.75	77.03	1.85
	30	447	1/1	13.75	32.51	7.36	60.70	1.87
	40	238	1/4	20	47.60	11.66	81.65	1.72

Table 4.2. Continued.

Station	Sample (cm)	$BF_{\#}$	Split	Initial volume (ml)	$BF_{\#V}$	Initial weight (g)	$BF_{\#W}$	$BF_{\#W}$ / $BF_{\#V}$
Izmit-deep	1	96	1/1	15	6.40	1.40	68.67	10.73
	2	44	1/1	15	2.93	2.50	17.63	6.01
	3	23	1/1	15	1.53	3.78	6.08	3.96
	4	7	1/1	17.5	0.40	3.79	1.85	4.62
	6	24	1/1	15	1.60	6.52	3.68	2.30
	8	88	1/1	18.75	4.69	8.70	10.12	2.16
	10	483	1/2	11.25	85.87	6.27	154.12	1.79
	15	309	1/4	14	88.29	6.73	183.55	2.08
	20	391	1/4	12	130.33	10.55	148.25	1.14
	30	565	1/8	20	226.00	15.89	284.51	1.26
	40	560	1/8	20	224.00	12.65	354.15	1.58
K40K46	1	328	1/4	16.25	80.74	7.91	165.80	2.05
	4	507	1/4	16.25	124.80	9.17	221.13	1.77
	8	1174	1/4	20	234.80	9.40	499.79	2.13
	15	281	1/8	21.5	104.56	10.20	220.41	2.11
	30	349	1/8	20	139.60	45.51*	61.35	0.44
K42K20	2	944	1/128	13.75	8787.78	6.07	19912.99	2.27
	4	812	1/256	13.75	15117.96	7.51	27671.62	1.83
	8	1068	1/256	13.75	19884.22	7.55	36227.38	1.82
	15	925	1/256	21.5	11013.95	9.21	25716.77	2.33
K49.5L04	1	931	1/256	16.5	14444.61	5.94	40117.15	2.78
	4	1874	1/128	21.5	11156.84	13.79	17389.59	1.56
	8	448	1/256	23	4986.43	17.42	6582.94	1.32
	15	680	1/256	22.5	7736.89	17.91	9718.08	1.26
K51.2K09	1	290	1/8	21.25	109.18	6.75	343.91	3.15
	4	297	1/8	22.5	105.60	9.64	246.47	2.33
	8	456	1/8	16.25	224.49	6.63	550.64	2.45
	15	397	1/2	16.25	48.86	8.95	88.70	1.82
	30	640	1/4	20	128.00	15.67	163.34	1.28
MM50	1	421	1/16	17	396.24	5.33	1264.03	3.19
	4	437	1/16	17.5	399.54	7.20	971.11	2.43
	8	314	1/16	17	295.53	9.37	536.47	1.82
	15	549	1/16	21.25	413.36	12.38	709.42	1.72
	30	404	1/8	20	161.60	16.37	197.46	1.22

Benthic foraminifera absolute abundances tend to increase with depth in core in most cores such as 2, 3 (21), 6; decrease downward in K49.5L04; and irregular in others such as 45C-2 and 5 (Figure 4.2). The downward increase in $BF_{\#V}$ is expected due to compaction as volume per unit mass sediment decrease downward; however, the increases and decreases are usually also seen in $BF_{\#W}$ (for 2021 samples, Table 4.2) therefore cannot only be attributed to compaction, and should be explained in terms of differences in sediment composition.

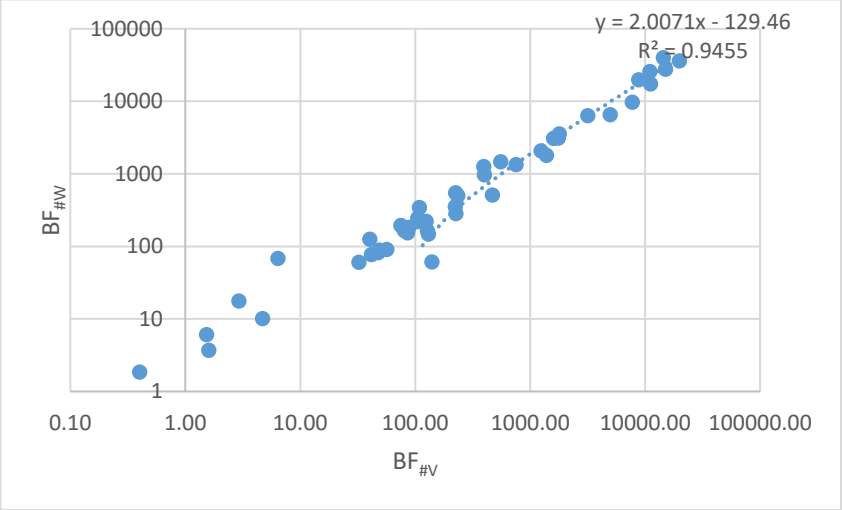


Figure 4.1. Correlation of $BF_{\#V}$ and $BF_{\#W}$ values in 2021 samples, plotted on log-log scale for better visibility.

Planktonic foraminiferal absolute abundances (volume normalized) are given in Table 4.3. $PF_{\#V}$ mostly follows the trend in $BF_{\#V}$, and the two are somewhat correlated (R^2= 0.68; see Figure 4.2). P% values usually occur within a site-specific range, rarely increasing or decreasing out of that range, indicating different sediment compositions.

Table 4.3. Number of benthic foraminifera ($PF_{\#}$) of the working split size, total absolute abundance of planktonic foraminifera normalized to 1 ml of sediment ($PF_{\#V}$) (see Split and Initial volume in Table 4.1 and Table 4.2), relative abundance of planktonic foraminifera in total foraminifera assemblage (P%), weight-wise ratio of material coarser than 63 μm in the sediment (Sand%, for 2021 samples only).

Station	Sample (cm)	$PF_{\#}$	$PF_{\#V}$	P%	Sand %
2	2	6	25.60	1.55	
	5	11	35.20	2.01	
	10	12	61.44	4.23	
	15	8	40.96	1.52	
	20	25	128.00	4.93	
	25	49	250.88	6.05	
	27	57	486.40	8.01	
4	4	31	39.68	10.40	
	8	16	10.24	2.72	
	15	69	22.08	5.97	
	30	162	103.68	20.12	
5	4	30	153.60	4.73	
	8	125	640.00	5.93	
	10	46	235.52	6.23	
	15	39	399.36	10.43	
	20	78	798.72	7.98	
	30	50	1024.00	10.66	
	40	49	1003.52	11.56	
6	4	49	250.88	8.93	
	8	57	291.84	7.57	
	15	76	389.12	7.18	
	30	133	1361.92	11.42	
7-2	4	93	119.04	13.27	
	8	128	327.68	14.83	
	15	169	865.28	11.99	
	30	488	2498.56	35.41	
8	4	155	24.80	36.90	
	8	343	109.76	37.98	
	15	394	252.16	55.73	
	30	1232	788.48	75.72	
1 (21)	1	7	27.57	1.70	3.26
	4	39	62.40	3.36	4.20
	8	18	38.40	1.19	3.18
	15	10	21.33	1.51	2.06
3 (21)	1	4	7.88	1.40	5.13
	4	18	28.80	3.68	13.63
	8	26	25.60	2.01	3.66
	15	20	23.27	1.31	2.31
45C	1	155	12.40	23.48	1.00
	4	310	27.56	26.84	0.69
	8	170	27.20	32.44	0.43

Table 4.3. Continued.

Station	Sample (cm)	$PF_{\#}$	$PF_{\#V}$	P%	Sand %
	15	308	197.12	29.50	2.10
	20	191	30.56	42.35	0.40
	30	471	34.25	51.31	0.61
	40	620	124.00	72.26	0.72
Izmit-deep	1	6	0.40	5.88	1.93
	2	5	0.33	10.20	0.40
	3	2	0.13	8.00	0.71
	4	0	0.00	0.00	1.06
	6	0	0.00	0.00	0.41
	8	2	0.11	2.22	0.31
	10	8	1.42	1.63	0.93
	15	9	2.57	2.83	1.50
	20	44	14.67	10.11	0.67
	30	16	6.40	2.75	0.42
	40	11	4.40	1.93	0.76
K40K46	1	836	205.78	71.82	0.64
	4	713	175.51	58.44	0.65
	8	1092	218.40	48.19	0.88
	15	455	169.30	61.82	0.68
	30	1246	498.40	78.12	0.21
K42K20	2	500	4654.55	34.63	9.77
	4	340	6330.18	29.51	9.68
	8	358	6665.31	25.11	7.31
	15	243	2893.40	20.80	13.39
K49.5L04	1	137	2125.58	12.83	12.24
	4	267	1589.58	12.47	9.32
	8	139	1547.13	23.68	6.12
	15	135	1536.00	16.56	6.35
K51.2K09	1	274	103.15	48.58	5.77
	4	292	103.82	49.58	6.44
	8	551	271.26	54.72	4.75
	15	993	122.22	71.44	0.56
	30	3352	670.40	83.97	0.48
MM50	1	9	8.47	2.09	10.11
	4	4	3.66	0.91	17.29
	8	2	1.88	0.63	2.92
	15	21	15.81	3.68	3.63
	30	27	10.80	6.26	1.53

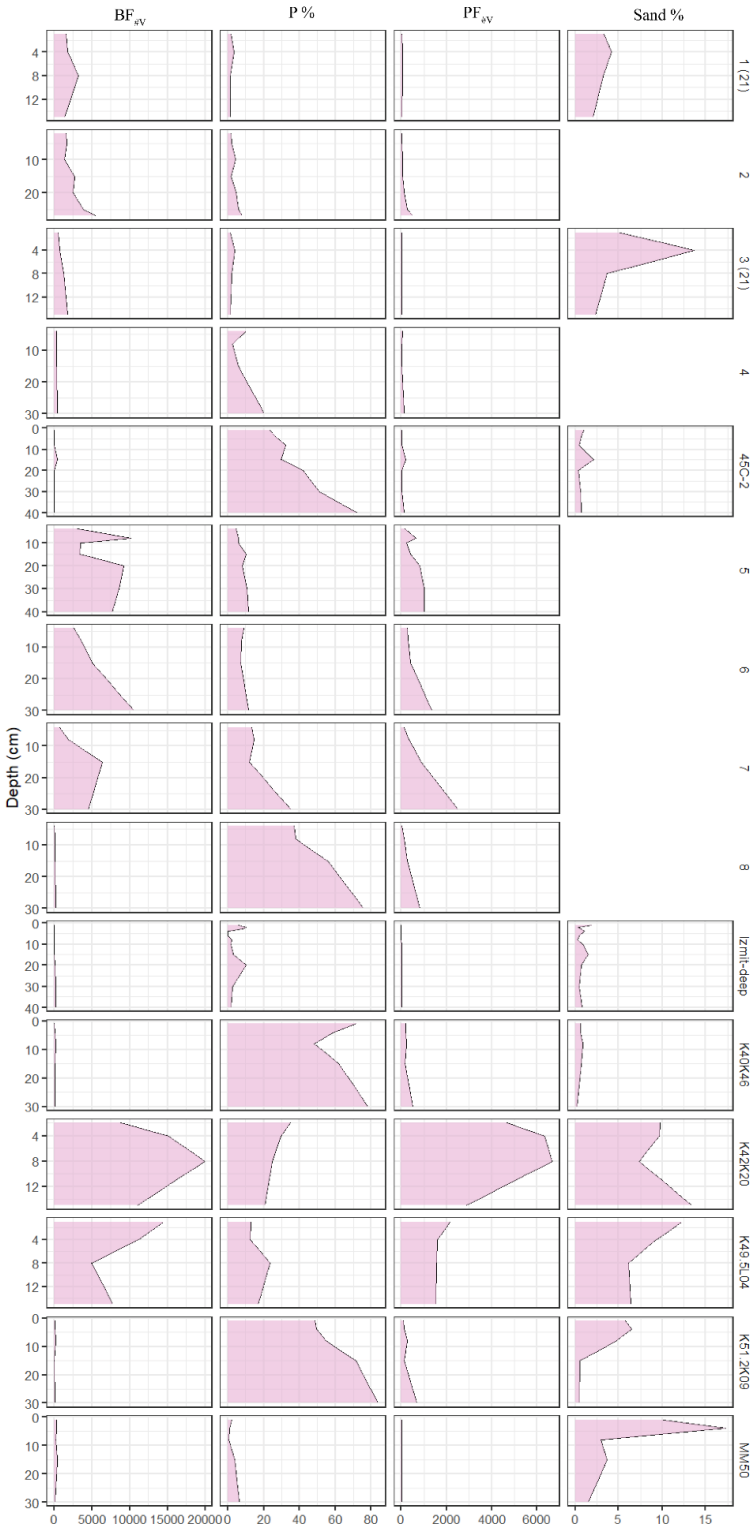


Figure 4.2. Total absolute benthic and planktonic foraminifera (volume normalized, $BF_{\#V}$ and $PF_{\#V}$), planktonic foraminifera ratio (P%), and sand content (Sand %, not present in stations 2, 4, 5, 6, 7, 8) in cores (ggplot2, Wickham, 2016).

4.2 Relative abundance changes in cores

Overall, the composition of frequent, abundant and dominant benthic foraminiferal taxa in the down-core samples are similar to the core-top samples (Section 3.3). Below, the changes in the cores are explained, accompanied by bar graphs showing the relative abundances of frequent, abundant and dominant taxa.

4.2.1 Station 2

Station 2 (Figure 4.3, Supplementary Table B.2) has 11-20% *Bolivina spathulata*, 10-16% *Paracassidulina minuta* and 5-9% *Bolivina* cf. *vadescens*. *Ammonia* spp. *Bulimina aculeata*, *Cassidulina laevigata*, *Discorbinella bertheloti*, *Eilohedra vitrea*, *Gyroidina umbonata*, *Nonionella iridea*, *Spiroplectinella wrighti* and *Valvulinearia bradyana* are frequent to abundant in four or more samples in the core.

The overall assamblage is very similar between the samples of the core, one small change happens in sample 20 cm, where *B.* cf. *vadescens* and *P. minuta* decrease in abundance, and representatives of Family Discorboidae increase. In addition, at and below this level, miliolid taxa are more abundant than the upper samples.

Both planktonic foraminifera ratio (P%, Table 4.3) and absolute abundance of benthic foraminifera ($BF_{\#V}$, Table 4.2) increase downcore steadily (Figure 4.2).

4.2.2 Station 4

P. minuta (17-21%) and *B. spathulata* (13-18%) are dominant in most samples, and *B.* cf. *vadescens* (6-16%) is highly abundant (Figure 4.4, Supplementary Table B.3). *Bolivina alata*, *Bolivina dilatata*, *Bolivina striatula*, *B. aculeata*, *Eilohedra vitrea*, *Nonionella iridea* and *Nonionella stella* are frequent to abundant in two or more samples in this core. 8 cm sample is marked with dominant *B.* cf. *vadescens*, while in the 30 cm sample *B. spathulata* is only abundant (<15%) and textularids, especially *S. writghti* are more abundant than upper samples. Bolivinids (in sum) are

of less abundance, while cassidulinids are more abundant in the 15 and 30 cm samples compared to upper two samples.

Both P% (Table 4.3) and $BF_{\#V}$ (Table 4.2) are fixed in the core, only changing very slightly (Figure 4.2).



Figure 4.3. Relative abundances of selected taxa in Station 2 sediment core. Panels from left to right: A: Bolivinitidae; B: Buliminoidea; C: Cassidulinoidea; D: Planorbulinoidea, Discorboidea, Rotaloidea; E: Nonionoidea, other Rotaliana, Spirillinida; F: Robertinida, Textulariana, Miliolida. Scales of x-axes of panels are the same. Y-axis not to scale. Taxa abbreviations as in Supplementary Table A.1.



Figure 4.4. Relative abundances of selected taxa in Station 4 sediment core. Panels from left to right: A: Bolivinitidae; B: Buliminoidea; C: Cassidulinoidea; D: Planorbulinoidea, Discorboidea, Rotaloidea; E: Nonionoidea, other Rotaliana, Spirillinida; F: Robertinida, Textulariana, Miliolida. Scales of x-axes of panels are the same. Y-axis not to scale. Taxa abbreviations as in Supplementary Table A.1.

4.2.3 Station 5

P. minuta (22-29%) is the only dominant taxon in this core; *B. spathulata* (10-13%) and *B.* cf. *vadescens* (5-7%) are abundant in all samples (Figure 4.5, Supplementary Table B.4). These are accompanied by frequent to abundant *E. vitrea* and *Globocassidulina subglobosa* in all samples, and *Bolivina dilatata*, *B. aculeata*,

Bulimina costata, *Gyroidina umbonata* abundant in three or more samples in the core.



Figure 4.5. Relative abundances of selected taxa in Station 5 sediment core. Panels from left to right: A: Bolivinitidae; B: Buliminoidea; C: Cassidulinoidea; D: Planorbulinoidea, Discorboidea, Rotaloidea; E: Nonionoidea, other Rotaliana, Spirillinida; F: Robertinida, Textulariana, Miliolida. Scales of x-axes of panels are the same. Y-axis not to scale. Taxa abbreviations as in Supplementary Table A.1.

P. minuta decreases downward while *G. subglobosa* increase, except for 40 cm sample where *P. minuta* is only of 22% abundance; in 40 cm sample Rotalioidea (in

total) holds 4% abundance. In 15 cm sample the abundance of *E. vitrea* is replaced by slight increase in *Hyalinea balthica*, *Elphidium* spp. and *S. wrighti*, while the buliminid assemblage changed from *B. aculeata* dominant to *B. costata* and *B. elongata* dominant. Otherwise, the assemblage in the core is quite steady.

P% (Table 4.3) increases downcore steadily. On the other hand, $BF_{\#V}$ (Table 4.2) is lower in samples 4, 10, 15 cm (3092-3543), but significantly higher in samples 8, 15, 20, 30 cm (7680-10147) (Figure 4.2). These differences in the absolute abundance are not reflected in the assemblage composition.

4.2.4 Station 6

P. minuta (22-27%) is dominant in all samples, *B. spathulata* is dominant (17-21%) in samples 8, 15, 30 cm samples, but abundant (14%) in 1 cm sample. *B. dilatata* and *B.* cf. *vadescens* are frequent-abundant (4-10%) (Figure 4.6, Supplementary Table B.5). *G. subglobosa* and *E. vitrea* are frequent in two or more samples; other bolivinids, cassidulinids, Planorbulinoidea and other Discorboidea are of frequent abundances in all samples.

Very little difference is observed between the core samples. Total bolivinid abundance slightly increases with depth while cassidulinids abundance decreases. In addition, Miliolida, Spirillinida, and *Nonionella iridea* increase in abundance downward while Planorbulinoidea decreases.

P% (Table 4.3) and $BF_{\#V}$ (Table 4.2) increase downward in the core steadily (Figure 4.2).

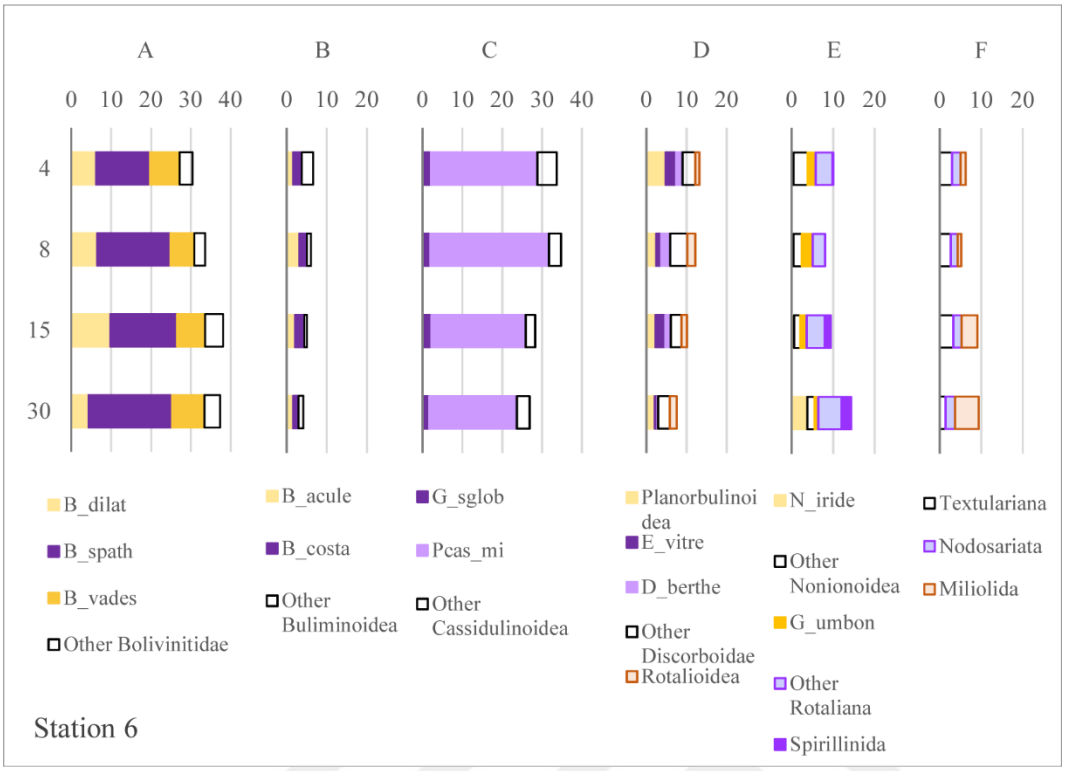


Figure 4.6. Relative abundances of selected taxa in Station 6 sediment core. Panels from left to right: A: Bolivinitidae; B: Buliminoidea; C: Cassidulinoidea; D: Planorbulinoidea, Discorboidea, Rotaloidea; E: Nonionoidea, other Rotaliana, Spirillinida; F: Robertinida, Textulariana, Miliolida. Scales of x-axes of panels are the same. Y-axis not to scale. Taxa abbreviations as in Supplementary Table A.1.

4.2.5 Station 7-2

P. minuta (18-18%) is dominant in all samples while *B. spathulata* (12-19%) and *B.* cf. *vadescens* (8-18%) are abundant to dominant: the dominant bolivinids changes from *B. spathulata* to *B.* cf. *vadescens* in the sample 30 cm (Figure 4.7, Supplementary Table B.6). These are accompanied by frequent to abundant B. dilatata and Eilohedra vitrea; frequent other bolivinids, G. subglobosa, Planorbulinoidea, other Discorboidea, other Nonionoidea and other Rotaliana in all samples.

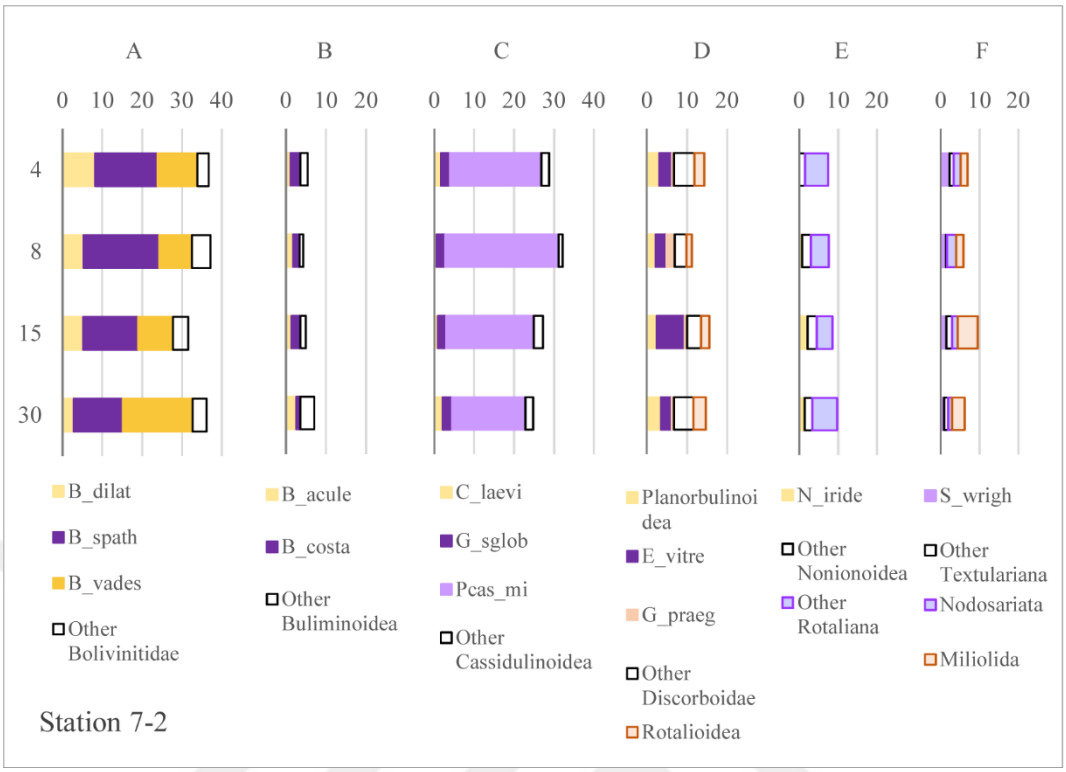


Figure 4.7. Relative abundances of selected taxa in Station 7-2 sediment core. Panels from left to right: A: Bolivinitidae; B: Buliminoidea; C: Cassidulinoidea; D: Planorbulinoidea, Discorboidea, Rotaloidea; E: Nonionoidea, other Rotaliana, Spirillinida; F: Robertinida, Textulariana, Miliolida. Scales of x-axes of panels are the same. Y-axis not to scale. Taxa abbreviations as in Supplementary Table A.1.

Downward changes are quite subtle in this core with both bolivinids and cassidulinids abundance decreasing slightly in 15 and 30 cm samples. P% (Table 4.3) and $BF_{\#V}$ (Table 4.2) increase downward in the core steadily (Figure 4.2).

4.2.6 Station 8

B. spathulata is dominant (22, 27%) in the upper two samples, abundant (14, 12%) in the 15 and 30 cm samples, while *B.* cf. *vadescens* is abundant (11, 10%) in the first two samples but is only frequent (4%) in 15 and 30 cm samples (Figure 4.8, Supplementary Table B.7). *P. minuta*, on the other hand, is dominant in all samples

(15-19%). These are accompanied by frequent to abundant *Bolivina alata* (3-6%), other miliolida (3-7%) and frequent Nodosariata (3-5%) in all samples. *Sigmoilopsis* sp. 1, *Siphonaperta* spp., *E. vitrea*, *Svratkina tuberculata*, *V. bradyana*, *Bolivina albatrossi*, *Bolivina striatula* and Textulariana are frequent in at least two samples; Bulimina costata is frequent to abundant in 15 and 30 cm samples.

The downward change is marked with decreased bolivinids abundances in the 15 and 30 cm samples, accompanied by slightly higher cassidulinid and *B. costata* abundances, and significantly higher miliolid abundances.

P% (Table 4.3) and $BF_{\#V}$ (Table 4.2) increase downward in the core steadily (Figure 4.2).

4.2.7 Station 1 (2021)

Both *B. spathulata* (23-25%) and *P. minuta* (15-20%) are dominant in this core, *B.* cf. *vadescens* (6-14%) is abundant (Figure 4.9, Supplementary Table B.8). *Bulimina elongata*, *C. laevigata*, *V. bradyana* are frequent to abundant in all samples, while *Ammonia* spp., *B. aculeata*, *B. marginata*, *E. vitrea*, Nonionoidea and Textulariana are frequent at least in two samples.

Difference between samples occur in *B.* cf. *vadescens*, which decreases in the 15 cm sample, instead *P. minuta* and Textulariana are increased. Miliolida is of very low abundance in this core.

Planktonic foraminifera (PF) (P%, 1.13-3.36%) and sand (Sand%, 2.06-4.20%) ratios are very low in this core and do not differ between the samples (Table 4.3, Figure 4.2). Absolute abundance of benthic foraminifera ($BF_{\#V}$) are similar in three samples (1390-1795) but higher in 8 cm sample (3182, Table 4.2, Figure 4.2) which conicides with a slight increase in bolinivids and slight decrease in cassidulinids (Figure 4.9).

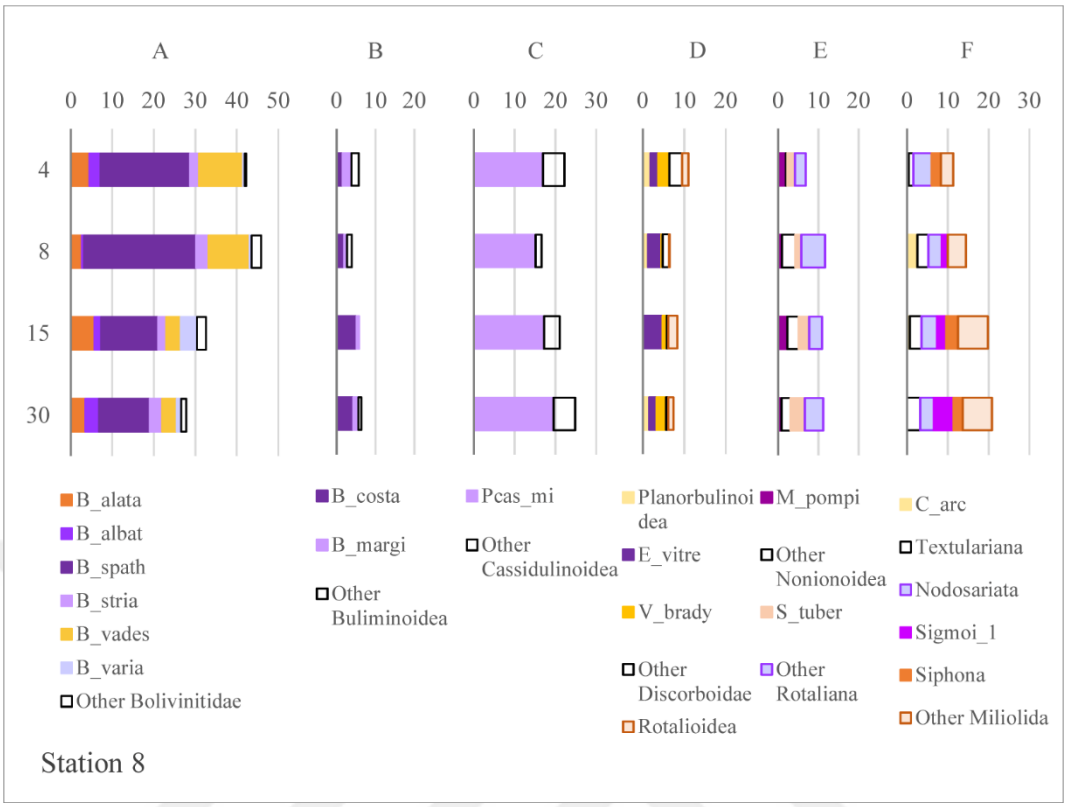


Figure 4.8. Relative abundances of selected taxa in Station 8 sediment core. Panels from left to right: A: Bolivinitidae; B: Buliminoidea; C: Cassidulinoidea; D: Planorbulinoidea, Discorboidea, Rotaloidea; E: Nonionoidea, other Rotaliana, Spirillinida; F: Robertinida, Textulariana, Miliolida. Scales of x-axes of panels are the same. Y-axis not to scale. Taxa abbreviations as in Supplementary Table A.1.

4.2.8 Station 3 (2021) – Izmit Bay shelf – 195 m

P. minuta and *B. spathulata* are dominant in all samples of this core while *B.* cf. *vadescens* is abundant (Figure 4.10, Supplementary Table B.9). These are accompanied by frequent Rotalioidae, *B. dilatata*, *B. elongata*, *E. vitrea*, *V. bradyana*, Nonionoidea, *Eubuliminella* sp., *G. umbonata*, *S. wrighti* in at least two samples. Other Bolivinitidae and other Buliminoidae are frequent in all the samples. There is not a significant difference in assemblage between the samples of the core.

PF (P%, 1.31-3.68%) and sand (Sand%, 2.31-13.63 %) ratios are very low in this core and do not differ between the samples, except for in the 4 cm sample where the sand ratio reaches 13.63%, and P% increases very slightly to 3.68% (Table 4.3, Figure 4.2). This change in S% is not accompanied by any assemblage changes, except for a very slight decrease in bolivinid taxa.

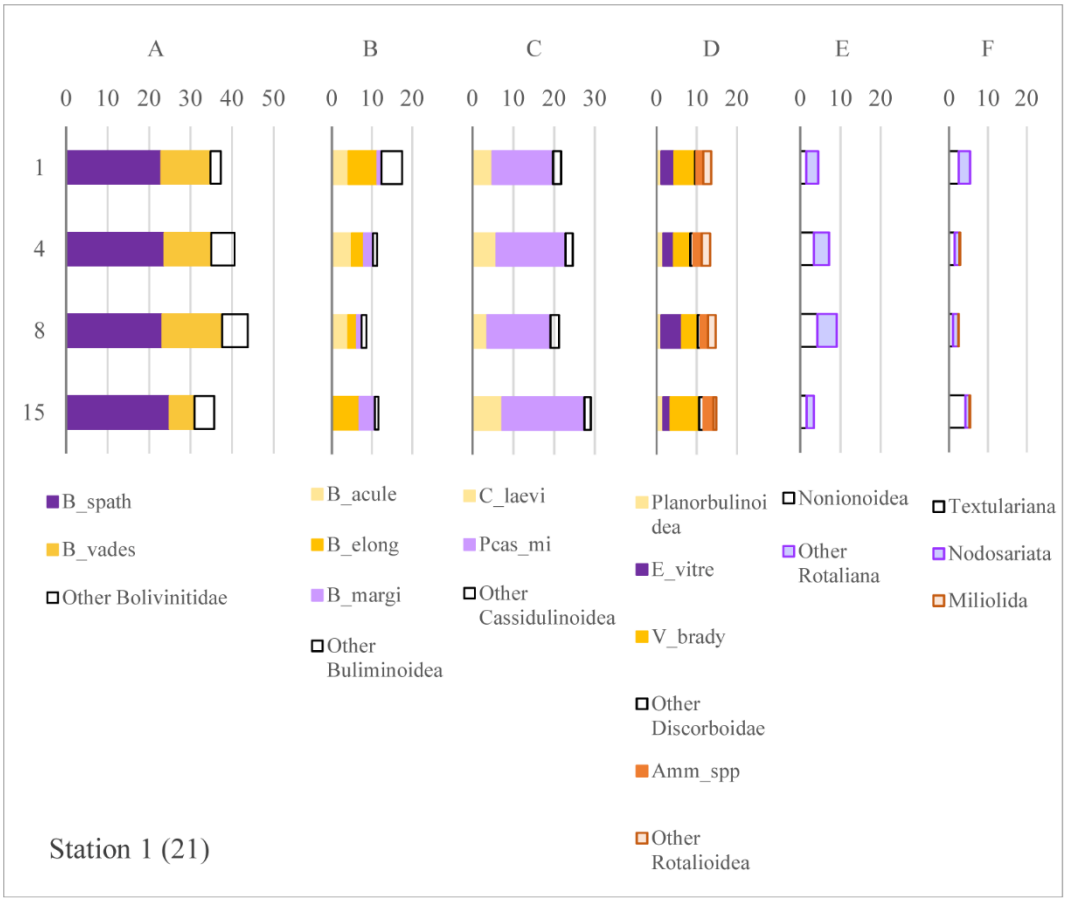


Figure 4.9. Relative abundances of selected taxa in Station 1 (21) sediment core. Panels from left to right: A: Bolivinitidae; B: Buliminoidea; C: Cassidulinoidea; D: Planorbulinoidea, Discorboidea, Rotaloidea; E: Nonionoidea, other Rotaliana, Spirillinida; F: Robertinida, Textulariana, Miliolida. Scales of x-axes of panels are the same. Y-axis not to scale. Taxa abbreviations as in Supplementary Table A.1.

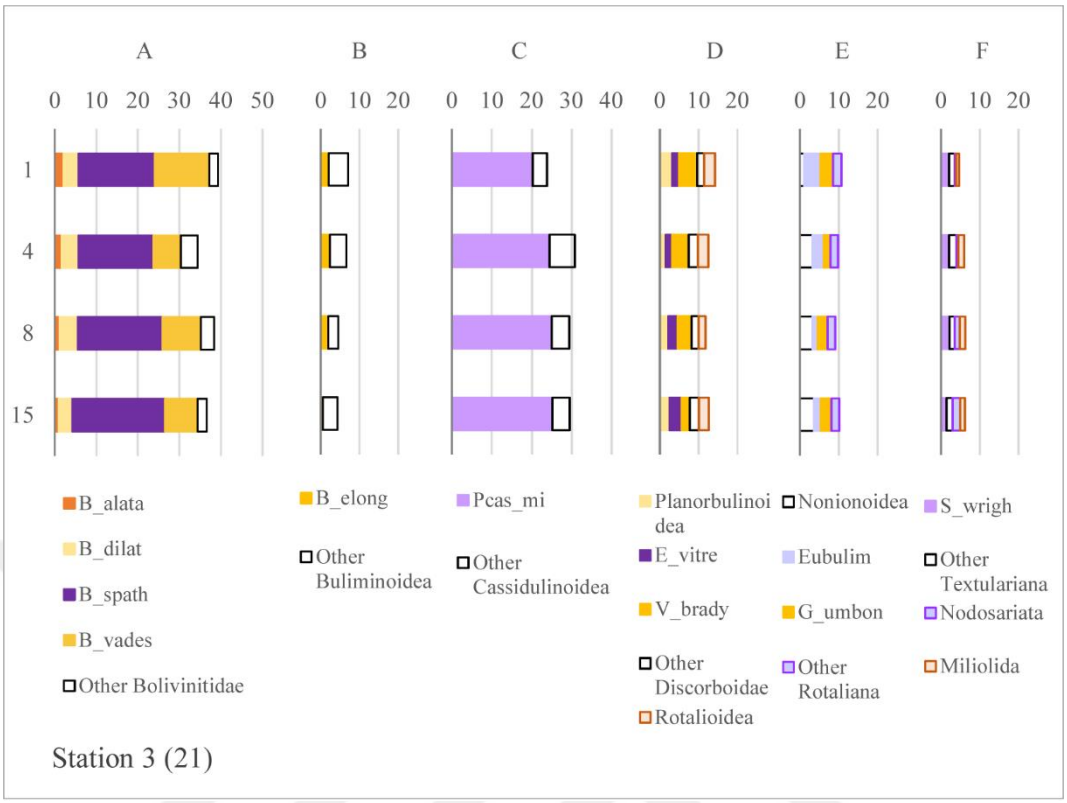


Figure 4.10. Relative abundances of selected taxa in Station 3 (21) sediment core. Panels from left to right: A: Bolivinitidae; B: Buliminoidea; C: Cassidulinoidea; D: Planorbulinoidea, Discorboidea, Rotaloidea; E: Nonionoidea, other Rotaliana, Spirillinida; F: Robertinida, Textulariana, Miliolida. Scales of x-axes of panels are the same. Y-axis not to scale. Taxa abbreviations as in Supplementary Table A.1.

4.2.9 45C-2

B. spathulata (8-23%) and *P. minuta* (12-39%) are both abundant to dominant in the core; while, *B.* cf. *vadescens* (3-9%) and B. costata (2-5%) are frequent to abundant (Figure 4.11, Supplementary Table B.10). These are accompanied by *B. dilatata*, *B. aculeata*, Planorbulinoidea, *V. bradyana*, *Melonis pompilioides* and Glabratellidae frequent or abundant in at least three samples.

Both *B. spathulata* and *P. minuta* decrease in abundance down-core, are dominant in the top 20 cm of the core, become only abundant in the 30 and 40 cm samples. *B.*

cf. *vadescens* also decreases downcore, and is only frequent in the 20, 30, 40 cm samples. these are replaced by abundant to dominant (12-17%) M. pompilioides in the 20, 30, 40 cm samples, increasing downward. These bottom three samples also have higher abundances of *V. bradyana*, *Rosalina bradyi*, Rotalioidea, Planorbulinoidea, Glabratellidae and other Rotaliana.

In 45C-2, PF ratio (P%, 23.48-72.26%) steadily increases downward, and sand (Sand%, 0.4-2.1%) ratio does not differ much between the samples (Table 4.3, Figure 4.2). the highest sand ratio (2.1%) occurs in sample 15 cm in which absolute abundances of both BF ($BF_{\#V}$, Table 4.2) and PF ($PF_{\#V}$, Table 4.3, Figure 4.2) are higher. 15 cm sample BF assemblage is practically the same as the samples above, however a shift in community structures occurs, and the assemblage of below lying samples are somewhat different (Figure 4.11).

4.2.10 Izmit-deep

The absolute abundance of benthic foraminifera in this core is very low (see Section 4.1) and although the whole samples were analyzed, a population of at least ~300 specimens were not reached in the top 8 cm of the core (Table 4.2). Therefore, the relative abundances of the foraminifera in these 8 cm may include a higher error margin.

Izmit-deep is characterized by the presence and abundance of *Virgulinella fragilis* in the top 10 cm of the core (Figure 4.12, Supplementary Table B.11). The abundance of this form peaks at 4 cm sample and is accompanied by *Ammonia* spp. and and *Bolivina* spp. The abundance of *V. fragilis* diminishes in 15 cm sample.



Figure 4.11. Relative abundances of selected taxa in 45C-2 sediment core. Panels from left to right: A: Bolivinitidae; B: Buliminoidea; C: Cassidulinoidea; D: Planorbulinoidea, Discorboidea, Rotaloidea; E: Nonionoidea, other Rotaliana, Spirillinida; F: Robertinida, Textulariana, Miliolida. Scales of x-axes of panels are the same. Y-axis not to scale. Taxa abbreviations as in Supplementary Table A.1.

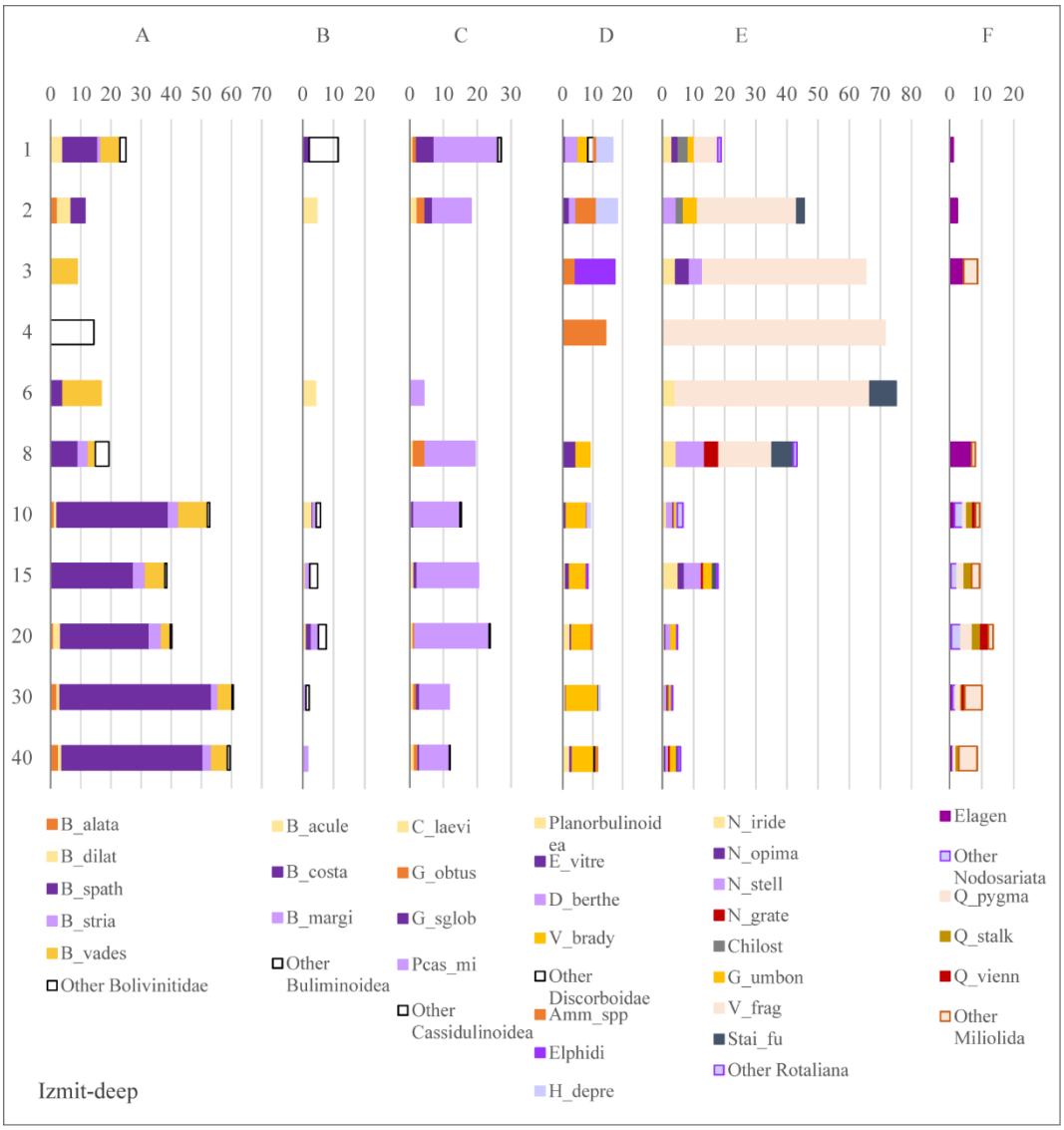


Figure 4.12. Relative abundances of selected taxa in Izmit-deep sediment core. Panels from left to right: A: Bolivinitidae; B: Buliminoidea; C: Cassidulinoidea; D: Planorbulinoidea, Discorboidea, Rotaloidea; E: Nonionoidea, other Rotaliana, Spirillinida; F: Robertinida, Textulariana, Miliolida. Scales of x-axes of panels are the same. Y-axis not to scale. Taxa abbreviations as in Supplementary Table A.1.

Samples 10 cm and below are similar to other stations with abundant to dominant *B. spathulata* (27-50%) and *P. minuta* (9-22%), and abundant *B.* cf. *vadescens* (3-10%). However, the abundance of *B. spathulata* is its highest among all studied samples in 30 and 40 cm samples (48-50%). In the top 8 cm of the core, the abundances of these

taxa vary highly. In samples 10 cm and below, the dominant forms are accompanied by abundant *V. bradyana* and frequent *B. striatula* in all samples, and some miliolids occur frequently. The upper samples, on the other hand, have various abundances of nonionoids, *Stainforthia fusiformis*, *Ammonia* spp., *Elphidium* spp. and *Haynesina* depressula.

Very low $BF_{\#V}$ (Table 4.2) and $PF_{\#V}$ (Table 4.3) are present in this core, both numbers increase downward starting at 10 cm sample (Figure 4.2). A shift in community structures is also seen at sample 10 cm (Figure 4.12).

4.2.11 K40K46

P. minuta (8-16%) is abundant in most samples in this core, becomes dominant in only sample 15 cm (Figure 4.13, Supplementary Table B.12). *B. spathulata* (13-31%) is moslty dominant, but only abundant in 1 and 30 cm samples. *B.* cf. *vadescens* (4-17%) is frequent in 1 cm sample, dominant in 8 cm sample and abundant in the others. These are accompanied by abundant *B. striatula* (7-11%) in all samples, frequent to dominant *Sigmoilopsis* sp. 1 (3-17%), and frequent to abundant *Sigmoilinita tenuis* (3-10%) in all samples. *B. alata*, *B. dilatata*, *B. costata*, *V. brady* and *M. pompilioides* occur in this core as frequent to abundant in at least three samples.

The sand ratio in the samples (Sand%, Table 4.3) is very low (0.21-0.88%). This core has high P% values (Table 4.3) throughout, decreasing slightly towards sample 8 cm, increasing afterwards; opposingly, $BF_{\#V}$ values increase in the same sample (Table 4.2, Figure 4.2). This shift is also mirrored in the BF assemblage composition: towards 8 cm sample, the bolivinid abundance increase as *Sigmoilopsis* sp. 1 and *S. tenuis* abundances decrease, the opposite occurs downward.

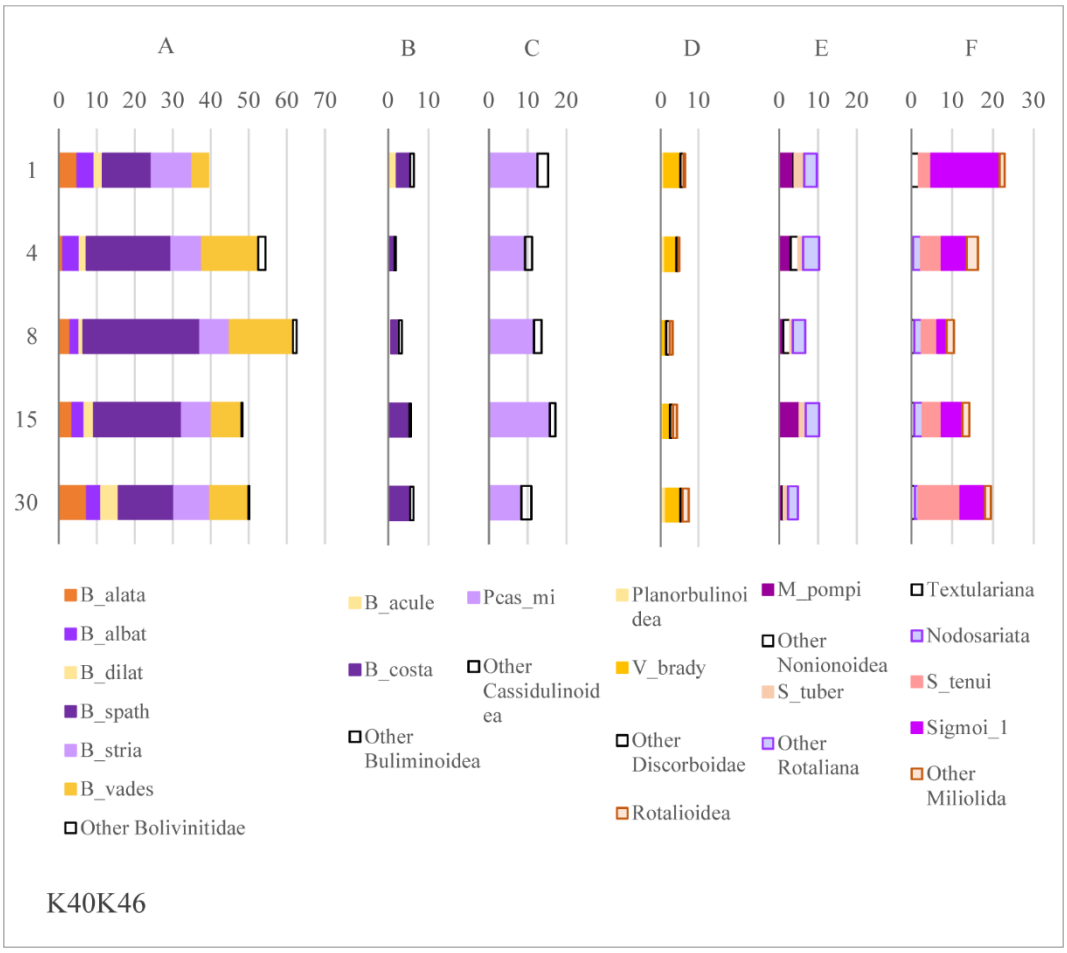


Figure 4.13. Relative abundances of selected taxa in K40K46 sediment core. Panels from left to right: A: Bolivinitidae; B: Buliminoidea; C: Cassidulinoidea; D: Planorbulinoidea, Discorboidea, Rotaloidea; E: Nonionoidea, other Rotaliana, Spirillinida; F: Robertinida, Textulariana, Miliolida. Scales of x-axes of panels are the same. Y-axis not to scale. Taxa abbreviations as in Supplementary Table A.1.

4.2.12 K42K20

P. minuta (23-29%) and *B. spathulata* (18-23%) are both dominant in the core, *B.* cf. *vadescens* (7-13%) is abundant (Figure 4.14, Supplementary Table B.13). *B. dilatata* (9-17%) is abundant in the top three samples, but is dominant in the 15 cm sample.

These are accompanied by frequent to abundance *B. costata* and *B. marginata* in all samples and frequent *H. marmarica* and *E. vitrea* in three samples.

Vertical change in *P. minuta* abundance is somewhat mirrored by change in buliminid abundance. Otherwise, the assemblages of this core are quite stable.

PF ratio (P%, Table 4.3) decreases downward in this core while the $BF_{\#V}$ (Table 4.2) and $PF_{\#V}$ (Table 4.3) increase toward 8 cm sample, and is lower in the 15 cm sample (Figure 4.2).

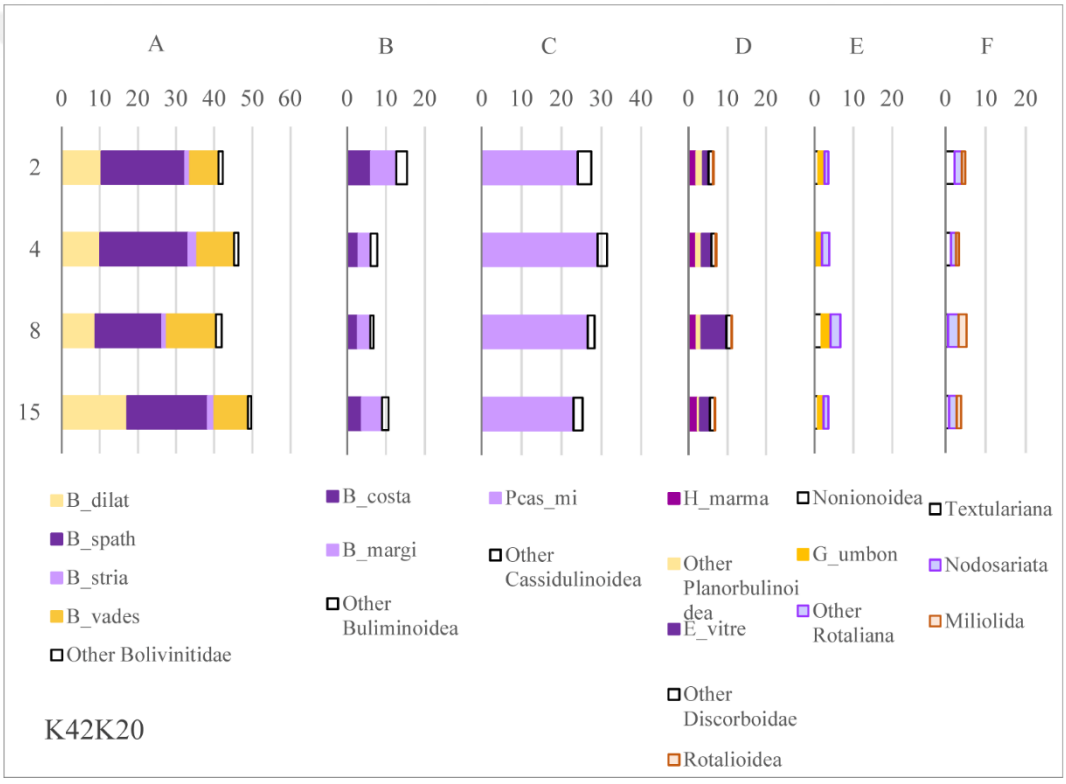


Figure 4.14. Relative abundances of selected taxa in K42K20 sediment core. Panels from left to right: A: Bolivinitidae; B: Buliminoidea; C: Cassidulinoidea; D: Planorbulinoidea, Discorboidea, Rotaloidea; E: Nonionoidea, other Rotaliana, Spirillinida; F: Robertinida, Textulariana, Miliolida. Scales of x-axes of panels are the same. Y-axis not to scale. Taxa abbreviations as in Supplementary Table A.1.

4.2.13 K49.5L04

P. minuta (29-37%) and *B. spathulata* (19-24%) are dominant and *B.* cf. *vadescens* is abundant in all samples of this core (Figure 4.15, Supplementary Table B.14). *B. dilatata* is frequent in all samples; *B. aculeata* is frequent in samples 4, 8, 15 and *B. elongata* is frequent in 1 cm sample. *E. vitrea* is frequent to abundant in three samples. Other than increase in *P. minuta* and *B. aculeata* and decrease in bolivinids in sample 8 cm, the assemblage is quite stable in the core. In the sample 8 cm, an increase in P% (Table 4.3) and decrease in $BF_{\#V}$ (Table 4.2) accompanies this change in assemblage (Figure 4.2). Sand content (Sand%, 6.12-12.24%, Table 4.3) is higher than most stations and decreases downward in this core (Figure 4.2).

4.2.14 K51.2K09

P. minuta (5-21%) and *B. spathulata* (8-18%), *B. inflata* (3-16%) are abundant to dominant in the core (Figure 4.16, Supplementary Table B.15). *B. dilatata* (4-10%) and *M. pompilioides* (3-12%) are frequent to abundant abundant in all samples. *B. marginata* and other Bolivinitida are frequent in all samples, while Texulariana, Nodosariata and Miliolida are of significant abundances (>2%) in almost all samples.

The assemblage in 4 and 8 cm samples are significantly different from others with *M. pompilioides* and *B. inflata* having higher abundances and *P. minuta* and *B. spathulata* having lower abundances. *B. inflata* is more abundant in the top part of the core (1,4,8 cm), while it is replaced by *B. costata* in the lower part (15 and 30 cm). *M. pompilioides* is also more abundant in the top part of the core than the lower part.

In 8 cm sample, the $BF_{\#V}$ is highest (Table 4.2). sand content (Sand%, Table 4.3) is higher in the upper part of the core (4.75-6.44% in samples 1, 4, 8 cm) but significantly lower in the lower part of the core (0.48-0.56 in 15 and 30 cm). P% increases steadily downward (Table 4.3, Figure 4.2).

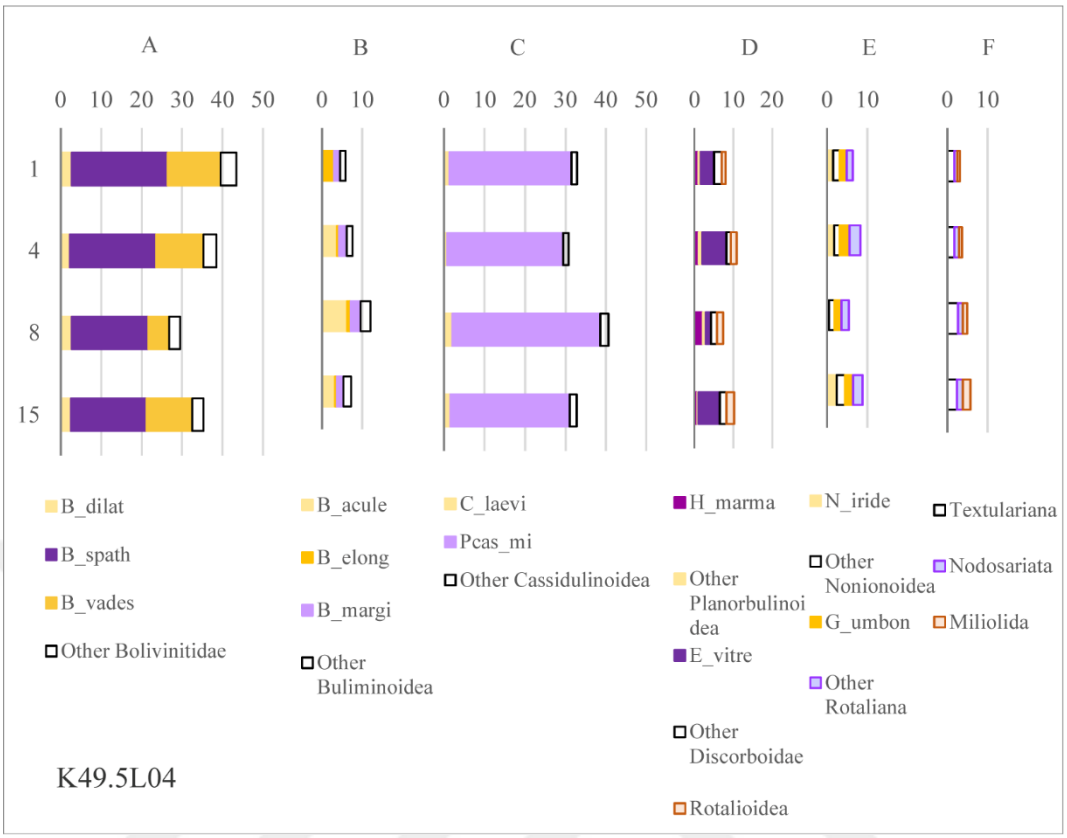


Figure 4.15. Relative abundances of selected taxa in K49.5L04 sediment core. Panels from left to right: A: Bolivinitidae; B: Buliminoidea; C: Cassidulinoidea; D: Planorbulinoidea, Discorboidea, Rotaloidea; E: Nonionoidea, other Rotaliana, Spirillinida; F: Robertinida, Textulariana, Miliolida. Scales of x-axes of panels are the same. Y-axis not to scale. Taxa abbreviations as in Supplementary Table A.1.

4.2.15 MM-50

In this core, no taxa with dominant abundance (>15%) are present (Figure 4.17, Supplementary Table B.16). *B. spathulata* (8-15%), *B.* cf. *vadescens* (5-12%), *B. aculeata* (6-10%), *C. laevigata* (5-10%) and *V. bradyana* (7-10%) are all abundant in all samples. *P. minuta* (2-6%) is only frequent to abundant in all samples. *Ammonia* spp., *Rectuvigerina phlegeri*, *Trifarina angulosa*, *Planorbulina mediterranensis*, *E. vitrea* and *N. iridea* are at least frequent in at least three samples,

and Miliolida and Textulariana reach substantial abundances (>2%) in at least four samples.

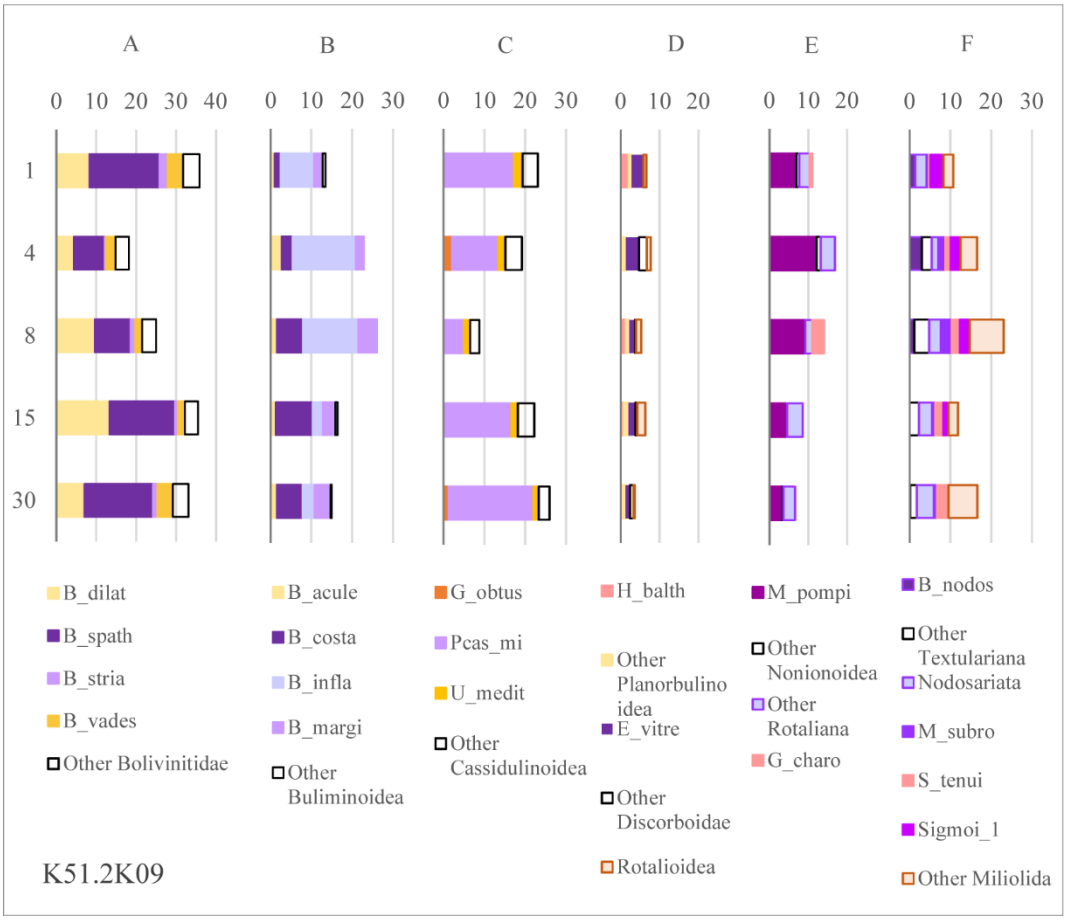


Figure 4.16. Relative abundances of selected taxa in K51.2K09 sediment core. Panels from left to right: A: Bolivinitidae; B: Buliminoidea; C: Cassidulinoidea; D: Planorbulinoidea, Discorboidea, Rotaloidea; E: Nonionoidea, other Rotaliana, Spirillinida; F: Robertinida, Textulariana, Miliolida. Scales of x-axes of panels are the same. Y-axis not to scale. Taxa abbreviations as in Supplementary Table A.1.

Bolivinitidae abundance do not change downcore, however, Buliminoidea abundance decreases remarkebly. Especially *R. phlegeri* and *B. elongata* are abundant (10% and 7% respectively) in the 1 cm sample, but decrease drastically in

the samples below. Cassidulinids and miliolids, especially *Quinqueloculina stalkeri*, also increase in abundance downcore while *Ammonia* spp. decrease.

The sand content (Sand%, Table 4.3, Figure 4.2) of the upper two samples are very high (10.11 and 17.29% respectively) and low in the lower samples (1.53-2.92%). P% is usually low (0.63-6.26%), highest in the 30 cm sample (Table 4.3) with lowest absolute abundance of BF (BF$_{\#V}$, Table 4.2, Figure 4.2).

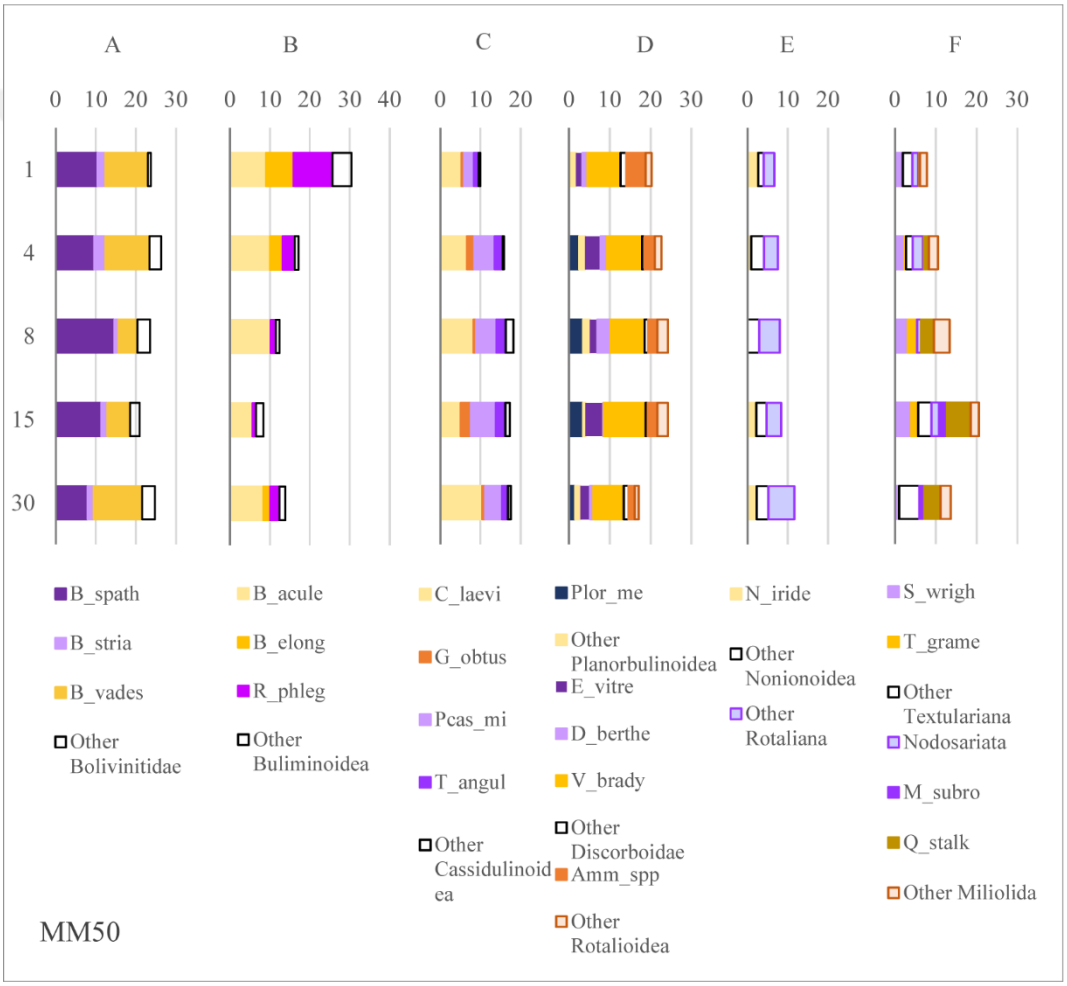


Figure 4.17. Relative abundances of selected taxa in MM50 sediment core. Panels from left to right: A: Bolivinitidae; B: Buliminoidea; C: Cassidulinoidea; D: Planorbulinoidea, Discorboidea, Rotaloidea; E: Nonionoidea, other Rotaliana, Spirillinida; F: Robertinida, Textulariana, Miliolida. Scales of x-axes of panels are the same. Y-axis not to scale. Taxa abbreviations as in Supplementary Table A.1.

CHAPTER 5

BENTHIC FORAMINIFERA ASSEMBLAGES OF THE SEA OF MARMARA: A COMPILATION OF QUANTITAVE DATA

In the Sea of Marmara, numereous quantitative benthic foraminiferal studies were conducted (Table 5.1). These studies were aimed to document the assemblages, the geographic distribution of taxa, the changes in assemblages in time, exploration of paleoenvironments and investigations of the effects of environmental variables on BF assemblages. This chapter aims to combine the quantitative data of these previously published research and evaluate the effect of sampling and processing differences on the reported assemblages, and provide an integrated, comprehensive account on the distribution of taxa.

5.1 Selection of studies

Table 5.1 lists the quantitative benthic foraminifera studies done in the Sea of Marmara, and their methodological details. From these studies, ten of them were selected for further analyses (Table 5.2). Selection of studies was made with consideration of sampling sites, counting method and total counted number of benthic foraminifera; further details for each study and the reason for their inclusion or exclusion are given below.

Alavi (1988, Code: SoM_13 in Table 5.1; Table 5.2) was the first to study benthic foraminifera of the Sea of Marmara and carried out quantitative analysis on two cores form the deep Çınarcık Basin. The counting was done on three size fractions separately (63-125, 125-250, >250 μm) with finer fractions being split (undisclosed number of times) when necessary. The reported results (census tables) are the summed numbers of counted foraminifera from the three size fractions, not corrected

Table 5.1. Counting and other method details of the quantitative benthic foraminifera studies of the Sea of Marmara.

Data Code	Reference	Type	Studied assemblage	Size fraction (μm)	Counting details
SoM_01	Fontanier et al., 2018	Core	Live (rose Bengal stained)	>125 & 63-125	Samples of 5.4 cm diameter and 0.5 or 1 cm thickness. Whole sample.
SoM_02	Phipps et al., 2010	Grab	Dead	>125	Initial sample size not reported. Samples split (undisclosed number of times). Agglutinant taxa omitted.
SoM_03	Kırcı-Elmas, 2006	Core	Undiff.	>125	Samples of 10 g dry sediment. Whole sample?
SoM_04	Akçer, 2003	Core	Undiff.	>40 (?)	Samples of 30 g wet sediment. Resieved after drying from an undisclosed sieve size. Counted once on counting tray and multiplied to reach the absolute abundance numbers.
SoM_05	Topkar, 2003	Core	Undiff.	>40	Samples of 15/30 g wet sediment. Counted once on counting tray and multiplied to reach the absolute abundance numbers.
SoM_06	Kırcı-Elmas, 2018	Grab	Undiff.	125	Samples of 10 g of dry sediment. Whole sample?
SoM_07	Kırcı-Elmas, 2013	Grab	Undiff.	>63 & >125	Samples of 10 g of dry sediment. Samples resieved after splitting (undisclosed number of times, to at least 300 individuals). Reported as relative abundances only.
SoM_08	Avşar, 2010	Grab	Undiff.	>63	Samples of 5 g dry sediment. Only about 300 individuals counted without splitting? .
SoM_09	Kırcı-Elmas et al., 2008	Core	Undiff.	>125	Samples of 2 cm slices or 10 g dry sediment. Whole sample?
SoM_10	Meriç and Algan, 2007	Core	Undiff.	>250	Cores from littoral areas. Samples of 50 g of wet sediment. <250 μm fraction never investigated. Whole sample?
SoM_11	Kaminski et al., 2002	Core	Undiff.	>125	Samples of 10 ml sediment. Whole sample.

Table 5.1 continued.

Data Code	Reference	Type	Studied assemblage	Size fraction (μm)	Counting details
SoM_12	Avşar et al., 2006	Core	Undiff.	>63	Samples of 5 g dry sediment. Whole sample.
SoM_13	Alavi, 1988	Core	Undiff.	>63	Samples of 4 ml wet sediment. Whole sample (>250, 125-250 and 63-125 treated separately and split if needed). Reported summed number of counted specimens.
SoM_14	Kam and Yümün, 2021	Core	Undiff.	>63	Samples of 15 g wet sediment. Whole sample?

for split size. This approach was applied to limit the overbearing dominance of small forms, however produces a faulty higher ratio of larger forms. Without knowing the split ratio applied to the sample size fractions, there is no way of understanding the underestimation of abundance these small taxa experienced in this analysis. Despite the very clear methodological difference, this study was included in further analyses since the number of samples coming from the deep basins are limited.

Kaminski et al. (2002, Code: SoM_11 in Table 5.1; Table 5.2) worked on four cores, but reported the results of only three from Prince Islands Shelf, southern exit of the Bosphorus and southern shelf edge. Except for some almost barren intervals, the number of counted foraminifera were adequate in the samples.

Akçer (2003, Code: SoM_04 in Table 5.1) was carried out on three cores coming from the Central High, Imralı Basin and Prince Islands Shelf. This study reported quantitative results obtained from 30 g of wet samples, over an undisclosed sieve size; any splitting, if done, was not mentioned, instead "counted once on counting tray and multiplied to reach the absolute abundance numbers" remark is added. Moreover, quantitative results (census tables) are identical for two of the studied cores. Akçer (2003) identified 44 and 28 species in the cores, and except for a few samples, the counted benthic foraminifera numbers are not adequate. Therefore, this study was omitted from further analyses.

Topkar (2003, Code: SoM_05 in Table 5.1) studied two cores from the Izmit Bay. They processes 15 or 30 g of wet samples, examined material coarser than 40 μm; however, the counting was done as in Akçer (2003) (Table 5.1). Topkar (2003) identified and quantified 71 and 75 species in the two cores. Although for most samples the reported "absolute abundances" are adequate, because the counting method is not reliable, this study was omitted from further analysis.

Kırcı-Elmas (2006, Code: SoM_03 in Table 5.1; Table 5.2) studied 6 cores from Central and Çınarcık basins, two of which were published separately in Kırcı-Elmas et al. (2008, Code: SoM_09 in Table 5.1; Table 5.2). Analyses were done on 10 g of dry sediment; although if and how much splitting was done was not mentioned, the census data were reported as normalized to 10 gr of dry sediment. To prevent duplication, Kırcı-Elmas et al. (2008) was used for the two cores present in both studies, and Kırcı-Elmas (2006) was limited to those which were not present in the 2008 publication.

Avşar et al. (2006, Code: SoM_12 in Table 5.1; Table 5.2) studied grab samples from the Erdek Bay, worked on 5 g of dry samples. All of the samples, except for one, produced benthic foraminifera numbers lower than 300 despite use of the full sample (no splitting). Avşar (2010; Code: SoM_08 in Table 5.1; Table 5.2) studied grab samples from the northern shelf, worked on 5 g of dry samples. No splitting was mentioned but "three hundred […] specimens were picked" from the whole samples. The smaller number of individuals in the former can be source of error, similarly, the picking in the latter may be biased (towards larger specimens or known taxa); yet, these two studies were included in the analyses nonetheless.

One study was carried out on cores taken from littoral areas (Meriç and Algan, 2007, Code: SoM_10 in Table 5.1). This study reported quantitative results obtained from 50 g of wet samples, above 250 μm sieve size, and eliminated from further analyses here due to large size fraction and also small number of benthic foraminifera counted from the samples (30 specimens in average).

Phipps et al. (2010, Code: SoM_02 in Table 5.1; Table 5.2) studied grab samples from the western part of the southern shelf to slope (west of Erdek Bay), samples were split an undisclosed amount of times, and both count data and relative abundances were reported. The data Phipps et al. (2010) reports omits the rose Bengal stained individuals (only reports dead assemblage) and agglutinant taxa (only report calcareous assemblage); yet it is included in the analyses nonetheless.

Kırcı-Elmas (2013, Code: SoM_07; and 2018, Code: SoM_06 in Table 5.1; Table 5.2) studied grab samples from all shelves (including the Bosphorus and Dardanelles) and the northern shelf respectively, from 10 g of dry samples. Kırcı-Elmas (2013) used two different size fractions (>63 and >125 μm) and split (undisclosed amount of times) the samples to include at least 300 specimens; reported only the relative abundance data. Kırcı-Elmas (2018), on the other hand, used >125 μm size fraction and counted foraminifera from the whole samples (no splitting). Although given only as relative abundances and there is no way of understanding the absolute abundances, the data of Kırcı-Elmas (2013) is included since it constitutes samples from various locations. Similarly, the data of Kırcı-Elmas (2018) is also included in further analyses despite the low total number of benthic foraminifera.

Fontanier et al. (2018, Code: SoM_01 in Table 5.1; Table 5.2) studied two short cores from the Çınarcık Basin and Central High, used two size fractions (63-125 and >125 μm), and reported the census data for the whole sample (no splitting), only for rose Bengal stained (assumed live) individuals. Although the reported numbers are very low for the Çınarcık Basin station, the data was included in the further analyses since this is the only quantitative live foraminifera study. The data of the Çınarcık Basin station was used as all levels lumped (1.5 cm of thickness).

Kam and Yümün (2021, Code: SoM_14 in Table 5.1) worked on cores from the nothern shelf (İstanbul, Silivri). From 15 g wet sediment, foraminifera were studied from the >63 μm size fraction. However, although they worked on cores, the levels (depth in core) of quantitative foraminiferal results are not included, therefore it

cannot be known if the data they report belong to a sum of all the core, or only a specific interval. Due to this discrepancy, this study was eliminated from further analysis.

5.2 Methodological and reporting differences between studies

Out of 11 publications included in this study, six of them were conducted on cores, and five of them were conducted on grab samples (Table 5.2, Figure 5.1). For the grab samples, the depth of sampling (sample thickness from surface to bottom of sampled interval) was not given for Avşar et al. (2006, SoM_12), Avşar (2010, SoM_08) and Phipps et al. (2010, SoM_02), given as upper 2 cm by Kırcı-Elmas (20013, SoM_07; 2018, SoM_06). The cores were sampled mostly every 10 cm, spanning mostly 2 cm thickness (Alavi, 1988, SoM_13; Kaminski et al., 2002, SoM_11; Kırcı-Elmas, 2006, SoM_03; Kırcı-Elmas, 2008, SoM_09), in 0.5 to 1 cm intervals (Fontanier et al., 2018) and with 1, 2, and 5 cm intervals (this study).

Nine of the studies were conducted on undifferentiated assemblage (i.e., any distinction between live and dead foraminifera was not done; Table 5.1, Table 5.2). Three of the studies used rose Bengal (rB) staining and one reported rB stained foraminifera numbers (Fontanier et al., 2018, SoM_01), one reported only non-stained numbers (Phipps et al., 2010, SoM_02), and this present study reported undifferentiated numbers (SoM_TS).

Table 5.2. Type of sample, amount of stations, locations, water depths, studied assemblage type (Live / Dead / Undifferentiated) and size fraction (coarser than 63 or 125 μm) of the analyzed quantitative benthic foraminifera studies.

Data Code	Reference	Type	Number of stations	Location	Depth (m)	L/D/U	Size fraction (μm)
SoM_01	Fontanier et al. 2018	Core	2	Çınarcık Basin and Central high	1237, 326	L	63
SoM_02	Phipps et al. 2010	Grab	30	Southwestern shelf to slope: west of Erdek Bay.	15-350	D	125
SoM_03	Kırcı-Elmas 2006	Core	4	Central Basin and Çınarcık Basin	700-1200	U	125
SoM_06	Kırcı-Elmas 2018	Grab	19	Northern Shelf: Tekirdağ, Silivri	15-70	U	125
SoM_07	Kırcı-Elmas 2013	Grab	23	All Marmara shelves, Dardanelles, Bosphorus	11-320	U	63
SoM_08	Avşar 2010	Grab	26	Northern Shelf: Tekirdağ, Silivri, İstanbul	13-111	U	63
SoM_09	Kırcı-Elmas et al. 2008	Core	2	Central Basin	703, 895	U	125
SoM_11	Kaminski et al. 2002	Core	3	Prince Islands shelf; southern exit of the Bosphorus; southern shelf edge	64-111	U	125
SoM_12	Avşar et al. 2006	Grab	15	Erdek Bay	28-57	U	63
SoM_13	Alavi, 1988	Core	2	Çınarcık Basin	1200	U	63
SoM_TS	This study	Core	18	Izmit Bay, Prince Islands Shelf, Çınarcık and Central Deep, Imralı Basin, southern shelf	53.5-1214	U	63

Five studies were conducted on >125 µm fraction, and four studies were conducted on >63 µm fraction (Table 5.1). The other two studies reported census data in two separate size fractions (Kırcı-Elmas, 2013, SoM_07, >63 and >125 µm; Fontanier et al., 2018, SoM_01, 63-125 and >125 µm; Table 5.1), for these studies >63 µm data were used (directly for SoM_07; by summing fractions for SoM_01 since no splitting was applied).

Kırcı-Elmas (2013, SoM_07) reported the data only as relative abundances, and Alavi (1988, SoM_13) reported the sum of counted specimens from different size fractions without correcting for split size. All other publications reported either the census data directly, or as normalized to the initial sample weight or volume (Table 5.1).

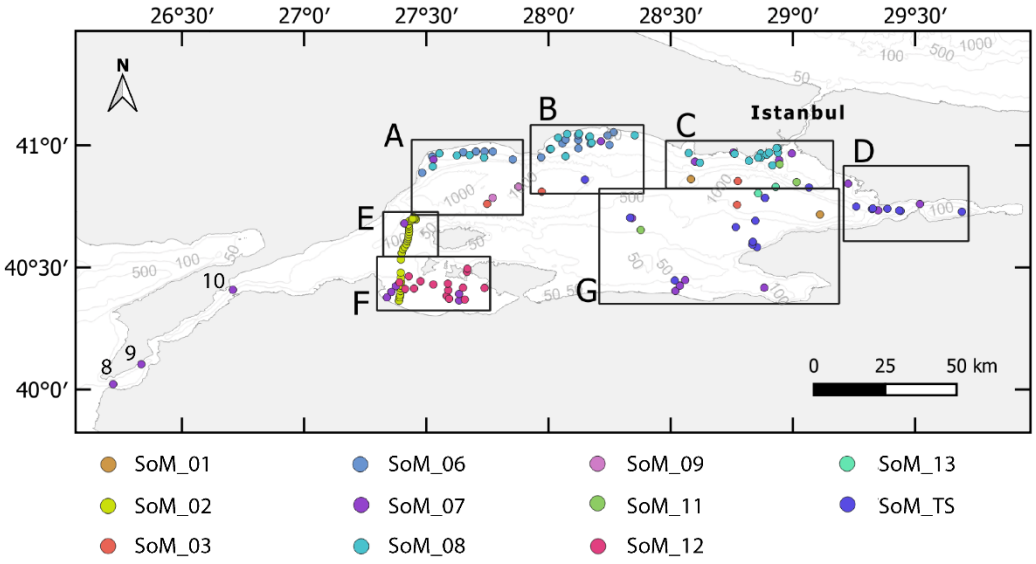


Figure 5.1. Location map of stations in analyzed studies (see Table 5.2 for references). Inset frames (A-G) show extents of maps A-G (continued on the text page).

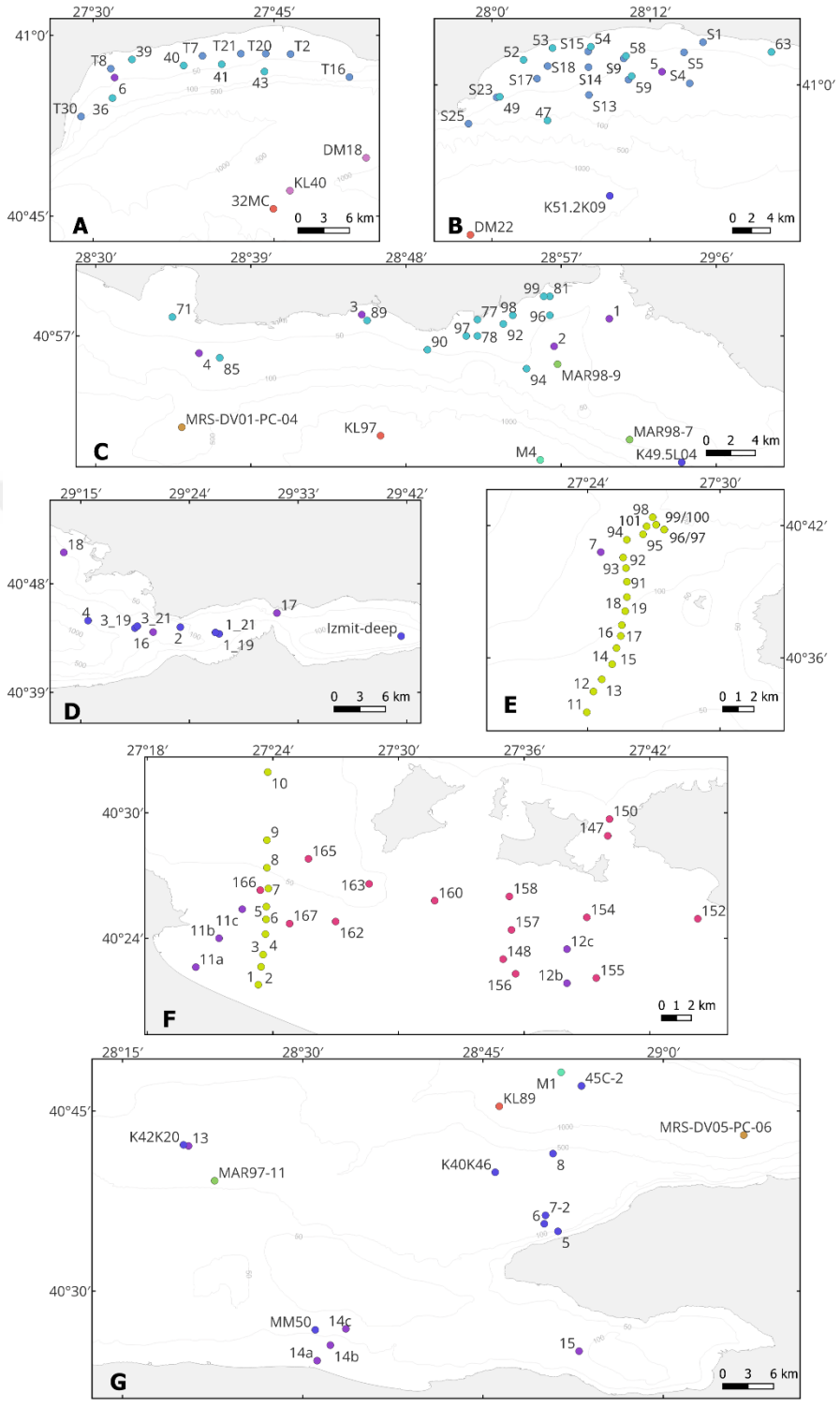


Figure 5.1. Continued.

The taxonomy of identified taxa was given in the publications in a few different formats. Some of the publications included a brief taxonomic list including only the original references to identified taxa (Fontanier et al., 2019, SoM_01, Kırcı-Elmas, 2018, SoM_06; Avşar, 2010, SoM_08; Avşar et al., 2006, SoM_12), and some only gave an incomplete list (Kırcı-Elmas, 2013, SoM_07). Some included only a reference to a previous work (Phipps et al., 2010, SoM_02; Alavi, 1988, SoM_13). Some included in a list a few more recent references including the page and figure numbers from the references showing their framework of the taxa, however not necessarily including all identified taxa (Kırcı-Elmas, 2006, SoM_03; Kırcı-Elmas et al., 2008, SoM_09; Kaminski et al., 2002, SoM_11). This study provided a detailed and comprehensive systematic taxonomy part complete with descriptions, taxonomic discussions and distinguishing features (see Chapter 8).

No publications gave a complete set of images for all identified taxa. Phipps et al. (2010, SoM_02) included no illustrations of taxa. Alavi (1988, SoM_13), Kaminski et al. (2002, SoM_11), Kırcı-Elmas (2006, SoM_03; 2013, SoM_07; 2018, SoM_06), Avşar et al. (2006_SoM_12), Kırcı-Elmas et al. (2008, SoM_09), Avşar (2010, SoM_08) and Fontanier et al. (2018, SoM_01) provided SEM illustrations only for a number of common or widely distributed taxa. This study included SEM figures and stereomicrographs for almost all taxa except for a few very rare ones.

Number of unidentified specimens were reported by about half of the studies (Phipps et al., 2010, SoM_02; Kırcı-Elmas, 2006, SoM_03, 2018, SoM_06, 2013, SoM_07; Kaminski et al., 2002, SoM_11 and this study). The relative abundances of the unidentified specimens are usually in 0-2% range, however higher numbers (10% in this study; 16.7% in SoM_11; 6.7% in SoM_03) are also present occasionally. The rest of the studies did not report the number of unidentified specimens.

5.3 Distribution of stations

Each study done on grab samples included 15 to 30 stations; each study done on cores included 2-6 stations; except this study which included 18 stations, however in three of these only the surface intervals were studied. In total, the data from 144 stations are compiled here (Table 5.2, Figure 5.1, Supplementary Table E.1). Shallowest of these stations is of 11 m water depth (Kırcı-Elmas, 2013, SoM_7, Station 14a), and the deepest is of 1237 m (Fontanier et al., 2018, SoM_1, MRS-DV05-PC-06). Most of the studied stations belong to the shelf: 102 stations were from water depths of 100 m or shallower (Figure 5.2.A). Sixteen stations from 100-200 m, seven stations from 200-300 m, five stations from 300-400 m and nine stations from >1000 m water depth were studied; there are no stations studied from 500-700 m and 900-1000 m water depth; minimum number of stations belong to 800-900 m (one station) and 400-500 m and 700-800 m (two stations each). Shelf stations (<100 m) were present in seven, stations form 100-200 m water depth were present in five, stations from 300-400 m water depth and >1000 m water depth were present in four, stations from 200-300 m and 700-800 m water depth were present in two studies and stations form 400-500 m and 800-900 m water depth were only present in one study (Figure 5.2.B).

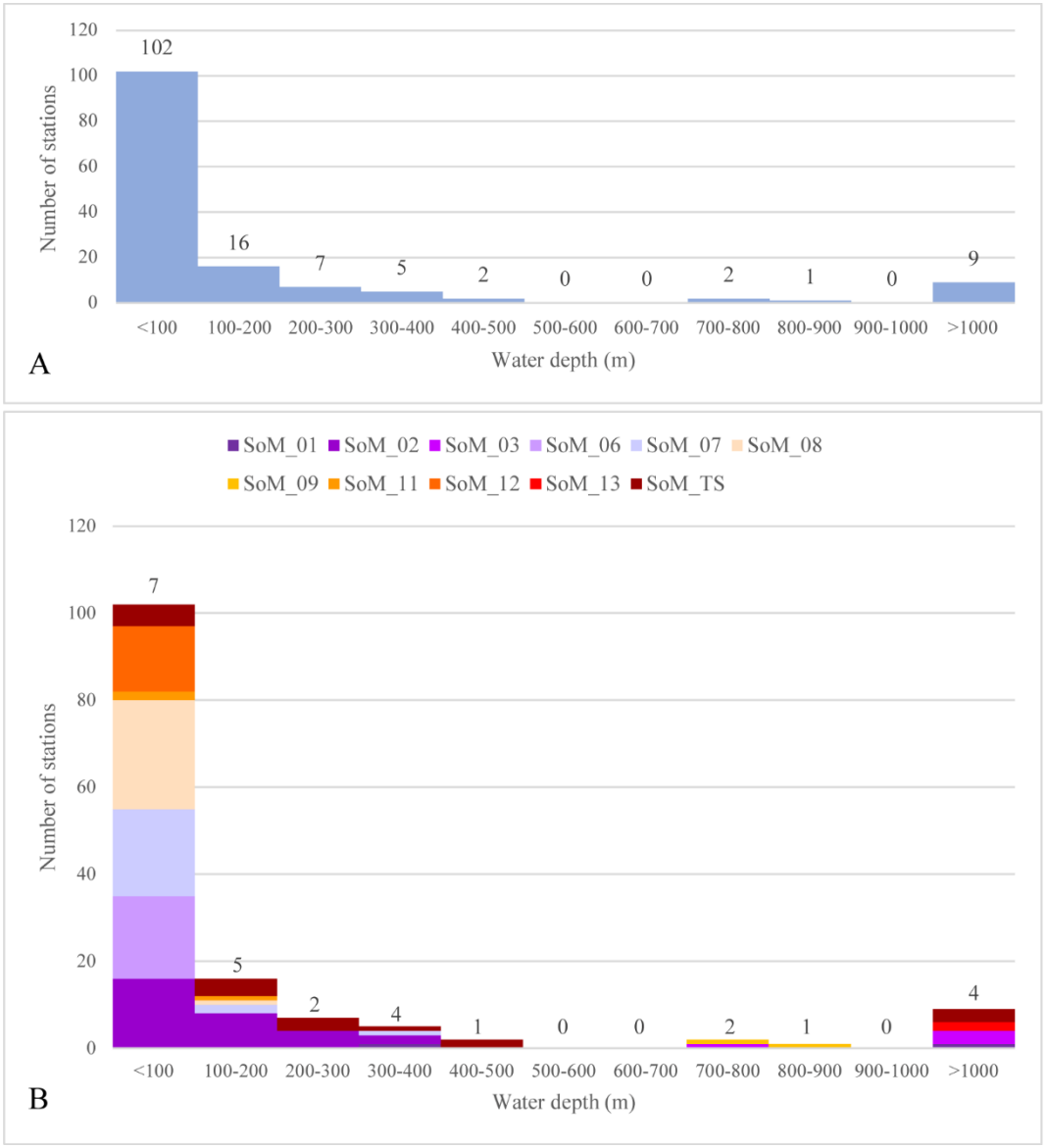


Figure 5.2. Number of stations with respect to water depth: A. histogram for all studies included here, number of stations present in every water depth bin labelled above columns; B. stacked histogram showing stations belonging to different studies, number of studies present in every water depth bin labelled above columns. Data codes as in Table 5.2.

Some parts of the Sea of Marmara are more densely studied (Figure 5.1, Table 5.3, Supplementary Table E.1, see Figure 1.4 for locations). Highest number of stations studied belong to the Erdek Bay (29); to the west, western Southern shelf (7) and

western Southern slope (15) also have high numbers of stations studied. The Southern shelf (Southern shelf west and central, Erdek Bay and Gemlik Bay combined) has 41 stations in total. Northern shelf (Tekirdağ, Silivri, İstanbul, Prince Islands combined) have in total 55 stations, 21 of which are from Silivri, and 18 from Istanbul. In the Çınarcık Basin 8, and in the Central Basin 5 stations are present, while there is no study conducted in the Tekirdağ Basin. The inner part of the Izmit Bay was only studied in this study (Izmit-deep station in the Karamürsel Basin), but the outer part was studied by two studies (a total of eight stations). There are three stations at Prince Islands shelf, two on the shelf and slope off Armutlu Peninsula, two in the Imralı Basin, one on the Central High, and three on central Southern slope. No quantitative study was conducted in the Bosphorus, but three stations are present in the Dardanelles.

Table 5.3. For each location (alphabetically ordered), number of studies, number of stations, the code of the studies (see Table 5.2 for references) and station names/numbers.

Number of Studies	Number of Stations	Location	Study (code)	Station
1	1	Armutlu shelf	SoM_TS	5
1	1	Armutlu slope	SoM_TS	6
3	5	Central Basin	SoM_03	DM22, 32MC
			SoM_09	DM18, KL40
			SoM_TS	K51.2K09
1	1	Central High	SoM_01	MRS-DV01-PC-04
4	8	Çınarcık Basin	SoM_01	MRS-DV05-PC-06
			SoM_03	KL89, KL97
			SoM_13	M1, M4
			SoM_TS	8, 45C-1, 45C-2
1	3	Dardanelles	SoM_07	8, 9, 10

Table 5.3. Continued.

Number of Studies	Number of Stations	Location	Study (code)	Station
3	29	Erdek Bay	SoM_02	1, 2, 3, 4, 5, 6, 7, 8, 9
			SoM_07	11a, 11b, 11c, 12b, 12c
			SoM_12	147, 148, 150, 152, 154, 155, 156, 157, 158, 160, 162, 163, 165, 166, 167
1	1	Gemlik Bay	SoM_07	15
1	2	Imralı Basin	SoM_TS	7-2, K40K46
3	18	Istanbul	SoM_07	1, 2, 3, 4
			SoM_08	71, 77, 78, 81, 85, 89, 90, 92, 94, 96, 97, 98, 99
			SoM_11	MAR98-9
2	9	Izmit Bay	SoM_07	16, 17
			SoM_TS	1_19, 2, 3_19, 4, 1_21, 3_21, Izmit-deep
3	3	Prince Islands	SoM_07	18
			SoM_11	MAR98-7
			SoM_TS	K49.5L04
3	21	Silivri	SoM_06	S23, S1, S4, S5, S8, S9, S13, S14, S15, S17, S18, S25
			SoM_07	5
			SoM_08	47, 49, 52, 53, 54, 58, 59, 63
2	4	Southern shelf (central)	SoM_07	14a, 14b, 14c
			SoM_TS	MM50
1	7	Southern shelf (west)	SoM_02	10, 11, 12, 13, 14, 15, 16
3	3	Southern slope (central)	SoM_07	13
			SoM_11	MAR97-11
			SoM_TS	K42K20
2	15	Southern slope (west)	SoM_02	17, 18, 19, 91, 92, 93, 94, 95, 96, 97, 98, 99, 100, 101
			SoM_7	7

Table 5.3. Continued.

Number of Studies	Number of Stations	Location	Study (code)	Station
3	13	Tekirdağ	SoM_06	T2, T7, T8, T16, T20, T21, T30
			SoM_07	6
			SoM_08	36, 39, 40, 41, 43

5.4 Taxonomic remarks and homogenization

Minimum of 13 (Fontanier et al., 2018, SoM_01) to maximum of 207 (Kırcı-Elmas, 2013, SoM_07) taxa were identified in the publications (Table 5.4).

Table 5.4. Total number of identified taxa (S_{TOT}), average species richness per sample (S_{AV} = (ΣS_i)/k, where S_i= species richness in ith sample, k= number of samples in the study) and number of average reported individuals per sample (N_{AV}= (ΣN_i)/k, where N_i= collected/reported number of individuals in ith sample) in the studied publications. See Table 5.2 for references.)

Data Code	S_{TOT}	S_{AV}	N_{AV}
SoM_01	13	4.50	158.50
SoM_02	211	62.17	670.30
SoM_03	99	15.28	212.52
SoM_06	198	74.42	3492.47
SoM_07	207	51.61	-
SoM_08	115	29.81	299.88
SoM_09	65	11.49	85.32
SoM_11	153	20.85	267.58
SoM_12	74	23.33	137.60
SoM_13	74	28.11	169.00
SoM_TS	164	54.12	596.96

The data for all studies were combined in order to evaluate the differences in assemblage composition and relative abundances between the studies, stations, water depths and locations. For this purpose, the sysnonymy of the taxa cited in the original publications needed to be checked and sorted (homogenization of taxonomic data). Most publications did not include a full list of taxonomy and illustrations of all identified taxa, but some did reference to previous publications for taxonomic framework (see Section 5.2); therefore, the trail of references were followed where necessary. The homogenization of census data included consideration for:

i. obvious name changes, e.g., *Bolivina* species with angular margins were previously regarded as a separate genus, *Brizalina*,

ii. lumping of subspecies and/or varieties; e.g., *Ammonia tepida* was separated to four types by (Phipps et al., 2010, SoM_02) which were lumped here under the species name,

iii. lumping or transferring of species left in open nomenclature or species groups under the genus; e.g., Kaminski et al. (2002, SoM_11) reported abundances of *Elphidium* sp. 2 Cimerman and Langer 1991, *Elphidium* sp. and *Elphidium* spp. separately, which were lumped here under the generic name as *Elphidium* spp.; however for some, lumping was not carried out, e.g., Alavi (1988) remarked the similarity and the diffuculty in distingusihing of *Bolivina spathulata* and *Bolivina dilatata*, especially for smaller (pre-adult) specimens, and presented the data for these two taxa separately for one core, while lumped them together for the other core under the name *'Bolivina dilatata* and *Brizalina spathulata'*; here, this lumped taxon of Alavi's is regarded under *B. spathulata* instead of *Bolivina* spp.,

iv. lumping of taxa whose names are commonly used interchangebly, e.g., all studies report the abundance of either *Cassidulina laevigata* or *Cassidulina carinata*, two taxa which are commonly considered synonymous (Milker and Schmiedl, 2012); only Kaminski et al. (2002, SoM_11) includes both taxa in one sample alone, therefore these two taxa

are regarded under the same name (*C. laevigata*) and the abundances of the two in the single sample (Kaminski et al, 2002, MAR98-7 sample 70 cm) were summed,

v. misidentifications when the taxonomic reference trail can be followed or the publication included taxonomic framework and/or illustrations for the taxon, e.g., *Gyroidina umbonata* is commonly misidentified as *Gyroidinoides lamarckiana* or *Gyroidina lamarckiana*.

These could only be done for the taxa identified and/or researched in this study; therefore perfect homogenization was not reached in the data set especially for miliolids, elphidiids, ammonias, in other words, shallow water dweller taxa. In addition, the taxonomic reference trail and illustrations proved short of useful in some occasions, preventing homogenization. For example, Kırcı-Elmas (2006, SoM_3), reported abundances of both *Cassidulina minuta* and *Cassidulina crassa*. The former here is regarded to belong to genus *Paracassidulina*, and the latter is the most common misidentification of *P. minuta*, and sometimes of *Globocassidulina oblonga* or *Cassidulina reniforme*. Since no comprehensive taxonomic details or illustrations are present for neither, their true identity remains obscure; therefore were left as originally cited. Ideally, the reference specimens for all publications would be studied and compared to reach a perfect homogenization in the data.

The synonymy table compiled in this way is presented in Supplementary Table E.2. After the homogenization, 437 separate taxa are present in the data set.

This table was constructed especially for the homogenization of the quantitative data, therefore some supraspecific taxa do appear instead of species where the identified species were not counted separately in this study (e.g., Ellipsolagenidae was left as a family level taxon in census data due to rarity, however, 16 different species were identified belonging to this family).

The systematic taxonomy for taxa identified in this study, and when applies, synonymy and comments on the identifications of the publications considered here, are given in detail in Chapter 8.

5.5 Absolute abundance and diversity in the surface samples

The absolute abundances cannot be calculated for the following publications: in Avşar et al. (2006, SoM_12) and Avşar (2010, SoM_08) the details of splitting are not shared; in Phipps et al. (2010, SoM_02) neither the initial sample size nor the splitting details are shared; in Kırcı-Elmas (2013, SoM_7) only relative abundances are published; in Alavi (1988, SoM_13) the reported census data is not corrected for size fraction.

Census data given by Kırcı-Elmas (2006, SoM_03; 2018, SoM_06) and Kırcı-Elmas et al. (2008, SoM_09) are normalized to an initial sample of 10 g (dry) and by Kaminski et al. (2002, SoM_12) to an initial sample of 10 ml, therefore can be used directly as absolute abundances. And census data given by Fontanier et al. (2018, SoM_1) can be used for calculating absolute abundances. Yet, these cannot be compared with each other since the absolute abundance in volume and weight differ (see Section 3.1 and Section 4.1).

The homogenized data set was filtered for the surface samples only (grab samples or topmost samples of cores; surface data set hereafter), resulted in a data set composed of 144 stations and 387 taxa.

Diversity indices in the surface samples are given in Supplementary Table E.3. In the surface data set, thirteen stations fewer than 100, ten have 100-200, eleven have 200-300 specimens (N). Remaining 110 stations have 300 or more specimens. The number of taxa (S) obtained amongst the recorded number of individuals (N), i.e., the counted or published (normalized to sample size) number of individuals (e.g., in SoM_03, SoM_06, see Table 5.1), have a significant logarithmic relationship (r^2=0.6568, p=2.837E-16, Figure 5.3). The increase in number of taxa with increasing specimen counts diminish distinctly after about 1000 individuals. This shows the importance of adequate sample size for use in statistical analysis. The stations with low specimen counts (see Supplementary Table E.3) present a larger

error margin in terms of species richness, and also in relative abundances; hence, should be treated with caution.

Species richness (S) in the Sea of Marmara changes in the range of 3 (SoM_07 station 14a) and 105 (SoM_06 station T8). Only six stations have 15 species or lower (SoM_01 stations MRS-DV01-PC-04 and MRS-DV05-PC-06, SoM_07 station 14a, SoM_08 station 52, SoM_12 stations 156 and 167), and only five stations have 90 species or higher (SoM_02 station 14, SoM_06 stations T2, T8, S4 and S25) (Figure 5.4).

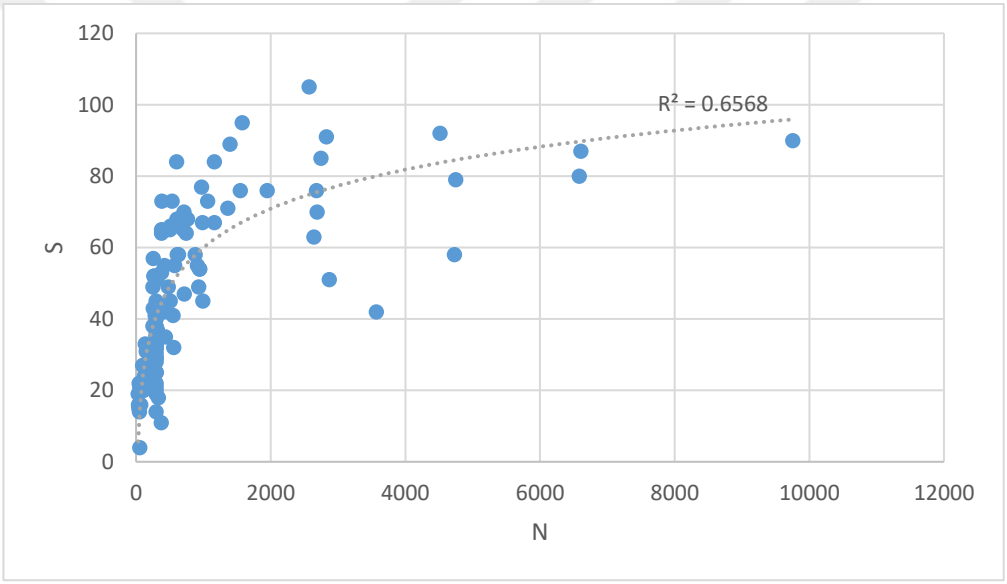


Figure 5.3. Relationship between number of counted individuals (N) and species richness (S) in the surface data set (see Supplementary Table E.3) excluding SoM_07.

Except for a few stations (SoM_01 stations MRS-DV01-PC-04 and MRS-DV05-PC-06, SoM_07 stations 11a and 14a) dominance (D) values are below 0.4 (Supplementary Table E.3.). The same stations also show low (<1.5) Shannon's diversity (H'). In a few stations (SoM_02 stations 4, 8, 101, SoM_06 station S1,

SoM_07 station 8) Shannon's diversity is unusually high (>3.5). Evenness values cover a very wide range of 0.14 to 0.86.

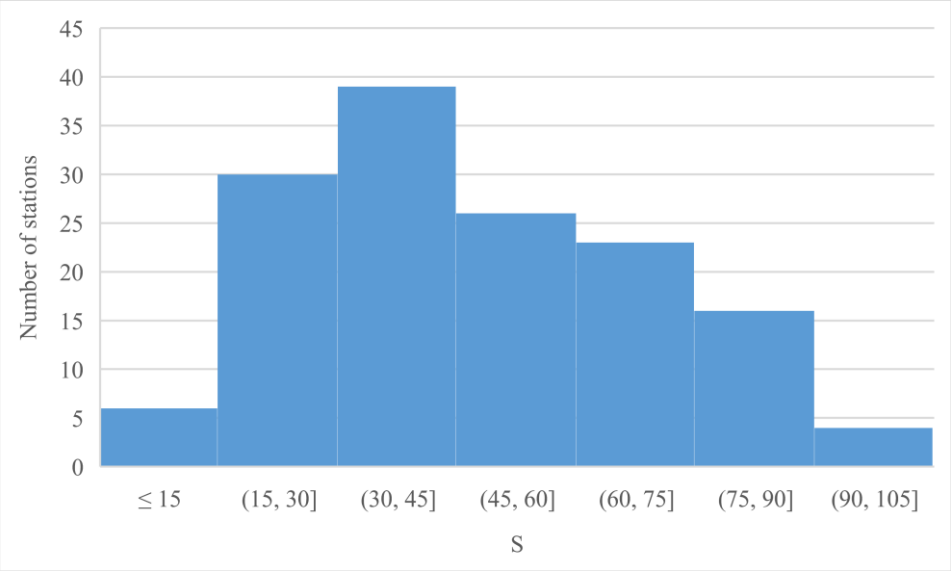


Figure 5.4. Histogram showing the species richness distribution amongst stations for surface data set.

Evenness (E) and dominance (D) are two values which range between 1/S (species richness) and 1, and should have an inverse relationship. Due to their different calculation methods (see Section 1.3.7) the relationship is not linear, and depends on S (Figure 5.5). Two of the stations with species richness lower than 16 are obvious outliers. One of these belong to Fontanier et al. (2018, SoM_01, MRS-DV05-PC-06, Çınarcık Deep) and the data is of live foraminiferal abundance. Both the species richness (S=4) and the counted number of foraminifera (N=54) are very low in the Çınarcık deep station (MRS-DV05-PC-06; note that the top three samples were lumped for the analysis forming a 1.5 cm thick top sample). The other outlier, Station 14a of Kırcı-Elmas (2013, SoM_07) is from the central Southern shelf, very close to the mouth of the Çapraz Stream, from 11 m water depth; the species richness is exceptionally low (S=3). Three of the stations are extreme cases. Central High station

MRS-DV01-PC-04 (SoM_01) is of low species richness (S=11) and high dominance; similarly, station 11a (SoM_07, near mouth of Biga Steam) also has low species richness (S=16) and high dominance; while, one Central Basin station, DM22 (SoM_03) is marked with very high evenness and very low dominance.

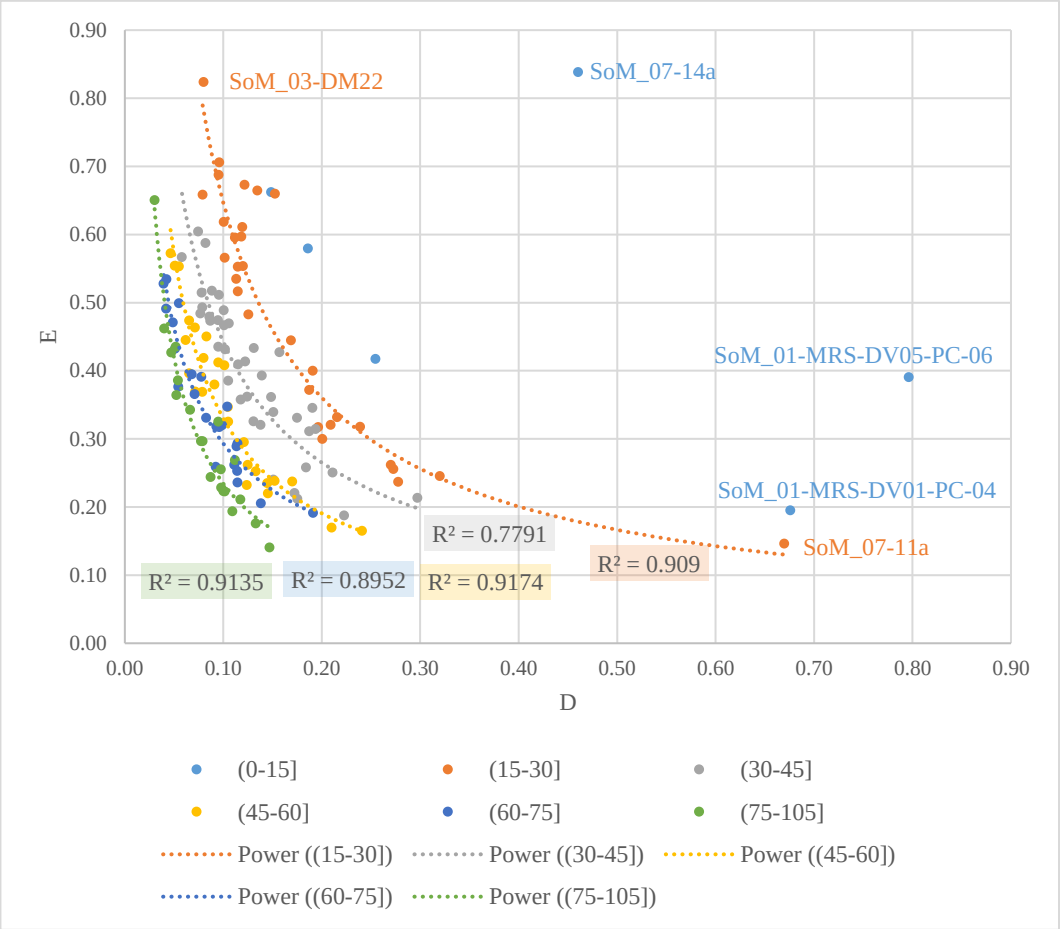


Figure 5.5. Relationship between dominance (D) and evenness (E) in the surface data set; different colors for different species richness intervals; trendlines (power) plotted and correlation coefficients indicated, except for 0-15 interval. Outlier and extreme stations labelled with data codes (Table 5.2) and station numbers.

None of the diversity indices (i.e., S, H', D, E) show any correlation with water depth (Figure 5.6).

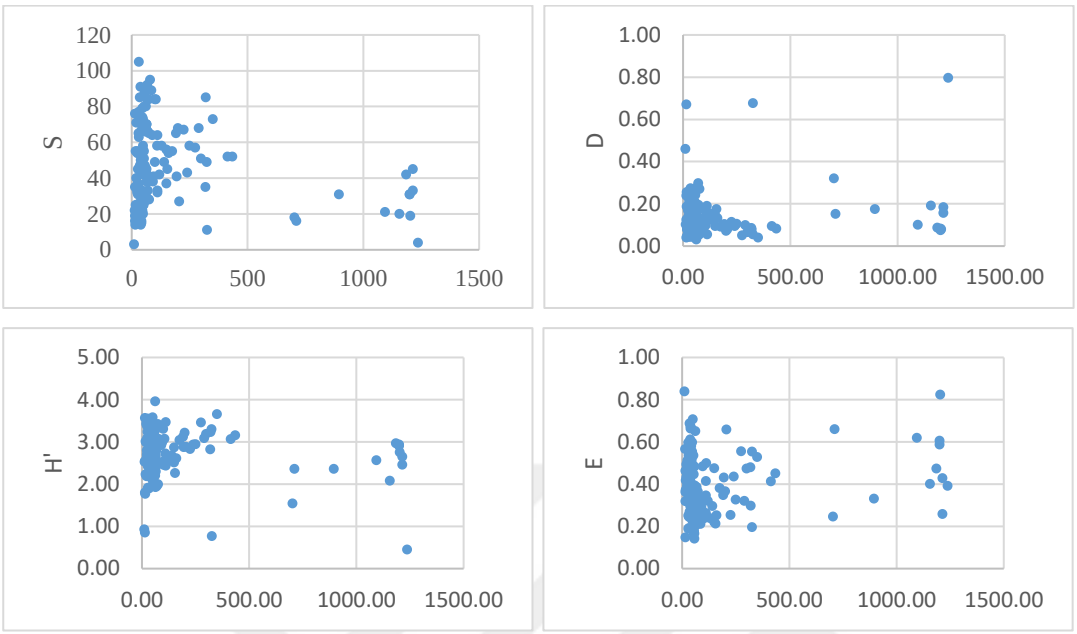


Figure 5.6. Species richness (S), dominance (D), Shannon's diversity (H') and evenness (E) values plotted against water depth (x-axes, meters).

The diversity indices in the surface data set as grouped by study (Figure 5.7), location (Figure 5.8) and water depth (Figure 5.9) are illustrated as Box and Whisker plots.

In the studies, the difference is evident especially in terms of species richness (Figure 5.7). The studies with higher number of stations (SoM_02, SoM_06, SoM_07, SoM_TS) recorded higher variation in and higher numbers of S. The other indices show even smaller differences between studies. One major difference is seen in SoM_01 which is the only live foraminifera (rB stained) study, which has very low S and H' and very high D. Studying of dead versus undifferentiated assemblages has no effect on these indices as SoM_02 is similar to other studies in terms of all. The studied size fraction did not make any difference in terms of S, D, H' and E.

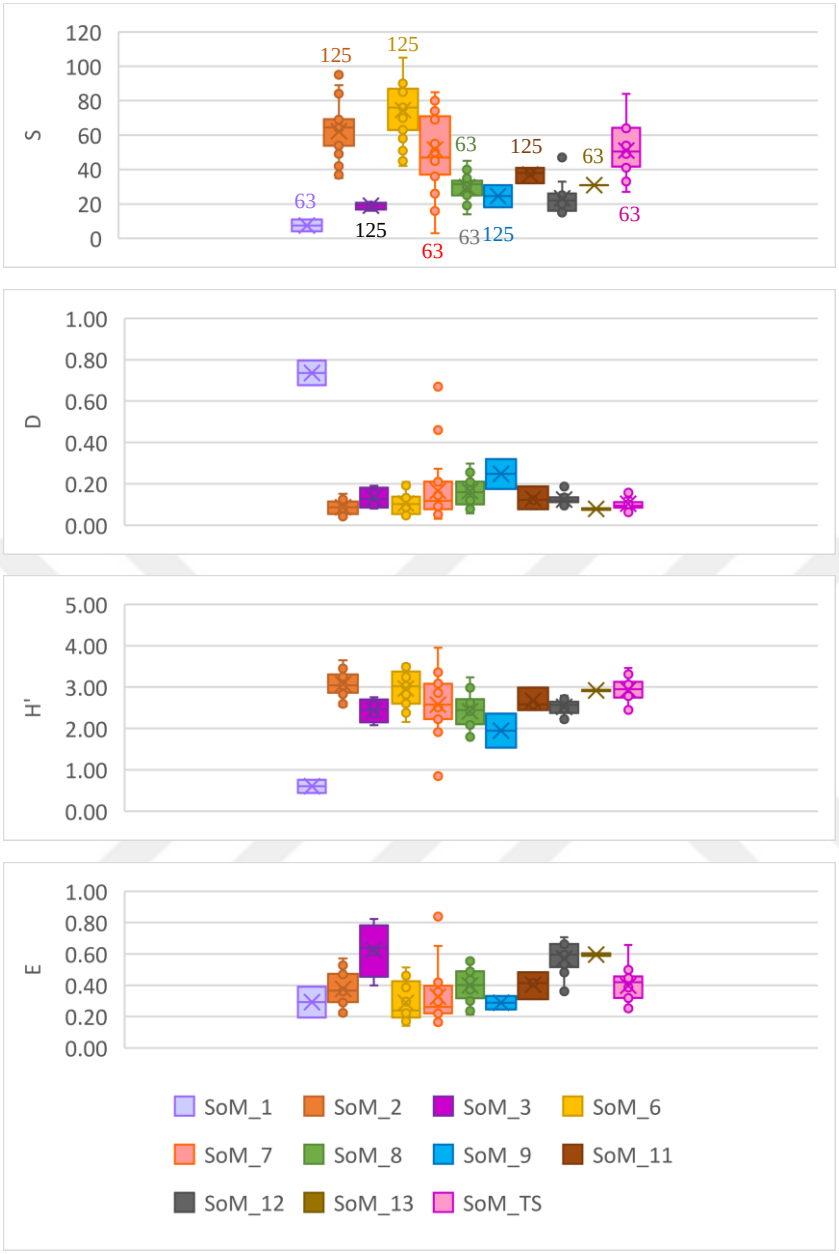


Figure 5.7. Box and Whisker plots for studies: species richness (S), dominance (D), Shannon's diversity (H') and evenness (E) values in the surface data set. Studied size fractions are noted in plot S. Table 5.2 for study references.

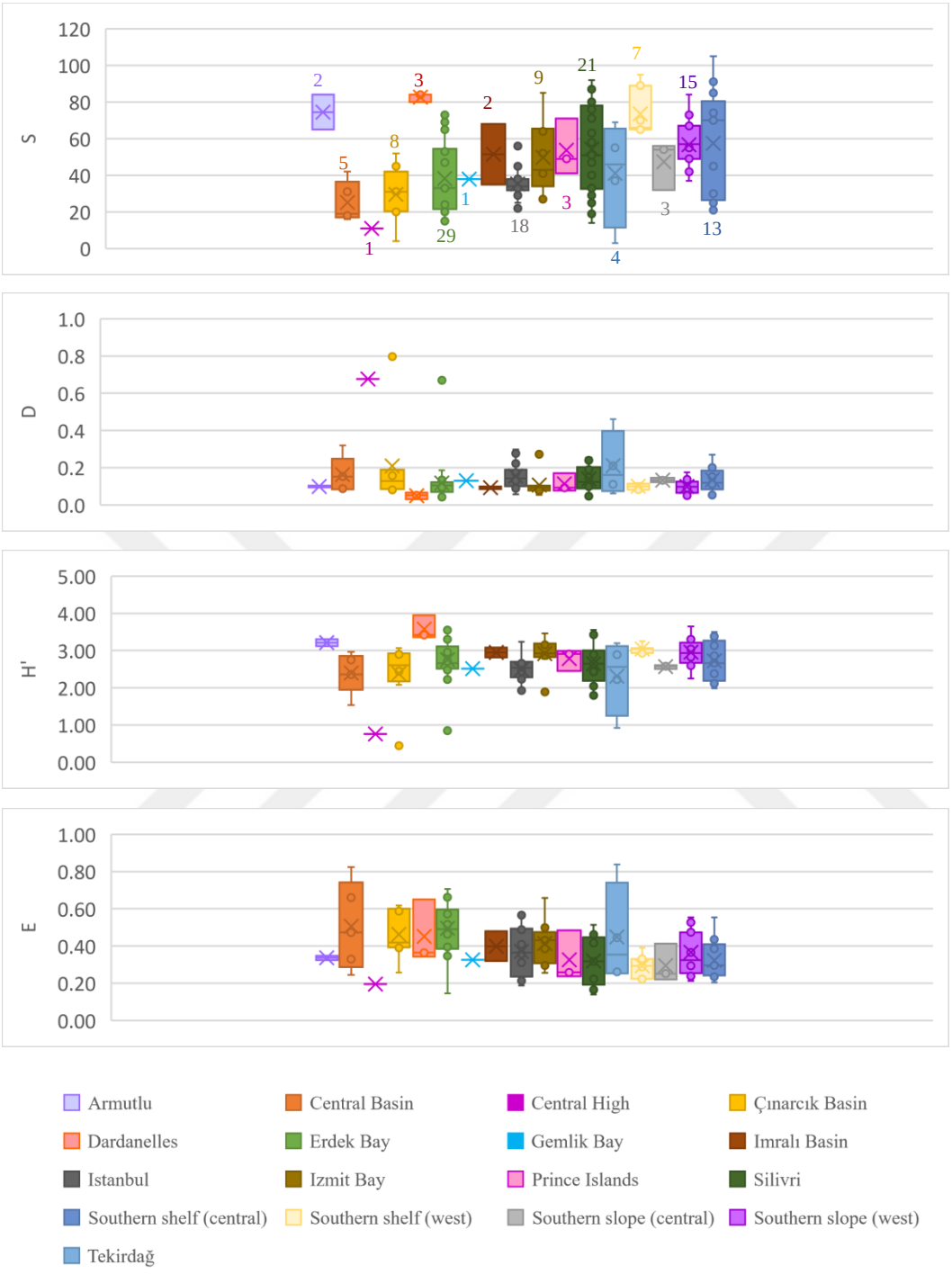


Figure 5.8. Box and Whisker plots for locations: species richness (S), dominance (D), Shannon's diversity (H') and evenness (E) values in the surface data set. Note Armutlu group includes both shelf and slope stations. Number of stations noted in plot S. Figure 1.4 for locations.

Location-wise grouping of diversity indices show slight differences in between locations especially for species richness (S; Figure 5.8). Armutlu and Dardanelles stations both have S values around 80; however, there are stations in Izmit Bay, Silivri, central Southern shelf, western Southern slope and Tekirdağ with similar S values as well. Lowest S values occur in Central High, Çınarcık Basin and central Southern shelf. The number of stations studied from locations vary greatly, however no relationship is seen between the number of stations and variation in S, showing that some locations may have included drastically different environments. In terms of dominance three stations are markedly different than the rest: MRS-DV01-PC-04 (Central High) and MRS-DV05-PC-06 (Çınarcık Basin) belong to SoM_01, the only study to report data of live foraminifera, and 11a (Erdek Bay) of SoM_07 is situated very close to the mouth of Biga Stream. Same stations are marked with low Shannon's index (H'). The highest evenness values (E) occur in the Central Basin (DM22, SoM_03) and central Southern shelf (14a, SoM_07, near mouth of Çapraz Stream).

Grouping of stations with respect to water depth produce only slight differences in between different depth ranges, only in species richness (S; Figure 5.9). The shelf (<100m) is marked with very high variation in S values, 100-200 and 200-300 m ranges are almost identical, 300-100 m water depth range is also large but a lower median, and the deepest stations (>1000 m) have the lowest median and cover a narrower range in the lower values.

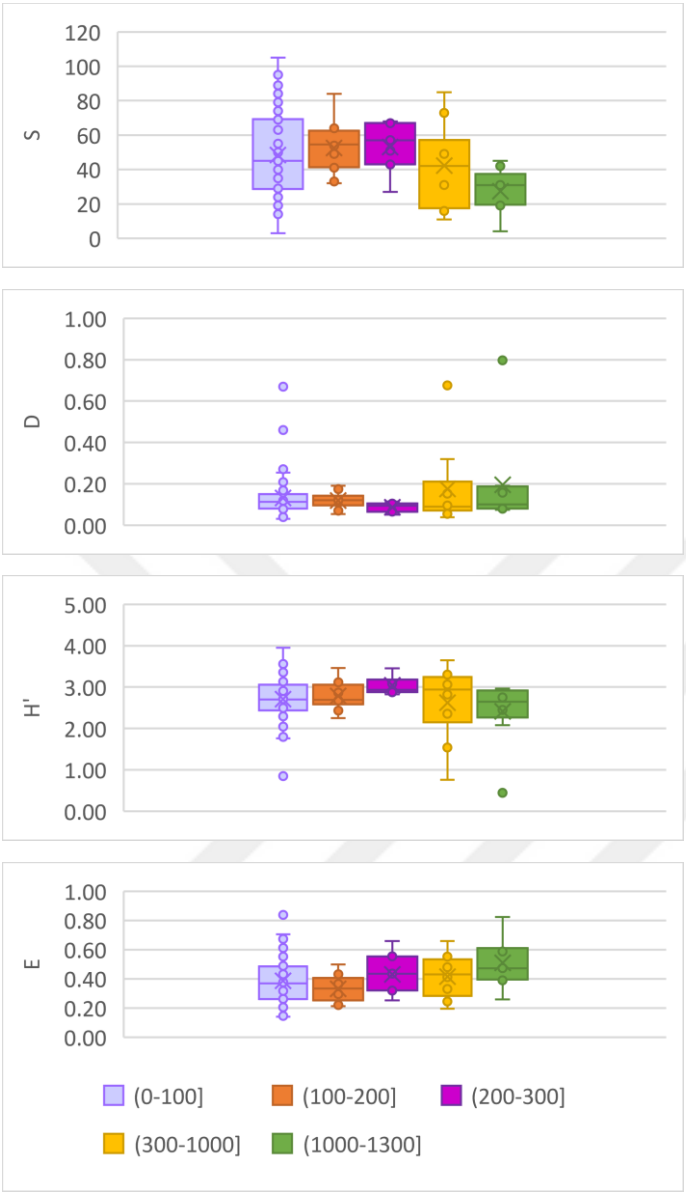


Figure 5.9. Box and Whisker plots for water depth ranges: species richness (S), dominance (D), Shannon's diversity (H') and evenness (E) values in the surface data set.

5.6 Relative abundances of taxa in the surface data set

The surface data set was investigated in terms of relative abundances of taxa. Among the 385 taxa present in the surface data set (after homogenization), only 16 of them occur with relative abundances more than 30% in at least one sample (Table 5.5). In 14 samples, the most dominant taxa occur with relative abundances higher than 40% (Table 5.6) These very dominant taxa are some *Ammonia*, *Bolivina*, *Bulimina* and cassidulinid species, *Asterigerinata mamilla*, *Elphidium crispum*, *Sigmoilinita tenuis* and *Uvigerina mediterranea*. 13 taxa occur with 15-30% abundances (dominant) and are *Aubignyna perlucida*, *Bolivina variabilis*, *Bulimina marginata*, *Chilostomella mediterranensis*, *Chilostomella ovoidea*, *Cribroelphidium poeyanum*, *Discorbinella bertheloti*, *Elphidium decipiens*, *Elphidium* spp., *Gyroidina umbonata*, *Lobatula lobatula*, *Melonis barleanum*, *Sigmoilopsis* spp. (Table 5.7).

Table 5.5. Number of taxa in relative abundance ranges for the surface data set.

Relative abundance range	Number of taxa
>30%	16
15-30%	12
10-15%	12
5-10%	38
2-5%	70
0-2%	237

Different *Ammonia* species occur abundantly (>5%) in some stations of SoM_02, SoM_07, SoM_08 and SoM_12 studies whose samples mostly come from the shelves of the Sea of Marmara. In other stations they are either absent or are of smaller abundances (usually <2%). In SoM_02, the stations in water depths shallower than 55m (Erdek Bay) have 6-55% *Ammonia* (total) abundance, below that threshold (western Southern shelf and slope) *Ammonia* abundance decreases to 4% and lower. In SoM_06, a few stations have abundant *Ammonia* (total), all of which

are shallower than 55 m, two of them from Tekirdağ, four from Silivri shelf. About half of the stations of SoM_07 have abundant *Ammonia* (total), these stations are of from shallow (<55m) shelves and one in Dardanelles (74 m). About half of the stations of SoM_8 have abundant *Ammonia* (total), only one of these stations are situated in Tekirdağ, the rest come from Istanbul and Silivri shallow shelves, except for two in Istanbul which are of deeper settings (>55m). In SoM_12 all stations (Erdek Bay) have abundant *Ammonia* (total) except for one station.

Table 5.6. Very dominant (>30%) taxa: their average (in stations they are present) and maximum abundances, the stations in which the taxa have their maximum abundance and the numbers of stations taxa are present in.

Taxon	Average	Max	Max in station	Number of stations
Ammonia compacta	6.14	37.00	SoM_08_53	80
Ammonia parkinsoniana	3.34	31.00	SoM_08_39	37
Ammonia tepida	4.64	81.70	SoM_07_11a	53
Ammonia spp.	3.07	62.50	SoM_07_14a	77
Asterigerinata mamilla	8.33	40.64	SoM_06_S14	59
Bolivina dilatata	3.52	30.97	SoM_03_KL89	90
Bolivina spathulata	13.54	50.00	SoM_08_90	109
Bolivina vadescens	10.33	88.89	SoM_01_MRS-DV05-PC-06	73
Bolivina spp.	4.38	39.92	SoM_11_MAR98-9	11
Bulimina aculeata	6.49	41.40	SoM_07_14b	105
Bulimina costata	4.40	39.69	SoM_09_DM18	67
Cassidulina laevigata	12.76	37.50	SoM_12_167	118
Elphidium crispum	6.00	40.33	SoM_08_52	59
Paracassidulina minuta	18.88	36.03	SoM_TS_45C-1	20
Sigmoilinita tenuis	1.62	34.29	SoM_03_32MC	85
Uvigerina mediterranea	3.34	46.39	SoM_09_KL40	32

Different *Elphidium* species are abundant (>5%) in the stations rarely. These stations occur in SoM_02, SoM_06, SoM_08 and SoM_12. In total, *Elphidium* genus is abundant in some stations of SoM_07 in addition to previously mentioned stations. The distribution of the total *Elphidium* abundance is very similar to that of *Ammonia*,

but it is abundant in fewer stations. In 62 stations *Elphidium* and *Ammonia* occur together with at least one of them being abundant (>5%), in 45 stations either one of them is more abundant with a difference of at least 4%, and in 17 stations their abundances are very close to each other. The dominant genus may differ between very close stations (e.g., of SoM_02, assemblage in stations 1 (15 m water depth) is dominated by genus *Ammonia* by a 55.3% abundance and *Elphidium* is of 9.8% abundance only while the assemblage in station 2 (18 m water depth) is dominated by *Elphidium* by a 31.2% relative abundance and *Ammonia* is of 23.2% abundance), showing the effect of competition between these shallow water dweller taxa. *Cribroelphidium poeyanum* is abundant in the Erdek Bay, up to 55 m water depth. It is most abundant station 157 (SoM_12, 22.3%). It is also present in the northern shelf stations, although abundant very rarely.

Table 5.7. Dominant (15-30%) taxa: their average (in stations they are present) and maximum abundances, the stations in which the taxa have their maximum abundance and the numbers of stations taxa are present in.

Taxon	Average	Max	Max in station	Number of stations
Aubignyna perlucida	2.10	15.34	SoM_2_3	32
Bulimina marginata	2.38	25.54	SoM_11_MAR97-11	107
Chilostomella mediterranensis	2.28	17.82	SoM_13_M4	29
Chilostomella ovoidea	2.04	25.66	SoM_3_KL89	21
Cribroelphidium poeyanum	2.70	22.31	SoM_12_157	88
Discorbinella bertheloti	3.03	23.32	SoM_12_166	107
Elphidium decipiens	4.21	15.07	SoM_2_2	13
Elphidium spp.	1.51	18.80	SoM_7_14a	62
Gyroidina umbonata	3.25	22.10	SoM_2_14	86
Lobatula lobatula	3.09	17.67	SoM_8_71	80
Melonis barleanum	1.58	16.67	SoM_3_KL97	39
Sigmoilopsis spp.	6.89	16.77	SoM_TS_K40K46	3

Aubignyna perlucida is present in 32 stations, abundant in only four stations: stations 1 (10.5%) and 3 (15.3%) of SoM_02, station 11b (12.8%) of SoM_07, and station

53 (8.7%) of SoM_08. In the rest of the stations the taxon is present, it is mostly rare or very rare (<2%). All four of the stations the taxon is abundant in are of 15-25 m water depth.

Asterigerinata mamilla is present in 59 stations, in 23 of which it is abundant (>5%). The highest relative abundance of the taxon comes from the Silivri shelf (SoM_06 station S14, 31 m water depth), a station where other shallow water dweller taxa (*Elphidium* and *Ammonia* especially) are of low abundances (<5%). All stations the taxon is abundant are on the northern shelf, except for one in Dardanelles (SoM_07 station 8) and one in the Erdek Bay (SoM_12 station 150). Except for the Dardanelles station, the taxon is abundant in water depths shallower than 55 m. *Asterigerinata adriatica* is also present in the shelf stations, but to a lesser abundance, it is frequent and, in a few stations, abundant between 30-60 m water depths.

In total, *Bolivina* genus is abundant in water depths deeper than 40 m, shallower than that, the genus is either not present, or present with only lower abundances (<5%); except for station 89 of SoM_08 (Istanbul, 19%), station 14b (central Southern shelf, 23.4%) and station 1 (Istanbul, 31%) of SoM_07, and station 5 of SoM_02 (Erdek Bay, 5.5%).

Bolivina spathulata is the usually most abundant of the genus, occurring with abundances up to 50%, most abundant in northern outer shelves (stations belonging to SoM_06, SoM_07, SoM_08).

Bolivina vadescens is the second most abundant taxon, however was misidentified in Kırcı-Elmas (2013, SoM_07) as *Bolivina variabilis* and in Kaminski et al. (2002, SoM_11) and Phipps et al. (2010, SoM_02) as *Brizalina catanensis*, and were probably included in other bolivinid taxa by other studies. It occurs up to 88.9% in the live assemblage (SoM_01, MRS-DV05-PC-06) in the Çınarcık Basin, and is abundant in the majority of the stations it was recorded. The possible lumping of the taxon in other studies prevent the visualization of the extent of the distribution of the taxon.

Bolivina dilatata occurs with mostly under 5% relative abundances, except for Çınarcık Basin stations of SoM_03 where 15-30% relative abundances are recorded, probably due to misidentification and lumping with *Bolivina spathulata*. In addition, Avşar et al. (2006, SoM_12) and Avşar (2010, SoM_08) did not record the taxon, most probably lumped it with *B. spathulata*. The taxon is abundant in several outer shelf and slope stations both from the north and from the south, and also deep Çınarcık and Central basins. Similar to the misidentification problems in *B. vadescens*, the extent of this taxon, too, cannot be determined as a result.

Bulimina species are abundant in most stations, except for shallow inner shelf stations both in the south and in the north. Interestingly, in total, genus *Bulimina* reaches >40% abundance in station 2 (Istanbul) and station 14b (central Southern shelf) of SoM_07, both are of 28 water depth. The other station with very high (>40%) *Bulimina* abundance is DM18 of SoM_9 in the deep Central Basin.

Bulimina inflata, a taxon identified only in SoM_11, SoM_13 and SoM_TS, is abundant only in the Central Basin (K51.2K09 of SoM_TS, 8.3%), occurring alongside *Bulimina costata* (a smaller costate buliminid) of rare abundances (<2%). High numbers for *B. costata* are reported by Kırcı-Elmas (2006, SoM_03) and Kırcı-Elmas et al. (2008, SoM_09) from the Central Basin (DM22, DM18 and KL40; 18.8, 39.7, 20.2% respectively) probably include both species (illustrations given by Kırcı-Elmas, 2006, belong to *B. inflata*) but the majority of the given abundances probably belong to *B. inflata*. *Bulimina aculeata* is abundant mostly in shelves, while *Bulimina costata* is recorded to be abundant in deeper (slope) settings.

Cassidulinids (genera *Cassidulina*, *Globocassidulina*, *Paracassidulina* in total), are abundant in the majority of the stations, with up to 41.5% abundance. Cassidulina laevigata was recorded to be abundant on the shelves and upper slopes with high abundances, except for very shallow inner parts (~<30 m); on the deeper slopes (~>150m), however, *C. laevigata* abundance decreases drastically to below 5%. In these deeper settings, *Paracassidulina minuta* is more abundant (up to 36%), however was recorded in the surface data set only in one study (SoM_TS), and was

probably reported as lumped with *C. laevigata*, or under the name *Cassidulina crassa* (e.g., Kaminski et al., 2002, SoM_11; taxon is here considered under *Globocassidulina*, not added as a synonym to *P. minuta* due to lack of distinguishing illustrative material). Nonetheless, the abundant distribution of *P. minuta* probably is restricted to the eastern part of the basin since in the western Southern slope the total cassidulinid abundance is quite low. *Globocassidulina subglobosa* is abundant in a few shelf stations.

Sigmoilinita tenuis, *Sigmoilopsis schlumbergeri* and *Sigmoilopsis* spp. are all abundantly present in deeper (>150 m) settings. *S. tenuis* is recorded from Central and Çınarcık basins (SoM_03, SoM_09, SoM_13). *S. schlumbergeri* is recorded from the Central Basin (SoM_03) and western Southern slope (SoM_02). *Sigmoilopsis* spp. is abundant (16%) only in the Imralı Basin (SoM_TS, station K40K46; taxon composed only of *Sigmoilopsis* sp. 1 in SoM_TS).

Uvigerina mediterranea is abundant in a few stations only. In the Central Basin (SoM_09, KL40) it occurs alongside with buliminids with 46.4% abundance. In other stations in Central Basin (SoM_03) and western Southern slope (SoM_02) the taxon is present below 10%.

Chilostomella species are abundant in three stations, all from the Çınarcık Basin, with 17-26% abundances (SoM_03, KL89; SoM_13 M1 and M4). These species may be synonyms.

Discorbinella bertheloti is abundant in 19 shelf stations with up to 23.3% (SoM_12 station 166, Erdek Bay) abundance, both in the north and in the south, in water depths between 40-70 m. In the other stations the taxon is present, its relative abundance rarely exceeds 2%.

Gyroidina umbonata is abundant in the western Southern shelf and slope (SoM_02), in Gemlik Bay (SoM_07 station 15) and in one station in Tekirdağ shelf (SoM_06 station T30).

Lobatula lobatula is abundantly present in the inner shelf stations of the northern shelf (in SoM_06 and SoM_08), and not present in deep Central and Çınarcık Basin stations. In other stations the taxon is present, its abundance rarely exceeds 2%.

Melonis species are abundant in deep Çınarcık and Central Basin stations (maximum 20.2% in total in SoM_03 station KL97). Genus is rare otherwise and not present in inner shelf settings. Interestingly, in one station in the Erdek Bay (SoM_12 station 148, 42 m water depth) *Melonis pompilioides* is present with 11.4% abundance.

Articulina tubulosa is present in the deep Çınarcık and Central Basin stations, and in two of these abundant (SoM_03 stations KL97 and DM22).

Cibicides species, especially *Cibicides advenum*, are present, and rarely abundant, in shelf and slope stations, up to 8%. Planorbulina mediterranensis present in outer shelf and upper slope settings, although rarely above 2%. *Hyalinea balthica* is more abundant in the outer shelf and upper slope stations, mostly in the southern part. *Hyalinea marmarica* was identified only by SoM_TS, and individuals belonging to *H. marmarica* may have been lumped with *H. balthica* in other studies, hindering the ability to evaluate their depth distribution.

Eilohedra vitrea is mostly present in water depths deeper than 55m, and is usually rare. The relative abundance of the taxon never exceeds 5%.

Globobulimina species are present mostly and more abundantly in deeper settings (below 100 m), although with abundances rarely above 2%.

Neoconorbina terquemi is present until 400 m water depth, but very rare except for the shallow shelves (40 m) where it is abundant up to 13.3% relative abundance. the taxon is more abundant in Silivri and Tekirdağ than Istanbul and Southern shelf.

Nonionoids (*Nonionella* and *Nonionoides*) are present throughout the depth gradient with up to 11.8% relative abundance. In the shallow shelf stations nonionoids are mostly represented by *Nonionella turgida* (may be synonymous with *Nonionella opima*), but in deeper parts they are more diverse.

Rectuvigerina phlegeri is present, but rarely abundant in stations deeper than 25 m. other than KL89 (Çınarcık Basin) of SoM_03, *R. phlegeri* is not present in deep basins. *Reussella spinulosa* is present in shelf stations, but rare; only abundant (5-6%) in three Erdek Bay stations. *Trifarina angulosa* is very rare, but present except for deep basins. *Virgulinella fragilis* is present in three stations, very rare in one (SoM_TS station 1 (19), outer Izmit Bay), and abundant in the others (SoM_1 station MRS-DV01-PC-04, Central High; SoM_TS station Izmit-deep, inner Izmit Bay, Karamürsel Basin).

Rosalina species are present in the shallow shelf (<55 m) stations, more abundant in the northern shelves; and more sporadically and rarer, in the outer shelf and upper slope stations. *Valvulineria bradyana* is present in stations deeper than 20 m, with abundances occasionally with abundances more than 10%.

Among the miliolids, *Miliolinella subrotunda* is present throughout the whole depth distribution but abundant in several shelf stations shallower than 40 m, and in one Central Basin station (SoM_03, DM22). *Quinqueloculina* species are sporadically present throughout the whole depth gradient, but more consistently present in the inner shelf; however, almost always rare with a few exception taxa. *Quinqueloculina seminula* is recorded abundantly (>5%) in several shelf stations shallower than 50 m. *Quinqueloculina pygmaea* and *Quinqueloculina stalkeri* are rare, but consistently present in outer shelf and upper slope stations. Spiroloculina species, especially Spiroloculina excavata are present throughout; S. excavata is the only representative of the genus to reach 5% abundance, in only one station (SoM_03 station 32MC).

Textularin taxa are present except for the shallowest 20 m, but are almost always very rare-rare. *Siphotextularia* spp. reaches 5% abundance in the Central Basin 32MC (SoM_03), *Spiroplectinella sagittula* is abundant (6,9%) in the Dardanelles (SoM_07 station 8), *Textularia bocki* is abundant in the central Southern slope (SoM_11 station MAR97-11).

5.7 Similarity of sites

Using the surface data set with relative abundances of the 384 taxa (excluding unidentified specimens) and 144 stations, a cluster analysis (UPGMA, Bray-Curtis dissimilarity index) was performed. The resulting dendrogram when cut from an arbitrary 32% similarity level resulted in 15 separate station clusters (Figure 5.10).

5.7.1 Cluster 1

Cluster 1 (Figure 5.10, Figure 5.11) includes stations MRS-DV01-PC-04 and MRS-DV05-PC-06 of Fontanier et al. (2018, SoM_01) from Central High and Çınarcık Basin respectively. The cluster separates from all other stations at about 5% similarity. This is the only live (rB stained) foraminifera study in the SoM and in both stations the species richness is very low, accompanied with very high relative abundances of *Bolivina vadescens* (88.8 and 81.6% respectively). This taxon never reaches that much abundance in the dead or undifferentiated assemblages, it is maximum 29.1% (station 1 of SoM_07, Kırcı-Elmas, 2013) abundant in the rest of the stations.

5.7.2 Cluster 2

Cluster 2 (Figure 5.10, Figure 5.11) is composed of station 1 of SoM_02 (Phipps et al., 2010), and stations 3, 14a, 17 and 11a of SoM_07 (Kırcı-Elmas, 2013). These stations are marked with very high abundances of genus *Ammonia*, accompanied by *Elphidium, Aubignyna perlucida* and *Porosononion granosum* in station SoM_02_1, by *Elphidium* in SoM_07_14a and SoM_07_17 and *Bulimina* in SoM_07_3. All of these stations come from <35 m water depths. More importantly they come from locations either very close to stream mouths (SoM_02_1 and SoM_07_11a from near

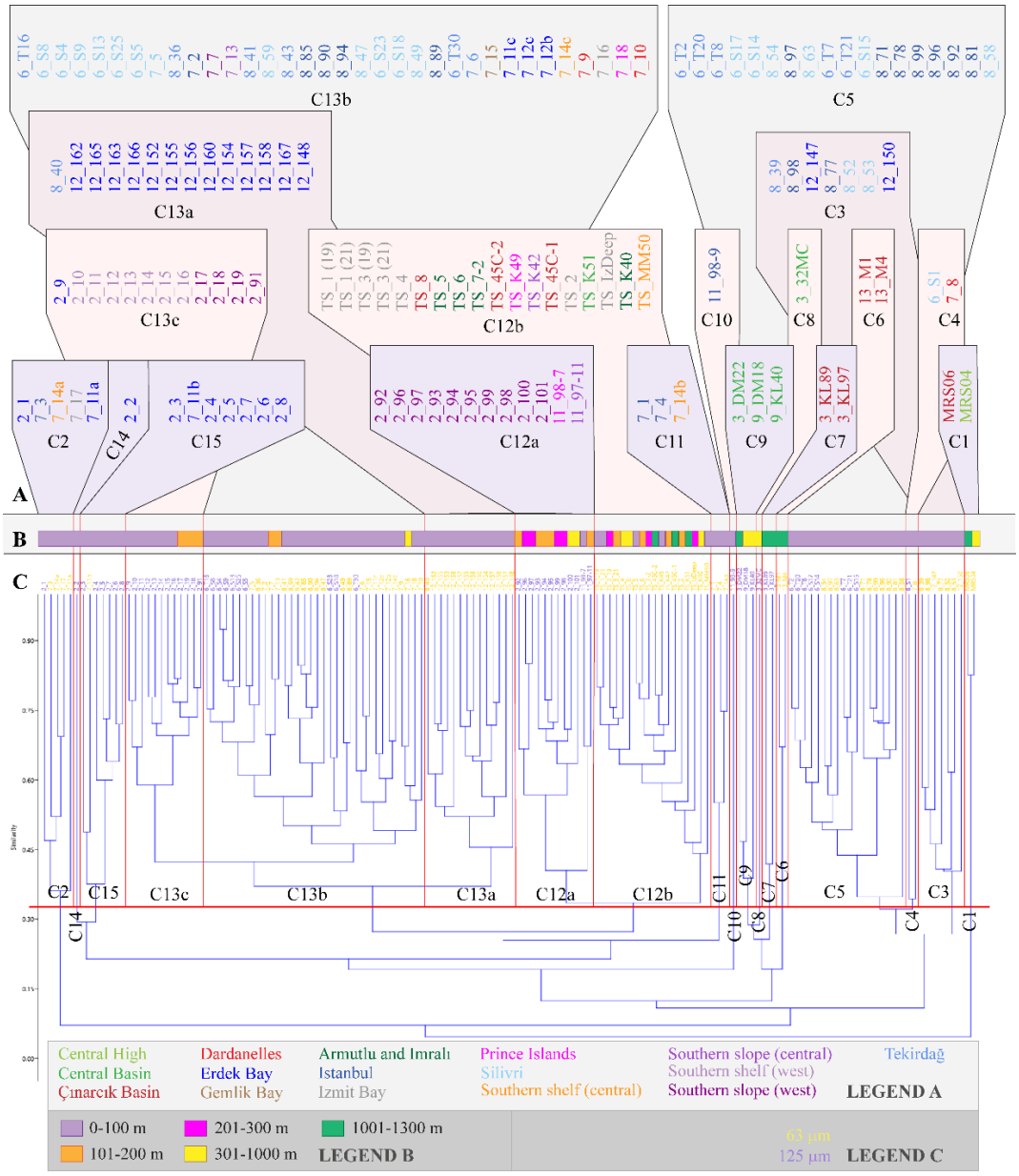


Figure 5.10. Dendrogram produced from the cluster analysis (hierarchical clustering, UPGMA, Bray-Curtis) of surface data set (384 taxa, 144 stations). A: Station numbers (shortened as "study code_station number", without using SoM prefix, and MAR prefix in SoM-11, MRS06: MRS-DV05-PC-06, MRS04: MRS-DV01-PC-04, TS_IzDeep: SoM_TS_Izmit-deep, other stations of this study shortened to first few characters only, see Table 5.2 for references) in clusters, colored according to location (see legend A); B: water depths the stations belong to (see legend B); C: dendrogram cut from about 32% similarity resulting in 15 separate clusters of stations, clusters and subclusters enumerated (as C#) starting from the root of the tree; station numbers colored according to studied size fraction (see legend C).

the mouth of Biga stream, SoM_07_14a from near the mouth of Çapraz stream, SoM_07_17 from near the mouth of Dil Stream-Dilderesi) or just outside the Küçükçekmece lagoon (SoM_07_3).

5.7.3 Clusters 3, 4, 5

Clusters 3, 4 and 5 are from shallow shelves (Figure 5.12).

Cluster 3 (Figure 5.10) is composed of samples from northern and southern shallow shelves. SoM_08 stations 39 (Tekirdağ), 52 and 53 (Silivri), 77 and 98 (Istanbul) come from the northern inner shelves of water depths shallower than 25 m, very close to the coast and city centers on the shores; and SoM_12 stations 147 and 150 come from between the Kapıdağ Peninsula (28 m) and Paşalimanı Island (35 m). The stations are all *Ammonia* and *Elphidium* dominated, with some also including abundant *Asterigerinata mamilla*, *Aubignyna perlucida*, *Cribroelphidium poeyanum*, *Lobatula lobatula*, *Miliolinella subrotunda*, *Pyrgo inornata*, *Rosalina bradyi* and *Siphonaperta aspera*. Cluster is most similar to Clusters 4 and 5.

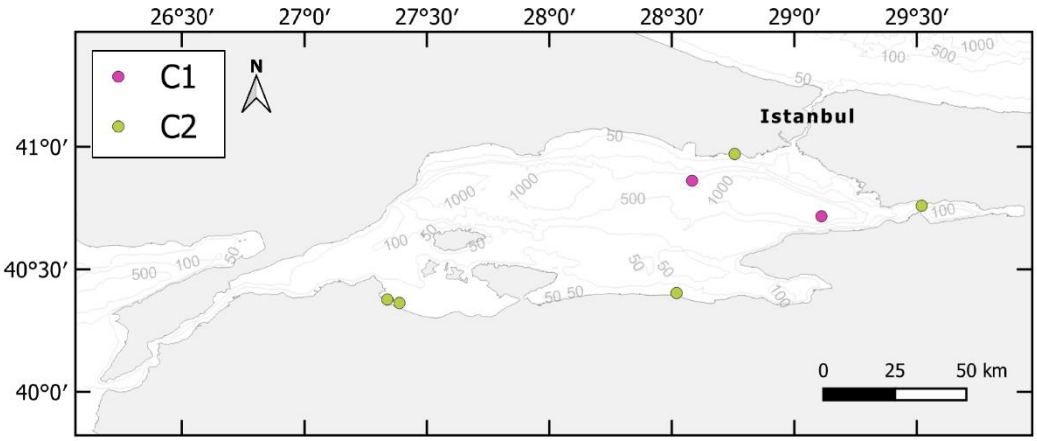


Figure 5.11. Location map of stations belonging to clusters 1 and 2 (see Figure 5.10 and Figure 5.1 for station names).

Cluster 4 (Figure 5.10) include SoM_06 station S1 (Silivri, 15 m, very close to the shore) and SoM_07 station 8 (Dardanelles, 62 m, the Mediterranean side). Both stations have very high species richness (76 and 80 respectively) and Shannon's diversity (3.56 and 3.95 respectively). No taxon is recorded to be more abundant than 11%. Elphidium spp. (9.2%) in SoM_06_S1 and *Asterigerinata mamilla* (10.4%) in SoM_7_8 are the most abundant taxa in the stations. Apart from them, assemblages include *Ammonia* species, *Cribroelphidium poeyanum*, *Lobatula lobatula*, *Neoconorbina terquemi*, *Quinqueloculina* species, *Rosalina bradyi*, *Sigmoilinita costata*, *Spiroplectinella sagittula* and *Triloculina marioni* in >2% abundances and other rare taxa. while in Silivri station miliolids are more abundant than textularins, in Dardanelles stations the situation is opposite. This cluster is most similar to Cluster 5.

Cluster 5 (Figure 5.10) includes stations from Tekirdağ, Silivri and Istanbul shelves from SoM_06 (Kırcı-Elmas, 2018) and SoM_08 (Avşar, 2010); all stations in SoM_06 in this cluster are of 20-40 m water depth, and in SoM_08 they are of 20-50 m water depth. The stations are different from all other by abundant to dominant *Asterigerinata mamilla* (minimum 6% in SoM_06_T21, maximum 40.6% in SoM_06_S14), accompanied by *Lobatula lobatula* (mostly above 5%, above 10% in about half of the stations), *Ammonia* species (rarely below 2% in total, mostly above 5%), and abundant *Elphidium* species.

5.7.4 Clusters 6, 7, 8, 9

Most deep basin stations are included in clusters 6, 7, 8 and 9 (Figure 5.13).

Cluster 6 (Figure 5.10) is composed of two Çınarcık Basin stations of Alavi (1988, SoM_13). The data was reported by Alavi by summing the counts coming from different size fractions and split to different ratios, without correcting for the split size. Due to this, the relative abundances of usually larger taxa (e.g., *Chilostomella mediterranensis* and *Nonionella opima*) are higher and usually smaller taxa (e.g.,

Paracassidulina minuta) are lower than the relative abundances in the other stations of the deep Çınarcık Basin. Nonetheless, the cluster is most similar to clusters 7, 8 and 9 which include deep Çınarcık and Central Basin stations.

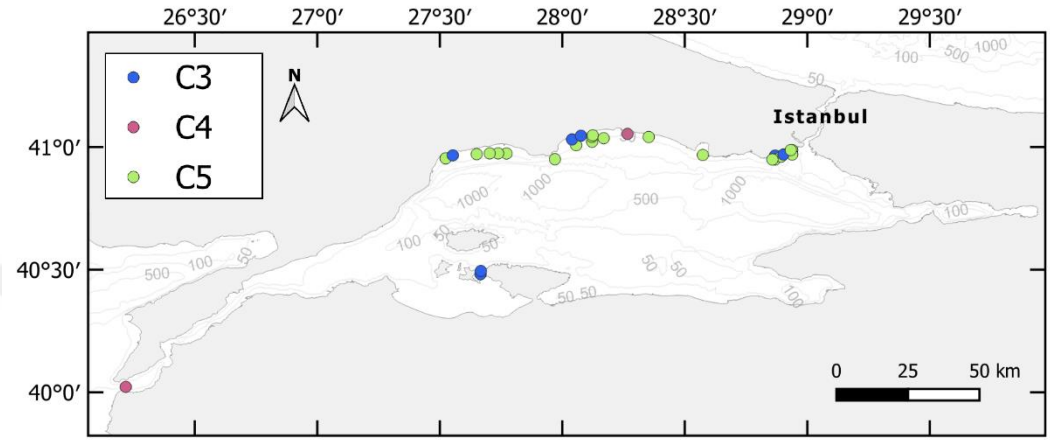


Figure 5.12. Location map of stations belonging to clusters 3, 4 and 5 (see Figure 5.10 and Figure 5.1 for station names).

Two deep Çınarcık Basin stations of Kırcı-Elmas (2006, SoM_03) make up the Cluster 7 (Figure 5.10). The assemblages of the two stations somewhat differ, but are similar in terms of dominance of Bolivina dilatata and the accompanying taxa. In KL89 assemblage is composed of very dominant *Bolivina dilatata* (30.1%) accompanied by abundant *Chilostomella ovoidea* (25.7%), *Bulimina marginata* (8%), *Sigmoilinita tenuis* (5.3%) and *Valvulineria bradyana* (13.3%); while in KL97 it consists of dominant *B. dilatata* (15.4%) and *Melonis barleeanum* (16.7%) accompanied by abundant *Bolivina alata* (10.7%), *S. tenuis* (13.1%) and *V. bradyana* (8.3%). *Bolivina spathulata* was not recorded in Kırcı-Elmas (2003), and may be lumped with *B. dilatata*, explaining these very high abundances of the otherwise rarely above 10% taxon.

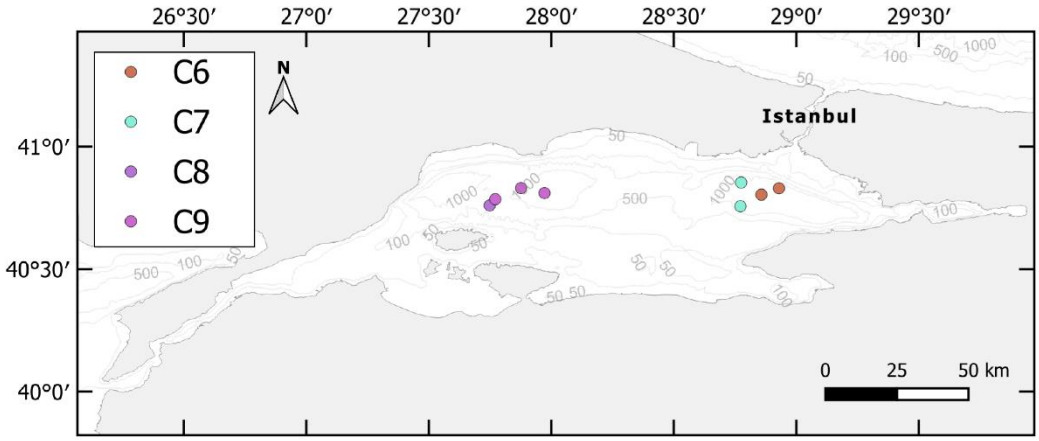


Figure 5.13. Location map of stations belonging to clusters 6, 7, 8 and 9 (see Figure 5.10 and Figure 5.1 for station names).

Clusters 8 and 9 include stations of Kırcı-Elmas (2006, SoM_03) and Kırcı-Elmas et al. (2008, SoM_06) coming from the Central Basin (Figure 5.10). Station 32MC (711 m, slope on the southern side) makes up the cluster 8, and stations DM22 (1203 m, basin floor), DM18 (895 m, a flat spot adjacent to the Western high) and KL40 (703 m, slope from the Western High) make up the cluster 9. These stations have in common abundant to very abundant *Bulimina* species, *Bulimina aculeata* (8.6%) for cluster 8 and *Bulimina costata* (minimum 18.8%) for cluster 9. Very dominant abundance of *Sigmoilinita tenuis* (34.2%) makes 32MC different from the cluster 9 in which *S. tenuis* abundance is around 10% in two, below 5% in one station. In addition, *Sigmoilopsis schlumbergeri, Siphotextularia* spp., *Spiroloculina excavata* are abundant in 32MC but rarer in cluster 9 stations. In KL40 *Uvigerina mediterranea* is the most abundant taxon (46.4%), in DM22 it is abundant but is absent in the other two stations.

5.7.5 Cluster 10

Cluster 10 is composed of only one station: MAR98-9 of Kaminski et al. (2002, SoM_11), a shelf station from Istanbul, of 64 m water depth (Figure 5.10, Figure

5.14). It is separated from other shelf stations due to the very dominant abundance of *Bolivina* spp.: the *Bolivina* genus in this station were counted without differentiating the species. The station is close to stations SoM_07_2 and SoM_08_94, both present in subcluster 13b with abundant *B. spathulata* and *B. dilatata*. In addition, Kaminski et al. (2002) report a high abundance of *Cassidulina crassa* (8.5%, here considered as *Globocassidulina crassa*, may be conspecific with *Paracassidulina minuta*), not present in the nearby stations (may be lumped with *Cassidulina laevigata*). The station is similar to the latter two otherwise; had the *Bolivina* species been counted separately, this station would most likely plot in the same cluster as the mentioned nearby stations. The assemblage in the station includes abundant *Bulimina aculeata, Bulimina elongata* and *Cassidulina laevigata*.

5.7.6 Cluster 11

Stations 1 (Istanbul, near Bosphorus, 28 m), 4 (Istanbul west, near Büyükçekmece, 50 m) and 14b (central Southern shelf, near mouth of Çapraz stream, 28 m) of Kırcı-Elmas (2013, SoM_07) make up the cluster 11 (Figure 5.10, Figure 5.14). These three stations from very different settings are combined together due to very high abundances of *B. aculeata* (31-41.4%) and *Bolivina vadescens* (12.3-29.1%, reported as *Bolivina variabilis*). Several taxa have different abundances in stations: *Ammonia tepida* is abundant in station 1 (14.2%) and *Cassidulina* is abundant in station 4 (11.4%) but rare to frequent in the other two; *Nonionella turgida* is abundant in stations 4 and 14b, but only frequent in station 1; *Rectuvigerina phlegeri* is of 4.9% in station 14b but not present in the other two.

5.7.7 Cluster 12

Cluster 12 is composed of two branches (subclusters) (Figure 5.10). Majority of the stations are from the slope setting (Figure 5.15).

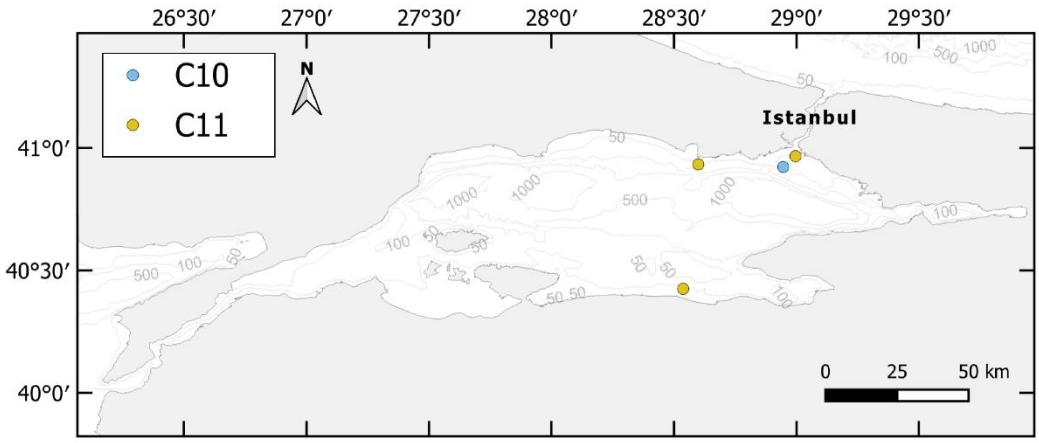


Figure 5.14. Location map of stations belonging to clusters 10 and 11 (see Figure 5.10 and Figure 5.1 for station names).

Subcluster 12a includes stations of Phipps et al. (2010, SoM_02, stations 92-101) from the western Southern shelf (below 140 m water depth), and two stations of Kaminski et al. (2002, SoM_11, stations MAR98-7from Prince Islands, 97 m, and MAR97-11 from central Southern upper slope, 111 m). These stations have significant *Bolivina spathulata* (5.5-25.9%, mostly above 10%), *Bulimina costata* (8.9-21.2% in SoM_02 stations), *Bulimina marginata* (6.9-25.5% in SoM_11 stations), *Bolivina vadescens* (3.2 to 24.9%, mostly 5-15%) abundances accompanied with *Uvigerina mediterranea*, *Gyroidina umbonata*, *Sigmoilopsis schlumbergeri*, *Hyalinea balthica* abundant in several stations.

Subcluster 12b is composed of the stations of this study, very similar to but differentiating from subcluster 12a by very high abundances of *Paracassidulina minuta*. The stations of this study come from various locations and water depths, however, the stations are not plotted with other stations of similar settings, instead are clumped together due to the presence and high abundance of *P. minuta*. The lack of identification of this taxon in the literature prevents the evaluation of this study's stations with respect to similarities to others. The similarities of stations of this study to each other were explored in Section 3.4.

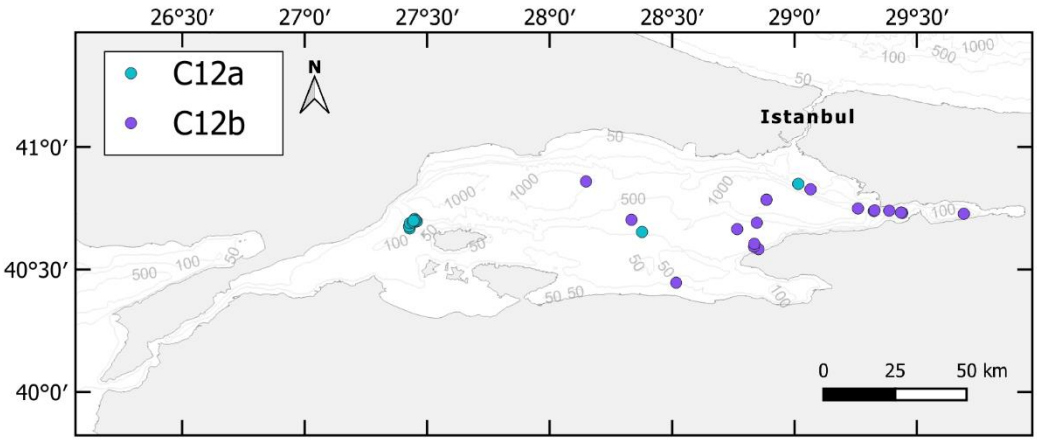


Figure 5.15. Location map of stations belonging to cluster 12 (see Figure 5.10 and Figure 5.1 for station names).

5.7.8 Cluster 13

Cluster 13 is composed of three branches (subclusters) and is the most crowded cluster (Figure 5.10). Cluster is composed of stations coming from the intermediate to outer shelf and uppermost slope (Figure 5.16).

Subcluster 13a includes station 40 from SoM_08 (Avşar, 2010) and almost all stations of SoM_12 (except two stations which were in cluster 3). These stations are from 37-57 m water depth, and except for SoM_08_40, all from the Erdek Bay. The assemblage in these stations include very high abundances of *C. laevigata* (11.4-37.5%) and *Ammonia compacta* (6.9-23.6%), accompanied by *Cribroelphidium poeyanum* (abundant in most stations, up to 22%), *B. spathulata* (abundant in half of the stations, up to 17%), *Bulimina marginata* (abundant in five stations), *D. bertheloti* (abundant in more than half of the stations, up to 23%), *Globocassidulina subglobosa* (abundant in four stations), *Quinqueloculina seminula* (abundant in four stations), *V. bradyana* (abundant in five stations).

Subcluster 13b includes 34 stations from SoM_06 (Kırcı-Elmas, 2018), SoM_07 (Kırcı-Elmas, 20013) and SoM_08 (Avşar, 2010) from northern and southern shelves and southern slope, from water depths 30-155 m. These stations have very high abundances of *C. laevigata* (7.3-33.4%, mostly above 15%), *B. spathulata* (1.9-47.6%, >15% in 20, <5% in 3 stations), *B. aculeata* (<5 in 9 stations, mostly 7-15%, up to 28.5%), accompanied by *B. vadescens* (is SoM_07, recorded as *B. variabilis*), *B. dilatata* (in SoM_06 and SoM_07 stations), *Discorbinella bertheloti* (mostly <5%, abundant in 8 stations), *V. bradyana* (abundant in 6 stations) and Ammonia compacta (abundant in 4 stations) in some stations.

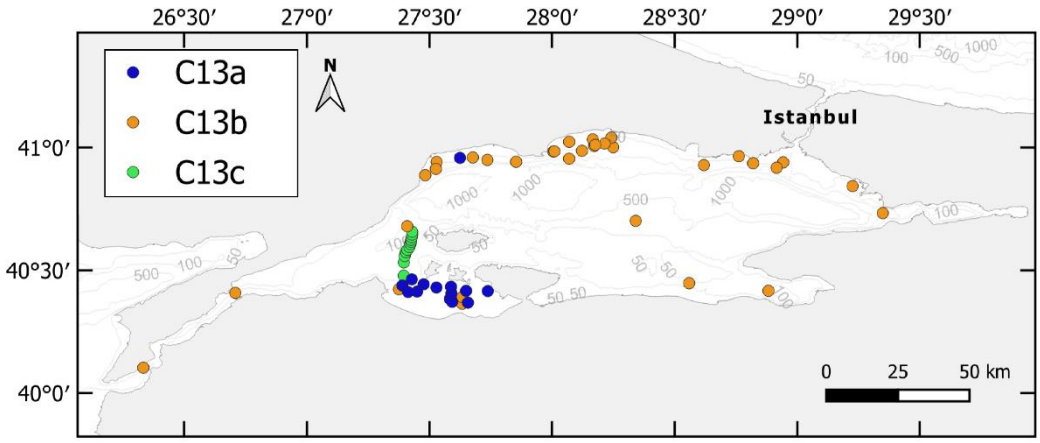


Figure 5.16. Location map of stations belonging to cluster 13 (see Figure 5.10 and Figure 5.1 for station names).

All stations in subcluster 13c come from Phipps et al. (2010, SoM_02), they are all from the Erdek Bay (SoM_08 station 9, just at the entrance of the bay) and western Southern shelf (SoM_08 stations 2 to 91) of 55-130 m water depth. These stations include abundant *C. laevigata* (14.2-32.6%, only three stations <15%) and *B. vadescens* (3.3-17.8%, only one station <5%), and *Gyroidina umbonata* (>5% except for three stations, >15% in three stations, up to 22.1%) accompanied by *B. aculeata* (abundant in shallower half of the stations, up to 9.8%), *B. dilatata* (abundant in half

of the station, up to 8.8%), *B. spathulata* (abundant in deeper half of the stations up to 10.4%) and frequent *Hyalinea balthica* (abundant in only three stations).

5.7.9 Clusters 14 and 15

Station 2 of Phipps et al. (2010, SoM_02) is the only station in cluster 14, while rest of the stations of SoM_2 along with station 11b of Kırcı-Elmas (2013, SoM_07) make up the cluster 15. These two clusters are most similar to each other (Figure 5.10). The stations are all situated in the Erdek Bay (Figure 5.17).

Cluster 14, station 2 of SoM_02, has abundant *Ammonia parkinsoniana* (14.3%), *Elphidium decipiens* (15%), *Elphidium crispum* (7.2%), *Neoconorbina terquemi* (8.9%), *Porosononion granosum* (11.6%).

Cluster 15 stations have abundant *B. aculeata* (>4%, up to 10.8%) and *Porosononion granosum* (5.6-13.2%), deeper stations have high *C. laevigata* abundance (8.4-12.6%; 1-3% in shallower stations), *E. decipiens* is present in all stations except for SoM_07_11b with abundances decreasing with depth (2.1-8.7%), *Reussella spinulosa* (abundant in only two stations) and *Rectuvigerina phlegeri* (<5%) are present in all stations, *V. bradyana* is present in all stations (1.4-6.7%, >2% except for two stations), *Nonionella turgida* is present in all stations with low abundances (<5%) except for SoM_07_11b (8%), *D. bertheloti* is abundant in stations SoM_02_8 and SoM_02_6 (8.5 and 11.7% respectively), *Cribroelphidium poeyanum* is low usually in abundance (0.6-2.5% in six stations, 7.4% in SoM_02_3) but present in all stations, *Cibicides advenum* is present except for shallowest two stations (SoM_02_3 and SoM_07_11b) and abundant (>5%) in two of the stations. *Asterigerinata adriatica*, *Aubignyna perlucida* and *Ammonia* species abundances interchange between stations, *Aubignyna perlucida* becomes abundant (15%) in SoM_02_3.

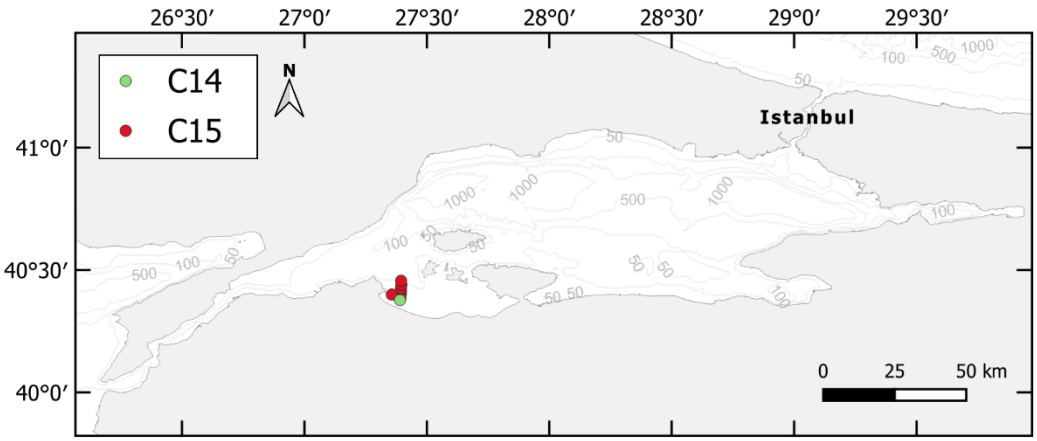


Figure 5.17. Location map of stations belonging to clusters 14 and 15 (see Figure 5.10 and Figure 5.1 for station names).

CHAPTER 6

FORAMINIFERA AS BIOTIC INDICES

Using biogenic components of ecosystems and recent sediments is done to assess the ecosystem health, ecologic quality, polution effects and degree and etc.; and also assigns predictive power to said biogenic components in terms of various environmental variables such as water depth, oxygenation levels, organic carbon flux; finally attributing them proxy status both for future and past projections. Assessment of such environmental variables in the geologic past is a worthy effort both for understanding the past and for exploring possible future outcomes. Foraminifera are one of these biogenic components on which much study has been conducted. Foraminifera are preferential in these types of studies due to their small size and high abundance in the modern sediment, and as fossils in older strata. They have been utilized in studies dealing with paleoenvironment due to specialized habitat preferences of taxa (i.e., certain water depth, temperature range etc.).

In recent sediments, work on foraminifera for environmental exploration and correlation is done in three different mediums: i. the chemistry of tests of a taxon, ii. the minute morphologic details of a taxon, and iii. the community structure, i.e., relative abundances of taxa or groups in a sample. This chapter is focused on the third. All of the indices covered here deal with relative abundances of groups of foraminiferal taxa, and the relationships of these relative abundances to environmental variables. Van der Zwaan et al. (1990) related the planktonic foraminiferal relative abundance to water depth; Corliss's (1895) approach argues a relationship between the benthic foraminiferal community structure and organic carbon flux; and Kaiho (1999) established a relationship between the benthic foraminiferal community structure and dissolved oxygen. Finally, Foram-AMBI (Alve et al., 2016; Jorissen et al., 2018) uses benthic foraminiferal community structure to asses and relate to ecological quality status of marine waters (EcoQS),

using total organic carbon in the sediment as the proxy for it. Although there are more biotic indices concerned with the benthic foraminiferal community structure (e.g., Sen Gupta et al., 1996; Bouchet et al., 2012; Dimiza et al., 2016) most of these are concerned with limited geographic coverage (e.g., only coastal settings and very shallow shelves) therefore are not considered to fit the dataset of this study. In this chapter, previously mentioned biotic indices concerned with the community structures of benthic foraminifera are explored, explained and applied in the Sea of Marmara.

6.1 Background

6.1.1 Planktonic foraminifera and water depth

The ratio of benthic and planktonic foraminifera was investigated in terms of the relationship to primary productivity and water depth as they are the two major controls on the amount of the food reaching the sea floor (Suess, 1980) which influences the benthic foraminiferal abundance (e.g., Berger and Diestar-Haas, 1988; Van der Zwaan et al., 1990; De Rijk et al., 1999).

Berger and Diestar-Haas (1988) proposed a relationship between the benthic/planktonic foraminifera ratio, water depth and distance from shore, indicating given the same productivity and other input related with food, the product of benthic/planktonic ratio, water depth, and distance to shore (BZ index) would be fixed. Any changes altering the fossil association (e.g., dissolution) or the living community (e.g., increase in food supply like lateral transport) would then be evident as changes in benthic/planktonic ratio, or the BZ index.

Van der Zwaan et al. (1990), building on Berger and Diestar-Haas's hypothesis, observed an exponential relationship between the planktonic foraminiferal relative abundance (in total foraminifera) and water depth, however the data was highly scattered. They stated that the scatter in the data could be minimized by removing

the infaunal (stress indicators) from the total foraminiferal number since their distribution is not directly dependent on the amount of the food reaching the sea floor, instead on the food buried in the sediment. The infaunal nature of the taxa was decided according to "general agreement" in literature, but they did not provide a list of taxa. With omission of infaunal foraminifera, the formula developed by Van der Zwaan et al. (1990, Equation 6.3, Figure 6.2) is confined to water depths between 30 and 1250 m. Van der Zwaan et al. (1990) further stated that any changes to in-situ assemblage (e.g., resedimentation, dissolution) have a large effect on the depth estimates, and also any samples deposited under anoxic or strongly dysoxic conditions should be avoided when attempting paleobathymetry estimations through %P* index in fossil material.

$$D = e^{(3.58718+(0.03534*\%P^*))} \quad \text{Equation 6.1}$$

De Rijk et al. (1999) also investigated the planktonic foraminiferal ratio (in total foraminiferal abundance) in terms of its relationship with depth, for the Mediterranean Sea. They produced two exponential best-fits for the data, one for the Eastern (Equation 6.2) and one for the Western part (Equation 6.3) of the Mediterranean Sea (Figure 6.2).

$$y = 24 * ln(x) - 81.9 \quad \text{Equation 6.2}$$

$$y = 21.1 * ln(x) - 64.1 \quad \text{Equation 6.3}$$

The regression curves proposed by Van der Zwaan et al. (1990) and De Rijk et al. (1999) are given in Figure 6.2. The three curves are especially similar in the lower planktonic foraminiferal ratio values, with higher planktonic foraminifera ratio values the difference between the regressions of become more evident, although it should be noted that the independent variable used by the two studies are different,

and in the plotted curves infaunal benthic foraminifera ratio was assumed zero hence making P% and %P* equal. Omission of infaunal benthics in Van Der Zwaan et al. (1990) increases the independent variable values by reducing the denominator, the difference is especially high between 100-1000 m water depths where infaunal benthic foraminifera ratio may be 30-90% (see fig. 6 therein). Therefore, although the regression curves appear similar, increasing differences towards the deeper settings stem from higher infaunal abundance.

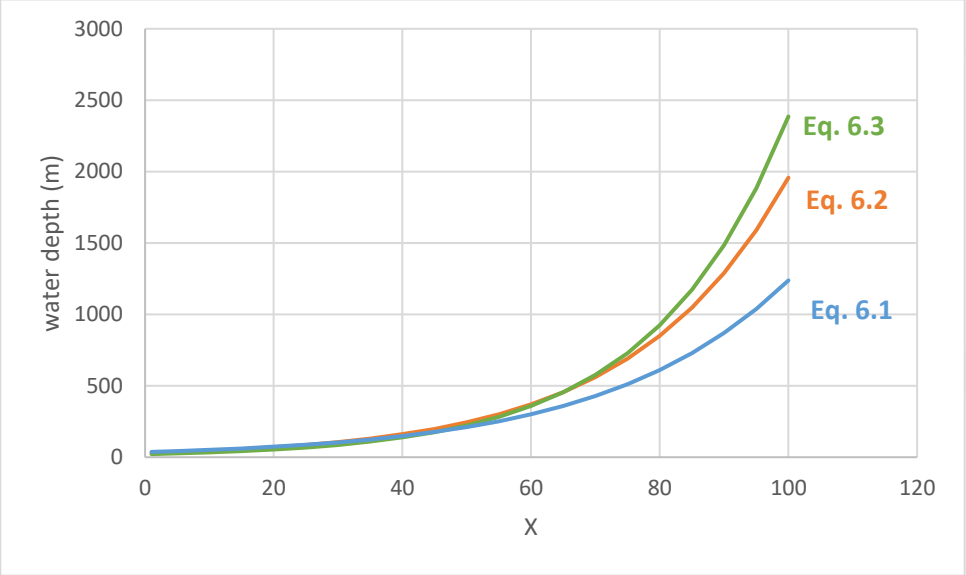


Figure 6.1. Plots of regression curves proposed by Van der Zwaan et al. (1990, Equation 6.1, with X = %P*) and De Rijk et al (1999, Equation 6.2 (east) and Equation 6.3 (west), with X = P%).

Recently, planktonic foraminifera ratio was used to determine not only paleobathymetry, but also the locations where the original foraminiferal assemblage was altered due to downslope transport, lateral advection, or dissolution (Tapia et al., 2022).

6.1.2 Benthic foraminifera and organic carbon flux

Corliss (1985) proposed a link between morphology and microhabitat preference of calcareous foraminifera (hyaline and porcelaneous test, not including agglutinated or organic walled taxa) in terms of preferred living depth with respect to sediment-water interface. Corliss (1985) based the hypothesis on previously published interspecific differences in stable isotopes interpreted to reflect living depth in the sediment, and their own quantitative work showing that different taxa having their maximum abundance at different depths in sediment, and correlated these findings with the test shape and porosity.

Building on Corliss (1985), Corliss and Chen (1988) proposed a morphotype-classification scheme (from total foraminiferal assemblage from surface sediments from the Norwegian Sea), was later utilized in the same way by Corliss and Fois (1990, for dead foraminiferal assemblage from surface sediments from the Gulf of Mexico) (Figure 6.2). All three studies are built on the assumption that infaunal living foraminifera are somehow more tolerant to or prefer the lower oxygen settings, and higher organic carbon flux. Corliss and Chen (1988) proposed that the major control on the community structure (i.e., ratio of infaunal and epifaunal benthic foraminifera) is organic carbon flux. The amount of carbon flux is loosely and inversely related to distance from shore, but positively related to total organic carbon content (TOC) in sediment (Corliss and Chen, 1988). Corliss and Chen (1988) concluded that epifaunal taxa dominate assemblages, i.e., epifaunal ratio in total benthic foraminifera number as percent (E%) is higher than 50%, where organic carbon flux is less than 3-6 g/m^2y.

Some examples of test shapes deemed infaunal and epifaunal are given in Figure 6.2 (Corliss, 1985; Corliss and Chen, 1988; Corliss and Fois, 1990). The miliolid taxa (Order Miliolida, porcelaneous test) were considered to be all epifaunal. Trochospiral taxa of planoconvex shapes with porous flat side, trochospiral taxa with rounded margins, and trochospiral taxa with angular margins were all considered to be epifaunal according to this scheme. On the other hand, all planispiral taxa, tests

with spherical outline, biserial enrolled lenticular taxa, biserial flattened taxa and taxa with cylindrical outline were all regarded to be infaunal. Corliss and Chen (1988) and Corliss and Fois (1990) remarked that chamber arrangement and porosity were also considered in their subdivision of morphotypes in addition to overall test shape unlike the previous morphotype studies such as Bernhard (1986).

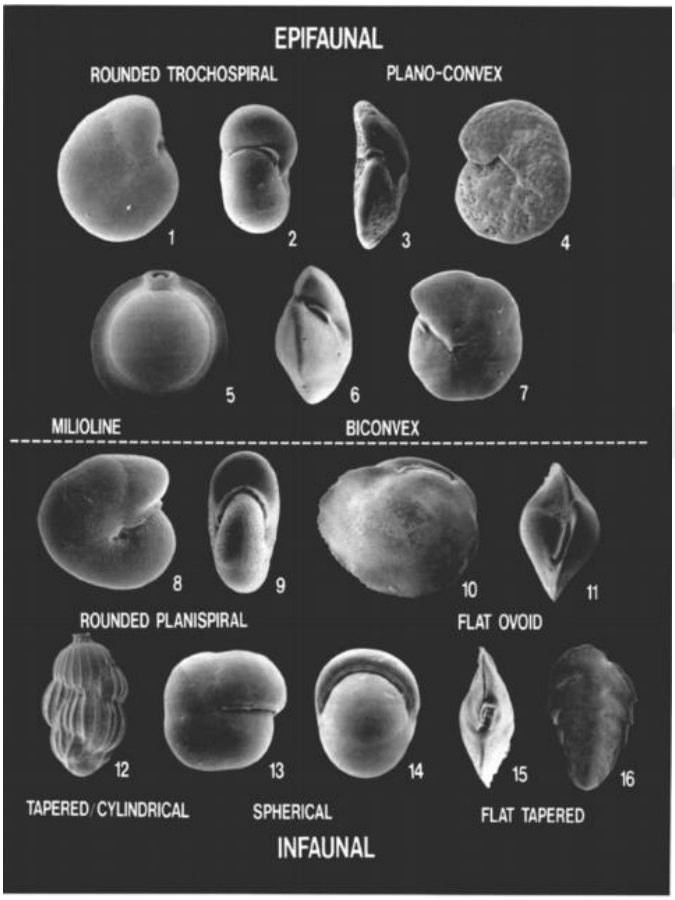


Figure 6.2. Foraminiferal morphotype classification scheme from Corliss and Chen (1988) and Corliss and Fois (1990).

6.1.3 Benthic foraminifera and dissolved oxygen: Benthic Foraminifera Oxygen Index

Kaiho (1994) grouped calcareous benthic foraminifera (hyaline and porcelaneous test, not including agglutinated or organic walled taxa) in terms of their tolerance to varied dissolved oxygen content. Three major groups Kaiho classified are Oxic, Suboxic and Dysoxic indicators, according to previous works dealing with the relationship between test morphology and oxygen levels, and microhabitat (i.e., infaunal vs. epifaunal living preferences). Using samples coming from various dissolved oxygen settings from world oceans and seas, Kaiho (1994) established the relationship of the previously proposed Benthic Foraminifera Oxygen Index (BFOI, Kaiho, 1989, 1991) and dissolved oxygen; and Kaiho (1999) further established the relationships between BFOI, dissolved oxygen, organic flux and primary productivity, concluding that although primary productivity and carbon flux do have local effects on dissolved oxygen and BFOI, the relationship (linear regression) between dissolved oxygen and BFOI is the highest. Kaiho (1999) also indicated that BFOI cannot be used to pinpoint a dissolved oxygen value, but instead can be used to differentiate different oxygenation levels (e.g., anoxic, suboxic, low oxic).

Kaiho (1994, 1999) used >63 μm fraction for the analysis. and separated the calcareous benthic foraminifera into five groups according to their size, morphology, and previously published habitat/microhabitat preferences, providing lists of taxa for their studied samples. These five groups are:

i. Oxic indicators: Large (>350 μm) forms with thick walls and planoconvex (e.g., *Cibicides*), biconvex, rounded trochospiral and spherical (e.g., *Globocassidulina subglobosa*) test shapes, and thick walled miliolids (e.g., *Pyrgo*, *Quinqueloculina*). These are allegedly absent from low-oxygen settings.

ii. Suboxic indicators A: Smaller representatives of oxic indicator taxa, they are assumed to be able to live under low-oxygen environments.

iii. Suboxic indicators B: Forms with intermediate morphologies of oxic and dysoxic indicators. *Lenticulina*; large *Nodosaria*, *Dentalina*, *Pleurostomella*; large, ornamented species of *Bulimina* and *Stilostomella*; rounded planispiral (e.g., *Melonis*), flat ovoid (e.g., large *Cassidulina*) and spherical forms (e.g., *Fissurina*); small and/or thin walled, planoconvex and biconvex trochospiral forms (e.g., *Rosalina*, *Nonion*); and *Uvigerina*, *Oridorsalis*, *Gyroidina*, *Gyroidinoides* and *Hoeglundina*. These are assumed to behave infaunal or epifaunal with regards to the bottom water oxygenation.

iv. Suboxic indicators C: Thin walled forms which are found in intermediate microhabitats between Suboxic B and Dysoxic groups: e.g., *Bulimina aculeata*, *Elphidium excavatum*, *Nonionella*.

v. Dysoxic indicators: Thin walled and flattened-elongate forms such as *Bolivina*, *Bulimina exilis*, small *Cassidulina*, *Chilostomella*, *Fursenkoina*, *Globobulimina*.

Using relative abundances of these five groups Kaiho's index BFOI is calculated by Equation 6.4 in case Oxic indicator taxa are present, and Equation 6.5 in case they are not (Kaiho, 1994). The BFOI when Oxic taxa are not present is calculated with all suboxic taxa (groups A, B and C) in Kaiho (1999; Equation 6.6).

$$BFOI = \frac{O}{O+D} * 100$$ where O = number of oxic indicators, D = number of dysoxic indicators — Equation 6.4

$$BFOI = (\left(\frac{I}{I+D}\right) - 1) * 50$$ where I = number of suboxic indicators A and B; D = number of dysoxic indicators — Equation 6.5

$$BFOI = (\left(\frac{S}{S+D}\right) - 1) * 50$$ where S= number of suboxic indicators; D = number of dysoxic indicators — Equation 6.6

In the Sea of Marmara, Kaminski (2012) utilized Kaiho's model on a depth transect (previously studied by Chendeş et al., 2004; Phipps et al., 2010). Kaminski (2002) grouped taxa in the five groups referring to Kaiho's (1994) work, widening the list given by Kaiho to include the taxa from the Sea of Marmara. In doing so Kaminski mostly followed the morphotype approach of Kaiho, however, used >125 µm fraction which can create an underrepresentation issue for the smaller taxa. Kaminski (2002) compared the calculated oxygen (from BFOI, using the linear relationship established in Kaiho, 1994) to measured values. Although for some of the dataset the calculated and measured values were similar, for most of the dataset the difference is significant.

6.1.4 Benthic foraminifera and ecological quality: Foram-AMBI

AMBI (AZTI Marine Biotic Index; Borja et al. 2000) was developed for coastal (estuarine and littoral, intertidal and subtidal areas of maximum ~35 m water depth), soft-bottom areas for macrozoobenthos, grouping the taxa in ecological groups with respect to their sensitiveness of a stress gradient, and using the relative abundances in a formula to obtain a Biotic Coefficient which correlates negatively with species richness, diversity, redox potential, organic matter content and dissolved oxygen. Alve et al. (2016) modified the methodology for benthic foraminifera of NE Atlantic and Arctic fjords (continental shelves and slopes) to develop Foram-AMBI using total organic carbon (TOC) as the stress gradient. Later, many studies were conducted using, improving, testing the Foram-AMBI from various geographic locations and depositional settings (e.g., Jorissen et al., 2018, Mediterranean; El Kateb et al., 2020, Gulf of Gabes, Tunusia; O'Malley et al., 2021, Gulf of Mexico; Bouchet et al., 2021, English Channel/European Atlantic coast and the Mediterranean Sea intertidal and transitional waters; Fossile et al., 2021, Southern Adriatic Sea; Nunes et al., 2023, Guanabara bay, SE Brazil).

The method, groups taxa with respect to their relative abundance distributions on a total organic carbon gradient (TOC, Figure 6.3), producing five different ecological

groups, and using the relative abundances of the groups in an equation to calculate a Biotic Coefficient (BC, Equation 6.7). The characteristics of the groups are summarized below (according to Alve et al., 2016 and Jorissen et al., 2018):

- Group I: Sensitive species: sensitive to organic matter enrichment, abundances decrease with increasing TOC, and are absent in strongly enriched areas. These are usually rare species whose abundance trends are difficult to observe due to their rarity.

- Group II: Indifferent species: usually occur in low abundances over a wide range of TOC, but absent in strongly enriched areas.

- Group III: Tolerant species (Alve et al. 2016) or Third-order opportunists (Jorissen et al. 2018): occur in low abundances in low-enrichment areas, but favor the first stages of organic enrichment.

- Group IV: Second-order opportunists: absent or rare (<2%) in low or moderate TOC, but increase in abundance with organic enrichment.

- Group V: First-order opportunists: absent or rare (<2%) in low or moderate TOC, but increase in abundance with organic enrichment. Their maximum abundance is closer to the maximum enrichment. These are the last taxa to occur before azoic conditions (i.e., maximum enrichment).

$$BC = \left\{ \begin{matrix} (0 * \%GI) + (1.5 * \%GII) + (3 * \%GII) + \\ (4.5 * \%GIV) + (6 * \%GV) \end{matrix} \right\} / 100 \qquad \text{Equation 6.7}$$

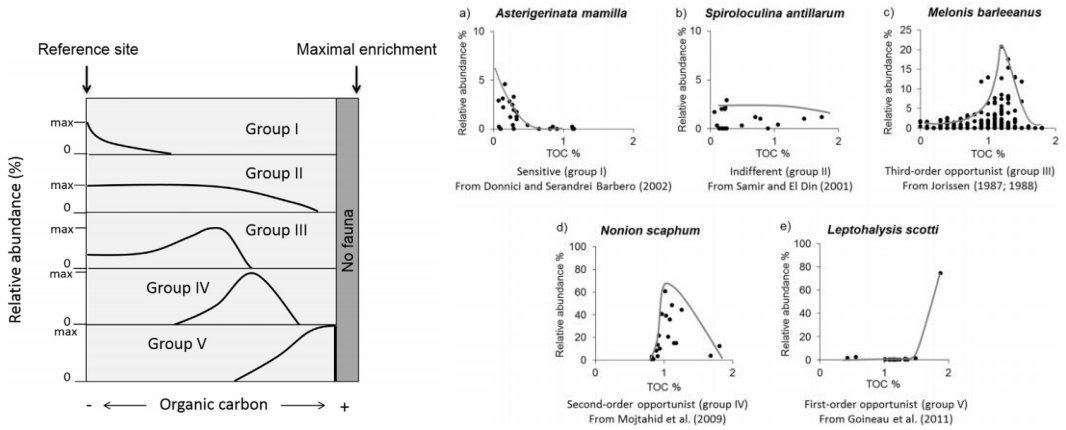


Figure 6.3. Left: relative abundance distributions of the different ecological groups and right: examples of relative abundances of taxa belonging to the said groups (Jorissen et al. 2018).

The index for the macrozoobenthos is available online as a calculation tool, including the database of species assignments to the ecological groups (https://ambi.azti.es/). Borja and Muxika (2005) presented the guidelines for the usage of the index. Two main guidelines state that the ecological group of the assigned taxa should not be altered for specific areas, and that if the abundance of not assigned taxa is greater than 50%, AMBI should not be used, and if it is greater than 20%, it should be regarded with caution due to larger error margin.

The first guideline mentioned above was disregarded in the benthic foraminiferal studies, with Jorissen et al. (2018), O'Malley et al. (2021) and Bouchet et al. (2021) compiling their own respective taxon assignments after the initial set of assignments by Alve et al. (2016); while other studies cited in previous paragraphs used the lists compiled by one of these publications. The summary of these four studies including the number of samples in their data sets, the water depth and TOC ranges, and the number of taxa they assign to ecological groups are given in Table 6.1.

Table 6.1. Summary of four Foram-AMBI publications which made species assignments to ecological groups (EG). LBF: living benthic foraminifera, TBF: total (living+dead) benthic foraminifera, V: validation, C: calibration. #: number of. [1]: Alve et al. 2016 (Shelf to upper slope; below halocline), [2]: Jorissen et al. 2018, [3]: O'Malley et al. 2021, [4-]: [4-1]: Bouchet et al. 2021: English Channel/European Atlantic intertidal and Transitional Waters (TWs), [4-2]: Mediterranean Sea intertidal and TWs.

Reference:		[1]	[2]	[3]	[4-1]	[4-2]
Location		NE Atlantic and Arctic Fjords	Mediterranean Sea	Gulf of Mexico	English Channel/European Atlantic	Mediterranean Sea
# C datasets		19	15	1	21	21
# V datasets		4	-	1	1	1
# C samples		289	608	52	587	301
# V samples		213	-	7	12	23
# Samples with LBF		C: 248 V: 154	138	59	599	324
# Samples with TBF		C: 41 V: 59	470	-	-	-
Water depth range (m)		~20-1200	~1-300	42-2975	-	-
TOC range (%)		0.03-6.00	0-20	~0-20 % (TOM)	0-16	0.07-17.8
# Identified species		419	493	239	-	-
# Total Assigned species		128	199	155	77	79
# Assigned species	EG I	65	79	21	22	42
	EG II	33	60	50	13	7
	EG III	27	46	36	23	17
	EG IV	1	12	29	6	4
	EG V	2	2	19	13	9

Considering that different taxa do occur in different geographical regions, it is plausible that different data sets could be formed, however, even the co-occurring taxa are evaluated to belong to different ecological groups (EG) in these four studies,

and even in the two datasets of Bouchet et al. (2021). After homogenization of the data by these four studies, 442 taxa in total form the master table (Supplementary Table F.1), after homogenization of data (Supplementary Table F.2 for the list of synonymous names). To exemplify the different assignments, the four species occurring in all five and 13 in four of the five datasets are given in Table 6.2, they are assigned to EG I, II and/or III by more than one, and differently by the others. Only 19 taxa occur in more than one data set with matching ecological group assignment in all datasets they occur; out of these, 17 of them were assigned to EGI, one to EGII, one to EGIII (Table 6.3).

Table 6.2. Ecological group assignments (in Arabic numerals) of species occurring in all five datasets. Agreeing assignments color matched. See Table 6.1 for references.

Species	[1]	[2]	[3]	[4-1]	[4-2]
Bolivina spathulata	3	3	2	3	4
Bolivina striatula	2	3	3	5	1
Bulimina marginata	3	3	2	4	2
Nonionella turgida	2	5	2	3	3
Bolivina dilatata	2	2		3	2
Bolivina pseudoplicata	2	2		2	5
Bulimina elongata	2	3		4	3
Buliminella elegantissima	3		5	3	3
Cassidulina carinata	1	4	2		1
Cibicides lobatulus	1	1		1	1
Cibicides refulgens	1	1	1		1
Epistominella vitrea	2	4	3	3	
Haynesina germanica		3	5	3	3
Quinqueloculina seminula	2	3		5	1
Spirillina vivipara	1	3		2	1
Stainforthia fusiformis	5	3		4	5
Textularia agglutinans	2	3	4		1

Table 6.3. The list of taxa occurring in more than one dataset with the same ecological group (EG) assignment. #: number of datasets. Ecological group assignments given in Arabic numerals.

Species	# dataset	Agreed EG
Adelosina longirostra	2	1
Adelosina mediterranensis	2	1
Asterigerinata mamilla	3	1
Astrononion stelligerum	2	1
Cibicides lobatulus	4	1
Cibicides refulgens	4	1
Cycloforina contorta	2	1
Elphidium complanatum	2	1
Elphidium crispum	2	1
Gavelinopsis praegeri	3	1
Neoconorbina terquemi	2	1
Peneroplis pertusus	3	1
Peneroplis planatus	3	1
Planorbulina mediterranensis	3	1
Quinqueloculina auberiana	2	1
Rosalina macropora	2	1
Sigmoilina costata	2	1
Bolivina subaenariensis	2	2
Bulimina aculeata	2	3

6.2 Applications

Above mentioned indices were applied to the data produced from the core-top samples (see Table 1.2 for the intervals topmost are samples confined to) of the studied 18 cores (see Chapter 3 and Supplementary Table C.1). For applications, only the taxa which are present in at least one sample with at least 2% abundance (>2% taxa) were used (see Section 3.4).

6.2.1 Planktonic foraminifera ratio and water depth

As stated in chapters 3 and 4, planktonic foraminifera ratio (in total foraminifera, P%) is usually higher in deeper (or more distant from shore) samples (Table 6.4). When the core-top samples' P% values are plotted against water depth (Figure 6.4A), there is only a slight correlation (R^2=0.39). The majority of the stations belong to water depths shallower than 450 m but span a large planktonic foraminiferal ratio values (1.17% in Station 3 (19) to 71.82% in K40K46, Table 6.4). The exponential best fit to the data is somewhat parallel to the regression curves of De Rijk et al. (1999, east: Equation 6.2, west: Equation 6.3, Figure 6.4B). The calculated water depth estimates with these two regression curves deviate greatly from the actual water depths, and are underestimated in all stations except for K40K46 (Table 6.4). The deviations are smaller in shallower sites, while increasing greatly with increasing water depth.

Following Van der Zwaan et al. (1990), the infaunal taxa were then removed from the total foraminifera abundance for calculation of the modified planktonic foraminiferal ratio (%P*) (Table 6.4). For the distinction between infaunal and epifaunal taxa, Corliss's (1985) scheme was used (see Section 6.2.2) since it is one of the references Van der Zwaan et al. (1990) referred to. According to the morphotype classification following Corliss (1985), the 12 taxa, which were assigned as epifaunal, constitutes only the 8-27% of the total abundance in the core-top samples here analyzed. The modified planktonic foraminiferal ratios (%P*) are significantly higher than unmodified ratio (P%, Table 6.4, Figure 6.5A), with the difference being smaller in lower and higher extremes of P% and larger in medium P% values (Figure 6.5B). A similar second-degree polynomial relationship occurs between the infaunal benthic foraminiferal ratio (I%) and the unmodified PF ratio (P%, Figure 6.5C). But a meaningful relationship between infaunal ratio and bottom depth was not observed (see Section 6.2.2).

Omitting the infaunal elements from the benthic foraminiferal sum provides a better correlation with water depth (Figure 6.6A, R^2=0.51), however, large differences in

estimated water depth (with the model of Van der Zwaan et al., 1990) with the actual water depth of the station occur in several stations (Table 6.4). The core-top sample of 45C-2 is underestimated by about 600 m, while the difference is almost halved in its sibling core 45C-1.

Table 6.4. Epifaunal ($BF_{\#E}$) and total benthic foraminifera ($BF_{\#}$) and planktonic foraminifera ($PF_{\#}$) numbers counted from working splits, calculated planktonic foraminifera abundance in total foraminifera (P%), calculated planktonic foraminifera ratio (%P*, according to Van der Zwaan et al., omitting infaunal benthics), measured water depth (m) and estimated water depths (EWD, m) following Equation 6.3 [1], Equation 6.2 [2], Equation 6.3 [3] in the core-top samples. Colors according to sample clusters (Figure 3.9).

Station	$BF_{\#E}$	$BF_{\#}$	$PF_{\#}$	P%	%P*	Measured water depth (m)	EWD [1]	EWD [2]	EWD [3]
1 (19)	169	1165	25	2.10	12.89	65	56.97	33.12	23.04
2	40	380	6	1.55	13.04	112	57.29	32.37	22.45
3 (19)	29	254	3	1.17	9.38	240	50.32	31.86	22.05
4	31	267	31	10.40	50.00	435	211.49	46.80	34.15
5	70	604	30	4.73	30.00	100	104.31	36.95	26.10
6	52	500	49	8.93	48.51	192	200.68	44.02	31.85
7	46	608	93	13.27	66.91	290	384.39	52.74	39.13
8	37	265	155	36.90	80.73	414	626.50	141.17	119.91
1 (21)	46	405	7	1.70	13.21	67	57.62	32.57	22.61
3 (21)	38	282	4	1.40	9.52	195	50.59	32.16	22.29
45C-1	12	136	116	46.03	90.63	1214	888.80	206.52	184.83
45C-2	39	505	155	23.48	79.90	1214	608.34	80.71	63.48
Izmit-deep	12	96	6	5.88	33.33	206	117.35	38.76	27.57
K40K46	90	328	836	71.82	90.28	318.5	878.05	604.86	627.48
K42K20	78	944	500	34.63	86.51	160	768.37	128.43	107.68
K49.5L04	74	931	137	12.83	64.93	100	358.44	51.78	38.32
K51.2K09	28	290	274	48.58	90.73	1185	892.05	229.68	208.57
MM50	76	421	9	2.09	10.59	53.5	52.53	33.10	23.03

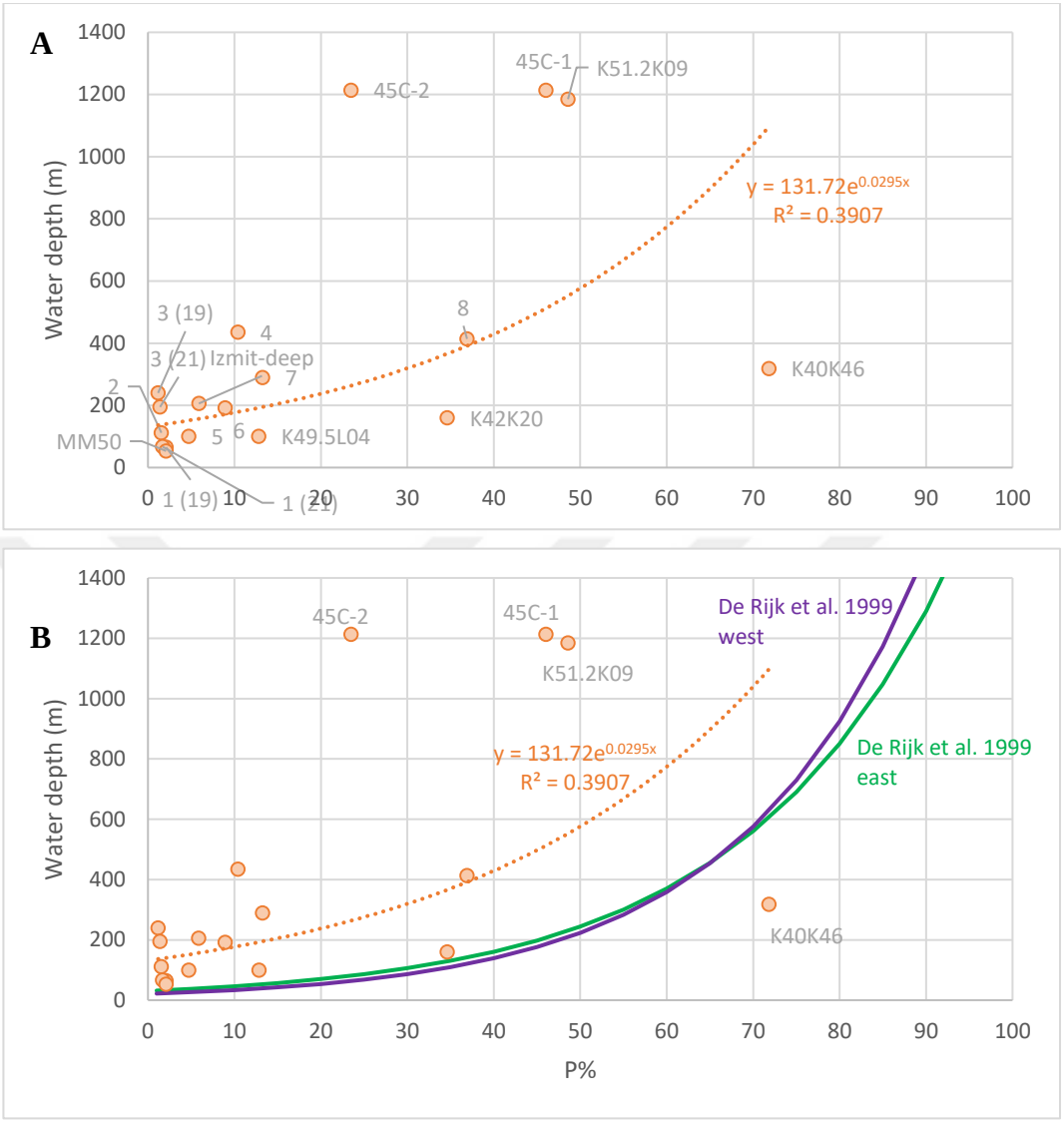


Figure 6.4. Scatter plot of (A) P% (horizontal) and water depth (m, vertical) and (B) regression curves of De Rijk et al. (1999) for the western and eastern Mediterranean Sea. R^2 value is indicated on exponential trend-line.

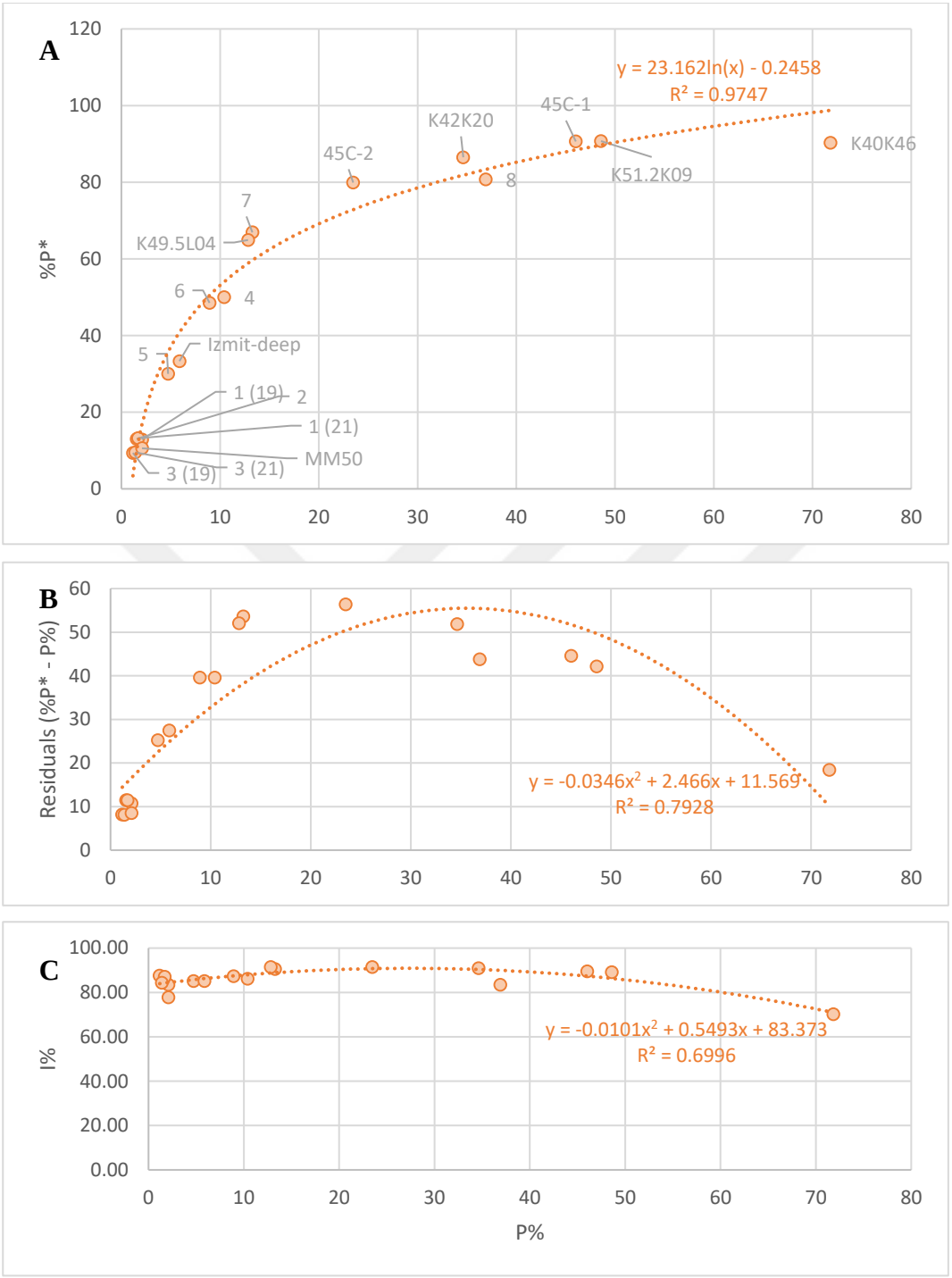


Figure 6.5. Scatter plots of (A) unmodified (P%) and modified (%P*) planktonic foraminiferal ratios in the core-top samples; (B) difference between the two PF ratios and (C) relative abundance of infaunal foraminifera (I%) against P%. R^2 values are indicated on trend-lines.

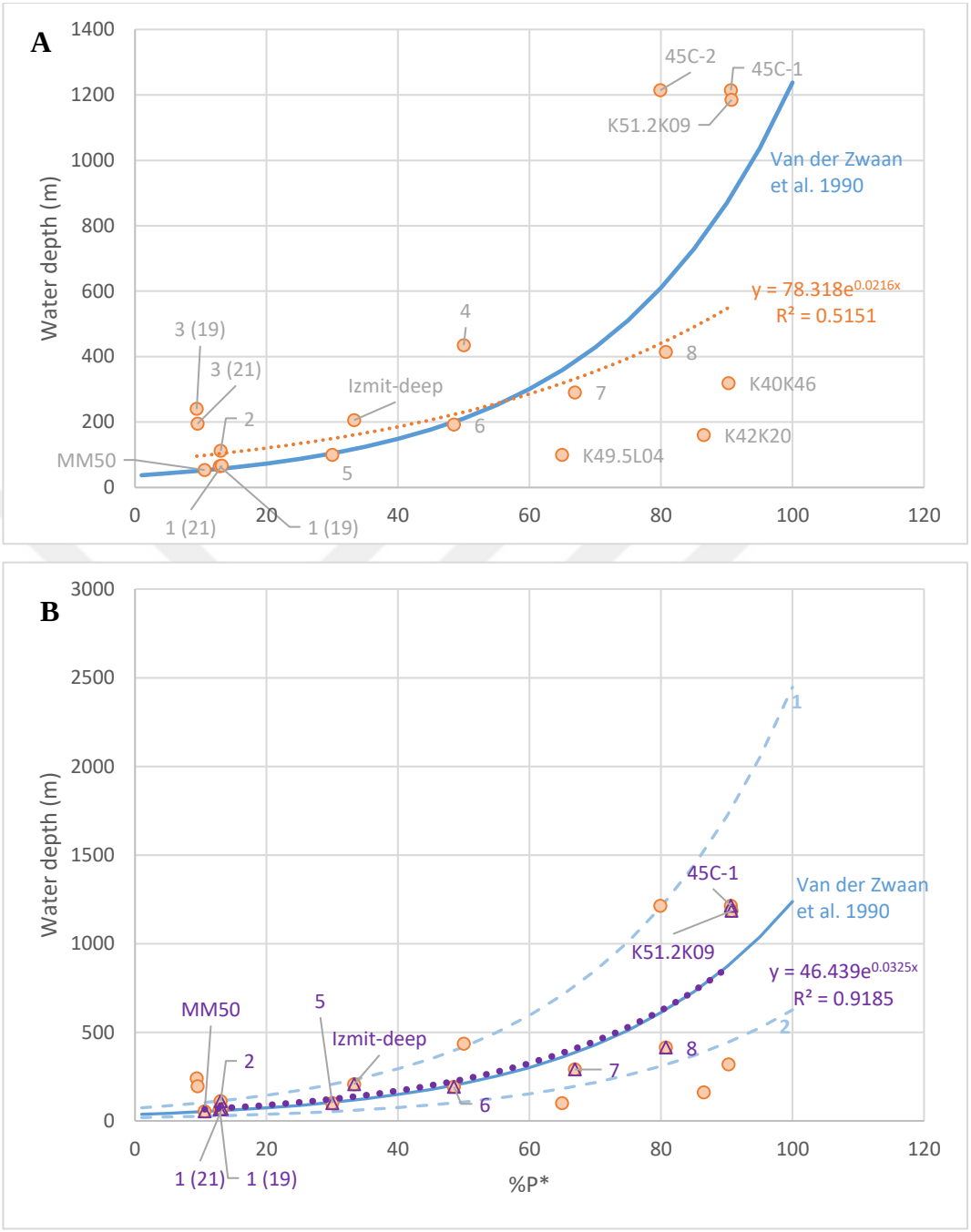


Figure 6.6. Scatter plots of %P* (horizontal) and water depth (m, vertical) and regression curve of Van der Zwaan et al. (1999). R^2 values are indicated on exponential trend-lines. (A): regression for the whole data set; (B). regression for stations marked with purple triangles, which remain in between the error margins 1 and 2 (light blue dashed lines, see text).

Similarly, a difference of about 600 m is also present for stations K40K46 and K42K20 (Figure 6.6A, Table 6.4). Smallest residuals are present in stations MM50, 1 (19), 1 (21), 5 and 6.

Since statistical details of the model was not provided by Van der Zwaan et al. (1990), a crude method for estimates for an error margin was applied by increasing and decreasing the intercept term in the model, forming the upper and lower bounds 1 and 2 in Figure 6.6B. At the level with 19% change in the intercept, 11 of the stations remain in between the bounds, and their regression provides a very high correlation coefficient. The resulting exponential regression is very similar to Van der Zwaan's (1990) model (Figure 6.6B).

Outlier stations are stations 3 (19), 3 (21), 4, 45C-2 which are underestimated, and K49.5L04, K42K20, K40K46 which are overestimated by Van der Zwaan's model (Table 6.4). Although the omission of taxa which were not assigned as infaunal or epifaunal (see Section 6.2.2) may be contributing to these residuals, these taxa make up only 7-20% of the total benthic foraminiferal abundance in the samples and are no more than 15% in these outlier stations. Had these unassigned taxa been epifaunal, it would only decrease the modified planktonic foraminiferal ratio (%P*), further increasing the underestimation of stations 3 (19), 3 (21), 4, 45C-2; and, the overestimated stations' (K49.5L04, K42K20, K40K46) estimated water depth would still be ~100-500 m deeper. Hence, the contribution of these unassigned taxa to the model cannot singlehandedly explain the large residuals in these outlier stations.

In both cores of the station 45C (deep Çınarcık Basin, very low bottom water dissolved oxygen, Table 2.2) the absolute abundances of both planktonic and benthic foraminifera are low (see Section 3.1); and the core-top samples of the two sibling cores (45C-1 and 45C-2, taken during the same multicorer cast) are somewhat different in terms of their planktonic foraminiferal ratio and their benthic foraminiferal assemblages (see Section 3.4). 45C-1 is poorer in terms of both planktonic and benthic foraminifera absolute abundances (Table 3.1, Table 3.2), and although the whole sample was processed, the counted benthic foraminifera number

did not reach the 250 BF individuals lower-limit, which may have created a larger error margin. The 250 lower-limit was met in 45C-2, here considered to represent a more complete and homogenous sampling. However, this is the sample which deviates greatly from the %P*-depth model. Although the lower number of BF collected from the core-top sample of 45C-1 prevents healthy interpretation of the BF assemblage, the difference between these two sibling samples may be due to patchiness (in-situ difference) and/or alteration of the assemblages via bottom processes.

Stations 3 (19 and 21) and 4, both off Izmit Bay with lower bottom water dissolved oxygen (Table 2.2), and of very similar benthic assemblage (see Section 3.4) are underestimated by the model about 150-200 m (Table 6.4). The modified ratio of planktonic foraminifera (%P*) are lower than what was expected by Van der Zwaan et al.'s (1990) model. This may mean that the standing stock of the planktonic foraminifera in that area is lower, the in-situ benthic foraminifera assemblage is denser with respect to PF abundance, or that the assemblages were altered by bottom processes. The BF absolute abundances are lower in these stations compared to the neighboring stations (Table 3.1, Table 3.2), which is expected under lower oxygen settings; however, neither the epifaunal foraminifera ratio (see Section 6.2.2) nor the benthic foraminiferal assemblage (see Section 3.4) are very different than the neighboring stations, increasing the possibility of alteration of the assemblage by bottom processes.

Among the overestimated stations, K49.5L04 and K42K20 are of higher sand content (Table 2.8). The benthic foraminiferal assemblage in these stations are similar to each other and stations off Izmit Bay (Figure 3.9, Figure 3.14); however, the absolute abundances of both benthic and planktonic foraminifera are highest in these two stations despite their shallow settings (Table 3.1, Table 3.2). The high foraminiferal abundances combined with high sand content may imply the alteration of the assemblages via winnowing, resulting in removal of small benthic individuals.

Station K40K46 in the Imralı Basin is in a setting with low bottom water dissolved oxygen (Table 2.2); however, it is the station with highest epifaunal foraminiferal ratio (see Section 6.2.2), and the planktonic foraminifera are comparatively rich so that it is one of the samples scoring highest in terms of the modified planktonic foraminiferal ratio (%P*, Figure 6.6A). The absolute abundance of benthic foraminifera is actually low (Table 3.1, Table 3.2) which is expected for a low-oxygen setting, but the high ratio of epifaunal taxa may indicate alteration of the assemblage by bottom processes.

6.2.2 Corliss's Morphotypes

Using lists and the outline of morphotypes given in Corliss and Chen (1988) and Corliss and Fois (1990), the >2% taxa identified in this study were classified into Corliss's proposed 9 morphotype classes, the textularin and unidentified taxa were not included in this classification (assigned 39 taxa; Table 6.5). For the taxa whose assignment was given in Corliss (1985), Corliss and Chen (1988) and Corliss and Fois (1990) were used as given, the others were assigned following the gross morphological properties and similarities to assigned taxa (Remarks in Table 6.5).

Table 6.6 lists the number of taxa belonging to morphotype classes and their average relative abundances in the core-top samples. Among these 39 assigned taxa, 12 of them belong to the tapered/cylindrical class, which is the most populated class of all. However, the class with highest relative abundance is the flattened tapered (composed of genus *Bolivina*) with 33.72%, followed by flattened ovoid class (composed of casidulin taxa) with 22.15%.

Table 6.5. Morphotype classification of the >2% taxa (see Section 3.4) in the core-top samples, except textularin and unidentified taxa. [1] Corliss and Chen, 1988; [2] Corliss and Fois, 1990; [3] Corliss, 1985; TS: this study. Morphotype classes abbreviations as in Table 6.6. Taxon abbreviations as in Supplementary Table A.1.

Taxon	[1]	[2]	TS	Remarks
Amm_spp			RT	
B_alata			FT	
B_albat		FT	FT	
B_vades			FT	
B_dilat			FT	
B_spath			FT	
B_stria			FT	
B_acule		TC	TC	
B_costa			TC	*Bulimina striata* var. *mexicana* Cushman classified as TC in [2]
B_elong			TC	
B_infla			TC	
B_margi	TC	TC	TC	
C_laevi	FO	FO	FO	
Chilost			TC	*Chilostomella oolina* Schwager classified as TC in [2]
D_berthe	PT	PT	PT	
E_vitre			BT	*Epistominella exigua* (Brady) classified as BT in [1]
Elphidi	RP	RP	RP	Several *Elphidium* species classified as RP in [1], [2]
Eubulim			TC	
G_praeg			BT	*Gavelinopsis translucens* (Phleger and Parker) classified as BT in [2]
Gbulimi			TC	*Globobulimina affinis* (d'Orbigny) considered infaunal in [3]
G_sglob	S	S	S	
G_umbon			RT	*Gyroidina lamarckiana* classified as RT in [1]; *Gyroidina orbicularis* (d'Orbigny) classified as RT in [1], [2]
H_depre		RP	RP	
H_balth	PT		PT	
H_marma			PT	
M_pompi		RP	RP	
N_iride			RP	
N_opima		RP	RP	
N_opima		RP	RP	
N_stell			RP	

Table 6.5. Continued.

Taxon	[1]	[2]	TS	Remarks
Pcas_mi			FO	*Cassidulina crassa* d'Orbigny classified as FO in [2]
R_phleg			TC	
S_tenui			M	*Sigmoilinita distorta* (Phleger & Parker) classified as M in [2]
Sigmoi_1			M	*Sigmoilopsis schlumbergeri* (Silvestri) classified as M in [2]
Siphona			M	*Siphonaperta horrida* (Cushman) classified as M in [2]
Stai_fu			TC	
S_tuber			RT	
U_medit			TC	*Uvigerina peregrina* Cushman classified as TC in [1], [2]
V_brady			RT	*Valvulineria candeiana* (d'Orbigny) classified as RT in [2]
V_frag			TC	

Table 6.6. Morphotype classes and abbreviations, the microhabitat they belong to, number of taxa assigned to (#) and average relative abundance of (Average %) each morphotype class.

Microhabitat	Morphotype class	Abbreviation	#	Average %
Epifaunal	Rounded trochospiral	RT	4	5.53
	Planoconvex trochospiral	PT	3	2.03
	Milioline	M	3	1.70
	Biconvex trochospiral	BT	2	2.79
Infaunal	Rounded planispiral	RP	6	4.81
	Tapered/Cylindrical	TC	12	11.38
	Flattened tapered	FT	6	33.72
	Spherical	S	1	1.43
	Flattened ovoid	FO	2	22.15

The relative abundances of the morphotype classes in the core-top samples are given in Table 6.7. Flattened tapered and flattened ovoid classes are those with highest relative abundance.

Table 6.7. Summed relative abundances of taxa assigned to different morphotype classes in core-top samples. Morphotype classes abbreviations as in Table 6.6. Colors according to sample clusters (Figure 3.9).

Station	RT	PT	M	BT	RP	TC	FT	S	FO
1 (19)	7.81	2.40	0.00	4.29	7.55	9.27	35.36	0.52	20.26
2	5.79	3.16	0.26	1.32	8.16	13.95	24.47	1.05	16.05
3 (19)	7.87	1.18	0.00	2.36	6.69	12.60	43.70	1.18	16.54
4	6.74	1.12	0.75	3.00	10.11	7.49	33.33	1.50	19.48
5	5.46	1.99	0.33	3.81	3.97	10.10	22.68	2.32	27.15
6	3.20	2.80	0.60	3.80	3.40	8.20	29.40	2.20	28.40
7	1.81	1.81	0.33	3.62	2.14	7.07	36.35	2.30	24.51
8	6.79	1.51	3.02	2.64	2.26	7.17	41.89	1.51	17.74
1 (21)	7.16	0.99	0.00	3.21	2.96	16.05	37.04	0.49	19.75
3 (21)	8.51	2.84	0.00	2.13	2.13	10.28	38.30	1.06	20.92
45C-1	2.94	2.21	0.00	3.68	4.41	8.09	22.79	1.47	38.97
45C-2	2.57	1.78	0.59	2.77	1.39	6.93	38.42	0.79	34.65
Izmit-deep	6.25	4.17	0.00	2.08	10.42	13.54	22.92	5.21	19.79
K40K46	7.01	0.00	19.82	0.61	4.27	7.32	39.33	0.91	12.80
K42K20	2.33	3.71	0.74	1.48	0.32	16.21	41.42	0.42	24.68
K49.5L04	2.69	1.07	0.54	3.65	3.76	6.34	42.00	0.97	31.47
K51.2K09	1.03	2.07	3.45	3.10	7.93	16.90	34.48	1.38	17.93
MM50	13.54	1.66	0.24	2.61	4.75	27.32	23.04	0.48	7.60

Relative abundances of total epifaunal and infaunal taxa are given in Table 6.8. In average, ~74% of the overall relative abundance belong to those taxa assigned to infaunal morphotype classes. The assigned taxa in total constitute 74.21% (Station 2) at minimum, 92.48% (K49.5L04) at maximum, in average ~86% of the total abundance. epifaunal (E%) and infaunal (I%) ratios, calculated as the ratio of total relative abundance of epifaunal (Tot EPIF) and infaunal (Tot INF) morphotype classes to total relative abundance of all assigned taxa (Tot), as percent. Minimum epifaunal ratio (E%) is recorded in two core-top samples: 45C-2 and K49.5L04 with 8.59%; while the maximum is found in station K40K46 with 29.80%.

Table 6.8. Summed relative abundances of epifaunal (Tot EPIF = RT + PT + M + BT) and infaunal taxa (Tot INF = RP + TC + FT + S + FO), total relative abundances (Tot) of the taxa used in this analysis, epifaunal (E%) and infaunal (I%) ratios in core-top samples. Colors according to sample clusters (Figure 3.9).

Station	Tot EPIF	Tot INF	Tot	E%	I%
1 (19)	14.51	72.96	87.47	16.58	83.42
2	10.53	63.68	74.21	14.18	85.82
3 (19)	11.42	80.71	92.13	12.39	87.61
4	11.61	71.91	83.52	13.90	86.10
5	11.59	66.23	77.81	14.89	85.11
6	10.40	71.60	82.00	12.68	87.32
7	7.57	72.37	79.93	9.47	90.53
8	13.96	70.57	84.53	16.52	83.48
1 (21)	11.36	76.30	87.65	12.96	87.04
3 (21)	13.48	72.70	86.17	15.64	84.36
45C-1	8.82	75.74	84.56	10.43	89.57
45C-2	7.72	82.18	89.90	8.59	91.41
Izmit-deep	12.50	71.88	84.38	14.81	85.19
K40K46	27.44	64.63	92.07	29.80	70.20
K42K20	8.26	83.05	91.31	9.05	90.95
K49.5L04	7.95	84.53	92.48	8.59	91.41
K51.2K09	9.66	78.62	88.28	10.94	89.06
MM50	18.05	63.18	81.24	22.22	77.78

Corliss (1985), Corliss and Chen (1988) and Corliss and Fois (1990) related the epifaunal and infaunal ratios of the samples to the organic carbon flux, and used sediment total organic carbon (TOC) as its proxy. To assess the relationship between the TOC and the E% and I% in the studied samples, the used TOC values are given in Table 3.7. For 2019 stations, the average values of lumped intervals (Table 1.2), and for stations 1 and 3 of 2021 sampling, only the top interval (1cm) TOC values of 2019 sampling were used. For other 2021 stations, data from Ergin and Yörük (1990) and Ergin et al. (1993) were used (Table 3.7).

Figure 6.7 shows the relationships between three environmental variables and the epifaunal and infaunal ratios. The linear correlations between total organic carbon (TOC), bottom water oxygen (DO), bottom depth (see Table 3.7) and epifaunal ratio

are with very low coefficients (R^2 = 0.0846, 0.0003, 0.0988 respectively), hence no relationship can be inferred. The lack of relationship between the environmental variables and the epifaunal and infaunal ratios can be attributed to: incorrect assignments of taxa to epifaunal and infaunal classes, lack of relationship between microhabitat preference and gross morphologic shape, lack of 'true' infaunal or epifaunal taxa, inability of the index to resolve this limited range of TOC.

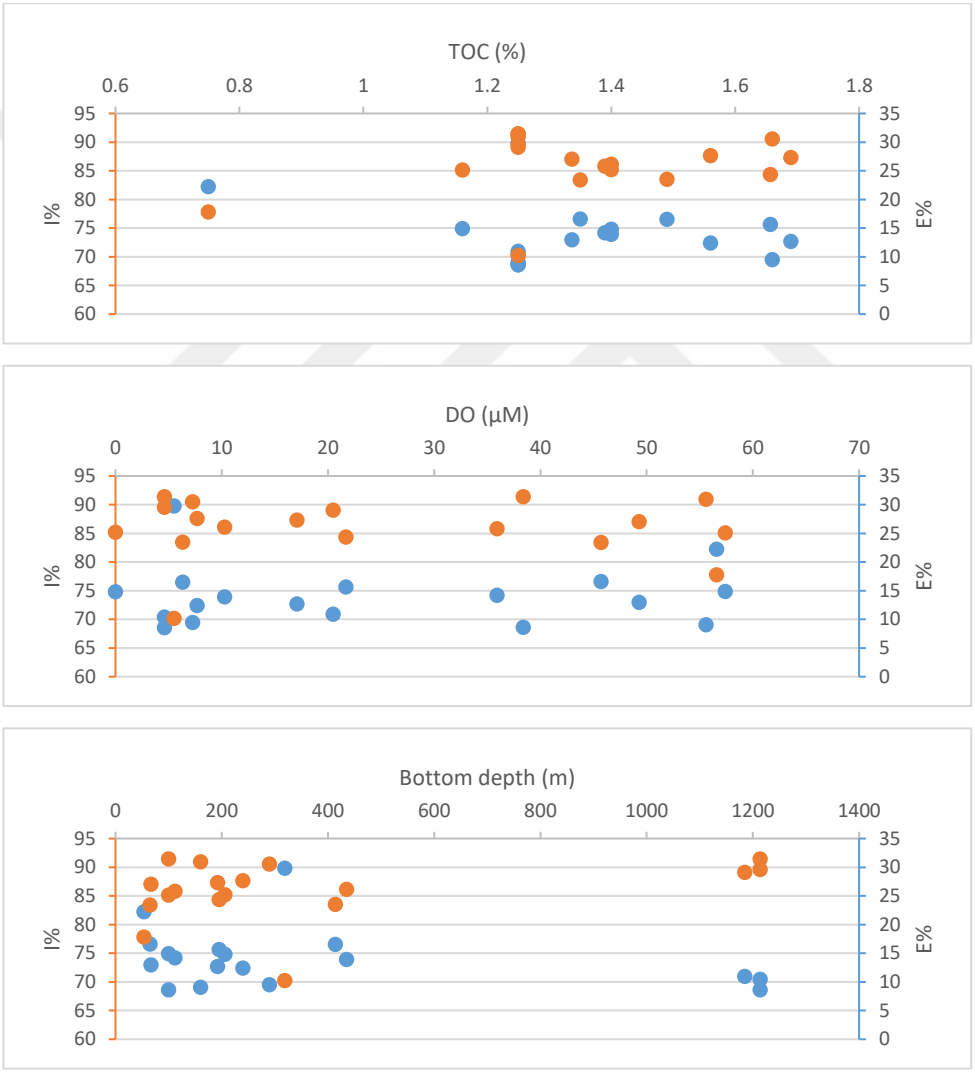


Figure 6.7. Scatter plots of total organic carbon (TOC), dissolved oxygen in bottom water (DO) and bottom depth vs. infaunal (I%) and epifaunal (E%) ratios.

6.2.3 Benthic Foraminifera Oxygen Index

Using the framework set up by Kaiho (1994, 1999) and the list of foraminiferal taxa by Kaminski (2012), the >2% taxa (except textularin and unidentified taxa) were classified into Oxic/Suboxic A, Suboxic B, Suboxic C and Dysoxic groups (Table 6.9). 33 of the >2% taxa were present in either one or both Kaiho (1994) and Kaminski (2012). Assignment criteria of the remaining six taxa are given in Table 6.9.

Table 6.9. Assignments of the >2% taxa (see Section 3.4) in the core-top samples, except textularin and unidentified taxa, into oxic, suboxic and dysoxic indicator groups. [1] Kaiho, 1994; [2] Kaminski, 2012; TS: this study. O: Oxic, S-A, B, C: Suboxic A, B and C; D: Dysoxic. Taxa abbreviations as in Supplementary Table A.1.

Taxon	[1]	[2]	TS	Remarks
Amm_spp		O, S-A	O, S-A	Several *Ammonia* species (thick walled) classified as O in [2]
B_alata	D	D	D	As *Bolivina* spp. in [1]
B_albat	D		D	As *Bolivina* spp. in [1]
B_vades	D	D	D	As *Bolivina* spp. in [1]; as *Brizalina catanensis* (Seguenza) in [2]
B_dilat	D	D	D	As *Bolivina* spp. in [1]
B_spath	D	D	D	As *Bolivina* spp. in [1]
B_stria	D	D	D	As *Bolivina* spp. in [1]
B_acule	S-C	S-C	S-C	
B_costa	S-B	S-B	S-B	As *Bulimina striata* d'Orbigny in [1]
B_elong		S-C	S-C	
B_infla			S-B	
B_margi		S-B	S-B	
C_laevi	S-B	D	S-B	as *Cassidulina* spp. in [1]; *Cassidulina carinata* Silvestri (thin walled variant) classified as D in [2]
Chilost	D		D	*Chilostomella oolina* Schwager and *C. ovoidea* Reuss classified as D in [1]; *Chilostomella mediterranensis* Cushman and Todd classified as D in [2]
D_berthe		O, S-A	O, S-A	
E_vitre	S-B	S-B	S-B	*Eilohedra nipponica* (Kuwano) classified as S-B in [1]

Table 6.9. Continued.

Taxon	[1]	[2]	TS	Remarks
Elphidi	S-C	O, S-A, S-B, S-C	S-B	*Elphidium excavatum* (Terquem) classified as S-C in [1]; several *Elphidium* species classified as O and several as S-B, *E. excavatum* in S-C in [2]
Eubulim	D		D	As *Bulimina exilis* in [1]
G_praeg		O, S-A	O, S-A	
Gbulimi	D	D	D	*Globobulimina affinis* (d'Orbigny), *G. auriculata* (Bailey), *G. pyrula* (d'Orbigny) classified as D in [1]; *G. affinis* and *G. turgida* (Bailey) classified as D in [2]
G_sglob	O, S-A	O, S-A	O, S-A	
G_umbon		S-B	S-B	*Gyroidina* spp. in classified as S-B in [1]; *Gyroidina multilocula* Coryell & Mossman (thin walled variant) classified as D in [1]
H_depre		S-B	S-B	
H_balth		S-B	S-B	
H_marma			S-B	Spezzaferri and Yanko-Hombach, 2007
M_pompi	S-B		S-B	As *Melonis* spp. in [1]; *Melonis barleanum* (Williamson) classified as S-B in [2]
N_iride	S-C		S-C	As *Nonionella* spp. in [1], [2]
N_opima	S-C		S-C	As *Nonionella* spp. in [1], [2]
N_stell	S-C	S-C	S-C	As *Nonionella* spp. in [1]
Pcas_mi	D		D	*Cassidulina tumida* Natland (thin wall, high porosity variants) classified as D in [1]; *Cassidulina carinata* Silvestri (thin walled variant) classified as D in [2]
R_phleg			S-B	
S_tenui		O, S-A	O, S-A	
Sigmoi_1			O, S-A	*Sigmoilopsis schlumbergeri* (Silvestri) classified as O in [2]
Siphona			O, S-A	
Stai_fu			S-B	Several *Stainforthia* species classified as S-B in [2]
S_tuber			S-B	
U_medit	S-B	S-B	S-B	As *Uvigerina* spp. in [1]
V_brady	S-B		S-B	As *Valvulineria* spp. in [1]; *Valvulineria complanata* (d'Orbigny) classified as S-B in [2]
V_frag			D	

Bulimina inflata (Seguenza) large, thick wall, highly porous, extremely different in these aspects from other Bulimina, more similar to *Uvigerina*. Since *Bulimina* species (except for B. aculeata) and *Uvigerina* spp. were considered to belong to Suboxic B group in Kaiho (1994), *B. inflata* is here classified as so as well. *Rectuvigerina phlegeri* Le Calvez is also considered to belong to Suboxic B group due to its morphologic similarities with these taxa.

Hyalinea marmarica Spezzaferri and Yanko-Hombach is here regarded to belong to Suboxic B group like its close relative *Hyalinea balthica* (Schröter). Spezzaferri and Yanko-Hombach (2007) reported the presence of *H. marmarica* in shallower waters and usually higher bottom water oxygenation conditions.

Siphonaperta spp. is placed under Oxic / Suboxic A group because many miliolid taxa, including *Sigmoilopsis schlumbergeri* (Silvestri), were considered to belong to oxic group by Kaminski (2012).

Svratkina tuberculata (Balkwill and Wright) is a low trochospiral, small taxon, and here it is considered to belong to Suboxic B group along with other small trochospiral taxa such as *Eilohedra vitrea* (Parker).

Virgulinella fragilis Grindell and Collen is a foraminifer which is specialized to survive in sulfidic bottom conditions (e.g., Bernhard 2003, Erbacher and Nelskamp 2006; see Section 7.3.6), therefore, it is here regarded to belong to Dysoxic group.

Oxic and Suboxic A groups are composed of the same set of taxa; however, differ in size since smaller individuals require less oxygen (Kaiho, 1994): oxic group is composed of the large specimens (larger than 350 μm), and the Suboxic A group includes the smaller individuals. However, Baas et al. (1998) stated that the small specimens of these taxa have been reported from well oxygenated bottom waters (Schönfeld, 1997); therefore, the Oxic group should not be limited by size, and Suboxic A group should be eliminated. Following Baas et al. (1998), and since such a size fractionation in the studied samples was not carried out, a further distinction in Oxic and Suboxic A groups was not done. In addition, among these taxa, large

individuals of *Ammonia* spp. were present in MM50 and Station 2, large individuals of *Sigmoilopsis* sp. 1 and *Sigmoilinita tenuis* were present in K40K46, and large individuals of *Globocassidulina subglobosa* were present in Station 5. Other than these, large individuals of these taxa were not present in the studied samples. Therefore, these Oxic / Suboxic A group taxa were treated either as Oxic group, or as Suboxic A group in the following calculations.

Table 6.10 gives the relative abundances of the different groups among the whole samples. In total, these taxa (39 >2% taxa except textularin and unidentified taxa) make up 74.21% (Station 2) at minimum, 92.48% (K49.5L04) at maximum, in average ~86% of the total abundance. The highest relative abundances in the samples belong to Dysoxic group. In most samples the Suboxic D group makes up for more than 50% of the relative abundance. the exceptions are MM50, in which the Suboxic D group is only 25.89%, and Station 2, in which the Suboxic D group is only 40.26%. Highest abundance of Suboxic B group is in sample K51.2K09 (28.28%), and highest abundance of Suboxic group C is in MM50 (19.71%). Oxic or Suboxic A group is most abundant in K40K46 (20.73%). Ratios of the different groups amongst the assigned taxa were calculated as percentages for use in BFOI calculations (Table 6.10, % columns).

Utilizing the three equations of Benthic Foraminifera Oxygen Index (BFOI) calculations (Equation 6.4, Equation 6.5, Equation 6.6) the BFOIs were calculated with assuming all Oxic/Suboxic A taxa belonged to Oxic group (BFOI(O), Equation 6.4), assuming all Oxic/Suboxic A taxa belonged to Suboxic A group and the Suboxic C group was not included in the calculations (BFOI(I), Equation 6.5), and assuming all Oxic/Suboxic A taxa belonged to Suboxic A group and the Suboxic C group was included in the calculations (BFOI(S), Equation 6.6) (Table 6.11). Resulting bottom water oxygenation settings of the samples according to Kaiho's subdivisions (1999, Table 6.12) are also noted for each BFOI calculations (Table 6.11). For comparison, measured bottom water dissolved oxygen and corresponding bottom water oxygen conditions are given in Table 6.13.

Table 6.10. Summed relative abundances of taxa assigned to different groups in core-top samples: O: Oxic; S-A, B, C: Suboxic A, B and C; S: Suboxic total; D: Dysoxic; total relative abundances of the groups; ratios of the groups in all assigned population (%). Colors according to sample clusters (Figure 3.9).

Station	Tot O / S-A	Tot S-B	Tot S-C	Tot D	Tot	O% / S-A%	S-B%	S-C%	S%	D%
1 (19)	3.61	20.43	11.24	52.19	87.47	4.12	23.36	12.86	40.33	59.67
2	6.84	14.21	12.89	40.26	74.21	9.22	19.15	17.38	45.74	54.26
3 (19)	5.51	13.39	10.63	62.60	92.13	5.98	14.53	11.54	32.05	67.95
4	5.99	13.11	11.61	52.81	83.52	7.17	15.70	13.90	36.77	63.23
5	5.63	15.73	6.62	49.83	77.81	7.23	20.21	8.51	35.96	64.04
6	5.60	14.80	4.00	57.60	82.00	6.83	18.05	4.88	29.76	70.24
7	4.28	12.83	2.30	60.53	79.93	5.35	16.05	2.88	24.28	75.72
8	7.17	15.85	0.38	61.13	84.53	8.48	18.75	0.45	27.68	72.32
1 (21)	2.47	19.51	12.59	53.09	87.65	2.82	22.25	14.37	39.44	60.56
3 (21)	3.55	15.25	4.61	62.77	86.17	4.12	17.70	5.35	27.16	72.84
45C-1	7.35	15.44	2.21	59.56	84.56	8.70	18.26	2.61	29.57	70.43
45C-2	3.76	9.70	2.57	73.86	89.90	4.19	10.79	2.86	17.84	82.16
Izmit-deep	11.46	14.58	6.25	52.08	84.38	13.58	17.28	7.41	38.27	61.73
K40K46	20.73	16.46	2.44	52.44	92.07	22.52	17.88	2.65	43.05	56.95
K42K20	2.33	20.02	3.07	65.89	91.31	2.55	21.93	3.36	27.84	72.16
K49.5L04	2.15	12.57	5.37	72.40	92.48	2.32	13.59	5.81	21.72	78.28
K51.2K09	4.83	28.28	1.38	53.79	88.28	5.47	32.03	1.56	39.06	60.94
MM50	7.60	28.03	19.71	25.89	81.24	9.36	34.50	24.27	68.13	31.87

Table 6.11. Results of BFOI calculations according to BFOI(O): Equation 6.4, BFOI(I): Equation 6.5, BFOI(S): Equation 6.6 and resulting bottom water oxygenation classes. Colors according to sample clusters (Figure 3.9).

Station	BFOI(O)		BFOI(I)		BFOI(S)	
1 (19)	6.46	Low oxic	-34.23	Suboxic	-29.83	Suboxic
2	14.53	Low oxic	-32.83	Suboxic	-27.13	Suboxic
3 (19)	8.09	Low oxic	-38.41	Suboxic	-33.97	Suboxic
4	10.19	Low oxic	-36.72	Suboxic	-31.61	Suboxic
5	10.15	Low oxic	-35.00	Suboxic	-32.02	Suboxic
6	8.86	Low oxic	-36.92	Suboxic	-35.12	Suboxic
7	6.60	Low oxic	-38.98	Suboxic	-37.86	Suboxic
8	10.50	Low oxic	-36.32	Suboxic	-36.16	Suboxic
1 (21)	4.44	Low oxic	-35.36	Suboxic	-30.28	Suboxic
3 (21)	5.35	Low oxic	-38.48	Suboxic	-36.42	Suboxic
45C-1	10.99	Low oxic	-36.16	Suboxic	-35.22	Suboxic
45C-2	4.85	Low oxic	-42.29	Dysoxic	-41.08	Dysoxic
Izmit-deep	18.03	Low oxic	-33.33	Suboxic	-30.86	Suboxic
K40K46	28.33	Medium oxic	-29.25	Suboxic	-28.48	Suboxic
K42K20	3.42	Low oxic	-37.33	Suboxic	-36.08	Suboxic
K49.5L04	2.88	Low oxic	-41.55	Dysoxic	-39.14	Suboxic
K51.2K09	8.24	Low oxic	-30.95	Suboxic	-30.47	Suboxic
MM50	22.70	Medium oxic	-21.04	Suboxic	-15.94	Suboxic

Table 6.12. Bottom water oxygen conditions subdivisions in terms of dissolved oxygen (DO ml/l and μM) and corresponding BFOI ranges (Kaiho, 1999).

Oxygen condition	DO (ml/l)	DO (μM)	BFOI
High oxic	>3.2	>142.9	50 – 100
Medium oxic	2.0–3.2	89.3–142.9	15 – 50
Low oxic	1.2–2.0	53.6–89.3	0 – 15
Suboxic	0.3–1.2	13.4–53.6	-40 – 0
Dysoxic	0.1–0.3	4.5–13.4	-50 – -40
Anoxic	< 0.1l	<4.5	-55 – -50

Table 6.13. Bottom depth, measured bottom water oxygen (DO ml/l and µM), corresponding oxygen conditions ([1] according to Kaiho, 1999, Table 6.12) and redox conditions ([2] Alımlı, 2022) and total organic carbon (TOC%). Colors according to sample clusters (Figure 3.9).

Station	Bottom depth (m)	DO (µM)	DO ml/l	[1]	[2]	TOC %
1 (19)	65	45.71	1.023488	Suboxic	Hypoxic	1.35
2	112	35.92	0.804281	Suboxic	Hypoxic	1.39
3 (19)	240	7.68	0.171962	Dysoxic	Suboxic	1.56
4	435	10.26	0.229731	Suboxic	Hypoxic	1.4
5	100	57.4	1.285238	Low oxic	Hypoxic	1.16
6	192	17.09	0.38266	Suboxic	Hypoxic	1.69
7	290	7.25	0.162334	Dysoxic	Suboxic	1.66
8	414	6.34	0.141958	Dysoxic	Suboxic	1.49
1 (21)	67	49.3	1.103871	Suboxic	Hypoxic	1.34
3 (21)	195	21.7	0.485883	Suboxic	Hypoxic	1.66
45C-1	1214	4.6	0.102998	Dysoxic	Suboxic	1.25
45C-2	1214	4.6	0.102998	Dysoxic	Suboxic	1.25
Izmit-deep	206	0	0	Anoxic	Sulfidic	1.40
K40K46	318.5	5.5	0.12315	Dysoxic	Suboxic	1.25
K42K20	160	55.6	1.244934	Low oxic	Hypoxic	1.25
K49.5L04	100	38.4	0.859811	Suboxic	Hypoxic	1.25
K51.2K09	1185	20.5	0.459013	Suboxic	Hypoxic	1.25
MM50	53.5	56.6	1.267325	Low oxic	Hypoxic	0.75

The three different calculations of BFOI include the relative abundance of different groups and result in drastically different numbers. BFOI(O), for which all Oxic/Suboxic A group was considered Oxic, results in positive numbers in the range of 2.88 (K49.5L04) – 28.33 (K40K46) which correspond to low oxic to medium oxic environments (Table 6.11). BFOI(I) and BFOI(S), on the other hand, result in negative numbers ranging between -41.29 (45C-2) and -21.04 (MM50) for the former, and -41.08 (45C-2) and -15.94 (MM50) for the latter, and correspond to dysoxic to suboxic environments (Table 6.11). The BFOI(O) and BFOI(I) results are taken as maximum and minimum possible values (since no size fractionation and distinction among Oxic and Suboxic groups was carried out), and the results are plotted against measured bottom water oxygen (Figure 6.8), showing the bottom

water oxygen conditions of only 11 core-top samples out of the studied 18 could be correctly identified if a distinction between Oxic and Suboxic A groups were made. These samples are 45C-2 as dysoxic; Station 6, K51.2K09, Station 3 (21), Station 2, K49.5L04, Station 1 (19) and Station 1 (21) as suboxic, and K42K20. MM50 and Station 5 as low oxic (in the order of increasing measured bottom water oxygen). Remaining 7 core-top samples, which come from anoxic (sulfidic) to dysoxic bottom water conditions (0-0.3 ml/l DO) cannot be identified as such via the BFOI, even the minimum BFOI (i.e., BFOI(I)) values are higher than anoxic-dysoxic range.

Kaiho (1999) stated that the BFOI cannot be used to pinpoint the bottom water oxygen as high accuracy numerical values, i.e., the correlation Kaiho (1994 and 1999) produced cannot be used as is. That is to say, BFOI can only separate different bottom water oxygen conditions such as oxic, suboxic, anoxic. Contrary to this, Kaminski (2012) did use the correlation of Kaiho (1994) to obtain "calculated" oxygen values and compared them to measured values, stating that the differentials are small enough. In Kaminski's study, all their samples were from oxic environments (>~1.2 ml/l DO), and their BFOI (BFOI(O)) were between 1.5 and 65. For the dissolved oxygen values between 1-2 ml/l, the calculated and measured oxygen values matched better than higher oxygen conditions. In addition, the top 40 m and 80-140 m (water depth) of their transect showed better correlation between calculated and measured DO values. Because Kaminski's study and this present study span different types of environments (oxic versus mostly suboxic), a comparison between the two will not be productive.

Nonetheless, had the size fractionation of the Oxic/Suboxic A group taxa were done, the results, at least for the oxic and suboxic stations (DO > 0.3 ml/l), could have been more accurate, and this result shows the applicability of BFOI, although to a limited extent. The taxa assigned to Oxic/Suboxic A group do not only occur in such environments, but also are present in lower oxygen settings (see the ~5% abundance of Oxic/Suboxic A group in dysoxic samples in Table 6.10). One extreme example is station K40K46 whose 20% of total foraminiferal abundance belongs to the Oxic/Suboxic A group taxa (Table 6.10).

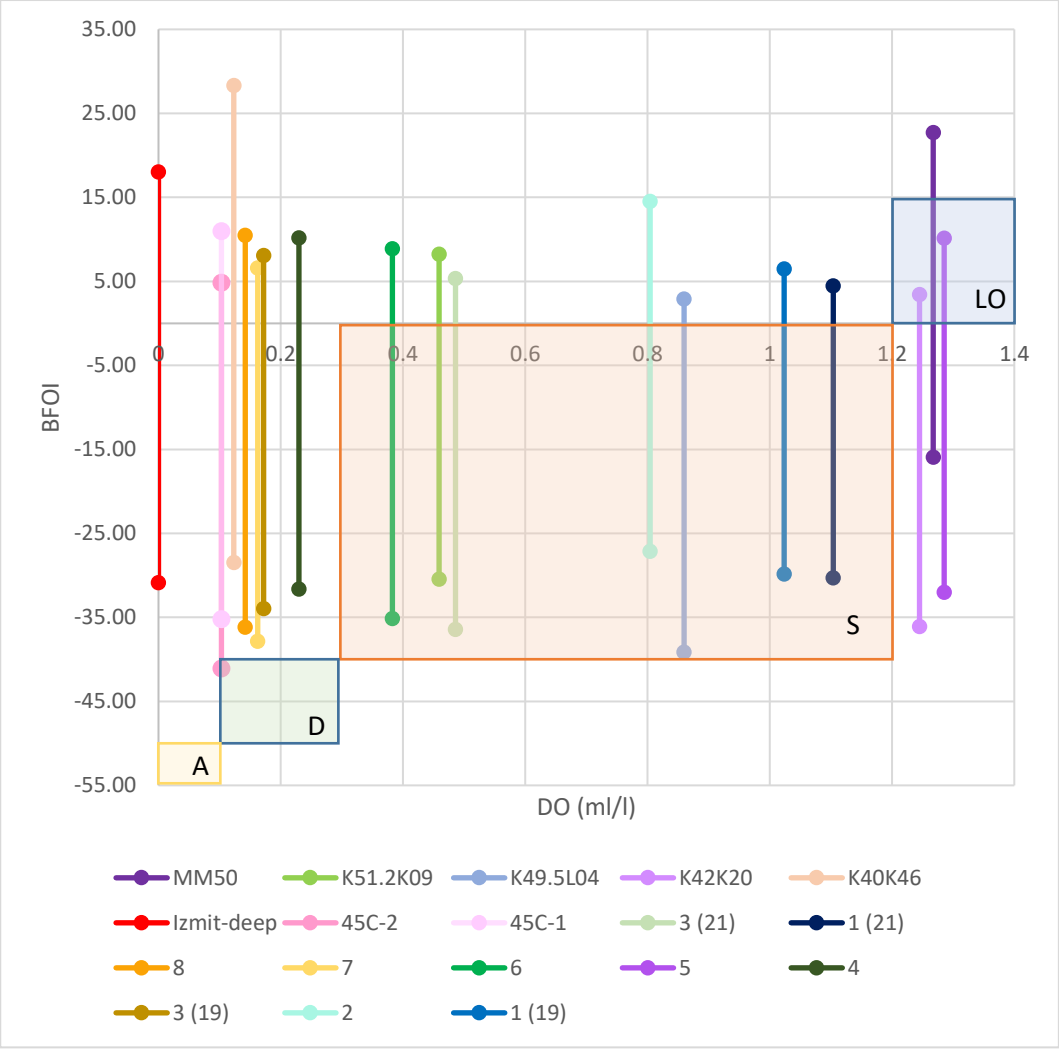


Figure 6.8. Maximum (O) and minimum (I) calculated BFOI values of the stations (Table 6.11) plotted against measured bottom water dissolved oxygen. Anoxic (A), dysoxic (D), suboxic (S) and low oxic (LO) ranges as given in Kaiho (1999) drawn on the plot.

6.2.4 Foram-AMBI

For the application and evaluation of Foram-AMBI (Alve et al., 2016), the taxa identified in this study were assigned to ecological groups for the core-top samples. Jorissen et al.'s (2018) assignments for the Mediterranean Sea was followed for the

most of the taxa; the assignments of the taxa which appear in that list with different names (synonyms and possible synonyms) and the assignment of several taxa which do not occur on Jorissen et al.'s list (mostly supraspecific taxa) are given in Table 6.14.

Since in the calculation of Foram-AMBI (Equation 6.7) the not-assigned taxa effectively act as EGI with zero (0) weight, and lower the Foram-AMBI value, leaving taxa unassigned was avoided as much as possible. For this purpose, *Ammonia* spp., *Elphidium* spp., Ellipsolagenidae, Glabratellidae, *Globobulimina* spp., *Pyrgo* spp., *Spirillina* spp. were assigned to either the EG of the only species or to an average of the species present in Jorissen et al.'s list (Table 6.14). *Bolivina* cf. *vadescens* and *Paracassidulina minuta*, two very abundant taxa, do not occur in Jorissen et al.'s list. Although in some publications the name *Bolivina catanensis* was used for individuals belonging to *B.* cf. *vadescens*, in the dataset of Jorissen et al. (2018) considered *B. catanensis* occurrences (assigned to EGI) came from Romano et al. (2009, 2013), who distinguished the taxon sensu Sgarrella and Moncharmont Zei (1993) which is not a synonym for *B.* cf. *vadescens* as distinguished here.

Table 6.14. Assignments of taxa to ecological groups (EG, in Arabic numerals) in this study [TS] and the reasoning (R) for those that differ from Jorissen et al. (2018, [2]) in name or assignment. M: mixed (for supraspecific assignments), *: see text for explanation.

Taxa [TS]	EG [TS]	Taxa [2]	EG [2]	R
Ammonia spp.	2	*Ammonia inflata*	2	M
		Ammonia compacta	3	
		Ammonia parkinsoniana	1	
		Ammonia tepida	4	
Ammoscalaria pseudospiralis	2	*Ammoscalaria foliaris*	2	
Articulina tubulosa	1	*Articulina mucrunata*	1	
Aubignyna perlucida	3	*Ammonia perlucida*	3	
Bolivina dilatata	2	*Bolivina dilatata*	2	
		Bolivina dilatata spathulata	1	
Bolivina spathulata	3	*Bolivina dilatata spathulata*	1	
		Bolivina spathulata	3	

Table 6.14. Continued.

Taxa [TS]	EG [TS]	Taxa [2]	EG [2]	R
Bolivina cf. *vadescens*	3			*
Bolivina spp.	3			*
Cassidulina laevigata	4	*Cassidulina carinata*	4	
		Cassidulina laevigata	4	
Eilohedra vitrea	4	*Epistominella vitrea*	4	
Elphidium spp.	2	12 *Elphidium* species	In 1-3 range	M
Ellipsolagenidae	2	*Fissurina orbignyana caribaea*	2	M
Glabratellidae	1	*Glabratella erecta*	1	M
		Glabratella hexacamerata	1	
Globobulimina spp.	2	*Globobulimina affinis*	2	
Globocassidulina oblonga	2	*Cassidulina oblonga*	2	
Haynesina depressula	2	*Elphidium depressulum*	2	
Lobatula lobatula	1	*Cibicides lobatulus*	1	
Melonis pompilioides	3	*Melonis barleeanus*	3	
Nonionella opima	5	*Nonionella opima*	4	*
		Nonionella turgida	5	
Paracassidulina minuta	3			*
Porosononion granosum	3	*Porosononion subgranosum*	3	
Pyrgo spp.	2	*Pyrgo oblonga*	2	M
Quinqueloculina schlumbergeri	3	*Quinqueloculina stelligera*	3	
Sigmoilinita costata	1	*Sigmoilina costata*	1	
Sigmoilopsis sp. 1	3	*Sigmoilopsis schlumbergeri*	3	
Spirillina spp.	3	*Spirillina vivipara*	3	M
Textularia gramen	3	*Textularia bocki*	3	
Textularia pala	1	*Textularia truncata*	1	
Virgulinella fragilis	5			*

Therefore *B.* cf. *vadescens* was not assigned to EGI, but instead to EGIII along with *Bolivina spathulata* due to its high abundance in the same stations with the latter (Table 6.14). Same approach was taken for *P. minuta*: since it is most abundant with *B. spathulata*, it was assigned the same group (Table 6.14). For *Bolivina* spp., an undifferentiated taxon used mostly for undistinguishable minute (juvenile) forms, EGIII was chosen since most of the individuals belonging to the genus are of *Bolivina spathulata* and *Bolivina* cf. *vadescens*, both assigned to EGIII (Table 6.14).

Nonionella turgida is one of the two EGV taxa in Jorissen et al. (2018), and *Nonionella opima*, which may be a synonym to *N. turgida* is assigned EGIV in Jorissen et al.'s list; therefore, for *N. opima* in this study, the worse condition (EGV) is chosen. Finally, *Virgulinella fragilis*, a taxon which appears abundantly only in sulfidic Izmit-deep station (Karamürsel Basin) was assigned to EGV (Table 6.14).

This way, from a total of 134 taxa (excluding unidentified and indeterminate taxa) identified in the core-top samples of the 18 studied stations, 74 were assigned to ecological groups (Table 6.15): EGI, EGII and EGIII each include 23 taxa, EGIV includes 3 taxa and EGV includes 2 taxa; and remaining 60 taxa are not assigned. The not assigned taxa make up the 4.9% to 21.2% of the total assemblage, is higher than 20% only in Station 2 (Figure 6.9A, Table 6.16), therefore the use of Foram-AMBI are in accordance with the guidelines of Borja and Muxika (2005).

By utilizing Equation 6.7 (Borja et al., 2000), the Foram-AMBI values were then calculated first by using the relative abundances of ecological groups as is (Figure 6.9A), and then by removing the not assigned taxa from the dataset and recalculating the relative abundances (Figure 6.9B) as proposed by Borja et al. (2012).

The calculated Foram-AMBI values are minimum 1.80 and maximum 2.36 by using the total assemblages; while, eliminating the not assigned taxa from the dataset the values become minimum 2.16 and maximum 2.69 (Table 6.16). The assemblage in all stations are dominated by EGIII. These values fall in the range of "slightly polluted" (1.2 to 3.3) in site pollution and the assemblage is "unbalanced" according to the AMBI classification of Borja et al. (2000).

Table 6.15. List of taxa assigned to ecological groups (EG, in Arabic numerals, color coded). Taxa abbreviations as in Supplementary Table A.1.

EG	Taxon
1	*A_tubul*
1	*Adelosi*
1	*Aster_m*
1	*Astro_s*
1	*B_vades*
1	*C_refulg*
1	*D_berthe*
1	*G_praeg*
1	*Glabra*
1	*L_lobat*
1	*M_subro*
1	*N_terqu*
1	*Plor_me*
1	*R_brady*
1	*R_globu*
1	*R_mpora*
1	*R_spinu*
1	*Ros_spp*
1	*S_costa*
1	*S_excav*
1	*T_pala*
1	*T_trica*
1	*T_trigo*
2	*A_pspir*
2	*Amm_spp*

EG	Taxon
2	*Amphi_1*
2	*Amphi_s*
2	*B_alata*
2	*B_costa*
2	*B_dilat*
2	*B_labia*
2	*B_nodos*
2	*B_pspli*
2	*B_varia*
2	*Elphidi*
2	*G_sglob*
2	*G_umbon*
2	*Gbulimi*
2	*Gcassid*
2	*H_balth*
2	*H_depre*
2	*N_grate*
2	*P_laevi*
2	*Pyrgo*
2	*T_angul*
2	*U_medit*
3	*A_perlu*
3	*Aster_a*
3	*B_acule*
3	*B_elong*

EG	Taxon
3	*B_margi*
3	*B_spath*
3	*B_stria*
3	*Bol_spp*
3	*C_invol*
3	*Celp_po*
3	*H_pacif*
3	*M_bulbo*
3	*M_pompi*
3	*Pcas_mi*
3	*Poros_g*
3	*Q_pygma*
3	*Q_schlu*
3	*R_phleg*
3	*Sigmoi_1*
3	*Spirill*
3	*Stai_fu*
3	*T_agglu*
3	*T_grame*
4	*C_laevi*
4	*E_vitre*
4	*V_brady*
5	*N_opima*
5	*V_frag*

The calculated Foram-AMBI values (after elimination of not assigned taxa) were investigated in terms of the relationships with environmental variables (Table 3.7). No relationship was discovered for the evaluated variables, except for a slight correlation with total organic carbon (TOC, R^2=0.3424, Figure 6.10). However, given that the species assignments were done with respect to the distribution of abundances of taxa along the TOC gradient, the relationship between the Foram-AMBI and TOC is poorer than expected.

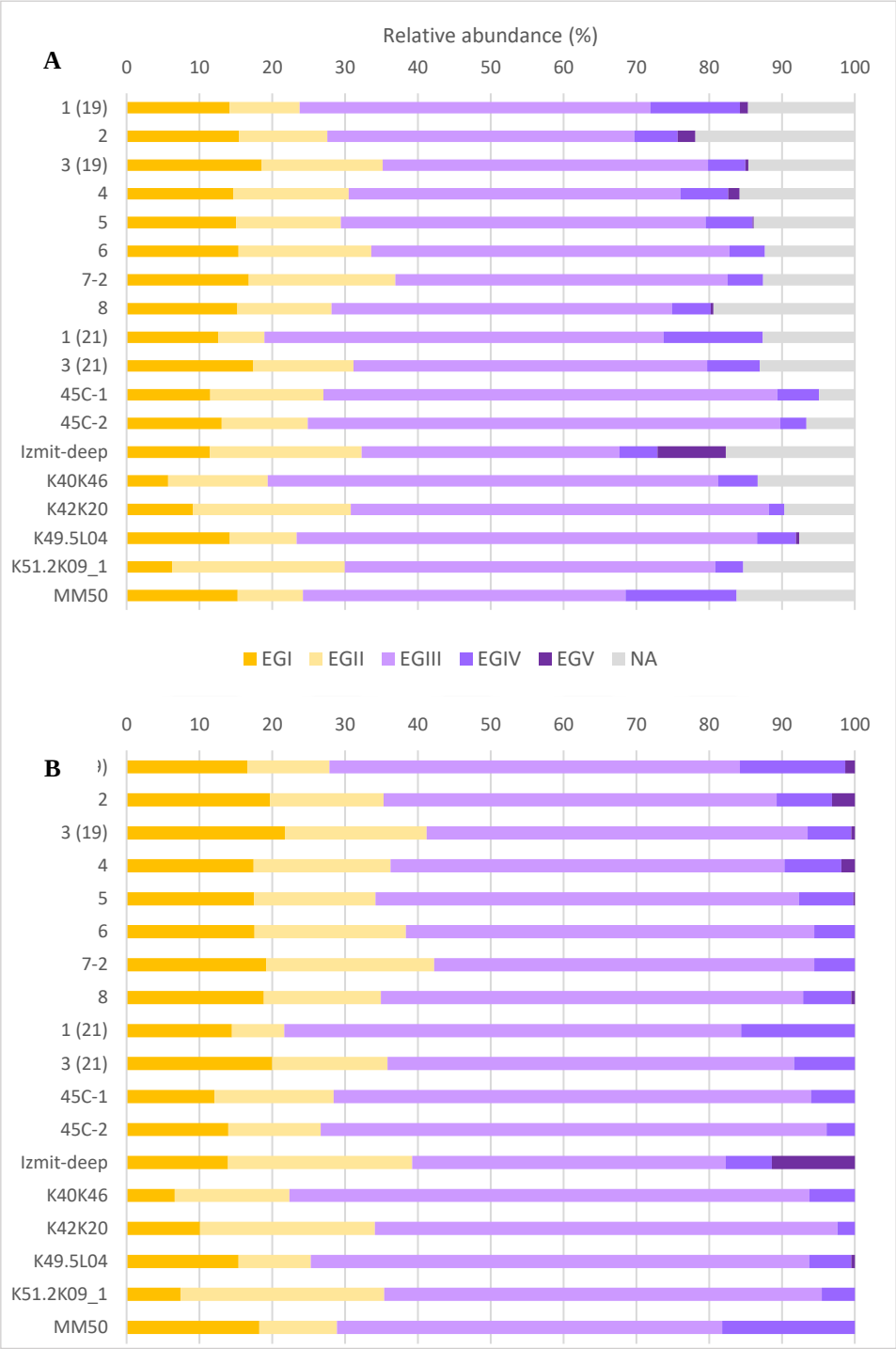


Figure 6.9. Relative abundances of ecological groups (EGI-V) and not assigned (NA) taxa in the core-top samples: A. in total assemblage, B. only among assigned taxa.

Table 6.16. Number of specimens (N, excluding unidentified and indeterminate taxa), ratio of not assigned taxa (NA%), calculated Foram-AMBI values for (1) using the total assemblage, and (2) using only the assigned taxa.

Station	N	NA (%)	Foram-AMBI (1)	Foram-AMBI (2)
1 (19)	1153	14.66	2.21	2.59
2	370	21.89	1.86	2.38
3 (19)	253	14.62	1.84	2.16
4	259	15.83	1.99	2.37
5	591	13.87	2.02	2.34
6	494	12.35	1.97	2.24
7-2	596	12.58	1.89	2.16
8	263	19.39	1.86	2.31
1 (21)	396	12.63	2.35	2.69
3 (21)	276	13.04	1.99	2.29
45C-1	122	4.92	2.36	2.48
45C-2	498	6.63	2.29	2.45
Izmit-deep	96	17.71	2.17	2.64
K40K46	315	13.33	2.30	2.66
K42K20	932	9.66	2.14	2.37
K49.5L04	916	7.64	2.30	2.49
K51.2K09_1	287	15.33	2.05	2.43
MM50	413	16.22	2.15	2.57

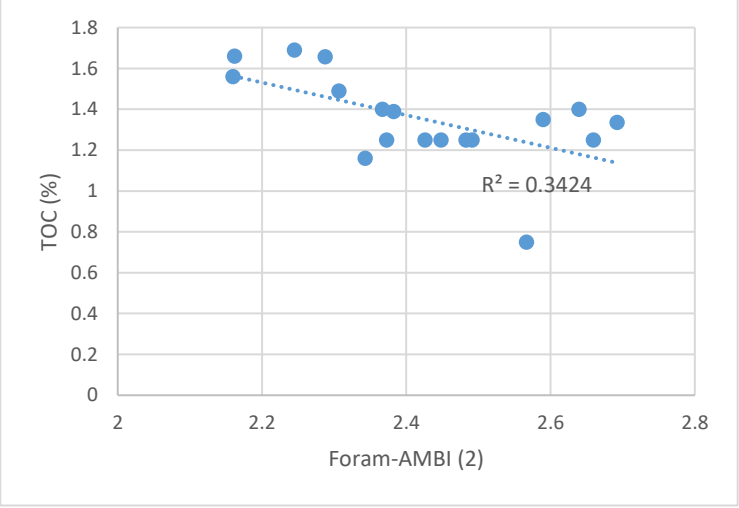


Figure 6.10. Scatter plot for total organic carbon (TOC%, see Table 3.7) and Foram-AMBI values calculated for only assigned taxa (see Table 6.16). A linear trend-line added and its correlation coefficient noted.

CHAPTER 7

A FORAMINIFERAL EVIDENCE FOR THE ESTABLISHMENT OF SULFIDIC BOTTOM WATER CONDITIONS IN THE KARAMÜRSEL BASIN AFTER THE '99 EARTHQUAKE

The Izmit-deep core from the Karamürsel Basin (Izmit Bay) was examined and the benthic foraminifera assemblage was quntified in detail. The core is remarkebly different from all other cores studied from SoM in that the benthic and planktonic foraminiferal absolute abundances are very low and a sulfidic water prone species, *Virgulinella fragilis*, is abundant in the top part of the core; but a normal SoM assemblage is present in the bottom part of the core. Due to this uniqueness the core was dated (AMS ^{14}C), and a hypothesis of its depositinal history was constructed.

7.1 Properties of the Karamürsel Basin and previous works

The Karamürsel basin floor is restricted by the North Anatolian Fault and en-echalon folds to the north, and to the south it is restricted by a paleo-shelf break (at about 72 m depth, paralleling the shore) which is mostly continuous on the eastern side, but is disrupted by mass movements on the western side (Cormier et al., 2006, Figure 7.1). The basin floor sedimens of the Karamürsel Basin are composed of tubiditic (sandy) units capped by muddy levels which include homogenites and hemipelagic facies (McHugh et al., 2006), strata progressively tilted toward north (towards North Anatolian Fault - NAF, Figure 7.2, Cormier et al., 2006). Surficial sediments of the basin floor are predominantly clay sized (Ergin and Yörük, 1990; Algan et al. 1999). According to Okyar et al. (2008) the Holocene sediments in the Gulf of Izmit are about 25 m thick maximum, and in the basin-floor of the Karamürsel Basin the Holocene succession is about 5 m thick.

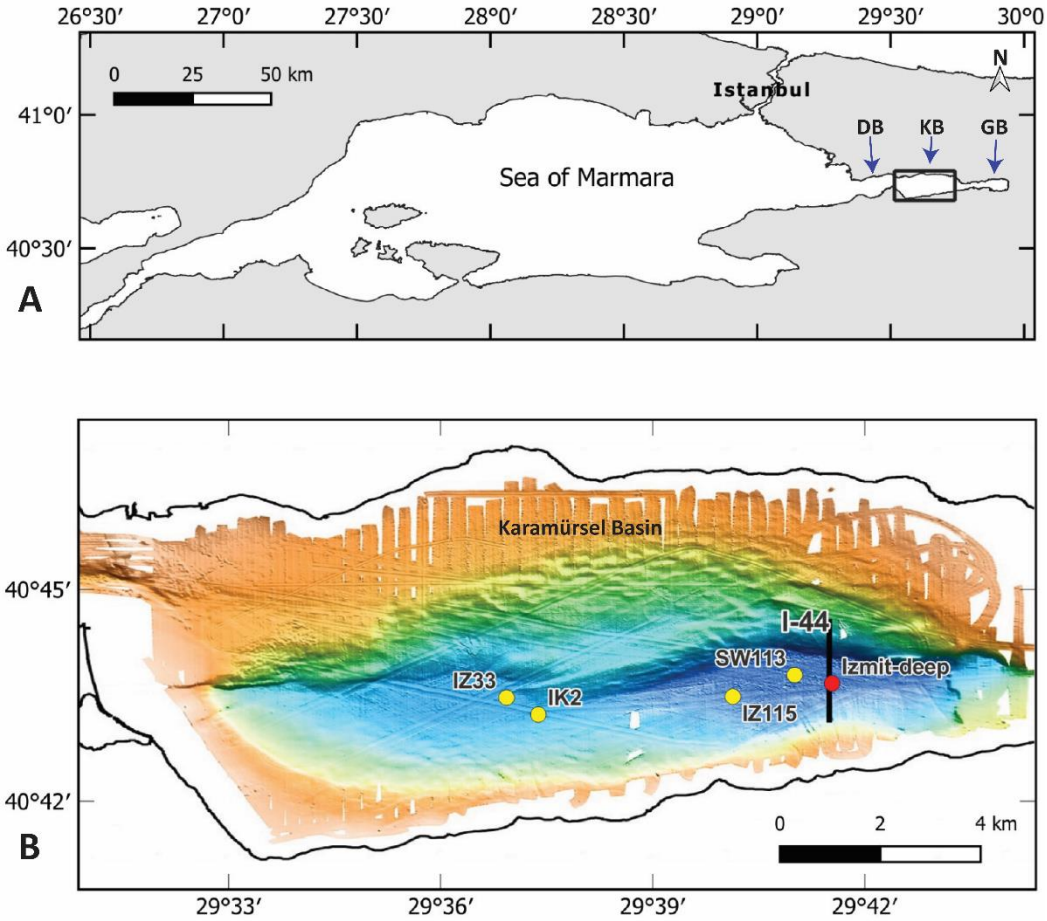


Figure 7.1. A. Locations of the Darıca, Karamürsel and Gölcük basins (DB, KB, GB respectively), black rectangle shows the extent of the map in B; B. Locations of dated cores, from west to east: IZ33 (McHugh et al., 2006; Gasperini et al., 2018), IK2 (Arslan Kaya, 2023b); IZ115 and SW113 (Çağatay et al. 2012); and Izmit-deep (this study); and the Chirp profile line I-44 (Figure 7.2) on multibeam bathymetry of Karamürsel Basin (Cormier et al., 2006).

Table 7.1 lists the coordinates and water depths of the cores from four publications from the same area (Karamürsel Basin, see locations on map, Figure 7.1). Three of these cores (IZ-33, McHugh et al., 2006 and Gasperini et al. 2018; and IZ-115 and SW-113, Çağatay et al. 2012) were applied dating methods (14C and/or Pb210&Cs), the other (IK-2, Arslan Kaya et al., 2023b) was only correlated lithologically with IZ-115. For all four of these cores, the turbidite-homogenite units were correlated with the historical earthquakes (Figure 7.3).

Table 7.1 Coordinates and water depth of cores from the Karamürsel Basin.

ID	Reference	Longitude	Latitude	Water depth (m)
IZ33	McHugh et al., 2006 and Gasperini et al., 2018	29.6155	40.7244	~160
IK2	Arslan Kaya, 2023b	29.623	40.7204	156
IZ115	Çağatay et al. 2012	29.6689	40.72464	199
SW113	Çağatay et al. 2012	29.6835	40.72974	210
Izmit-deep	This study	29.69232	40.72777	206

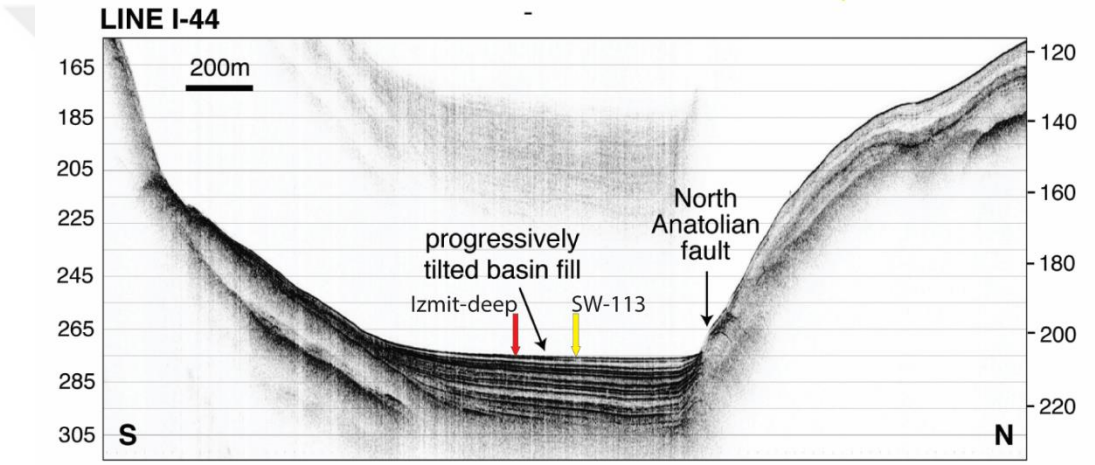


Figure 7.2. Line I-44 chirp profile: flat bottom of the central basin; note how beds become progressively tilted toward the North Anatolian Fault (Cormier et al., 2006). Positions of Izmit-deep (red arrow) and SW-113 (yellow arrow) cores projected onto the line of section are shown.

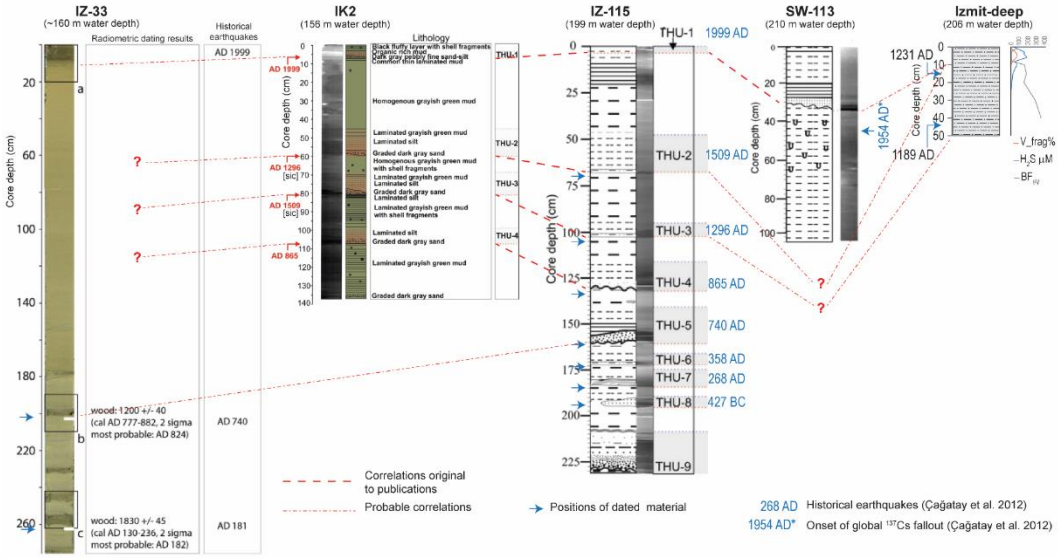


Figure 7.3. Cores from the Karamürsel Basin. Correlated historical earthquake dates in IZ-115 and 1954 AD (by ^{137}Cs isotope) in SW-113 are directly taken from Çağatay et al. (2012). Blue arrows show positions of dated material. Relative abundance of *V. fragilis* (V_frag%), hydrogen sulfide concentration (H_2S µM) and total benthic foraminiferal abundance (weight normalized: $BF_{\#V}$) given for Izmit-deep core. Red dashed lines for correlations made by original authors; red dash-dot lines with arrow heads and question marks added for visualization of probable continuations. Y-axis same throughout. See Figure 7.1and Table 7.1 for locations and references.

7.2 Turbidite-Homogenite Units (THUs) in the Karamürsel Basin

Homogenite term was first used for homogeneous reflectors in seismic section which corresponds to predominantly structureless mud layers associated with turbidites in the Mediterranean Sea (Kastens and Cita, 1981; Heike, 1984; McHugh et al., 2006). They may be mud-turbidites or distal turbiditic facies. They may include some lamination; however, they rarely contain foraminifers which distinguishes them from hemipelagic deposition (McHugh et al., 2014, Bektaş et al., 2024). These mud-rich homogenites may take months to settle from suspension (McHugh et al., 2006).

The turbidite-homogenite units (THUs) term in the recent paleoseismology studies is being used to represent turbiditic units composed of sand-rich (thin) bottom

lamellae overlain by structureless mud-rich (thicker) homogenite part, which is ideally overlain by hemipelagic sedimentation (e.g., Çağatay et al., 2012). In the Sea of Marmara, at the bottom of the THU units, the sand-rich laminations are usually thin (e.g., 5-10 cm, McHugh et al., 2006; 1-5 cm in IZ-115, Çağatay et al., 2012) or there may be only silt increase with minor sand contribution, with the base of the units being usually somewhat scoured (Çağatay et al. 2012). These sand- or silt- rich layers may be accompanied by slight increase in density and increase in magnetic susceptibility. The following units are mud-rich homogenites.

The distinction between homogenites and hemipelagic sedimentation is not stratightforward, may as well be gradational (Goldfinger, 2011). There are no globally applicable criteria yet for the distinction of homogenite and hemipelagite, and it should be done with a site-specific set of criteria (Goldfinger, 2011). Some of these criteria are grain size, density, magnetic susceptibility and elemental concentrations; other criteria may be bioturbation and biogenic composition (or lack thereof). Bioturbation occurs in hemipelagic deposits, but is only restricted to the uppermost part of the homogenite where the sediment can be bioturbated after recolonization (Goldfinger, 2011; Bektaş et al., 2024); however, if the homogenite is not thick enough, bioturbation will mix all of it down to the coarse grained trubidite. Biogenic composition (foraminifera) is also lacking in the homogenites since the deposition is so fast and the grain size is so fine (Anschutz et al., 2002; Bolliet et al., 2014; Bektaş et al., 2024), only the bottom sandy part include foraminifera (allochthonous); however, again, if the homogenite is not thick enough the whole thickness may be recolonized by infaunal taxa and lose this signal. In addition, any post-depositionional changes (i.e., winnowing and dissolution) can alter the biogenic composition (e.g., foraminiferal assemblage) of the hemipelagic deposits, making it difficult to distinguish from homogenites (Hayward et al., 2019b).

Çağatay et al. (2012) described nine THUs going back to 427 BC at about 2 m depth in the core IZ-115 (Figure 7.3). In IZ-115 the last (most recent) turbidite-homogenite unit (THU-1) is ascribed to 1999 Izmit earthquake and only encompasses about 4 cm

of sediment at the top of the core while in the nearby core SW-113 this event produced about 30 cm of deposition with an erosional base. SW-113 is located to the north east of IZ-115, and is at a slightly deeper setting. To the west, core IK2 (Arslan Kaya et al., 2023b) was correlated to IZ-115 by means of lithostratigraphy and the THU-1 constitute about top 8 cm of the core. Lastly in IZ33 (McHugh et al., 2006 and Gasperini et al., 2018), the seismoturbidite encompassing the top ~10 cm of the core is ascribed tentatively to 1999 earthquake.

THU-2, 3 and 4 described in IZ-115 are dated to correspond to 1509, 1296 and 865 AD earthquakes (Figure 7.3, Çağatay et al., 2012) and only occur in one other core: IK2 (which is correlated only by means of lithostratigraphy, Arslan Kaya et al., 2023b). In IZ-33 (very close to IK2) these earthquakes are not represented by THUs (McHugh et al., 2006; Gasperini et al., 2018). In SW-113, these events are outside the bounds of the core (Çağatay et al., 2012). THU-5 is described in IZ-33 and IZ-115 and dated to 740 AD earthquake (McHugh et al., 2006; Çağatay et al., 2012), in other cores it is outside the bounds of the cores.

Not considering the westernmost core (IZ-33), the thicknesses between bases of THU's (i.e., the whole turbidite+homogenite+hemipelagite succession) seem to get thicker eastward (Figure 7.3). This may be due to erosion of the top of the successions (hemipelagic deposits and/or homogenites) just below the following turbidite, or because the depocenter is in the vicinity of SW-113, which sits at the deepest part (210 m) of the basin, and IK-2 and IZ-115 are on a slight slope facing east toward SW-113 (Figure 7.1). Still, the "natural" thickness of the depostis in SW-113 do not preclude the erosion hypothesis.

7.3 Properties of the Izmit-deep core

Below, several properties of the core are given. These properties are later used in the interpretation of the core in terms of the nature of deposits.

7.3.1 Sand content

The sandy intervals of THUs may be of various thicknesses, usually in centimeter scale (as can be seen in Figure 7.3). However, there may be sand – mud alternations in those turbidite sections and in actuality the sand levels maybe only as thick as millimeters.

In Izmit-deep core, there is not a grain size analysis of enough of a high resolution, therefore detection of such fine sand laminations is impossible. The sand content (weight% material coarser than 63 μm) of the samples is the only grain size measure, given below in Figure 7.4. The samples are about 0.75 % sand in average, and the values change between 0.31% and 1.93%. Only up to 2% by weight of the samples are sand sized. This figure includes both siliciclastic and biogenic material, as well as organic debris and mud clumps (which did now wash out).

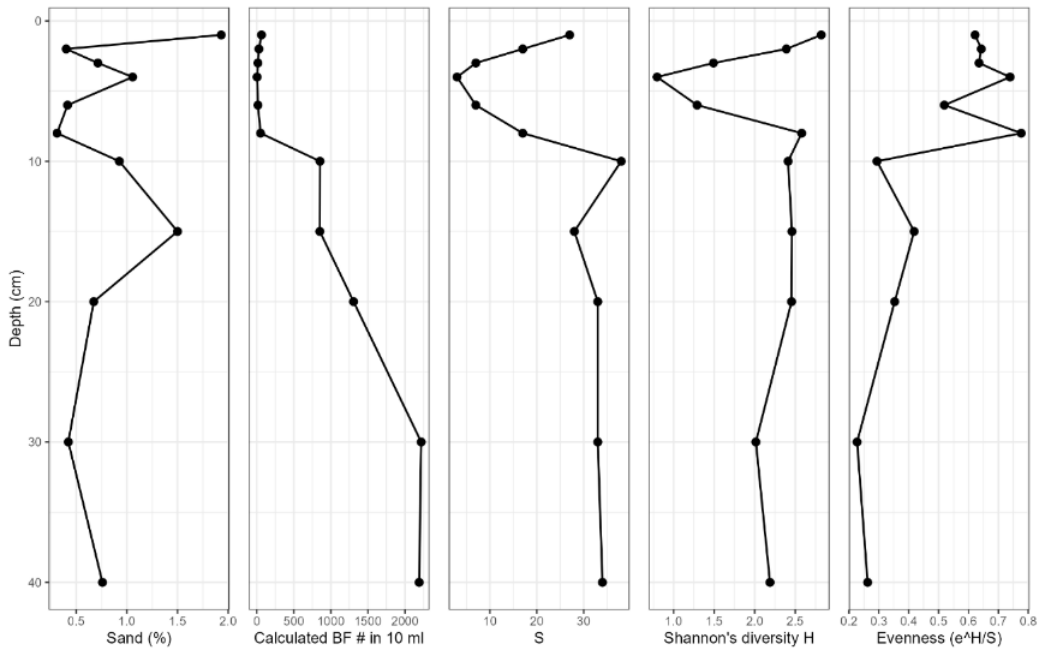


Figure 7.4. Sand content (% weight), calculated benthic foraminifera number in 10 ml of sediment, species richness, Shannon's diversity and evenness in the Izmit-deep core.

7.3.2 Bottom and pore water chemistry (Alımlı, 2022)

The most striking feature of the bottom water properties of the Izmit-deep station is the high concentration of H2S and absence of dissolved oxygen. Alımlı (2022) reported the bottom water and pore water properties of the station. H_2S is 30 µM and NH_4 is 1.5 µM in the bottom water. In addition, the pore waters of the core include very low levels of dissolved iron (up to 3 µM) and low NO_3. NH_4 increases downward in the core with a change in gradient at 15 cm, while H_2S increases towards 6 cm sample, then decreases down, diminishing after 15 cm sample (Figure 7.5). According to Alımlı (2022) the change in gradient in NH_4 and the absence of H_2S below 15 cm indicates different redox conditions in the bottom part of the core.

7.3.3 Sedimentation rate

^{14}C ages of the 15 cm and 45 cm samples, 1231 AD ± 22 and 1189 AD ± 22 are very close to each other. Assuming the succession between samples do not include breaks in sedimentation, these results mean a sedimentation rate of 0.8 cm/yr (35 cm sediment deposition in 42 years) which is very high compared to the literature (0.07 cm/yr, Ergin and Yörük, 1990; 0.36 cm/yr, Çağatay et al., 2012). But the number agrees with 0.5-1 cm/yr figure for the depocenters of turbiditic material (McHugh et al., 2006) and exactly matches the 0.8 cm/yr figure of Sorichetta et al. (2010). The 10 cm of the core (post 1231 AD) is also very short to be a result of continuous hemipelagic sedimentation after 1231 AD, which would make up a 0.013 cm/y sedimentation rate (10 cm of sediment deposition in 790 y).

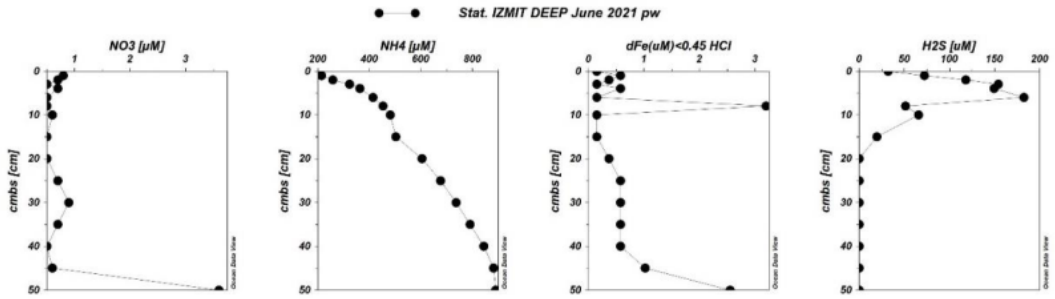


Figure 7.5. Pore water properties of the core Izmit-deep (Alımlı, 2022).

7.3.4 Benthic foraminifera absolute abundance

Throughout the Izmit-deep core, change in absolute benthic (total: live+dead) foraminifera abundance ($BF_{\#W}$: normalized to 1-gram dry sediment) is significant (Figure 7.6). $BF_{\#W}$ in the Izmit-deep core is higher in the bottom part (bottom to 10 cm). In 40 cm sample the $BF_{\#W}$ is 346.6, which is similar to the number in the surface sample of Central Deep station (K51.2K09 1 cm: $BF_{\#W}$ =341.54; See Section 3.1). From 40 cm to 10 cm (153.2) benthic foraminifera number decreases two-fold, however, from 10 cm to 8 cm (11) the decrease is even higher (more than 10-fold). From there to 4 cm the $BF_{\#W}$ decreases even further down to 1.8, then it increases upward and is 68.7 in the surface sample.

Live benthic foraminifera abundance is almost zero in this core. Apart from one specimen in sample 10 cm, no stained foraminifera were found. Yet, all of the individuals belonging to *Virgulinella fragilis* Grindell and Collen, and very few of other taxa were found to be pink tinted, which is taken to be an evidence for, although little, some organic tissue being present in the tests at the time of sampling.

7.3.5 Planktonic foraminifera absolute abundance

Planktonic foraminiferal abundance (number in gram dry sediment) in the Izmit-deep core is almost zero (Figure 7.6). Very low abundance of planktonic foraminifera in the whole Karamürsel Basin is evident in that even the ^{14}C dating of cores form the basin were carried out from benthic foraminifera, mollusk shells and wood (McHugh et al., 2006; Çağatay et al., 2012) instead of planktonic foraminifera which is the actual preferred medium for such analysis. In addition, Kırcı-Elmas et al. (2021) studied cores on top of the 64 m deep ridge separating Karamürsel Basin from the Western (Darıca) Basin and reported that planktonic foraminifera are very rare. Although recent studies show that planktonic foraminifera do not perform daily (diurnal) vertical migration (Meilland et al., 2019), they do migrate through the water column during their life cycle (Pratch et al., 2019); therefore, this ridge separating the Karamürsel and Darıca basins may be a natural barrier for planktonic foraminifera preventing them from entering the bay. Another possible reason for their near absence in the basin may be due to the upper water column circulation; since planktonic foraminifera are passive floaters, diminished upper layer circulation entering the bay (Algan et al., 1999; Mutlu et al., 2024) would mean lower numbers of planktonic foraminifera entering the bay. The very low number of planktonic foraminifera must be due to a combination of factors such as upper water column properties and competition with other zooplankton, in addition to the sill depth.

Planktonic foraminifera absolute abundance ($PF_{\#W}$) in the samples, although with extremely smaller numbers, show a similar distribution as benthic foraminifera abundance (Figure 7.6). At the top 1 cm, $PF_{\#W}$ is the highest (4.3), halves in the second sample (2), and between 0-1 individuals per g dry sediment for the rest of the core.

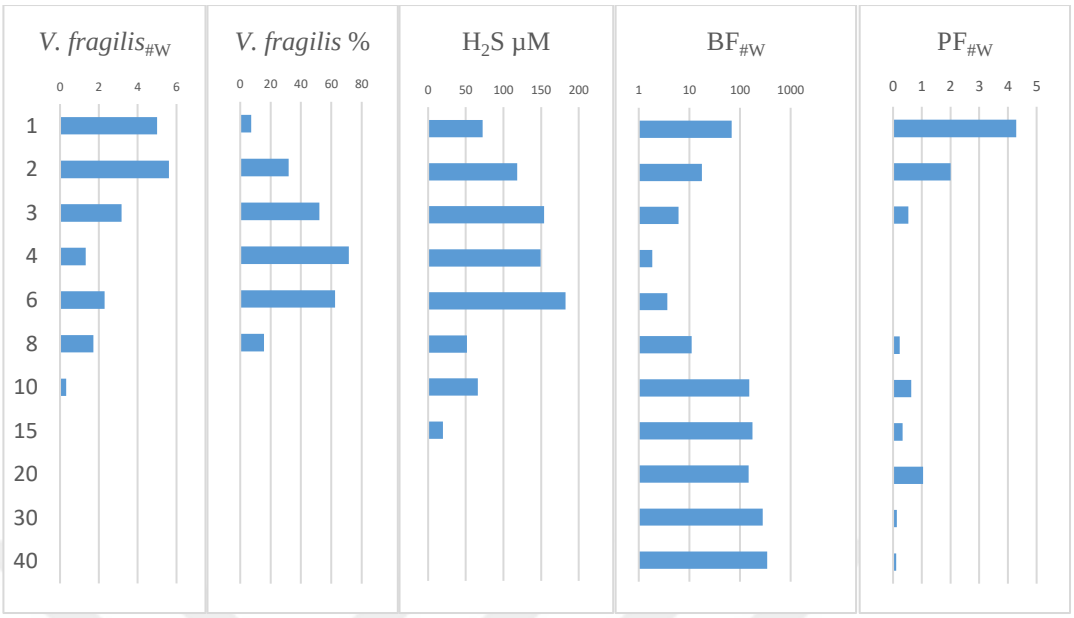


Figure 7.6. Absolute (number in gram dry sediment) and relative (%) abundances of *Virgulinella fragilis*, H_2S content of pore water (µM), absolute abundance of benthic foraminifera (x-axis log scale) and planktonic foraminifera (number in gram dry sediment). Y-axis not to scale.

7.3.6 Benthic foraminifera assemblage

Benthic foraminifera assemblage (relative abundances of taxa) of the core is given in Figure 4.12. The core is characterized by the presence and abundance of *Virgulinella fragilis* Grindell and Collen in the top 10 cm of the core. The abundance of this form peaks at 4 cm sample (3.5 cm depth in core) and is accompanied by some *Ammonia* spp. and *Bolivina* spp. Relative abundance of *V. fragilis* decrease towards sample 10 cm, and the taxon is absent in the samples below this level. Below 10 cm, the assemblage is dominated by *Bolivina* species (*Bolivina spathulata* (Williamson), *Bolivina dilatata* Reuss, *Bolivina* cf. *vadescens* Cushman) and *Paracassidulina minuta* (Cushman), accompanied by some *Valvulineria bradyana* (Fornasini) and *Nonionella* spp.

Although most foraminifera can tolerate temporary adverse conditions and are much more resilient than macrozoobenthos, in sulfidic environments they are usually absent, or represented only by some very specialized taxa (Levin et al., 2009). One of those specialized taxa is *V. fragilis* which usually lives under anoxic and sulfidic bottom water conditions, commonly associated with sulfate oxidizing bacterial mats (such as *Beggiatoa*) (e.g., Bernhard 2003, Erbacher and Nelskamp 2006, Leiter and Altenbach 2010, Takata et al. 2003, 2005a, 2005b, 2006, 2014, Cardich et al. 2012). The species is found to host kleptoplasts, and symbiotic bacteria (δ-proteobacteria) which are sulfate reducers (Tsuchiya et al. 2015). Although the precise functions and pathways in the molecular level are not well understood, the endobionts allow *V. fragilis* the potential to live under a wide range of environmental conditions (Bernhard 2008, Bernhard et al. 2018, Tsuchiya et al. 2015). Previously, rose Bengal stained individuals of *V. fragilis* was found in the Sea of Marmara on Central High (329 m water depth) from an area with large filamentous bacterial mat (Fontanier et al., 2018).

The similarities of samples were investigated with cluster analyses calculated from the relative and absolute abundances of taxa which present near identical dendrograms (Figure 7.7).

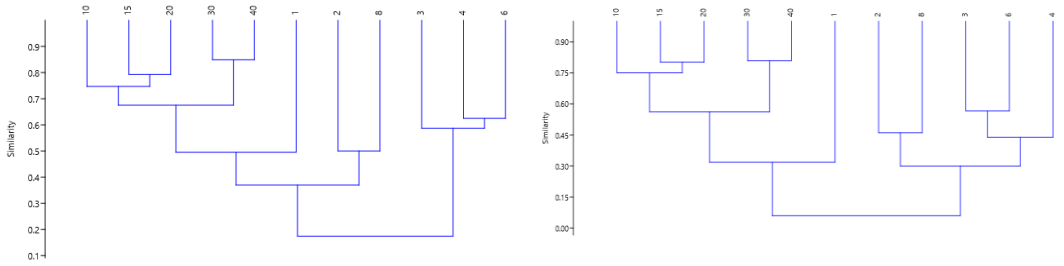


Figure 7.7. Cluster analysis (UPGMA, Bray-Curtis) calculated from left: relative abundances of taxa, right: absolute abundances of taxa (number in gram dry sediment).

Three main groups of samples occur according to the cluster analyses: group 1: samples 3, 4, and 6 with very high *V. fragilis* (>50%) and only very few (2-6) other taxa; group 2: samples 2 and 8 with lower *V. fragilis* and low number (16) of other taxa; group 3: all other samples with low or no *V. fragilis* and high number (>26) of other taxa with higher abundances. Although *V. fragilis* is the main divide in this grouping, differences in other taxa such as *Bolivina spathulata* (Williamson) and *Bolivina dilatata* Reuss, *Paracassidulina minuta* (Cushman), *Nonionella* spp. and *Valvulineria bradyana* (Fornasini) also play a role.

The assemblage in group 3 samples are in fact more similar to other Marmara surface samples rather than group 1 or 2 samples from the same core (Figure 7.8). On the other hand, group 1 and 2 samples are highly different from the rest of the Sea of Marmara samples.

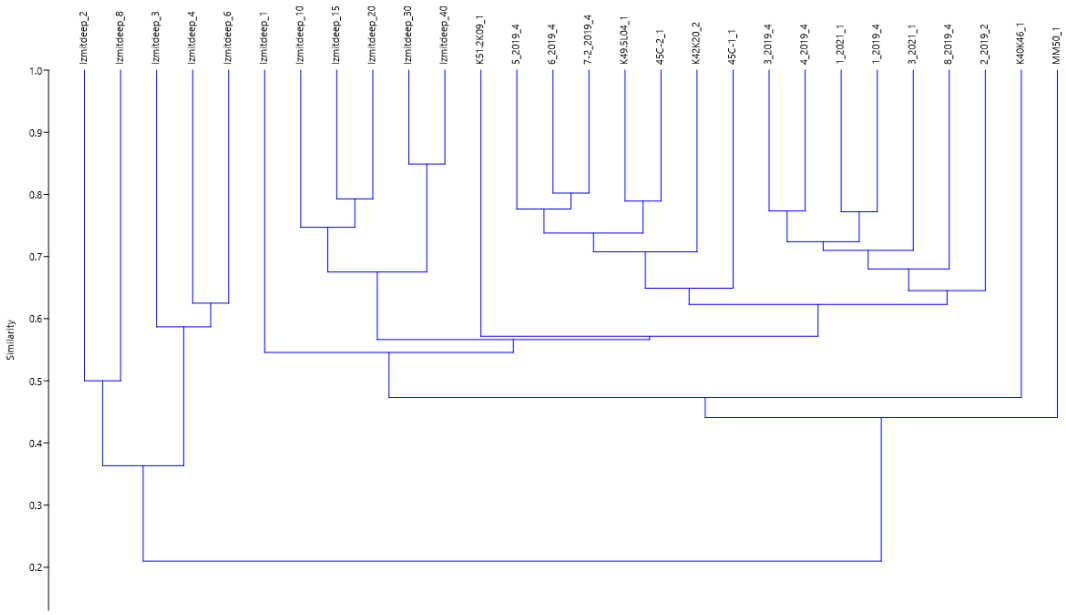


Figure 7.8. Cluster analysis (UPGMA, Bray-Curtis) calculated from relative abundances of taxa for the Izmit-deep core samples and surface samples from all stations.

7.3.7 Radiocarbon dating

The uncalibrated, δ13C corrected radiocarbon ages (BP) of the two samples of Izmit-deep core (15 cm and 45 cm) provided by TÜBİTAK-MAM are given in Table 7.2.

Table 7.2 Radiocarbon dating results as reported by the lab (TÜBİTAK-MAM).

Lab #	Sample #	14 C age (BP)	Sample type	Pretreatment
TÜBİTAK - 3254	Izmit-deep 15 cm	1266±22	Sediment	Acid washing
TÜBİTAK - 3255	Izmit-deep 45 cm	1311±22	Sediment	Acid washing

Calibration of conventional ^{14}C ages were done by using OxCal (v4.4.4; Bronk Ramsey, 1995, 2009, 2021) and CALIB (rev8.2, Stuvier and Remier, 1993, 2020) programs with marine calibration curve of Heaton et al. (2020; marine20.14c) and using marine reservoir correction value (ΔR = -63±40) from the Sea of Marmara (Sinai et al. 2000: site number 28) as recalculated for use with Marine20 curve (Heaton et al. 2020) in the online marine reservoir correction data-base (map no 243; http://calib.org/marine/ accessed on April 1st, 2024; Reimer and Reimer, 2001).

Calibration by OxCal and CALIB programs resulted in slightly different figures (2-5 years difference) (Table 7.3). These differences are very small when the error margin of 14C dating is considered. Hence, the calibrated ages given by CALIB program was chosen (Table 7.4).

7.4 Subdivisions of the Izmit-deep core

Considering the properties of the Izmit-deep core explained above, the core can be subdivided to four distinct intervals: interval A) from bottom of the core to top of sample 30 cm, interval B) up to top of sample 15 cm; interval C) up to top of sample 2 cm, interval D) top 1 cm. The characteristics of these intervals are as follows:

Table 7.3 Calibration results of ^{14}C dates of Izmit-deep samples by OxCal (posterior probability) and CALIB software.

			OxCal (cal AD)				CALIB (cal AD)				
Sample (cm)	14C BP		68.30%		95.40%		68.30%		95.40%		Median probability
15	1266	±22	1166	1306	1066	1372	1165	1304	1067	1369	1231
45	1311	±22	1122	1274	1040	1320	1123	1273	1039	1317	1189

Table 7.4 Uncalibrated (^{14}C BP), and calibrated (CALIB) ages for two bulk samples from the Izmit-deep core. Calibration curves and reservoir correction values as explained in the text.

Sample	^{14}C (BP)	68.30% (AD)		95.40% (AD)		Median (AD)
15 cm	1266 ± 22	1165	1304	1067	1369	1231
45 cm	1311 ± 22	1123	1273	1039	1317	1189

7.4.1 Interval A

The bottom two samples (40 and 30 cm) have high absolute benthic foraminifera abundance ($BF_{\#W}$, Figure 7.6) and similar benthic foraminifera assemblage (Figure 7.7): these two samples are clearly linked. Benthic foraminifera assemblage is most similar to, apart from interval B samples from the same core, surface sample of Central-deep station (K51.2K09; Figure 7.8), but is significantly different in terms of very high (~50%) abundances of opportunistic *Bolivina spathulata* (Williamson) and *Bolivina dilatata* Reuss. The assemblage is indicative of deep marine setting as evidenced by absence (or near absence) of shallow shelf taxa like rosalinids, ammonias, and cibicids (Figure 4.12, Supplementary Table B.11). In this interval the $PF_{\#W}$ values are near zero (Figure 7.6), in addition the sand content is also very low

(Figure 7.4). Radiocarbon dating results show that sample 45 cm (foraminiferal study was not conducted) belongs to 1189 AD (Table 7.4).

7.4.2 Interval B

Samples 20 and 15 cm (from top of interval A to top of sample 15 cm) make up the second interval. This interval has high $BF_{\#W}$ numbers, although lower than interval A samples (Figure 7.6), and a benthic foraminifera assemblage similar to the rest of the Sea of Marmara (Figure 7.8). The assemblage is different from the assemblage of interval A by lower relative abundances of *B. spathulata* (Williamson) and *B. dilatata* Reuss, compensated by higher relative abundances of the other dominant opportunistic taxa: *Paracassidulina minuta* (Cushman). The interval also has slightly higher relative abundances of miliolid taxa (Figure 4.12, Supplementary Table B.11) which usually inhabit inner shelf environments; therefore, may be allochthonous (e.g., *Quinqueloculina* spp. found most abundant in inner shelf station MM-50). The H_2S content in the core first appears in sample 15 cm, and the change in gradient in NH_4 also occurs in that level (Figure 7.5). Sand content is slightly higher in sample 15 cm but still very low (Figure 7.4). Radiocarbon dating results show that sample 15 cm belongs to 1231 AD (Table 7.4).

7.4.3 Interval C

This interval is composed of three subsections numbered from I to III from older to younger:

I. Sample 10 cm represents the bottom of the interval C. The benthic foraminiferal assemblage in this sample is similar to that of interval B (Figure 7.7), but with higher *B. spathulata* (Williamson) and *B. dilatata* Reuss (though not as high as interval A), slightly lower *Paracassidulina minuta* (Cushman), minor possibly allochthonous rosalinids and miliolids. The species richness is slightly higher than interval B (Figure 7.4) with previously

absent species having trace abundances (may be also allochthonous). The $BF_{\#W}$ of the sample is similar to that of interval B too, and the $PF_{\#W}$ is very low (Figure 7.6). The presence of *V. fragilis* although in low abundances (Figure 7.6, Figure 4.12), and the difference in pore water geochemistry (H_2S increases in this sample, Figure 7.5) separate this sample from the underlying samples, and group it with the overlying succession.

II. Samples 8 to 4 cm are second subsection of this interval. An increasing trend in absolute abundance of *V. fragilis*$_{\#W}$, a drastically lowered $BF_{\#W}$, and (near) absent $PF_{\#W}$ characterize this subinterval (Figure 7.6). In addition, H_2S values are high, having the maximum in sample 6 cm (Figure 7.6, Figure 7.5). Benthic foraminifera assemblage is drastically different than below lying intervals with very high *V. fragilis* relative abundances, and very few other taxa (Figure 4.12, Figure 7.7). However, the assemblage comparison is not very healthy since the number of studied foraminifera despite the use of the whole samples (about 15ml) are very low.

III. Samples 3 and 2 cm make up the uppermost subsection of this interval. Absolute abundance of *V. fragilis*$_{\#W}$ further increases, and the $BF_{\#W}$ and $PF_{\#W}$ start to increase as well (Figure 7.6). This results in lowered *V. fragilis* relative abundances (Figure 7.6), however, the assemblage is still highly differentiated from samples of intervals A and B (Figure 7.7). H_2S decrease upward (Figure 7.5).

7.4.4 Interval D

Interval D includes the topmost sample. The benthic foraminiferal assemblage is more similar to that of interval A and B; however, the sample also includes minor, possibly allochthonous specimens (cibicids). The absolute abundance of *V. fragilis*$_{\#W}$ is a little lower than sample 2 cm (Figure 7.6). The $BF_{\#W}$ is significantly higher than intervals C2 and C3 but still not as high as samples of interval A and B and the $PF_{\#W}$ is the highest in this sample (Figure 7.6).

7.5 Depositional interpretation of the Izmit-deep core

7.5.1 Intervals A and B

According to grain size, foraminiferal assemblage and abundance, and geochemical properties explained above, the main divide in the core is located between samples 15 and 10 cm. Alımlı (2022) remarked the change in NH_4 gradient as well as the H_2S curve in sample 15 cm and noted that the redox conditions of the bottom part of the core (intervals A and B) must be different than today's configuration (Figure 7.5). The sulfidic bottom water conditions in the Karamürsel Basin is formed after the 1999 earthquake according to Balkıs (2003). Therefore, the upper part of the core (above 15 cm with high H_2S) was most probably deposited after the '99 earthquake. Below 15 cm, the absence of H_2S indicates bottom water conditions which were not sulfidic. Moreover, the BF assemblage indicates a highly stressed and suboxic deep marine environment, apart from minor shelf taxa which are probably allochthonous. The higher $BF_{\#W}$ in these samples (intervals A and B), along with the bioturbated, pre-'99 earthquake deposits in a nearby core (WS-113, Çağatay et al., 2012, Figure 7.3) also suggest non-sulfidic bottom water conditions.

Intervals A and B have slightly different BF assemblages (Figure 4.12, Figure 7.7, Supplementary Table B.11). In the interval B, *B. spathulata* and *B. dilatata* combined relative abundances are lower and *P. minuta* relative abundance is higher compared to the interval A. These taxa are opportunistic, thriving in stressed (high food, low oxygen) environments, and they are the dominant taxa in the Sea of Marmara in outer shelf and deeper settings (see Section 3.4). The controlling factor of dominance of one or the other is obscure but may be environmental (e.g., difference in quality of food). If the intervals A and B are assumed to be hemipelagic depositions, the change in BF assemblage should correspond to a change in environmental conditions. However, the $PF_{\#W}$ values are significantly low in these intervals (Figure 7.6). Planktonic foraminifera abundance is found to be near zero in turbidites and homogenites (Anschutz et al., 2002) which hints at the probability that

these intervals are in fact not solely hemipelagic. Yet, it should be kept in mind that the PF abundance in the Karamürsel Basin is already very low (Kırcı-Elmas et al., 2021) as shown in the topmost sample of the core which is assumed hemipelagic (see below). Moreover, the fact that the radiocarbon dating resulted in a very high sedimentation rate between 45-15 cm of the core (see Section 7.3.3) further increases the possibility of these intervals to have a mass flow (turbiditic) component. If that is the case, the difference in BF assemblages as well as $BF_{\#W}$ between interval A and B (Figure 7.6) show that these intervals were fed from different sources. This may be because these two intervals are products of successive mass flows (asynchronic), or two different mass flows produced by the same event (synchronic).

Considering the documented and dated seismoturbidites form the Karamürsel Basin (see Section 7.2) the closest historical earthquake to the dates obtained from the Izmit-deep core is 1296 AD (Çağatay et al., 2012). This date fits in the 68.3% confidence interval of the 15 cm sample age and 95.4% confidence interval for the 45 cm sample (Table 7.4). Therefore, it is plausible that these two intervals are synchronic and are seismoturbidites belonging to 1296 AD earthquake, but deposited by mass flows from two different sources. In that case, it is only expected that the ages obtained from the samples are older than the event itself since radiocarbon dates from bulk sediment samples may have up to thousands of years of offset due to incorporation of carbon from various sources (e.g., Berg et al., 2020, Strunk et al., 2020, Hansen et al., 2022). This creates an error in dating especially in mass flow cases where abundant old organic carbon mobilizes downslope and deposit without much in-situ organic carbon present, hence appear older than deposition age.

In conclusion, interval A and B may be two different turbiditic fluxes mobilized synchronously due to the 1296 AD earthquake. Interval A was sourced from a slightly older level composed of mostly deep marine sediment, including a BF assemblage with a higher *Bolivina* spp. relative abundance. On the other hand, interval B was sourced from a slightly younger level, also composed of deep marine sediment but maybe shallower than the source of interval A, including a BF assemblage with a lower *Bolivina* spp. relative abundance and minor contribution

from shelf taxa. Both of these two source sites may be situated along the landslide prone paleo-shelf edge and slope bounding the southern margin of the basin floor (Cormier et al., 2006). These two fluxes reached the area separately. Firstly, interval A got deposited as mostly silt-rich turbidite base layer, on top of which interval B was deposited also as a silt-rich turbidite base layer. The clay dominant portion of the mobilized sediment were most probably mixed, and deposited later on top of interval B as homogenites. This portion, along with all post 1296 AD sediment was eroded away before the deposition of interval C after the ’99 earthquake.

The basin floor is tilted towards north where Izmit-deep station (206 m water depth) is located (Cormier et al., 2006; Sorichetta et al., 2010). Çağatay et al. (2012) proved the presence of pre-1999 hemipelagic sediments (bioturbated mud) in the core SW-113, which is situated in a slightly deeper setting (210 m water depth) to northwest of Izmit-deep core. This slight slope may explain the erosion of post 1296 AD deposits in Izmit-deep core. The sediment may be mobilized from the site of Izmit-deep station due to disturbances (seismic or otherwise) and got deposited further down-slope.

7.5.2 Interval C

Interval C is interpreted to be the turbidite-homogenite unit belonging to the ’99 earthquake. Interval C1 (sample 10 cm) may be the silt-rich base layer of the turbidite. The higher $BF_{\#W}$ supports this interpretation (Figure 7.6). The BF assemblage in sample 10 cm is similar to that of interval B (Figure 4.12, Figure 7.7); therefore, it may be sourced from a similar setting as the source of interval B. Upwards, in intervals C2 (samples 8, 6, 4 cm) and C1 (samples 3 and 2 cm) the $BF_{\#W}$ and $PF_{\#W}$ figures are significantly smaller, especially in samples 6 and 4 cm. Hence, the rest of the interval C may be the homogenite settled from the turbiditic cloud. For the upper part (interval C3), slightly higher $BF_{\#W}$ and $PF_{\#W}$ may be due to i. slow recolonization of this environment by infaunal taxa after homogenite deposition, or ii. downward transport of tests due to bioturbation, or both.

According to Sorichetta et al. (2010) the topmost layer of the basin floor sediments in the Karamürsel Basin is significantly tilted (0.16° towards north); the magnitude of the tilt brings forth the interpretation that the topmost layer predates ’99 earthquake which tilted the basin floor sediments but did not cause a large turbidite. This interpretation is contradicting with the findings of Çağatay et al. (2012) who dated the core SW-113 via 137Cs and proved the presence of a turbidite layer of 32.5 cm thickness belonging to ’99 earthquake in that core. The THU attributed to the ’99 earthquake is further correlated with other three cores west of SW-113, although with progressively smaller thickness (McHugh et al., 2006; Çağatay et al., 2012, Gasperini et al., 2018; Arslan Kaya et al., 2023b). The 9 cm thick interval (interval C) ascribed here to the ’99 earthquake is compatible with the geometry of the basin and the thicknesses of the ’99 turbidite in other cores. As the basin slopes northward and SW-113 is in a slightly deeper setting (210 m) than Izmit-deep (206 m), a thinner turbiditic deposit in this core is plausible.

7.5.3 Interval D

The topmost sample (sample 1 cm) most probably represents the most recent hemipelagic deposition since ’99 earthquake. The $BF_{\#W}$ is lower than that of the turbiditic intervals A, B, and C1, while the $PF_{\#W}$ is highest of the core hinting towards an in-situ sedimentation (Figure 7.6). The BF assemblage is of a deep marine-stressed environment, and the presence of *V. fragilis* in high numbers (absolute abundance) is in alignment with high concentration of H_2S in the bottom water. These *V. fragilis* individuals, although not vividly pink-red stained, are pink tinted which shows that probably these specimens were not transported from elsewhere (and older strata), instead they are in-situ; and although were not live at the time of sampling, they still had some organic tissue inside the test to be colored slightly. Similarly, pink tinted *V. fragilis* individuals found in other (deeper) samples probably show the infaunal distribution of the taxon: i.e., these individuals belong to the hemipelagic deposition post ’99, but have colonized the homogenite and turbidite

levels. The fact that no vividly pink-stained foraminifera were found in the sample may mean that the standing stock is very low. Moreover, the relatively higher $BF_{\#W}$ in this interval along with the absence of stained tests may indicate a high seasonal variation in foraminiferal abundance.

The hemipelagic deposition above the ’99 turbidite was found to be 4 cm thick in SW-113 (Çağatay et al., 2012) in which the sand content (up to 25%) was composed mainly of plant material. This thickness is compatible with 1 cm hemipelagic thickness in Izmit-deep core.

7.6 Summary

Izmit-deep station is situated on the basin floor of the Karamürsel Basin. The benthic foraminiferal absolute abundance, planktonic foraminiferal absolute abundance, benthic foraminiferal assemblage, sand content, pore water chemistry and radiocarbon dating results were used to interpret the core’s depositional setting. Four intervals were distinguished in the core, A to D from bottom to top. Interval A and B represent two different but synchronous mass flows most probably related to 1296 AD earthquake. Both units show that the bottom water conditions during their original deposition were not sulfidic, but highly stressed. Interval B is assumed incomplete with a significant hiatus between top of this interval and interval C. Interval C is a turbidite-homogenite sequence related to the ’99 earthquake. Topmost interval, interval D is composed of the post ’99 hemipelagic deposition on top of the homogenite. Both intervals C and D were deposited under sulfidic conditions as evident from the presence of *Virgulinella fragilis*, a benthic foraminifer specialized to live under such conditions.

CHAPTER 8

SYSTEMATIC TAXONOMY

Foraminifera are classified according to their chamber arrangement, wall structure, position and morphology of the apertures, overall test shape, morphology of the sutures and chambers, and other details such as surface ornamentation. By comparing the morphotypes encountered in this study to previous publications (historical and recent, especially those dealing with Mediterranean foraminifera) the benthic foraminifera in this study were identified. In this study, one in superfamily (Polymorphinoidea), one in family (Glabratellidae), seven in genus (*Adelosina* spp., *Ammonia* spp., *Dentalina* spp., *Elphidium* spp., *Globobulimina* spp., *Laevidentalina* spp., *Pullenia* spp.) and 163 in species level, in total 172 taxa were identified; 165 of them were illustrated using a stereomicroscope equipped with a camera, and a scanning electron microscope (Supplementary Table G.1). Details of the equipment used for illustration can be found in Section 1.3.5.

For identification of the taxa, main sources used are Loeblich and Tappan (1964, 1988), Cimerman and Langer (1991), Sgarrella and Moncharmont Zei (1993), Sakınç (2008), Milker and Schmiedl (2012), Meriç et al. (2014). In addition to these, identifications in the publications which dealt with benthic foraminifera of the Sea of Marmara (e.g., Kaminski et al., 2002; Kırcı-Elmas, 2018), older compilations (e.g., Cushman's Pacific and Atlantic monographs: such as 1910, 1922a, 1923) and original descriptions of taxa (Ellis and Messina Foraminifera catalogues, and when available, original publications) were utilized. For generic and suprageneric classification of taxa, an up to date online database (WoRMS Editorial Board, 2025, World Register of Marine Species: WoRMS) was used in addition to Loeblich and Tappan (1988). The supraordinal classification of foraminifera follows Pawlowski et al. (2013).

This chapter includes the descriptions, taxonomic overviews, and distinguishing criteria for the identified benthic foraminiferal taxa. The ordering of the following text is alphabetical in each rank. The same ordering is used, as much as possible, in the organization of plates. Summary table for the taxonomy of the identified benthic foraminiferal taxa are also given in the same order (Supplementary Table G.1).

Two different types of plates accompany this text (Appendix G, Plate 1-48): one composed of SEM figures (odd numbered plates), one composed of stereomicrographs (even numbered plates); each set of SEM and stereomicrograph plates feature the same taxa. Most of the specimens imaged via the SEM also have stereomicrographs, sometimes a suite of stereomicrographs from different angles are present for the same specimen. Specimens are marked with a specimen number (starting with IS_, stands for 'Imaging Specimens') noted in plate explanations, so that images of the same specimen can be compared.

The synonym lists are comprehensive; include the original description of taxa, some major name changes, and further references which paint a picture of the current understanding of the taxon. On the left hand side of the synonym list some notes are given when necessary, their meanings are as follows:

- 'non': misidentification, incorrect use of name,
- 'part': reference partially correctly identified the taxon; usually a paranthesis follows this kind of synonym indicating which figures are misidentifications as '(not fig….)',
- '?': uncertain reference, either due to lack of clarity (some characteristic feature is not shown/explained) or may be an extreme case of morphologic variation,
- '*': reference features a special character, e.g., a test elongated more than in other references.

For suprageneric levels, a small remark is made only when necessary. Genus levels include the original authorage, and the type taxon given with the original name and

the accepted name if the species name changed later. Description and taxonomic remarks are given when necessary.

CLASS GLOBOTHALAMEA Pawlowski, Holzmann & Tyszka, 2013

ORDER ROBERTINIDA Loeblich & Tappan, 1984

Order Robertinida comprises the taxa with aragonitic wall structure.

SUBORDER ROBERTININA Loeblich & Tappan, 1984

Superfamily Ceratobuliminoidea Cushman, 1927

Family Creatobuliminidae Cushman, 1927

Subfamily Ceratobulimininae Cushman, 1927

Genus *Ceratolamarckina* Troelsen, 1954

1954 *Ceratobulimina (Ceratolamarckina)* – Troelsen: p. 452

Type: *Ceratolamarckina tuberculata* (Brotzen, 1948, p. 124)

Low trochospirally coiled forms with few, inflated, rapidly enlarging chambers. Sutures depressed on both sides. Umbilicus open and may have tubercules. Internal partition attached at the umbilical side, not attached at the spiral side, going up only to the bottom of the intercameral foramen. Septal face with apertural bulge situated ventrally. Aperture an interiomarginal arch between the umbilicus and the margin of the apertural bulge, limited on one side where the septal face connects to the earlier whorl, on the other where the internal partition attaches the outer wall. Secondary aperture on septal face, a rounded opening above the internal partition. When a new chamber is added apertural bulge is replaced by a thin plate closing the main aperture and the intercameral opening is formed above the internal partition by resorption.

Ceratolamarckina arctica (Green, 1959)

Plate 1 Figures 1-3; Plate 2 Figures 1-8

1959 *Ceratobulimina arctica* – Green: p. 78, pl.1 fig. 1a-c

1960 *Ceratobulimina arctica* – Green, p. 71, pl. 1 fig. 1a-c

part 1991 *Robertinoides charlottensis* (Cushman); Scott and Vilks, p. 32, pl. 3 fig. 16 (?), 20-23 (not fig. 15, 17-19)

1993 *Ceratobulimina arctica* Green; Sgarrella and Moncharmont Zei, p. 242, pl. 25 fig. 8-9

2020 *Ceratobulimina arctica* (Green); Jennings et al., pl. 2 fig. 10a-b

Test small, very low trochospiral with 2-5 chambers following a spherical proloculus arranged in a dextral half-coil. Chambers lengthen radially very rapidly so that the length of the final chamber is about 4/5 of the whole test. Outline slightly lobulate. Margin rounded. Spiral side with very slightly depressed and slightly curved sutures; umbilical side with straight to very slightly curved sutures which are almost flush at the periphery but depressed at the umbilicus producing bulbous shapes at the umbilical end of the chambers. Umbilicus wide and with granulate pustules. Aperture an interiomarginal, umbilical arch and an accessory areal aperture in some specimens present on the septal face as a rounded opening located centrally. An internal partition limits the umbilical bulb of the chamber in the direction of coiling, and the interiomarginal aperture is situated between the the connection point of the internal partition and the connection point of the septal face to the proloculus. Connection point of the internal partition, as a short linear dent oblique to the septal face, can only be observed on the last formed chamber since the next chamber always cover the umbilical aperture of the previous one. Internal partition is not attached to the dorsal side, on the ventral side the connection suture (dent) goes up a short distance (radially). Areal aperture is a secondary element produced after the next chamber is built and the umbilical aperture of the previous chamber is closed. Test

is aragonitic, very thin and fragile, transparent; surface is smooth and shiny except for the pustulose umbilicus.

Troelsen (1954) rergarded the forming of areal septal aperture of the ceratobuliminids as a secondary event happening after the closure of the main aperture while the addition of the new chamber. The fact that there are specimens in the studied material both with and without the areal aperture strengthens Troelsen's theory. Those found with the areal aperture must be missing at least one chamber.

The aperture of *Ceratobulimina*, the genus under which this taxon was originally described, is more of an elongated slit adjacent to the internal partition which reaches and connects to the dorsal (spiral) side of the chamber; however, in this taxon the aperture is interiomarginal and the internal partition do not connect to the dorsal side, which is a feature of *Ceratolamarckina* (Troelsen, 1954). In addition, the umbilical pustules are a marked feature for the genus *Ceratolamarckiana* (Loeblich and Tappan, 1988, p. 441). Because of these morphologic criteria, this taxon is moved to genus *Ceratolamarkiana*, despite it being considered extinct (Loeblich and Tappan, 1988).

The taxon (as *Ceratobulimina arctica*) was described from the Arctic Ocean, and is recorded from recent deep sea sediments (>500 m; Lagoe 1979, Scott and Vilks, 1991; Wollenburg and Mackensen, 1998, 2009), as well as from Pleistocene deposits (O'Neil 1981). According to Heinz et al. (2001), this species lives also in the Mediterranean (Gulf of Lions, 911 m water depth) as a deep infaunal taxon; Sgarrella and Moncharmont Zei (1993) recorded this taxon from the Gulf of Naples. Due its small size and highly fragile test, it was propably either not preserved or overlooked in most studies outside the Arctic Ocean, and in older strata.

Scott and Vilks (1991) regarded this taxon as a pre-adult state for *Robertinoides charlottensis* (Cushman). They illustrated specimens as a growth gradational series noting that the groove in the *C. arctica* (formed by the attachment of the internal plate at the umbilical side of the last formed chamber) becomes the slit-like aperture of the adult *R. charlottensis*. They also mention the absence of umbilical pustules in

R. charlottensis, which are interpreted to be lost during ontogeny. Nonetheless, they fail to discern the very obvious chamber arrangement differences between the two taxa. *R. charlottensis* is a high trochospiral form as other Robertinininae, the spire is made up of two chamber series (one primary, one secondary) coiling tightly so that originally Cushman (1925) mistook the form as biserial enrolled and described it under genus *Cassidulina*. The holotype images of an adult specimen (by Smithsonian National Museum of Natural History Department of Paleobiology Collections, Catalogue number USNM CC 1546, access via http://n2t.net/ark:/65665/398a592a6-75ff-4b87-902b-75b69439edfb) clearly shows the apperant biseriality and pointed proloculus with high spire in *R. charlottensis*. The chamberlet feature of this superfamily is very muted in *C. arctica* with very little surficial evidence of the internal partition (see holotype image by Smithsonian National Museum of Natural History Department of Paleobiology Collections, Catalogue number USNM MO 689641, access via http://n2t.net/ark:/65665/320275d58-093f-4359-a8b0-e09292539aa1) which makes this taxon exceptionally different than *R. charlottensis*. Identification of Scott and Vilks (1991) of *R. charlottensis* may be not correct either considering the illustrations of the taxon are much smaller and stouter than the type.

Taxon is very easily distinguished from others by its small size, only very few radially elongate chambers and very transparent, thin and fragile test over all other characteristics.

Superfamily Robertinoidea Reuss, 1850

Family Robertinidae Reuss, 1850

Subfamily Robertininae Reuss, 1850

Genus *Robertinoides* Höglund, 1947

1947 *Robertinoides* – Höglund, p. 222

Type: *Bulimina normani* Goës (1894, p. 47, pl. 9 fig. 437-438)

Test ovate, apex (the initial end of test) pointed. Chambers composed of two halves, separated by an internal diaphragm, coiled trochospirally. Main apertures made up of two openings, one slit at the intracameral suture, the other slit more central on the apertural face of the distal half of the chamber, interiomarginal, vertical to the suture. The proximal half of the next chamber gets situated covering the main apertures on the distal half of the previous chamber. An accessory aperture, a triangular opening, present at the junction of the intracameral suture of the ultimate chamber and the main suture between the penultimate and ultimate chambers; previous accessory apertures blocked by following chambers. Surface smooth.

The taxonomy and complex interior of the genus was described and illustrated in detail by Höglund (1947) and compared to genus *Robertina* which has a single main aperture (vertical slit) as opposed to double aperture of *Robertina*. Due to their double main apertures, Höglund (1947) argues that all forms described and illustrated by Cushman and Parker (1936) should be included in *Robertinoides* instead. Among those, *Robertina translucens* Cushman and Parker was originally described and illustrated to hold a "very small and inconspicuous secondary aperture", yet, the holotype of the taxon (see holotype image by Smithsonian National Museum of Natural History Department of Paleobiology Collections, Catalogue number USNM CC 23672, access via http://n2t.net/ark:/65665/m34c760c83-126f-490e-98ef-8d84925ef9e8) has only a single primary aperture, and therefore should remain in *Robertina*.

Robertinoides bradyi (Cushman and Parker, 1936)

Plate 2 Figure 9

part 1884 *Bulimina subteres* Brady; Brady, p. 403, pl. 50 fig. 18 (not 17)

1936 *Robertina bradyi* – Cushman and Parker, p. 99, pl. 16 fig. 9a, b

1994 *Robertinoides bradyi* Cushman and Parker; Jones, p. 55, pl. 50 fig. 18

1980 *Robertina translucens* Cushman and Parker; Alavi, p. 76, pl. 23 fig. 3

2004 *Robertina translucens* Cushman and Parker; Chendeş et al., pl. 1 fig. 17

Test ovate, apex (the initial end of test) pointed, widening towards the apertural end, tapering. Chambers composed of two halves, separated by an internal diaphragm, coiled trochospirally, 4-5 in the last whorl. Intracameral sutures shallowly depressed, limbate; sutures between chambers more depressed. Vertical part of the main aperture near parallel to the long axis, narrow; the slit at the intracameral suture less obvious. Accessory aperture on the adapertural side of the test small, triangular. Surface smooth, test transparent, fragile.

Brady (1881) named *Bulimina subteres* with references to the illustrations of *Bulimina elegantissima* d'Orbigny by Brady (1878, p. 436, pl. 21 fig. 12) and *Bulimina presli* Reuss var. *elegantissima* d'Orbigny by Parker and Jones (1865, p. 374, pl. 15 fig. 13-17). Considering the wide morphologic variety and differences in the referenced illustrations and Brady's own illustrations (in 1884, pl. 50 fig. 17-18), Cushman and Parker (1936) indicated that the name *B. subteres* was invalid, and that Brady's fig. 18 (in pl. 50) was identical to their new species *Robertina bradyi*. Taxon was transferred to genus *Robertinoides* due to the presence of double main aperture (Höglund, 1947).

Forms previously attributed to *Robertina translucens* Cushman and Parker by Alavi (1980) and Chendeş et al. (2004) do not belong in *R. translucens* due to presence of the double main aperture, but carry characteristics of *R. bradyi* instead.

This form is even rarer than *R. pumilum* in the Sea of Marmara, and the juveniles of these two forms cannot be distinguished, therefore were treated as one group in census counts. Adult individuals are fatter than *R. pumilum*, and the vertical portion of the aperture is near parallel the long axis.

Robertinoides pumilum Höglund, 1947

Plate 1 Figures 4-6; Plate 2 Figures 10-15

1947 *Robertinoides pumilum* – Höglund, p. 227, pl. 18 fig. 5

1980 *Robertina* sp. Daniels; Alavi, p. 76, pl. 24 fig. 3, 7

2012 *Robertina translucens* Cushman and Parker; Milker and Schmiedl, p. 80, fig. 19.17-18

2015 *Robertinoides pumilum* Höglund; Spezzaferri et al., pl. 18, fig. 8

Test ovate, apex (the initial end of test) pointed, somewhat widening towards the apertural end, slightly tapering to more or less cylindrical. Chambers composed of two halves, separated by an internal diaphragm, coiled trochospirally, 4-5 in the last whorl. Intracameral sutures shallowly depressed, limbate; sutures between chambers more depressed. Vertical part of the main aperture oblique to the long axis, short, do not extend beyond the halfway point on the apertural face, wider; the slit at the intracameral suture less obvious, narrower, longer. Accessory aperture on the adapertural side of the test small, triangular. Surface smooth, test transparent, fragile.

Taxon is similar to *Robertinoides bradyi* (Cushman and Parker) in many aspects, but the general form is more elongate and the vertical portion of the main aperture is wider and oblique to the long axis instead of near parallel. *Robertina translucens* Cushman and Parker is also a similar taxon, however lacks the double main aperture.

Individuals attributed to *Robertina* sp. Daniels by Alavi (1980) and *R. translucens* Cushman and Parker by Milker and Schmiedl (2012) are identical to the individuals assigned in this study to *R. pumilum*.

Most of the studied *Robertinoides* in the Sea of Marmara belong to this taxon. They are easily distinguished from all other taxa by the characteristic chamber shape and coiling. Adult specimens of *R. pumilum* is different from *R. bradyi* by a more elongate, narrower outline and more oblique and wider vertical portion of the main aperture.

SUBCLASS ROTALIANA Mikhalevich, 1980

ORDER ROTALIIDA Lankester, 1885

Order Rotaliida comprises the taxa with calcitic hyaline wall structure.

Superfamily Asterigerinoidea d'Orbigny, 1839

Family Asterigerinatidae d'Orbigny, 1839

Genus *Asterigerinata* Bermúdez, 1949

1949 *Asterigerinata* Bermúdez: p. 266

Type: *Asterigerinata dominicana* Bermúdez, 1949 (p. 266; pl.16, fig. 37-39)

Test conical, trochospiral; spiral side evolute, umbilical side involute; margin angular. Chambers crescentic, rapidly growing in size (tangential dimension) so that the last chamber occupies almost 1/3-1/2 of the periphery. Umbilicus covered by flaps (cover plates) producing a rosette shape and secondary chamberlets (between the chamber and the flap), but lack secondary apertures. Aperture an interiomargial arch.

Asterigerinata adriatica Haake, 1977

Plate 1 Figures 7-10; Plate 2 Figures 16-21

1977 *Asterigerinata adriatica* – Haake, p. 69, pl. 3 fig. 1-5

1991 *Asterigerinata* sp. 1; Cimerman and Langer, p. 73, pl. 82 fig. 5, 6

2012 *Asterigerinata adriatica* Haake; Milker and Schmiedl, p. 111, fig. 25.7-9

Test conical, trochospiral; spiral side evolute, umbilical side involute; margin angular, carinate with heavy concentration of pustules. Chambers crescentic, rapidly growing in size (tangential dimension) so that the last chamber occupies almost 1/3-1/2 of the periphery; outer margins of chamber with conical pustules so that the spiral side is pustulose. Umbilicus covered by flaps (cover plates) producing a rosette shape and secondary chamberlets. Aperture an interiomargial arch. Surface of the spiral pustulose, on the umbilical side surface smooth; a few coarse pores present on cover plates.

Asterigerinata sp. 1 of Cimerman and Langer (1991) is very similar to this form. Although the taxon's most prominent feature is the pustulose spiral side, images shared by Milker and Schmiedl (2012, especially fig. 25.9) are less densely ornamented.

This taxon is only found rarely in the material examined, and usually as juveniles.

Asterigerinata mamilla (Williamson, 1858)

Plate 1 Figures 11-15; Plate 2 Figures 22-28

1858 *Rotalina mamilla* – Williamson: p. 54, pl. 4, fig. 109-111

1991 *Asterigerinata mamilla* (Williamson); Cimerman and Langer, p. 73, pl. 82 fig. 1-4

? 2008 *Asterigerinata mamilla* (Williamson); Sakınç, pl. 17 fig. 2.

2012 *Asterigerinata mamilla* (Williamson); Milker and Schmiedl, 2012; p. 111, fig. 25.10-13

Test conical: concavoconvex to planoconvex, trochospiral; spiral side evolute, umbilical side involute; margin angular, strongly keeled. Chambers crescentic, rapidly growing in size (tangential dimension) so that the last chamber occupies almost 1/3-1/2 of the periphery; in smaller specimens width of chambers smaller. In adult specimens outline non-lobulate, in juveniles more lobulate. Umbilicus covered by flaps (cover plates) producing a rosette shape and secondary chamberlets (between the chamber and the flap), but lack secondary apertures. Aperture an interiomargial arch. Surface smooth; a row for pores present on the spiral side parallel the outer margin of chambers; on the umbilical side a few large pores present on the cover plates.

On the spiral side, chambers are tangentially elongated with varying breadth on the radial dimension. In adult specimens with narrower crescentic chambers the spiral side is very similar to that of *Neoconorbina terquemi* (Rhezak), but the umbilical sides of the two taxa are distinctly different. Yet, when the umbilical sides are

damaged, the distinction of these forms is only available via the pore structure on the spiral side. The pores of *A. mamilla* are in a regular row near the outer margin of the chamber while *N. terquemi* has less regular and smaller pores. The image for *A. mamilla* given by Sakınç (2008) is more in-line with the description of *N. terquemi*.

The forms found in our material are usually small (pre-adult) with wider (in the radial dimension) chambers on the spiral side which provides the taxon a superficial similarity some rosalinid taxa; the taxon is distinguished from them by its very distinctive aperture.

Superfamily Bolivinitoidea Cushman, 1927

Family Bolivinitidae Cushman, 1927

Subfamily Bolivinitinae Cushman, 1927

Genus *Bolivina* d'Orbigny, 1839a

1839a *Bolivina* d'Orbigny: p. 61.

Type: *Bolivina plicata* d'Orbigny, 1839a (p. 62, pl. VIII, fig. 4-7)

Chamber arrangement is biserial. Test shape may be spathulate (tapering towards the proloculus) or elongate (with more or less parallel sides) with carinate to rounded edges. Chambers vary in shape and size from nearly globular to wide and low with sutures depressed to flush. Aperture interiomarginal, an arch which is generally elongated, with a rim in some species, with an internal toothplate that connects the apertures of the earlier chambers; the toothplate, being an internal feature, rarely discernible from the outside of the test. Surface smooth to ornamented with coarse pits, straight costae or irregular striae.

Originally, Costa (1856, p. 300, pl. 15, fig. 1-2, type taxon: *Brizalina aenariensis* Costa) distinguished their new genus *Brizalina* from d'Orbigny's *Bolivina* by the internal "double siphons", probably a misconception of the toothplate system which runs inside the test connecting the apertures of the chambers. Traditionally in

practice, these genera were distinguished by the shape of test margins which is rounded-subrounded for *Bolivina* and subangular to carinate for *Brizalina*. Other than this feature, the test characteristics are the same for the two genera. According to Ertan, et al. (2004) the distinction between genera *Bolivina* and *Brizalina* is not supported by genetic studies. Therefore, here, they are treated as synonyms.

Bolivina alata (Seguenza, 1862a)

Plate 3 Figures 1-5; Plate 4 Figures 1-5

1862a *Vulvulina alata* Seguenza, p. 115, pl. 2 fig. 5

1875 *Bolivina beyrichi* Reuss, var. *carinata*; Hantken, p. 64, pl. 7 fig. 12

1884 *Bolivina beyrichi*, var. *alata* Seguenza; Brady, p. 422, pl. 53 fig. 2-4

1893 *Bolivina (Vulvulina) alata* Seguenza; Egger, p. 296, pl. 7 fig. 27

1911 *Bolivina beyrichi* Reuss, var. *alata* (Seguenza); Cushman, p. 35, fig. 57

1922a *Bolivina beyrichi* Reuss, var. *alata* (Seguenza); Cushman, p. 30, pl. 8 fig. 3

1960 *Bolivina alata* (Seguenza); Hofker, p. 248, fig. 85-88

1991 *Brizalina alata* (Seguenza); Cimerman and Langer, p. 59, pl. 6 fig. 12-14

2002 *Brizalina alata* (Seguenza); Kaminski et al., p. 188, pl. 2 fig. 12

2005 *Brizalina alata* (Seguenza); Meriç et al., pl. 3 fig. 5

2008 *Brizalina alata* (Seguenza); Sakınç, pl. 12 fig. 4-5

2014a *Brizalina alata* (Seguenza); Meriç et al., pl. 49 fig. 13-17

Form elongate, flaring; compressed, with carinate margins. Chambers as tall as wide; grow more rapidly in length as added. Chamber overlaps in the median (axial) part

of the test is quite large, especially in large (adult) forms the last chamber tends to cover a great portion of the previous chamber's periphery. Keel continues around the whole chamber margin, rimming the aperture, merging with the carina of the previous chamber, extending toward the initial part of the test as pseudospines. Sutures are shallowly depressed and curved. Aperture interiomarginal, elongate, rimmed on both sides. Surface is smooth, distinctly perforated except for the sutures and carina; test transparent.

The species is most similar to *Bolivina beyrichi* Reuss (1851), of which, many authors regarded *B. alata* to be a variety (e.g., Hantken, 1875; Brady, 1884, Cushman, 1911, 1922a). The chamber shape and arrangement and growth rates are similar in the two species, as well as the surface porosity; however, the keeled margin only occurs in *B. alata*.

The form is very distinct in morphology, even the pre-adult or broken forms can be readily distinguished. The surface porosity, thinness of the test, curvature of the sutures and most importantly the wide keel can be observed even in specimens with as few as 3-4 chamber pairs.

Bolivina albatrossi Cushman, 1922

Plate 3 Figures 6-9; Plate 4 Figures 6-9

1922a *Bolivina albatrossi* – Cushman, p. 31, pl. 6 fig. 4

1989 *Bolivina albatrossi* Cushman; Gary et al., pl.1 fig. 1-4

1993 *Bolivina albatrossi* Cushman; Sgarrella and Moncharmont Zei, p. 207, pl. 14 fig. 7

Test ovoid-elliptical in frontal view, sides parallel; edges subrounded to rounded. Sutures oblique, obscured by fine reticulations on the surface. Aperture interiomarginal. Test transparent; surface rough except for the top halves of last chamber pair which are smooth.

Cushman's (1922a) accompanying drawing shows the stout shape of the form very well, however said reticulations are not well illustrated. SEM images of Gary et al. (1989) show in high detail the reticulations, also the morphologic variety of the species.

The form is distinguished from other *Bolivina* by shiny surface, especially so in the latter part of the two chambers which are unornamented, even in smaller (juvenile) specimens, and ovoid-elliptical shape. Form is usually represented by small individuals, only in very few samples large individuals were encountered.

Bolivina dilatata Reuss, 1850

Plate 5 Figures 1-7; Plate 6 Figures 1-9

1850 *Bolivina dilatata* Reuss, p. 381, pl. 48 fig. 15

1937 *Bolivina dilatata* Reuss; Cushman, p. 78, pl. 9 fig. 17-20

1980 *Bolivina* "*dilatata dilatatissima*" Parker; Alavi, **p**. 43, pl. 26 fig. 1, 8

1980 *Bolivina* cf. *robusta* Brady; Alavi, **p**. 43, pl. 24 fig. 11

1991 *Brizalina dilatata* (Reuss); Cimerman and Langer, p. 59, pl. 62 fig. 2

2002 *Brizalina dilatata* (Reuss); Kaminski et al., pl. II/13

2008 *Brizalina dilatata* (Reuss); Sakınç, pl. 12/6-7

2012 *Brizalina dilatata* (Reuss); Milker and Schmiedl, p. 81, fig. 19.30

2016 *Bolivina dilatata* Reuss; Lei and Li, p. 203, fig. 2

2016 *Bolivina robusta* Brady; Lei and Li, p. 204, fig. 4

2016 *Bolivina spathulata* (Williamson); Lei and Li, p. 206, fig. 5

Test is large, elongate, flaring; aboral part bluntly rounded with a large proloculus, sides may become parallel for the last two pair of chambers. Margins bluntly carinate, the carina continues around the proloculus, may produce a very small spinal

projection; carina continues up to the oral side for the very last adult chamber pair in complete specimens. Periphery mostly non-lobate. Sutures initially highly curved, get straighter towards the oral end; a few finger-like downward projections present concentrated near the median line, more prominently seen in the adult part of the test. Sutures mostly flush with the test except for the outer margins where they may become somewhat depressed. Chambers low and broad, initially curved around the curve of the large proloculus, later getting straighter; acutely angled to the median line. Surface mostly smooth except for a very slight roughness concentrated on and near the median line produced by the finger-like projections; pores may align to give the test a finely striate appearance. Aperture interiomarginal, rimmed on one side. Test porous; porosity is adjacent to the sutures in the initial part, later covers the whole chamber, except for the slightly roughened areas on the median line; wall thick.

Bolivina dilatata and *Bolivina spathulata* are very similar in most aspects: the test is flaring, usually an inequal rhomboid, the edges are pinched and/or carinate usually with very little, if any, lobulation, the sutures are mostly flush, and the surface is mostly smooth. In the literature these names are used somewhat interchangeably, or the taxa are noted to have morphologic gradation (Alavi, 1988; Barmawidjaja, 1991; Dimiza et al., 2020; Lyu et la., 2022), or completely confused with each other. However, subtle differences do allow to differentiate these taxa. *Bolivina dilatata* has a larger initial part: a larger proloculus and wider initial chambers; however, if the initial part is broken, the width and length of the rest of the tests are similar for these taxa: both may be widely flaring, or narrow and with somewhat parallel sides towards the oral end. Both have oblique sutures, but *B. dilatata* has more curved sutures for the initial part and digitate overlaps are present in later chambers; if those are somewhat obscured, the distinction is almost impossible. Both taxa have pinched/carinate edges, with the angularity continuing up the apertural face in only the youngest of adult chambers in complete individuals; but in *B. dilatata*, the angularity (carina) also wraps around the proloculus.

The digitate overlaps on sutures are mostly obscure in SEM images since they provide almost no surface elevation difference; they are best observed in stereomicrographs. They are best illustrated on line drawings of Cushman (1937) and stereomicrographs in Lei and Li (2016). The digitate overlaps are also present in the specimens illustrated for *B. spathulata* of Lei and Li (2016, fig. 5) which fits better with this taxon instead. In the SEM images provided by Sakınç (2008) and Kaminski et al. (2002) these overlaps are faintly observable. The specimens referred to *Bolivina* cf. *robusta* and *Bolivina* "*dilatata dilatatissima*" by Alavi (1980) and to *Bolivina robusta* by Lei and Li (2016) are considered to belong to this taxon instead. They are just shorter forms (6-7 pairs of chambers, probably not fully mature) with the same kind of sutural details.

The taxon is distinguished from most other biserial taxa by its larger size. The adult specimens are distinguished from *B. spathulata* by digitate overlaps on sutures which are flush with the test. Smaller specimens are distinguished from smaller representatives of *B. spathulata* by larger proloculus and broader and more curved initial serial chambers. Form is distinguished from *Bolivina alata* by its flush sutures and low and broad chambers, as well as by not possessing a well-defined carina that extends into spinal projections.

Bolivina pseudoplicata Heron-Allen and Earland, 1930

Plate 3 Figures 10-12; Plate 4 Figures 10-12

1930 *Bolivina pseudoplicata* – Heron-Allen and Earland, p. 81, pl. 3 fig. 36-40

1937 *Bolivina pseudoplicata* Heron-Allen and Earland; Cushman, p. 166, pl. 19 fig. 12-20

1978 *Bolivina pseudoplicata* Heron-Allen and Earland; Wright, p. 711, pl. 2 fig. 6-7

1991 *Bolivina pseudoplicata* Heron-Allen and Earland; Cimerman and Langer, p. 58, pl. 61 fig. 1-3

1991 *Bolivina pseudoplicata* Heron-Allen and Earland; Rasmussen, fig. 6.11

1993 *Bolivina pseudoplicata* Heron-Allen and Earland; Sgarrella and Moncharmont Zei, p. 208, pl. 14 figs. 9, 10

2003 *Bolivina pseudoplicata* Heron-Allen and Earland; Murray, fig. 5.17

2008 *Bolivina pseudoplicata* Heron-Allen and Earland; Sakınç, pl. 12 fig. 2-3

2012 *Bolivina plicatella* Cushman; Milker and Schmiedl, p. 80, fig. 19.21

non 2012 *Bolivina pseudoplicata* Heron-Allen and Earland; Milker and Schmiedl, p. 80, fig. 19.22-23

Test is small, longer than wide. Edges are rounded-subrounded, very faintly lobulate. Sutures are oblique, depressed when not obscured by costae-like features which project downward toward the proloculus: the projections align to produce the costae-like features spanning almost the whole test vertically. Test is porous, porosity especially observable on the last two chambers' upper parts where the costae-like features are absent and the pores are surrounded by polygonal ridges. Aperture is interiomarginal, loop-shaped.

Bolivina plicata d'Orbigny (1839a, p. 62, pl. 8, fig. 4-7) originally described from Chile (Eastern Pacific) is a widely misidentified taxon in the literature with most of the references given to it actually belonging to either *Bolivina plicatella* Cushman or *Bolivina pseudoplicata* Heron-Allen and Earland. The confusion is due to its holotype being missing and the fact that the illustrations given by d'Orbigny are highly schematic. This produces an important problem in taxonomy, given that *B. plicata* is the type taxon to genus *Bolivina*. Depiction of *B. plicata* in Reyment (1983) from the same area as the original description of the species, and the assignment of

neotype by Revets (1996) from the same sample d'Orbigny described his taxon, are probably the most accurate representations of the taxon. Both Reyment (1983) and Revets (1996) illustrate and describe an elongate, fully porous form with vertical costae-like features almost spanning the whole test. The costae-like features are produced by the ruffling of the outer walls, merging with the ruffling of the walls of the previous chamber in the series (Reyment, 1983), a feature similar to retral processes in elphidiids, producing the zig-zagging plicate riblets. Both *Bolivina pseudoplicata* and *Bolivina plicatella* are depicted (in their original descriptions) with similar plicate riblets produced (apparently) with similar ruffling of the outer walls.

Bolivina plicatella Cushman (1930a: p. 46, pl. 8, fig. 10 a-b) was described from fossil material (Miocene, Choctowhatchee marl) and most its citation also comes from fossil (mostly Miocene) material although recent representatives are noted to exist (Cushman, 1937). On the other hand, *Bolivina pseudoplicata* Heron-Allen and Earland was described from the northern Atlantic (British Isles). Cuhsman (1937) remarks that the plication in *Bolivina plicatella* is subtler, and the depressions between the plications in *Bolivina pseudoplicata* are cut deeper. Original depictions of the forms are quite similar and the different volume of the plications Cushman remarks are not distinguishable from given illustrations. It seems the distinction between these species is confined to the age of the strata specimens were found from (e.g., Wright, 1978; Verhallen, 1991) and the two species may as well be synonyms.

Except for Milker and Schmiedl (2012) no other recent foraminifera publication which reported both of these species were encountered during this study. All other accounts of this taxon under the name of *Bolivina pseudoplicata* from recent sediments agree mostly in morphology although with some variation in the strength of the ornamentations (costae, plicae), and what Milker and Schmiedl (2012) describe and illustrate with the name *Bolivina plicatella* fit well with those. However, the illustrations given for *Bolivina pseudoplicata* by Milker and Schmiedl (2012) are of a more robust form with distinctly sharper and disorganized surface ornamentations which probably do not belong to this taxon.

Most of the specimens assigned here have two longitudinal ridges clearly observable with the stereomicroscope. Size-wise the form is similar to *Bolivina albatrossi* and *Bolivina variabilis*, but wider; under the stereomicroscope the taxon is distinguishable by its surface ornamentation when it is clearly visible, but for smaller specimens, surface only appears "rugose" in which case they are differentiated from *B. albatrossi* and *B. variabilis* by the surface ornamentation being coarser and obstructing the visibility of the sutures more.

Bolivina spathulata (Williamson, 1858)

Plate 5 Figures 9-17; Plate 6 Figures 10-21

1858 *Textularia variabilis* var. *spathulata* Williamson, p. 76, fig. 164-165

1937 *Bolivina spathulata* Williamson; Cushman, p. 162, pl. 15 fig. 20-24

? 1980 *Bolivina dilatata* Reuss; Alavi, **p**. 43, pl. 25 fig. 3

1980 *Bolivina spathulata* (Williamson); Alavi, **p**. 44, pl. 24 fig. 8, pl. 25 fig. 9-11 (not 5), pl. 27 fig. 12-13

1980 *Bolivina* sp. – Alavi, p. 44, pl. 24 fig. 13-14

1991 *Brizalina spathulata* (Williamson); Cimerman and Langer, p. 60, pl. 62 fig. 3-5

1991 *Brizalina* sp. 1 – Cimerman and Langer, p. 60, pl. 62 fig. 10

2002 *Brizalina spathulata* (Williamson); Kaminski et al. pl. 2 fig. 9

2002 *Brizalina* sp. – Kaminski et al., pl. 2 fig. 14

2005 *Brizalina spathulata* (Williamson); Meriç et al., pl. 3 fig. 6

2008 *Brizalina spathulata* (Williamson); Sakınç, pl. 12 fig. 8-9

2012 *Brizalina spathulata* (Williamson); Milker and Schmiedl, p. 82, fig. 20.1

2014a *Brizalina spathulata* (Williamson); Meriç et al., pl. 50 fig. 2-5

2018 *Brizalina spathulata* (Williamson); Kırcı-Elmas, fig. 3.11

Test elongate, flaring; aboral part bluntly pointed, flaring towards the oral part; sides may become somewhat parallel for the last two pair of chambers. Margins acutely angled and usually carinate; carina or acutely pinched margin continues up to the oral side for the very last adult chamber pair in complete specimens. Periphery usually not lobate. Sutures straight to slightly curved, flush with surface except for the outer margins where they may become slightly depressed. Chambers low and broad, growing steadily as added; acutely angled to the median line. Surface smooth. Test porous on outer chamber walls, non-porous on the thin sutures.

Williamson's (1858) type describes curved sutures, however the later publications cited above interpret the taxon with straighter sutures, curving usually confined to near the outer margins. Although the periphery is mostly non-lobulate, some lobulation is seen in some individuals (e.g., Kırcı-Elmas, 2018). In addition, the angular margins are sometimes thinly carinated, and this carina is serrated (confined to chambers, not continuous through the sutures as in *Brizalina* sp. Kaminski et al. 2002) in some individuals. See *Bolivina dilatata* Reuss above for further discussion with regard to distinction from that taxon.

The taxon is distinguished from other biserial taxa by its larger size. From *B. dilatata* it is different by simple sutures (no digitate overlaps) and smaller initial part. In addition, *B. spathulata* is more commonly less flaring and narrower than *B. dilatata*.

Bolivina striatula Cushman, 1922b

Plate 3 Figures 17-21; Plate 4 Figures 17-24

1922b *Bolivina striatula* Cushman, p. 27, pl. 3 fig. 10

1936 *Bolivina striatula* Cushman var. *spinata* Cushman, p. 59, pl. 8 fig. 9

1947 *Bolivina* cf. *striatula* Cushman; Höglund, **p**. 266, pl. 24 fig. 4; pl. 32 fig. 14-15; text-figs. 277, 278, 287

1958 *Bolivina attica* Parker, p. 259, pl. 2 fig. 12-14

1960 *Bolivina striatula* Cushman; Hofker, p. 251, fig. 106

non 1973 *Brizalina striatula* (Cushman); Van Voorthuysen, p. 40, pl. 2 fig. 16

1973 *Brizalina attica* (Parker); Van Voorthuysen, p. 40, pl. 2 fig. 10

1980 *Bolivina attica* Parker; Alavi, p. 42, pl. 25 fig. 7a, 8; pl. 26 fig. 13

1991 *Brizalina striatula* (Cushman); Cimerman and Langer, p. 60, pl. 62 fig. 6-9

1993 *Bolivina striatula* Cushman; Sgarrella and Moncharmont Zei, p. 210, pl. 14 fig. 16

2002 *Brizalina striatula* (Cushman); Kaminski et al., p. 188, pl. 2 fig. 10

2008 *Brizalina striatula* (Cushman); Sakınç, pl. 12 fig. 10-11

2012 *Brizalina striatula* (Cushman); Milker and Schmiedl, 2012; p. 82, fig. 20.3

2014a *Brizalina striatula* (Cushman); Meriç et al., pl. 50 fig. 6

Test elongate, tapering towards the initial chamber but with almost parallel sides for most of the test; edges angular, initial chamber with a downward pointing, short spine. Initial portion of the test (about up to 3/4 of the adult forms) ornamented with thin, parallel costae. Sutures shallowly depressed to flush, slightly curved; obscured in the ornamented part. Aperture interiomarginal, rimmed from both sides in mature specimens by the extension of the angular margins. Surface smooth except for the costae in the initial part of the test; costae may be very shallow (in more compressed specimens) or elevated (in more robust specimens).

The original description of the taxon does not possess the spine feature, and exclusively remarks the shallowness of the striations (Cushman, 1922b) which is clearly seen in the SEM image of the holotype (by Smithsonian National Museum of Natural History Department of Paleobiology Collections, Catalogue number USNM

CC 1089, access via http://n2t.net/ark:/65665/3f9d51afb-4496-447a-8434-b4ba04b71b06). Later, Cushman (1936) described a variety of the taxon (*Bolivina striatula* var. *spinata*) which is distinct from its parent taxon by the presence of an acerose spine on the proloculus and being more tapering (see holotype image by Smithsonian National Museum of Natural History Department of Paleobiology Collections, Catalogue number USNM PP 26212, access via http://n2t.net/ark:/65665/35774c4d7-ae2f-4770-874d-c125bca345b7). Höglund (1947), remarked on the variable expression of both the costae (shallow and indistinct to strong-more elevated and longer) and the terminal spine (a slight protuberance to distinctly formed and long spine), described their taxon (marked cf. for measure) with the synonymy of both the parent taxon and the variety. Höglund assigned the degree of tapering of the test and the strength of costae as well as length and development of spine to generational differences.

Both varieties (with or without spine) can be found in the literature addressed as *Bolivina striatula* Cushman. For example; Cimerman and Langer (1991) and Milker and Schmiedl (2012) provide illustrations of specimens with no spine on the proloculus and do not mention such feature in their descriptions; while Kaminski et al. (2002) and Meriç et al. (2014a) both provide images of specimens with distinct spine on the proloculus. Considering the conventional use of the species *Bolivina striatula* already includes the types with spine on the proloculus, here, the variety *Bolivina striatula* var. *spinata* is taken as a synonym for this taxon.

A similar form is Parker's (1958) *Bolivina attica* which is described to possess a spine on the proloculus as the major difference from *Bolivina striatula* Cushman. Apart from Alavi (1980), Van Voorthuysen (1973) and Musco (2012), this taxon is very rarely referred to in the literature and as only in name (no accompanying description). Examining the holotype images (by Smithsonian National Museum of Natural History Department of Paleobiology Collections, Catalogue number USNM PR 6123, access via http://n2t.net/ark:/65665/3ec02cd4e-8cca-48c3-8ce4-13172946d701), its resemblance to *Bolivina striatula* var. *spinata* is clear, and here taken as a synonym of that taxon. The SEM image given by Sgarrella and

Moncharmont Zei (1993, pl. 14, fig. 11) for *B. attica* is a misidentification since it is much shorter and wider, has less developed angularity on the edges of the later portion of the test, and the striations are very faint.

The form can be readily distinguished from other bolivinids via the overall shape, presence of costae on the older portion of the test and the spine on the proloculus. Some variations in the strength (elevation) of the costae and the roundness of margins are observed in studied individuals. The elevation of the costae varies in individuals from slightly elevated (perceivable only on sutures) to elevated (clearly continuous for all its length). The roundness of the margins in the earlier portion of the test (first few pairs of chambers) varies from angular to subrounded. Although most of the studied individuals are elongate with more or less parallel sides (after a few pairs of initial chambers), a few individuals with stronger tapered shape with otherwise similar characteristics were also encountered; this shape variation is probably due to generational differences (Höglund, 1947). Forms, even when broken or pre-adult are easily distinguished with these characteristics.

Bolivina subspinescens Cushman, 1922a

Plate 3 Figures 25-28; Plate 4 Figures 25-29

	1884	*Bolivina textularioides* Reuss; Brady, p. 419, pl. 52 fig. 24-25
	1888	*Bolivina textularioides* Reuss; Brady, Parker and Jones, p. 221, pl. 43 fig. 1
?	1911	*Bolivina spinescens* – Cushman, p. 46, fig. 76
	1922a	*Bolivina subspinescens* – Cushman, p. 48, pl. 7 fig. 5
	1937	*Bolivina subspinescens* Cushman; Cushman, p.157, pl. 19 fig. 1-3
?	1937	*Bolivina spinescens* Cushman; Cushman, p. 142, pl. 18 fig. 17-19
	1985	*Bolivina subspinescens* Cushman; Hermelin and Scott, p. 204, pl. 3 fig. 2

1990 *Bolivina spinescens* Cushman; Hasegawa et al., p. 476, pl. 3 fig. 9

1990 *Bolivina subspinescens* Cushman; Hasegawa et al., p. 476, pl. 3 fig. 10

1992 *Bolivina subspinescens* Cushman; Timm, p. 44, pl. 5 fig. 6 a and b

1993 *Bolivina subspinescens* Cushman; Sgarrella and Moncharmont Zei, p. 210, pl. 14 fig. 12, 13

2008 *Bolivina subspinescens* Cushman; Leiter, p. 24, pl. 3 fig. 4

2008 *Bolivina subspinescens* Cushman; Sakınç, pl. 12 fig. 12-13

2010 *Bolivina spinescens* (Cushman); Margreth, p. 113, pl. 24 fig. 7

2010 *Bolivina subspinescens* Cushman; Margreth, p. 114, pl. 24 fig. 8

2012 *Bolivina subspinescens* Cushman; Milker and Schmiedl, p. 81, fig. 19.24

Test tapering, elongate; edge rounded; periphery lobulate; proloculus with apiculate spine. Chambers grow rapidly as added, inflated. Sutures deep, oblique. Aperture wide, ovate with a toothplate that does not stick out of the aperture. Surface rugged by fine to coarse pore pits and occasional minute spines, especially so near the bases of the chambers.

*Belorussiella textilarioides (*Reuss, 1863; originally described as *Bolivina textilarioides*) is an agglutinant form remarked to have "roughened surface" which was attributed by Reuss to erosion on an erroneously assumed hyaline test, and placed under genus *Bolivina*. Hence, the taxon was mistakenly used for hyaline forms of similar overall shape with slightly ornamented surfaces. Some accounts of *Belorussiella textilarioides* are synonymized into *Cassidelina spinescens* (Cushman, 1911; originally described as *Bolivina spinescens*) and *Bolivina subspinescens* Cushman (1922a) (Cushman, 1937). Of these records *Bolivina textilarioides* (Brady, 1884, pl. LII, fig. 24-25) stands out since it appears in synonym lists of both of the

taxa (Cushman, 1937) creating confusion in the concepts of both taxa. The two taxa are quite similar with elongate, tapering shapes, rounded edges, lobulate peripheries, inflated chambers, depressed sutures, surface ornamentations ("minutely spinose or granular", Cushman, 1911, 1922a, 1937) and a large and loop shaped aperture. Cushman (1922a) remarks that the chambers are more pronouncedly angular in *B. subspinescens* than in *C. spinescens*, however the angularity of chambers of *B. subspinescens* are taken as intraspecific variation in Cushman (1937). Moreover, the extent of surface roughness is illustrated to be limited to just above the sutures in *C. spinescens*. Meanwhile, a larger portion of the basal parts of the chambers in *B. subspinescens* are illustrated to be ornamented; however, variability of the ornamentations, with some specimens being completely clear while others being entirely covered with ornamentations, is also remarked (Cushman, 1937). These two features are the only ones distinguishing these two species, yet, these features of *C. spinescens* appear to be in the intraspecific variation of *B. subspinescens*. Considering the taxonomic confusion mentioned above and the overall similarity of these forms, their synonymy requires further studies. Moreover, replacement of *spinescens* (Cushman, 1911) into the genus *Cassidelina* (WoRMS Editorial Board, 2025, see https://www.marinespecies.org/aphia.php?p=taxdetails&id=490037), a genus with wide and ovate aperture with a spoon-like large toothplate, grants a need for further investigation for the replacement of *B. subspinescens*, which possesses a very similar aperture, as well.

Other references to *B. subspinescens* show some variation in the degree of surface ornamentation. These ornamentations occur as only large pore pits (Hasegawa et al., 1990), large pore pits accompanied by thin and vaguely observable spinose projections (Timm, 1992; Sgarrella and Moncharmont Zei, 1993; Leiter, 2008; Sakınç, 2008), and smaller pore pits (Milker and Schmiedl, 2012). The extent of the porosity also show variability as occurring only in the basal part of the chambers for the whole test (Hasegawa et al., 1990; Timm, 1992, adult specimen in pl. 5 fig. 6a; Leiter, 2008; Milker and Schmiedl, 2012) to covering almost the whole test except for the upper portions of the last formed pair of chambers (Timm, 1992, juvenile

specimen in pl. 5 fig. 6a; Sgarrella and Moncharmont Zei, 1993; Sakınç, 2008). Overall test shape also varies from thin and elongate (Hasegawa et al., 1990; Sgarrella and Moncharmont Zei, 1993; Leier, 2008; Sakınç, 2008; Milker and Schmiedl, 2012) to broader (Hermelin and Scott 1985; Timm, 1992; Margreth, 2010) forms. References to taxon *C. spinescens* in Hasegawa et al. (1990) and Margreth (2010) are very similar to *B. subspinescens* as depicted by Milker and Schmiedl (2012), and may as well be considered in this taxon's morphological variability.

An aspect which was not remarked by Cushman (1937), or in the description of the form by Milker and Schmiedl (2012) is a spine projection on the proloculus. Although short, a spine is present on the holotype (see holotype image by Smithsonian National Museum of Natural History Department of Paleobiology Collections, Catalogue number USNM CC 17080, access via http://n2t.net/ark:/65665/314633318-d9af-4dfb-bca8-826cd2698463); a similar short projection is seen in all other references cited above, and two publications show individuals with longer spine on the proloculus (Hermelin and Scott 1985; Timm, 1992, adult specimen in pl. 5 fig. 6a). Like the morphology of the aperture, which is the same for all mentioned references, this basal projection is another feature which fits in the description of genus *Cassidelina*. However, without detailed examination of the aperture, it is preferred here to keep the original name *Bolivina subspinescens* instead of replacement of this taxon into genus *Cassidelina*.

Taxon is different from other bolivinids by its generally smaller size, lobulate periphery, ornamented surface, dull appearance and large aperture.

Bolivina cf. *vadescens* Cushman, 1933a

Plate 3 Figures 29-34; Plate 4 Figures 30-35

	1947	*Bolivina* cf. *vadescens* Cushman; Höglund, p. 265, pl. 24 fig. 6
?	1984	*Bolivina catanensis* Seguenza; Brun et al., p. 22, pl. 10 fig. 34 a-h
	2002	*Brizalina catanensis* (Seguenza); Kaminski et al., pl.2 fig. 11

2012 *Bolivina catanensis* Seguenza; Mendes et al., fig. 2.6a-b

2012 *Bolivina ordinaria* Phleger and Parker; Mendes et al., fig. 2.8a-f

2013 *Bolivina variabilis* (Williamson); Kırcı-Elmas, fig. 5.1

2014a *Brizalina earlandi* (Parr); Meriç et al., pl. 49 fig. 18-20

2016 *Bolivina ordinaria* Phleger and Parker; Martins et al., pl. 3 fig. 12

2018 *Bolivina vadescens* Cushman; Fontanier et al., fig. 4 A-C

2021 *Bolivina ordinaria* Phleger and Parker; Kırcı-Elmas et al., fig. 5 h-i

Test medium in size, elongate, tapering in the earlier portion of the test, later, sides becoming almost parallel. Margins are subrounded (especially in the early portion of the test) to angular. Chambers wider than high, getting regularly higher as added; inflated especially in the median part. Sutures curved, sigmoid, depressed in the adult chambers, especially so in the median part, getting shallower near the margins; very shallow to flush in the earlier portion of the test; less curved (closer to horizontal) in shorter and more flaring specimens. Aperture usual bolivine type. Apertural end of the test broadly oval. Wall transparent, surface densely porous and usually shiny. Surface porosity may be limited to the basal parts of the chambers or may cover the whole chamber.

This taxon was recorded under several names: *Bolivina vadescens* Cushman (Höglund, 1947: as *cf.*; Fontanier et al., 2018), *Bolivina variabilis* Williamson (Kırcı-Elmas, 2013), *Brizalina earlandii* (Parr) (Meriç et al., 2014a), *Bolivina catanensis* Seguenza (1862a) (Brun et al., 1984; Kaminski et al,2002; Mendes et al., 2012), *Bolivina ordinaria* Phleger and Parker (Mendes et al., 2012; Martins et al., 2016; Kırcı-Elmas et al. 2021). In all these accounts the figured individuals are distinct with porous tests with distinctly angular margins and sigmoid and depressed sutures. These characters do not agree with none of the assigned names: *Bolivina vadescens* has flush sutures (Cushman, 1933a, p. 81, pl. 8, fig. 11 a and b; see holotype image by Smithsonian National Museum of Natural History Department of Paleobiology

Collections, Catalogue number USNM CC 19014, access via http://n2t.net/ark:/65665/35935c63d-5d0d-46fb-9f35-3a31b54d473b); *Bolivina variabilis* has large polygonal pore pits, almost horizontal sutures, and rounded margins (Williamson, 1858); *Bolivina earlandii* has taller than wide chambers and rounded margins (Parr, 1950); *Bolivina catanensis* has a distinctly carinate edge, shallowly depressed sutures and a sparse surface porosity, more akin to *Bolivina spathulata* (Seguenza, 1862a); and *Bolivina ordinaria* has strongly limbate and opaque sutures which are not as depressed (Phleger and Parker, 1951; see holotype image by Smithsonian National Museum of Natural History Department of Paleobiology Collections, Catalogue number USNM PAL 369353, access via http://n2t.net/ark:/65665/3aa6e46ce-bbff-4074-a48a-b9c0d639384e).

This taxon is quite abundant in the Sea of Marmara, however, other than the above cited names, it is probably lumped in with other bolivinids. In the absence of a better fitting name, and regarding the most similarities with Cushman's taxon, here it is left in open nomenclature.

The form is easily distinguished from other bolivinids by its shiny surface, transparent and porous test, elongate shape, inflated chambers and distinct suture shape. The pre-adult forms are found to have less curved and less depressed sutures and more rounded margins, but the test porosity and chamber inflation distinguish them.

Bolivina variabilis (Williamson, 1858)

Plate 3 Figures 13-16; Plate 4 Figures 13-16

1858 *Textularia variabilis* – Williamson, p. 76, fig. 162-163

1866 *Textilaria globigera* Schwager, p. 252, pl. 7 fig. 100

1933a *Bolivina globulosa* Cushman, p. 80, pl. 8 fig. 9a and b

part 1937 *Bolivina variabilis* (Williamson); Cushman, p. 158, pl. 16 fig. 6, 12, 14 (not fig. 13)

1965 *Bolivina variabilis* (Williamson); Phleger, p. 51, pl. 1 fig. 8

1970 *Bolivina variabilis* (Williamson); Sliter, p. 166, pl. 5 fig.4; pl. 6 fig.13

1978 *Bolivina variabilis* (Williamson); Wright, p. 712, pl. 2 fig. 19-20

? 1980 *Bolivina variabilis* (Williamson); Alavi, p. 44, pl. 25 fig.1

1980 *Bolivina variabilis* (Williamson); Boltovskoy et al., p. 18, pl. 4 fig. 14

1991 *Bolivina variabilis* (Williamson); Cimerman and Langer; p. 59, pl. 61 fig. 7-8

1999 *Bolivina variabilis* (Williamson); Lipps and Langer, pl. 1 fig. 3

2001 *Brizalina variabilis* (Williamson); Alve and Murray et al., pl. 2 fig. 56

2004 *Bolivina variabilis* (Williamson); Ertan et al., pl. 1

2009 *Bolivina variabilis* (Williamson); Darling et al., fig. S1, S4, SI Text

2012 *Bolivina variabilis* (Williamson); Milker and Schmiedl, p. 81, fig. 19.25-26

2017 *Bolivina variabilis/Steprochilus* complex; Kucera et al., fig. 7, Supplementary Material 4

2018 *Bolivina variabilis* (Williamson); Romano et al., pl. 1 fig. 8

2019 *Bolivina variabilis* (Williamson); Little and van Hengstum, fig. 3.6

2020 *Bolivina variabilis* (Williamson); Aiello, p. 10, fig. 3.10

2022 *Bolivina variabilis* (Williamson); Meilland, p. 5, pl. 2-right

Test small to medium size, elongate; edges subrounded-rounded. Chambers commonly with basal extensions (similar to retral processes). Sutures curved (arcuate to sinusoidal) with changing degree of digitate overlaps; commonly obscured by surface ornamentation. Aperture interiomarginal. Surface punctate with

large pore pits and almost reticulate patterns produced by merging of the polygonal rims of the pores and digitate basal lobes of chambers, especially in the initial part of the test.

As the name was taken to be the evidence of it, the taxon was treated in the literature as with high intraspecific morphological variation; however, Williamson (1858) named their taxon *variabilis*, not because of the variation they observed in their *variabilis* typica, but because they assumed the three varieties they also defined in the same publication (*variabilis* var. *difformis*, *variabilis* var. *laevigata*, *variabilis* var. *spathulata*) as belonging to the same species. The description of typica indicates slender forms with slightly lobulate margins, depressed and usually arcuate sutures, chambers of equal length and breadth, and coarsely pitted surface. The taxon concept was interpreted differently by many authors which do not align with the original description (e.g., Cushman, 1942; Debenay, 2012; Kırcı-Elmas, 2013); nevertheless, the concept used here follows the descriptions and illustrations in the publications cited above. Among these cited publications, still a considerable morphologic flexibility occurs, most of all in terms of the presence and development of the basal lobes and the reticulate surface.

Darling et al. (2009) state that *Streptochilus globigerus* (Schwager, 1866; originally described as *Textilaria globigera*) and *Streptochilus globosus* (Cushman, 1933a; originally described as *Bolivina globulosa*) are the same species as *Bolivina variabilis* according to molecular (genetic) studies, a tychopelagic (able to live as both plankton and benthos) taxon which may be the link in the transition from benthic to planktonic mode of life (Darling et al. 2009; Kucera et al., 2017). The scope of the morphologic variation in *B. variabilis* is well documented in Kucera et al. (2017, taxon referred as *Bolivina variabilis/Streptochilus* complex) for the individuals recovered from plankton tows, and in Darling et al. (2009).

The form is similar to *Bolivina compacta* Sidebottom in terms of elongate test and pitted – punctate surface; smoother individuals of *B. variabilis* may be confused with *B. compacta* (Sliter, 1970; Wright, 1978; Alavi, 1980). The form is also similar to

Bolivina pseudoplicata Heron-Allen and Earland (1930) in terms of its ornamented surface; forms of *B. pseudoplicata* with less pronounced vertical costae may be confused with *B. variabilis* (Wright, 1978). Here, the individuals with punctate surface, if two zigzagging vertical costae were not observed with the stereomicroscope, were placed under *B. variabilis*, hence this taxon may include specimens which would be assigned to *B. compacta* or *B. pseudoplicata*.

This taxon is distinguishable from others by its punctate and sometimes rugose surface and dull appearance, and usually smaller size.

Bolivinellina **Saidova, 1975**

Bolivinellina sp.

Plate 5 Figures 18-21; Plate 6 Figures 22-25

Test slender with elliptical cross section, biserial with the last chamber tending uniserial. Outline mostly non-lobulate. Chambers lower in the initial part, getting higher as added. Sutures oblique, simple. Wall transparent, very thin. Surface smooth, lower half of chambers porous. Aperture bolivine-type, interiomarginal loop in the biserial part, terminal in the uniserial last chamber.

Most of the specimens belonging to this taxon were found as broken either at the initial end or the oral end, or both, with 6-7 chamber pairs. The wall is transparent and very thin compared to other *Bolivina*. Very few forms were found with adult uniserial chamber on which the aperture becomes terminal rather than interiomarginal like other *Bolivina*. A similar feature, although not present in the description, is found in *Bolivina humilis* (Cushman and McCulloch, 1942, pl. 26 fig. 6), however that taxon is longer (8-10 chamber pairs) and broader according to type illustrations. *Bolivinellina pacifica* is also similar in terms of shallowness of the sutures and H/W ratio of chambers, however is also very long (~10 chamber pairs) and a uniserial tendency or terminal aperture are not mentioned for the type (Cushman and McCulloch, 1942). *Bolivinellina pescicula* holotype (as illustrated in

Loeblich and Tappan, 1988) is the most fitting to our taxon, but the uniserial tendency is not included in the generic description.

Taxon is distinguished from other biserial taxa by the transparent and shiny, very slender test, shallow to flush sutures between higher than wide chambers and distinct porosity on the lower half of the chambers.

Subfamily Fursenkoininae Loeblich & Tappan, 1961

Genus *Fursenkoina* Loeblich & Tappan, 1961

1961 Fursenkoina – Loeblich and Tappan, p. 314

Type: *Virgulina squamosa* d'Orbigny in Deshayes (1832, p. 1127)

Test elongate, with ovate to rounded transverse section, twisted biserial. Chambers usually taller than wide, somewhat inflated. Aperture narrow, comma shaped, with internal toothplate. Wall hyaline, optically granular; surface smooth.

The twist in biseriality gives an irregular look to especially the initial part of the test. A similar irregular look is also present in *Stainforthia*, whose initial portion is triserial. These two genera are commonly confused with each other. Two main distinctions between the genera are wall type and apertural character. *Fursenkoina* has an optically granular wall while *Stainforthia* has radial (Loeblich and Tappan, 1961; Hofker, 1956). However, the apertural characteristics are much less clear and may become highly similar. *Fursenkoina* usually develops a narrow, long, slit-like aperture, while the aperture of *Stainforthia* is produced in a wider, ovate depression and may develop terminally in adult specimens. The toothplate in *Fursenkoina* may be extending through the apertural opening and may be dentate (Loeblich and Tappan, 1964).

Genera *Cassidella* Hofker and *Virgulina* d'Orbigny are considered to be synonyms of *Fursenkoina* (Hofker, 1956, Revets, 1996). Many species originally described under *Virgulina* belong to either *Fursenkoina* or *Stainforthia*.

Fursenkoina schreibersiana (Cžjžek, 1848)

Plate 5 Figures 22-24; Plate 6 Figures 26-29

	1848	*Virgulina schreibersiana* – Cžjžek, p. 147, pl. 13 fig. 18-23
non	1884	*Virgulina schreibersiana* Cžjžek; Brady, p. 414, pl. 52 fig. 1-3
non	1893	*Virgulina schreibersiana* Cžjžek; Egger, p. 290, pl. 8 fig. 93-95
	1980	*Fursenkoina schreibersiana* (Cžjžek); Alavi, p. 70, pl. 37 fig. 8
part	1985	*Fursenkoina acuta* (d'Orbigny); Papp and Schmid, p. 82, pl. 75 fig. 2-6 (fig. 1 ?)
	1991	*Fursenkoina acuta* (d'Orbigny); Cimerman and Langer, p. 64, pl. 67 fig. 1, 2
	1994	*Fursenkoina acuta* (d'Orbigny); Knudsen and Seidenkrantz, pl. 3 fig. 8-11, 18
	1996	*Fursenkoina squamosa* (d'Orbigny); Revets, p. 12, pl. 8 fig. 1-4
?	1996	*Fursenkoina schreibersiana* (Cžjžek); Revets, p. 12, pl. 8 fig. 5-8
	2006	*Fursenkoina acuta* (d'Orbigny); Avşar et al., pl. 2 fig. 8
	2008	*Fursenkoina acuta* (d'Orbigny); Sakınç, pl. 14 fig. 8
	2012	*Fursenkoina acuta* (d'Orbigny); Milker and Schmiedl, p. 92, fig. 21.10-11

Test oblong, somewhat compressed; both apertural and adapertural poles rounded. Chambers somewhat inflated, embracing, biserially arranged with a very significant twist so that the two series cannot be traced easily. Sutures depressed. Aperture narrow, long, rimmed on one side with a lip and equipped with a serrated toothplate which extends out the apertural opening. Surface smooth, shiny; test translucent, whitish.

D'Orbigny (1846, p. 234, pl. 13, fig. 4,5, pl. 14, fig. 5-7) described *Polymorphina acuta* as an elongated, biserial form with a large radiate aperture, later renamed as *Polymorphina subacuta* by d'Orbigny (1852, p. 159). The name *Polymorphina acuta* was previously given to another taxon by d'Orbigny (1826, p. 99; nomen nudum), described briefly ("espèce très-allongée") in d'Orbigny (1852, p. 160) with reference to the former publication, later illustrated by Fornasini (1900, p. 135, tf. 1), and renamed by Haynes (1958, p. 13, pl. 5 fig. 4) as *Polymorphina eolithiformis*. The former (*P. subacuta* d'Orbigny, 1852 = *P. acuta* d'Orbigny, 1846) was later studied by Papp and Schmid (1985). They note that in the original material of d'Orbigny only a few individuals, which are deemed juvenile, match the illustrations given in 1846. The rest of the specimens were larger and all of the specimens were considered identical to *Virgulina schreibersiana* Čžjžek. Papp and Schmid (1985) further note that the apertures of the specimens were not radiate like d'Orbigny indicated, but rather slit-like; and proposed that the valid name of the taxon to be *Fursenkoina acuta* (d'Orbigny, 1846). Though, the SEM images given by Papp and Schmid (1985) are quite different than d'Orbigny's illustrations for the taxon, not only in terms of apertural morphology, but also in terms of chamber arrangement. D'Orbigny's illustrations do not depict the irregularly twisted nature of the earlier chambers. On the other hand, the SEM images given by Papp and Schmid (1985) are near identical to Čžjžek's (1848). Judging by the illustrations, the synonymy of d'Orbigny's *P. acuta* (1846) and Čžjžek's *V. schreibersiana* is questionable. Yet, the name *Fursenkoina acuta* (d'Orbigny) is widely used for this morphospecies (see above cited synonymy).

Čžjžek (1848) denoted that *V. schreibersiana* is different from *Virgulina squamosa* d'Orbigny due to more bulbous chambers and rounded initial end. The illustrations Revets (1996) attributed to *Fursenkoina squamosa* (d'Orbigny) fits better to Čžjžek's taxon instead, and are very similar to accounts cited in the synonymy here. Alavi (1980) noted that individuals intermediate between *F. schreibersiana* and *F. squamosa* were present, and that these two species may be synonymous.

Papp and Schmid (1985) and Cimerman and Langer (1991) illustrate very tall individuals among shorter ones. The more elongate specimens (with more numerous chambers) are more distinctly biserial in the later part of the test. In this study, only short individuals were found in which only the twisted portion with more embracing chambers were present.

The aperture on the specimens investigated here are all narrow, one side rimmed with a narrow lip, and at the apex a small portion of the serrated toothplate sticks out. A similar feature of the toothplate is observable in figures of Cimerman and Langer (1991), Knudsen and Seidenkrantz (1994), and Milker and Schmiedl (2012).

The wall of the taxon is considerably less transparent than *Stainforthia* and has more of a frosted look. The elongate and enveloping earlier chambers and irregular (twisted) arrangement distinguishes this taxon from others.

Superfamily Buliminoidea Jones, 1875 (fide Loeblich and Tappan, 1984)

Family Buliminidae Jones, 1875 (fide Loeblich and Tappan, 1984)

Triserial forms with loop-shaped aperture with an internal tooth plate.

Genus *Bulimina* d'Orbigny, 1826

1826 *Bulimina* – d'Orbigny, p. 269

Type: *Bulimina marginata* d'Orbigny (1826, p. 269, pl. 12 fig. 10-12)

Test usually somewhat conical to elongate; chambers triserially arranged with various degree of overlap. Sutures usually distinct, depressed, unless obstructed by surface ornamentation. Surface smooth or may be ornamented with spines or costae. Aperture interiomarginal, situated in a shallow depression, ovate; an internal toothplate provides a loop surrounding the opening. Test transparent, to translucent and yellowish; surface usually shiny.

Taxonomy and history of buliminids are highly convoluted. High intraspecific morphologic variation occurs in populations blurring the limits of morphospecies.

Bulimina aculeata d'Orbigny, 1826

Plate 7 Figures 1-7; Plate 8 Figures 1-8

1826 *Bulimina aculeata* – d'Orbigny, p. 269, no. 7

1871 *Bulimina aculeata* d'Orbigny; Parker et al., p. 72, N° 70, fig. 128

1884 *Bulimina aculeata* d'Orbigny; Brady, p. 406, pl. 51 fig. 7-9

1911 *Bulimina aculeata* d'Orbigny; Cushman, p. 86, fig. 139

1922a *Bulimina aculeata* d'Orbigny; Cushman, p. 96, pl. 22 fig. 1-2

2006 *Bulimina marginata* d'Orbigny; Avşar et al., pl. 2 fig. 5

2008 *Bulimina elongata* d'Orbigny; Sakınç, pl. 13 fig. 12

2012 *Bulimina aculeata* d'Orbigny; Milker and Schmiedl, p. 87, fig. 20.19

2014a *Bulimina aculeata* d'Orbigny; Meriç et al., pl. 50 fig. 20-21

Test may be short or elongate. Chambers triserially arranged; triseriality becomes somewhat irregular towards the younger chambers in elongate specimens. Chambers very enveloping in earlier chambers, becoming less so towards the younger ones in elongate specimens. Sutures depressed. Aperture a regular buliminid loop. Surface smooth other than spines concentrated especially on the earlier chambers; spines conical, may be stout, but at least a few of them situated on or near the proloculus are longer; directed outwards with an acute angle to the long axis.

Jorissen (1988) considered all non-costate buliminids under the name *Bulimina marginata* and distinguished forma *aculeata* due to density of spines and absence of undercut margins of chambers. He remarked that forma *aculeata* has a triangular transverse section. Triangular transverse section is observed in this study only in shorter (may be juvenile) specimens; in more elongate forms the upper part of the test has a more rounded transverse section. Jorissen (1988) marked similar elongate forms as elongate variants of forma *aculeata*. Such elongate forms were sometimes attributed to *Bulimina elongata* d'Orbigny (e.g., Sakınç, 2008, pl. 13 fig. 12),

however here considered to belong to *B. aculeata* due to clearly observable spines on the earlier chambers. Brady (1884) noted that the later chambers of *B. aculeata* may be completely smooth, a feature also observed in this study.

Tsuchiya et al. (2008) showed that the spines on *Bulimina aculeata* are directed away from the coiling axis as opposed to *Bulimina marginata* d'Orbigny in which the spines are more or less parallel to the long axis. The length of the test in Tsuchiya et al.'s studied *B. aculeata* population is quite constant with all illustrated specimens having a more or less conical-fat shape which is not much taller than wide. These specimens may be juvenile representatives of the taxon.

B. marginata differs from this taxon by its spines being aligned on the carinate edge of the chambers. The spines on this taxon may or may not be aligned in a row, and the chamber edges are never carinated and never undercut. *B. elongata* is different from this taxon by a more elongate shape, but, more importantly the near absence of spines. The juveniles of this taxon are very similar to that of *B. elongata*, but is distinguished by the presence of spines.

Bulimina costata d'Orbigny, 1852

Plate 7 Figures 18-21; Plate 8 Figures 24-28

1826 *Bulimina costata* – d'Orbigny, p. 269 n° 1 [nomen nudum]

1852 *Bulimina costata* – d'Orbigny, p. 194

1947 *Bulimina costata* d'Orbigny; Cushman and Parker, p. 115, pl. 27 fig. 2-3

1980 *Bulimina costata* d'Orbigny; Alavi, p. 41, pl. 23 fig. 1, pl. 24 fig. 5

1991 *Bulimina* cf. *alazaensis* Cushman; Cimerman and Langer, p. 62, pl. 64 fig. 1-2

1993 *Bulimina costata* d'Orbigny; Sgarrella and Moncharmont Zei, p. 211, pl. 15 fig. 3

2012 *Bulimina costata* d'Orbigny; Milker and Schmiedl, p. 87, fig. 20.20

Test conical-elongate; earlier whorls increasing in diameter rapidly, in later whorls test may become more cylindrical than conical. Chambers triserially arranged, globular; bottom margins of chambers undercut, somewhat carinated, especially so in younger chambers; in later chambers undercut margins may disappear and may only be confined to some costae. Sutures depressed, obscured by surface ornamentation. Aperture a buliminid loop. Surface ornamented with high and strong, longitudinal costae except for the top halves of the last formed chambers which are smooth; surface between costae smooth and shiny. Costae continuous through several chambers, extend into spines pointing downward. Test transparent, finely porous.

D'Orbigny (1826) proposed the names *Bulimina costata* and *striata* (p. 269 n° 2) for fossil and recent forms respectively, but provided no descriptions or illustrations (nomen nudum). *B. striata* was illustrated in Guérin-Méneville (1832, p. 9, pl. 2, fig. 16), and *B. costata* was illustrated in d'Orbigny (1852), both without descriptions, and with near identical illustrations. According to Cushman and Parker (1947), *B. striata* has a basal spine which is not present in *B. costata*.

Bulimina buchiana d'Orbigny, another costate buliminid, differs from *B. costata* by its "non-keeled whorls near the sutures", pointing towards the lack of undercut and carinated chamber margins (d'Orbigny, 1846). Such undercut margins are illustrated for *B. striata* (Guérin-Méneville, 1832) and *B. costata* (d'Orbigny, 1852), and is present in the above cited more recent literature, although sometimes somewhat muted in the latest chambers, contrary to original illustrations. In this study, individuals referred to this taxon also possesses undercut and carinated chamber margins in the earlier whorls, but in more elongate specimens this feature is somewhat lost and only confined to breaks in some costae at the sutures.

Taxon is distinguished from the other costate buliminid *Bulimina inflata* by its usually smaller diameter and smoother test (finer porosity).

Bulimina elongata d'Orbigny, 1846

Plate 7 Figures 8-10; Plate 8 Figures 9-13

1846 *Bulimina elongata* – d'Orbigny, p. 187, pl. 11, figs. 19, 20

1980 *Bulimina elongata* d'Orbigny; Alavi, p. 45, pl. 22 fig. 11, pl. 23 fig. 8

1991 *Bulimina elongata* d'Orbigny; Cimerman and Langer, p. 62, pl. 64 fig. 3-8

? 2012 *Bulimina elongata* d'Orbigny; Milker and Schmiedl, p. 88, fig. 20.21

Test elongate, slender. Chambers triserially arranged; triseriality becomes somewhat irregular towards the younger chambers. Sutures depressed. Aperture a regular buliminid loop. Surface smooth other than very rare, very short spines.

Taxon is distinguished from other buliminids by being (almost) totally smooth, having an elongate test (H>>W) and somewhat lax coiling in the upper half of the test.

Bulimina inflata Seguenza, 1862a

Plate 7 Figures 22-25; Plate 8 Figures 29-36

1862a *Bulimina inflata* – Seguenza, p. 109, pl. 1 fig. 10

? 1884 *Bulimina inflata* Seguenza; Brady, p. 406, pl. 51 fig. 10-13

1980 *Bulimina inflata* Seguenza; Alavi, p. 46, pl. 23 fig. 4 [sic. Should be 5]

1993 *Bulimina inflata* Seguenza; Sgarrella and Moncharmont Zei, pl. 15 fig. 2

Test large, conical-elongate; earlier whorls increasing in diameter rapidly, in later whorls test may become more cylindrical than conical. Chambers triserially arranged, globular; bottom margins of chambers may appear undercut due to breaks in costae. Sutures slightly depressed, highly obscured by surface ornamentation.

Aperture a buliminid loop. Surface punctate with coarse pores, ornamented with longitudinal costae which are usually confined to chambers but may align to give a continuous appearance. Costae extend into spines pointing downward. Test thick, transparent, coarsely porous, giving a sugary appearance.

Brady (1884) provided illustrations and description for *B. inflata*, noting that it being a taxon of intermediate morphology linking *Bulimina aculeata* d'Orbigny and *Bulimina buchiana* d'Orbigny. Brady's illustrations were later classified under *Bulimina mexicana* Cushman by Jones (1994). *B. mexicana* has stronger costae according to Cushman (1922a; as variety of *B. inflata*), and the costae end in spines according to Cushman (1947; as variety of *B. striata*); nonetheless, *B. mexicana* (see holotype image by Smithsonian National Museum of Natural History Department of Paleobiology Collections, Catalogue number USNM PP 16402a, access via http://n2t.net/ark:/65665/m3a117ffcb-aa4e-4ac1-9350-d4c4d92deb2e) is significantly different from *B. inflata* since the former lacks the prominent coarse porosity of the latter which is distinctly illustrated and noted in the original description (Seguenza, 1862a). Brady's illustrations are very much in line with the original description of *B. inflata*, although the porosity is not depicted.

The form is distinguished from *B. costata* very easily by the very coarse porosity; in addition, the costae are lower and somewhat more irregular in shape, and the circumference of the test is usually greater. Sgarrella and Moncharmont Zei (1993) indicated that the juveniles of B. costata and B. inflata were difficult to distinguish, however, the porosity and width of the test are characters present even in the smallest specimens encountered in this study.

Bulimina marginata d’Orbigny, 1826

Plate 7 Figures 11-17; Plate 8 Figures 14-23

1826 *Bulimina marginata* – d'Orbigny, p. 269, pl. 12 fig. 10-12

1858 *Bulimina pupoides* var. *marginata* – Williamson, p. 62, fig. 126-127

1911 *Bulimina marginata* d'Orbigny; Cushman, p. 83, fig. 136

1922a *Bulimina marginata* d'Orbigny; Cushman, p. 91, pl. 21 fig. 4-5

1980 *Bulimina marginata* d'Orbigny; Alavi, p. 46, pl. 22 fig. 12

1991 *Bulimina marginata* d'Orbigny; Cimerman and Langer, p. 62, pl. 64 fig. 9-11

1993 *Bulimina marginata* d'Orbigny; Sgarrella and Moncharmont Zei, p. 212, pl. 15 fig. 5-7

non 2006 *Bulimina marginata* d'Orbigny; Avşar et al., pl. 2 fig. 5

2008 *Bulimina marginata* d'Orbigny; Sakınç, pl. 13 fig. 14-15

2012 *Bulimina marginata* d'Orbigny; Milker and Schmiedl, p. 88, fig. 20.23

2014a *Bulimina marginata* d'Orbigny; Meriç et al., pl. 51 fig. 11-13

Test conical; earlier whorls increasing in diameter rapidly, later whorls may become more cylindrical than conical in elongate specimens. Chambers triserially arranged, globular; bottom margins of chambers undercut providing a keeled edge. Sutures depressed. Aperture a buliminid loop. Surface smooth other than a row of spines situated at the keeled edge of chambers; spines directed downward parallel to the long axis. Test transparent, surface smooth, shiny.

Three main varieties occur in the *Bulimina marginata* population. The classic (sensu stricto) variety is with short tests, very well defined keeled and spinose margins and wide shoulders (undercut portions) occurring in all chambers (Plate 7 Figures 12-13; Plate 8 Figures 15-19). The elongate variety is with less wide shoulders and the shoulders and keeled margins disappear in the later chambers while having a more cylindrical shape (Plate 7 Figures 11; Plate 8 Figures 14). The pyramidal variety is with a more regular triseries and very small spines at the carinated edges, with triangular cross section in larger specimens (Plate 7 Figures 14-17; Plate 8 Figures 20-23). This variety may be considered under *Bulimina denudata* Cushman and

Parker (1938). Other than the classical variety, the other forms are very rare, hence were not treated separately.

Taxon is very easily distinguished by its carinate and spinose chamber margins.

Family Buliminellidae Hofker, 1951a

Genus *Buliminella* Cushman, 1911

1911 *Buliminella* – Cushman, p. 88

Type: *Bulimina elegantissima* d'Orbigny (1839a, p. 51, pl. 7 fig. 13-14)

Test elongate; tall (in the direction of long axis) and narrow chambers coiled in a high trochospire of only up to about three whorls; sutures shallowly depressed; aperture a loop in the depressed apertural face.

Cushman (1911) originally included *Bulimina subtere*s Brady, *Bulimina declivis* Reuss and *Bulimina contraria* Reuss in this genus due to long and obliquely coiled chambers and seemingly bulimin-like aperture; however, all of these taxa are now considered in Order Robertinida due to aragonitic wall structure.

Buliminella elegantissima (d'Orbigny, 1839a)

1839a *Bulimina elegantissima* – d'Orbigny, p. 51, pl. 7 fig. 13-14

1858 *Bulimina elegantissima* d'Orbigny; Williamson, p. 64, fig. 134-135

1884 *Bulimina elegantissima* d'Orbigny; Brady, p. 402, pl. 50 fig. 20-22

1947 *Buliminella elegantissima* d'Orbigny; Cushman and Parker, p. 67, pl. 17 fig. 10-12

1980 *Buliminella elegantissima* d'Orbigny; Alavi, p. 41

2016 *Buliminella elegantissima* d'Orbigny; Lei and Li, p. 224, fig. 14

Test small, fusiform. Chambers tall (in the direction of long axis) and narrow, numerous, situated obliquely to the long axis, coiled tightly, forming about two-three

whorls las of which is mostly involute. Sutures indistinct, shallow. Aperture interiomarginal, a loop, situated in a depression on the apertural face. Surface smooth; test translucent, whitish.

Buliminella multicamerata Cushman and Parker is a quite similar species in terms of numerous tall and narrow, tightly coiled chambers, but the apertural character is distinctly different and is accepted to belong to genus *Elonglobula* Finlay (Revets, 1993a). Alavi (1980, p. 41, pl. 24 fig. 6, pl. 22 fig. 6) reports a form he attributed to *Buliminella* sp., it probably belongs to genus *Elonglobula* instead.

This taxon is extremely rare in the Sea of Marmara, yet highly recognizable due to very distinct morphology.

Family Reussellidae Cushman, 1933c

Genus *Reussella* Galloway, 1933

1933 *Reussella* – Galloway, p. 360

Type: *Verneuilina spinulosa* Reuss (1850, p. 374 pl. 47 fig. 12)

Reussella spinulosa (Reuss, 1850)

Plate 9 Figure 7; Plate 10 Figures 8-9

1850 *Verneuilina spinulosa* – Reuss, p. 374, pl. 47, fig. 12

1988 *Reussella spinulosa* (Reuss) – Loeblich and Tappan, p. 527, pl. 575 fig. 9-12

Test pyramidal, triserial, with triangular transverse section. Edges angular, carinate. Sutures thickened, somewhat raised, with spinose, downward pointing projections at the corners. Aperture an interiomarginal slit, with an internal toothplate. Chamber surfaces porous, pustulose; sutures non-porous. Test transparent.

Taxon is quite rare in the Sea of Marmara, but is easily distinguished by its strictly triangular transverse section from other triserial taxa.

Family Siphogenerinoididae Saidova, 1981

Genus *Rectuvigerina* Mathews, 1945

1945 *Rectuvigerina*– Mathews, p. 590

Type: *Rectuvigerina multicostata* (Cushman & Jarvis, 1929, p. 14, pl. 3 fig. 6)

The genus is distinct with triserial to biserial to uniserial chamber arrangement, aperture produced on a short neck and with an internal toothplate, and costate ornamentations. The ornamentations are isolated on separate chambers, and do not cover the whole chamber; the areas near the sutures are unornamented.

The systematic placement of this genus is currently under Family Siphogenerinoididae, Superfamily Buliminoidea, apart from other triserial and necked taxa, namely genera *Trifarina* and *Uvigerina*. According to a genetic study, genus *Rectuvigerina* is more closely related to Uvigerinidae (Schweizer et al., 2005).

Rectuvigerina phlegeri Le Calvez, 1959

Plate 9 Figures 1-6; Plate 10 Figures 1-7

1959 *Rectuvigerina phlegeri* – Le Calvez in Berthois and Le Calvez, p. 363, pl. 1 fig. 11

1992 *Rectuvigerina phlegeri* Le Calvez; Schiebel, p. 55, pl. 3 fig. 10 a-d

? 1992 *Rectuvigerina bononiensis* (Fornasini); Schiebel, p. 54, pl. 3 fig. 8

2008 *Rectuvigerina phlegeri* Le Calvez; Sakınç, pl. 13 fig. 5-6

2012 *Rectuvigerina phlegeri* Le Calvez; Milker and Schmiedl, p. 86, fig. 20.18

? 2012 *Rectuvigerina bononiensis* (Fornasini); Milker and Schmiedl, 2012; p. 86, fig. 20.17

2014a *Rectuvigerina phlegeri* Le Calvez; Meriç et al., p. 222, pl. 50 fig. 15-18

Test elongate; chambers triserial to biserial to uniserially arranged. Chambers inflated; sutures depressed. Sutures become horizontal in the uniserial portion. Aperture produced on a short neck, kind of centered even in the initial triserial or biserial part of the test. Surface ornamented with fine longitudinal costae isolated on separate chambers, diminishing towards the top of the chambers. Costae may extend downward into thin and short spines.

Form is prominent with a short initial (triserial) part, followed by a prominent biserial stage and one-two uniserial chambers (Le Calvez in Berthois and Le Calvez, 1959).

Milker and Schmiedl (2012) report *Rectuvigerina bononiensis* (Fornasini, 1888) in addition to *R. phlegeri* from the Mediterranean recent fauna. They remark that *R. bononiensis* has a triserial to biserial chamber arrangement. Their illustration of the species is of a small specimen, and is exactly the same as *R. phlegeri* except the test is finished at the biserial stage, and the chambers appear to be a bit more elongated than what they show for *R. phlegeri*. Similarly, Schiebel (1992) also report a *R. bononiensis*. In their remarks they note that some of the adult forms of this taxon has the final chamber as uniserial. In Schiebel's (1992) illustrations, too, other than the previously mentioned chamber elongation, all other aspects of the specimens are exactly same as *R. phlegeri*.

The nature of the initial chamber arrangement of *R. bononiensis* is proven to be polymorphine-mode (chambers with 144 degrees apart) instead of triserial (Haunold, 1990); however, it impossible to judge from the illustrations given by Milker and Schmiedl (2012) and Schiebel (1992); their assignment, therefore, cannot be verified by this aspect. However, specimens of *R. bononiensis* illustrated in these two publications are different from Fornasini (1888 and 1898) and fossil material (e.g., Pellegrino et al., 2020) in more ways: costae are less numerous, test is less robust, outline more lobulate, chambers more elongate. These aspects are more akin to *R. phlegeri* more than they are to *R. bononiensis*. Moreover, *R. bononiensis* is considered extinct (Zachariasse and Lourens, 2022).

Small, pre-biserial stage specimens (e.g., Plate 9 Figures 5-6; Plate 10 Figures 5-7) are very close to what Milker and Schmiedl (2012) put as *R. bononiensis*. Small forms, when apertural end is broken, resemble *Bulimina costata* and *Trifarina angulosa*, and can be distinguished by the shape of chambers from the former and by the presence of costae from the latter.

Superfamily Cassidulinoidea d'Orbigny, 1839

Family Cassidulinidae d'Orbigny, 1839

Genus *Cassidulina* d'Orbigny, 1826

1826 *Cassidulina* – d'Orbigny, p. 282

Type: *Cassidulina laevigata* d'Orbigny (1826, p. 282, pl. 15 fig. 4-5)

This genus is characterized by biserial planispirally enrolled forms with a slit-like aperture almost parallel to the outer margin of the chamber. The aperture is accompanied by an elongate apertural plate at the lower margin of the aperture. Test is constructed from granular hyaline material, translucent.

A very similar genus, *Islandiella* Nørvang (1958) is different from *Cassidulina* by its aperture (no apertural plate, but a rim) and wall material (radial) (Nomura, 1983; Ovsepyan and Taldenkova, 2019).

Cassidulina laevigata d'Orbigny, 1826

Plate 11 Figures 1-12; Plate 12 Figures 1-7

1826 *Cassidulina laevigata* – d'Orbigny, p. 282, pl. 15 fig. 4, 5

1858 *Cassidulina laevigata* d'Orbigny; Williamson, p. 68, fig. 141-142

1884 *Cassidulina laevigata* d'Orbigny; Brady, p. 428, pl. 54 fig. 1-3

1896 *Cassidulina laevigata* d'Orbigny var. *carinata* – Silvestri, p. 104, pl. 2 fig. 10a-c

1991 *Cassidulina laevigata* d'Orbigny; Cimerman and Langer, p. 61, pl. 63 fig. 1-3

1993 *Cassidulina carinata* Silvestri; Sgarrella and Moncharmont Zei, p. 236, pl. 23 fig. 8-9

2008 *Cassidulina carinata* Silvestri; Sakınç, pl. 12 fig. 15-16

2012 *Cassidulina laevigata* d'Orbigny; Milker and Schmiedl, p. 84, fig. 20.5-6

2014a *Cassidulina carinata* Silvestri; Meriç et al., pl. 50 fig. 7-10

Test lenticular, biconvex, biserial and planispirally enrolled, involute. Rounded in frontal view, may be slightly lobulate or not lobulate; edge angular, sometimes distinctly keeled. Chambers elongate, curved. The chamber margins of the opposite series small and triangular at the periphery. Sutures curved, flush to very slightly depressed, especially near the periphery. Aperture a narrow arc parallel to the outer margin, with a wide flap. Chamber walls porous, sutures non-porous, non-porous boss-like areas may be present at the umbilici. Surface smooth.

Cassidulina laevigata d'Orbigny and *Cassidulina carinata* Silvestri are two very similar forms, and were considered synonymous by several authors (e.g., Milker and Schmiedl, 2012). *C. carinata* was originally described as a variety of *C. laevigata* which possesses wide, prominent keel. Presence of an umbonal boss was remarked by Parker (1954, p. 535) for *C. carinata*.

In the population examined from the Sea of Marmara, most individuals here attributed to *C. laevigata* are very small, i.e., juveniles. Only in a few stations mature specimens were encountered. Among these large individuals two main varieties occur: one with angular periphery and no umbonal boss (*laevigata*-type), the other with a more prominent keel (sometimes serrated) and a small umbonal boss (*carinata*-type). Because the small individuals are impossible to sort into one or the other, these two groups are lumped together in this study.

Taxon is distinguished from other cassidulinids by its lenticular shape and angular margin.

Genus *Globocassidulina* Voloshinova, 1960

1960 *Globocassidulina* – Voloshinova, p. 58

Type: *Globocassidulina subglobosa* (Brady, 1881, p.60)

This genus is characterized by biserial planispirally enrolled chamber arrangement and slit like or tri-partite aperture which is perpendicular or acutely angled to the outer margin of the penultimate chamber.

Globocassidulina oblonga (Reuss, 1850)

Plate 11 Figures 30-32; Plate 12 Figures 27-31

1850 *Cassidulina oblonga* – Reuss, p. 12, pl. 3 fig. 5, 6

1980 *Globocassidulina oblonga* (Reuss); Alavi, p. 71, pl. 36 fig. 1, 8

2008 *Globocassidulina subglobosa* (Brady); Sakınç, pl. 13 fig. 1-2

2012 *Globocassidulina oblonga* (Reuss); Milker and Schmiedl, p. 85, fig. 20.10-12

2013 *Globocassidulina subglobosa* (Brady); Kırcı-Elmas, fig. 5.5

2014a *Globocassidulina subglobosa* (Brady); Meriç et al., pl. 50 fig. 11-12

Test large, biserial-enrolled, somewhat compressed and globular. Peripheral margin is broadly rounded. Sutures flush. Aperture tri-partite with basal branch shorter (sometimes undistinguishable) than areal branch, accompanied with apertural flaps on both sides. Walls thick, visibly coarsely porous, surface smooth.

Some researchers considered *Cassidulina crassa* d'Orbigny sensu stricto a synonym to *oblonga* (e.g., Cushman, 1911).

This form is very similar to *Globocassidulina subglobosa*, and frequently lumped under that name. These are forms which are more compressed than *G. subglobosa*, and have a more ovate shape on frontal views. The aperture is similar to that in *G. subglobosa* but the apertural face less angled to the plane of coiling. In addition, this taxon is larger, and the porosity is more distinct.

Globocassidulina cf. *obtusa* sensu Sejrup and Guilbault (1980)

Plate 11 Figures 26-29; Plate 12 Figures 21-26

? 1858 *Cassidulina obtusa* – Williamson, p. 69, fig. 143-144

1932 *Cassidulina crassa* d'Orbigny; Heron-Allen and Earland, p. 357, pl. 9 fig. 29-31 (not 26-28 and 32-33)

1980 *Cassidulina obtusa* Williamson; Sejrup and Guilbault, fig. 2 A-E

2003 *Cassidulina obtusa* Williamson; Murray, fig. 6.11-12

2012 *Cassidulina obtusa* Williamson; Milker and Schmiedl, p. 84, fig. 20.7-8

2016 *Cassidulina crassa* d'Orbigny; Lei and Li, p. 212, fig. 8 a-d (not e-g)

Test small, biserial enrolled, compressed, frontal and edge views usually both ovate. Periphery very slightly lobulated, chambers inflated and ovate with slightly depressed sutures. About three-four chambers visible on both sides, with the chambers of the opposite series only seen at and near the outer margin as small triangular chambers. Edge subrounded-rounded, except the last formed chamber on which the apertural face and the outer wall make a more angular edge. Apertural face curved with a fold in the central part. Aperture nearly triangular, at the interiomarginal position: elongated at the base of the apertural face (basal apertural branch) and going a short distance up perpendicular to the bottom of the aperture up the apertural face situated at the fold of the apertural face (areal apertural branch sensu Nomura, 1983). Test translucent, walls fairly thin, surface smooth.

In the original description Williamson (1858) makes a comparison to *Cassidulina crassa* d'Orbigny and emphasizes the difference in the aperture as *C. crassa* with a 'triangular' aperture while *C. obtusa* was described to have an elongated arch shaped aperture. In addition to the described arch-shaped aperture, Sejrup and Guilbault (1980) interpret the taxon with a fold on the apertural face at which a small vertical extension of aperture "may" sit. This feature is not present in the original description; therefore, Sejrup and Guilbault's interpretation of the taxon was followed.

This form is very similar to *Paracassidulina minuta*, especially the smaller representatives of it, but *G.* cf. *obtusa* is a bit fatter and the aperture is distinctly different. This form is also very similar to smaller individuals of *Globocassidulina subglobosa*, but has deeper sutures, more inflated chambers and more of an ovate shape.

Globocassidulina subglobosa Brady, 1881

Plate 11 Figures 22-25; Plate 12 Figures 15-20

1884 *Cassidulina subglobosa* – Brady, p. 430, pl. 54 fig. 17 a-c

1911 *Cassidulina subglobosa* Brady; Cushman, p. 98, fig. 152

1980 *Globocassidulina subglobosa* (Brady); Alavi, p. 71, pl. 36 fig. 4, pl. 37 fig. 4

1991 *Globocassidulina subglobosa* (Brady); Cimerman and Langer, p. 61, pl. 63 fig 4-6

1993 *Globocassidulina subglobosa* (Brady); Sgarrella and Moncharmont Zei, p. 236, pl. 24 fig. 1-2

2012 *Globocassidulina subglobosa* (Brady); Milker and Schmiedl, p. 85, fig. 20.13-14

2014a *Globocassidulina subglobosa* (Brady); Meriç et al., pl. 50 fig. 14 (not 11, 12)

Test small, biserial, enrolled with globular shape. Margin broadly rounded, so much so, in smaller individuals the form nears spherical. Sutures flush, or nearly so. Aperture situated in an interiomarginal position, an ovate opening almost perpendicular to the suture between the last chamber and the penultimate chamber, surrounded by a lip.

The form is similar to *Globocassidulina* cf. *obtusa* but has less depressed sutures, and for larger specimens, more visibly porous test; also, the aperture is more oval than tri-partite (shorter basal apertural branch). In addition, the apertural face is angled (nearing perpendicular) with respect to plane of coiling instead of nearing parallel in *G*. cf. *obtusa*.

The form is also similar to *Globocassidulina oblonga*, but is usually smaller, sutures are more depressed, and the test is more finely porous. Moreover, the aperture in *G. oblonga* usually has a longer basal branch.

Genus *Paracassidulina* Nomura, 1983

1983 *Paracassidulina* – Nomura, p. 94

Type: *Globocassidulina nipponensis* Eade (1969, p. 65, 66, pl. 13 fig. 1-4)

Genus is characterized by biserial enrolled coiling, interiomarginal, long, slit-like aperture accompanied by an apertural rim covering the base of the aperture.

Paracassidulina minuta (Cushman, 1933a)

Plate 11 Figures 13-21; Plate 12 Figures 8-14

? 1911 *Cassidulina crassa* d'Orbigny – Cushman, p. 97, fig. 151

1933a *Cassidulina minuta* – Cushman, p. 92, pl. 10 fig. 3a–c

? 1945 *Cassidulina crassa* d'Orbigny; Cushman, fig. 18-19

1993 *Cassidulina crassa* d'Orbigny; Sgarrella and Moncharmont Zei, p. 236, pl. 23 fig. 10-11

2008 *Cassidulina crassa* d'Orbigny; Sakınç, pl. 12 fig. 14

2016 *Globocassidulina minuta* (Cushman); Martins et al., fig. 5.4 a-b

Test small, biserial enrolled, compressed. Rounded in frontal view, ovate in edge view. Periphery very slightly lobulated, chambers inflated and ovate (bean-shaped) with depressed, curved sutures in between. About four chambers visible on both sides, with the chambers of the opposite series only seen at and near the outer margin as small triangular chambers. Edge subrounded, except the last formed chamber on which the apertural face and the outer wall make a more angular margin. Apertural face is more or less parallel to the plane of coiling. Aperture elongated, at the interiomarginal position, with a thin lip (apertural ridge *sensu* Nomura, 1983) covering the bottom part of the chamber. Test translucent, walls fairly thin; surface smooth.

Forms of similar morphologies were reported under, but definitely do not belong to the taxon *Cassidulina crassa* d'Orbigny (1839a). D'Orbigny's species is specifically described with a triangle-like aperture (i.e., *Globocassidulina*-type aperture) situated at the central part of the apertural face (Sejrup and Guilbault, 1980; Nomura, 1983), making those references listed above with elongate, crescent-shaped, slit-like apertures (*Paracassidulina*-type, Nomura, 1983) misidentifications. The morphologies encountered in the samples, and those references above, fit very well under *Cassidulina minuta* Cushman (1933a). Although it is described as a small form, some of the references illustrate larger specimens (e.g., Cushman, 1911; Sakınç, 2008), however, overall morphology is the same. I have encountered specimens of various sizes, although almost never larger than ~300 μm with the same morphologic characters with one exception: the margin tends to be more angular in larger individuals. The original description of *Cassidulina obtusa* (Williamson, 1858) is also very similar to our material, however, that taxon is mostly interpreted differently in the literature (see *Globocassidulina* cf. *obtusa* sensu Sejrup and Guilbault) which do not fit the specimens regarded here.

Only a few studies from the Sea of Marmara record this taxon, under the name *Cassidulina crassa* d'Orbigny (Kırcı-Elmas, 2006, 2013, 2018; Kırcı-Elmas et al., 2008, 2021: as *Globocassidulina crassa*; Kaminski et al., 2002; Sakınç, 2008). Although some studies do include a *Cassidulina minuta* Cushman (Kırcı-Elmas, 2006; Kırcı-Elmas et al. 2021 as *Globocassidulina minuta*) in addition to *Cassidulina crassa*, they do not provide any images or descriptions of either taxa. Moreover, they followed the latter taxon interpretation as in Sgarrella and Moncharmont Zei (1993) (Kırcı-Elmas, 2018) which is here considered in the synonymy of *P. minuta*.

Paracassidulina neocarinata (Thalmann, 1950) is also a similar taxon, but it is different from *minuta* by its carinated edge and usually larger size (Cushman, 1922a).

This form is easily distinguished from *Cassidulina* species by its inflated chambers and depressed sutures, and usually small size. It is very similar to *G.* cf. *obtusa* (sensu Sejrup and Guilbault), but the latter is different by its broader periphery, more ovate frontal view, and most importantly, the fold in the apertural face.

Family Globobuliminidae Hofker, 1956

The family was attributed to Cushman (1927) by Holzman and Pawlowski (2017) but was previously formed by Hofker (1956).

Genus *Globobulimina* Cushman, 1927

Plate 9 Figures 16-22; Plate 10 Figures 18-26

1927 *Globobulimina* – Cushman, p. 67

Type: *Globobulimina pacifica* Cushman (1927, p. 67, pl. 14 fig. 12)

Test large, globular-ovate with very rapid chamber growth rate. Chambers very enveloping, triserially arranged. Aperture loop shaped with surrounding toothplate. Wall perforated, appears sugary; surface smooth.

Because globobulimins were very infrequently encountered in this study, they were not distinguished specifically, but grouped as *Globobulimina* spp.

Family Sphaeroidinidae Cushman, 1927

Genus *Sphaeroidina* d'Orbigny, 1826

1826 *Sphaeroidina* – d'Orbigny, p. 267

Type: *Sphaeroidina bulloides* d'Orbigny, 1826 (p. 267, no. 65); in Deshayes, 1832 (p. 966)

This taxon is characterized by globular tests with strongly enveloping hemispherical chambers which are arranged so that only a few (~3) chambers are seen from the outside.

Sphaeroidina bulloides d'Orbigny in Deshayes, 1832

Plate 9 Figures 13-15; Plate 10 Figures 15-17

1826 *Sphaeroidina bulloides* – d'Orbigny: p. 267

1832 *Sphaeroidina bulloides* d'Orbigny; Deshayes, p. 966

1988 *Sphaeroidina bulloides* d'Orbigny; Loeblich and Tappan, p. 564, pl. 617 fig. 1-6

2012 *Sphaeroidina bulloides* d'Orbigny; Milker and Schmiedl, p. 100, fig. 23.3-4

Test globular with strongly embracing hemispherical chambers. Sutures depressed. Only three-tour chambers visible from the outside. Aperture interiomarginal, situated at the junction point where the last three chambers meet, partially covered by a toothplate. Wall shiny with a white hue, minutely perforated.

Recognition of the form is very easy by its globigerid-like overall outer shape, but solid and smooth wall structure.

Family Uvigerinidae Haeckel, 1894

Subfamily Angulogerininae Galloway, 1933

Genus *Trifarina* Cushman, 1923

1923 *Trifarina* – Cushman: p. 99

Type: *Trifarina bradyi* Cushman, 1923 (p. 99, pl. 22 fig. 3, 9)

1927 *Angulogerina* – Cushman: p. 69

Type: *Uvigerina angulosa* Williamson, 1858 (p. 67, pl. 5 fig. 140)

This genus is characterized by an elongate test with a triangular cross section. Chamber arrangement is triserial, tending towards biserial and uniserial in de adult chambers. Three corners of the test are angular, carinated, at least for a few last formed chambers. The aperture is produced on a short neck and provided with a toothplate. The test surface is ornamented with discontinuous longitudinal costae and pustules.

This genus is considered to be synonymous with *Angulogerina* Cushman (1927), which do not have a tendency for becoming uniserial (Loeblich and Tappan, 1964).

Trifarina angulosa (Williamson, 1858)

Plate 9 Figures 8-12; Plate 10 Figures 10-14

1858 *Uvigerina angulosa* – Williamson: p. 67, pl. 5 fig. 140

1958 *Angulogerina angulosa* (Williamson); Parker, p. 259, pl. 2 fig. 1, 2

1991 *Angulogerina angulosa* (Williamson); Cimerman and Langer, p. 62, pl. 66 fig. 3-4

2003 *Trifarina angulosa* (Williamson); Murray, p. 26, fig. 10, no. 5

2008 *Angulogerina angulosa* (Williamson); Sakınç, pl. 14 fig. 4-5

2012 *Angulogerina angulosa* (Williamson); Milker and Schmiedl, p. 90, fig. 21.2-4

Test slender, initially triserial, later tending biserial. earlier part with more rounded edges and more distinct sutures between fairly inflated chambers, later edges becoming angular, even carinated. Aperture terminal, produced on a neck. Surface pustulose throughout, with some longitudinal, fine, discontinuous costae occurring on later chambers.

Small specimens may resemble *Bulimina* spp. and *Rectuvigerina* spp., especially if the apertural end is broken, however the pustulose surface and angular lateral margins of chambers distinguishes the form from the latter two.

Subfamily Uvigerininae Haeckel, 1894

Genus *Uvigerina* d'Orbigny, 1826

1826 *Uvigerina* – d'Orbigny: p. 268

Type: *Uvigerina pygmaea* d'Orbigny, 1826 (p. 269 n° 2 Model n° 67, pl. 12 fig. 8-9

This genus is characterized by triserial coiling, costate and/or pustulate surface and a terminal aperture with a neck and a hemicylindrical toothplate. A similarly costate and necked form *Rectuvigerina* is different from *Uvigerina* in that it is smaller, has thinner walls, and changes chamber arrangement to biserial and uniserial in the adult part.

Uvigerina mediterranea Hofker, 1932

Plate 9 Figures 23-26; Plate 10 Figures 27-31

1884 *Uvigerina pygmaea* d'Orbigny; Brady, p. 575, pl. 74 fig. 11, 12

1932 *Uvigerina mediterranea* – Hofker: pp. 118- 121, fig. 32

1991 *Uvigerina mediterranea* Hofker; Cimerman and Langer, p. 62, pl. 65 fig. 7-9

1993 *Uvigerina mediterranea* Hofker; Sgarrella and Moncharmont Zei, p. 214, pl. 16 fig. 1-2

2012 *Uvigerina mediterranea* Hofker; Milker and Schmiedl, p. 90, fig. 20.28

2014a *Uvigerina mediterranea* Hofker; Meriç et al., pl. 52 fig. 6-8

Test fat and large, completely triserial. Chambers inflated, overlapping; sutures shallowly depressed. Aperture produced on a short neck and provided with a toothplate. Surface ornamented with longitudinal costae which do not cross sutures.

According to Fontanier et al. (2002) *U. mediterranea* can be distinguished from *Uvigerina peregrina* Cushman by i. larger, bulkier test, ii. more widely separated, smaller number of costae, iii. more regular (continuous) costae, iv. smooth surface between costae. *U. peregrina* has pustulose ornamentation in between its costae and also the costae are less continuous. In addition, although not always, *U. mediterranea* is remarked to have a better developed neck with a prominent lip which sits in kind of a depression on the last formed chamber, while the neck of *U. peregrina* is located at the highest point of the test. Distinguishing this taxon may prove more difficult for microspheric *U. mediterranea*.

U. mediterranenea occur almost only in the Central Deep (Station K51.2K09) in the Sea of Marmara, along with other large taxa (such as *Bulimina inflata* Seguenza and *Melonis* spp.), while *U. peregrina* is not present. In the Mediterranean Sea, on the other hand, both *U. mediterranea* and *U. peregrina* occur together.

Small specimens of *U. mediterranenea*, especially those with only 2-5 chambers can be distinguished from *B. inflata*, by the presence of neck and the characteristic wall. The wall in *B. inflata* is always coarsely porous (even in the young), giving a sugary appearance to the test, however, in *U. mediterranea* wall is always smooth, whitish, and appears more homogeneous due to smaller pores.

Superfamily Chilostomelloidea Brady, 1881

Family Chilostomellidae Brady, 1881

Subfamily Chilostomellinae Brady, 1881

Genus *Chilostomella* Reuss in Cžjžek, 1849

1849 *Chilostomella* – Reuss in Cžjžek, 1849: p. 50

Type: *Chilostomella ovoidea* Reuss, 1850 (p. 380, pl. 48 fig. 12)

The genus is characterized by ovoid-cylindrical-fusiform tests with two strongly embracing chambers per whorl and slit like aperture which produces an arc near one pole of the test.

Chilostomella sp. 1

Plate 13 Figures 1-6; Plate 14 Figures 1-5

2008 *Chilostomella mediterranensis* Cushman and Todd; Sakınç, pl. 17 fig. 8-9

Test ovoid-fusiform with circular transverse section. Initial chambers are faintly seen on one side; last formed pair of chambers enclose the other side. Sutures very shallow, indistinct. Aperture situated near the pole, on the side of the test; a narrow interiomarginal slit, appearing as an arch due to the curvature of the chamber and the test; margin of aperture serrated. Wall thin, transparent to somewhat translucent; surface smooth, shiny.

Three species of the genus are mentioned in the Mediterranean literature: *Chilostomella ovoidea* Reuss, *Chilostomella oolina* Schwager and *Chilostomella mediterranensis* (e.g., Mullineaux and Lohmann, 1981; Caralp, 1988), associated with globobuliminids, sapropel deposition and anoxic conditions. The specific distinction in the genus usually comprises the comparisons of overall test shape; and aperture location and shape (Cushman and Todd, 1949). *C. oolina* is an elongated, cylindrical form. *C. ovoidea* and *C. mediterranensis*, on the other hand, are ovoid or

fusiform. In addition, aperture in *C. ovoidea* is longer and more slit-like while in *C. mediterranensis* it is shorter and more open, with a lip that flares outwards more pronouncedly than other taxa of the genus. Cushman and Todd (1949) mentions the likeness of *C. mediterranensis* to *Chilostomella cylindroides* Reuss, another ovoid form, but remarks that the outward flaring of the lip in *C. mediterranensis* distinguishes this genus. Considering that chilostomellids are although not rare, but fairly uncommon, the inter- and intra-specific morphologic variety and presence of intermediate forms are lacking. The modern representatives of the genus may represent cryptic species according to genetic studies (Grimm et al. 2007).

The individuals encountered in this study has distinctly serrate apertural margin; such a feature is not mentioned or illustrated in any of the *Chilostomella* species reported from the Mediterranean Sea. The same feature is clearly present in the individuals attributed to *C. mediterranensis* by Sakınç (pl. 17 fig. 8-9). These specimens clearly belong to Genus Chilostomella, however, are probably a distinct and separate species.

Taxon is easily distinguished from other foraminifera by the overall ovoid shape and thin, transparent to translucent, finely perforate test walls, even for pre-adult or broken forms.

Family Gavelinellidae Hofker, 1956

Subfamily Gavelinellinae Hofker, 1956

Genus *Gyroidina* d'Orbigny, 1826

1826 *Gyroidina* – d'Orbigny, p. 278

Type: *Gyroidina orbicularis* d'Orbigny in Parker, Jones & Brady (1865, pl. 3 fig. 85)

The genus is characterized by trochospiral coiling with an evolute spiral and involute umbilical side, optically granular and porous wall structure, closed umbilicus and interiomarginal slit aperture.

Gyroidina umbonata (Silvestri, 1898)

Plate 13 Figures 7-11; Plate 14 Figures 6-10

1898 *Rotalia soldanii* d'Orbigny var. *umbonata* – Silvestri: p. 329, pl. 6 fig. 14

1991 *Gyroidinoides lamarckiana* (d'Orbigny); Cimerman and Langer, p. 75, pl. 85 fig. 7-8 (not fig. 9)

2002 *Gyroidinoides lamarckiana* (d'Orbigny); Kaminski et al., pl. 4 fig. 11-12

2008 *Gyroidinoides lamarckiana* (d'Orbigny); Sakınç, pl. 17 fig. 8-9

2012 *Gyroidinoides umbonata* (Silvestri); Milker and Schmiedl, p. 116 fig. 26.22-23

2013 *Gyroidina umbonata* (Silvestri); Kırcı-Elmas, fig. 6.4

2014a *Gyroidina umbonata* (Silvestri); Meriç et al., p. 226, pl. 72 fig. 10

Test low trochospiral with strongly convex, involute umbilical side and flat to slightly convex, evolute spiral side. Outline lobulate, peripheral margin rounded. Chambers trapezoidal on the spiral side, separated by depressed, slightly curved sutures; triangular on the umbilical side, separated by depressed, nearly radial sutures; 5-6 chambers in the last whorl. Umbilicus closed by successive chambers, only a shallow depression remains where chambers meet. Apertural face almost perpendicular to the outer margin of the test; aperture is interiomarginal, umbilical-extraumbilical slit rimmed by a lip. Small accessory apertures present on the spiral side where the intercameral suture meets the spiral suture. Wall translucent, generally whitish, thin; surface smooth, dull.

In the literature the taxon was previously reported under the name *Gyroidinoides lamarckiana* (d'Orbigny) which is a distinctly different taxon with high number of chambers in the last whorl and a non-lobulate periphery.

Generic placement of the taxon should be in *Gyroidina* d'Orbigny, not *Gyroidinoides* Brotzen due to the nature of the umbilicus being closed instead of open and partially covered with umbilical flaps.

The whitish look of the test material, as well as lobulate nature of the form is very distinguishing even for juvenile specimens. *Aubignyna perlucida* may occur similar from the spiral side, but the umbilical side of that taxon is not as convex, the sutures are covered with granular-pustulose material, and the test is more transparent.

Family Svratkinidae Bugrova, 1989

Genus *Svratkina* Pokorný, 1956

1956 *Svratkina* – Pokorný, p. 257

Type: *Svratkina australiensis* (Chapman, Parr & Collins, 1934, p. 563, pl. 8 fig. 9 a-c)

Trochospiral forms with biconvex test, involute spiral and evolute umbilical side. Test surface with large pustules. Aperture an oblique opening on the umbilical side.

Svratkina tuberculata (Balkwill and Wright, 1885)

Plate 13 Figures 12-17; Plate 14 Figures 11-12

1885 *Discorbina tuberculata* – Balkwill and Wright, p. 350, pl. 13 fig. 28-30

1980 *Svratkina tuberculata* (Balkwill and Wright); Alavi, p. 74, pl. 29 fig. 8, 12

1992 *Eponides tuberculata* (Balkwill and Wright); Schiebel, p. 66, pl. 4 fig. 4 a-b

Test small, low trochospiral with evolute spiral and involute umbilical sides. Outline very slightly lobulate; chambers grow gradually with last chamber occupying up to a quarter of the test; periphery rounded. Aperture an interiomarginal opening.

Surface of the spiral side covered with coarse and blunt, short, tubular pustules (tubercules) which are denser on the spiral side; surface near the umbilicus smooth. Wall quite thick and translucent, usually has a yellowish hue.

It is very easily distinguished from other biconvex forms by its small size and coarse tubercules on the spiral side.

Superfamily Discorbinelloidea Sigal, 1952

Family Discorbinellidae Sigal, 1952

Genus *Discorbinella* Cushman and Martin, 1935

1935 *Discorbinella* – Cushman and Martin, p. 89

Type: *Discorbinella montereyensis* Cushman and Martin (1935, p. 89, pl. 14 fig. 13)

Test planoconvex, trochospiral, may be carinate. Spiral side convex, umbilical side flat. Both sides semi-evolute. Chambers on the umbilical (flat) side with umbilical flaps. Aperture an interiomarginal equatorial short arch with a lip, continuing under the umbilical flaps. Test finely perforate.

Genera *Discorbinella* Cushman and Martin and *Hanzawaia* Asano are near identical in most respects. Their synonymy should be considered (Jones, 1994).

Discorbinella bertheloti (d'Orbigny, 1839c)

Plate 15 Figures 15-18; Plate 16 Figures 13-18

1839c *Rosalina bertheloti* – d'Orbigny, p. 135, pl. 1 fig. 28-30

1884 *Discorbina bertheloti* (d'Orbigny); Brady, p. 650, pl. 89 fig. 10-12

1978 *Hanzawaia boueana* (d'Orbigny); Wright, pl. 5 fig. 12-14

1987 *Hanzawaia boueana* (d'Orbigny); Jorissen, pl. 3 fig. 10

1991 *Discorbinella bertheloti* (d'Orbigny); Cimerman and Langer, p. 70, pl. 86 fig. 1-4

1993 *Discorbinella bertheloti* (d'Orbigny); Sgarrella and Moncharmont Zei, p.216, pl. 16 fig. 11-12

1994 *Discorbinella bertheloti* (d'Orbigny); Jones, p. 95, pl. 89 fig. 10-12

2008 *Discorbinella bertheloti* (d'Orbigny); Sakınç, pl. 15 fig. 10-11

2012 *Discorbinella bertheloti* (d'Orbigny); Milker and Schmiedl, p. 104, fig. 23.29-30

2014a *Discorbinella bertheloti* (d'Orbigny); Meriç et al., pl. 59 fig. 2-6

Test ovate in outline; low trochospiral, about 1.5-2 whorls; planoconvex to slightly concavoconvex; both sides semi-evolute; carinate. Chambers 7-9 in the last whorl, rapidly enlarging. Sutures distinctly curved on both sides; flush to almost flush on the flat (or concave) umbilical side. Sutures on the convex spiral side thickened and flush or slightly raised for the inner part of the test, thinner in the younger part of the test and may be slightly depressed for the last few chambers. On the flat (umbilical) side chambers have umbilical flap extensions covering a portion of the earlier whorl; on the convex (spiral) side umbilicus depressed, chambers never cover the central clear boss-like feature (proloculus?). Aperture interiomarginal, at the periphery, a narrow and low arch accompanied by a strong lip, continuing on the flat (umbilical) side under the umbilical flaps following the spiral suture. Test densely perforated, especially so for the convex (spiral) side except for the sutures, keel and umbilical flaps, very glassy and transparent; surface smooth, flat (umbilical) side especially shiny.

Some researchers (e.g., Wright, 1978) attributed identical specimens to *Hanzawaia boueana* (d'Orbigny) which is a very similar taxon. Its synonymy to this taxon should be further investigated.

The overall look of the test, especially porosity, the glassy nature, and the planoconvex-concavoconvex nature is very similar in *Planodiscorbis rarescens* (Brady). Especially the pre-adult specimens may be almost impossible to tell apart. This taxon is different than *P. rarescens* in that sutures on the convex side are

thickened, keel is usually narrower, the number of chambers in the whorl is higher, and the convex side is always semi-evolute.

Taxon is similar to cibicids due to the planoconvex nature, but the convexity in planoconvex cibicids are just the opposite of this taxon (i.e., the flat side is spiral side in cibicids, while the convex side is the spiral side in this taxon). Moreover, the wall of cibicids are usually less transparent, and the chamber arrangement not semi-evolute.

Family Pseudoparrellidae Voloshinova, 1952

Genus *Eilohedra* Lipps, 1965

1965 *Eilohedra* – Lipps; p. 124, fig. 3

Type: *Epistominella levicula* (Resig, 1958, p. 304, text-fig. 16)

Small, trochospiral forms with hyaline wall structure and smooth test surface. Spiral side evolute and convex, umbilical side involute and flat or convex. Aperture a slit extending along the basal suture and continuing up the apertural face.

Eilohedra vitrea (Parker, 1953)

Plate 13 Figures 18-22; Plate 14 Figures 13-20

1953 *Epistominella vitrea* – Parker in Parker et al., p. 9, pl. 4 fig. 34-36, 40-41

1958 *Epistominella levicula* – Resig, p. 304, text-fig. 16

2012 *Epistominella vitrea* Parker; Mendes et al., fig. 4.1 a-b

2019 *Eilohedra vitrea* (Parker); Melis et al., fig. S1, 13-14

Test small, somewhat lensoidal, trochospiral, compact; spiral side evolute, umbilical side involute. Chambers about 5-6 in the last whorl; triangular on umbilical side, growing gradually as added; on the spiral side inner whorls very small. Sutures depressed on umbilical side, flush on spiral side. Umbilicus closed, a shallow

depression. Aperture at a near equatorial, interiomarginal position, perpendicular to the suture between the last chamber and the previous whorl. Test very transparent, surface smooth.

Epistominella exigua (Brady, 1884) is similar to *E. vitrea*, and the names are used in the literature somewhat interchangeably. The size and overall shape, as well as chamber arrangements agree to a degree, but, *E. exigua* has a sharp (angular) margin, and a smaller number of chambers in the last whorl. This taxon was not encountered in the studied samples.

All encountered *E. vitrea* specimens were minute, even when reached full adult size. The last whorl has 6-6.5 chambers and the margin is rounded-subrounded. Some individuals are higher trochospiral, with a more pinched, but still subrounded outer margin.

The apertural extension on the apertural face perpendicular to the last suture is clear in most of the specimens and is the most important distinguishing factor.

The rarity of this form in the Sea of Marmara literature is probably due to studied size-fraction. This small form's abundance can be seen in the fine fraction (63-125 μm).

Superfamily Discorboidea Ehrenberg, 1838 (fide Loeblich and Tappan, 1984)

Test low trochospiral; wall perforate, hyaline, optically radial; aperture interiomarginal, on the umbilical side.

Family Bagginidae Cushman, 1927

Subfamily Serovaininae Sliter, 1968

Genus *Rotamorphina* Finlay, 1939

1939 *Rotamorphina* – Finlay, p. 325

Type: *Rotamorphina cushmani* Finlay (1939, p. 325, pl. 28 fig. 130-133)

Test trochospiral, biconvex; umbilical side involute, spiral side evolute. About 6-7 chambers in each whorl. Umbilicus covered by umbilical flaps. Aperture an umbilical-extraumbilical arch covered by umbilical flaps. Test thin, surface smooth.

This genus is considered extinct (Loeblich and Tappan, 1988). The following species was tentatively put under this genus by its author.

Rotamorphina? *involuta* Parker, 1958

Plate 13 Figures 23-25; Plate 14 Figures 21-23

1958 *Rotamorphina*? *involuta* – Parker, p. 274, pl. 4 fig. 28-30

1993 *Rotamorphina*? *involuta* Parker; Sgarrella and Moncharmont Zei, p. 219, pl. 19 fig. 1-3

Test small, compact, very low trochospiral; periphery broadly rounded, outline lobulate. Spiral side semi-involute, umbilical side involute. 5-6 chambers in the last whorl, rapidly growing in size. Sutures radial, shallowly depressed on both sides. Umbilicus closed with wide, triangular umbilical flaps. Aperture most probably an umbilical-extraumbilical arch, but obscured by the umbilical flaps. Test coarsely porous on the spiral side, central part on the umbilical side non-porous; surface smooth.

The generic position of the taxon is questionable. Parker (1958) remarked that the taxon differs from the typical *Rotamorphina* by the semi-involute spiral side, and hence attributed this taxon to this genus only tentatively.

Taxon is quite rare, but is easily distinguished from others by its small size, very low and faint trochospiral coiling, and coarsely perforated test.

Family Cancrisidae Chapman, Parr and Collins, 1934

Genus *Cancris* de Monfort, 1808

1808 *Cancris* – de Monfort, p. 267

Type: *Cancris auriculatus* de Montfort (1808, p. 267) = *Nautilus auricula* Fichtel and Moll (1798, p. 108, pl. 20 fig. a-f)

Test trochospiral, biconvex, with carinated edge. Chambers elongate (in the radial dimension), curved, increasing in size somewhat rapidly. Umbilicus partially covered by umbilical flaps of chambers. Test porous, transparent; surface smooth.

Cancris auricula (Fichtel and Moll, 1798)

1798 *Nautilus auricula* – Fichtel and Moll, p. 108, pl. 20 fig. a-f

1808 *Cancris auriculatus* – de Montfort, p. 267

1884 *Pulvinulina auricula* (Fichtel and Moll); Brady, p. 688, pl. 106 fig. 4

1931 *Cancris auricula* (Fichtel and Moll); Cushman, p. 72, pl. 15 fig. 1

Test large, low trochospiral, lensoidal; umbilical side involute with low convexity, spiral side evolute and slightly convex; margin sharply angular. Chambers longer radially than tangentially, increase in size somewhat rapidly; somewhat inflated on the umbilical side. Sutures curved backwards on spiral side, nearly flush; near radial on umbilical side, depressed near the umbilicus, near flush near the periphery. Umbilicus depressed, umbilical shoulders of chambers imperforate, flaps attached to the umbilical ends of the chambers cover the umbilicus. Aperture an interiomarginal, umbilical-extraumbilical arch. Surface smooth; test coarsely and densely porous except for the sutures, umbilical shoulders and flaps and the apertural face; transparent.

This taxon is so rare in the Sea of Marmara it was recorded only in Station 2 and is represented by a single specimen. The test is quite distinctive in the adult, very similar to *Valvulineria bradyana*, except is lenticular with a sharp, carinated margin.

Genus *Valvulineria* Cushman, 1926a

1926a *Valvulineria* – Cushman, p. 59

Type: *Valvulineria californica* Cushman (1926a, p. 60, pl. 9, fig. 1 a-c)

Low trochospiral forms with hyaline, porous test, evolute spiral and involute umbilical side. Umbilicus depressed, but covered with umbilical flaps. Aperture an umbilical-extraumbilical arch.

Valvulineria bradyana (Fornasini, 1900)

Plate 15 Figures 7-14; Plate 16 Figures 7-12

1900 *Discorbina bradyana* – Fornasini, p. 393, text fig. 43

1991 *Valvulineria bradyana* (Fornasini); Cimerman and Langer, p. 64, pl. 67 figs. 8-10

1993 *Valvulineria bradyana* (Fornasini); Sgarrella and Moncharmont Zei, p. 220, pl. 18 fig. 1-2

2012 *Valvulineria complanata* (d'Orbigny, 1846); Milker and Schmiedl, p. 93, fig. 21.16-17

2004 *Valvulineria bradyana* (Fornasini); Chendeş et al., pl. 2 fig. 12

2006 *Valvulineria bradyana* (Fornasini); Avşar et al., pl. 2 fig. 9-10

2014a *Valvulineria bradyana* (Fornasini); Meriç et al., pl. 53 fig. 2-5

Test large, low trochospiral; umbilical side involute with low convexity, spiral side evolute and near planar or slightly convex. Chambers increase in size gradually. Sutures curved on spiral side, almost flush; near radial on umbilical side, depressed especially near the umbilicus. Umbilicus depressed, umbilical shoulders of chambers imperforate, flaps may be attached to the umbilical ends of the chambers, covering the umbilicus. Aperture an interiomarginal, umbilical-extraumbilical arch. Surface smooth; test coarsely and densely porous except for the sutures, umbilical shoulders and flaps and the apertural face.

According to Parker (1958), Rasmussen (2005) and Milker and Schmiedl (2012) this taxon is a junior synonym to fossil *Valvulineria complanata* (d'Orbigny, 1846). The

synonymy cannot be confirmed without the examination of the type material. Hence, here, the name widely used for the recent forms is employed.

This species is quite distinct with thick but transparent and shiny shell which is coarsely porous except for sutures, apertural face, and umbilical shoulders and flaps. The juveniles of the species do not have such distinct flaps, but the imperforate umbilical shoulders are enough to detect them.

Family Rosalinidae Reiss, 1963

Genus *Gavelinopsis* Hofker, 1951a

1951a *Gavelinopsis* – Hofker, p. 485

Type: *Discorbina praegeri* Heron-Allen & Earland (1913, p. 122 pl. 10 fig. 8-10)

Test planoconvex to slightly biconvex; trochospiral; spiral side evolute, umbilical side involute; margin angular, carinate. Chambers crescentic on the spiral side, triangular on the umbilical side with umbilical extensions. Sutures flush on the spiral side, depressed and radial on the umbilical side. Umbilicus with an umbilical plug. Aperture an interiomarginal, extraumbilical slit, bounded above by a lip. Test hyaline, finely perforate on the umbilical side except for the keel, sutures, umbilical flaps and umbilical plug. Surface smooth.

Gavelinopsis praegeri (Heron-Allen and Earland, 1913)

Plate 15 Figures 1-6; Plate 16 Figures 1-5

1913 *Discorbina praegeri* – Heron-Allen and Earland: p. 122, pl. 10 fig. 8-10

1964 *Gavelinopsis praegeri* (Heron-Allen and Earland); Loeblich and Tappan, p. C579, fig. 465,4

1988 *Gavelinopsis praegeri* (Heron-Allen and Earland); Loeblich and Tappan, p. 560, pl. 608 fig. 6-12

1991 *Gavelinopsis praegeri* (Heron-Allen and Earland); Cimerman and Langer, p. 66, pl. 70 fig. 3-4

1993 *Gavelinopsis praegeri* (Heron-Allen and Earland); Sgarrella and Moncharmont Zei, p. 46, pl. 4 fig. 6

2012 *Gavelinopsis praegeri* (Heron-Allen and Earland); Milker and Schmiedl, p. 97, fig. 22.3-4

2014a *Gavelinopsis praegeri* (Heron-Allen and Earland); Meriç et al., pl. 55 fig. 1

Test planoconvex; trochospiral with evolute spiral side and involute umbilical side; of about three whorls; margin somewhat angular, bluntly carinate. Chambers crescentic on the spiral side, 5-6 in the last whorl; triangular and slightly inflated on the umbilical side with umbilical flaps extending towards but not fusing to an umbilical plug. On the sutures spiral side curved and flush, except for last couple of sutures which may be slightly depressed; on the umbilical side sutures depressed, radial, may be very gently curved. Umbilicus with a central plug, detached from umbilical flaps. Aperture an interiomarginal extraumbilical low arch with a lip. Test transparent; finely perforate near the outer margins of the chambers, especially on the umbilical side; surface smooth, shiny. A brown hue is observed in the earlier whorls of most of the encountered specimens.

Taxon is distinguished from others by its large size, bluntly carinate periphery, planoconvex shape and distinct umbilical plug. *Rosalina williamsoni* (Chapman and Parr) is highly similar to especially juveniles of this taxon; however, *R. williamsoni* is distinctly concavoconvex while this taxon is planoconvex. Juveniles of this taxon may even have a somewhat convex umbilical side (Plate 16 Figures 1, 2).

Genus *Neoconorbina* Hofker, 1951b

1951b *Neoconorbina* – Hofker, p. 357

Type: *Rosalina orbicularis* Terquem (1876, p. 166 pl. 9 fig. 4; junior homonym of *Rosalina orbicularis* d'Orbigny, 1850) = *Discorbina terquemi* Rzehak (1888, p. 228)

Test concavoconvex, outline circular; trochospiral with convex spiral and concave umbilical sides; margin angular, carinate. Chambers crescentic, very long (tangentially) and low (radially), growing in size rapidly, final chamber in adults occupying most of the periphery. Sutures strongly curved on both sides. Umbilicus depressed, covered partially by successive umbilical flaps of chambers. Test perforate, coarser perforations on the umbilical side; surface smooth.

In Hofker (1951b) no description of the genus is supplied; however, in Hofker (1951a) a description is given with type taxon as *Neoconorbina pacifica* Hofker. See Loeblich and Tappan (1964, p. C582) for details.

Neoconorbina terquemi (Rzehak, 1888)

Plate 15 Figures 19-21; Plate 16 Figures 19-23

1876 *Rosalina orbicularis* – Terquem, p. 166 pl. 9 fig. 4

1888 *Discorbina terquemi* – Rzehak, p. 228

1964 *Neoconorbina terquemi* (Rzehak); Loeblich and Tappan, p. C582, fig. 457,5

1991 *Neoconorbina terquemi* (Rzehak); Cimerman and Langer, p. 66, pl. 70 fig. 5-7

2008 *Neoconorbina terquemi* (Rzehak); Sakınç, pl. 15 fig. 3

? 2008 *Asterigerinata mamilla* (Williamson); Sakınç, pl. 17 fig. 2.

2012 *Neoconorbina terquemi* (Rzehak); Milker and Schmiedl, p. 97, fig. 22.5-6

2014a *Neoconorbina terquemi* (Rzehak); Meriç et al., pl. 55 fig. 2-5

Test concavoconvex, outline circular; trochospiral with convex spiral and concave umbilical sides; margin angular, carinate. Chambers crescentic, very long (tangentially) and low (radially), growing in size rapidly, final chamber in adults occupying most of the periphery. Sutures strongly curved on both sides. Umbilicus depressed, covered partially by successive umbilical flaps of chambers. Test perforate, more densely but finely on spiral side, may become a couple of rows of pores parallel the outer margin; coarser perforations on the umbilical side; surface smooth.

Taxon is easily distinguished from others by its very long, crescentic chambers. *Asterigerinata mamilla* (Williamson) may resemble this taxon, but is usually is higher conical, and pore distribution is different. *Spirorbina*? spp. may also be similar; however, the chambers are less elongated and the umbilicus is filled with pustules in that taxon.

Genus *Planodiscorbis* Bermúdez, 1952

1952 *Planodiscorbis* – Bermúdez, p. 40

Type: *Discorbina rarescens* Brady (1884, p. 651, pl. 90 fig. 2-3)

Test planoconvex, trochospiral; spiral side flat to slightly concave, umbilical side convex. Chambers small in number, rapidly growing in size as added, last chamber very large. On spiral side arrangement is semi-evolute with flaps on inner margins of chambers covering partially the previous whorl. Umbilicus closed by successive chambers. Aperture a slit on the spiral side, located between the periphery and the proximal margin of the chamber. Test hyaline, transparent.

The apertural characteristics of this genus, and of the type species *Planodiscorbis rarescens* (Brady), are somewhat inconsistent in the literature. Brady's figures (1884, pl. 90 fig. 2-3) show a convex umbilical side for the taxon with only slightly curved sutures, and a flat to concave spiral side which is semi-evolute with flap-like extensions ("valvular lobes") on the inner margin of the chambers covering a portion of the inner whorl; the aperture is not described by Brady, however the illustration

(pl. 90 fig. 2-a of Brady, 1884) shows an opening on the flat (spiral) side beneath the distal edge of the last formed chamber. The aperture of the genus (and the typetaxon) is described to be "a slit along the whorl on the dorsal [flat, spiral] side" of the test by Bermúdez (1952, translation). Loeblich and Tappan (1964) assigned the specimen Brady illustrated (pl. 90 fig. 2) as lectotype, however, in their recreation of the illustrations a curious, proximally directed curve is present on the distal suture of the last chamber on the umbilical side, where an umbilical extraumbilical arched aperture would normally be. In addition to this discrepancy, Loeblich and Tappan (1988), although clearly indicating in writing the position of the aperture as on the spiral side, include *Planodiscorbita* McCulloch, whose aperture is on the umbilical (convex) side, as a synonym to *Planodiscorbis*. According to the position of the aperture, *Planodiscorbita* should not be considered a synonym to this taxon.

Another discrepancy with regards to the aperture occurs in *Planodiscorbis* sp. nov. Jones (1994) which was originally attributed to *Discorbina bertheloti* var. *baconica* Hantken by Brady (1884, pl. 90 fig. 1). Here, this taxon is taken as a synonym to *P. rarescens* despite the difference in apertural characteristics, which are interpreted as ontogenic changes. See *Planodiscorbis rarescens* (Brady, 1884) below for further discussion.

Hansen and Revets (1992) in their revision of Discorbidae, Rosalinidae, and Rotaliidae kept *Planodiscorbis* as an incertae sedis taxon. Here the genus is placed under Family Rosalinidae following Loeblich and Tappan (1988); however, the great similarities between this genus and *Discorbinella* may grant this genus replacement into Family Discorbinellidae.

Planodiscorbis rarescens (Brady, 1884)

Plate 17 Figures 1-4; Plate 18 Figures 1-6

1884 *Discorbina rarescens*– Brady, p. 651, pl. 90 fig. 2-3

1884 *Discorbina berthelothi* var. *baconica* Hantken; Brady, p. 651, pl. 90 fig. 1

1952 *Planodiscorbis rarescens* (Brady); Bermúdez, p. 40, pl. 4 fig. 6-7

1964 *Planodiscorbis rarescens* (Brady); Loeblich and Tappan, p. C583, fig. 458,3

non 1992 *Planodiscorbis rarescens* (Brady); Hansen and Revets, p. 177, pl. 7 fig. 4-6, 9

1994 *Planodiscorbis rarescens* (Brady); Jones, p. 95, pl. 90 fig. 2-3

1994 *Planodiscorbis* sp. nov.; Jones, p. 95, pl. 90 fig. 1

Test ovate in outline; low trochospiral, about 1.5-2 whorls; planoconvex to slightly concavoconvex; flat (spiral) side semi-evolute, convex (umbilical) side involute; carinate. 5-6 chambers in the last whorl, rapidly enlarging; last chamber very large, constitutes a quarter to half of the surface area on the convex side. Sutures distinctly curved on the flat side, flush to almost flush; depressed, radial or slightly curved on the convex side. On the flat (spiral) side, chambers have extensions (flaps) covering a portion of the earlier whorl and the aperture; umbilicus covered by successive chambers on the convex (umbilical) side. In the adult, aperture only on the spiral side, under the flaps of the chambers, does not reach the periphery; in pre-adult specimens aperture reaches the periphery and is extended to the umbilical side slightly as a short arch. Keel wide, transparent, non-porous; continuous for the whole periphery in adult tests, interrupted by the peripheral aperture in pre-adult specimens. Test densely and finely perforated, especially so for the convex (umbilical) side, except for the keel and umbilical flaps, very glassy and transparent; surface smooth, flat side especially shiny.

The illustrations given for this taxon in Hansen and Revets (1992) are of an almost conical specimen; neither this shape, test porosity, nor the arrangement on the spiral side agree with the type description or type figures.

The adult specimens are identical with the type figures, and, although rare in the Sea of Marmara, the morphology is highly characteristic and easily distinguished from other taxa. *Discorbinella bertheloti* (d'Orbigny) is a similar taxon due to its

planoconvex shape, semi involute, nearly identical flat side, and very glassy test, but is different from this taxon due to higher number of chambers in the last whorl, semi-evolute convex side, thickened sutures, less prominent keel and equatorial aperture. However, the pre-adult specimens of these two taxa are very similar and very difficult to tell apart.

Discorbina bertheloti var. *baconica* Hantken sensu Brady (1884 = *Planodiscorbis* sp. nov. by Jones, 1994) is depicted with a morphology very similar to *P. rarescens*: an involute convex side, small number of chambers in the last whorl, chambers with high growth rate and significantly large last chamber; however, holds an equatorial arched aperture just as in *D. bertheloti*. Identical specimens of various sizes were recovered from the studied material, and thought to be non-complete representatives of this taxon. This interpretation is further backed by Plate 17 Figure 1 where an individual whose last chamber was broken can be seen, the lip of the arched aperture on the interiomarginal equatorial position is visible. Hence, loss of the equatorial aperture only occurs in the last formed chamber.

Genus *Rosalina* d'Orbigny, 1826

1826 *Rosalina* – d'Orbigny, p. 271

Type: *Rosalina globularis* d'Orbigny (1826, p.271)

Test low trochospiral, planoconvex to concavoconvex; convex spiral side evolute, umbilical side involute; margin subacute. Chambers semilunate to semicircular on the spiral side, triangular on the umbilical side, rapidly growing in size. Chambers with triangular umbilical flaps on the umbilical side; umbilicus open. Aperture interiomarginal on the umbilical side, near the periphery; secondary apertures occur on the proximal side of the folia. Test densely and distinctly perforate.

Rosalina bradyi (Cushman, 1915)

Plate 17 Figures 12-16; Plate 18 Figures 14-18

1884 *Discorbina globularis* d'Orbigny; Brady, p. 634, pl. 86 fig. 8

1915 *Rosalina globularis* (d'Orbigny) var. *bradyi* – Cushman, p. 12, pl. 8 fig. 1

1987 *Rosalina bradyi* Cushman; Jorissen, p. 41, pl. 3 fig. 6

1991 *Rosalina bradyi* Cushman; Cimerman and Langer, p. 66, pl. 71 fig. 1-5

2012 *Rosalina bradyi* Cushman; Milker and Schmiedl, p. 98, fig. 22.11-14

part 2014a *Rosalina bradyi* Cushman; Meriç et al. pl. 55 fig. 6-9, 13 (not fig. 10-12)

Test low trochospiral; spiral side convex, evolute; umbilical side flat to slightly concave, involute. Margin subrounded. About 5 chambers in the last whorl, rapidly growing in size. Sutures flush to very slightly depressed, curved on the spiral side, flush and indistinct on the umbilical side. Chambers with triangular umbilical flaps (folium) on the umbilical side, umbilical flaps distinctly separated. Aperture an interiomarginal extraumbilical arch, secondary apertures present on proximal side of folia. Test densely perforate on the spiral side, imperforate on umbilical side. Surface smooth.

Meriç et al. (2014a) included specimens with thickened imperforate sutures on the spiral side to this taxon (pl. 55 fig. 10-12 therein) which should be placed under *Rosalina macropora* (Hofker) instead.

Taxon is distinguished from *R. macropora* (Hofker) by its thinner sutures; from *Rosalina globularis* d'Orbigny by its imperforate umbilical side and triangular folia.

Rosalina globularis d'Orbigny, 1826

Plate 17 Figures 5-10; Plate 18 Figures 7-12

1826 *Rosalina globularis* – d'Orbigny, p. 271, pl. 13 figs. 1-4

2008 *Rosalina globularis* d'Orbigny; Sakınç, pl. 15 fig. 8-9

1993 *Rosalina globularis* d'Orbigny; Sgarrella and Moncharmont Zei, p. 219, pl. 17 fig. 7-8

2012 *Rosalina globularis* d'Orbigny; Milker and Schmiedl, p. 98, fig. 22.15-16

Test low trochospiral; spiral side convex, evolute; umbilical side umbilicate, involute. Margin subrounded-rounded. About 5 chambers in the last whorl, inflated, rapidly growing in size. Sutures depressed, gently curved on both sides. Chambers with small triangular umbilical flaps (folium) on the umbilical side, umbilical flaps distinctly separated; much of the umbilicus not covered by folia. Aperture an interiomarginal extraumbilical arch with a lip on the upper margin, secondary apertures present on proximal side of folia. Test transparent, densely and coarsely perforate on both sides except for the folia and apertural face; the initial whorl on the spiral side may also be imperforate. Surface smooth, especially shiny at the center where the imperforate initial whorls are present.

Sgarrella and Moncharmont Zei (1993) illustrated specimens which have more inflated chambers than most other references.

The chambers of this taxon are more inflated on the umbilical side with respect to *Rosalina bradyi* (Cushman), and the folia are distinctly shorter and cover a much less distance on the umbilicus. Taxon is distinguished from others by its densely and coarsely perforate test, inflated chambers and open umbilicus.

Rosalina macropora (Hofker, 1951a)

Plate 17 Figure 11; Plate 18 Figure 13

1951a *Discopulvinulina macropora* – Hofker, p. 460, figs. 312, 313

1991 *Rosalina macropora* (Hofker) – Cimerman and Langer, p. 67, pl. 71 figs. 6, 7

part 2014a *Rosalina bradyi* Cushman; Meriç et al. pl. 55 fig. 10-12 (not fig. 6-9, 13)

2014a *Rosalina macropora* (Hofker); Meriç et al. pl. 56 fig. 10-14

Test low trochospiral; spiral side convex, evolute; umbilical side involute. Margin subrounded. About 5 chambers in the last whorl, rapidly growing in size. Sutures thickened and imperforate on the spiral side, gently curved on both sides. Chambers with triangular umbilical flaps (folium) on the umbilical side. Aperture an interiomarginal extraumbilical arch, secondary apertures present on proximal side of folia. Test densely and coarsely perforate on the spiral side except for the thickened intercameral and spiral sutures; imperforate on umbilical side. Surface smooth.

This taxon is distinguished from others by the very distinctly thickened sutures on the spiral side. Otherwise, the taxon is very similar to *Rosalina bradyi* (Cushman).

Rosalina williamsoni (Chapman and Parr in Parr,1932)

Plate 17 Figures 17-22; Plate 18 Figures 19-24

1858 *Rotalina nitida* – Williamson, p. 54, fig. 106-108

1932 *Discorbis williamsoni* – Chapman and Parr, in Parr, p. 226, pl. 21 fig. 25

1937 *Discorbis williamsoni* Chapman and Parr; Chapman and Parr, p. 105, pl. 8 fig. 23

2012 *Discorbis williamsoni* Chapman and Parr; Milker and Schmiedl, p. 95, fig. 22.1-2

Test concavoconvex, small; trochospiral, about two whorls; spiral side evolute and convex, umbilical side involute and concave; margin angular, carinate. 5 chambers in the last whorl, gradually growing in size; the last chamber occupies up to 1/4 of the test periphery. Chambers crescentic on the spiral side, triangular on the umbilical side; umbilical flaps present on umbilical margins of chambers. Sutures flush, indistinct on the spiral side, depressed and slightly curved on the umbilical side. Umbilicus with a small, central umbilical knob, umbilical flaps of chambers extend towards the knob but do not merge with it. Aperture an interiomarginal

extraumbilical arch, closed by successive chambers; accessory apertures beneath umbilical flaps. Test thin, fragile, very transparent; minutely perforated on the umbilical side; surface smooth, shiny.

Taxon was previously regarded to belong to genus *Discorbis*, however, since the umbilical flaps do not form "chamberlets" as in *Discorbis*, and chamber interiors are not subdivided, the taxon is replaced to *Rosalina* (following Murray, 1991). However, the taxon does not have the characteristic coarsely perforate wall of the genus *Rosalina*, therefore generic attribution of the taxon may be subject to change.

Taxon is distinguished from others by its very shiny and smooth test, small size, umbilical knob and fragility. Due to the smooth and convex spiral side and the knob in the umbilicus, the taxon is highly similar to *Gavelinopsis praegeri* (Heron-Allen and Earland), but different from that taxon, the overall size is smaller, the umbilical side is distinctly concave and the margin is more thinly carinate.

Genus *Spirorbina* Sellier de Civrieux, 1977

1977 *Spirorbina* – Sellier de Civrieux, p. 35

Type: *Spirorbina simplex* Sellier de Civrieux (1977)

Test low conical, planoconvex to concavoconvex; trochospiral with flat to gently concave umbilical and convex spiral side; outline circular, non-lobulate; margin angular. Chambers semilunate on both sides. Sutures flush and strongly curved on both sides. Umbilical side partially evolute, umbilicus wide. Aperture an interiomarginal slit on the umbilical side, starting from near the periphery, continuing along the spiral suture towards the earlier chambers. Test translucent; finely perforate on spiral side, more coarsely and sparsely perforate on umbilical side.

Spirorbina? sp.

Plate 15 Figures 22-23; Plate 16 Figures 24-25

2012 *Spirorbina?* sp. 1 – Milker and Schmiedl, p. 99, fig. 22.22-23

Test small, low conical, concavoconvex; trochospiral with gently concave umbilical and convex spiral side; outline circular, non-lobulate; margin angular. Chambers semilunate on both sides. Sutures flush and strongly curved on both sides. Umbilical side partially evolute, umbilicus wide, umbilical area filled with pustules. Aperture an interiomarginal slit on the umbilical side, starting from near the periphery, continuing along the spiral suture towards the earlier chambers. Test translucent; finely perforate on spiral side, more coarsely and sparsely perforate on umbilical side. Surface smooth other than the umbilical pustules, dull due to porosity.

The specimens encountered in this study agree highly with Milker and Schmiedl's (2012) taxon. Taxon is only tentatively put under Spirorbina, and differs from it due to the umbilical pustules.

Taxon is very similar to *Neoconorbina terquemi* (Rzehak) in its concavoconvex shape, but the chambers are much shorter, and the umbilicus of this taxon is filled with pustules.

Superfamily Glabratelloidea Loeblich & Tappan, 1964

Family Glabratellidae Loeblich & Tappan, 1964

Plate 19 Figures 1-12; Plate 20 Figures 1-12

Test low or high trochospiral, with evolute, convex spiral side and involute umbilical side. Test optically radial, perforate. Surface of umbilical side with pustules and radial grooves. Aperture interiomarginal on the umbilical side in the adult, but during plastogamy umbilical regions of test get resorbed leaving a central round opening.

The representatives of this family in the Sea of Marmara are highly diverse, yet so rare, they were not studied below the family level.

Superfamily Nonionoidea Schultze, 1854

Family Astrononionidae Cushman & Edwards, 1937

Genus *Astrononion* Cushman and Edwards, 1937

1937 *Astrononion* – Cushman and Edwards, p. 30

Type: *Nonionina stelligera* d'Orbigny (1939c, p. 128, pl. 3 fig. 1, 2)

Test planispiral, involute, laterally compressed, with rounded periphery. Sutures partially covered by sutural plates, extending from the umbilici towards the periphery, attached at the distal part, open at the proximal part as supplementary apertures. Aperture interiomarginal, equatorial, extending between the two umbilici. Test densely perforate, surface smooth.

Cushman and Edwards (1937) termed the sutural plates as chamberlets, and put together all planispiral taxa with such features under *Astrononion*. Some of these taxa regarded to belong to *Astrononion* Cushman and Edwards (1937) are now considered as type-taxa for other nonionoid genera (such as *Laminononion*, *Fijinonion*) distinguished from *Astrononion* by the shape and extend of the sutural plates and accompanying supplementary apertures.

Astrononion stelligerum (d'Orbigny, 1839c)

Plate 19 Figures 21-24; Plate 20 Figures 23-27

1839c *Nonionina stelligera* – d'Orbigny, p. 128, pl. 3 fig. 1-2

part 1884 *Nonionina stelligera* d'Orbigny; Brady, p. 728, pl. 109 fig. 3-4 (not fig. 5)

1937 *Astrononion stelligerum* (d'Orbigny); Cushman and Edwards, p. 31, pl 3 fig. 7

1991 *Astrononion stelligerum* (d'Orbigny); Cimerman and Langer, p. 74, pl. 84 fig. 13-15

2008 *Asterinonion* [sic] *stelligerum* (d'Orbigny); Sakınç, pl. 17 fig. 6-7

non 2012 *Astrononion stelligerum* (d'Orbigny); Milker and Schmiedl, p. 112, fig. 26.7-8

2014a *Astrononion stelligerum* (d'Orbigny); Meriç et al., pl. 71 fig. 9-13

Test planispiral, involute, biconvex; periphery non-lobulate or very slightly lobulate, margin rounded. 9 chambers in the last whorl, somewhat inflated. Sutures curved backwards; flush at the periphery; narrowly incised otherwise; covered by sutural plates for about half the distance from the umbilicus to the periphery. Umbilicus shallowly depressed. Aperture an interiomarginal slit extending from one umbilicus to the other; supplementary apertures present at the proximal margins of the sutural plates. Test perforate except for the sutural plates, sutures, and the apertural face; surface smooth.

The outline of the form is non-lobulate or very slightly lobulate as described by d'Orbigny (1839c). The specimens illustrated by Milker and Schmiedl (2012) are of a lobulate form with a distinctly rounded apertural face, should belong to another species.

According to the number of chambers and the shape and extend of the sutural plates *Astrononion australe* Cushman and Edwards is a very similar taxon; but is somewhat fatter, and slightly more lobulate.

The umbilici of *Astrononion stelligerum* can be open and depressed (e.g., Meriç et al., 2014a, pl. 71 fig. 8, 13) or may be closed by fusing of the sutural plates (e.g., Cimerman and Langer, 1991, pl. 84 fig. 15). All the specimens examined in this study have shallowly depressed, open umbilici.

The taxon is easily distinguished from other taxa by the presence of the sutural plates. The juveniles of this taxon are most similar to the juveniles of *Melonis pompilioides* (Fichtel and Moll), but even those can be distinguished by the presence of the sutural plates on incised sutures.

Family Melonidae Holzmann & Pawlowski, 2017

Genus *Melonis* de Monfort, 1808

1808 *Melonis* – de Monfort, p. 66

Type: *Nautilus pompilioides* Fichtel and Moll (1798, p. 31, pl. 2 fig. a-c)

Test robust, biumbilicate, with open and deep umbilici. Periphery rounded. 10-12 chambers in the last whorl. Sutures radial, straight to slightly curved, and thickened. Aperture a slit extending from one umbilicus to the other and remaining open around the umbilical margin with distinct lip. Surface coarsely perforate except for the apertural face, sutures and umbilical rim.

Melonis pompilioides (Fichtel and Moll, 1798)

Plate 19 Figures 13-20; Plate 20 Figures 13-22

1798 *Nautilus pompilioides* – Fichtel and Moll, p. 31, pl. 2 fig. a-c

1846 *Nonionina soldanii* – d'Orbigny, p. 109, pl. 5 fig. 15-16

1851 *Nonionina affinis* – Reuss, p. 72, pl. 5 fig. 32

1858 *Melonis barleeanus* – Williamson, p. 32, pl. 3, figs. 68, 69

1958 *Melonis sphaeroides* – Voloshinova, p. 153, pl. 3, fig. 10

1984 *Melonis pompilioides* (Fichtel and Moll); Rögl and Hansen, p. 30, pl. 2 fig. 1-2, pl.3 fig. 1

1991 *Melonis pompilioides* (Fichtel and Moll); Cimerman and Langer, p. 77, pl. 85 fig. 1-4

1993 *Melonis barleeanum* (Williamson); Sgarrella and Moncharmont Zei, p. 242, pl. 26 fig. 1-2

1993 *Melonis pompilioides* (Fichtel and Moll); Sgarrella and Moncharmont Zei, p. 242, pl. 26 fig. 5-6

2012 *Melonis affinis* (Reuss); Milker and Schmiedl, p. 115, fig. 26.9-10

2014a *Melonis pompilioides* (Fichtel and Moll); Meriç et al., pl. 71 fig. 14-24

Test planispiral, involute, biconvex, with open and depressed, small umbilici; periphery non-lobulate, margin subrounded to rounded. 10-11 chambers in the last

whorl, not inflated. Sutures flush, thick, limbate, radial, non-porous. Umbilicus open and deep in the adult, surrounded by non-porous umbilical margins of the chambers; closed in juvenile. Aperture an interiomarginal slit extending from one umbilicus to the other, accompanied by a lip on the upper margin. Test thick; coarsely perforated except for the sutures, umbilical margins of the chambers and the apertural face; surface smooth.

These are planispiral forms with perforated test. The earlier part of the test with subrounded periphery, later becomes more rounded as the chamber size in axial dimension increases gradually. The sutures are gently curved to straight, thickened. The umbilical ends of the chambers are fitted with an imperforate structure (flap) which merge around the umbilicus looking like a hollow cylindrical umbilical knob.

Melonis pompilioides (Fichtel and Moll), *Melonis soldanii* (d'Orbigny), *Melonis affinis* (Reuss), *Melonis barleeanus* (Williamson) and *Melonis sphaeroides* Voloshinova are considered synonyms and/or ecophenotypes (see discussion in Van Morkhoven et al., 1986, pp. 74, 76). Although there are some publications which did distinguish these taxa (e.g., Milker and Schmiedl, 2012; Houlbourn et al. 2013), here they are considered synonymous.

In the studied material, fatter individuals (*M. pompilioides*-type) and thinner individuals (*M. barleeanus*-type) are found together. The distinction between the adult end-members of these two types can only be done by the width of the test and the apertural face, and the shape of the edge; these characters are highly variable, and, other than these characters the two types are identical. The juvenile forms are always with a narrowly rounded edge, and cannot be assigned to one type or the other. In addition, the depressed umbilici are never developed in the juvenile specimens.

Taxon is easily distinguished from other taxa by its large size, very distinct, thick and limbate sutures, and coarsely porous test. *Astrononion stelligerum* (d'Orbigny) may appear similar, but is distinguished by the flaps over its incised sutures. The

juveniles of the taxon are somewhat different than their adult counterparts in that the umbilici are not depressed and open, but closed.

Family Nonionidae Schultze, 1854

Genus *Nonionella* Cushman, 1926a

1926a *Nonionella* – Cushman, p. 64

Type: *Nonionella miocenica* Cushman (1926a, p. 64)

Test auriculate, low trochospiral; spiral side evolute; umbilical side involute. Chambers radially elongated and increasing rapidly in length (radial dimension); umbilical margins of chambers with umbilical flap, may be very inflated (bulge), covering the umbilicus completely. Test thin, whitish, translucent, optically granular; surface smooth.

Nonionella iridea Heron-Allen and Earland, 1932

Plate 21 Figures 11-17; Plate 22 Figures 22-32

1932 *Nonionella iridea* – Heron-Allen and Earland, p. 438, pl. 16 fig. 14-16

2008 *Nonionella iridea* Heron-Allen and Earland; Lobegeier and Sen Gupta, pl. 2 fig. 9

part 2012 *Nonionella iridea* Heron-Allen and Earland; Mendes et al., fig. 4.2a and c (not fig. 4. 2b)

Test small, ovate, periphery rounded; outline non-lobulate to very slightly lobulate; low trochospiral; spiral side evolute, last whorl somewhat detached; umbilical side involute. Chambers growing gradually in size; about 6-7 in the last whorl. Chambers have a small inflated lobe extension (bulge) on the umbilical side, only partially covering the umbilicus. Sutures depressed, nearly radial, slightly curved. Umbilicus open, depressed, partially covered by umbilical bulges. Aperture an equatorial arch, but obscure. Test whitish, translucent so that the apertural face of the earlier

chambers can be seen from the side in well preserved specimens, minutely perforate; surface smooth.

The chambers of this taxon are more equidimensional than most nonionids, may become wider (tangentially) in some specimens. The umbilical bulge is quite small, not extending over the umbilicus, only partially covering it; this feature makes this taxon similar to *Nonionoides*; however, there are no pustules in the umbilicus or the sutures. According to these characters, this taxon may belong to another nonionid genus.

The small size of this taxon, and the fact that the juveniles of all nonionids are highly similar, are probably the two reasons for this taxon's very rare occurrence in Mediterranean benthic foraminifera literature. The partially covered umbilicus of this taxon distinguishes it from the juveniles of other nonionids.

Nonionella opima Cushman, 1947

Plate 21 Figures 1-5; Plate 22 Figures 1-10

part 1884 *Nonionina turgida* (Williamson); Brady, pl. 109 fig. 19 (not fig. 17-18)

part 1930b *Nonionella turgida* (Williamson); Cushman, pl. 6 fig. 4 (not fig. 1-3)

1947 *Nonionella opima* – Cushman, p. 90, pl. 20 fig. 1-3

1991 *Nonionella opima* Cushman; Cimerman and Langer, p. 74, pl. 84 fig. 1-3

1991 *Nonionella turgida* (Williamson); Cimerman and Langer, p. 74, pl. 84 fig. 6-8

1993 *Nonionella turgida* (Williamson); Sgarrella and Moncharmont Zei, p. 240, pl. 24 fig. 5

2008 *Nonionella turgida* (Williamson); Sakınç, pl. 17 fig. 5

part 2012 *Nonionella turgida* (Williamson); Milker and Schmiedl, p. 112, fig. 26.1-6

2014a *Nonionella turgida* (Williamson); Meriç et al., pl. 71 fig. 4-8

Test ovate, large, thick; periphery rounded; outline non-lobulate; low trochospiral; spiral side evolute, umbilical side involute. Chambers elongate (in the radial dimension) and low (in tangential dimension); growing rapidly in size, especially radially and in thickness (parallel coiling axis); last chamber fairly large, covering about half the surface on the umbilical side; about 8 in the last whorl. Chambers have an inflated lobe extension (bulge) on the umbilical side, covering the umbilicus and central portions of earlier chambers. Sutures depressed, but shallowly; flush to almost flush for the earlier part of the test. Umbilicus covered by successive umbilical extensions (bulges) of chambers. Aperture an equatorial arch, but obscure. Test whitish, translucent so that the apertural face of the earlier chambers can be seen from the side in well preserved specimens, minutely perforate; surface smooth.

This taxon is commonly recorded under the name *Nonionella turgida* (Williamson) (see references cited above). Williamson's taxon is less inflated and thick, and the chambers are narrower, more elongate, and higher in number with respect to *Nonionella opima* Cushman according to the type illustrations (Williamson, 1858, p. 50, pl. 4 fig. 95–97). Brady's interpretation of this taxon (a symmetrical form which sometimes may occur as asymmetrical) and the illustrations he provides seems like the main point of confusion (1884, p. 731, pl. 109 fig. 17-19). Brady's two illustrations depict such a symmetrical variant (fig. 17 and 18), but the third image (fig. 19) clearly do not belong with the rest. These symmetrical illustrations were reprinted by Cushman (1930b, pl. 6 fig. 2) under *N. turgida*; an illustration of an asymmetrical form was also given in the same plate (fig. 4). Neither the symmetrical nor the asymmetrical forms given by Brady (1884) and Cushman (1930b) can be classified under *N. turgida*. Though, the asymmetrical forms, as well as the forms attributed to *N. turgida* by the references cited above, can be referred to *N. opima* due to large umbilical bulge covering the umbilicus and large last chamber.

In the adult, the taxon is distinguished from other nonionids by its fat build and large and inflated umbilical bulge covering the umbilicus. The bulge is attached to the previous chambers with finger like projections which remain under the bulge unlike *Nonionella stella* Cushman and Moyer in which the finger like projections remains visible in umbilical view. Smaller, juvenile specimens are more difficult to distinguish: the bulge is respectively smaller and less inflated, the form is thinner, therefore they are similar to juveniles of *N. stella*. However, the sutures of the earlier chambers in that taxon are more depressed, and chambers are less elongate.

Nonionella stella Cushman and Moyer, 1930

Plate 21 Figures 6-10; Plate 22 Figures 11-21

1930 *Nonionella miocenica* var. *stella* – Cushman & Moyer, p. 56, pl. 7 fig. 17

1993 *Nonionella stella* Cushman and Moyer; Sgarrella and Moncharmont Zei, p. 240, pl. 24 fig. 6

2012 *Nonionella stella* Cushman and Moyer; Mendes et al., fig. 4.3

part 2012 *Nonionella iridea* Heron-Allen and Earland; Mendes et al., fig. 4.2b (not fig. 4. 2a and c)

Test ovate, periphery rounded; outline non-lobulate to very slightly lobulate (especially for the last chamber); low trochospiral; spiral side evolute, last whorl somewhat detached; umbilical side involute. Chambers elongate (in the radial dimension) and low (in tangential dimension); growing gradually in size; about 8 in the last whorl. Chambers have an inflated lobe extension (bulge) on the umbilical side, covering the umbilicus and central portions of earlier chambers, attached to previous chambers with finger like projections; projections coincide with the sutures. Sutures depressed, nearly radial, slightly curved. Umbilicus covered by successive umbilical bulges. Aperture an equatorial arch, but obscure. Test whitish, translucent

so that the apertural face of the earlier chambers can be seen from the side in well preserved specimens, minutely perforate; surface smooth.

The taxon is different from *Nonionella miocenica* Cushman by less numerous chambers and the finger like projection on the umbilical bulge.

The taxon is distinguished from other nonionids by the less elongate (relatively more equidimensional chambers) and the distinctive umbilical bulge with clear finger like projections. Very small specimens may look alike *Nonionella iridea* Heron-Allen and Earland and juveniles of *Nonionoides minuta* (Parker) due to more equidimensional chambers; however, the former has a very small umbilical bulge which only partially closes the umbilicus and the latter has an open umbilicus while the umbilicus of *N. stella* is completely covered by an umbilical bulge even in the juvenile.

Nonionoides **Saidova, 1975**

1975 *Nonionoides* – Saidova, p. 248

Type: *Nonionina grateloupi* d'Orbigny (1826, p. 294; nomen nudum) = *Nonionina grateloupii* d'Orbigny (1839b, p. 46, pl. 6 fig. 6-7)

Test auriculate, very low trochospiral; spiral side evolute, umbilical side involute. Chambers increase in length (radial dimension) rapidly. Umbilicus open, deep. Pustules present in and around the umbilicus, in the spiral suture and adjacent to the aperture; larger pustules (polyps) may be present at the umbilical ends of the chambers surrounding the umbilicus. Aperture equatorial. Test thin, whitish, optically granular, translucent; surface smooth other than the pustules.

Nonionoides grateloupii (d'Orbigny, 1839b)

Plate 21 Figures 18-23; Plate 22 Figures 33-40

1826 *Nonionina grateloupi* – d'Orbigny, p. 294 [nomen nudum]

1839b *Nonionina grateloupii* – d'Orbigny, p. 46, pl. 6 fig. 6-7

1904 *Nonionina grateloupi* d'Orbigny; Fornasini, p. 12, pl. 3 fig. 5

1930b *Nonion grateloupi* (d'Orbigny); Cushman, p.10, pl. 3 fig. 9-11, pl. 4 fig. 1-4

1982 *Pseudononion grateloupi* (d'Orbigny); Saunders and Mueller-Merz; p. 266, pl. 4 fig. 30-33

part 2012 *Nonionella turgida* (Williamson); Milker and Schmiedl, fig. 26.5-6 (not fig. 26.1-4)

Test ovate, compressed, periphery rounded; outline non-lobulate; very low trochospiral; spiral side evolute, umbilical side involute. Chambers elongate (in the radial dimension) and low (in tangential dimension); growing rapidly in length. Inner margin of chambers on the umbilical side inflated as a bulge, situated to the side of the umbilicus. Sutures radial, depressed near the umbilicus, becomes flush at the periphery. Umbilicus open, depressed, some small and some elongated pustules (polyps) situated in the umbilicus. Aperture an equatorial arch, but obscure. Test minutely perforated, translucent, whitish; surface smooth other than some umbilical polyps and smaller pustules in the umbilicus, in the suture between whorls, and the apertural face rimming the aperture.

The taxon was first recorded by d'Orbigny (1826), but no description or illustrations were provided (nomen nudum). Later it was described by d'Orbigny (1939b), but the name was written as ending with double i ("*grateloupii*") instead of a single i ("*grateloupi*") as was written in 1826 publication. Later usage of the name was the latter as the taxon was referred to the 1826 publication. Since the correct reference should be d'Orbigny (1939b), the name also should occur as it was reported in there.

The original depiction of the form (d'Orbigny, 1939b; Fornasini, 1904) is quite primitive. Cushman's (1930b) series of illustrations (including the original type figure) shows great variety, but lacks the fine details such as the pustules. The SEM illustrations given by Saunders and Mueller-Merz (1982) depict forms very similar to the ones examined in this study. The thickness of the test (and the last chamber;

in the direction parallel to the coiling axis) and the number of chambers in the last whorl are here taken as intraspecific variations.

Pseudononion japonicum Asano (=*Nonionella atlantica* Cushman) is different in that it is bilaterally more symmetrical, spiral side more involute, the pustules are denser and also present in the intercameral sutures (Saunders and Mueller-Merz, 1982).

The pustules on this taxon are less densely arranged than *Nonionella minuta* (Parker, see below), and the umbilical polyps are smaller and less conspicuous. The chamber growth rate and the auriculate shape greatly resembles *Nonionella opima* Cushman, but that taxon is much fatter, and also the umbilicus of that taxon is covered by large umbilical bulge. the auriculate shape and open umbilicus differentiates this taxon from other nonionids. The juveniles of this taxon are distinguished from the juveniles of other nonionids by the open umbilicus, thin build, and flush sutures.

Nonionoides minuta (Parker, 1954)

Plate 21 Figures 24-28; Plate 22 Figures 41-45

1954 *Valvulineria minuta* – Parker, p. 527, pl. 9, figs. 4-6

1980 *Valvulineria minuta* Parker; Alavi, p. 52, pl. 26 fig. 6, pl. 27 fig. 9, pl. 28 fig. 7

1993 *Valvulineria minuta* Parker; Sgarrella and Moncharmont Zei, p. 220, pl. 18 fig. 3-4

1994 *Valvulineria minuta* (Schubert); Loeblich and Tappan, p. 135, pl. 268 fig. 4-6

2012 *Valvulineria minuta* Parker; Milker and Schmiedl, p. 94, fig. 21.18-19

Test medium sized, low trochospiral with evolute spiral and involute umbilical side. Wall translucent, minutely perforate. Outline very slightly lobulate, lobulation more

prominent in larger individuals. Chambers inflated, globular, increasing gradually as added; about 7 in the last whorl. Sutures thinly depressed, near radial on both sides. Umbilicus wide and partially closed by somewhat overlapping polyps (elongate pustules) pointing towards the center of the umbilicus. Aperture an interiomarginal equatorial arch whose extension towards the umbilicus is obscured (not observed) due to umbilical pustules. Test minutely perforated, translucent, whitish; surface smooth other than umbilical polyps and some smaller pustules in the umbilicus, in the sutures of the younger chambers on the spiral side, and the apertural face rimming the aperture.

The commonly used name for the taxon, *Valvulineria minuta*, was given to two similar taxa independently. *Discorbina rugosa* var. *minuta* of Schubert (1904, p. 420) was originally described as a variety of *Valvulineria rugosa* (d'Orbigny, originally described under genus *Rosalina*). Schubert refers to Brady (1884, p. 652, pl. 91, fig. 4) in his description who depicted "smaller" individuals with a narrower umbilicus and a less lobulate periphery than the typical. Umbilical flaps depicted in Brady's illustrations are overlapping, convex and very similar to those in *V. rugosa* and *Valvulineria bradyana* (Fornasini). Parker (1954) described a *Valvulineria minuta* independently which differs from Schubert's taxon by a wider umbilicus and smaller (narrower) umbilical "flap" only occurring in the last chamber.

Loeblich and Tappan (1994) included Parker's taxon in the synonymy of Schubert's; nonetheless, the SEM illustrations they provide are more fitting with Parker's type. Identical to the specimens examined in this study, the umbilical "flaps" in the illustrations given in above cited publications are less like curved surfaces (typical umbilical flaps in *Valvulineria*), and more like elongate pustules with blunt and rounded ends, here termed as umbilical polyps.

The wall of the individuals studied is more similar to that of *Nonionella* than *Valvulineria* due to being minutely perforate and (probably) optically granular. The smaller (juvenile) individuals are very similar to small *Nonionella* and *Nonionoides* specimens (especially *Nonionella iridea*). In addition, the pustules in the umbilicus,

in the sutures of the younger chambers on the spiral side, and the apertural face rimming the aperture are also features that do not belong to *Valvulineria*, instead are seen in Family Nonionidae. The same pustules and umbilical polyps are present in individuals illustrated by Alavi (1980), Sgarrella and Moncharmont Zei (1993), and Loeblich and Tappan (1994); while, the specimens illustrated by Milker and Schmiedl (2012) agree with the rest of the cited material in most aspects, the pustules are not observable, those specimens may belong to juvenile representatives. Very similar elongate umbilical polyps are present in *Nonionoides grateloupii* (d'Orbigny) (see Saunders and Mueller-Merz, 1982, pl. 4 fig. 31b, 33).

The true identity of Parker's taxon cannot be proven unless the type specimens themselves are examined, yet, since many researchers opted to use the name, here this form is also attributed to Parker's taxon. Moreover, due to above mentioned morphological criteria, especially the wall type, the pustules and polyps, as well as the open umbilicus, taxon is moved to genus *Nonionoides*.

Adults of the taxon is easily distinguished from other nonionids by the lack of umbilical extensions of chambers, the more equilateral dimensions of chambers, and wide umbilicus. Juveniles of the nonionids are very difficult to distinguish from each other; however, the open umbilicus are still observable in the juveniles of this taxon.

Family Pulleniidae Schwager, 1877

Subfamily Pulleniinae Schwager, 1877

Genus *Pullenia* Parker & Jones in Carpenter et al., 1862

1862 *Pullenia* – Parker & Jones in Carpenter et al., p. 184

Type: *Nonionina bulloides* d'Orbigny (1846, p. 107, pl. 7 fig. 9–10)

Test planispiral, involute; globular to compressed; peripheral margin rounded; outline lobulate. Chambers three to six in the last whorl, triangular. Sutures flush to depressed. Aperture interiomarginal, slit-like, spans the whole distance between umbilici. Test finely perforate; surface smooth.

Pullenia spp.

Plate 19 Figures 25-27; Plate 20 Figures 28-30

Test planispiral, involute, laterally compressed; peripheral margin rounded; outline lobulate. Chambers four or five in the last whorl, triangular. Sutures depressed. Umbilici closed, slightly depressed. Aperture interiomarginal, slit-like, spans the whole distance between umbilici. Test finely perforate; surface smooth.

The two very similar lobulate *Pullenia* species, namely *Pullenia quadriloba* Reuss (four chambers in the last whorl) and *Pullenia quinqueloba* (Reuss; five chambers in the last whorl) are treated together in this study.

Superfamily Planorbulinoidea Schwager, 1877

Family Cibicididae Cushman, 1927

Genus *Cibicides* de Monfort, 1808

1808 Cibicides – de Monfort, p. 122

Type: *Cibicides refulgens* de Monfort (1808, p. 123)

Test low trochospiral with planoconvex to biconvex shape and angular/carinated periphery. Umbilical side involute, spiral side evolute, may be semi evolute. Aperture an interiomarginal equatorial arch which continues onto the spiral side at the spiral suture.

Truncatulina d'Orbigny is, to most part, synonymized with the present genus.

Historically the planoconvex morphotypes were classified under *Cibicides*, and the biconvex forms under *Cibicidoides* Thalmann. Genetic studies, on the other hand, argue that the test morphology cannot be a distinguishing feature on generic level (Schweizer et al. 2009).

Cibicides refulgens de Montfort, 1808

Plate 23 Figures 8-10; Plate 24 Figures 7-11

1808 *Cibicides refulgens* – de Montfort, p. 123

1991 *Cibicides refulgens* Montfort; Cimerman and Langer, p. 70, pl. 75 fig. 5-9

1991 *Cibicides advenum* (d'Orbigny); Cimerman and Langer, p. 70, pl. 74 fig. 8-10

2009 *Cibicides refulgens* de Montfort; Schweizer et al., fig. 1m-n

2012 *Cibicides refulgens* de Montfort; Milker and Schmiedl, p. 107, fig. 24.14-16

2014a *Cibicides advenum* d'Orbigny; Meriç et al., pl. 59 fig. 15-18

Test planoconvex, with flat, evolute spiral side and convex, involute umbilical side; margin angular; outline non-lobulate. Chambers about 9 in the last whorl, coiled around a central umbonal boss on the umbilical side. Sutures curved and thickened on the spiral side, limbate and flush on the umbilical side. Aperture an interiomarginal, equatorial arch accompanied by a lip; the aperture also extends onto the spiral side along the spiral suture. Test porous, especially so on the spiral side, translucent; surface smooth.

The porosity of the test is probably variable between individuals and may be responsive to ecological conditions. The individuals illustrated by Milker and Schmiedl (2012) are finely perforate; while, Cimerman and Langer (1991) give illustrations of rather porous (on both sides) specimens. Individuals examined in this study are porous on the spiral side, however the umbilical side is usually found to be more finely or sparsely perforated. In addition, most of the individuals in this study have an umbilical boss, of which no mention was found in the studied literature. Similar boss-like features were also seen in *Lobatula lobatula* (Walker and Jacob) specimens, especially in smaller (juvenile) individuals. Due to differences in

porosity and the presence of the umbilical boss, the assignment of this taxon is only done tentatively.

Cibicides advena (d'Orbigny) is a very similar species, and may be a synonym to this taxon. Meriç et al. (2014a) illustrated identical specimens under the name *C. advena*.

Taxon is distinguished from others by a coarsely porous, flat spiral side; less visibly porous, convex umbilical side, and non-lobulate periphery. Juveniles and non-lobulate varieties of *Lobatula lobatula* (Walker and Jacob) is very similar to this taxon, but they usually have a smaller number of chambers in the last whorl.

Genus *Lobatula* Fleming, 1828

1828 *Lobatula* – Fleming, p. 232

Type: *Lobatula vulgaris* Fleming (1828, p. 2322) = *Lobatula lobatula* (Walker and Jackob, 1798, p. 642, pl. 14, fig. 36)

Test planoconvex; spiral side flat, umbilical side convex; outline mostly lobulate; periphery rounded to angular, carinate. Aperture an equatorial arch with a lip, continuing along the spiral suture. Test coarsely perforate except for the keel and the area adjacent to the aperture.

Genetic studies of Schweizer et al. (2009) show that genus *Lobatula* is invalid, and they propose that *Lobatula lobatula* be replaced into genus *Cibicidoides* Thalmann. Due to wide usage of the taxon, the name *Lobatula* is retained here contrary to Schweizer et al.'s proposition.

Lobatula lobatula (Walker and Jackob, in Kanmacher, 1798)

Plate 23 Figures 1-7; Plate 24 Figures 1-6

1798 *Nautilus lobatulus* – Walker and Jacob; in Kanmacher, p. 642, pl. 14, fig. 36

1828 *Lobatula vulgaris* – Fleming; p. 232

1988 *Lobatula lobatula* (Walker and Jacob); Loeblich and Tappan, p. 168, pl. 637, figs. 10-13

1991 *Lobatula lobatula* (Walker and Jacob); Cimerman and Langer, p. 71, pl. 75 fig. 1-4

2009 *Cibicidoides lobatululus* (Walker and Jacob); Schweizer et al., fig. 1a-h

2012 *Lobatula lobatula* (Walker and Jacob); Milker and Schmiedl, p. 107, fig. 24.17-20

2014a *Lobatula lobatula* (Walker and Jacob); Meriç et al., pl. 60 fig. 2-14

Test planoconvex; spiral side flat or may be concave; umbilical side gently convex. Periphery may be non-lobulate, or may be highly and irregularly lobulate. Edge angular, usually carinated. Chambers 7-8 in the last whorl, may be rapidly and irregularly increasing in size. Umbilicus with an imperforate boss in the young, last whorl of chambers cover the umbilical boss. Aperture an interiomarginal equatorial arch with a lip; aperture extends along the spiral suture.

The intraspecific variation is quite large in this taxon as the outline can be lobulate or non-lobulate, and the non-lobulate forms can be misidentified as *Cibicides refulgen*s de Monfort (Brady, 1884; Schweizer et al., 2009). *C. refulgens* is different from the present taxon in that the porosity on the umbilical side is finer, and the last whorl contains slightly more numerous chambers.

Family Planorbulinidae Schwager, 1877

Genus *Hyalinea* Hofker, 1951a

1951a *Hyalinea* – Hofker, p. 416, 508, 513

Type: *Nautilus balthicus* Schröter (1783, p. 20, pl. 1, fig. 2)

Test discoidal, very low trochospiral, appears almost planispiral; laterally compressed, almost symmetrical; semi-evolute on both sides. Periphery with a thick

imperforate band (keel). Chambers with umbilical extensions (folium) on both sides of the test. Sutures usually thickened and raised. Aperture an interiomarginal equatorial arch with a lip. Supplementary apertures occur under the folium on both sides of the test. Surface smooth except for occasional pustules in umbilical region.

Hyalinea balthica (Schröter, 1783)

Plate 23 Figures 21-23; Plate 24 Figures 27-34

	1783	*Nautilus balthicus* – Schröter: p. 20, pl. 1, fig. 2
	1991	*Hyalinea balthica* (Schroeder); Hermelin, pl. 1
	2007	*Hyalinea balthica* (Schröter); Spezzaferri and Yanko-Hombach, p. 3, pl. 1 fig. 1, 3a–b, pl. 2 fig. 2a–c, 4a–b, 5a–c
part	2008	*Hyalinea balthica* (Schröter); Sakınç, pl. 16 fig. 1-2, (not pl. 15 fig. 12)
	2012	*Hyalinea balthica* (Schröter); Milker and Schmiedl, p. 93, fig. 24.1-2
part	2014a	*Hyalinea balthica* (Schröter); Meriç et al., pl. 59 fig. 7, 9-10 (not fig. 8)

Test discoidal, nearly planispiral, semi-evolute on both sides. Outline non-lobulate; periphery with thick, subrounded keel. Chambers 8-12 in the last whorl, usually not inflated, last few may be slightly inflated; inner margins of chambers with umbilical extensions (folium) which cover part of the earlier whorl. Sutures thickened, imperforate, mostly radial, raised or flush at least in the earlier part of the test, last few may be thinner and depressed. Umbilici not depressed, inner whorls can be seen partially. Aperture a short interiomarginal equatorial arch, bounded above by a raised lip. Supplementary apertures occur on both sides of the test under the folium. Test finely perforate except for the sutures, keel, folium and apertural face; optically radial, transparent; surface smooth.

Taxon is easily distinguished from others by its near-symmetrical sides, semi-evolute, almost planispiral coiling and thick and limbate sutures. *Hyalinea marmarica* Spezzaferri and Yanko-Hombach is a very similar taxon and it cooccurs in the Sea of Marmara with *H. balthica*. *H. balthica* is different from *H. marmarica* in terms of higher number of chambers in the last whorl, and thick and raised sutures. The pre-adult representatives of these two taxa are highly similar and if smaller than ~1.5 whorls they cannot be differentiated.

Hyalinea marmarica Spezzaferri and Yanko-Hombach, 2007

Plate 23 Figures 18-20; Plate 24 Figures 20-26

	2007	*Hyalinea marmarica* – Spezzaferri and Yanko-Hombach, p. 3, pl. 1 fig. 2a–e, 4a–d, pl. 2 fig. 1a–c
	2002	*Hyalinea balthica* (Schröter); Kaminski et al., pl. 3 fig. 13
part	2008	*Hyalinea balthica* (Schröter); Sakınç, pl. 15 fig. 12, (not pl. 16 fig. 1-2)
part	2014a	*Hyalinea balthica* (Schröter); Meriç et al., pl. 59 fig. 8 (not fig. 7, 9-10)

Test discoidal, nearly planispiral, semi-evolute on both sides. Outline somewhat lobulate; periphery with thick, subrounded keel. Chambers 6-8 in the last whorl, somewhat inflated; inner margins of chambers with umbilical extensions (folium) which cover part of the earlier whorl. Sutures thickened, imperforate, gently curved, depressed especially for the last few, earlier ones may be somewhat raised. Umbilici slightly depressed, inner whorls can be seen partially. Aperture a short interiomarginal equatorial arch, bounded above by a raised lip. Supplementary apertures occur on both sides of the test under the folium. Small accessory apertures at the periphery where the sutures meet the keel present. Test finely perforate except for the sutures, keel, folium and apertural face; optically radial, transparent; surface smooth.

The representatives of this taxon were mostly lumped under *H. balthica* in the literature (see above given synonymy).

Taxon is easily distinguished from others by its near-symmetrical sides, semi-evolute, almost planispiral coiling and mostly depressed sutures. *Hyalinea balthica* (Schröter) is a very similar taxon and it cooccurs in the Sea of Marmara with *H. marmarica*. *H. marmarica* has fewer number of chambers in the last whorl, and almost all of the sutures on this taxon are depressed. In addition, although cannot be observed under stereomicroscope, *H. marmarica* has accessory aperture at the periphery unlike *H. balthica.* The pre-adult representatives of these two taxa are highly similar and if smaller than ~1.5 whorls they cannot be differentiated (Plate 23 Figures 16-17; Plate 24 Figures 17-19).

Genus *Planorbulina* d'Orbigny, 1826

Planorbulina mediterranensis d'Orbigny, 1826

Plate 23 Figures 11-15; Plate 24 Figures 12-16

1826 *Planorbulina mediterranensis* – d'Orbigny, p. 280, pl. 15 fig. 4-6

2012 *Planorbulina mediterranensis* d'Orbigny; Milker and Schmiedl, p. 108, fig. 24.21-24

1991 *Planorbulina mediterranensis* d'Orbigny; Cimerman and Langer, p. 71, pl. 78 fig. 1-8

Test discoidal; early stage of 1-1.5 whorls trochospiral as in *Cibicides* and *Lobatula*, later proliferating. Spiral (attached) side flat or in the shape of the substrate, evolute, with flush, thickened sutures. Umbilical side evolute with depressed sutures. Proliferating chambers with two interiomarginal equatorial apertures on opposite margins of chamber, accompanied with raised lips. Test transparent, optically radial; both sides coarsely perforate; surface smooth.

The initial, trochospiral portion of the tests usually have a yellowish-brown hue. The juveniles of 1-1.5 whorls are very similar to *Cibicides* and *Lobatula* juveniles, but

are more lobulate, mostly evolute, and the umbilicus is with a large umbilical boss-like feature.

The taxon is easily distinguished by its very characteristic discoidal shape.

Superfamily Rotaloidea Ehrenberg, 1839

Family Ammoniidae Saidova, 1981

Genus *Ammonia* Brünnich, 1771

Plate 27 Figures 1-15; Plate 28A Figures 1-10; Plate 28-B Figures 1-6

1771 *Ammonia* – Brünnich, p. 232

Type: *Nautilus beccarii* Linnaeus (1758, p. 710)

Test large, trochospiral, biconvex; spiral side evolute, umbilical side involute. Umbilicus may have an umbilical plug. Sutures on the umbilical side incised, may appear feathered with transverse fissures; further protrusions may occur near the umbilicus. Test optically radial, translucent for the chamber walls due to dense porosity, transparent for the sutures.

The taxonomy of this genus and the validity and the practicality of the species attributed to this genus has been a topic of vast research amongst taxonomists and geneticists (Pawlowski et al., 1995; Debenay et al., 1998; Holzmann and Pawlowski, 2000; Hayward et al., 2004; Hayward et al., 2019a, 2021). In previous studies, several morphospecies of *Ammonia* were recorded from the Sea of Marmara, namely *Ammonia ammoniformis* (d'Orbigny), *Ammonia beccarii* (Linnaeus), *Ammonia compacta* (Hofker), *Ammonia falsobeccarii* (Rouvillois), *Ammonia inflata* (Seguenza), *Ammonia novoeuxinica* Yanko, *Ammonia parasovica* Shchedrina & Mayer, *Ammonia parkinsoniana* (d'Orbigny), *Ammonia tepida* (Cushman).

This taxon is only regarded at the generic level due to the rarity of this shallow water genus in the studied samples which come mainly from deeper settings. Adult specimens belonging to this genus were recovered from only few stations (Station 1,

2 and MM-50), in other stations only small (juvenile, only up to about 1 whorl big) representatives were found. These juvenile specimens in the deeper stations may be reworked, transported.

Taxon is distinguished from other taxa by its fat and biconvex shape and distinct umbilical plug (and other umbilical protrusions).

Family Elphidiidae Galloway, 1933

Subfamily Elphidiinae Galloway, 1933

Genus *Cribroelphidium* Cushman and Brönnimann, 1948

1948 *Cribroelphidium* – Cushman and Brönnimann, p.18

Type: *Cribroelphidium vadescens* Cushman and Brönnimann (1948, p. 18 pl. 4 fig. 5)

Test planispiral, involute, with rounded margin. Sutures with ponticuli (as in *Elphidium*). Umbilici with an imperforate boss on which openings may be present. Aperture a row of interiomarginal openings, some areal openings may also be present. Test optically radial, densely perforate other than the umbilical boss and the apertural face; surface smooth.

Cribroelphidium poeyanum (d'Orbigny, 1839b)

Plate 25 Figures 19-22; Plate 26 Figures 18-22

1839b *Polystomella poeyana* – d'Orbigny, p. 55, pl. 6 fig. 25-26

2008 *Cribroelphidium poeyanum* d'Orbigny; Sakınç, pl. 19 fig. 3-4

2014a *Cribroelphidium poeyanum* (d'Orbigny); Meriç et al., pl. 78 fig. 6-12

Test planispiral, involute, laterally compressed, with rounded margin. Sutures radial, may be slightly depressed, with several ponticuli; between the ponticuli remaining openings small. Umbilici very slightly depressed, with an imperforate boss on which only several large ovate openings present. Aperture a row of interiomarginal

openings, some areal openings may also be present. Test optically radial, densely perforate other than the umbilical boss and the apertural face; surface smooth.

Taxon is easily distinguished from *Elphidium* by its rounded margin instead of a carinate one, and from *Porosononion* by lack of umbilical pustules.

Genus *Elphidium* de Monfort, 1808

Plate 25 Figures 1-18; Plate 26 Figures 1-17

1808 *Elphidium* – de Monfort, p. 14

Type: *Nautilus macellus* var. *beta* Fichtel & Moll (1798, p. 68, pl. 10 fig. h–k)

Test lensoidal to discoidal, planispiral, both sides involute, biumbonate. Periphery carinate. Chambers low (tangentially), elongate (radially), numerous in the last whorl. Sutures curved, sometimes very strongly, incised, with transverse structures (ponticuli, retral processes; and fossettes). Test optically radial, surface may have pustules or spiraling ridges.

In previous studies, many morphospecies of *Elphidium* were recorded from the Sea of Marmara, most commonly *Elphidium aculeatum* (d'Orbigny), *Elphidium advenum* (Cushman), *Elphidium complanatum* (d'Orbigny).

This taxon is only regarded at the generic level due to the rarity of this shallow water genus in the studied samples which come mainly from deeper settings. Adult specimens belonging to this genus were recovered from only few stations (Station 2, 5, and MM-50), in other stations only small (juvenile, only up to about 1 whorl big) representatives were found. These juvenile specimens in the deeper stations may be reworked, transported.

Taxon is distinguished from other taxa by its larger size and very distinct transverse structures on incised sutures for adult specimens. Juvenile specimens, too, hold the same morphology, however, the smooth ones with lower number of ponticuli are very similar to *Porosononion simplex* (Cushman) and may be impossible to

distinguish from it under stereomicroscope. *Cribroelphidium* is a very similar genus, but the margin is not carinated and instead subrounded-rounded.

Genus *Porosononion* Putrya in Voloshinova, 1958

1958 *Porosononion* - Putrya in Voloshinova, p. 135

Type: *Nonionina subgranosa* Egger (1857, p. 299 pl. 14 fig. 16-18)

Test planispiral, involute; margin rounded. Sutures radial, incised, filled with pustules. Umbilici with pustules, and one or a few larger plugs. Aperture interioaerial rounded openings. Test optically radial, perforate. Sutures, umbilici and interiomarginal area adjacent to the aperture(s) with pustules.

According to Loeblich and Tappan (1988), *Porosononion* is a synonym of *Cribroelphidium*.

Porosononion granosum (d'Orbigny, 1846)

Plate 25 Figures 23-27; Plate 26 Figures 23-27

1846 *Nonionina granosa* – d'Orbigny, p. 110 pl. 5 fig. 19-20

? 1857 *Nonionina subgranosa* – Egger, p. 299 pl. 14 fig. 16-18

? 1991 *Porosononion* sp. 1 – Cimerman and Langer, p. 81, pl. 84 fig. 9-12

1993 *Elphidium granosum* (d'Orbigny); Sgarrella and Moncharmont Zei, p. 229, pl. 21 fig. 1-2

2008 *Elphidium granosum* (d'Orbigny); Sakınç, pl. 19 fig. 9-10

2012 *Elphidium granosum* (d'Orbigny); Milker and Schmiedl, p. 121, fig. 27.17-18

2014a *Porosononion subgranosum* (Egger); Meriç et al., pl. 78 fig. 13-18

2021 *Porosononion subgranosus* (Egger); Kırcı-Elmas et al., fig. 8d

Test planispiral, involute; periphery rounded. Chambers 7-10 in the last whorl, somewhat inflated. Sutures radial, incised, filled with pustules. Umbilici slightly depressed; one or a few plugs may be present. Aperture inconspicuous, small several rounded interiomarginal openings. Test optically radial, densely and coarsely perforated except for the apertural face; chamber walls smooth, sutures, umbilici and apertural region pustulose.

Porosononion subgranosum (Egger) is described to have 12 in the last whorl (Egger, 1857), while d'Orbigny's taxon is originally described with 8. The two taxa are not considered synonymous in the literature, however, vary similar specimens with various numbers of chambers in the last whorl can be found under the two names. In the studied material, it was observed that smaller specimens were of fewer chambers and larger specimens with larger number of chambers, and a gradation between the two extremes were also seen. Therefore, here they are considered together, under the name of d'Orbigny's taxon. The synonymy of the two taxa should be further investigated.

Taxon is easily distinguished from others by its planispiral nature, quite transparent and densely perforate test, and above all else, the pustulose umbilici. *Cribroelphidium poeyanum* (d'Orbigny) is a similarly planispiral and perforate form, however the whole test is smoother than the present taxon.

Porosononion simplex (Cushman, 1933b)

Plate 27 Figures 19-20

1933b *Elphidium simplex* – Cushman, p. 52, pl. 12, figs. 8, 9

2012 *Haynesina simplex* (Cushman); Milker and Schmiedl, p. 112, fig. 25.19-20

Test small, planispiral, involute. Margin subangular to subrounded. Sutures curved, incised, filled with pustules. Umbilici with umbilical knob, umbilical area pustulose. Aperture inconspicuous, interiomarginal area pustulose. Test optically radial,

transparent; surface smooth other than sutures, umbilici and interiomarginal area adjacent to the aperture which are pustulose.

The taxon was previously regarded under genus *Haynesina*; however, it does not constitute a slit aperture as in *Haynesina*.

The pustulose nature may give the sutures, especially in smaller individuals, the illusion of ponticuli as in *Elphidium*. Distinguishing the juveniles of this taxon from smooth walled *Elphidium* proves near impossible under stereomicroscope.

The taxon is distinguished from others by its umbilical boss and curved incised sutures.

Family Haynesinidae Mikhalevich, 2013

Genus *Aubignyna* Margerel, 1970

1970 *Aubignyna*– Margerel, p. 60

Type: *Aubignyna mariei* – Margerel (1970, p. 60-64, pl. 1, figs 1-8, pl. 2, figs 1-10, text-fig. 2) = *Rotalia perlucida* – Heron-Allen and Earland (1913, p. 139, pl. 13 fig. 7-9)

Test trochospiral, edge rounded. Spiral side evolute, with somewhat depressed sutures; umbilical side involute with depressed, incised sutures in which granular material (pustules) are densely present. Umbilicus closed, depressed, also pustulose. Aperture interiomarginal, pustulose surface present near aperture, pustules obscuring the opening. Surface smooth other than the pustules. Test transparent, optically radial.

Aubignyna perlucida (Heron-Allen and Earland, 1913)

Plate 27 Figures 21-22; Plate 28-B Figure 10

1913 *Rotalia perlucida* – Heron-Allen and Earland, p. 139, pl. 13 fig. 7-9

1969 *Buccella planidorso* – Atkinson, p. 535, fig. 6.3a-c

1970 *Aubignyna mariei* – Margerel, p. 60-64, pl. 1, figs 1-8, pl. 2, figs 1-10, text-fig. 2

2000 *Aubignyna perlucida* (Heron-Allen and Earland); Murray et al., p. 61, pl. 1 fig. 1-14; fig. 1d

part? 2008 *Aubignyna perlucida* (Heron-Allen and Earland); Sakınç, pl. 18 fig. 2-3 (fig. 1 ?)

part? 2014a *Aubignyna perlucida* (Heron-Allen and Earland); Meriç et al., pl. 72 fig. 12-15 (fig. 11, 16-17 ?)

Test medium in size; low trochospiral, umbilical and spiral views with more or less rounded outline; edge rounded; spiral side evolute, slightly convex; umbilical side involute, slightly concave. Chambers somewhat inflated; 6-7 chambers in the last whorl, about 1,5 whorls in total. Sutures slightly depressed and curved on spiral side, more prominently depressed and filled with pustules on umbilical side. Aperture an interiomarginal slit, but obscured by pustules. Test porous, transparent; surface smooth other than the granular material (pustules) present in the umbilicus, sutures on the umbilical side and around the aperture.

Murray et al. (2000) remark that adults of this taxon never exceed 1.5 whorls but are comparatively larger (>300 μm). The individuals examined in this study are mostly juveniles, but the adult forms of about 1.5 whorls were also found, but never larger than 250 μm. Sakınç (2008) and Meriç et al. (2014a) illustrated the spiral sides of larger specimens which has more than two whorls; attribution of those specimens to this taxon is questionable.

The form is quite rare in the Sea of Marmara. The overall shape is similar to *Gyroidina umbonata* (Silvestri), but differs from that taxon by its transparent wall, slightly concave umbilical side, and surface ornamentation.

Genus *Haynesina* Banner and Culver, 1978

1978 *Haynesina* – Banner and Culver, p. 184

Type: *Nonionina germanica* Ehrenberg (1840, p. 23)

Test planispiral, involute, biumbilicate; periphery rounded. Sutures gently curved and deeply incised near the umbilicus, becoming near flush near the periphery. Aperture an interiomarginal arch, but may be obscured by pustules. Surface smooth except for pustules in the sutures, around the umbilici and the aperture. No ponticuli or fossettes appear at the sutures.

Haynesina depressula (Walker and Jacob, in Kanmacher 1798)

Plate 27 Figures 16-18; Plate 28-B Figures 7-9

1798 *Nautilus depressulus* – Walker and Jacob, in Kanmacher, p. 641, pl. 14, fig. 33

1991 *Haynesina depressula* (Walker and Jacob); Cimerman and Langer, p. 81, pl. 83 fig. 1-4

2008 *Nonion depressulum* Walker and Jacop [sic]; Sakınç, pl. 17 fig. 3-4

2012 *Haynesina depressula* (Walker and Jacob); Milker and Schmiedl, p. 112, fig. 25.17-18

Test moderately compressed, planispiral, involute, biumbilicate. Periphery rounded-subrounded. Chambers 8-10 in the last whorl. Sutures gently curved and deeply incised near the umbilicus, becoming near flush near the periphery. Aperture an interiomarginal arch, but may be obscured by pustules. Surface smooth except for pustules in the sutures, around the umbilici and the aperture.

Taxon is distinguished from others by its biumbilicate nature and numerous chambers in the last whorl.

Superfamily Siphoninoidea Cushman, 1927

Family Siphoninidae Cushman, 1927

Genus *Siphonina* Reuss, 1850

1850 *Siphonina* – Reuss, p. 372

Type: *Siphonina fimbriata* Reuss (1850, p. 372, pl. 47 fig. 6) = *Rotalina reticulata* Czjzek (1848, p. 145, pl. 8, figs. 7-9)

Test trochospiral, biconvex, lensoidal; outline nearly circular; margin carinate. Chambers crescentic. Umbilical side involute, umbilicus closed. Aperture peripheral, produced on an ovate neck with an everted rim, directed slightly towards the umbilical side. Test optically radial, coarsely perforate; surface smooth or may be with radial striae or pustules.

Siphonina reticulata (Czjzek, 1848)

Plate 27 Figures 23-25; Plate 28-B Figures 11-13

1848 *Rotalina reticulata* – Czjzek, p. 145, pl. 8, figs. 7-9

1931 *Siphonina reticulata* (Czjzek); Cushman, p. 68, pl. 14, fig. 1

1991 *Siphonina reticulata* (Czjzek); Cimerman and Langer, p. 69, pl. 73 fig. 11-13

1993 *Siphonina reticulata* (Czjzek); Sgarrella and Moncharmont Zei, p. 222, pl. 19 fig.7-8

2012 *Siphonina reticulata* (Czjzek); Milker and Schmiedl, p. 103, fig. 24.24-26

2014a *Siphonina reticulata* (Czjzek); Meriç et al., pl. 58 fig. 8-10

Test trochospiral, biconvex, lensoidal; outline nearly circular; margin carinate. Chambers crescentic. Sutures indistinct on both sides. Umbilical side involute, umbilicus closed. Aperture peripheral, produced on an ovate neck with an everted rim, directed slightly towards the umbilical side. Test optically radial, coarsely perforate near the sutures and at the keel; surface smooth, shiny.

The taxon is very easily distinguished from all others by its lenticular shape and necked, peripheral aperture.

Superfamily Turrilinoidea Cushman, 1927

Family Stainfothiidae Reiss, 1963

Genus *Hopkinsina Howe & Wallace, 1932*

1932 *Hopkinsina* – Howe and Wallace, p. 61

Type: *Hopkinsina danvillensis* Howe and Wallace (1932)

Test fusiform, triserial to biserial. Chambers inflated, sutures depressed. Aperture terminal, produced.

Hopkinsina pacifica Cushman, 1933a

Plate 29 Figures 12-13; Plate 30 Figures 22-23

1933a *Hopkinsina pacifica* – Cushman, p. 86, pl. 8 fig. 16

? 1944 *Hopkinsina pacifica* var. *atlantica* – Cushman, p. 30, pl. 4 fig. 1

1992 *Hopkinsina pacifica* Cushman; Barmawidjaja et al., pl. 3 fig. 6-9

1999 *Spiroloxosloma glabra* (Millett); Hayward et al., p. 131, pl. 9 fig. 5

2001 *Hopkinsina atlantica* Cushman; Debenay et al., pl. 4 fig. 14

2005 *Hopkinsina pacifica* Cushman; Ernst et al., pl. 1 E-F

2008 *Hopkinsina pacifica* Cushman; Frontalini and Coccioni, pl. 1 fig. 11

2012 *Hopkinsina atlantica* Cushman; Mendes et al., fig. 3.5

2016 *Hopkinsina pacifica* Cushman; Martins et al., pl. 7 fig. 6

Test fusiform, slightly compressed. Chambers globular, arranged initially triserially, later becoming biserial, twisted. Sutures depressed. Aperture apparently terminal, situated at the apex of the test, adjacent to the suture; partially surrounded by a tall collar (horse-shoe shaped neck), provided with a toothplate that extends out the

apertural opening. Test translucent, whitish; surface dull, minutely pustulose, pustules may appear to be ordered in vertical rows.

The taxon is most similar to *Hopkinsina pacifica* Cushman and *Hopkinsina atlantica* Cushman. Original description of *Hopkinsina pacifica* indicates a form with smooth surface (Cushman, 1933a); however, the SEM image of the holotype clearly shows a minutely pustulose surface (see image by Smithsonian National Museum of Natural History Department of Paleobiology Collections, Catalogue number USNM CC 17513, access via http://n2t.net/ark:/65665/376b94889-d862-4a9b-b757-646b9271f5b4). *Hopkinsina atlantica* Cushman, originally described as a variety of *H. pacifica*, is a very similar species, described as being smaller than *H. pacifica*, having more elongated chambers and being more twisted (Cushman, 1944). Cushman (1944) notes that *H. pacifica* is only present in the tropical Pacific, while the variety *H. atlantica* was only found in one station in the Atlantic. The synonymy of these two taxa are should be investigated.

More recent accounts of *H. pacifica* from the Mediterranean Sea (see synonymy above) all depict forms with minutely pustulose surface. Some of these accounts are more elongated than others and the type. Similar forms were also attributed to *H. atlantica* (see synonymy above). Hayward et al. (1999) illustrated a very similar specimen attributed to *Spiroloxosloma (Hopkinsinella) glabra* (Millett), that image also clearly shows the toothplate extending out the aperture.

Taxon is similar to *Stainforhia fusiformis*, but is differentiated from it by the pustulose surface which appear opaquer and more whitish under the stereomicroscope, and the very clearly produced aperture.

Genus *Stainforhia* Hofker, 1956

1956 *Stainforthia* – Hofker, p. 908

Type: *Virgulina concava* Höglund (1947, p. 257, pl. 23 fig. 3-4, pl. 32 fig. 4-7, t-fig. 273-275)

Test initially triserial, later twisted biserial. chambers longer than wide, inflated; sutures depressed. Aperture situated in a concave depression on the apertural face, may become terminal in adult, a loop, equipped with a toothplate. Test optically radial, densely porous; surface smooth.

Stainforthia fusiformis (Williamson, 1858)

Plate 29 Figures 8-11; Plate 30 Figures 12-21

1858 *Bulimina pupoides* var. *fusiformis* – Williamson, p. 63, fig 129-130

2001 *Stainforthia fusiformis* (Williamson); Gooday and Alve, pl. 3, 4

2015 *Stainforthia fusiformis* (Williamson); Spezzaferri et al., pl. 22 fig. 2

Test small, somewhat ovate, tapering towards both poles, proloculus without a spine. Chambers inflated, usually longer than wide, arranged triserially at first (for a few chambers), later twisted biserial. Sutures depressed. Aperture situated in a wide concavity in the apertural face or is slightly produced terminally in the adult; a small loop rimmed by a tooth plate whose free part may extend out the aperture and is dentate. Surface smooth, shiny; test transparent to somewhat translucent, minutely and densely perforated, the proloculus and the early sutures distinctly transparent (optically radial).

Some specimens were found to be more elongated in outline, with less elongated chambers, and less twist in the biseriality. The aperture on these elongate varieties are narrower, however, still situated in a depression on the apertural face. These specimens, though may belong to another species of Stainforthia, are here included in this taxon due to having an identical wall type and juvenile phase.

The terminal aperture is only recovered in a handful of specimens in this study. Most specimens were found to be damaged due to the fragility of the test.

Taxon is distinguished from other *Stainforthia* by distinct fusiform shape, small size, and more transparent test.

Stainforthia? sp.

Plate 29 Figures 1-7; Plate 30 Figures 1-11

1980 *Stainforthia concava* (Höglund); Alavi, p. 47, pl. 22 fig. 5, pl. 23 fig. 10

2008 *Stainforthia concava* (Höglund); Sakınç, pl. 13 fig. 3-4

part 2014a *Fursenkoina acuta* (d'Orbigny); Meriç et al., pl. 52 fig. 20-23 (non fig. 19)

Test elongate, compressed; tapering towards the initial portion, proloculus with a spine; broadening towards the apertural end; biserial, may be twisted; rarely, initial portion may be triserial for a few chambers; a larger and a smaller varieties present. Chambers somewhat inflated, taller than wide. Sutures depressed. In smaller variety the aperture is wide, in larger variety narrow and slit like, more akin to the aperture of *Fursenkoina*. Test translucent, frosted due to dense porosity; surface smooth.

The two varieties are very much alike in all aspects except size and the apertural character. Since a size gradation between the two varieties were observed, these specimens here are considered as one taxon. The taxon is tentatively and questionably regarded under genus *Stainforthia* due to similarities with *Stainforthia concava* (Höglund) and *Stainforthia loeblichi* (Feyling-Hanssen).

Family Turrilinidae Cushman, 1927

Genus *Eubuliminella* Revets, 1993b

1993b *Eubuliminella* – Revets, p. 141

Type: *Bulimina elegans* var. *exilis* Brady (1884, p. 399, pI. 50, figs. 5,6)

Test conical to fusiform, high trochospiral with four to five chambers per whorl, may become triserial. Chambers inflated, sutures depressed. Aperture a loop with a cristate toothplate. Test densely porous except for at or near the sutures which are transparent and non-porous; surface smooth.

Eubuliminella sp.

Plate 29 Figures 14-17; Plate 30 Figures 24-27

Test conical, tapering towards the initial part; proloculus with a spine. Chambers inflated, high trochospiral, about four chambers per whorl, may be triserial later. Sutures depressed. Aperture an interiomarginal loop, provided with a toothplate whose free edge is serrated. Surface smooth, shiny; test mostly translucent and finely porous except for the upper parts of the chambers and the sutures which are transparent and non-porous.

Brady (1884, p. 399, pl. 50 fig. 5-6) described *Bulimina elegans* var. *exilis* as very regularly triserial, and illustrated highly elongate and slender specimens. Cushman's (1922a, p. 106, pl. 17, fig. 7-12) illustrations of the taxon depict fatter specimens with a high trochospiral arrangement with four chambers in the last whorl (see pl. 17 fig. 7-8 therein, especially similar to material from this study) but the description indicates triseriality. Revets (1993b, pl. 1 fig. 1-7) examined the type material and lectotypes for the taxon and erected the genus *Eubuliminella* with *Eubuliminella exilis* (Brady) as the type species for quadro- or penta-serial forms which may reduce to triserial with maturity, with cristate toothplate partially surrounding the aperture. The SEM images provided by Revets (1993b) of the chosen lectotype and paralectotypes for *Eubulimina exilis* are thinner than the material of the present study, however the cristate toothplate and the non-porous sutures characteristic of the genus are represented in the studied material.

Taxon is very easily distinguished by the quadroserial chamber arrangement, distinct spine on the proloculus, and the distinct non-porous sutures. The overall morphology is similar to buliminids, but the aperture of the taxon is distinctly wider.

Superfamily Virgulinelloidea Loeblich & Tappan, 1984

Family Virgulinellidae Loeblich & Tappan, 1984

Genus *Virgulinella* Cushman, 1932

1932 *Virgulinella* – Cushman, p. 9

Type: *Virgulina pertusa* Reuss (1861, p. 362, pl. 2 fig. 16)

Test fusiform-ovate, with ovate to rounded transverse section. Chambers triserially arranged, may become twisted biserial in adult; inflated, with finger-like extensions of basal part of the chambers extending over the sutures and reaching the top part of the previous whorl. Sutures depressed. Main aperture a narrow loop with a toothplate, accessory sutural apertures present between finger-like processes. Surface smooth.

Virgulinella fragilis Grindell and Collen, 1976

Plate 29 Figures 18-19; Plate 30 Figures 30-34

1959 *Virgulina (Virgulinella) pertusa* Reuss; Lankford, pl. 3 fig. 3

1976 *Virgulinella fragilis* – Grindell and Collen, p. 274, pl. 1 fig. 1-8

1999 *Virgulinella fragilis* Grindell and Collen; Hayward et al., p. 136, pl. 9 fig. 32-33

2003 *Virgulinella fragilis* Grindell and Collen; Bernhard, fig. 1 C-D

2004 *Virgulinella fragilis* Grindell and Collen; Ertan et al., pl. 1

2005a *Virgulinella fragilis* Grindell and Collen; Takata et al., fig. 2.1

2005b *Virgulinella fragilis* Grindell and Collen; Takata et al., pl. 1 fig. 2

2009 *Virgulinella fragilis* Grindell and Collen; Tsuchiya et al., pl. 1

2018 *Virgulinella fragilis* Grindell and Collen; Fontanier et al., fig. 4 F

Test ovate, taller than wide, tapering towards the proloculus. Chambers inflated, triserially arranged. Sutures depressed, distinct with several basal extensions from younger chambers extending to top of the chambers of the previous whorl, and sutural openings in between. Aperture loop shaped, with tooth-plate. Test extremely thin and fragile, transparent; surface smooth, shiny.

Lankford (1959) report a *Virgulina (Virgulinella) pertusa* from the east of the Mississippi Delta margin from recent sediments. The illustration Lankford provides depict a short form with only a few well separated processes on the sutures. *V. pertusa* (Reuss) on the other hand is a form with very numerous and small processes. What Lankford illustrated, most probably, belongs to this taxon instead.

Taxon is quite interesting in terms of its ecology, i.e., affinity with sulfur bacteria and eutrophic and hypoxic bottom conditions and patchy geographic distribution (e.g., Bernhard, 2003; Takata et al., 2005b). *V. fragilis* was recorded from the Sea of Marmara previously by Fontanier et al. (2018).

The form is quite unique with its distinct sutures, sutural openings and intervening processes, and very thin and fragile test wall. The form is very rarely found as whole due to extreme fragility.

SUBCLASS TEXTULARIANA Mikhalevich, 1980

Test agglutinated, multilocular, may be coiled or uncoiled.

ORDER LITUOLIDA Lankester, 1885

SUBORDER LITUOLINA Lankester, 1885

Superfamily Lituloidea Blainville, 1827

Family Discamminidae Mikhalevich, 1980

Genus *Ammoscalaria* Höglund, 1947

1947 *Ammoscalaria* – Höglund: p. 151

Type: *Ammoscalaria tenuimargo* (Brady, 1882, p. 715; type figures in Brady, 1884, p. 303, pl. 33 fig. 13-16)

The genus is characterized by planispiral to uniserial coiling with coarsely agglutinated walls. Septa are of organic material, rarely and sparsely agglutinated,

sutures indistinct. Intercameral foramen a simple areal opening. Main aperture terminal on a produced neck.

Ammoscalaria pseudospiralis (Williamson, 1858)

Plate 33 Figures 1-7; Plate 34 Figures 1-6

1858 *Proteonina pseudospiralis* – Williamson: p. 2, pl. 1 fig. 2-3

1884 *Haplophragmium pseudospirale* (Williamson); Brady, p. 302, pl. 33 fig. 1-4

1947 *Ammoscalaria pseudospiralis* (Williamson); Höglund, p. 159, pl. 31 fig. 1 a-p

1991 *Ammoscalaria pseudospiralis* (Williamson); Cimerman and Langer, 1991; p. 18, pl. 5 fig. 4-6

2004 *Ammoscalaria pseudospiralis* (Williamson); Chendeş et al., pl. 1 fig. 3

2008 *Ammoscalaria pseudoscalaris* [*sic*] (Williamson); Sakınç, pl. 1/4

2014a *Ammoscalaria pseudospiralis* (Williamson); Meriç et al., pl. 2 fig. 3

2016 *Ammoscalaria pseudospiralis* (Williamson); Lei and Li, p. 24 fig. 8 - 9

Test large, very thin (compressed), initial part discoidal, biumbilicate and planispiral, later rectilinear. Sutures indistinct. Aperture a circular, small, areal opening. Surface rough, wall coarsely agglutinated.

The form is characterized by a planispiral to uniserial test made of coarsely arenaceous material. The septa are mostly of organic material and very thin, usually not agglutinated (Loeblich and Tappan, 1988). Intercameral apertures are round with a slight neck (Höglund, 1947). The last chamber is more finely agglutinated and with thinner wall, getting narrower distally towards the true aperture, forming a neck (Höglund, 1947).

This taxon is similar to *Glaphyrammina americana* (Cushman, 1910) in surface texture, wall make-up and gross chamber arrangement; however, the planispiral portion of the test is larger in *G. americana* while the rectilinear portion makes up at least half of the test in *A. pseudospiralis*. Another distinction is that the aperture of *G. americana* is an elongated slit covering almost the whole breadth of the septal face of the uniserial last chamber.

All specimens from the Sea of Marmara were incomplete: broken so that either only the planispiral portion remains or as only few rectilinear chambers intact. Only very few relatively more complete individuals were found in which the spiral portion was as tall as the rectilinear portion. No completely intact specimens were found, therefore the very different last chamber and the apertural characteristic of the taxon were not observed. Nonetheless, the intercameral openings on a few of the broken individuals were observed, situated centrally on the apertural face, a round opening; therefore, the taxon is referred to *A. pseudospiralis* instead of *G. americana*.

Discammina compressa (Göes, 1882) is another similar flattened taxon, but usually is composed of siliceous spicules and a brown matrix. In addition, the form is semi-involute, planispirally coiled with only one (if any) uncoiled chambers; and the last several chambers are more inflated. The specimens from the Sea of Marmara never have such inflated chambers. Meriç et al. (2014a) provides three images for *Discammina compressa*, all of them side views, not showing the edge profile or the aperture. These images do resemble the illustrations given by Loeblich and Tappan (1964) for *D. compressa*, but neither has incorporated siliceous spicules. Especially one of Meriç et al.'s images (2014a, pl. 2 fig. 6) resembles the forms described here; however, without the apertural view referring it as belonging to *A. pseudospiralis* instead cannot be done confidently.

The individuals belonging to this taxon are quite easily distinguished from others by the large and thin (discoidal) dimensions and very coarse agglutinated test.

Family Haplophragmoididae Maync, 1952 (fide Loeblich and Tappan, 1984)

Genus *Labrospira* Höglund, 1947

These are large planispiral forms with coarsely agglutinated tests and an elongate aperture just above the interiomarginal position, both borders with a lip.

Labrospira kosterensis Höglund, 1947

1947 *Labrospira kosterensis* – Höglund, p. 147, p1. 11 figs. 4 a, b, tf. 130, 131

1991 *Labrospira kosterensis* Höglund; Cimerman and Langer, p. 18, pl. 4 fig. 11-13

Test planispiral, involute with 5 chambers in the last whorl. Chambers slightly inflated; sutures radial, depressed. Aperture nearly at the interiomarginal position, a little above the suture, an ellipse with long axis parallel to the coiling axis, rimmed from above and below. Surface smooth, shiny.

Höglund (1947) remarks that the test is brown in color, but all specimens here included are white-grayish.

SUBORDER SPIROPLECTAMMININA Mikhalevich, 1992

Superfamily Spiroplectamminoidea Cushman, 1927

Family Spiroplectamminidae Cushman, 1927

Subfamily Morulaeplectinae Saidova, 1981

Genus *Morulaeplecta* Höglund, 1947

Morulaeplecta bulbosa Höglund, 1947

Plate 31 Figure 1; Plate 32 Figure 1

1947 *Morulaeplecta bulbosa* – Höglund, p. 165, text-fig. 142, pl. 12 fig. 2

1992 *Morulaeplecta bulbosa* Höglund; Barmawidjaja et al., pl. 1 fig. 5-7

1993 *Spiroplectinella earlandii* (Parker); Sgarrella and Moncharmont Zei, p. 161, pl. 3 fig. 1-3

1999 *Textularia earlandii* Parker; Hayward et al. p. 90, pl. 2 fig. 22-23

2003 *Morulaeplecta bulbosa* Höglund; Murray, p. 13, fig. 3.4-5

2010 *Morulaeplecta bulbosa* Höglund; Alve and Goldstein, pl. 2 fig. 1-3

2011 *Morulaeplecta bulbosa* Höglund; Murray and Alve, fig. 18.7

Test small, elongated, nearly cylindrical, a little wider than thick. Lateral margins rounded. Initial portion of test bulbous with one or two offset chambers situated at another plane than the plane of biseriality; these chambers are invisible in frontal view, but discernable in edge view; test later regularly biserial. Chambers globular; sutures horizontal, depressed; outline lobulate. Aperture an interiomarginal low arch, slightly offset from center. Wall agglutinated, thin, fragile; surface rough.

The initial part of this taxon includes offset chamber(s). Such offset chambers in elongate textularins occur in *Morulaeplecta bulbosa* Höglund as coiled chambers surrounding the proloculus and in genus *Lacroixina cochleata* (Lacroix, 1932) as two pairs of chambers surrounding the proloculus (Höglund, 1947, p. 165; p. 183). The latter form has near terminal, necked aperture even in the young (see line drawings of sections in Höglund, 1947, text-fig. 160) which is very different from the present taxon. Another elongate textularin, *Textularia earlandi* Parker (1952) (=*Textularia tenuissima* Earland, 1933) identical to the present taxon in most respects, except for the initial portion of the test which is planispiral, arranged in the plane of biseriality, hence do not produce a protrusion in the initial part like the present taxon. *Textularia porrecta* Brady (1884) is also an elongate textularin and is greatly similar, however that taxon is biserial throughout.

The initial portions of the forms given under *Textularia* (or *Spiroplectinella*) *earlandii* by Sgarrella and Moncharmont Zei (1993) and Hayward et al. (1999) both have the mentioned protrusion identical to the studied material here. That initial portion of the test was remarked to be of an undefined arrangement by Höglund

(1947) due to the difficulty of observation. According to Loeblich and Tappan (1964, p. C251) that initial portion is streptospiral. Due to the small size and coarse agglutination (with respect to test size) the exact nature of the initial portion could not be observed in this study.

The test is extremely fragile. The last chamber of the specimen chosen for this very rare taxon was broken during the photographing with the stereomicroscope.

Taxon is easily distinguished from most other agglutinant taxa by its slender form and very thin wall.

Subfamily Spiroplectammininae Cushman, 1927

Genus *Spiroplectinella* Kisel'man, 1972

1972 *Spiroplectinella* – Kisel'man, p. 135

Type: *Spiroplecta wrighti* Silvestri (1903, p. 59, p. 60 tf. 1-6)

Taxon is characterized by a planispiral initial part followed by a flaring biserial adult part. Biserial part has an elongated diamond (lozenge) cross section. The edges are angular – carinated. The wall is finely agglutinated and smoothly finished. The aperture is interiomarginal, symmetrical low arch.

The wall texture, in terms of porosity, is non-canaliculate (sensu Loeblich and Tappan, 1988), in other words non-pseudoporous (sensu Hottinger et al., 1990 and references therein). Pseudoporous (canaliculate) agglutinated wall occurs in, for example, Family Textulariidae, and is described to include linear or anastomosing elongate and thin pores in the agglutinated wall structure, closed from the inside by organic lining and from the outside by outer agglutinated layer (Hottinger et al., 1990).

Spiroplectinella wrighti (Silvestri, 1903)

Plate 31 Figures 2-7; Plate 32 Figures 2-8

*part 1884 *Textularia sagittula* Defrance; Brady, p. 361, pl. 42 fig. 17*, 18

	1891	*Spiroplecta sagittula* (Defrance), sp.; Wright, p. 471
	1903	*Spiroplecta wrighti* – Silvestri, p. 59, fig. 1-6
	1913	*Spiroplecta wrighti* Silvestri; Heron-Allen and Earland, p. 57
?	1922a	*Spiroplecta wrightii* [sic] Silvestri; Cushman, p. 5 pl. 4 fig. 5-8
?part	1930	*Textularia sagittula* Defrance; Heron-Allen and Earland, p.72
	1987	*Textularia sagittula* Defrance; Jorissen, pl. 3 fig. 12
*	1991	*Spiroplectinella wrighti* (Silvestri); Cimerman and Langer, p. 20, pl. 6 fig. 1-4
	1991	*Spiroplectinella sagittula* (d'Orbigny); Cimerman and Langer, p. 19, pl. 6 fig. 5-6
	1991	*Spiroplectinella* cf. *S. taiwanica* (Chang); Cimerman and Langer, p. 19, pl. 6 fig. 7-9
	1993	*Spiroplectinella wrighti* (Silvestri); Sgarrella and Moncharmont Zei, p.161, pl. 3 fig. 13
	1994	*Spiroplectinella wrighti* (Silvestri); Loeblich and Tappan, p. 20 pl. 15 fig. 15-18
	2002	*Spirorutilus* spp.; Kaminski et al., p. 195, pl. 1 fig. 3-4
?part	2002	*Textularia* sp. Kaminski et al., p. 195, pl. 1 fig. 7 (non fig. 8)
*part	2012	*Spiroplectinella sagittula* s.l. (Defrance); Milker and Schmiedl, p. 34, fig. 9.19, 20*, 21
	2012	*Spiroplectinella* sp. 1; Milker and Schmiedl, p. 34, fig. 9.22
	2012	*Spiroplectinella* sp. 2; Milker and Schmiedl, p. 34, fig. 9.23-24
*part	2014a	*Spiroplectinella sagittula* (d'Orbigny); Meriç et al., pl. 3 fig. 2*, 3-6, 7*, 8-14

2021 *Textularia sagittula* Defrance; Kırcı-Elmas et al., fig. 9-h

Test triangular, initially planispiral, later biserial, biserial part flaring. In microspheric specimens the initial planispiral portion very small, giving the test a pointed apex; in megalospheric specimens the planispiral portion larger making the test apex broadly rounded. Test compressed, an elongate lozenge shape in cross section, margins narrowly angular, outline non-lobulate. The planispiral portion of 3-4 chambers (a half whorl) with flush and indistinct, radial sutures; in the biserial portion chambers low and broad, sutures flush to very slightly depressed, nearly horizontal, may be slightly curved. Wall mostly finely agglutinated, coarse grains present on the median line; yellowish in color, opaque; surface almost smooth, only slight elevation differences between the grains occur. Aperture an interiomarginal symmetrical low arch.

Individuals belonging to this taxon were recorded under *Textularia sagittula* d'Orbigny (1839c) or *Textularia sagittula* Defrance (1824). Wright (1891) noted that all the individuals they recognized as *Spiroplecta sagittula* (Defrance) had planispiral initial portions: in the microspheric ones smaller, in the megalospheric ones larger. Silvestri (1903) assigned these forms with initial planispiral portions to a new species: *Spiroplecta wrighti*. *Textularia sagittula* Defrance, the typetaxon of the genus *Textularia*, do not possess a planispiral initial part, is more elongate, has more inflated chambers and depressed sutures, chamber shapes are more equidimensional than the present taxon, and is significantly larger (about 2-3 mm in length; see neotype by Loeblich and Tappan, 1985 and discussion in 1964). According to Silvestri (1903), many accounts attributed to the name *Textularia sagittula* Defrance (e.g., Brady, 1884, pl. 42 fig. 18) are of wide, flaring and carinated forms that should belong to *S. wrighti* instead. The confusion between *sagittula* and *wrighti* occurred due to the varied emphasis put on the initial planispiral stage in textularin foraminifera (for example Heron-Allen and Earland, 1913 separating the two taxa, but Heron-Allen and Earland, 1930 keeping them under *Textularia sagittula* as different generations). Loeblich and Tappan designated a neotype for *T. sagittula* (1985, p. 205) showing clearly and very distinctly that the two taxa are not

conspecific, not even congeneric (see discussion in Loeblich and Tappan, 1964 p. C253, fig. 165, 1a-c).

Even more confusion is present concerning the original reference of *sagittula*. WoRMS (2025, https://www.marinespecies.org/aphia.php?p=taxdetails&id= 114285) accept Defrance as the original authority, however some publications refer to d'Orbigny as the original author of *sagittula* (e.g., Cimerman and Langer, 1991; Meriç et al., 2014a). D'Orbigny (1839, p. 138, pl. 1 fig. 19-21) took the original ownership of the taxon and noted the first description as *Polymorphum sagittulum* Soldani. Soldani (1780, no 154, p. 120, pl. 14 fig. 74) gives a brief account of a very small, pine nut shaped fossil from Italy under the name *Sagittulae*. D'Orbigny's illustration is similar to Defrance's, however in his discussion he included that Defrance's type not being identical to Soldani's. Nonetheless, Soldani's illustrations are very crude, and cannot be included in neither.

The confusion between these taxa is still evident in the recent literature despite Silvestri's (1903) and Loeblich and Tappan's (1964, 1985) efforts. Jorissen (1987) and Milker and Schmiedl (2012) took Silvestri's and Defrance's taxa as synonymous; Cimerman and Langer (1991) gave highly similar illustrations for both *Spiroplectinella sagittula* (d'Orbigny) and *Spiroplectinella wrighti* (Silvestri); Meriç et al. (2014a) treated *Spiroplectinella sagittula* (d'Orbigny) and *Textularia sagittula* (Defrance) separately.

The references and figures given with a star (*) in the above given list of synonyms are of taller individuals whose upper half has almost parallel sides and more depressed sutures. These forms may be truly adult forms of the taxon due to the facts that these individuals were given along with specimens of *Spiroplectinella wrighti* sensu stricto (i.e., specimens with elongated rhomboidal cross section with flush or very slightly depressed sutures) and that the lower half of the said taller specimens are identical to *S. wrighti* s.s.; however, their resemblance to *T. sagittula* Defrance s.s. cannot be refuted, and the SEM illustrations are not adequate to assess the

planispiral initial whorl for certain identification. In the material examined for this study, no such tall specimens were found.

The specimens attributed to *Spiroplectinella* cf. *S. taiwanica* (Chang) by Cimerman and Langer (1991) should belong to this taxon instead. That taxon is more distinctly thinly carinate with irregular edges (see Hottinger et al., 1990). Kaminski et al. (2002) recorded this present taxon under the name *Spirorutilus* spp. with a reference to *S. sagittula* sensu Cimerman and Langer (1991), noting that *sagittula* could not be transferred to another genus due to being the typetaxon of *Textularia*. Kaminski et al. (2002) also illustrated a *Textularia* sp. which is identical to the present taxon except that the chamber arrangement in the initial part on the SEM illustration cannot be determined with certainty.

Taxon is very easily distinguished especially when megalospheric by its broadly rounded base at which the carinate edges on these initial planispiral chambers are most often pronouncedly lighter in color. The diagnostic initial planispiral portion of the test is best visible when the specimens are wetted. The wall texture of the taxon is smoother than most representatives of the genus *Textularia*, and composed of mostly calcitic grains with minor inclusion of opaque minerals. The aperture of the taxon is a low and relatively wide arch, always positioned symmetrically unlike some *Textularia* whose aperture may be offset to one side.

SUBORDER VERNEUILININA Kaminski and Mikhalevich in Kaminski, 2004

Superfamily Verneuilinoidea Cushman, 1911

Family Prolixoplectidae Loeblich & Tappan, 1985

Genus *Eggerelloides* Haynes, 1973

1973 *Eggerelloides* – Haynes, p. 44

Type: *Bulimina scabra* Williamson (1858, p 65, pl. 5 fig. 136, 137)

Eggerelloides scabrus (Williamson, 1858)

Plate 33 Figure 16; Plate 34 Figure 19

1858 *Bulimina scabra* – Williamson, p. 65, pl. 5 fig. 136, 137 [figure caption as *B. arenacea*]

1947 *Eggerella scabra* (Williamson); Höglund, p. 191, pl. 13 fig. 12-14, tf. 162-165

1991 *Eggerelloides scabrus* (Williamson); Cimerman and Langer, p. 21, pl. 8 fig. 7

2010 *Eggerelloides scaber* (Williamson); Alve and Goldstein, pl. 2 fig. 7

Test conical, trochospiral to triserial. Chambers inflated, globular; sutures depressed. Aperture an interiomarginal arch. Wall coarsely agglutinant; surface slightly rough.

Höglund (1947) notes that the wall texture is variable according to water depth, with shallower settings including individuals with finer grained wall texture and deeper settings with coarser. Alve and Goldstein (2010) indicate that the juvenile *Liebusella goesi* Höglund is identical with the present taxon.

The taxon is rare in the Sea of Marmara. It is easily distinguished from other textularin forms by its triserial chamber arrangement and globular chambers.

ORDER TEXTULARIIDA Lankester, 1885

SUBORDER TEXTULARIINA Delage & Hérouard, 1896

Superfamily Eggerelloidea Cushman, 1937

Family Pseudogaudrynidae Loeblich & Tappan, 1985

Subfamily Pseudogaudryninae Loeblich & Tappan, 1985

Genus *Pseudoclavulina* Cushman, 1936

1936 *Pseudoclavulina* – Cushman, p. 16

Type: *Clavulina clavata* Cushman (1926b, p. 589)

Pseudoclavulina crustata Cushman, 1936

Plate 33 Figures 13-14; Plate 34 Figure 18

1936 *Pseudoclavulina crustata* – Cushman, p. 19, pl. 3 fig. 12

1991 *Pseudoclavulina crustata* Cushman; Cimerman and Langer, p. 23, pl. 11 fig. 9 -10

1993 *Clavulina crustata* (Cushman); Sgarrella and Moncharmont Zei, p. 167, pl. 4 fig. 10

2012 *Pseudoclavulina crustata* Cushman; Milker and Schmiedl, p. 42 fig. 11.4-6

Test large, elongate, initially triserial, later uniserial. Triserial portion with triangular cross section, edges narrowly rounded, faces flat to slightly concave. Uniserial portion with subcylindrical chambers. Sutures horizontal, indistinct. Aperture interiomarginal in the triserial phase, terminal on a neck in the uniserial phase. Wall coarsely agglutinated, surface very rough.

Most specimens belonging to this taxon were found as broken. The triangular pyramidal initial phase is very distinct in terms of morphology as well as size.

A number of broken pieces belonging to the septa of the rectilinear portion was found in the samples. Their identity (weather as *Bigenerina nodosaria* or *Pseudoclavulina crustata*) was determined in terms of size differences: this present taxon has a larger diameter.

Superfamily Textularioidea Ehrenberg, 1838

Family Textulariidae Ehrenberg, 1838

Subfamily Siphotextulariinae Loeblich and Tappan, 1985

Genus *Siphoscutula* Loeblich and Tappan, 1985

1985 *Siphoscutula* – Loeblich and Tappan, p. 206

Type: *Siphoscutula leroyi* Loeblich & Tappan (1985, p. 206)

Test biserial with diamond shaped cross section and angular lateral margins. Aperture a rounded, slightly produced opening above the base of the apertural face.

Siphoscutula? sp. 1

Plate 33 Figure 15; Plate 34 Figures 16-17

Test triangular, cross section diamond shaped with narrowly subrounded lateral margins. Chambers low, broad, last pair taller than the rest; sutures flush. Aperture a rounded-oval areal opening nearly central on the apertural face, above the suture, slightly offset to the side, encircled with elevated rim as in *Siphotextularia*. Wall coarsely agglutinated; surface rough.

The form highly resembles the biserial portion of *Bigenerina nodosaria* d'Orbigny in size and outline, but that taxon has interiomarginal arched aperture in the biserial stage (Loeblich and Tappan, 1964, p. C254, fig. 165.14). The siphotextularin aperture places this taxon into Subfamily Siphtotextulariinae. It differs from *Siphotextularia* by its more of a lozenge cross section instead of a quadrate one. Genus *Spiroscutula* is the most similar with respect to the cross-section shape and the apertural character, but differs in that it is finely agglutinated and the chamber growth rate is much higher (Loeblich and Tappan, 1985, p. 206). Form is distinguished from *Textularia* by the rounded and rimmed aperture and by being somewhat more flattened at the median line.

Genus *Siphotextularia* Finlay, 1939

1939 *Siphotextularia* – Finlay, p. 510

Type: *Siphotextularia wairoana* Finlay (1939, p. 511, pl. 68 fig. 2)

Test biserial, cross section quadrangular. Aperture asymmetrical, areal, oval, with distinct lip or produced on a tubular neck. Walls canaliculate, finely agglutinated.

Siphotextularia concava (Karrer, 1868)

Plate 31 Figures 8-11; Plate 32 Figures 9-12

1868 *Plecanium concavum* – Karrer, p. 129, pl. 1, fig. 3

part 1884 *Textularia concava* (Karrer), sp.; Brady, p. 360, pl. 42, figs. 14 (non pl. 42 fig. 13 and non pl. 43 fig. 11)

1911 *Textularia concava* (Karrer); Cushman, pp. 22-23, text-fig. 38

1991 *Siphotextularia concava* (Karrer); Cimerman and Langer, p. 23, pl. 12 fig. 4-6

1993 *Siphotextularia concava* (Karrer); Sgarrella and Moncharmont Zei, p. 166, pl. 3 fig. 12

2008 *Siphotextularia concava* (Karrer); Sakınç, pl. 2 fig. 4-5

2012 *Siphotextularia concava* (Karrer); Milker and Schmiedl, p. 40, fig. 10.25-26

? 2012 *Siphotextularia flintii* (Cushman); Milker and Schmiedl, p. 40, fig. 11.1-3

part 2014a *Siphotextularia concava* (Karrer); Meriç et al., pl. 6 fig. 11, 14-17 (non fig. 12-13)

Test triangular in frontal view, higher than wide; cross section quadrate with concave sides and rounded edges. Test biserial, sometimes twisted; with oblique, straight, more or less depressed sutures. Chambers low and broad, quadrate; 6-8 pairs; last pair inflated to some extent. Aperture an asymmetrically located elliptical opening surrounded by a continuous raised lip at or slightly above the interiomarginal position. Wall composed of mostly fine-grained material bound together with calcite cement, finely porous, thin. Surface dull.

The number of chamber pairs in the taxon commonly varies between six to eight; however, one of Cimerman and Langer's illustrations (1991, pl. 12 fig. 6) depict a specimen with 10 chamber pairs.

The inflation of the chambers and the depression of the sutures are here considered variable. Individuals illustrated by Brady (1884), Cimerman and Langer (1991) and Milker and Schmiedl (2012) have almost flush sutures while those by Sgarrella and Moncharmont Zei (1993), Sakınç (2008) and Meriç et al. (2014a) have more inflated chambers and more depressed sutures. Nonetheless, the main specific characters of the elongate ovate aperture and concave sides are all present in all these references.

Rana (2009) considered *Textularia concava* sensu Cushman (1911, p. 22 fig. 38) under synonymy of *Siphotextularia pseudoconcava* Zheng, yet that form illustrated by Cushman perfectly fits in the variation of the present taxon.

Milker and Schmiedl (2012, p. 40, fig. 11.1-3) illustrate two specimens under the name *Siphotextularia flintii* (Cushman), reported as different from *S. concava* by more inflated chambers and a more rounded periphery. Cushman's taxon (originally described as *Textularia flintii*, 1911, p. 21 fig. 36) is accepted under the genus *Karrerotextularia* (Zheng and Fu, 2008), a genus distinguished from *Siphotextularia* by lips below and above a slit-like interiomarginal aperture instead of a continuous raised rim in the latter (Loeblich and Tappan, 1988, p. 174), a character visible in Cushman's depiction of his taxon. These Milker and Schmiedl's specimens differ from Cushman's taxon by the lower number of chambers (8 instead of >10 in Cushman's) as well as the continuous raised rim around the ovate aperture. The apertural characteristic puts Milker and Schmiedl's illustrated specimens firmly in genus *Siphotextularia*, and maybe even in the variation of this present taxon.

One of Brady's illustrations under the name *Textularia concava* (1884, pl. 43 fig. 11) belongs to *Siphotextularia rolshauseni* Phleger & Parker (Jones, 1994); and another one (1884, pl. 42 fig. 13) is illustrated as having a simple, interiomarginal, low arch aperture and do not belong to this taxon. Brady's (1884, pl. 42) fig. 14 depicts a specimen with very sharp margins on the four corners different than the

other cited references and the material examined from the Sea of Marmara whose corners are somewhat rounded. Two specimens illustrated by Meriç et al. (20014, pl. 6 fig. 12-13) do not belong in this taxon due to much elongate test with more numerous chambers, and may belong to *Siphotextularia caroliana* Cushman instead.

The taxon is very easily distinguished from other biserial textularins by its fine-grained wall structure, dull surface, low and broad chambers, oblique sutures, concave sides, quadrate cross section, and, most importantly, the very specific oval aperture with encircling raised rim, even in the smallest (juvenile) specimens.

Subfamily Textulariinae Ehrenberg, 1838

Genus *Bigenerina* d'Orbigny, 1826

1826 *Bigenerina* – d'Orbigny, p. 261

Type: *Bigenerina nodosaria* d'Orbigny (1826, p. 261, pl. 11 fig. 9-12)

Bigenerina nodosaria d'Orbigny, 1826

Plate 33 Figures 8-12; Plate 34 Figures 7-15

1826 *Bigenerina nodosaria* – d'Orbigny, p. 261, pl. 11 fig. 9-12

1884 *Bigenerina nodosaria* d'Orbigny; Brady, p. 369, pl. 44 fig. 14-18

1911 *Bigenerina nodosaria* d'Orbigny; Cushman, p. 27, fig. 46-48

1991 *Bigenerina* ? *nodosaria* d'Orbigny; Cimerman and Langer, p. 21, pl 9 fig. 1-6

2008 *Bigenerina nodosaria* d'Orbigny; Sakınç, pl. 1 fig. 8-9

2014a *Bigenerina nodosaria* d'Orbigny; Meriç et al., pl. 4 fig. 10-15

Test elongate; initially biserial, triangular; later uniserial, rectilinear. Biserial stage with low and broad chambers, increasing in both dimensions as added; last pair of biserial chambers higher than previous ones. Rectilinear stage with subcylindrical chambers, slightly narrower than or equal to the top of the biserial phase in diameter.

Sutures indistinct in both phases, horizontal. Aperture an areal opening, terminal and on a neck in the rectilinear portion; basal (textularin) in the biserial portion. Wall coarsely agglutinated, surface rough.

The genus is described without a toothplate (see Loeblich and Tappan, 1988, p. 172). Cimerman and Langer (1991) illustrate a broken rectilinear portion of an individual with a toothplate (pl. 9 fig. 4); but the toothplate is not observable on the X-ray images (pl. 9 fig. 2, 3).

The shape of the aperture is variable: trigonal (Cimerman and Langer, 1991, pl. 9 fig. 5; Hofker, 1968, p.16), or oval-rounded (d'Orbigny, 1826, p. 261; Cushman, 1911, p. 27). In the studied material a high number of apertural faces from the rectilinear portion were found as fragments. On these intercameral septa the shape of the aperture is either rounded or ovate, always produced on a rim.

Hofker (1968) illustrated a series of specimens which they distinguished to be different generations of *Bigenerina nodosaria*. Of those, in the illustrations given for A1 and A2 generations (pl. 1 fig. 26-29; pl. 2 fig. 1-3) the diameter of the rectilinear portion is narrower than or equal to the top of the biserial phase as in our specimens and other references listed above. However, the illustrations given for the B generation have a minute biserial phase, and the diameter of the rectilinear portion greatly exceeds that of the top of the biserial phase; such forms were not encountered in this study. In addition, the biserial phase in A1 and A2 generation illustrations of Hofker are significantly shorter than that of ours.

Genus *Textularia* Defrance, 1824

1824 *Textularia* – Defrance, p. 177

Type: *Textularia sagittula* Defrance (1824, p. 177)

Test biserial throughout, wall canaliculate (sensu Loeblich and Tappan, 1988), aperture an interiomarginal arch.

The aperture in most representatives of this genus is found to be not symmetrically located, but slightly offset towards the margin. This criterion was used to distinguish it from the smaller (juvenile) individuals of *Spiroplectinella* where the initial planispiral portion of the test in *Spiroplectinella* cannot be observed.

Very small individuals (of 3-6 chambers) belonging to this genus cannot be differentiated into species, hence were left under Textulariana indeterminate.

Textularia agglutinans d'Orbigny, 1839b

Plate 31 Figure 12; Plate 32 Figure 13

	1839b	*Textularia agglutinans* – d'Orbigny, p. 144, pl. 1 figs 17-18, 32-34
part	1884	*Textularia agglutinans* d'Orbigny; Brady, p. 363, pl. 43 fig. 1-3 (non fig. 12)
	1991	*Textularia agglutinans* d'Orbigny; Cimerman and Langer, p. 21, pl. 10 fig. 1-2
	2008	*Textularia agglutinans* d'Orbigny; Sakınç, pl. 1 fig. 10-11
	2012	*Textularia agglutinans* d'Orbigny; Milker and Schmiedl, p. 38, fig. 10.15-16
?	2014a	*Textularia agglutinans* d'Orbigny; Meriç et al., pl. 4 fig. 16

Test elongate, triangular at the bottom half, sides nearly parallel at the top half. Margins narrowly subrounded; margins of last pair of chambers more rounded. Chambers high and wide, last two inflated at the top; sutures barely distinct due to coarse agglutination. Aperture an interiomarginal low arch. Wall coarsely agglutinated, surface rough.

The lower half of the test is very similar to *Textularia gramen* d'Orbigny in every aspect except that it is flaring with a lower angle than the latter. In the upper part of the test width increase as chambers added is even smaller so that the sides are nearly parallel in truly mature tests.

The pinching of the margins in the lower half of the test is a variable feature. Brady (1884) illustrated specimens with rounded margins throughout just like the original description of d'Orbigny (1839b). Later references to the taxon, though, all show somewhat narrower margins for the lower half of the test (e.g., Cimerman and Langer, 1991). Most of the references to the taxon has coarsely agglutinated wall; however, Meriç et al. (2014a) illustrated a specimen with finer agglutination, which may or may not be conspecific. The last chamber of the test may be slightly offset towards the center as illustrated by Brady (1884, pl. 43 fig. 1a).

The taxon is distinguished from *Textularia gramen* by larger size, more elongate test and occasionally coarser agglutination; however, when the test is pre-adult so that only the lower half is present distinction between *T. gramen* and *T. agglutinans* is near impossible.

Textularia gramen d'Orbigny, 1846

Plate 31 Figures 13-18; Plate 32 Figures 14-19

	1846	*Textularia gramen* – d'Orbigny; p. 248, pl. 15 fig. 4–6
part	1991	*Textularia bocki* Höglund; Cimerman and Langer, p. 21, pl 10, fig. 5-6
	1993	*Textularia calva* Lalicker; Sgarrella and Moncharmont Zei, p. 164, pl. 3 fig. 11
	2008	*Textularia bocki* Hoeglund; Sakınç, pl. 1 fig. 12
	2008	*Textularia calva* (Lalicker, 1935); Sakınç, pl. 1 fig. 13-14
	2008	*Textularia conica* d'Orbigny; Sakınç, pl. 1 fig. 15
	2012	*Textularia calva* Lalicker; Milker and Schmiedl, p. 39, fig. 10.17
	2012	*Textularia gramen* d'Orbigny; Milker and Schmiedl, p. 39, fig. 10.19-20
part	2014a	*Textularia bocki* Höglund; Meriç et al., pl. 5 fig. 7-8

Test triangular with subangular to pinched lateral margins. Chambers low and broad, but the last pair are very inflated at the top. Sutures slightly oblique, slightly depressed, but mostly inconspicuous due to the coarse agglutination of the test. Aperture an interiomarginal low arch, positioned slightly asymmetrically. Wall coarsely agglutinated, surface rough.

Specimens illustrated under *Textularia gramen* d'Orbigny by Milker and Schmiedl (2012) are identical to the present taxon. In addition, specimens attributed to *Textularia bocki* Höglund (Cimerman and Langer, 1991; Sakınç, 2008, Meriç et al. 2014a), *Textularia calva* Lalicker (Sgarrella and Moncharmont Zei, 1993; Sakınç, 2008; Milker and Schmiedl, 2012), and *Textularia conica* d'Orbigny (Sakınç, 2008) are very similar to the present taxon in terms of the flushness of the sutures, coarse agglutination of the wall, pinching of the lateral margins and the shape of the aperture; and are considered conspecific here. *Textularia bocki* Höglund (1947) is different from the present taxon by finer agglutination of the wall, the smoother finish of the surface, and the wider and lower aperture. *Textularia calva* Lalicker (1935) is similar in terms of the coarse agglutination and indistinct sutures, but different from the present taxon by the round cross section of the top part of the test, almost equal width and breadth (i.e., conical shape), and the wider and lower aperture. Finally, *Textularia conica* d'Orbigny (1839b) is significantly different in that its top margins of the last pair of chambers are not rounded, but truncated.

A wide variety of H/W ratios are found in the studied material. The coarsely agglutinated nature and the rough surface easily distinguishes this taxon from *Textularia* sp. 1.

Textularia pala Czjzek, 1848

1848 *Textularia pala* – Czjzek, p. 148 pl. 13 fig. 25-27

? 1991 *Textularia truncata* Höglund; Cimerman and Langer, p. 22, pl. 12 fig. 1-3

? 1993 *Textularia pala* Czjzek; Sgarrella and Moncharmont Zei, p. 166, pl. 3 fig. 8

non 2008 *Textularia pala* Czjzek; Sakınç, pl. 2 fig. 1-2

2012 *Textularia pala* Czjzek; Milker and Schmiedl, p. 40, fig. 10.22-22

non 2014a *Textularia pala* Czjzek; Meriç et al., pl. 5 fig. 14

Test small, triangular in frontal view, rapidly flaring. Lateral margins carinated, angular. Chambers low, broad; getting greatly broader as added; tops of the last pair not inflated, flat or gently curved; top margins of the last pair angular. Sutures slightly depressed. Aperture an interiomarginal low arch. Wall finely agglutinated, surface smooth.

The chamber growth rate is very high so that the lateral margins may become concave as in Milker and Schmiedl (2102). Milker and Schmiedl (2012) considered the forms referred to *Textularia truncata* Höglund by Cimerman and Langer (1991) as synonymous with their *Textularia pala*. Cimerman and Langer's illustrations show specimens with a distinctly lower growth rate. The two mentioned taxa are highly similar in their smooth and finely agglutinated surface as well as the truncate top surface of the top pair of chambers (see Czjzek, 1848 and Höglund, 1947), their possible synonymy should be noted. Two main differences are evident in the original descriptions: i. *T. pala* is much broader and thinner than *T. truncata*, ii. chambers of *T. pala* are lower and broader than *T. truncata*.

Number of chambers are much higher in the original description of *T. pala* than it is shown by Milker and Schmiedl, or material of this study.

Textularia conica d'Orbigny is similar to what is recorded here, but is more coarsely agglutinated and with a rougher surface (e.g., d'Orbigny, 1839b; Milker and Schmiedl, 2012).

Taxon is easily distinguished from other *Textularia* by its small size, truncate top margin of the chambers and rapidly flaring test.

Textularia sp. 1

Plate 31 Figures 19-20; Plate 32 Figures 20-21

Test small, short, flaring. Lateral margins sharply angular; chambers low and broad except for the last pair which are inflated at the top; sutures slightly depressed, horizontal. Aperture an interiomarginal low arch, positioned slightly asymmetrically. Wall is finely agglutinated except for the sharp margins where coarser sediments are affixed.

The taxon is very similar in general shape to *Textularia gramen* d'Orbigny, however usually is smaller, and has a smoother surface.

CLASS MONOTHALAMEA Haeckel, 1862
(as emended by Pawlowski et al., 2013)

ORDER ASTRORHIZIDA Lankester, 1885

SUBORDER SACCAMMININA Lankester, 1885

Superfamily Saccamminoidea Brady, 1884

Family Saccamminidae Brady, 1884

Subfamily Saccammininae Brady, 1884

Genus *Lagenammina* Rhumbler, 1911

1911 *Lagenammina* – Rhumbler, pp. 92, 111

Type: *Lagenammina laguncula* Rhumbler (1911, pp. 92, 111)

Lagenammina arenulata (Skinner, 1961)

Plate 39 Figure 18; Plate 40 Figure 20

1884 *Reophax difflugiformis* (Brady); Brady, p. 290, pl. 30 fig. 5 (non fig. 1-4)

1953 *Proteonina atlantica* (Cushman); Parker et al., p. 11, pl. 1 fig. 4

1961 *Lagenammina difflugiformis arenulata* – Skinner, p. 1239

1973 *Lagenammina atlantica* (Cushman); Lankford and Phleger, pl. 1 fig. 1

1991 *Lagenammina atlantica* (Cushman); Cimerman and Langer, p. 15, pl. 1 fig. 1-3

1993 *Lagenammina atlantica* (Cushman); Sgarrella and Moncharmont Zei, p. 152, pl. 1 fig. 13

1994 *Lagenammina arenulata* (Skinner); Jones, pl. 30 fig. 5

Test unilocular, flask shaped, with a widely rounded bottom and a tapering top, with a narrow, cylindrical neck. Wall is arenaceous, composed of sand particles irrespective of material: both lithogenic (quartz and plagioclase grains and lithic fragments) and biogenic (pelecypod debris) grains cemented together with a whitish (calcitic?) cement; very coarse grains used in the main chamber body, finer grains used in the neck. Aperture rounded, at the end of the neck.

This taxon was reported under *Lagenammina atlantica* (Cushman) by many authors, e.g., Parker et al. 1953; Lankford and Phleger, 1973; Cimerman and Langer, 1991; Sgarrella and Moncharmont Zei, 1993. All of these accounts illustrate a form with a neck, however the original description (Cushman, 1944; see holotype image by Smithsonian National Museum of Natural History Department of Paleobiology Collections, Catalogue number USNM CC 40517, access via http://n2t.net/ark:/65665/3638d3ce2-6a5a-43f0-bb45-8c9526da8846) clearly depicts a form which tapers towards the aperture yet does not possess a neck.

Lagenammina arenulata differs from *L. atlantica* mainly by having a neck; in addition, the wall is composed of much coarser material in *L. arenulata*. *Lagenammina difflugiformis* (Brady) is different from the present species by its wall structure which is finer and more uniform in terms of used grain size.

The taxon is found in only two stations: Station 5 and 7-2.

CLASS NODOSARIATA Mikhalevich, 1993 emend. Rigaud et al., 2015

ORDER NODOSARIIDA Calkins, 1926

Superfamily Nodosarioidea Ehrenberg, 1838

Family Lagenidae Reuss, 1862a

These are unilocular forms with circular cross section and necked aperture.

Genus Hyalinonetrion Patterson & Richardson, 1988

1988 *Hyalinonetrion* – Patterson & Richardson: p. 242

Synonyms: *Amphorina* d'Orbigny, C., 1849, vol. 5, p. 666 (not *Amphorina* de Quatrefages)

Type: *Hyalinonetrion sahulense* Patterson & Richardson (1988, p. 243, fig. 5-6) accepted as *Hyalinonetrion gracillimum* (Seguenza, 1862b)

Elongate, spindle shaped forms with long neck at the end of which the aperture is situated with a phialine lip (everted rim). Test is hyaline and imperforate with smooth surface.

Hyalinonetrion gracillimum Seguenza (1862b)

Plate 35 Figure 1; Plate 36 Figure 1

1862b *Amphorina gracillima*– Seguenza, p. 51, pl. 1 fig. 37

part 1884 *Lagena gracillima* (Seguenza); Brady, p. 456, pl. 56 fig. 19-22, 24-28 (not fig. 23)

1923 *Lagena gracillima* (Seguenza); Cushman, p. 23, pl.4 fig. 5

1991 *Hyalinonetrion gracillimum* (Seguenza); Cimerman and Langer, p. 52, pl. 55 fig. 1-2

1994 *Procerolagena gracillima* (Seguenza); Jones, p. 62, pl. 56 fig. 19-22, 24-28 (not 29)

2012 *Hyalinonetrion gracillimum* (Seguenza); Milker and Schmiedl, p. 74, fig. 18.30

2014a *Hyalinonetrion gracillimum* (Seguenza); Meriç et al., pl. 47 fig. 1

Test small, spindle shaped, elongate, tapering at both ends, widest part slightly closer to the aboral pole. Cross section circular. Apertural pole extends into a long tube at the end of which the aperture is situated accompanied by an everted rim. The adapertural pole also extends into a long tube, yet shorter than the apertural tube, and is closed. Wall transparent-translucent; surface smooth.

Brady (1884) considered the adapertural tube to be open in this taxon, however Cushman (1923) regarded the open ended individuals as broken and the adapertural end to be originally closed.

A similar taxon is *Lagena napolitana* Boltovskoy & Giussani de Kahn, (1983; originally described as *Amphorina elongata* Costa, 1856; considering the long, slender adapertural end of the form it probably fits better under *Hyalinonetrion*) which is a slenderer-more cylindrical taxon. *Hyalinonetrion elongatum* (Ehrenberg, 1844) is a taxon even slenderer.

Another similar taxon is *Hyalinonetrion clavatum* (d'Orbigny, 1846), whose adapertural pole extends into a tube of variable length (Cushman, 1923, p. 10), shorter than that of *H. gracillimum*. Alavi (1988) considered these taxa to be separate; however, Alavi (1980) noted that these two are closely allied. Brady (1884) illustrates a wide variety of morphologies for *H. gracillimum* some of which may be attributed to *H. clavatum* instead due to shorter adapertural tube. Illustrations given by Cimerman and Langer (1991), Milker and Schmiedl (2012) and Meriç et al. (2014a) are also of individuals with short adapertural tube. Without examination of these illustrated individuals it is impossible to infer weather these are just broken specimens or are indeed with shorter, intact adapertural tube. Considering the high

degree of morphologic similarities in between these species and possible synonymy, and the fact that all publications from the Sea of Marmara attributed these specimens to Seguenza's taxon, the same naming was followed for literary cohesion.

The very few individuals examined from the Sea of Marmara are all broken either at one end or both. The from is easily distinguished from other Lagenidae by its elongate-fusiform shape, distinct tapering at the adapertural end, and very smooth surface.

Genus *Lagena* Walker & Jacob, 1798

1798 *Lagena* – Walker and Jacob, in Kanmacher, p. 634

Type: *Lagena sulcata* (Walker and Jacob, 1798, in Kanmacher, p. 634i pl. 14 fig. 5)

Test usually flask – vase – tear-drop shaped with a long neck at the end of which the aperture is situated with a phialine lip (everted rim); adapertural pole usually broadly rounded, rarely with a stout spine. Surface smooth to costate, sometimes hispid; wall transparent-translucent.

Specimens from the Sea of Marmara belonging to this genus are very few and small, inhibiting specific recognition. Most encountered morphotypes are given below. Other individuals of this genus and specimens which are unassignable to a species are lumped into *Lagena* spp. in counting splits.

Lagena hispidula Cushman, 1913

Plate 35 Figure 3; Plate 36 Figures 4-5

part 1884 *Lagena laevis* (Montagu) – Brady, p. 455, pl. 56 fig. 10-11

1913 *Lagena hispidula* – Cushman, p. 14, pl. 5 fig. 2-3

1923 *Lagena laevis* (Montagu) var. *nebulosa* – Cushman, p. 29, pl. 5 fig. 4-5

1994 *Lagena hispidula* Cushman; Jones, p. 62, pl. 56 fig. 10-11

2008 *Lagena nebulosa* Cushman; Sakınç, pl. 10 fig. 12

non 2014a *Lagena nebulosa* Cushman; Meriç et al., pl. 47 fig. 5

Test small, globose, with a long and slender neck. Surface hispid, causing the test to look more whitish and opaquer.

Brady (1884) considered this morphotype a part of *Lagena laevis* (Montagu); however, that form has smooth surface in contrast to hispid surface of this taxon. Cushman, referring to the same figures of Brady (1884) described two different names in 1913 (*Lagena hispidula*) and 1923 (*Lagena laevis* var. *nebulosa*). Sakınç (2008), as well as other publications from the Sea of Marmara (Kırcı-Elmas, 2006, 2013; Kırcı-Elmas et al., 2008; Phipps et al., 2010) used the latter name (*L. nebulosa* Cushman), yet, the name *Lagena hispidula* should take precedence.

Meriç et al. (2014a) illustrates a form with hispid surface but with distinct spiral ridges on the neck which should belong to *L. hispida* Reuss (1863) instead. *L. hispidula* is different than *L. hispida* in that the hispid ornamentation is finer in the former, and spiral ridges are present on the neck of the latter.

All specimens belonging to this taxon were found with somewhat broken necks, however on the remaining neck portions no evidence of spiral ridges were observed. Although high variation in chamber shape is reported (Cushman, 1923), all specimens belonging to this taxon were with almost spherical chambers. This form is distinguished from other *Lagena* by its cloudy – translucent – whitish test and globose body which transitions into the slim neck pretty drastically.

Lagena interrupta Williamson, 1848

Plate 35 Figure 2; Plate 36 Figures 2-3

1848 *Lagena striata* (Montagu) var. a. *interrupta*– Williamson, p. 14, pl. 1 fig. 7

1973 *Lagena sulcata* (Walker and Jacob) var. *interrupta* (Williamson); Haynes, p. 92, pl. 12 fig. 10

non 2014a *Lagena interrupta* Williamson; Meriç et al., pl. 47 fig. 3

Test small, tear drop shaped with a short neck, distinctly costate. Costa are smooth, linear and situated regularly with the same spacing throughout. About half of the costae starts from the adapertural pole which is broadly rounded. Among those, about half of them traverse the whole test reaching the top of the neck (first order), others end just below the neck (second order). Rest of the costae are shorter, spanning various distances between the poles (third order). Costae are situated with a repeating pattern (1^{st}, 3^{rd}, 2^{nd}, 3^{rd}, 1^{st}…). All costae are almost of same height (in the radial dimension) but the longest ones are slightly higher and shortest ones are slightly lower. 1^{st} degree costae are higher especially at the body to neck transition giving the test a more regularly flaring shape. Regions between the costae are smooth. Wall whiteish, only slightly translucent, and resembles that of *Amphicoryna* (maybe due to taphonomic processes). Aperture terminal.

Lagena sulcata var. *alticostata* Cushman (1913) is very similar in the fashion of the costae, but the dominant ones (longest, those that span the whole test) are indicated to be plate-like (higher in the radial dimension). *Lagena sulcata* var. *torquiformis* (Haynes) is also a very similar form; however, the neck is longer and the dominant costae wraps around the neck in a spiral.

Original description of the form includes that all the costae are of different lengths (Williamson, 1848). *L. interrupta* sensu Haynes (1973) is more irregular in terms of the mentioned repeating pattern of costae. *L. interrupta* given in Meriç et al. (2014a), with fine costae and hexagonal patterns on the neck, clearly belongs to *L. striata* (d'Orbigny) instead.

The form is distinguished from *Lagena* sp. 1 by its smaller size, more pronounced costae, and shorter neck.

Lagena perlucida (Montagu 1803)

Plate 35 Figure 4; Plate 36 Figures 6-7

	1803	*Vermiculum perlucidum* – Montagu, p. 525, pl. 14 fig. 3
	1848	*Lagena striata* var. *perlucida* – Williamson, p. 15, pl. 1 fig. 11
non	1858	*Lagena vulgaris* var. *perlucida* – Williamson, p. 5, fig. 7-8
	1858	*Lagena vulgaris* var. *semistriata* – Williamson, p. 6, fig. 9
non	1923	*Lagena perlucida* (Montagu); Cushman, p. 46, pl. 8 fig. 12-13
	1923	*Lagena semistriata* Williamson; Cushman, p. 50, pl. 9 fig. 15
	1973	*Lagena perlucida* (Montagu); Haynes, p. 86, pl. 12 fig. 5, pl. 13 fig. 5
part	1984	*Lagena semistriata* (Williamson) subsp. *dorbignyi*; Jones, p. 133, pl. 7 fig. 14
part	1991	*Lagena* sp. 2 – Cimerman and Langer, p. 53, pl. 55 fig. 10
?	2008	*Lagena semistriata* Williamson; Sakınç, pl. 10 fig. 13-14
	2014a	*Lagena semistriata* Williamson; Meriç et al., pl. 47 fig. 6

Test tear drop shaped: broadest point much closer to the adapertural pole, gradually but somewhat rapidly tapers towards the neck transition. Neck also tapering, almost as long as the chamber. Basal part of the test decorated with several short, blunt costae that diminish upwards; some of them reappear just at the neck transition and span the neck as faint features. The very basal parts of the costae are slightly higher (in radial dimension). Wall transparent, aperture terminal with everted rim.

Although Montagu's description (1803) depicts a form with costae spanning the whole chamber, the taxon was later interpreted to hold forms with costae that diminish upwards, ending below the neck transition (Williamson, 1848; Haynes, 1973). It is confused with *Lagena semistriata* Williamson, a more cylindrical form

with costae that abruptly terminates somewhere below the neck transition, and with smooth neck (Williamson, 1848). Montagu's description for *L. perlucida* also do not include costae on the neck; however, Haynes (1973) describes forms with costae, even sometimes slightly spiral, on the necks. Most references after Williamson's (1858) swapping of the definitions of these taxa (with respect to Williamson, 1848), refer similar forms to *L. semistriata* instead. Very similar forms are reported under *L. semistriata* as cited above.

The form is distinguished from *L. semistriata* by its bottom-heavy distinct shape.

Lagena strumosa Reuss, 1863

Plate 35 Figure 5; Plate 36 Figures 8-9

	1858	*Lagena strumosa* – Reuss; p. 434
	1863	*Lagena strumosa* – Reuss, p. 328, pl. 4, fig. 49
?	1913	*Lagena striata* (d'Orbigny) var. *strumosa* Reuss – Cushman, p. 20, pl. 7 fig. 7-10
?	2012	*Lagena strumosa* Reuss; Milker and Schmiedl, p. 75, fig. 18.34
	2014a	*Lagena strumosa* Reuss; Meriç et al., pl. 47 fig. 10-13

Test globose with a stout adapertural spine and an elongate neck, distinctly costate. Costae are mostly confined to the lower half of the chamber and do not continue down to the spine or up to the neck. Neck is slightly tapering upwards, has annual ring-like ornamentation. Surface is smooth other than the costae.

Lagena annellatrachia Loeblich and Tappan (1994) is the most similar taxon but is different in that it has higher number of costae which span the whole chamber, and the surface between costae may be hispid. Original description of *L. strumosa* includes the remark that the costae may span the whole chamber (below the neck) or just be confined to the lower half (Reuss, 1863). Loeblich and Tappan (1994) also remark that the neck of the *L. strumosa* is smooth instead of the annulate neck of

their taxon; however, the original description does not make a remark to that aspect and the line illustration is not sufficient to make out this fine detail (Reuss, 1863). Individuals of *L. strumosa* illustrated by Cushman (1913) and Milker and Schmiedl (2012) are of wholly costate individuals which may be attributed to both of these taxa. Individuals illustrated by Meriç et al. (2014a) agrees completely with our specimens.

The form is fatter and larger than most other *Lagena*.

Lagena cf. *annellatrachia* Loeblich and Tappan, 1994

Plate 35 Figure 6; Plate 36 Figure 10

? 1994 *Lagena annellatrachia* – Loeblich and Tappan, p. 77, pl. 142 fig. 1-8, 11, 12

Test globose with a stout adapertural spine and an elongate neck, distinctly costate. Costae are mostly confined to the lower half of the chamber and do not continue down to the spine or up to the neck. Neck is slightly tapering upwards, has annual ring-like ornamentation. Surface between the costae is hispid, costae are rugged.

Test is very similar to *Lagena strumosa* Reuss, however the costae are more rugged, present as discontinuous blades at some parts of the test, and the surface between the costae are hispid. The form most resembles *L. annellatrachia* Loeblich and Tappan (1994) but is different from it by shorter and fewer costae.

The wall of this taxon is different from quite transparent *L. strumosa* by being more translucent, whiter, due to the hispid nature of the surface. In addition, this taxon is larger than *L. strumosa*.

Lagena cf. *laevis* Montagu 1803

Plate 35 Figure 7; Plate 36 Figure 11

? 1803 *Serpula* (*Lagena) laevis ovalis* – Montagu, p. 524

? 2008 *Lagena laevis* (Montagu); Sakınç, pl. 10 fig. 9-11

? 2014a *Lagena laevis* (Montagu); Meriç et al., pl. 47 fig. 4

Test an elongate vase shaped, with a rounded base, a very long neck terminated with an aperture and everted rim, a tear drop shaped chamber whose widest part is closer to the base than the neck transition. Surface smooth other than minute radial costa situated only at the base, forming small downward pointing flanges.

Original description of *Lagena laevis* (Montagu, 1803) do not include a type figure, and only gives a brief description of a smooth form with long neck. It appears that researchers used this name for smooth, elongate *Lagena* after Williamson (1848, and 1858 under *Lagena vulgaris* typica). Cushman (1923) and Haynes (1973) both share depictions of totally smooth forms.

Both Sakınç (2008) and Meriç et al. (2014a) illustrate specimens which almost perfectly fit with *L. laevis* references cited in the paragraph above, except for the base of the forms. In Meriç et al. (2014a) the form has a slight indentation as a ring at the base and a small protrusion, and in Sakınç et al. (2008) all three figures are of specimens apparently broken at the adapertural pole.

The radial small flanges at the base makes this form different than *Lagena laevis sensu stricto*. *Lagena oceanica* (Albani, 1974) is similar in that respect but the costae continue up the shell a little longer in that taxon. *Lagena setigera* (Millett, 1901) is another similarly shaped and similarly smooth taxon; however, the protrusions in that taxon are illustrated to be quite elongated, like thin spines. *Lagena tenuis* (Bornemann, 1855) is also very similar, described to have 5-7 short costae at the base which may go up the sides a short way. Having found only very few specimens, assigning these to any of these taxa cannot be done with confidence. Therefore, these specimens are left in open nomenclature under the mostly used name *L. laevis*.

Lagena sp. 1

Plate 35 Figure 8; Plate 36 Figure 12

part 1991 *Lagena* sp. 2 – Cimerman and Langer, p. 53, pl. 55 fig. 9

Test elongate, tear-drop shaped with a short and slender neck, distinctly costate. Costae are smooth, linear, of various lengths and locations on the test, more or less regularly spaced. Mostly, a costa starting at the top of or just below the neck, ending somewhere before reaching the base, is alternated by a costa starting at or near the base, ending somewhere before reaching the neck. Base is rounded, some of the costae gets slightly higher at the base forming small flanges. Wall transparent. Aperture terminal at the end of the neck.

This taxon agrees with Lagena sp. 2 of Cimerman and Langer (1991) in terms of overall shape of the test. In addition, although the number and size of the costae are slightly different, the offset and alternating nature of them, as well as the small flanges at the base are the same with the specimen illustrated by Cimerman and Langer (1991, pl. 55 fig. 9). The other specimen illustrated under that name (pl. 55 fig. 8) possibly belongs to *Lagena perlucida* (Montagu).

Taxon is similar to *L. interrupta* Williamson but is slenderer, the costae are of a less regular pattern, small flanges are present at the adapertural pole, and the body to neck transition is more abrupt.

Lagena sp. 2

Plate 35 Figure 9; Plate 36 Figures 13-14

Test slender, tear-drop shaped with a short and slender neck. Base broadly rounded, and decorated with a few (~6) costae which continue up the sides a very short distance, and are elongated downward to form small flanges. The neck is also decorated with a few subtle costae starting just below the body-neck transition, slightly spiraling up. Rest of the test smooth.

Taxon is similar to *Lagena semistriata sensu* Jones (1994, pl. 57 fig. 14), however the neck of that taxon is non-costate. *Lagena doveyensis* Haynes (1973) is also similar, but in addition to its neck being non-costate, its costae at the base are more numerous and finer. *Lagena perlucida* Montagu is similar in that the neck is costate;

however, that taxon also has more numerous and longer costae near the base and on the sides.

Family Nodosariidae Ehrenberg, 1838

Multilocular uniserial, or rarely biserial in part, rarely unilocular forms with hyaline, monolamellar or orthomonolamellar calcitic wall.

Subfamily Nodosariinae Ehrenberg, 1838

Genus *Dentalina* Risso, 1826

1826 *Dentalina* – Risso, p. 16

Type: *Dentalina cuvieri* (d'Orbigny, 1826, p. 255 n° 45)

Test elongate, may be arcuate; chambers uniserial with oblique to horizontal sutures; aperture radiate, surface vertically costate.

Dentalina spp.

Plate 35 Figure 24; Plate 36 Figure 37

Test rectilinear, circular in cross section, elongate, slender. Surface with vertical costae.

Only fragments of rectilinearly arranged, costate forms were found in the material from the Sea of Marmara, they are lumped in *Dentalina* spp. The genus is different from *Laevidentalina* by its costate surface, from *Pyramidulina* by slower growth rate of chambers, from *Marginulina* by a more central location of the aperture instead of at the dorsal angle.

Genus *Enantiodentalina* Marie, 1941

1941 *Enantiodentalina* – Marie, p. 149

Type: *Enantiodentalina communis* Marie (1941, p. 150, pl. 19 fig. 204-211)

Test elongate, early few chambers with biserial arrangement, later uniserial, rectilinear, may be arcuate; sutures usually flush, oblique; aperture radiate; surface smooth.

Enantiodentalina timorensis Loeblich and Tappan, 1994

Plate 35 Figure 23; Plate 36 Figures 38-41

part? 1991 *Astacolus crepidulus* (Fichtel and Moll); Cimerman and Langer, p. 52, pl. 54 fig. 14 (non fig. 10-13)

1994 *Enantiodentalina timorensis* – Loeblich and Tappan, p. 64, pl. 115 fig. 16-21

? 2014a *Dentalina inornata* d'Orbigny; Meriç et al., pl. 44 fig. 4-6

Test elongate, subcylindrical, slightly arcuate. Cross section sub-circular: one edge more constricted. In side view, the margin closer to the aperture (dorsal) is concave, non-lobulate, and narrowly rounded in section, the other margin is more lobulate, convex, and broadly rounded. In edge view both sides slightly lobulate. First two chambers in biserial arrangement; later chambers (about four in number) growing gradually both in diameter and in height, rectilinearly arranged. Chambers partially overlapping, covering the aperture of the previous chamber; subcylindrical in shape with oblique sutures between. Sutures slightly depressed, more so in the adult, make about 45° with the concave margin. Aperture terminal, on a short conical neck, radiate. Previous apertures are situated just adjacent to the dorsal margin Proloculus with a very short downward projecting spine. Test transparent, shiny, surface smooth.

The biserial arrangement of the initial chambers is characteristic for the genus *Enantiodentalina*. Although the genus was described to hold forms with nearly circular cross-section, some species (e.g., *Enantiodentalina timorensis* Loeblich and Tappan and *Enantiodentalina muraii* Uchio) diverge from that. *Enantiodentalina muraii* Uchai is different from *E. timorensis* by its shorter from and less arcuate

shape (Loeblich ant Tappan, 1994). The dorsal margin is narrower and convex in the genus *Astacolus*. *Chrysalogonium atlanticum* (Cushman, 1947, p. 90, pl. 19 fig. 10) is also similarly arcuate, concave at the dorsal margin, but the aperture in that species is on an elongated, slim neck. *Laevidentalina* can also be arcuate and with non-central aperture, but does not show biseriality and the sutures are mostly less oblique.

The X-ray image attributed to *Astacolus crepidulus* (Fichtel and Moll) by Cimerman and Langer (1991, pl 54 fig. 14) is arcuate in the opposite direction for that genus. Similarly, specimens attributed to *Dentalina inornata* d'Orbigny by Meriç et al. (2014a, pl. 44 fig. 4-6) all have concave dorsal sides and highly oblique sutures unlike that attributed taxon. Although the biseriality in the initial part is not observable in either of those specimens, they better fit in this present taxon.

Taxon is distinguished from other rectilinear nodosarids by a biserial phase in the juvenile, a concavely arched dorsal side and radiate terminal aperture which is adjacent to the dorsal side.

Genus *Grigelis* Mikhalevich, 1981

1981 *Grigelis* – Mikhalevich, p. 35

Type: *Grigelis pyrula* (d'Orbigny, 1826, p. 253 n° 13)

Test elongate, rectilinear-curvilinear, chambers globular to pyriform to spindle-shaped, separated by narrow necks; aperture on an elongate narrow neck, radial; surface smooth to longitudinally costate.

Grigelis orectus Loeblich and Tappan, 1994

Plate 35 Figures 21-22; Plate 36 Figures 32-33

1988 *Grigelis guttifera* (D'Orbigny); Loeblich and Tappan, p. 396, pl. 441, fig. 2-3

1994 *Grigelis orectus* – Loeblich and Tappan, p. 64 pl. 115 fig. 22

2008 *Dentalina guttifera* d'Orbigny; Sakınç, pl. 9 fig. 3

2014a *Dentalina guttifera* d'Orbigny; Meriç et al., pl. 44 fig. 3

2014a *Laevidentalina inflexa* (Reuss); Meriç et al. pl. 44 fig. 8

Test rectilinear with pyriform chambers and intervening slender, elongate necks. Sutures indistinct both in SEM illustrations and under light microscope. Form was never found intact, only broken one-two chamber pieces were studied. Test transparent, surface smooth, shiny.

Genus *Grigelis* is characterized by uniserially arranged chambers which are well separated from each other by long, narrow necks; a terminal, radial aperture and an elongate spine on the proloculus (Loeblich and Tappan, 1988, p. 396). Specimens belonging to *Grigelis orectus* was previously erroneously mainly attributed to *Dentalina guttifera* d'Orbigny and *Nodosaria pyrula* d'Orbigny; neither of these taxa hold such elongate necks between the chambers (Loeblich and Tappan, 1994, and references therein). The species is distinct with pyriform chambers, elongate necks between chambers, a very elongate spine on the proloculus, a radial, terminal aperture on the slender and elongate neck, a smooth surface. The necks between the chambers distinguish this genus from other rectilinear nodosarids, while the chamber shapes and smooth surface distinguish this species from other species of the genus.

The illustration for *Dentalina guttifera* by Sakınç (2008) is of only two chambers, broken from both sides, but the shapes of the chambers and the length of the neck are characteristic for *Grigelis orectus* instead. Similarly, individuals attributed to *Dentalina guttifera* and *Laevidentalina inflexa* (Reuss) by Meriç et al. (2014a) are of *Grigelis orectus*, the characteristic aperture in the former, the characteristic elongate spine on the proloculus in the latter being visible on the given illustrations.

Having found only broken specimens (two chambers at most), examination of the aperture or the proloculus was not possible. Other criteria are in perfect agreement, yet, the assignment of these individuals to *Grigelis orectus* is done somewhat tentatively.

Genus *Laevidentalina* Loeblich & Tappan, 1986

1986 *Laevidentalina* - Loeblich and Tappan, p. 242

Type: *Laevidentalina aphelis* Loeblich and Tappan (1986, p. 243 fig. 1-3)

Test elongate, arcuate; chambers uniserial with oblique to horizontal sutures; aperture radiate, surface smooth.

Laevidentalina spp.

Plate 35 Figure 25-26; Plate 36 Figures 34-35

Test elongate, cylindrical, somewhat arcuate. Chambers rectilinearly arranged with a little curving. Chambers increase in height more prominently than in diameter as added. Sutures horizontal or close to horizontal, almost flush in the earlier part of the test, more constricting between the adult chambers. Aperture radiate, produced on an offset neck. Proloculus with a short spine. Surface smooth, test translucent-transparent, wall thick.

A few broken individuals of above characteristics are lumped in *Laevidentalina* spp. The genus differs from *Dentalina* by its smooth surface, from *Enantiodentalina* by having no biserial phase, from *Astacolus* by not being obviously enrolled.

ORDER POLYMORPHINIDA Mikhalevich, 1980

SUBORDER POLYMORPHININA Mikhalevich, 1980

Superfamily Polymorphinoidea

Some rare specimens with unknown affinity (Plate 39 Figures 2-5; Plate 40 Figures 9-14) are left in superfamily level. They may belong to Family Glandulinidae and/or Polymorphinidae. They are hyaline, smooth, two-three chambered, globular to compressed forms, with almost flush sutures, rapidly growing chambers, radiate, terminal, slightly produced aperture. Presence of entosolenian tube (characteristic of Glandulinidae) is obscure, so is the nature of the chamber arrangement considering only two-three chambered forms were found.

Family Ellipsolagenidae Silvestri, 1923

Subfamily Ellipsolageninae Silvestri, 1923

Bilaterally symmetrical forms with round to slit-like aperture with entosolenian tube.

Genus *Fissurina* Reuss, 1850

1850 *Fissurina* – Reuss, p. 366

Type: Fissurina laevigata Reuss (1850, p. 366, pl. 46 fig. 1)

Circular to ovate to quadrangular tests, compressed, may be carinate; surface may be smooth or punctate; aperture terminal, oval or slit-like, with free or attached entosolenian tube.

Fissurina annectens (Burrows and Holland in Jones 1895)

Plate 37 Figures 1-4; Plate 38 Figures 1-4

1895 *Lagena annectens* Burrows and Holland; Jones TR, p. 203, pl. 7 fig. 11

non 1994 *Fissurina annectens* (Burrows and Holland); Jones RW, pl. 59 fig. 7, 15

Test small, tear-drop shaped with a circular chamber and a broadly rounded apertural protrusion in frontal view, compressed, both sides convex with ellipsoidal cross section. Edges non-carinate, broadly rounded. Narrow translucent bands of higher porosity lay parallel to the outer outline, disconnected near the neck, may be connected at the adapertural part forming a horse-shoe shape. These translucent bands are also very faintly depressed. Aperture a slit between broadly rounded lips, opening to a short, central entosolenian tube. Surface smooth, transparent other than the translucent narrow bands. Adapertural pole may be slightly indented or may be fitted with a very short spine.

Jones (RW, 1994) considered Brady's illustrations (1884, pl. 59 fig. 7, 15) of *Lagena quadricostulata* Reuss to be included in *Fissurina annectens*, however when Brady's explanation is considered it is obvious that these cannot be synonymous with this taxon. The lateral bands are described to be depressed with costae present on both sides of the depression (more like *Fissurina subrevertens*), and the aperture is described to be terminal circular (Brady, 1884, p. 486). The original description in Jones (TR, 1895) also includes one of Brady's illustrations (fig. 15); however, notes that the depressions ("sulci") in the fossil forms are probably due to taphonomic changes and that the recent forms only have "frosted bands". Due to the difference in apertural characteristics, Brady's specimens are not considered to belong to this taxon.

This taxon is distinguished from other slit-apertured *Fissurina* by its smaller size and the very distinct narrow translucent bands parallel the outer margin.

Fissurina castanea (Flint, 1899)

Plate 37 Figures 5-6; Plate 38 Figures 5-6

?	1884	*Lagena fimbriata* (Brady); Brady, p. 486, pl. 60 fig. 26; non fig. 27-28
	1884	*Lagena fimbriata* (Brady); Balkwill and Millett, p. 82 pl. 2 fig. 5
	1899	*Lagena castanea* – Flint, p. 307, pl. 54 fig. 3
	1993	*Fissurina castanea* (Flint); Sgarrella and Moncharmont Zei, p. 201, pl. 13 fig. 10
non	1984	*Fissurina castanea* (Flint); Jones, pl. 3 fig. 1
?	1994	*Fissurina* sp. nov. (7) – Jones, p. 70, pl. 60 fig. 26
	2008	*Fissurina castanea* (Flint); Sakınç, pl. 11 fig. 6

Test small, nearly circular in frontal view, with a slightly produced neck and a broadly rounded base; cross section elliptical; not carinate. Surface smooth other

than the ovate area wrapping around the base which is hispid, and bordered by a continuous flange. Aperture terminal, a narrow-elongate ovate opening bordered between equally produced lips, linked to an entosolenian tube. Test transparent other than the hispid ovate basal part which appears whitish.

In the original description of *Fissurina castanea* (Flint) the basal features (mentioned here as flanges) are described as "keels or wings […] extending about half the circumference of the test"; a hispid nature to the area between these features is not noted. In addition, any linear decorations of these "keels" are also not indicated. In the Sea of Marmara material studied here, these basal flanges were always found as broken; from the type figures of Flint it is obvious that most of those specimens also have broken "keels". Sakınç (2008) provides an illustration of a specimen with intact basal flanges with faint radial lineations, Sgarrella and Moncharmont Zei (1993) on the other hand provides an illustration of a specimen with smooth flanges.

Fissurina fimbriata (Brady, 1881) is a form described to include all morphologies, entosolenian and ectosolenian alike, "furnished with a deep vertical wing, encircling the oval base" (Brady, 1884). The mentioned deep vertical wing has radial lineations ("parallel tubuli", Brady, 1884) and is taken to be the main distinctive feature of the taxon. The three figures attached to this taxon in Brady (1884, pl. 60) are drastically different from each other, one more circular (fig. 28), one more elongated (fig. 26) and one with a continuous keel surrounding the test, wider around the long neck, more akin to *Lagenosolenia*. Jones (1994) regarded the former as *Fissurina* sp. nov. (7), and the latter two as *Fissurina fimbriata* (sensu stricto) despite the very obvious apertural characteristic differences. The more circular one, *Fissurina* sp. nov. (7) of Jones (1994), may belong to this taxon instead.

Referring to the original description of *F. fimbriata* (Brady, 1881) which do not include the type figures, Balkwill and Millett (1884) illustrated a specimen almost identical to ours. That specimen has no radial lineations on the mostly broken basal flange, and the area between the flange appears hispid. The lineations of the basal

flange and the hispidity of the area between the flange are here treated as non-descriptive characters.

The specimen illustrated by Jones (1984) for *Fissurina castanea* (Flint) do not possess a basal flange, therefore do not belong to this taxon.

This taxon is quite rare in the Sea of Marmara but has a wide geographic distribution, and one of the most frequently encountered Nodosarids. They are always found with broken flanges. The form is quite distinct with its near circular outline and the hispid basal area which stands out by being whitish in contrast to the transparent rest of the test.

Fissurina laevigata Reuss, 1850

Plate 37 Figures 7-8; Plate 38 Figures 7-8

1850 *Fissurina laevigata*– Reuss, p. 366, pl. 46 fig. 1

1884 *Lagena laevigata* Reuss; Brady, p. 473, pl. 114 fig. 8

1994 *Fissurina laevigata* Reuss; Jones, p. 113, pl. 114 fig. 8

2012 *Fissurina crebra* (Matthes); Milker and Schmiedl, p. 78, fig. 19.7

Test circular, with a broad and long apertural protrusion, compressed, margins subrounded to subangular, sides broadly convex. A broad and short protrusion on the adapertural pole is faintly present. Aperture a long and narrow slit in between apertural lips. Surface with slight hispidity around the neck. Test transparent other than the hispid portion on the neck which is opaquer.

Fissurina laevigata Reuss is illustrated with a shorter neck than the present species, otherwise there is total agreement. *Fissurina laevigata* subsp. *labiata* (Buchner) sensu Boltovskoy and Guissani de Kahn (1983) is also similar; especially so in the elongate nature of the lips and variable size of "spine" on the adapertural pole, but it is more elongate. The illustration of *Fissurina crebra* (Matthes) sensu Milker and Schmiedl (2012); although noted to be carinate, appears non-carinate just like the

present species. Moreover, is hispid around the neck area. The length of the lips and the hispidity of the surface may be intraspecific variations.

The taxon is distinguished from similar other *Fissurina* with elongated lips and slit aperture by its non-carinate periphery, broadly circular outline except the wide apertural protrusion, and smooth surface other than the hispidity at the neck.

Fissurina neptuni (Buchner, 1940)

Plate 37 Figures 9-10; Plate 38 Figures 9-11

1940 *Lagena neptuni*– Buchner, p. 484, pl. 15 fig. 294-296

2008 *Fissurina neptuni* (Buchner); Sakınç, pl. 11 fig. 8

2014a *Fissurina neptuni* (Buchner); Meriç et al., pl. 48 fig. 16

Test egg shaped in frontal view, composed of a circular chamber, a wide keel and a gradually tapering neck with rounded top. The keel widens into spines at the base of the form, one at the center (adapertural pole) and two symmetrically to the sides of the first. Spines elongated somewhat radially. Keel divides into two with a shallow groove between them right above the lateral spines, encircles test upwards with a constant width and becomes the apertural lip. Chamber inflated, sides convex. Outer margin of the chamber, just next to the keel, is a wide U-shaped translucent band with denser porosity. Aperture a slit in between elongated rounded lips, opening into a short entosolenian tube. Surface smooth, transparent except for the U-shaped translucent band.

The studied individuals agree perfectly with Buchner's original illustrations. The U-shaped band of higher porosity looks translucent under reflected light, also is of a lighter shade in the SEM illustrations, and is quite a distinct character. A similar character is described for *Fissurina lucida* (Williamson); however, that species is non-carinate and more elongated.

Fissurina spinosa (Sidebottom, 1912) is a similar species with three spines, however, the position of the lateral spines is more outwardly, spines are somewhat more

elongated, U-shaped translucent band and the bifurcation of the keel towards the aperture are not present; in addition, a slightly raised margin of the chamber is present just adjacent to the inner margin of the keel (Sidebottom, 1912, p. 402 pl. 17 fig. 16, 17; Loeblich and Tappan, 1994).

The taxon is distinguished from other slit-apertured *Fissurina* by its distinct carina, the three wide spines on the basal part and the U shaped wide translucent band on the chamber.

Fissurina robusta Zheng, 1979

Plate 37 Figures 11-12; Plate 38 Figures 12-13

1979 *Fissurina robusta* – Zheng, p. 153, pl. 13 fig. 11

? 1983 *Fissurina laevigata* Reuss f. *labiata* Buchner; Boltovskoy and Guissani de Kahn, p. 30, pl. 2 fig. 8, 9

1991 *Fissurina lucida* (Williamson); Cimerman and Langer, p. 55, pl. 59 fig 1

1994 *Fissurina lucida* (Williamson); Loeblich and Tappan, p. 90, pl 156 fig. 1-3

1994 *Fissurina robusta* Zheng; Loeblich and Tappan, p. 90, pl 158 fig. 5-8

2008 *Fissurina lucida* (Williamson); Sakınç, pl. 11 fig. 7

Test elongate, chamber oval and apertural protrusion rounded at the top, compressed with convex sides, non-carinate. Base rounded, with a very small indentation. Edges are broadly rounded, cross section ellipsoidal. Aperture a narrow slit between produced round lips, width of the apertural protrusion variable. Surface smooth, transparent, shiny.

Fissurina labiata is described to hold a narrow keel, a horse-shoe shaped whitish band parallel the outer margin, and a small basal spine (“mucro”; Williamson, 1848, p. 17, pl. 2, fig. 17). These features make this form distinctly different than the

present taxon. Those given under this name by Cimerman and Langer (1991), Loeblich and Tappan (1994), and Sakınç (2008) all have rounded margins, and no trace of the horse-shoe shaped band or the mucro; those accounts are very similar to this present taxon, although the specimens examined here were slightly more elongated.

These specimens fit best under the name *Fissurina robusta* Zheng (as cited in Loeblich and Tappan, 1994), other than being a little smaller. *Fissurina robusta* (Buchner, 1940) is also very similar but has a circular cross section, therefore may belong to *Pseudoolina* instead. The account of *Fissurina laevigata* Reuss f. *labiata* Buchner by Boltovskoy and Guissani de Kahn (1983), regarded as belonging to *Fissurina robusta* Zheng by Loeblich and Tappan (1994), is also very similar to the present species except for the adapertural elongation (spine) on that taxon.

The form is different from other *Fissurina* by its slender-elongate shape, non-carinate margins and completely smooth and transparent test.

Fissurina variocarinata (Buchner, 1940)

Plate 37 Figures 13-14; Plate 38 Figures 14-15

1940 *Lagena annectens* f. *variocarinata*– Buchner, p. 482, pl. 15, fig. 279-283

1983 *Fissurina annectens variocarinata* (Buchner); Boltovskoy and Guissani de Kahn, p. 301, pl. 2 fig. 1-2

Test egg to tear-drop shaped in frontal view, composed of a circular chamber, a wide surrounding keel and a gradually tapering neck with rounded top. At the adapertural pole the keel extends downward forming a small spine. Chamber inflated, sides convex. Transition from keel to chamber is drastic with a shallow depression forming as a narrow translucent band at the outer margins of the chamber except for the chamber – neck transition and the adapertural pole. Aperture a slit in between elongated, rounded lips. Surface smooth to very shallowly pitted, transparent.

The original description in Buchner (1940) illustrates a narrow keel for the taxon with a slight indentation around the outer margin of the chamber, adjacent to the keel. This latter feature is similar to that of *Fissurina annectens* under which *F. variocarinata* was described as a variety. This slight indentation is as a narrow translucent band under reflected light, and also provides a subtle hue change in SEM illustrations. Different from the type and from specimens of Boltovskoy and Guissani de Kahn (1983) our specimens are fitted with a wider keel and a very small spine at the adapertural pole.

This taxon is distinguished from other *Fissurina* with slit aperture by its broadly circular chamber, wide, rounded apertural protrusion and keel of constant width.

Fissurina sp. 1

Plate 37 Figures 15-17; Plate 38 Figures 16-18

Test small, circular, tricarinate, compressed, both sides broadly convex. All three keels are blunt. Main keel encircles the whole chamber and surrounds the lensoidal aperture as a rim. Minor keels are positioned near the outer margin, dissipate towards the neck, and join the main keel at the adapertural pole. Neck very short and wide, aperture terminal, opening into a short and central entosolenian tube. Surface smooth or may be faintly costate: costae few in number, restricted to the adapertural part, dissipating upwards. Test transparent, shiny.

Forms illustrated under the name *Fissurina sidebottomi* (Buchner) and *Fissurina* sp. A in Meriç et al. (2014a, pl. 49 fig. 1-2) are similar to this taxon in overall shape, however a third, smaller keel per side is present just next to the main keel and the surface is pitted in both. *Fissurina sidebottomi* sensu stricto is indeed a circular form but holds only one main keel, hence very different from what Meriç et al. (2014a) illustrated and this present taxon.

The aperture on this taxon is situated at the terminal end of a very short neck, and of a wide lens shape. Ovoid apertures are indeed included in genus *Fissurina* description; however, this shape is very different than the more common slit-like

aperture. *Fissurina alveata* (McCulloch, sensu Loeblich and Tappan, 1994) has a similarly shaped aperture, and also a similarly shaped test, however the minor keels on that taxon are very short and they do not merge at the adapertural pole with the main keel.

Fissurina faba (Balkwill & Millett, 1884) is a similarly circular form with a very short neck, however the surface of that taxon is indicated to be roughened, and the form is non-carinate.

Although the type illustration (*Oolina fasciata*, Egger, 1857, p. 270, pl. 5, figs. 12) is misleading, the account of *Lagena fasciata* (Egger) by Reuss (1863, p. 323, pl. 2 fig. 24) is probably the closest to this present taxon. However, later use of this taxon (Boltovskoy and Guissani de Kahn, 1983; Milker and Schmiedl, 2012) includes forms with lateral depressions (more akin to *Fissurina surebvertens* Parr) instead of the clearly described (by Reuss, 1863) lateral carina. Considering this confusion in the literature, this taxon is left in open nomenclature.

The taxon is distinguished from *Fissurina* sp. 2 by its non-pitted surface, smaller size and more circular shape. It is distinguished from the tricarinate *Palliolatella* sp. by is smaller size and more inflated shape, as well as the bluntness of the main keel.

Fissurina sp. 2

Plate 37 Figures 18-19; Plate 38 Figures 19-20

Test pear shaped with truncate apertural margin, tricarinate, compressed, both sides broadly convex. All three keels are blunt. Main keel wider, encircles the whole chamber and surrounds the lensoidal aperture as a rim. Minor keels are narrower and shallower, positioned parallel the outer margin, terminate just below the aperture, and join the main keel at the adapertural pole with a vertical irregular protrusion. Neck tapers towards the terminal aperture gradually, aperture opening into a short and central entosolenian tube. Surface smooth between the keels, irregularly and coarsely pitted otherwise. Test transparent, dull due to pitted nature.

Fissurina contusa Parr (1945) is a similarly pitted form, however it is more of a circular-ellipsoidal shaped than pyriform. Another form with rough surface is *Fissurina lacunata* (Burrows and Holland, in Jones, 1895) however surface pattern is coarser than present taxon. *Fissurina sidebottomi* (Buchner) and *Fissurina* sp. A in Meriç et al. (2014a, pl. 49 fig. 1-2) are very similar in terms of surface pattern to this taxon, however those are circular forms with very short neck. *Fissurina macropunctata* Jones (1984) most resembles this present taxon, however the area between the keels are also pitted in that taxon. That feature may as well be an intraspecific variation; however, the assignment cannot be done with confidence therefore it is left in open nomenclature.

Similar to *Fissurina* sp. 1, the aperture of this taxon is wide lens shape; however, the transition from chamber to neck is more gradual and the neck is longer. In addition, the surface is pitted in this taxon.

Fissurina sp. 3

Plate 37 Figure 20; Plate 38 Figure 21

The test is small, broadly ovate in frontal view, compressed with low convex sides, bicarinate with a narrow groove in between the ragged keels. Aperture a terminal slit on a very short neck, opening into an entosolenian tube which is central for half of the length of the test and bends away from the center downward. Surface hispid at the lower half of the test, appear whitish and dull under reflected light, otherwise transparent and shiny.

Both the ragged double keel and the surface hispidity are curious features, not common to *Fissurina*, and distinguish this form from other *Fissurina*.

Fissurina sp. 4

Plate 37 Figure 21; Plate 38 Figure 22

Test elongate, ovoid, compressed, both sides convex. Curved depressions present laterally, parallel the outer margin, starting a little above the base, terminating before

reaching the neck. Aperture a slit between slightly produced, broadly rounded lips. Surface smooth, test transparent, shiny.

This taxon is similar to *Fissurina fasciata* sensu Boltovskoy and Guissani de Kahn (1983) and Milker and Schmiedl (2012), but it is more elongated and lacks the median groove. Descriptions and illustrations of both references are not in agreement with the type of that taxon (Egger, 1857, p. 270, pl. 5, figs. 12) or Reuss's interpretation (1863, p. 323, pl. 2 fig. 24) that shows lateral carina, not depressions. The lateral depressions and median groove are features in line with *Fissurina subrevertens* Parr (1950).

This taxon is very similar to *Fissurina quadrata* (Williamson, 1858) in terms of the short neck, lateral depressions, rounded edges and elongate test, but that taxon is distinctly quadrate while *Fissurina* sp. 4 is more ovate. *Fissurina quadricostulata* (Reuss, 1870) is also a similar taxon but described to have "ribs" running parallel the margin, instead of the depression on this form.

This taxon is easily distinguished from *Fissurina annectens* by its ovate shape, and from *Fissurina lucida* by the lateral depressions.

Genus *Lagenosolenia* McCulloch, 1977

1977 *Lagenosolenia* – McCulloch

Type: *Lagenosolenia falcata* (Chaster, 1892)

Ovate-elongate tests, compressed, may have one or more keels, aperture terminal occasionally with phialine lip.

Lagenosolenia strigimarginata Loeblich and Tappan, 1994

Plate 37 Figure 22; Plate 38 Figure 23

1994 *Lagenasolenia strigimarginata* – Loeblich and Tappan, p. 93, pl. 161 fig. 9-10

Test tear-drop shaped with a truncated top and broadly rounded base, quadrocarinate, compressed so that sides are mostly planar. One inner and one outer keel decorate the periphery of the form on each side; on edge view the keel are symmetrical with a deep groove in between the inner (more central) ones. Outer keels surround the chamber in an egg shape; neck is surrounded on two sides by the larger (inner) keels which results in the tear-drop outline. Surface smooth, finely perforated, test whitish and opaquer around the keels and more transparent at the center. Aperture terminal on top of the long, slender neck, opening into a short, central entosolenian tube.

The form is nearly identical to the type description of *Lagenosolenia strigimarginata*, but is slightly smaller. It is distinguished from other decorated unilocular nodosarids in the Sea of Marmara by its distinct tear-drop shape and arrangement of keels.

Genus *Palliolatella* Patterson & Richardson, 1987

1987 *Palliolatella* – Patterson and Richardson, p. 219

Type: *Palliolatella avita* Patterson & Richardson, 1987 (p. 219, pl. 2 fig. 4-7; pl. 5 fig. 3, 4)

Elongate, ovate tests, compressed, usually with more than one keel with main keel forming a hood around the neck.

Palliolatella sp.

Plate 37 Figure 23; Plate 38 Figure 24

? 2008 *Palliolatella orbignyana* (Seguenza); Sakınç, pl. 11 fig. 9

? 2014a *Fissurina orbignyana* (Seguenza); Meriç et al., pl. 48 fig. 17-18

? 2014a *Parafissurina lateralis* (Cushman); Meriç et al., pl. 49 fig. 3-4

Test circular with a slightly produced apertural part, tricarinate, compressed, both sides slightly convex. Outline with a thin and wide, central keel surrounding the chamber and recurving downward at the vicinity of the neck, providing rimmed

margins to the lensoidal aperture. One more narrower keel present on each side of the test as almost a complete circle near the outer edge of the chamber, disconnected only at the short neck, connecting to the lip formed by the central keel. Surface smooth, finely perforate, transparent and shiny.

The tricarinate nature, the merging of the inner keel to the outer keel at the neck, and the recurved lips formed by the central keel, as well as the gross circular outline are identical with this form in the illustrations of *Palliolatella orbignyana* (Seguenza) by Sakınç (2008) and *Fissurina orbignyana* (Seguenza) and *Parafissurina lateralis* (Cushman) by Meriç et al. (2014a); however, the inner keels are much wider in all three than this taxon. Seguenza's taxon was illustrated by Milker and Schmiedl (2012, referred to as *Fissurina orbignyana*) with a more coarsely perforated surface and no recurved portion of the main keel around the neck, otherwise is very similar to previously mentioned references. Cimerman and Langer (1991), on the other hand, provide an interpretation for Seguenza's taxon (as *Palliolatella orbignyana*) which includes a pitted surface (coarsely porous) and much less developed inner keels. These two accounts agree with this taxon even less.

The form illustrated here is a little asymmetrical which may be due to any test deformations or anomalies; however, may also be genuine. In which case the aperture is not terminal, but is subterminal and the form should then be referred to *Pseudofissurina* instead. The absence of more material inhibits certainty of identification.

Subfamily Oolininae Loeblich & Tappan, 1961

Radially symmetrical forms with radiate to round aperture with entosolenian tube.

Genus *Anturina* Jones, 1984

1984 *Anturina*– Jones, p. 99

Type: *Anturina haynesi* Jones (1984, p. 100; holotype: Oolina laevigata d'Orbigny in Haynes, 1973, p. 108, pl. 14 fig. 11)

Test globular, inflated, aperture radiate, with an entosolenian tube.

Anturina haynesi Jones, 1984

Plate 39 Figure 1; Plate 40 Figure 1

1973 *Oolina laevigata* d'Orbigny; Haynes, p. 108, pl. 14 fig. 11

1984 *Anturina haynesi* – Jones, p. 100

Test egg-shaped with a broadly rounded base, a rounded cross section and a tapering top. Aperture radiate, terminal. Surface smooth, translucent, dull.

Jones described the species designating the holotype as the illustration of Haynes (1973) of *Oolina laevigata* d'Orbigny. In Haynes's description a "trace of entosolenian tube" is mentioned. According to Knight (1986), such an entosolenian tube is not present, but a disc at the interior end of the neck (endodisc) is. According to this criterion, Revets (2005) proposed to transfer this genus to Family Lagenidae, and questioned its synonymy with the genus *Reussoolina*. Following the original reference, here the taxon is retained in Oolininae.

Taxon is very similar to *Polymorphina* and *Globulina* and is distinguished from them due to its unilocular nature. Taxon is distinguished from other globose Ellipsolagenidae by being smooth and not possessing a neck.

Genus *Favulina* Patterson and Richardson, 1988

1988 *Favulina* – Patterson and Richardson, p. 249

Type: *Favulina hexagona* (Williamson, 1848, p. 20, pl. 2 fig. 23)

Test tear-drop shaped with circular cross section, and a short neck. Aperture terminal with a short entosolenian tube. Surface with polygonal reticulations.

Favulina hexagona (Williamson, 1848)

Plate 35 Figures 10-12; Plate 36 Figures 16-18

1848 *Entosolenia squamosa*, var. γ, *hexagona* – Williamson, p. 20, pl. 2 fig. 23

1999 *Oolina hexagona* (Williamson); Hayward et al., p. 122, pl. 8 fig. 2

2008 *Favulina hexagona* (Williamson); Sakınç, pl. 11 fig. 2-3

2012 *Favulina hexagona* (Williamson); Milker and Schmiedl, p. 77, fig. 19.4

2016 *Favulina hexagona* (Williamson); Margerel, p. 564, fig. 2A-I

Test pyriform (pear-shaped): base broadly rounded and apertural pole tapers to a small neck on top of which a circular aperture is present. Surface of the test is decorated with ridges that form large pentagonal to hexagonal depressions: at the equatorial part more regularly hexagonal, towards the base and the neck the shape distorts into pentagons. Wall thick; ridges smooth; surface smooth other than the ridges, shiny, translucent. Neck very short.

The form is very distinct with its fat shape and coarse decorations. Other similarly decorated forms include *Favulina foveolata* (Seguenza) which is shorter (more globose) with a wide and short rim around the aperture and *Favulina squamosa* (Montagu) whose decorations are finer, less pronouncedly hexagonal, and more regularly arranged in vertical rows.

A very short entosolenian tube with a rim on the internal end of the tube is mentioned for the genus (Margerel, 2016), however due to the thickness of the wall this feature was not observed in the specimens investigated.

The form is distinguished from other globular nodosarids by its distinct fat, pear shape and hexagonal decorations.

Subfamily Parafissurininae Jones, 1984

Bilaterally symmetrical forms with asymmetrical aperture with entosolenian tube.

Genus *Parafissurina* Parr, 1947

1947 *Parafissurina* – Parr, p. 123

Type: *Parafissurina ventricosa* (Silvestri, 1904)

Tests ovoid to circular in frontal outline, compressed, ovoid to lenticular in edge view. Edges may be broadly rounded or carinate. May have basal spines. Surface smooth. Aperture subterminal, slit-like between asymmetrically produced lips: one lip extending longer to form a hood over the aperture. Entosolenian tube attached to the side with the hood.

Parafissurina basispinata McCulloch, 1977

Plate 37 Figures 27-30; Plate 38 Figures 28-31

1977 *Parafissurina basispinata* – McCulloch, p. 139, pl. 72 fig. 1-3

1994 *Parafissurina basispinata* McCulloch; Loeblich and Tappan, p. 94, pl. 162 fig. 1-5

non 1995 *Fissurina basispinata* – Yassini and Jones, p. 122, fig. 462, 465

2006 *Parafissurina staphyllearia* (Schwager); Avşar et al., pl. 1 fig. 18

2008 *Parafissurina staphyllearia* (Schwager); Sakınç, pl. 11 fig. 10

2021 *Fissurina staphyllearia* Schwager; Kırcı-Elmas et al., fig. 7b

Test circular with a broad apertural protrusion in frontal view, carinate, and compressed with a lensoidal cross section. The keel is mostly of constant width. At the basal part it extends into basal spines, four or five in number, not necessarily symmetrical. At the apertural part the keel surrounds the crescentic subterminal aperture by forming the two asymmetrical lips one of which hovers over the other

forming a hood over the aperture. Surface finely and regularly porous, smooth, transparent, shiny.

A form with numerous basal spines is *Fissurina staphyllearia* Schwager; the outline of the form as well as the placement of the spines (see Brady, 1884, p. 474, Pl. 59, fig. 8-11) are very similar to this taxon; however, that taxon do not possess a hooded aperture (and belongs to *Fissurina*) or a keel. Individuals attributed to that taxon by Avşar et al. (2006), Sakınç (2008) and Kırcı-Elmas et al. (2021) all illustrate distinctly carinate specimens, and should belong to *Parafissurina basispinata* instead.

Parafissurina basispinata McCulloch is a carinate, circular *Parafissurina* with a few spines at the basal part which may or may not be symmetrical (Loeblich and Tappan, 1994). This account is in perfect agreement with the studied material. The width of the keel is a varying feature.

Fissurina basispinata Yassini and Jones (1995) is a completely different form with a fissurine aperture, longitudinal costae, and only one central adapertural spine.

The form is distinguished from other Parafissurina by its basal spines. Even if the spines are broken, this taxon is easily distinguished by the interrupted and segmented look of the keel at the basal part in contrast to the complete uninterrupted keel of *Parafissurina curvitubulosa*.

Parafissurina lata (Wiesner, 1931)

Plate 37 Figures 25-26; Plate 38 Figures 25-27

? 1884 *Lagena marginata* W. and J.; Balkwill and Millett, p. 81, pl. 3 fig. 2

1931 *Ellipsolagena lata* – Wiesner, p. 126, pl. 24 fig. K, L

1983 *Parafissurina lata* (Wiesner); Boltovskoy and Guissani de Kahn, p. 303 pl. 1 fig. 23-25

? 1994 *Parafissurina curvitubulosa* (McCulloch); Loeblich and Tappan, p. 94, pl. 162 fig. 6-12

2012 *Parafissurina lateralis* (Cushman) var. *carinata* (Buchner); Milker and Schmiedl, p. 79, fig. 19.14

Test nearly circular, compressed, carinate; cross section lensoidal; on edge view slightly asymmetrically biconvex. Keel surrounds the whole test periphery with nearly constant width, usually wide, occasionally narrower. Test transparent, surface smooth, shiny. Keel non-porous, center of the test non-porous, the porosity of the test increases towards the margins of the test forming a wide U-shaped band. Aperture a crescentic slit on one side of the test, developed between margins which are asymmetrically produced slightly above the circular outline of the test; opening to an entosolenian tube attached to the side opposite the aperture for almost the whole length of the test.

The illustrated specimen attributed to *Lagena marginata* W. and J. by Balkwill and Millett (1884) is equipped with a *Parafissurina*-type aperture, and a wholly attached entosolenian tube as apparent on the illustration. As no reference other than author initials are provided in Balkwill and Millett (1884), the true meaning of the attributed taxon cannot be evaluated. Nonetheless, the name was later attributed to Walker and Boys (1784) by Cushman (1923) who provided no references while discussing the difference of "many references to this species in the literature" and the type illustrations of Walker and Boys. Walker and Boys's (1784) taxon is of a tear-drop shaped, keeled *Fissurina*, while the form Cushman (1923) refers to under this name is nearly perfectly circular with a significantly wider keel. *Fissurina marginata* is now attributed to Montagu (1803; Hayward et al., 1999) who actually used the name with reference to Walker and Boys (1784). Regardless of the referred type material, this current conception of the taxon (see Hayward et al., 1999, p. 119, pl. 7 fig. 22-23) is more similar to Cushman's *Lagena marginata* variety, a circular fissurine form with a keel surrounding the whole chamber, unrelated to the present taxon. The

characters of the taxon as illustrated by Balkwill and Millett (1884) are very much in line with this present taxon instead of instead of any *marginata* referenced above.

The specimens attributed to *Parafissurina curvitubulosa* (McCulloch) by Loeblich and Tappan (1994) are similarly keeled forms with parafissurine-tpe aperture. These have nothing to do with the original description of *Fissurina curvitubulosa* (McCulloch, 1977, p. 100, pl. 65 fig. 4-5) which is clearly a *Fissurina* with a terminal aperture. *F. curvitubulosa* is distinct in that its entosolenian tube diverts from the median drastically at about the center of the test and directs toward a margin. The use of this name by Loeblich and Tappan (1994) implies that their taxon, too, has a diverting entosolenian tube, a feature which cannot be seen in SEM images. This present taxon does not have such a diverting entosolenian tube.

The circular outline and the near constant width of surrounding keel in *Parafissurina lateralis* (Cushman) var. *carinata* (Buchner) as used in Milker and Schmiedl (2012), are identical to this taxon and should belong here instead.

The taxon is distinguished from other *Parafissurina* by its smooth keel of constant width and near circular outline. Width of the keel variable, may be quite narrow.

ORDER VAGINULINIDA Mikhalevich, 1993

Family Vaginulinidae Reuss, 1860

Partially or totally enrolled forms, laterally compressed, with radiate or cribrate terminal aperture.

Subfamily Lenticulininae Chapman, Parr & Collins, 1934

Genus *Lenticulina* Lamarck, 1804

1804 *Lenticulina* – Lamarck, p. 186

Type: *Lenticulina rotulata* (Lamarck, 1804, p. 188, pl. 62 fig. 11 – plates published in 1806: Annales du Muséum d'histoire naturelle V. 8)

Planispiral, involute forms with equatorial aperture situated at the outermost margin, producing a protrusion here. Outline circular, periphery usually carinated, surface usually smooth.

Lenticulina cultrata (de Monfort, 1808)

Plate 39 Figures 7-9; Plate 40 Figures 9-14

1808 *Robulus cultratus* – de Montfort, p. 215, figure on p. 214

1991 *Lenticulina cultrata* (Monfort) – Cimerman and Langer, p. 51, pl. 53 fig. 5-6

2008 *Lenticulina cultrata* (Monfort) – Sakınç, pl. 9 fig. 11-12

Test planispiral, involute; or in some individuals semi-involute, lenticular, biumbonate, strongly carinate; outline non-lobulate. 5-8 triangular chambers in the last whorl, growing gradually in size. Sutures limbate, flush with the surface, slightly curved, tangential to the central umbo. Central umbo of clear wall material, allows the large proloculus, or, in semi-involute individuals, the inner part of the previous whorl to be seen. Keel wide, strong, from transparent test material. Apertural face concave with angular margins. Aperture at the dorsal angle, a few radial slits, and a central slit at the outside margin of the apertural face. Surface smooth, shiny.

The exact shape of the aperture is somewhat different than that illustrated by Cimerman and Langer (1991) which possesses a series of thin radiate slits at the outside margin in addition to the central slit aperture with distinctly developed lips. Those illustrated by Sakınç (2008) from the Sea of Marmara are very similar to the present taxon. *Lenticulina iota* (Cushman, 1923) is a similar taxon with a very wide keel, but the keel in that taxon gets wider towards the earlier chambers. *Lenticulina limbosa* (Reuss, 1863, as *Robulina limbosa*) was described with a wide keel, much like the present taxon, however the number of chambers in the last whorl in that taxon is larger (9-10). Cushman's account for *L. limbosa* (Cushman, 1933b, p. 3, pl. 1 fig. 4-6, pl. 2 fig. 5, as *Robulus limbosus*), is composed of illustrations very similar

to the series of figures given for this present taxon in almost every respect except the keel, and the taxon is noted to be strongly keeled; however, the depictions show a significantly narrower keel than the original description of Reuss and this present taxon.

Taxon is distinguished by its wider keel and more circular outline from other lenticulinids.

Lenticulina gibba (d'Orbigny, 1839b)

Plate 39 Figure 6; Plate 40 Figures 6-8

1839b *Cristellaria gibba* – d'Orbigny, p. 40 pl. 7 fig. 20-21

1991 *Lenticulina gibba* (d'Orbigny); Cimerman and Langer, p. 51, pl. 53 fig. 7-11

? 2008 *Lenticulina gibba* (d'Orbigny); Sakınç, pl. 9 fig. 13

Test small, only of about one whorl, planispiral, involute, lenticular, biconvex, carinate; outline non-lobulate. About 5 triangular chambers in the last whorl, growing rapidly in height, so that the apertural face is as tall as the previous whorl. Sutures limbate, slightly curved backwards, flush with the surface. Keel narrow, indistinct, transparent, locations of the previous apertures clearly observable at the inner margin. Apertural face tall, flat, with subrounded margins. Aperture a central slit at the outside margin of the apertural face with raised lateral lips, and two other slits at the outer margin, starting from the dorsal angle situated to the sides of the keel. Surface smooth, shiny.

D'Orbigny (1839b) described *Cristellaria gibba* as an oblong, subcarinate form (p. 40 pl. 7 fig. 20-21). The drawings given depict a rapidly flaring form. Cimerman and Langer's (1991) account for the taxon includes a series of images highly similar to ours in terms of apertural characteristics and general chamber growth rate. D'Orbigny indicated his taxon to have about 10 chambers, Cimerman and Langer's account give no information on this and it is impossible to deduce from the SEM

images due to the flush nature of the sutures. Due to mentioned similarities, the present taxon is considered to juvenile representatives of *L. gibba*.

The taxon is distinguished from others by its indistinct keel and flat apertural face.

Lenticulina cf. *nitida* (Brady, 1884)

Plate 39 Figure 10; Plate 40 Figure 17

1884 *Cristellaria nitida* (d'Orbigny); Brady, p. 549, pl. 70 fig. 2

Test planispiral, involute, lenticular, biconvex, carinate; outline slightly lobulate for the last two chambers. About 6 triangular chambers in the last whorl, growing rapidly in height, so that the apertural face is as tall as the previous whorl. Sutures limbate, slightly curved backwards, almost merging at the indistinct central umbo; flush with the surface for the most part, last suture slightly depressed. Keel wide, transparent, locations of the previous apertures clearly observable at the inner margin. Apertural face tall, concave, with sharply angular margins. Aperture radiate at the dorsal angle, produced, and an additional central slit at the outside margin of the apertural face with prominent lateral lips. Surface smooth, shiny.

D'Orbigny (1826) described a *Cristellaria nitida* (p. 291, no. 5), based on Soldani's "*Nautili Lituitati"* (1798, pl. 56 fig. O, P). The original illustration of Soldani's is the type figure. That illustration shows a spirally coiled, flaring form whose chambers get increasingly longer radially, coiled evolutely, and the sutures are clearly depicted as raised. Brady's (1884) interpretation of the taxon is drastically different than Soldani's depiction, with its less lobulate outline, higher (tangentially) chambers, not raised sutures (except for the oldest suture of the last whorl), involute coiling and a prominent keel. Brady's taxon, hence, must be a different taxon than that of Soldanii's and d'Orbigny's taxon, which is most probably not a lenticulinid.

This present taxon is nearly identical to Brady's, other than the single raised suture in the last whorl which is not present in this form. Therefore, this taxon is only marked as *L.* cf. *nitida*.

Taxon is different than other lenticulinids by its slightly lobutale outline, marked keel of uniform width, rapidly growing chambers, and concave apertural face.

Lenticulina sp. 1

Plate 39 Figure 11; Plate 40 Figures 18-19

Test small, only of about 3-4 chambers, planispiral, lenticular, biconvex; outline non-lobulate. Chambers triangular. Sutures slightly curved, flush with the surface. Periphery narrowly subangular but not carinate. Apertural face tall, with rounded margins. Aperture slightly produced at the dorsal angle, probably radiate. Surface smooth, shiny.

Being of very few chambers, these forms are clearly juvenile specimens belonging to genus *Lenticulina*; however, their identity cannot be determined. This is the most abundantly found lenticulinid in the Sea of Marmara.

Genus *Neolenticulina* McCulloch, 1977

Neolenticulina variabilis (Reuss, 1850)

Plate 39 Figures 12-13; Plate 40 Figures 15-16

	1850	*Cristellaria variabilis* – Reuss, p. 369, pl. 46, figs. 15, 16
	1866	*Cristellaria peregrina* – Schwager, p. 245, pl. 7, fig. 8
part	1884	*Cristellaria variabilis* Reuss – Brady, p. 541, pl. 68 fig. 11 (? fig. 12-16)
part	1951	*Neolenticulina peregrina* (Schwager); Phleger and Parker, p. 9, pl. 4 fig. 20
part	1977	*Neolenticulina chathamensis* – McCulloch, p. 8, pl. 94 fig. 11 (? fig. 12)
	1993	*Neolenticulina peregrina* (Schwager); Sgarrella and Moncharmont Zei, p.195, pl. 12 fig. 4

part 1994 *Neolenticulina variabilis* – Jones, p. 80, pl. 68 fig. 11 (? fig. 12-16)

2008 *Neolenticulina peregrina* (Schwager); Sakınç, pl. 9 fig. 15-16

2012 *Neolenticulina peregrina* (Schwager); Milker and Schmiedl, p. 73, fig. 18.21

2014a *Neolenticulina peregrina* (Schwager); Meriç et al., pl. 45 fig. 9

In juveniles, test triangular in outline with curved sides, planispiral, involute; compressed with lenticular cross section. three chambers in the last whorl, triangular, much embracing, with angular dorsal periphery. Angular margin continues the whole test. Sutures shallowly depressed to flush. Aperture radiate on the dorsal angle as a glassy cone, barely protrudes; locations of the previous two apertures make up the other two vertices of the test, visible as glassy triangular parts under reflected light; a slight notch on the surface present at the corner, left by the covering of the penultimate aperture by the ultimate chamber. Surface smooth, test transparent, shiny.

In adults, later chambers are also enrolled planispirally but tend to uncoil slightly. Last chamber triangular or broadly ovate in outline; aperture terminal, almost cribrate; apertural face do not exist, instead the whole margin of the final chamber sharply angular or even carinate.

This present taxon most resembles the juvenile condition of *Neolenticulina chathamensis* McCulloch (1977, p. 8, pl. 94 fig. 11) who regarded their taxon separate from *Neolenticulina peregrina* (as *Cristellaria peregrina*, Schwager, 1866, p. 245 pl. 7 fig. 89), and the latter to be confined as a fossil taxon. The difference between them according to McCulloch is that the latter is quadrate with constant thickness while McCulloch's taxon is biconcave. The biconcavity in McCulloch's taxon (1977, p. 8, pl. 94 fig. 12) comes from the depression of the sutures in the adult chambers; similarly, depression of the last suture is higher in Schwager's taxon forming a break in the convexity in edge view, making these two accounts highly similar. Considering the original descriptions and illustrations of the two taxa, the

main striking differences are i. the shape of the ultimate chamber which is more rounded than triangular in Schwager's taxon and ii. the width and extend of the keel which is of more uniform width and surrounds the whole test in Schwager's taxon while more confined to the latter chambers and somewhat narrower in McCulloch's.

Brady (1884, p. 541, pl. 68 fig. 11-16) regarded *N. peregrina* and *Neolenticulina variabilis* (as *Cristellaria variabilis*, Reuss, 1850, p. 369, pl. 46, figs. 15, 16) as synonyms, and, plus, different stages of life. One of Reuss's *Neolenticulina variabilis* illustrations (1850, fig. 16) is quite different with higher number of chambers and a slower rate of chamber growth; the other illustration, on the other hand, is indeed similar to Schwager's taxon, but is shown to have a narrow apertural face instead of the carinate margin Schwager's taxon has. These two features may be attributable to incorrect depiction, then, the synonymy would necessitate Reuss's name to take precedence.

Brady's (1884) series of illustrations for different life stages indicate the width and extend of the keel changes throughout growth, and may also be variable between individuals. Similarly, the shape of the ultimate chamber is taken as intraspecific variation. These variations are evident in the illustrations given for *Neolenticulina peregrina* (Schwager) by more recent references (e.g., Sgarrella and Moncharmont Zei, 1993, with a broadly rounded ultimate chamber and a keel encircling the whole test; Milker and Schmiedl, 2012 with a keel mostly confined to the triangular ultimate chamber; Meriç et al., 2014a, with a highly elongated and narrow-tall final chamber). On the other hand, the aperture on the curvilinear chambers of the above mentioned three taxa are strikingly similar: closely appressed cribrate on somewhat produced necks appearing radiate. The cribrate aperture on the genus *Cribrolenticulina* is reported to be confined to the last chamber, previous chambers having a simple aperture (Haman, 1978, p. 90). A similar phenomenon may be present in *Neolenticulina* as well. The illustrated juvenile stages do not possess the characteristic cribrate aperture (e.g., McCulloch, 1977, pl. 94 fig. 11; Brady, 1884, p. 541, pl. 68 fig. 11); it appears the aperture gains its characteristic nature after the planispiral-involute juvenile phase, of three or so chambers, is completed.

Here, these three taxa are regarded as synonyms to which the present taxon belong. The taxon is mostly represented by juvenile triangular specimens of two different sizes: i. small with about 125 μm in diameter, ii. larger with about 300 μm in diameter; interpreted as different sexual generations.

Taxon is easily distinguished from other lenticulinids by its near-triangular outline in the juvenile; and involute coiling of few chambers the last whorl with the last chamber being distinctly larger and tending to uncoil in the adult.

Genus *Saracenaria* Defrance, 1824

1824 *Saracenaria* – Defrance, p. 176

Type: *Saracenaria italica* Defrance (1824, p. 177)

Planispirally enrolled to rectilinear, uniserial forms with triangular cross section which may be carinate at all three edges, flaring chambers, flat apertural face, and radiate aperture which may develop on a neck.

Saracenaria sp.

Plate 35 Figure 27; Plate 36 Figure 42

Form broken, only apertural end with 2.5 chambers remaining. Test large, with triangular cross section with rounded corners. Chambers rectilinear. Aperture radiate, with one longer arm more prominent on the outside corner of the triangular apertural face. Surface smooth, shiny, wall thick.

No intact specimens were found in the Sea of Marmara material, however the triangular shape of the test, as well as the large dimensions and the apertural characteristics are very much in line with the genus *Saracenaria*. *Saracenaria italica* (Defrance, 1824) is the most resembling taxon and was recorded from the Sea of Marmara by Sakınç (2008, pl. 45 fig. 10); however, having studied only very few broken specimens it is left in open nomenclature.

Subfamily Marginulininae Wedekind, 1937

Forms which may have slightly enrolled initial part, later becoming rectilinear, with rounded or flattened cross section.

Genus *Amphicoryna* Schlumberger in Milne-Edwards, 1881

1881 *Amphicoryna* – Schlumberger in Milne-Edwards, p. 881

Type: *Amphicoryna scalaris* (Batsch, 1791, p. 2, pl. 2 fig. 4a-b)

Rectilinear, uniserial, apiculate forms which may have initial astacoline coiling (microspheric generations). Chambers globular; aperture radiate on an elongate neck; surface may be vertically costate or pustulose.

Amphicoryna scalaris (Batsch, 1791)

Plate 35 Figures 13-16; Plate 36 Figures 19-24

1791 *Nautilus* (*Ortoceras*) *scalaris* – Batsch, p. 2, pl. 2 fig. 4a-b

part 1884 *Nodosaria scalaris*, Batsch; Brady, p. 510, pl. 63 fig. 29-31 (not fig. 28)

1988 *Amphicoryna scalaris* (Batsch); Loeblich and Tappan, p. 116, pl. 450 fig. 11-14

part 1991 *Amphicoryna scalaris* (Batsch); Cimerman and Langer, p. 52, pl. 54 fig. 1-5, 9 (not fig. 6-8)

1993 *Amphicoryna scalaris* (Batsch); Sgarrella and Moncharmont Zei, p. 191, pl. 11 fig.2-3

part 2008 *Amphicoryna scalaris* (Batsch); Sakınç, pl. 10 fig. 1, 2, 4 (not fig. 3)

2012 *Amphicoryna scalaris* (Batsch); Milker and Schmiedl, p. 73, fig. 18.22-25

part 2014a *Amphicoryna scalaris* (Batsch); Meriç et al., pl. 45 fig. 11-13, 17, 18 (not fig. 14-16)

Test large, uniserial, distinctly costate; adapertural part with a stout spine, apertural part with a neck. In microspheric generation initial chambers triangular, added with slight coiling (astacoline), forming a distinct keel at the dorsal side, later chambers globular-spherical, added rectilinearly; in megalospheric generation triangular astacoline phase missing. In triangular phase sutures indistinct, oblique, linear on two flat sides adjacent to the keel, and on the other side chambers a little inflated and sutures depressed, horizontal. Sutures distinct, depressed, horizontal in globular phase. Globular chambers overlapping so that each chamber includes the neck part of the previous one, chamber growth rate variable. In megalospheric forms the second chamber is often much shorter than the proloculus, but is of almost the same diameter with it. Later chambers increase in diameter slowly but regularly, in height more rapidly. In triangular phase, the costae on the two flat sides are elongate, oblique, parallel to sutures; on the side with inflated chambers costae are vertical. In globular phase, the costae are distinct, high, mostly vertical, rarely coiling; either spanning the whole chamber starting at the base of the chamber, or more rarely, continuous through the sutures; some costae may be fragmented into rows of elongate blades. Neck elongate, decorated with complete or fragmented annulate rings; aperture terminal, at the end of the neck, radiate. Surface smooth other than the costae; wall thick, appearing whitish under reflected light.

This taxon appears to be used as a lump taxon of many highly similar morphologies. For example, Brady (1884) included forms with smooth (pl. 63, fig. 28) and annulate (fig. 29-31) necks alike in their account of the taxon; that specimen with the smooth neck was later resorted into *Amphicoryna leurodeira* Loeblich and Tappan (1994). Loeblich and Tappan (1994) noted *A. scalaris* to have a smooth neck while discussing the distinguishing features of *Amphicoryna separans* (Brady). Contrarily, Cushman (1913) illustrated a specimen with annulate neck and regularly increasing chamber dimensions. In addition, Cushman (1923) remarked that they did not find the taxon sensu stricto in the Atlantic, and that the further studies of the vast reference list for the taxon should reveal more than one species.

Recent references for the taxon also include different morphotypes: for example, specimens that clearly belong to *A. separans* (Cimerman and Langer, 1991, pl. 54 fig. 6, 7; Sakınç, 2008, pl. 10 fig. 3; Meriç et al., 2014a, pl. 45 fig. 16). Two most prominent features of *A. separans* is the long neck that separates the ultimate chamber from the earlier (3-4 chambers long) part of the test, and shallower, less constricted sutures in the earlier part of the test. Previously cited material all show those characteristics.

Taxon is distinguished by its large size, strongly costate surface, an astacoline coil in microspheric specimens, a variable growth rate throughout the test and a neck with annular rings.

Amphicoryna sp. 1

Plate 35 Figure 17; Plate 36 Figures 25-27

part 1991 *Amphicoryna scalaris* (Batsch); Cimerman and Langer, p. 52, pl. 54 fig. 8 (not fig. 1-7, 9)

2002 *Amphicoryna proxima* (Silvestri); Kaminski et al., pl. 2 fig 5 [sic, should be 4]

? 2014a *Amphicoryna scalaris* (Batsch); Meriç et al., pl. 45 fig. 14 (not fig. 11-13, 15-18)

Test bilocular, proloculus with a stout spine and second chamber with a prominent long neck. Chambers globular, costate. Costae slim and low, numerous, diminish below the neck; they are most prominent on the basal part of the second chamber. The neck may be smooth or faintly annulate. The end of the neck is slightly widened with the radial aperture. Surface smooth other than the costae, test transparent.

Above listed characteristics fit very well with the definition of the genus *Amphicoryna*. Similar forms were previously reported under *Amphicoryna scalaris* and *Amphicoryna proxima* (Silvestri). Due to the weakness of the costae and the difference in size, these forms are not included in *Amphicoryna scalaris*.

Amphicoryna proxima is also different in that some of its costae continue up the neck, reaching the widened part. Kaminski et al.'s depiction of *A. proxima* has an annular neck which is more fitting in this taxon instead. One specimen illustrated by Meriç et al. (2014a) under *A. scalaris* is as small and with as weak costae as the present species; although it is trilocular, that specimen, too, may belong here instead.

Due to the differences on the neck, *Amphicoryna* sp. 1 and 2 are kept separate here. This taxon is different from other *Amphicoryna* by its bilocular nature, very weak costae, smooth to annulate neck, and small size.

Amphicoryna sp. 2

Plate 35 Figure 18; Plate 36 Figures 28-29

?	1872	*Nodosaria proxima* – Silvestri, p. 63, pl. 7 [sic, should be 6] fig. 138-147
?	2004	*Amphicoryna proxima* (Silvestri); Popescu and Crihan, pl. 4 fig. 7-8
part	2014a	*Amphicoryna scalaris* (Batsch); Meriç et al., pl. 45 fig. 15 (not fig. 11-14, 16-18)

Test composed of three chambers, proloculus with a very short spine, last chamber with a long and slim neck. Proloculus and the second chamber are globular, last chamber more pyriform and may be slightly offset. Form costate, costae more prominent on the basal parts of the chambers. Costae slim, low; a few of the costae stronger, reach the top of the neck. Top of the neck is widened with the radiate aperture. Surface smooth other than the costae, test transparent.

Silvestri's taxon carries a high resemblance to this present taxon. It is described as bi- or trilocular, costate, with a pyriform last formed chamber and an elongate neck. However, the size difference is significant. Silvestri (1872) gives length dimensions of 1.5 mm for the largest (trilocular) form while noting the length of the other forms as variable between 0.35 to 0.80 mm. The forms investigated here are all of about

0.35 mm in length. This may be just intraspecific variation; however, it is restricting from confidently assigning these specimens to Silvestri's taxon.

The illustrated specimen of *A. proxima* by Popescu and Crihan (2004) is highly similar to ours despite being bilocular. One very significant difference is the strength of the costae which makes the synonymy between these taxa questionable. One specimen illustrated under *A. scalaris* by Meriç et al. (2014a) is also very similar with a pyriform last chamber, weak costae and smooth-costate neck and can be considered to belong to this taxon instead.

Taxon is easily distinguished from Amphicoryna sp. 1 by its larger overall size, however the first two chambers are smaller than that of *Amphicoryna* sp. 1. It is different from other *Amphicoryna* by its small size, trilocular nature, pyriform shape of the last chamber and weak costae some of which decorate the neck.

Genus *Astacolus* de Monfort, 1808

1808 *Astacolus* – de Monfort, p. 262

Type: *Astacolus crepidula* (Fichtel & Moll, 1798, p. 107, pl. 19 fig. g-i)

Test arcuate, early portion enrolled; compressed rounded or angular dorsal periphery, radiate aperture and smooth surface.

Astacolus crepidula (Fichtel and Moll, 1798)

Plate 35 Figures 19; Plate 36 Figures 30-31

1798 *Nautilus crepidula* – Fichtel and Moll, p. 107, pl. 19 fig. g-i

1884 *Cristellaria crepidula*, Fichtel and Moll; Brady, p. 542, pl. 67 fig. 17, 19-20, pl. 68 fig. 1-2

1923 *Cristellaria crepidula* (Fichtel and Moll), Cushman, p. 117 pl. 35 fig. 3, 4

? 1988 *Astacolus crepidulus* (Fichtel and Moll); Loeblich and Tappan, p. 410, pl. 450, figs. 7-10

part 1991 *Astacolus crepidulus* (Fichtel and Moll); Cimerman and Langer, p. 52, pl. 54 fig. 10-13 (not fig. 14)

1994 *Astacolus crepidulus* (Fichtel and Moll); Loeblich and Tappan, p. 72, pl. 130 fig. 1-10

2008 *Astacolus crepidulus* (Fichtel and Moll); Sakınç, pl. 10 fig. 5-6

Test semi-ovate in side view, compressed, dorsal margin subrounded. Earlier chambers in a planispiral roll, later becoming curvilinear. Sutures radial, nearly straight, nearly flush, chambers not inflated. Aperture radial, on the dorsal angle, slightly produced. Surface smooth, test transparent.

This taxon is described to have 12-13 chambers in a planispiral to rectilinear-arcuate arrangement (Fichtel and Moll, 1798), however, fewer number of chambers are reported in the literature (e.g., Cimerman and Langer, 1991). Cimerman and Langer (1991) pointed out that the aperture of this taxon is cross-shaped, however other references (cited above) illustrate radiate apertures with more than four arms. This feature is here taken as an intraspecific variation.

The taxon is similar to *Saracenaria latifrons* (Brady) but the latter has carinate edges and a dorsal keel (Brady, 1884, p. 544, pl. 68 fig. 19; Cushman, 1923, p. 117 pl. 35 fig. 3, 4).

No complete individuals were found in the studied material, only broken specimens with 5-6 chambers intact were seen. The enrolling and the chamber shape in the studied specimens are all indicative of *A. crepidulus*.

Astacolus? sp. 1

Plate 35 Figures 20; Plate 36 Figure 36

Test small, elongate, arcuate, compressed with subrounded dorsal margin. Chambers slightly enrolled, curvilinearly added so that the dorsal margin is slightly convex. Chambers slightly inflated; sutures slightly depressed, oblique. Apertural face somewhat triangular, aperture at the dorsal angle, radiate. Test transparent, surface smooth.

This taxon is assigned under genus *Astacolus* due to curvilinear – slightly enrolled chamber arrangement, smooth surface, and subrounded dorsal margin. The somewhat triangular apertural face and cross section is reminiscent of *Saracenaria*, however that genus is mostly larger, significantly wider, and most often with a dorsal keel. Genus *Vaginulina* is also very similar, however it is ovate in section unlike the present taxon.

Specimens belonging to this taxon are only of a few chambers (3-5), and may be juveniles. They are usually with a comparatively large proloculus, they may also belong to a megalospheric generation. Taxon is distinguished from other curvilinear-compressed nodosarids by its slightly enrolled arrangement. The chambers are more inflated than those in *Astacolus crepidula*.

CLASS TUBOTHALAMEA Pawlowski, Holzmann and Tyszka, 2013

ORDER MILIOLIDA Delage & Hérouard, 1896

These forms have porcelaneous tests with occasional agglutinated grains incorporated.

SUBORDER MILIOLINA

Superfamily Cornuspiroidea Schultze, 1854

Family Cornuspiridae Schultze, 1854

Genus *Cornuspira* Schultze, 1854

Cornuspira involvens (Reuss, 1850)

Plate 42 Figure 31

1850 *Operculina involvens* – Reuss, p. 370, pl. 46 fig. 30 [sic. should be 20].

1884 *Cornuspira involvens* Reuss; Brady, p. 200, pl. 11 fig. 1-3

Form circular in outline, discoidal, with rounded periphery. Undivided tube enrolled mostly planispirally, may result in somewhat asymmetrical sides. Tube diameter increasing gradually, partially embracing the previous whorl. Aperture open end of tube. Test milky white, translucent; surface smooth.

Only small representatives of the taxon were found in this study. In contrast to transparent test and sugary look of the surface (due to porosity) of *Spirillina*, this taxon has a milky white and smooth test.

Superfamily Miliolidea Ehrenberg, 1839 (fide Loeblich and Tappan, 1988)

Family Cribrolinoididae Haynes, 1981

Genus *Adelosina* d'Orbigny, 1826

Plate 41 Figures 1-7; Plate 42 Figures 1-8

1826 *Adelosina* – d'Orbigny, p. 303

Type: *Adelosina laevigata* d'Orbigny (1826, p. 304)

The megalospheric ones of these forms have a planispirally enrolled early phase, later phase quinqueloculine, with an aperture produced on a neck. The microspheric forms are quinqueloculine throughout.

Several specimens of different growth stages are classified as *Adelosina* spp. All of the individuals encountered in this study are carinate, either completely smooth or

only faintly striated, and may belong to *Adelosina cliarensis* (Heron-Allen and Earland, 1930, p. 58, pl. 3, figs 26-31) and or *Adelosina laevigata* (d'Orbigny). No strongly costate *Adelosina* were found.

Family Hauerinidae Schwager, 1876

Subfamily Hauerininae Schwager, 1876

Genus *Cycloforina* Łuczkowska, 1972

1972 *Cycloforina* – Łuczkowska, p. 367

Type: *Quinqueloculina contorta* d'Orbigny (1846, p. 298, pl. 20 fig. 4-6)

Cycloforina rugosa (d'Orbigny, 1852)

Plate 41 Figures 10-12; Plate 42 Figures 12-14

1826 *Quinqueloculina rugosa* – d'Orbigny, p. 302 [nomen nudum]

1852 *Quinqueloculina rugosa* – d'Orbigny, p. 195

1893 *Quinqueloculina rugosa* d'Orbigny; Schlumberger, p. 68, pl. 2 [sic., should be 4] fig. 91-93, tf. 18-19

1905 *Quinqueloculina rugosa* d'Orbigny; Fornasini, p. 66, pl. 3 fig. 13

1991 *Cycloforina rugosa* (d'Orbigny); Cimerman and Langer, p. 33, pl. 28 fig. 3-4

2014a *Cycloforina rugosa* (d'Orbigny); Meriç et al., pl. 17 fig. 15

Test elongate, fusiform. Chamber arrangement quinqueloculine with three chambers on one side and four on the other side visible. Chambers with truncate outer margin with angular edges; chamber cross sections somewhat rectangular. Sutures depressed. Aperture produced on a neck, with a small tooth. Surface dull, rough, with fine grained agglutinated coating; coating composed mostly of calcitic grains; color yellowish.

Although the name was first used in d'Orbigny (1826) it was not accompanied by a description or an illustration. D'Orbigny (1852) is the first publication with a description attached, given as "*espèce bicarénée*", hence the taxon is attributed to that publication. The type description and figure are referred to Fornasini (1905) fide Ellis and Messina.

Schlumberger (1893) illustrated two transverse sections, one with chambers with distinctly doubly carinate outer margins (fig. 18), one with chambers with angular chamber edges (fig. 19). The individuals assigned to this taxon in this study are more similar to the latter, identical to Cimerman and Langer (1991).

The taxon is easily distinguished from other miliolids by its dull and rough surface, and necked aperture. It is different from *Cycloforina tenuicollis* (Wiesner) by its less angular margins and less depressed sutures.

Cycloforina tenuicollis (Wiesner, 1923)

Plate 41 Figures 8-9; Plate 42 Figures 9-11

1923 *Miliolina tenuicollis* – Wiesner, p. 44, 48, pl. 6 fig. 66 [fide Ellis and Messina]

1991 *Cycloforina tenuicollis* (Wiesner); Cimerman and Langer, p. 33, pl. 28 fig. 5-6

1993 *Cycloforina tenuicollis* (Wiesner); Sgarrella and Moncharmont Zei, p. 175, pl. 6 fig. 10-11

2008 *Cycloforina tenuicollis* (Wiesner); Sakınç, pl. 5 fig. 1-2

2012 *Cycloforina ? tenuicollis* (Wiesner); Milker and Schmiedl, p. 53, fig. 14.8

2014a *Cycloforina tenuicollis* (Wiesner); Meriç et al., pl. 17 fig. 16-17

Test elongate, fusiform. Chamber arrangement quinqueloculine with three chambers on one side and four on the other side visible. Chambers with truncate outer margin

with distinctly sharply angular edges; chamber cross sections somewhat trapezoidal. Sutures depressed. Aperture produced on a long neck, with a small tooth. Surface dull, rough, with fine grained agglutinated coating; coating composed mostly of calcitic grains; color yellowish.

Milker and Schmiedl (2012) questioned the generic position of the taxon claiming that the non-striate surface of the taxon as well as the long neck renders it not belonging to *Cycloforina* according to the description of Loeblich and Tappan (1988); however, said description of the genus do not include any limitation to the surface structure or the neck for the genus.

Taxon is different from other miliolids in terms of the dull and rough surface and distinctly angular chamber margins. The sutures are more depressed, angularity at the chamber margins is more distinct, and the neck is longer in this taxon with respect to *Cycloforina rugosa* (d'Orbigny).

Genus *Quinqueloculina* d'Orbigny, 1826

1826 *Quinqueloculina*– d'Orbigny, p. 301

Type: *Serpula seminulum* Linnaeus (1758, p. 786, p1. 2 fig. 1)

Quinqueloculina bosciana d'Orbigny, 1839b

Plate 41 Figures 13-14; Plate 42 Figures 15-16

1839b *Quinqueloculina bosciana* – d'Orbigny, p. 191, pl. 11, fig. 22-24

1991 *Quinqueloculina bosciana* d'Orbigny; Cimerman and Langer, p. 36, pl. 33 fig. 5-7

1993 *Quinqueloculina bosciana* d'Orbigny; Sgarrella and Moncharmont Zei, 93, p. 170, pl. 6 fig. 8-9

Test small, slim; with oval cross section; compressed; margins rounded. Three chambers on one side and four on the other side visible. Sutures almost flush to very shallowly depressed. Inner chambers oblique to the last two chambers, producing

oblique sutures. Aperture small, nearly circular, very slightly produced, with small tooth. Surface smooth; wall white, opaque, occasionally translucent.

The form is easily distinguished from other *Quinqueloculina* by its slender shape, oblique sutures, and very small aperture.

Quinqueloculina pygmaea Reuss, 1850

Plate 41 Figures 22-25; Plate 42 Figures 26-30

1850 *Quinqueloculina pygmaea* – Reuss, p. 384, pl. 50 fig. 3

1993 *Quinqueloculina pygmaea* Reuss; Sgarrella and Moncharmont Zei, p. 174, pl. 7 fig. 2

Test small, ovate, subcylindrical; cross section nearly circular. Three chambers on one side and four on the other side visible. Sutures depressed, nearly vertical. Aperture oblique to the long axis, ovate, not produced; with small simple tooth. Surface smooth, shiny; wall white, somewhat translucent.

The taxon is distinguished from other *Quinqueloculina* by its small size, nearly circular cross section and almost vertical, depressed sutures.

Quinqueloculina schlumbergeri (Wiesner, 1923)

Plate 41 Figures 15-17; Plate 42 Figures 17-19

1893 *Quinqueloculina stelligera* – Schlumberger, p. 68, pl. 2 figs 58-59, tf. 17

non 1913 *Miliolina stelligera* Schlumberger; Heron-Allen and Earland, p. 31; 187; pl. 1 fig. 14-15

1923 *Miliolina schlumbergeri* – Wiesner, p. 49, pl. 6 fig. 73

non 1929 *Quinqueloculina stelligera* Schlumberger; Cushman, p. 28, pl. 3 fig. 3-4

1930 *Miliolina schlumbergeri* – Heron-Allen and Earland, p. 58 pl. 2 fig. 16-19

1991 *Quinqueloculina stelligera* Schlumberger; Cimerman and Langer, p. 38, pl. 34 fig. 13-15

1993 *Quinqueloculina stelligera* Schlumberger; Sgarrella and Moncharmont Zei, p. 175, pl. 6 fig. 13-14

2012 *Quinqueloculina stelligera* Schlumberger; Milker and Schmiedl, p. 59, fig. 16.1-4

non 2014a *Quinqueloculina stelligera* Schlumberger; Meriç et al., pl. 25 fig. 2-3

Test ovate elongate to somewhat quadrate in frontal view. Three chambers on one side and four on the other side visible; chambers with triangular cross section whose outer edge is carinated so that the cross section of the whole form is like a five-cornered star. Sutures depressed. Aperture on a short neck, situated somewhat centrally on the oral pole; circular, surrounded by a lip and with a small tooth. Wall translucent except for the carinated edges of chambers; surface shiny, but somewhat irregular with sparse, shallow longitudinal grooves in larger specimens.

Due to the name *Quinqueloculina stelligera* Schlumberger (1893) being a homonym of the Eocene taxon *Quinqueloculina stelligera* Terquem (1882), Wiesner (1923) renamed the species as *Quinqueloculina schlumbergeri*. Independently, Heron-Allen and Earland (1930) gave the same name to the taxon as well.

Specimens attributed to *Q. stelligera* Schlumberger by Heron-Allen and Earland (1913) were later assigned to their new species *Adelosina cliarensis* (Heron-Allen and Earland, 1930; originally described as *Miliolina cliarensis*). Cushman (1929) noted that the individuals he assigned to *Q. stelligera* Schlumberger is more akin to Heron-Allen and Earland's (1913) interpretation; however, the illustrations he gives are clearly of a quinqueloculine form with an elongate neck, and probably belong to *Cycloforina* instead.

Forms attributed to *Quinqueloculina stelligera* Schlumberger by Meriç et al. (2014a) are of fatter forms with distinctly rugose surface and lacking the characteristic neck of this taxon, and do not belong in this taxon.

Identical forms were recorded under the name *Quinqueloculina stelligera* Schlumberger by Cimerman and Langer (1991), Sgarrella and Moncharmont Zei (1993) and Milker and Schmiedl (2012). The shallow longitudinal grooves on the surface are not present in the texts of the descriptions, but are depicted in the illustrations of most of the above given references.

Form is easily distinguished from other *Quinqueloculina* by its ovate-quadrangular test, strongly developed carinate edges of the chambers which are translucent except for the opaque carina, and the nearly centrally located stout neck.

Quinqueloculina seminulum? (Linnaeus, 1758)

Plate 43 Figure 1; Plate 44-A Figure 1

?	1758	*Serpula seminulum* – Linnaeus, p. 786, p1. 2 fig. 1
?	1884	*Miliolina seminulum* Linné; Brady, p. 157, pl. 5 fig. 6
?	1964	*Quinqueloculina seminulum* (Linné); Loeblich and Tappan, p. C458, fig. 349.1
?	1991	*Quinqueloculina seminula* (Linnaeus); Cimerman and Langer, p. 38, pl. 34 fig. 9 -12
?	2012	*Quinqueloculina seminula* (Linné); Milker and Schmiedl, p. 59, fig. 15.30-31
non	2014a	*Quinqueloculina seminula* (Linné); Meriç et al., pl. 24 fig. 10-17
non	2014b	*Quinqueloculina seminula* (Linné); Meriç et al., pl.1 fig. 11-13

Test ovate in frontal view, somewhat triangular in transverse section. Edges rounded-subrounded. Three chambers on one side and four on the other side visible; inner chambers slightly inflated. Sutures depressed. Aperture flush, more or less in line

with the outline of the test; ovate; with a simple tooth. Wall opaque; surface shiny, very smooth.

This present taxon differs from the *Quinqueloculina seminulum* sensu stricto slightly due to the inflation of the inner chambers which may or may not be an intraspecific variation. See *Quinqueloculina viennensis* below for a further discussion with regards to the morphologic comparisons and taxonomic history.

Taxon is distinguished from other *Quinqueloculina* by its large size and smooth surface and from *Quinqueloculina viennensis* by its rounded edges of chambers.

Quinqueloculina stalkeri Loeblich and Tappan, 1953

Plate 41 Figures 18-21; Plate 42 Figures 20-25

1953 *Quinqueloculina stalkeri* – Loeblich and Tappan, p. 40, pl. 5 fig. 5-9

1993 *Quinqueloculina stalkeri* Loeblich and Tappan; Sgarrella and Moncharmont Zei, p. 174, pl. 5 fig. 13-14

2008 *Quinqueloculina stalkeri* Loeblich and Tappan; Sakınç, pl. 6 fig. 1-2

2014a *Quinqueloculina stalkeri* Loeblich and Tappan; Meriç et al., pl. 25 fig. 1

Test fusiform, broader at the middle, tapering towards the poles. Three chambers on one side and four on the other side visible. Sutures distinctly depressed. Aperture a circular opening produced on a short neck, with an everted rim and small tooth. Surface dull, white; wall somewhat translucent, with a fine grained coating mostly of calcitic origin.

The necks of the studied individuals are longer than what is depicted in the original description by Loeblich and Tappan (1953); this taxon most resembles the

Loeblich and Tappan (1953) illustrated five individuals as holo- and paratypes of the taxon. The holotype (pl. 5 fig. 9; also image by Smithsonian National Museum of Natural History Department of Paleobiology Collections, Catalogue number USNM

PR 2036, access via http://n2t.net/ark:/65665/3bc5a62a7-0b78-499c-b595-ec4c13bf571f) is wider and slightly larger than the others, the neck is not well developed and is depicted with a very fine grained agglutinated coating as opposed to the paratypes on which the agglutinated coating is not illustrated and the necks and everted rims are well developed. These differences may require the splitting of a new taxon which is represented by the paratypes of Loeblich and Tappan; in which case the present taxon would belong to the new species.

The present taxon most resembles the paratype with the longest neck (pl. 5 fig. 6 of Loeblich and Tappan, 1953). The agglutinant material is mostly calcitic, other types of very fine grains are only very sparse, and the wall is usually thinner (and smoother) on the last chamber. Individuals identical to the present taxon were recorded by Sgarrella and Moncharmont Zei (1993), Sakınç (2008), and Meriç et al. (2014a) from the Mediterranean Sea and the Sea of Marmara under the same name.

Quinqueloculina vandiemeniensis Loeblich and Tappan, 1994

Plate 43 Figures 7-8; Plate 44-A Figures 8-9

1993 *Quinqueloculina lata* Terquem; Sgarrella and Moncharmont Zei, p. 172, pl. 5 fig. 15

1994 *Quinqueloculina vandiemeniensis* – Loeblich and Tappan, p. 51 pl. 83 fig. 1-3

Test small; quadrate in frontal view; margins narrowly subrounded-subacute. Adapertural pole broadly rounded, apertural pole somewhat truncate. Three chambers on one side and four on the other side visible. Sutures slightly depressed, indistinct. Aperture an ovate opening with a very slightly protruding, short, Y-shaped, bifid tooth. Surface smooth, highly polished; wall opaque, occasionally locally translucent.

Quinqueloculina lata Terquem is a very similar form in general quadrangular shape. The studied individuals are smaller (about 300 μm) with respect to *Quinqueloculina*

lata (Terquem, 1876: height: 0.96 mm). Moreover, *Q. lata* is described to have a simple tooth (Terquem, 1876; Heron-Allen and Earland, 1930; Le Calvez, 1958). However, the illustration attributed to *Quinqueloculina lata* Terquem by Sgarrella and Moncharmont Zei (1993) appears to have a short, bifid tooth, as do the material of this study. *Quinqueloculina vandiemeniensis* Loeblich and Tappan is identical to this present one with the quadrangular shape, subacute periphery and bifid tooth.

The form is distinct from other *Quinqueloculina* by its quadrangular shape, very shallow sutures and highly polished surface.

Quinqueloculina viennensis Le Calvez and Le Calvez, 1958

Plate 43 Figures 2-6; Plate 44-A Figures 2-7

1884 *Miliolina cuvieriana* d'Orbigny; Brady, p. 162, pl. 5 fig. 12

1958 *Quinqueloculina viennensis* – Le Calvez and Le Calvez, p. 187, pl. 5 fig. 42, 44-45

1993 *Quinqueloculina viennensis* Le Calvez and Le Calvez; Sgarrella and Moncharmont Zei, p. 176, pl. 7 fig. 8

1994 *Quinqueloculina lamarckiana* d'Orbigny; Jones, p. 21, pl. 5 fig. 12

2014a *Quinqueloculina seminula* (Linné); Meriç et al., pl. 24 fig. 10-17

2014b *Quinqueloculina seminula* (Linné); Meriç et al., pl.1 fig. 11-13

Test ovate in frontal view, triangular in transverse section. Edges narrowly subrounded to sharply angular. Three chambers on one side and four on the other side visible; the margins of the inner chambers occasionally and locally stick out sharply, protruding slightly next to the sutures. Sutures slightly depressed. Aperture flush, more or less in line with the outline of the test; ovate; with a simple tooth. Wall opaque; surface shiny, very smooth.

Le Calvez and Le Calvez (1958) described the taxon taking the individuals assigned to *Miliolina cuvieriana* d'Orbigny (1839b, p. 162, pl. 5 fig. 12) by Brady (1884) as

not belonging to *cuvieriana* due to surface ornamentation and apertural characteristics, and took them as synonymous to their taxon instead. Brady's illustrations are of a specimen which do not have striations on the surface as d'Orbigny's description of *cuvieriana* suggests. The same illustrations of Brady's were later assigned to *Quinqueloculina lamarckiana* d'Orbigny (1839b, p. 189, pl. 11, figs 14, 15) by Jones (1994) who claimed the two taxa to be synonymous (following Brady) and proposed that the name *lamarckiana* to have precedence since they were described in the same publication and *lamarckiana* came a page before *cuvieriana*. Said illustrations of Brady do not belong to *Q. lamarckiana* since it was described with a somewhat produced aperture (d'Orbigny, 1839b). They also do not belong to *Q. cuvieriana* on the surface ornamentation basis Le Calvez and Le Calvez (1958) discussed; however, apertural characteristics are identical contrary to Le Calvez and Le Calvez's account.

The angularity of the margins of the chambers varies in the population; according to Le Calvez and Le Calvez (1958) individuals from the deeper waters exhibit sharper chamber margins taking on the appearance of a keel. Indeed, specimens with sharply angular margins as well as less angular, more subrounded margins for the last two chambers of the tests were encountered; although, the ecological, or rather water depth preference of the two end-points of the morphological variety of the taxon could not be deciphered. The inner chambers, on the other hand, are always with a sharply angular margin and this sharp margin always sticks out at least for one of the inner chambers.

Quinqueloculina seminulum (Linnaeus, 1758) is a similar species in the overall ovate and compact shape, subrounded-oval aperture, simple tooth, smooth surface and similar size (~500 μm), as is widely used in the literature. The original description of *Q. seminulum* (as *Serpula seminulum*) by Linnaeus do not include such details as to the chamber arrangement or apertural modifications as expected, and accompanying illustrations can belong to many miliolid foraminiferal taxa. Brady (1884, p. 157, pl. 5 fig. 6) gave a comprehensive synonym list and the history of the

taxon as the lump-name for quinqueloculins with a smooth surface. Brady's illustrations and interpretation provide the basis of the modern understanding of the taxon. Later, Loeblich and Tappan (1964) established a neotype for *Q. seminulum* (p. C458, fig. 349.1; also, image by Smithsonian National Museum of Natural History Department of Paleobiology Collections, Catalogue number USNM MO 689756, access via http://n2t.net/ark:/65665/35b139c63-c752-4777-8ed4-628577451f33). Both Brady's and Loeblich and Tappan's illustrations indicate a compact form, taller than wide, and with rounded margins to the chambers despite an overall triangular transverse section. The sutures in Loeblich and Tappan's neotype are more depressed than that of *Q. viennensis*, and the margins of the inner chambers never sharply peak out like *Q. viennensis*; Nevertheless, the fine details of these, most probably closely related, taxa were ignored and there is some confusion in the literature regarding these two taxa.

Quinqueloculina viennensis is easily distinguished from other *Quinqueloculina* by its large size, very smooth and shiny surface and angular margins of the chambers at least for the inner chambers.

Quinqueloculina sp. 1

Plate 43 Figure 9; Plate 44-B Figure 1

Test subquadrate in frontal view, ovate in transverse section. Three chambers on one side and four on the other side visible. Sutures slightly depressed. Aperture a wide, semicircular opening, somewhat in line with the outline of the test; with protruding, short, simple tooth. Surface striate with very shallow, indistinct, longitudinal striations, shiny; wall opaque, occasionally locally translucent.

Taxon is similar to *Quinqueloculina milletti* (Wiesner) sensu Boltovskoy et al. (1980, p. 46, pl. 28 fig. 13-17) and Sgarrella and Moncharmont Zei (1993, p. 172, pl. 7 fig. 7). Those identifications do not belong to Wiesner's taxon (1912, p. 237) which is based on the incorrect identifications of *Miliolina bosciana* d'Orbigny by Millett (1898, p. 267, pl. 6 fig. 1) depicted to be equipped with a short neck and an everted

rim. Individuals illustrated by Boltovskoy et al. (1980) and Sgarrella and Moncharmont Zei (1993) instead have an aperture identical to the present taxon. Nonetheless, keeping the taxon in open nomenclature was preferred.

Form is similar to *Quinqueloculina vandiemeniensis* Loeblich and Tappan (1994), but is fatter, has a more rounded outline, chamber margins rounded instead of pinched and the aperture is oblique to the longitudinal axis instead of being perpendicular to it.

Quinqueloculina sp. 2

Plate 43 Figures 11-12; Plate 44-B Figures 4-5

Test fat, as wide as tall, somewhat circular. Three chambers on one side and four on the other side visible. Margins of chambers locally angular, especially at the central part. Sutures depressed, mostly distinct. Aperture a nearly circular opening, surrounded by an indistinct rim, directed in the direction of coiling, positioned past the longitudinal axis; with a short, bifid tooth. Surface striate with very shallow, indistinct, longitudinal striations, shiny; wall opaque, especially so at the angular margins, occasionally locally translucent.

The form is distinctly different from other *Quinqueloculina* by its fat build and is more circular outline rather than being elongated and ovate. In addition, the apertural end of the last chamber is tubular and wraps around the periphery for a short distance. The taxon is tentatively put under *Quinqueloculina* for its quinqueloculine chamber arrangement, however may belong to another genus in the Family.

Quinqueloculina? sp. 3

Plate 43 Figures 13-15; Plate 44-B Figures 6-8

Test large; ovate in frontal view; nearly subtriangular-subcircular in transverse section. Three chambers on one side and four on the other side visible; chambers inflated. Sutures depressed, distinct, mostly vertical, following parallel to the outline of the test. Aperture a domed opening, surrounded above by an indistinct rim; with

a short, narrow, thin flap (?). Surface dull with hispidity; wall mostly opaque, locally translucent.

The taxon is distinguished by its large size from most other *Quinqueloculina*, and from *Quinqueloculina viennensis* and *Q. seminula*? by its dull surface and deep sutures. The aperture of the taxon is also distinct: the "flap" is quite thin and motley found as broken. The taxon is tentatively put under *Quinqueloculina* for its apparently quinqueloculine chamber arrangement.

Subfamily Miliolinellinae Vella, 1957

Genus *Biloculinella* Wiesner, 1931

1931 *Biloculinella* – Wiesner, p. 69

Type: *Biloculina labiata* Schlumberger (1891, p. 556, t-fig. 13-14, pl. 9 fig. 60-62)

Test ovate, compressed, may be with carinate or angular edges. Chamber arrangement biloculine in the adult so that only two chambers visible from the outside. Aperture a thin crescentic slit, with a wide apertural flap.

The position of the aperture and the last chamber may not be perfectly symmetrical due to inner quinqueloculine arranged chambers. Aperture is similar to that of *Miliolinella*, but the flap-like tooth in that genus is smaller and the aperture itself is a larger opening.

Genus *Pyrgo* is very similar in most aspects except for the aperture which is more open and is accompanied by a short bifid tooth.

Biloculinella globula (Bornemann, 1855)

Plate 43 Figures 19-21; Plate 44-B Figures 14-16

1855 *Biloculina globulus* – Bornemann, p. 349, pl. 19, fig. 3

1891 *Biloculina globulus* Bornemann; Schlumberger, p. 576, pl. 12 fig. 97-100, t-fig. 42-44

non 1921 *Biloculina globulus* Bornemann; Cushman, p. 474, pl. 95 fig. 2

1958 *Biloculinella globula* (Bornemann); Le Calvez and Le Calvez, p. 201, pl. 7 fig. 76

1991 *Biloculinella globula* (Bornemann); Cimerman and Langer, p. 40, pl. 36 fig. 1-2

Test large, globular; periphery rounded. Two chambers visible from the outside, inflated. Sutures somewhat depressed. Aperture a crescentic slit with a concave apertural flap. Surface smooth.

Biloculinella subsphaerica (Wiesner, 1923) is a similarly globular species, however the aperture is considerably longer and thinner. On the other hand, the aperture in this taxon is shorter (about half of the width of the test) and less obstructed (Le Calvez and Le Calvez, 1958).

The form attributed to Bornemann's taxon by Cushman (1921) has a wide bifid tooth, and hence is not a *Biloculinella*, instead belongs to *Pyrgo subsphaerica* (d'Orbigny, 1839b, originally described as *Biloculina subsphaerica*).

This taxon is the largest of the *Biloculinella* found in the Sea of Marmara, and is different from other *Biloculinella* by its rounded periphery other than its size. The form resembles the largest specimens of *Miliolinella subrotunda* (Montagu) due to its rounded periphery and apertural similarities, but in that taxon at least three chambers are visible from the outside and the aperture is more open.

Biloculinella labiata (Schlumberger, 1891)

1891 *Biloculina labiata* – Schlumberger, p. 556, pl. 9 fig. 60-62, t-fig. 13-14

1923 *Biloculina labiata* Schlumberger var. *simplex* – Wiesner, p. 89, pl. 18 fig. 261

1958 *Biloculinella labiata* var. *simplex* (Wiesner); Le Calvez and Le Calvez, p. 202, pl. 16 fig. 193, 194

1991 *Biloculinella labiata* (Schlumberger); Cimerman and Langer, p. 40, pl. 36 fig. 12

2008 *Biloculinella labiata* (Schlumberger); Sakınç, pl. 6 fig. 11

Test ovate in frontal view, somewhat compressed in edge view. Periphery subangular to carinate. Two chambers visible from the outside, sutures distinct. Aperture a crescentic, narrow, terminal slit, with a wide apertural flap. Surface smooth.

Wiesner (1923) produced four varieties of Schlumberger's taxon, three of the varieties (*elongata*, *depressa*, *subsphaerica*) are substantially different from *B. labiata*; while, *simplex* being identical to Schlumberger's.

Biloculinella depressa (Wiesner) is very similar to *Biloculinella labiata*, the former is more compressed and with strongly angular-carinate periphery. The outline of the test in frontal view ranges from ovoid, but never as narrow and elongate as *Biloculinella elongata* (Wiesner), to almost perfectly circular. *Biloculinella subsphaerica* (Wiesner) is rather fat, usually larger, and the periphery is exclusively rounded.

Genus *Miliolinella* Wiesner, 1931

1931 *Miliolinella* – Wiesner, p. 63, 65, 107 [fide Loeblich and Tappan, 1988]

Type: *Vermiculum subrotundum* Montagu (1803, p. 521)

Test ovate, somewhat compressed, with rounded periphery. Chambers initially quinqueloculine, later nearly planispiral. Two to seven chambers visible from the exterior. Aperture crescentic with a broad, low apertural flap.

The aperture is similar to that of *Biloculinella*, but the flap is much smaller and the aperture itself is wider.

Miliolinella elongata Kruit, 1955

1955 *Miliolinella circularis* (Bornemann) var. *elongata* – Kruit, p. 110, pl. 1, fig. 15

1991 *Miliolinella elongata* Kruit; Cimerman and Langer, p. 41, pl. 37, fig. 8

1993 *Miliolinella circularis elongata* Kruit; Sgarrella and Moncharmont Zei, 1993, p. 187, pl. 10 fig. 5

2012 *Miliolinella elongata* Kruit; Milker and Schmiedl, p. 62, fig. 16.23-24

Test small, ovate, taller than wide, compressed. Periphery rounded. Three chambers visible on the exterior. Sutures shallow, distinct. Aperture terminal, a crescentic slit, with a concave apertural flap. Surface smooth, shiny.

The position of the aperture is slightly lower in the original description (Kruit, 1955) and Cimerman and Langer (1991). The apertures of the specimens examined in this study are positioned at the highest point of the test, similar to figures given by Sgarrella and Moncharmont Zei (1993) and Milker and Schmiedl (2012).

Taxon is significantly more elongated than *Miliolinella subrotunda* (Montagu). It is different from *Pyrgo elongata* (d'Orbigny) by its apertural flap and by having more than two chambers visible from the outside.

Miliolinella subrotunda (Montagu, 1803)

Plate 43 Figures 16-18; Plate 44-B Figures 9-13

1803 *Vermiculum subrotundum* – Montagu, p. 521

1991 *Miliolinella subrotunda* (Montagu); Cimerman and Langer, p. 42, pl. 38 fig. 4-9

2008 *Miliolinella subrotunda* (Montagu); Sakınç, pl. 7 fig. 4

Test globular, ovate to circular in frontal view, somewhat compressed. Three to four chambers visible from the exterior. Sutures slightly depressed. Aperture terminal, crescentic, with a broad, usually concave, low apertural flap. Surface smooth.

The outline of the test is various, between nearly circular to ovate (taller than wide) while the transverse section is ovate, but is slightly asymmetrical. The inner chambers are positioned oblique to the long axis; in the smaller (pre-mature) individuals the obliquity is much more pronounced.

The taxon is different from *Biloculinella globula* Bornemann by having more than two chambers visible from the outside, and from *Miliolinella elongata* Kruit by being more equidimensional.

Genus *Pseudotriloculina* Cherif, 1970

1970 *Pseudotriloculina* – Cherif, p. 112

Type: *Triloculina laevigata* d'Orbigny in Schlumberger (1893)

Test ovate with rounded periphery. Three chambers visible from the outside. Aperture a high, narrow arch with a protruding tooth.

Poignant (2019) indicated that the subgenus *Quinqueloculina* (*Pseudotriloculina*) Cherif (1970) was in fact identical to genus *Affinetrina* Łuczkowska (1972) and that the latter name should be used because when *Pseudotriloculina* was raised to genus level by Loeblich and Tappan (1988), the type taxon was incorrectly given as *Triloculina lecalvezae* Kaasschieter (1961, p. 166, pl. 5 fig. 16; taken as synonymous to *Triloculina laevigata* d'Orbigny, see Poignant (2019)).

Here, it is proposed to keep the generic name *Pseudotriloculina* since it takes precedence by being an earlier publication, with the type taxon as *Triloculina laevigata* d'Orbigny in Schlumberger (1893) as it was originally assigned by Cherif (1970).

Pseudotriloculina laevigata (d'Orbigny in Schlumberger, 1893)

Plate 43 Figure 10; Plate 44-B Figures 2-3

1826 *Triloculina laevigata* – d'Orbigny, p. 300 [nomen nudum]

non 1878 *Triloculina laevigata* d'Orbigny; Terquem, p. 57, pl. 5 fig. 20-21

1893 *Triloculina laevigata* d'Orbigny – Schlumberger, p. 63, t-fig. 9-10, pl. 1 fig. 45-47

1905 *Triloculina laevigata* d'Orbigny; Fornasini, p. 61, pl. 1 fig. 10

1958 *Triloculina laevigata* d'Orbigny; Le Calvez and Le Calvez, p. 192, pl. 6 fig. 62-64

1991 *Pseudotriloculina laevigata* d'Orbigny; Cimerman and Langer, p. 43, pl. 39 fig. 8-12

part 1991 *Quinqueloculina laevigata* d'Orbigny; Cimerman and Langer, p. 37, pl. 33 fig. 8, 9, 11

Test elongate, sides nearly parallel; somewhat compressed with ovate cross section. Three chambers visible from the outside. Sutures indistinct. Aperture an elongate arch, oblique to the long axis of the test, with a long, protruding tooth. Surface smooth.

The long and highly confusing history of the systematics of this taxon is well established by Poignant (2019). As shown by Poignant (2019), although they are widely considered to be synonymous (Loeblich and Tappan, 1988), *Triloculina laevigata* d'Orbigny (1826) and *Triloculina lecalvezae* Kaasschieter (1961) are two distinct and separate taxa.

D'Orbigny's name is a nomen nudum: does not have a description or type figure; yet, is widely used as is (e.g., Cimerman and Langer, 1991), sensu Schlumberger (1893) and Fornasini (1905) who based their descriptions and illustrations on the unpublished drawings of d'Orbigny. The name should be referred as

Pseudotriloculina laevigata (d'Orbigny in Schlumberger, 1893) as it is the earliest account of the taxon.

According to Poignant (2019) *Triloculina laevigata* d'Orbigny (1826) and *Affinetrina alcidi* Lévy et al. (1992) are synonyms. Since d'Orbigny's name is invalid, Poignant (2019) proposed the use of the latter name for this taxon which would create a taxonomic problem since d'Orbigny's taxon is the typetaxon of the genus *Pseudotriloculina*. See above for the discussion of generic placement of this taxon and naming of the genus.

Pseudotriloculina oblonga (Montagu) and *P. laevigata* are two very similar taxa whose synonymy should be investigated further. According to Le Calvez and Le Calvez (1958) the two names were previously used incorrectly or interchangeably. They attribute this confusion to Terquem's (1878) misinterpretation of the taxon (which later was used in the synonymy of *Triloculina lecalvezae* Kaasschieter (1961) and is identical to Kaasschieter's chosen holotype). Here, Le Calvez and Le Calvez (1958) and Cimerman and Langer (1991) are followed in the distinction of these two species: *P. laevigata* is more elongate with more parallel sides, while *P. oblonga* is more ovate and stouter.

Triloculina laevigata d'Orbigny is a homonym of *Triloculina laevigata* Bornemann (1855), however, the latter is clearly a *Miliolinella* with an apertural flap, and is considered to be synonymous with *Miliolinella enoplostoma* (Reuss).

The assignment of the individuals *Quinqueloculina laevigata* d'Orbigny (1839c) in Cimerman and Langer (1991) is probably a misidentification and those better belong in this taxon instead. They indicate that only three chambers are visible from the outside and the aperture is a high arch with a long, simple, protruding tooth, align closely with the features of *P. laevigata*, and very different than *Q. laevigata* d'Orbigny which has a T-shaped bifid tooth and five chambers visible from the outside.

Taxon is distinguished from other miliolid taxa by having three chambers visible from the outside, having an ovate cross section (instead of triangular as in *Triloculina*), having a narrow but high arched aperture with a long, protruding tooth.

Genus *Pyrgo* Defrance, 1824

1824 *Pyrgo* – Defrance, p. 273

Type: *Pyrgo laevis* Defrance (1824, p. 273, pl. 88 fig. 2)

Test ovate, compressed, may be with carinate or angular edges. Chamber arrangement biloculine in the adult so that only two chambers visible from the outside. Aperture with a bifid tooth.

The position of the aperture and the last chamber may not be perfectly symmetrical due to inner quinqueloculine arranged chambers.

Genus *Biloculinella* is very similar in most aspects except for the aperture which is crescentic-slit like and accompanied with a wide apertural flap instead of a short tooth.

Pyrgo anomala (Schlumberger, 1891)

Plate 43 Figures 24-26; Plate 44-B Figures 19-20

1891 *Biloculina anomala* – Schlumberger, p. 569, pl. 11 fig. 84-86; pl. 12 fig. 101

1991 *Pyrgo anomala* (Schlumberger); Cimerman and Langer, p. 44, pl. 41 fig. 3-5

Test oval in lateral view, somewhat taller than wide. Only two chambers visible from the outside; chambers inflated. Sutures depressed, somewhat sinusoidal in edge view. Aperture nearly rounded, partly covered by the broad, flap-like tooth. Surface smooth, shiny; test opaque.

The tooth in this taxon is mostly found to be broken, hence its original shape, which may aid in specific identification, was not well observed. These smooth and less slender (see *Pyrgo elongata*) types of the genus are tentatively collected under *Pyrgo anomala* in this study. The synonymy of the smooth and relatively fat types of this genus, namely this taxon and *Pyrgo inornata* (d'Orbigny), *Pyrgo fischeri* (Schlumberger) and *Pyrgo clypeata* (d'Orbigny) needs further research.

The taxon is different from *P. elongata* (d'Orbigny) by its larger size, wider test, and wider tooth.

Pyrgo elongata (d'Orbigny, 1826)

Plate 43 Figures 22-24; Plate 44-B Figures 17-18

1826 *Biloculina elongata* – d'Orbigny, p. 298 n° 4

1884 *Biloculina elongata* d'Orbigny; Brady, p. 144, pl. 2 fig. 9

1891 *Biloculina elongata* d'Orbigny; Schlumberger, p. 571, pl. 11 fig. 87-88; pl. 12 fig. 89

1908 *Biloculina elongata* d'Orbigny; Fornasini, p. 47, pl. 3 fig. 10-11

1991 *Pyrgo elongata* (d'Orbigny); Cimerman and Langer, p. 44, pl. 41 fig. 6-8

2008 *Pyrgo elongata* (d'Orbigny); Sakınç, pl. 7 fig. 11

Test ovate, elongate in lateral view; as wide as thick; twice as tall as wide. Only two chambers visible from the outside; chambers inflated. Sutures depressed, sinusoidal in edge view. Aperture nearly rounded, partly covered by the tooth. Surface smooth, shiny; test opaque.

The tooth is described/illustrated to be broad and rounded by above given references; unlike the specimens, which have relatively smaller tooth, here attributed to this species.

Pyrgo oblonga (d'Orbigny, 1839b) is a similar species whose possible synonymy to this species was questioned by Fornasini (1908). According to d'Orbigny (1839b) *oblonga* is wider than *elongata*; moreover, it is illustrated with a tooth whose distal edge is sinusoidal unlike *elongata* which has a rounded tooth.

Taxon is distinguished from others of the genus by its elongate, ovate shape.

Genus *Triloculina* d'Orbigny, 1826

1826 *Triloculina* – d'Orbigny, p. 209

Type: *Miliolites trigonula* Lamarck (1804, p. 351)

Test triangular to subtriangular in section. Chamber arrangement trilocular in adult so that only three chambers visible from the exterior. Aperture terminal, rounded with a short bifid tooth.

Triloculina tricarinata (d'Orbigny in Deshayes, 1832)

Plate 45 Figure 1; Plate 46 Figure 1

1826 *Triloculina tricarinata* – d'Orbigny, p. 299 [nomen nudum]

1832 *Triloculina tricarinata* d'Orbigny; Deshayes, p. 1052

1884 *Miliolina tricarinata* d'Orbigny; Brady, p. 165, pl. 3 fig. 17

1991 *Triloculina tricarinata* d'Orbigny; Cimerman and Langer, p. 46, pl. 44 fig. 3-4

1993 *Triloculina tricarinata* d'Orbigny; Sgarrella and Moncharmont Zei, p. 187, pl. 9 fig. 14-15

2008 *Triloculina tricarinata* d'Orbigny; Sakınç, pl. 8 fig. 3

? 2014a *Triloculina tricarinata* d'Orbigny; Meriç et al., pl. 32 fig. 15-18 [sic, should be 14-17]

Test nearly triangular in transverse section, oval in frontal view. Chambers overlapping, only three visible from the exterior; outer chamber wall flat with two edges sharply carinated. Three longitudinal keels on the test: two belonging to the last chamber, one belonging to the penultimate chamber; three faces of the test nearly flat. Sutures distinct, only slightly depressed. Aperture terminal, rounded, with a bifid, Y or T shaped tooth. Surface smooth.

Triloculina adriatica Le Calvez and Le Calvez (1958) is very similar due to the angular margins and flat faces of the test, but the edges are not truly keeled, the apertural tooth is blunter and the surface is very finely striated (Cimerman and Langer, 1991).

T. tricarinata illustrated by Meriç et al. (2014a) are of fatter individuals with less distinctly carinate edges and may not belong in this taxon.

Form is easily distinguished from other *Triloculina* by its sharply carinate edges.

Triloculina trigonula (Lamarck, 1804)

Plate 45 Figure 2; Plate 46 Figure 2

1804 *Miliolites trigonula* – Lamarck, p. 351

1826 *Triloculina trigonula* Lamarck; d'Orbigny, p. 299

1832 *Triloculina trigonula* d'Orbigny; Deshayes, p. 1051

1884 *Miliolina trigonula* Lamarck; Brady, p. 164, pl. 3 fig. 14-16

1964 *Triloculina trigonula* Lamarck; Loeblich and Tappan, fig. 354.4

1993 *Triloculina trigonula* Lamarck; Sgarrella and Moncharmont Zei, p. 187, pl. 10 fig. 1

2014a *Triloculina trigonula* Lamarck; Meriç et al., pl. 33 fig. 1

Test nearly triangular in transverse section, oval in frontal view. Chambers overlapping, only three visible from the exterior; chambers somewhat inflated.

Margins of chambers rounded; three faces of the test somewhat convex. Sutures depressed. Aperture terminal, rounded, with a bifid tooth. Surface smooth.

Taxon is different from *Triloculina tricarinata* by its rounded edges instead of sharply carinate ones, more convex chambers and depressed sutures.

Subfamily Sigmoilinitinae Łuczkowska, 1974

Genus *Sigmoilina* Schlumberger, 1887

1887 *Sigmoilina* – Schlumberger, p. 475

Type: *Planispirina sigmoidea* Brady (1884, p. 197, pl. 2 fig. 1-3, t-fig. 5c)

Test circular-ovate in frontal view, lensoidal, apertural and adapertural poles may be slightly acuminate. Two chambers per whorl arranged nearly planispirally, subsequent chambers placing slightly to one side of the previous whorl so that two sigmoid chamber sets occur in transverse section. Lateral extensions of chamber walls cover the previous chambers forming a lensoidal shape, though, the lateral surfaces are not strictly convex, but somewhat sigmoid themselves reflecting the sigmoidal chamber arrangement. Sutures indistinct. Aperture terminal, semi-circular, with an apertural flap. Surface very smooth, shiny.

Genus *Sigmoilina* Schlumberger (1887) was created to hold forms with sigmoid chamber arrangement, i.e., chambers of one-half coil in length arranged as per two in a coil, diverting from true planispirality so that in transverse section two sigmoidal series of chambers can be seen (at least for the inner portion). Schlumberger (1887) included *sigmoidea* Brady, *celata* Costa (sensu Brady, 1884), *edwardsi* Schlumberger, *secans* d'Orbigny, and *tenuis* Czjzek in his new genus.

It should be noted that Schlumberger (1887) used the generic name as *Planispirina* in the descriptions of the taxa in the text, while using either *Sigmoilina* or *Sigmoilina* (*Planispirina*) in the figure captions and plate explanations for the three taxa he examined in that publication (i.e., *sigmoidea* Brady, *celata* Costa (sensu Brady) and *edwardsi* Schlumberger); while using the name *Sigmoilina* for the species he

included in his new genus only at the very end of the paper. Considering that he intended the new supra-specific taxon to be a genus, the names of the said taxa are here referred with his new generic name despite the contrary use in his text.

The five taxa Schlumberger included in his new genus hold a great deal of variety in terms of wall structure (agglutinant incorporation vs. non), lateral chamber wall extension (present to non) and apertural shape and modifications (crescentic like *Biloculinella*, produced on a neck, not-produced). This variety was later subdivided by different authors into several different genera (Table 8.1), such as *Sigmoilopsis* Finlay (1947) for agglutinated forms, and *Sigmoilinita* Seiglie (1965), and *Spirosigmoilina* Parr (1942) for forms with later planispiral arrangement or tendencies and no chamber wall extensions, effectively narrowing the definition of *Sigmoilina*. The narrowed definition, as portrayed by Loeblich and Tappan (1988), then only includes *Sigmoilina sigmoidea* (Brady) from the original five proposed by Schlumberger in this genus.

Loeblich and Tappan (1988) remark in their diagnosis of *Sigmoilina* that the lateral extensions of the chambers cover the earlier chambers obstructing the visibility of the earlier chambers ('involuteness' in a sense) and sutures, producing a biloculine exterior look. Moreover, according to Loeblich and Tappan (1988) the aperture of *Sigmoilina* is with a small tooth, contrary to Schlumberger's (1887) interpretation and depiction of the typetaxon (see further under *Sigmoilina sigmoidea* (Brady) below). Regardless of the apertural character, solely the 'involuteness' of the test, require a significant overhaul of the species currently accepted under *Sigmoilina*, most of which do not possess the 'involute' character. Such an endeavor is out of the scope of the current work.

Nonetheless, here, genus *Sigmoilina* is taken as described by Loeblich and Tappan (1988). The sigmoid taxa without the 'involute' character are transferred under *Sigmoilinita* Seiglie.

Table 8.1. Five daughter taxa of *Sigmoilina* as listed by Schlumberger (1887), prominent changes in generic and specific attribution, and accepted names by WoRMS (2025).

Original	Schlumberger, 1887	Other	Accepted (WoRMS)
Spiroloculina celata Costa (sensu Brady as *Planispirina celata*)	*Sigmoilina celata* (Costa sensu Brady)	*Sigmoilina schlumbergeri* Silvestri: Silvestri, 1904	*Sigmoilopsis schlumbergeri* (Silvestri)
Sigmoilina edwardsi Schlumberger	*Sigmoilina edwardsi* Schlumberger	*Sigmella edwardsi* (Schlumberger): Mikhalevich, 1983	*Novosigmella edwardsi* (Schlumberger)
Quinqueloculina secans d'Orbigny	*Sigmoilina secans* (d'Orbigny)	*Massilina secans* (d'Orbigny): Schlumberger, 1893	*Massilina secans* (d'Orbigny)
Planispirina sigmoidea Brady	*Sigmoilina sigmoidea* (Brady)		*Sigmoilina sigmoidea* (Brady)
Quinqueloculina tenuis Czjzek	*Sigmoilina tenuis* (Czjzek)	See *Sigmoilinita tenuis* (Czjzek) for discussion	*Spirosigmoilina tenuis* (Czjzek)

Sigmoilina sigmoidea Brady, 1884

Plate 45 Figure 15; Plate 46 Figure 20

1884 *Planispirina sigmoidea* – Brady, p. 197, pl. 2 fig. 1-3, t-fig. 5c

1887 *Sigmoilina sigmoidea* (Brady); Schlumberger, p. 476, pl. 7 fig. 9-11

* 1917 *Sigmoilina sigmoidea* (Brady); Cushman, p. 61, pl. 24 fig. 2-3

* 1964 *Sigmoilina sigmoidea* (Brady); Loeblich and Tappan, p. C465 fig. 353.1

1993 *Sigmoilina sigmoidea* (Brady); Sgarrella and Moncharmont Zei, p. 184, pl. 9 fig. 13

2008 *Sigmoilina sigmoidea* (Brady); Sakınç, pl. 8 fig. 9

2014a *Sigmoilina sigmoidea* (Brady); Meriç et al., pl. 33 fig. 8-11

Test nearly circular in frontal view, biconvex. Chambers arranged in sigmoid fashion so that transverse section shows two sets of chambers following a sigmoid curve. Chamber walls extended laterally and cover the earlier chambers so that only two chambers are visible externally. Sutures very slightly depressed if any. Aperture terminal, crescentic, with a semi-circular flap. Test white, opaque; surface smooth, shiny.

Loeblich and Tappan (1988) remark a small tooth for the genus *Sigmoilina*, and hypotype assigned by Loeblich and Tappan (1964) agrees with the original description (Brady, 1884). Brady's (1884) description lacks any detail for the aperture other than "curved transverse orifice"; and illustrations inaccurately depict the aperture with a modification which may be interpreted as a flap or a tooth; same inaccurate depiction of the aperture is repeated in Cushman (1917) and Loeblich and Tappan (1964). Schlumberger's (1887) illustrations, on the other hand, clearly depict an apertural flap, noted as "semi-lunar" in the text. Moreover, the periphery (outer margins of the last two chambers) are noted to be "thin and slightly rounded" by Brady (1884) while depicted as sharply angular in Cushman (1917) and Loeblich and Tappan (1964). Schlumberger, on the other hand, illustrated the periphery as narrowly rounded. One other discrepancy between the original and Schlumberger's interpretation is the overall shape in frontal view which is more circular in Schlumberger (1887) while being more acuminate at the apertural and adapertural poles in the original (and Cushman, 1917; and Loeblich and Tappan, 1964).

Brady noted a genetic relationship between *sigmoidea* and the planispiral taxa *contraria* d'Orbigny and *exigua*. Brady considered the chamber arrangement of *sigmoidea* to be modified-planispiral, but unlike others of the genus (*Planispirina*), with only two chambers per whorl; and asymmetrically involute (lateral chamber extensions only to one side) due to the sigmoid modification of the planispirality. The compared taxa *contraria* d'Orbigny and *exigua* Brady are currently referred

under genus *Nummoloculina* and both taxa are with a semi-circular apertural flap, enhancing the accuracy of Schlumberger's interpretation of the taxon.

Later accounts of the species cited above in the synonym list show forms with a semi-lunar flap, circular outline and rounded periphery, identical to Schlumberger's account of the species. Here, this interpretation of the taxon is followed.

Taxon is distinguished from *Sigmoilinita* by its 'involute' nature. Due to its lensoidal shape and apertural flap it is similar to *Biloculinella* and *Miliolinella*. Yet, *Biloculinella* is usually lensoidal in the opposite plane, and *Miliolinella* has more than two chambers visible externally.

Genus *Sigmoilinita* Seiglie, 1965

1965 *Sigmoilinita* – Seiglie, p. 72

Type: *Quinqueloculina tenuis* Czjzek (1848, p. 149, pl. 13 fig. 31–34)

Test ovate in frontal view; compressed. Chambers arranged in a sigmoid pattern, at least for the initial part, later may become planispiral. Chambers walls without lateral extensions so that earlier chambers and sutures are not obstructed. Sutures distinct. Aperture produced on a neck, may or may not be rimmed.

Spirosigmoilina Parr (1942) and *Sigmoilinita* Seiglie (1965) are two genera with sigmoid to planispiral chamber arrangement with distinct sutures and no lateral chamber wall extensions covering the earlier chambers (as in *Sigmoilina*). *Sigmoilinita* is specified to bear a necked aperture (Seiglie, 1965); while no criteria were set for *Spirosigmoilina*; however, the typetaxon (*Spiroloculina tateana* Howchin) has an arched aperture which is not produced on a neck. Jones (1994) considered *Sigmoilinita* a junior synonym to *Spirosigmoilina*, this view is not followed here due to very different apertural characteristics. Unless the presence of the apertural neck is deemed not a defining character in generic level, these two genera cannot be considered synonyms.

Some taxa, previously attributed to *Sigmoilina* Schlumberger are here transferred to this genus since they lack the 'involuteness' characteristic of that genus.

Sigmoilinita costata (Schlumberger, 1893)

Plate 45 Figure 4; Plate 46 Figure 4

1893 *Sigmoilina costata* – Schlumberger, p. 61, pl. 1, figs. 51, 52; text-fig. 4

1993 *Sigmoilina costata* Schlumberger; Sgarrella and Moncharmont Zei, p. 184, pl. 9 fig. 6-8

Test elongate, slender, compressed. Chambers few, coiled in a slight sigmoid fashion. Sutures deep, distinct. Aperture situated on a long neck, small. Surface with numerous longitudinal costae, otherwise smooth.

This taxon is usually regarded under *Sigmoilina* in the literature; however, here considered to belong to *Sigmoilinita* due to lack of 'involuteness' (see *Sigmoilina* Schlumberger above). The sutures in this taxon and *Sigmoilinita grata* (Terquem) are very well depressed unlike *Sigmoilinita distorta* (Phleger and Parker).

This taxon and *S. grata* are very much alike due to the slender and costate nature of the test; however, the costae on this taxon is much finer, and the spaces between costae are very smooth. Moreover, the aperture of *S. grata* is more pronouncedly rimmed.

Sigmoilinita distorta (Phleger and Parker, 1951)

Plate 45 Figures 5-9; Plate 46 Figures 5-11

1951 *Sigmoilina distorta* – Phleger and Parker, p. 8, pl. 4, figs. 3-5

1993 *Sigmoilina distorta* Phleger and Parker; Sgarrella and Moncharmont Zei, p. 184, pl.9 fig. 5

2008 *Sigmoilina distorta* Phleger and Parker; Kırcı-Elmas et al., pl. 2 fig. 7

Test ovate in frontal view; compressed. Chambers arranged in a sigmoidal fashion, later may become planispiral for a couple of whorls. Chambers low, narrow and elongated. Sutures deep, distinct. Aperture terminal, slightly produced, rounded. Surface smooth, shiny.

This taxon is usually regarded under *Sigmoilina* in the literature; however, here considered to belong to *Sigmoilinita* due to lack of 'involuteness' (see *Sigmoilina* Schlumberger above). The chambers are indeed more embracing than *Sigmoilinita tenuis* (Czjzek), but never truly cover the earlier whorls as in *Sigmoilina sigmoidea* (Brady).

S. tenuis is a very similar form, but is different from this present taxon by having a more pronounced planispiral stage, by being more compressed, and having a dull surface. The surface of the present taxon is very shiny, very similar to the surface of *S. sigmoidea*.

Sigmoilinita grata (Terquem, 1878)

Plate 45 Figure 3; Plate 46 Figure 3

1878 *Sigmoilina grata* – Terquem, p. 55 pl. 5 fig. 14-15

1993 *Sigmoilina grata* Terquem; Sgarrella and Moncharmont Zei, p. 184, pl. 9 fig. 9

Test elongate, slender, compressed. Chambers few, coiled in a slight sigmoid fashion. Sutures deep, distinct. Aperture situated on a long neck, small. Surface with numerous longitudinal costae, otherwise smooth.

This taxon is usually regarded under *Sigmoilina* in the literature; however, here considered to belong to *Sigmoilinita* due to lack of 'involuteness' (see *Sigmoilina* Schlumberger above). The sutures in this taxon and *Sigmoilinita costata* (Schlumberger) are very well depressed unlike *Sigmoilinita distorta* (Phleger and Parker).

This taxon differs from *S. costata* by having a coarser and fewer costae, and having a less smooth surface in between the costae. Moreover, the costae are not perfectly linear and continuous, but have some wiggle and breaks. In addition, the aperture of this taxon is with a clear everted rim.

Sigmoilinita tenuis (Czjzek, 1848)

Plate 45 Figures 10-14; Plate 46 Figures 12-19

1848 *Quinqueloculina tenuis* – Czjzek, p. 149, pl. 13, fig. 31-34

1884 *Spiroloculina tenuis* (Czjzek); Brady, p. 152, pl. 10 fig. 7-11

1951 *Sigmoilina tenuis* (Czjzek); Phleger and Parker, p. 8, pl. 4 fig. 7

1991 *Sigmoilinita tenuis* (Czjzek); Cimerman and Langer, p. 48, pl. 45 fig. 7-10

1993 *Sigmoilina tenuis* (Czjzek); Sgarrella and Moncharmont Zei, p. 185, pl. 8 fig. 8

1994 *Spirosigmoilina tenuis* (Czjzek); Jones, p. 26, pl. 10 figs. 7-11

2008 *Sigmoilina tenuis* (Czjzek); Sakınç, pl. 8 fig. 10-11

2014a *Sigmoilinita tenuis* (Czjzek); Meriç et al., pl. 34 fig. 10-11

Test ovate in frontal view; compressed. Chambers initially arranged in a sigmoidal fashion, later becoming planispiral. Chambers low, narrow and elongated. Sutures deep, distinct. Aperture terminal, slightly produced, rounded. Surface smooth, dull.

Finlay (1947) included *Quinqueloculina tenuis* Czjzek in *Sigmoilopsis*; however, this taxon has very little (if any) agglutinant incorporation in the test, therefore do not belong in that genus.

Sigmoilina distorta Phleger and Parker is a similarly sigmoid form, with less developed planispiral portion and more embracing chambers, less depressed sutures and shinier surface. The juveniles of these two taxa are very similar, but

Spirosigmoilina tenuis juveniles can be distinguished by their dull surfaces, and usually more narrow chambers. The adult form is more akin to *Spiroloculina* with its compressed nature, but the inner sigmoid chambers differentiate this taxon from that genus.

Subfamily Sigmoilopsinae Vella, 1957

Genus *Sigmoilopsis* Finlay, 1947

1947 *Sigmoilopsis* – Finlay, p. 270

Type: *Sigmoilina schlumbergeri* Silvestri (1904, p. 267; type figures in Schlumberger, 1887, pl. 7 fig. 12-14, t-fig. 6-7)

Test oblong in lateral view; somewhat lensoidal; apertural and adapertural poles may be acuminate. Chambers arranged in sigmoid fashion. Sutures usually indistinct. Aperture terminal, rounded, may or may not be developed on a short neck. Wall porcelaneous, with significant amount of agglutinated material incorporated.

Finlay (1947) introduced *Sigmoilopsis* on the basis of wall structure as a genus for taxa previously regarded under Sigmoilina, but with agglutinant incorporation in the porcelaneous test material. *Sigmoilopsis* remains the sole taxon of Subfamily Sigmoilopsinae, distinguished from Subfamily Sigmoilinitinae by agglutinant incorporation in the test (Loeblich and Tappan, 1988). The addition of agglutinated material to the test wall is a widely occurring phenomenon in miliolid taxa (Rigaud and Martini, 2016), and does not always grant supra-specific level distinction, for example some species of *Quinqueloculina* do possess agglutinated coating, while genus *Siphonaperta* is reserved for quinqueloculine forms with agglutinant incorporation. The importance of agglutinant incorporation in porcelaneous tests in phylogeny remains ambiguous, and requires further studies, especially studies run on genetic material (DNA and/or RNA).

Sigmoilopsis sp. 1

Plate 45 Figure 19-21; Plate 46 Figure 26-31

Test ovate with acuminate poles in frontal view; asymmetrically lensoidal in apertural view. Chambers arranged so that they form two sigmoid sets in transverse section, creating the asymmetry in the apertural view. Sutures indistinct. Wall porcelaneous with fine agglutination, mostly composed of light colored grains (calcite and quartz). Aperture terminal, ovate, with a short bifid tooth. Color yellowish, darker for the inner chambers, lighter in the last formed two chambers.

The form is asymmetrically lensoidal just like *Sigmoilina*: the lateral surfaces do not form a strict convex curve, but are somewhat sigmoid themselves reflecting the sigmoidal chamber arrangement. Due to the agglutinated nature of the form the sutures of are indistinct.

Sigmoilopsis schlumbergeri (Silvestri, 1904, p. 267; type figure in Schlumberger, 1887, as *Sigmoilina (Planispirina) celata*, p. 481, pl. 7 fig. 12-14) is the closest taxon; however, it is a significantly large form (up to 2 mm length) as opposed to our specimens of about 250-300 μm length. Therefore, the taxon is here left in open nomenclature. The similarity of our specimens to the illustrations given under *S. schlumbergeri* by Van Morkhoven et al. (1986, p. 57, pl. 18), Phleger and Parker (1951, p. 8, pl. 4, figs. 6), and Cimerman and Langer (1991, p. 48, pl. 46 fig. 10-14) should be noted. Some coarsely agglutinated forms with very distinct necked apertures were incorrectly included in *Sigmoilopsis schlumbergeri* in the literature, they should be referred as *Siphonaperta horrida* (Cushman) (see below).

Subfamily Siphonapertinae Saidova, 1975

Genus *Siphonaperta* Vella, 1957

Siphonaperta horrida (Cushman, 1947)

Plate 45 Figures 16-18; Plate 46 Figures 21-25

1947 *Quinqueloculina horrida* – Cushman, p. 88, pl. 19, fig. 1

1951 *Quinqueloculina horrida* Cushman*;* Phleger and Parker, p. 7, pl. 3 fig. 18-19

1993 *Sigmoilopsis schlumbergeri* (Silvestri); Sgarrella and Moncharmont Zei, p. 185, pl. 9 fig. 4

2008 *Sigmoilopsis schlumbergeri* (Silvestri); Kırcı-Elmas et al., pl 2 fig. 9

2008 *Sigmoilopsis schlumbergeri* (Silvestri); Sakınç, pl. 8 fig. 12

2012 *Siphonaperta horrida* (Cushman); Milker and Schmiedl, p. 52, fig. 13.24

2012 *Sigmoilopsis schlumbergeri* (Silvestri); Milker and Schmiedl, p. 71, fig. 18. 7-8

2017 *Siphonaperta horrida* (Cushman); Al-Wosabi et al., p. 396, fig. 4.12

Test ovate in frontal view; somewhat triangular in section. Chambers with quinqueloculine arrangement. Sutures indistinct. Wall porcelaneous with coarse agglutination with grains of various origin. Aperture produced on a neck, ovate, rimmed, with a short bifid tooth.

In the literature, the taxon was confused with *Sigmoilopsis schlumbergeri* (Silvestri). The coarse agglutination of the wall obscuring the chamber arrangement is probably the main reason for the confusion. However, *Siphonaperta horrida* (Cushman) is somewhat triangular in section: i.e., one side convex, while the other nearly flat, just like most quinqueloculine forms. *S. schlumbergeri*, on the other hand, is asymmetrically biconvex due to sigmoidal coiling (like *Sigmoilina sigmoidea* Brady). Moreover, the coarse agglutination and longer (more pronounced) neck of the taxon distinguishes it from *S. schlumbergeri*. Above cited *S. schlumbergeri*

accounts belong to coarsely agglutinated forms with a distinct neck, which should belong to this taxon instead.

Cushman (1947) described the taxon as small but gave an average dimension of 0.50 μm length. In the examined material, forms of about 150 mm to 600 mm length were present.

Subfamily Tubinellinae Rhumbler, 1906

Genus *Articulina* d'Orbigny, 1826

1826 *Articulina* – d'Orbigny, p. 300

Type: *Articulina nitida* d'Orbigny in Guérin-Méneville (1832, p. 10, pl. 3 fig. 9)

Test elongate, with quinqueloculine initial portion, and following rectilinear portion. Aperture at the end of tubular chamber, rimmed. Surface smooth or longitudinally costate.

Articulina tubulosa (Seguenza, 1862a)

Plate 47 Figures 1-5; Plate 48 Figures 1-5

1862a *Quinqueloculina tubulosa* – Seguenza, p. 119, pl. 2, fig. 8, 8a, 8b

1981 *Articulina tubulosa* (Seguenza); Mullineaux and Lohmann, pl. 3 fig. 8-9

1984 *Articulina tubulosa* (Seguenza); Ross and Kennett, pl. 1, fig. 7-8

1993 *Articulina tubulosa* (Seguenza); Sgarrella and Moncharmont Zei, p. 190, pl. 10 fig. 11

Test elongate. Initially coiled in a quinqueloculine pattern, later chambers rectilinear. Chamber margins angular in quinqueloculine section. Rectilinear chambers tubular, with circular transverse section, the widest point near the suture, thinning upward. Sutures distinct. Aperture a wide neck between coiled and uncoiled sections, the end

of tubular chamber for the rectilinear chambers. Test locally translucent, surface smooth.

This taxon is common in deep water assemblages (Sgarrella and Moncharmont Zei, 1993 and references therein).

Genus *Rectospiroloculina* McCulloch is similar, but has a spiroloculine initial portion, instead of quinqueloculine.

Form is quite fragile and rarely found as complete. The rectilinear chambers are dislodged easily, and found in samples separate from the initial quinqueloculine stage. The initial portion of the test can be distinguished from other quinqueloculine forms by the wide necked aperture.

Family Spiroloculinidae Wiesner, 1920

Genus *Spiroloculina* d'Orbigny, 1826

1826 *Spiroloculina* - d'Orbigny, p. 298

Type: *Spiroloculina depressa* d'Orbigny (1826, p. 298 n° 1)

The form is fusiform with chambers which are truncated so that the form has two carinated edges on both sides. The chamber arrangement is planispiral in the adult phase and evolute. The aperture is slightly produced. According to the thickness of the chambers and the height/width ratio of the form I hesitantly classify these under this taxon.

Spiroloculina cymbium d'Orbigny, 1839c

Plate 47 Figure 7; Plate 48 Figure 7

1839c *Spiroloculina cymbium* – d'Orbigny, p. 140 pl. 3 fig. 5-6

1991 *Spiroloculina cymbium*, d'Orbigny; Cimerman and Langer, p. 29, pl. 22 fig. 1-4

1993 *Spiroloculina rostrata* Reuss; Sgarrella and Moncharmont Zei, p. 169, pl. 5 fig. 5

2008 *Spiroloculina cymbium* d'Orbigny; Sakınç, pl. 4 fig. 1-2

Test ovate in frontal view, longer than wide, with apertural and adapertural poles acuminate; discoidal, thin, with truncated edges. Chambers coiled in spiroloculine fashion, quadrate in section, not embracing. Chamber thickness (dimension parallel to axis of coiling) increases very gradually so that the two faces of the test are very slightly concave. Outer chamber edges truncate and slightly concave, margins carinate. Sutures vaguely distinct, thinly and shallowly depressed. Aperture terminal, produced on a neck. Surface slightly roughened by shallow grooves.

The original description of *Spiroloculina cymbium* is more exaggerated in terms of the concave faces and edges. The concavity in the examined specimens are very slight. *Spiroloculina communis* Cushman and Todd and *Spiroloculina angulosa* d'Orbigny in Fornasini are similarly necked taxa with concave faces; the concavity is even more pronounced in both of them. *Spiroloculina dilatata* d'Orbigny is also similar, but the faces are flat in that taxon, and the aperture is not necked.

Sgarrella and Moncharmont Zei (1993) attributed identical specimens to *Spiroloculina rostrata* Reuss. That taxon is described by Reuss to have one longitudinal groove on the faces of the last two chambers, which is missing in Sgarrella and Moncharmont Zei's (1993) specimen.

The taxon is distinguished from other *Spiroloculina* by its rough surface and very shallow sutures.

Spiroloculina excavata d'Orbigny, 1826

Plate 47 Figures 8-10; Plate 48 Figures 8-11

1826 *Spiroloculina excavata* – d'Orbigny, p. 271, pl. 16, figs. 19-21

1991 *Spiroloculina excavata,* d'Orbigny; Cimerman and Langer, p. 30, pl. 23 fig. 1-3

2012 *Spiroloculina excavata,* d'Orbigny; Milker and Schmiedl, p. 50, fig. 13. 3-4

2014a *Spiroloculina excavata,* d'Orbigny; Meriç et al., pl. 14 fig. 4-8

Test near circular in frontal view, with apertural and adapertural poles only slightly acuminate; discoidal, thick, with truncated edges. Chambers coiled in spiroloculine fashion, quadrate in section, not embracing. Chamber thickness (dimension parallel to axis of coiling) increase as chambers are added, so that the two faces of the test are concave. Outer chamber edges truncate and flat, margins distinctly carinate. Sutures limbate, vaguely distinct, somewhat depressed. Aperture terminal, oblique to the long axis, almost in line with the outline of the test, with a distinct, bifid tooth. Surface smooth.

Taxon is easily distinguished from other *Spiroloculina* by its thick, near circular test, and distinctly concave faces.

Spiroloculina tenuiseptata Brady, 1884

Plate 47 Figures 11-12; Plate 48 Figures 12-13

1884 *Spiroloculina tenuiseptata* – Brady, p. 153, pl. 10 fig. 5 (?6)

1991 *Spiroloculina tenuiseptata* Brady; Cimerman and Langer, p. 31, pl. 24 fig. 6-9

2012 *Spiroloculina tenuiseptata* Brady; Milker and Schmiedl, p. 50, fig. 13.7-8

2014a *Spiroloculina tenuiseptata* Brady; Meriç et al., pl. 15 fig. 1-7

Test elongate, longer than wide, with acuminate apertural and adapertural poles; discoidal, thin, with truncated edges. Chambers coiled in spiroloculine fashion, quadrate in section, not embracing, thin (in the radial dimension). Chamber thickness (dimension parallel to axis of coiling) increase gradually as chambers are added, so that the two faces of the test are concave. Outer chamber edges truncate and flat,

margins distinctly carinate; carina significantly elevated. Sutures depressed. Aperture terminal, produced, oblong. Surface somewhat rough.

The original description (Brady, 1884, fig. 6) show a form whose last whorl is detached. This may be an aberrant form belonging to this taxon, or may be a different taxon.

The taxon is distinguished from other *Spiroloculina* with significantly elevated carina.

Spiroloculina sp. 1

Plate 47 Figures 13-14; Plate 48 Figures 14-15

Test ovate in frontal view, longer than wide; discoidal. Chambers coiled in spiroloculine fashion, quadrate in section with rounded corners, not embracing. Chamber thickness (dimension parallel to axis of coiling) increase slowly as chambers are added, so that the two faces of the test are slightly concave. Outer chamber edges truncate but somewhat rounded, margins rounded, not carinate. Sutures depressed. Aperture terminal, oblique to the long axis, very slightly produced, almost in line with test outline; with a small tooth. Surface smooth.

The taxon is tentatively placed under *Spiroloculina,* however may belong to another genus since it does not possess the characteristic carinate edges.

Taxon is different from other *Spiroloculina* by its rounded, not carinate edges.

SUBORDER NUBECULARIINA Jones in Griffith & Henfrey, 1875

Superfamily Nubecularioidea JONES IN GRIFFITH & HENFREY, 1875

Family Ophthalmidiidae Wiesner, 1920

Genus *Cornuloculina* Burbach, 1886

Cornuloculina inconstans (Brady, 1879)

Plate 47 Figure 6; Plate 48 Figure 6

1879 *Hauerina inconstans* – Brady, p. 267

1884 *Ophthalmidium inconstans* Brady; Brady, p. 189, pl. 12 fig. 5, 7-8

1994 *Cornuloculina inconstans* (Brady); Jones, p. 27, pl. 12 fig. 5, 7-8

Test discoidal, very thin, near circular in frontal view. Chambers very low, about one-half coil in length; coiled around the proloculus planispirally. Chambers with thin and wide peripheral extension, producing wide depressed areas in between whorls, and an outer keel. Chamber height increases towards the aperture. Aperture open end of chamber (?) with two longitudinal, short partitions.

The form is always found as damaged, especially so for the thin outer keel. Brady (1884) describes mature specimens to have more than two chambers in the later whorls. The specimens examined in this study are pre-adult individuals with maximum of two chambers per whorl in the outermost whorls.

The taxon differs from all other miliolids by its very thin discoidal shape.

ORDER SPRIRILLINIDA Hohenegger & Piller, 1975

SUBORDER AMMODISCINA Mikhalevich, 1980

Superfamily Ammodiscoidea Reuss, 1862b

Family Ammodiscidae Reuss, 1862b

Subfamily Usbekistaniinae Vyalov, 1968

Genus *Glomospira* Rzehak, 1885

Glomospira charoides (Jones and Parker, 1860)

Plate 39 Figures 22-25; Plate 40 Figures 28-31

1860 *Trochammina squamata* Jones and Parker var. *charoides* – Jones and Parker, p. 304

1884 *Ammodiscus charoides* Jones and Parker; Brady, p. 334, pl. 38, fig. 10-16

1947 *Glomospira charoides* Jones and Parker; Höglund, p. 129, pl. 3 fig. 11, tf. 103

1991 *Repmanina charoides* (Jones and Parker); Cimerman and Langer, p. 17, pl. 3 fig. 6-9

2005 *Glomospira charoides* Jones and Parker; Panieri et al., pl. 1 fig. 7

2012 *Repmanina charoides* (Jones and Parker); Milker and Schmiedl, p. 32, fig. 9.6-7

Test small, globular, composed of a second tubular chamber coiled around a proloculus. Coiling is as a tight spiral forming almost a sphere around the proloculus, then turning coiling direction for another layer of spiral coiling. The last layer may or may not be completely covering the whole test. Tube inner cross section rounded. Sutures (between adjacent whorls) are very slightly depressed if any. Aperture open end of tube. Wall finely agglutinant in a red-brown cement. Surface smooth. Color red.

This taxon is very rare in the Sea of Marmara, found only in the Central Deep in this study.

Taxon is easily distinguished from others by its red color, almost spherical shape and very small size. It is usually found as damaged.

Glomospira gordialis (Jones and Parker, 1860)

1860 *Trochammina squamata* Jones and Parker var. *gordialis* – Jones and Parker, p. 304

1884 *Ammodiscus gordialis* Jones and Parker; Brady, p. 333, pl. 38, fig. 7-9

1991 *Glomospira gordialis* (Jones and Parker); Cimerman and Langer, p. 17, pl. 3 fig. 4-5

2005 *Glomospira gordialis* Jones and Parker; Panieri et al., pl. 1 fig. 8

Test nearly discoidal, composed of a second tubular chamber coiled around a proloculus. Coiling streptospiral at first, later tending to be planispiral but still irregular. Tube inner cross section rounded; sutures (between adjacent whorls) depressed. Aperture open end of tube. Wall finely agglutinated in a reddish-yellowish cement. Surface smooth. Color red-yellow.

This taxon is very rare in the Sea of Marmara, found only in the Central Deep in this study.

Taxon is easily distinguished from others by its red to yellow color, and spherical to discoidal irregular shape.

SUBORDER SPIRILLININA Hohenegger & Piller, 1975

Family Patellinidae Rhumbler, 1906

Subfamily Patellininae Rhumbler, 1906

Genus *Patellina* Williamson, 1858

Patellina corrugata Williamson, 1858

Plate 39 Figures 19-21; Plate 40 Figures 25-27

1858 *Patellina corrugata* – Williamson, p. 46, pl. 3, figs. 86–89, 89a

1884 *Patellina corrugata*, Williamson; Brady, p. 634, pl. 86, fig. 1-7

1991 *Patellina corrugata*, Williamson; Cimerman and Langer, p. 24, pl. 14 fig. 7-12

2008 *Patellina corrugata*, Williamson; Sakınç, pl. 2 fig. 7-8

2014a *Patellina corrugata*, Williamson; Meriç et al., pl. 7 fig. 10-12

Test circular in outline, sometimes oblong; conical with convex spiral side and concave umbilical side; edge sharply angular. Juvenile test is a coiled, undivided tube, as in *Spirillina*, but later trochospiral with two chambers per whorl. Chambers crescentic, with internal radiate partitions starting from the outer margin of the chamber but not reaching the umbilical margin. Umbilicus concave, closed by lamellae of successive chambers; rimmed by the last two crescentic chambers; a spiral groove present at the umbilicus on the covering lamellae per each chamber visible. On the spiral side, the portion of the outer margins of the chambers which sit between whorls are slightly raised, intercameral parts (between two successive chambers of the same whorl) less distinct. Spiral surface finely pitted (porous?) except for the non-porous raised sutures; on the umbilical side of the chambers, internal partitions provide radial ripples along the edge, umbilical lamellae non-porous, smooth. Internal partitions limbate, flush with the test on the spiral side, very well observed under reflected light.

Patellina formosa Heron-Allen and Earland (1932, p. 406, pl. 13, figs 23-25) is a similar taxon, but has a larger undivided tube portion; moreover, the initial tube in that taxon has internal partitions.

Family Spirillinidae Reuss & Fritsch, 1861 (fide Loeblich and Tappan, 1988)

Genus *Spirillina* Ehrenberg, 1843

Tightly planispirally coiled undivided hyaline tube.

Spirillina vivipara Ehrenberg, 1843

Plate 39 Figures 16-17; Plate 40 Figures 21-22

	1843	*Spirillina vivipara* – Ehrenberg; p. 422, pl. 3, vii Vera-Cruz, fig. 41
part	1884	*Spirillina vivipara* Ehrenberg; Brady, p. 630, pl. 85 fig. 1-4 (not fig. 5)
?part	1915	*Spirillina vivipara* Ehrenberg; Heron-Allen and Earland, p. 683, pl. 51, fig. 19-21 (not fig. 22-23)
	1991	*Spirillina vivipara* Ehrenberg; Cimerman and Langer, p. 24, pl. 14 fig. 4-6
	1993	*Spirillina vivipara* Ehrenberg; Sgarrella and Moncharmont Zei, p. 226, pl. 20 fig. 2
	2008	*Spirillina vivipara* Ehrenberg; Sakınç, pl. 2 fig. 6
non	2014a	*Spirillina vivipara* Ehrenberg; Meriç et al., pl. 7 fig. 8-9

Test circular, discoidal, both sides planar; composed of a planispirally coiled tube, non-septate. Edge rounded, slightly sloping; curved on the spiral side, flatter on the umbilical side, so that the widest part of the test is closer to the umbilical side. Both sides evolute, spiral side a little more embracing (due to the sloping of the outer edge of tube) producing the illusion of a slight convexity; umbilical side completely flat. Spiral suture shallowly depressed on the spiral side, flush on the umbilical side. Aperture as open end of the tube, apertural plane slightly oblique to the plane of coiling so that the opening is visible on the umbilical side but invisible on the spiral side. Test coarsely and densely porous on umbilical side, producing a rough surface, making the test translucent; porosity sparse on the spiral side, surface smooth other

than some radial ripples (growth lines?) which are more prominent on the last whorl, more transparent.

The porosity of the surface and the concavity of the sides are variable features. Cimerman and Langer (1991) provide illustrations for a form with a planar spiral side and a more densely perforate spiral side, while Brady includes forms with slightly concave umbilical (fig. 2) or spiral (fig. 3) sides alike into the taxon. Meriç et al. (2014a) illustrate specimens with distinctly angular margins (truncate periphery) which do not belong in this taxon and should be referred to *Spirillina limbata* Brady instead. Heron-Allen and Earland's depiction of the taxon (1915, p. 683, pl. 51, fig. 19-21; not fig. 22-23) is more concavo-convex with the umbilical side being concave and only a couple of whorls clearly illustrated; this specimen, too, may be unrelated to this taxon, and may be evaluated in the synonymy of *Spirillina* sp. 1 below.

Taxon is easily distinguished by its large diameter with respect to very low thickness, discoidal shape and glossy, mostly transparent test.

In the studied material some *Spirillina* with slightly convex spiral sides were also obtained. They are not included in this taxon due to their convex spiral side, instead they were identified only to generic level as *Spirillina* spp.

Spirillina sp. 1

Plate 39 Figures 14-15; Plate 40 Figures 23-24

?part 1915 *Spirillina vivipara* Ehrenberg; Heron-Allen and Earland, p. 683, pl. 51, fig. 19-21 (non fig. 22-23)

Test small, circular, may be slightly oblong, discoidal, umbilical side slightly concave; composed of a planispirally coiled tube, non-septate. Edge rounded. Coiling turns slightly downward for the last whorl. Spiral side as in *Spirillina vivipara*; umbilical side with only a few whorls visible at the outer margin, innermost part visible at the concave umbilicus. Spiral suture shallowly depressed on the spiral

side, flush on the umbilical side. Aperture not distinguished, but probably opens toward the umbilicus. Test coarsely and densely porous on both sides, surface smooth other than the porosity, transparent, shiny.

Above diagnosis, especially with regard to the coiling type, fits well under the description of *Turrispirillina*, as well as they may be juvenile *Spirillina*. Therefore, since only juvenile (small) individuals were recovered, the affiliation of these forms cannot be confidently put: they are left in open nomenclature.

CHAPTER 9

DISCUSSION AND CONCLUSION

9.1 Environmental preferences of selected taxa identified in this study

Bolivina spathulata, and most other bolivinids are considered to be tolerant to low- to suboxic conditions and high organic content in the sediment due to their ability to live infaunally (e.g., Corliss, 1985; Jorissen, 1987; Kaiho, 1994). These taxa are usually found in deeper settings, where other, less hypoxia tolerant taxa cannot live and compete with these opportunistic forms. Bolivinids are abundant in most locations in the Sea of Marmara, especially so in the outer shelf and deeper environments (Kaminski et al., 2002; Phipps et al., 2010, see Chapter 5) where permanent suboxic conditions are present.

Cassidulinids are similarly widely considered opportunistic and infaunal (e.g., Corliss, 1985; Jorissen, 1987; Kaiho, 1994). *Paracassidulina minuta* is found to be very abundant and even dominant in some stations in this study, especially in the deep Çınarcık Basin; however, the taxon was distinguished only by a few studies (see Chapter 5), and most likely was recorded under the name *Cassidulina crassa* (Kaminski et al., 2002), or possibly even lumped with *Cassidulina laevigata*. The latter was found to be abundant only on some shelf stations in this study (e.g., MM50), but some of the stations (30-150 m) from the literature (e.g., Kırcı-Elmas, 2013) include very abundant (up to ~30%) *Cassidulina laevigata*.

B. spathulata, *Bolivina* cf. *vadescens*, and *P. minuta* are the three most dominant taxa among the studied samples (see Chapter 3). Their distribution in the studied samples, all from water depths deeper than 50 m, is not fully controlled by any of the environmental variables examined in this study (bottom depth, bottom water dissolved oxygen, bottom water and pore water nitrite, pore water phosphate and ammonium, Table 3.7) according to the CCA analyses (see Section 3.5, Figure 3.17,

Figure 3.18). However, the relative abundance of *P. minuta*, especially, creates a distinction between the two clusters of samples (see Section 3.4). On the other hand, the lack of identification of the form in the literature (see Chapter 5), prevents the exploration of its true geographic distribution. The highest abundances of *P. minuta* occur in the two samples of station 45C (>30%, deep Çınarcık Basin), therefore in the CCA analyses, the taxon is located in the direction of bottom depth (Figure 3.17, Figure 3.18).

The abundance and size of *Melonis barleeanum* were found to be related to organic matter enrichment (Caralp, 1989a); the taxon prefers somewhat altered organic matter (Caralp, 1989b). The taxon is found to be abundant in areas of active bottom currents (Murray, 1984). Although they were treated separately in the meta-analysis (Chapter 5) *Melonis barleeanum* is here regarded to be synonymous with *Melonis pompilioides* (following Van Morkhoven et al., 1986). In the deep Central and Çınarcık basins, these taxa (either one or both) were recorded to be abundant (Alavi, 1988; Kırcı-Elmas, 2006; Kırcı-Elmas et al., 2008, this study). *M. pompilioides* individuals recovered from the K51.2K09 core (Central Basin) are especially large with respect to other stations. However, the TOC content of the station is below average (1.25 μM, Ergin et al., 1993, Table 3.7), therefore the abundance of this taxon in this station is less likely to be related to organic matter enrichment and more likely to be related to the type of organic matter (i.e., labile or refractory/altered) or bottom current activity. Here, Murray's remark about the active bottom currents should be taken with caution, since the overall the circulation in the deep basins in the Sea of Marmara is quite limited; however, considering the proximity of the Central Basin to the Dardanelles (source of saline waters and deep circulation), and the faster renewal of bottom waters in the Central Basin with respect to the Çınarcık Basin (Beşiktepe et al., 1994), the higher abundances of this deep sea taxon in the west is plausible. *M. pompilioides*'s abundance is especially high in 4 and 8 cm samples of the core, along with *Bulimina inflata*. Two other taxa, although with lower abundances *Sigmoilopsis* sp. 1 and *Sigmoilinita tenuis* occur together with *M. pompilioides* and *B. inflata* in the Central Basin station K51.2K09. These two taxa

are of higher abundances also in the Imralı Basin station K40K46, and to some extent in Station 8 and 45C, accompanying *M. pompilioides*. Co-occurring of these taxa wih *M. pompilioides* may mean that they have similar environmental preferences and are in competition with each other.

Rectuvigerina phlegeri is known to prefer sandy substrates (e.g., Frezza and Carboni, 2009) and is most abundant in station MM-50 with about 10% sand content in the core-top sample. Another notable occurrence of this taxon (2.6% in core-top sample) is in station 2, where gravel size coated grains are abundant. According to the CCA analyses (Figure 3.17, Figure 3.18), the optimum abundance of this taxon occurs in sites with higher dissolved oxygen and bottom water nitrite.

Virgulinella fragilis, although it also may inhabit well-ventilated environments, thrives, and sometimes dominates anoxic and sulfidic bottom water conditions, especially in and around sulfate oxidizing bacterial mats (such as *Beggiatoa*) (e.g., Bernhard, 2003; Erbacher and Nelskamp, 2006; Leiter and Altenbach, 2010; Takata et al., 2003, 2005a, 2005b, 2006, 2014; Cardich et al., 2012). The species is found to host kleptoplasts, and symbiotic sulfate-reducing bacteria (Tsuchiya et al., 2015), these endobionts give *V. fragilis* the opportunity to inhabit wide ranges of environmental gradients (Bernhard and Bowser, 2008; Bernhard et al., 2018; Tsuchiya et al., 2015). The taxon was recorded in the live assemblage from a core from the Central High (Fontanier et al., 2018, 8.5% in the core-top sample), and was present in a few of the studied samples in this study, only as one or two individuals except for in the Izmit-deep core (Karamürsel Basin) where it dominates the assemblage (i.e., >15%) in samples 2, 3, 4, 6, 8 cm. The basin has sulfidic bottom water conditions (Alımlı, 2022) which became prevalent after the '99 earthquake (see Chapter 7), allowing this opportunistic species to become more abundant while the other, less tolerant taxa were eliminated from the assemblage.

Stainforthia fusiformis is an opportunistic form which is present and abundant in low-suboxic and organic enriched basins and physically disturbed sediments, indicative of rapidly changing conditions, especially abundant in NW Europe

shelves, especially in fjords (Alve, 1994, 2003; Koho and Piña-Ochoa, 2011). This taxon sequesters chloroplasts from diatoms (Bernhard and Bowser, 1999) and can colonize previously anoxic environments rapidly. *S. fusiformis* is quite rare in the Sea of Marmara, recorded only in this study, usually with abundances <1%. Its highest abundance is in the Izmit-deep core, in samples 6 and 8 cm (8.3%, 6.8% respectively). These samples are very poor in terms of benthic foraminifera, and the occurrence of *S. fusiformis* along with *V. fragilis* is indicative of the anoxic – sulfidic conditions.

9.2 Changes in the vertical dimension for the studied cores

No significant changes were discovered in the majority of the cores in terms of changes in the benthic foraminiferal assemblage, absolute abundances of BF and PF, ratio of planktonic foraminifera in total foraminifera assemblage (P%) and sand content of the samples. Five stations, however, showed some changes along the core. These were interpreted in terms of changes in the depositional and environmental setting.

9.2.1 Station 8

Station 8 core from the Çınarcık Basin, to the north of Armutlu Peninsula, includes a shift in assemblage in terms of the relative abundances of *Sigmoilopsis* sp. 1 and *Siphonaperta* spp. and bolivinids (Figure 4.8). In the bottom half of the core these taxa, along with other miliolids are more abundant and they decrease towards the top of the core as bolivinids increase in abundance. *Sigmoilopsis* sp. 1 is found with *Sigmoilinita tenuis*, *Melonis pompilioides*, and *Bulimina inflata* in the Imralı Basin (K40K46) and the deep Central Basin (K51.2K09), and may be in competition with these taxa, sharing similar preferences, showing a change in food quantity and quality upwards. In addition, P% is higher in the lower part of the core, decreasing upwards (Table 4.3). Since planktonic foraminifera are heterotrophic, they are easily

affected by primary productivity, and a decrease in P% (ratio of planktonic foraminifera in total foraminifera) may signal a drop in primary productivity which in turn means less organic flux to the basin floor, and in turn decreasing abundances of the mentioned taxa. A similar approach was formulated by Berger and diester-Haass (1988) for use of BF/PF ratio for paleoproductivity applications. A more in-depth analysis concerned with primary productivity, organic flux to the sea bottom and the abundances of these taxa is a necessary next step.

9.2.2 45C-2

The core from the Çınarcık Basin have a shift in assemblage around the 15 cm sample (Figure 4.11). Below, the assemblage is similar to the top half of the core from the Central Basin (K51.2K09) with abundant *M. pompilioides* and some (only up to 2.9% in the 40 cm sample) *B. inflata*. From bottom to 15 cm *M. pompilioides* decreases significantly, while *Paracassidulina minuta* and bolivinids increase in abundance. The shift in the assemblage at 15 cm sample is accompanied by slightly increased sand content (Sand%= 2%), and the bottom half of the core is higher in P% as well. In addition, in the bottom half, Discorboidea (e.g., *Valvulineria bradyana*), miliolids and Rotaloidea are more abundant with respect to the upper half. This shift from a *Melonis* assemblage to a *P. minuta* assemblage may indicate a gradual change in the quantity and quality of food reaching the basin floor (see previous section 9.1).

9.2.3 Izmit-deep

Izmit-deep core, explored in detail in Chapter 7, situated at the floor of the Karamürsel Basin (Izmit Bay), is significantly different from all other studied stations due to i. very low BF and PF abundance in the top 8 cm of the core, ii. low diversity in terms of species richness and ii. presence and abundance of *V. fragilis*, an opportunistic taxon which persists under sulfidic conditions. From bottom to top,

the assemblage changes from being quite similar to normal deep water (outer shelf and deeper) Marmara assemblage, to being low diversity and low abundance, *V. fragilis* dominated assemblage (Figure 4.12). The change in assemblage, combined with the radiocarbon dating results, grain size, P% and BF and PF absolute abundances, the depositional history of the core was interpreted to be that of a thick turbiditic deposit, winnowed (eroded) for the most part, creating a hiatus, overlain by another turbiditic deposit inferred to belong to '99 earthquake after which the prevalent sulfidic bottom water condition was established.

A similar approach in the detection of turbidites via foraminiferal quantitative data was applied by Hayward et al. (2019b). In their study, the numbers of BF in different size fractions were obtained and compared. Although no such size fractionation was carried out in this study, the results obtained from the Izmit-deep core show that the quantitative foraminiferal data may prove useful in such applications.

9.2.4 K40K46

The station in the Imralı Basin (K40K46), is different from all other studied stations due to high abundances of *Sigmoilinita tenuis* and *Sigmoilopsis* sp. 1 (Figure 3.9). These two exchange abundances upcore, but, both of them decrease from the bottom of the core towards the sample 8 cm while bolivinids increase in abundance; above 8 cm the opposite occurs (Figure 4.13). Similar high abundances of *S. tenuis* and *Sigmoilopsis schlumbergeri* (may be synonymous with *Sigmoilopsis* sp. 1) were recorded from the deep Central and Çınarcık basins (Alavi, 1988; Kırcı-Elmas, 2006; Kırcı-Elmas et al., 2008). In K51.2K09 these taxa accompany the *Melonis pompilioides* assemblage (see below). In the Imralı Basin, *M. pompilioides* is present, but not as abundant. *S. tenuis* and *Sigmoilopsis* sp. 1 may be in competition with each other, and *M. pompilioides*, and may have similar preferences in terms of food quality and quantity. Then, the shift in assemblage from bottom to 8 cm may indicate a decrease in food influx to the bottom, and from 8 cm to top, an increase. In the core, from bottom to 8 cm a decrease, then to top, an increase in P% is also

seen (Table 4.3). As in Station 8, the P% data supports the change in food quantity interpretation.

9.2.5 K51.2K09

The core from the Central Basin (K51.2K09, Figure 4.16) is different from most other stations in terms of benthic foraminiferal assemblage which includes high abundances of *M. pompilioides* and *B. inflata* especially so in the top three samples (1, 4, 8 cm). Downcore, the abundances of these forms decrease, and instead bolivinids and cassidulinids increase. This may be a result in the change of bottom circulation, since *M. pompilioides* and *B. inflata* are more abundant in areas were bottom currents are more active (Murray, 1994), or a change in the quantity and quality of food reaching the deep basin.

9.2.6 MM50

In the core from the central Southern shelf (MM50, Figure 4.17), an increase in *Rectuvigerina phlegeri* in the top two samples (1, 4 cm), accompanied by a decrease in miliolids, especially *Quinqueloculina stalkeri*, is seen. *R. phlegeri* is known to be more abundant in sediments with higher sand content (e.g., Frezza and Carboni, 2009), indeed, the sand content (Sand%) is higher in the top two samples. The two nearby grab samples of Kırcı-Elmas (2013) also have somewhat higher relative abundances of *R. phlegeri* than most other stations in the SoM, yet, not abundant (i.e., <5%). The relationship of this taxon with grain size may indicate a higher sediment influx from the Çapraz Stream for the top part of the core.

9.3 Need for taxonomic review and establishment of a solid framework

In Chapter 5 a detailed meta-analysis of the literature of the quantitative benthic foraminiferal studies in the SoM is presented. The lack of reporting of the initial

sample sizes (Phipps et al., 2010, SoM_02) or the split amounts (Phipps et al., 2010, SoM_02), or reporting of only the weight or volume of the samples either wet or dry (e.g., Alavi, 1988, SoM_13; Avşar, 2010, SoM_08) or only the relative abundances (Kırcı-Elmas, 2013, SoM_07) prevents the usage of the data in terms of absolute abundances for comparisons between studies and stations. Therefore, the compiled data was analyzed only in terms of the BF assemblages, i.e., the relative abundances of taxa, resulting in 15 distinct stations clusters (Figure 5.10), allowing the determination of several biofacies belts. However, more importantly, the analysis showed differences in methodologies and reporting of data and the lack of a cohesive taxonomic framework.

The studied size fractions in the analyzed publications were either coarser than 125 μm or 63 μm. The cluster dendrogram in Figure 5.10 shows that the studied size fraction has no major effect on the grouping of stations. Since Bray-Curtis dissimilarity index used in the cluster analysis is inherently weighted by the relative abundances of taxa, the majority of the dissimilarity is produced by the differences in relative abundances of very highly abundant taxa: i.e., the clusters are formed around very dominant (>30%) and dominant (15-30%) taxa. The rare taxa are less significant in this approach. Most of the dominant and very dominant taxa are also relatively larger in size, their abundance can only increase in the 125 μm fraction due to the underestimation of (loss of) smaller taxa. For example, *Eilohedra vitrea*, a widely distributed taxon, mostly of rare abundances, is recorded in the core-top samples of this study, conducted from >63 μm fraction, as having a maximum of 4.1% (SoM_TS_1_19, Izmit Bay) abundance. Phipps et al. (2010), on the other hand, in their study from the size fraction >125 μm, only recorded this taxon up to 2.4% (SoM_02_11, just outside of Erdek Bay). Indeed, this difference is small, and cannot be surely and fully attributed to the size fraction difference. Although, when combined, such small differences in the relative abundances of the small taxa may add to significant differences. There is no way of assuming or generalizing how much of a difference analyzed size fraction can produce without conducting counting on both fractions in the same sample and comparing directly. Kırcı-Elmas (2013)

previously conducted quantitative analysis on the two size fractions separately and stated that the assemblage composition was not affected by the size fractions.

The counting methods and initial sample sizes vary among the studies analyzed (Table 5.1). Most of the studies either used the whole samples, or split the samples to obtain aliquots of about 300 benthic foraminiferal individuals and reported directly or as normalized counts, but always as the whole for the studied size fraction. The opposite was carried out by Alavi (1988, SoM_13) where he studied size fractions separately, and reported the sum of the separate fractions without normalizing to the initial sample size. This approach was to diminish the dominance of the small but abundant taxa, somewhat akin to a biomass calculation. Yet, this approach overestimates the dominance of already dominant and already large taxa, e.g., *Bolivina spathulata* while the truly dominant smaller taxon *Paracassidulina minuta* is heavily underestimated. The latter was found to be very dominant (>30%) in both samples from the Çınarcık Basin (45C-1, 45C-2) in this study; however, in Alavi (1988) it is only 4.6% and 8% abundant in the two cores from the same area. This difference in the counting methodology provides a big difference in the data and plots these two stations as a different cluster (cluster C6, Figure 5.10).

Another checked methodology difference is the evaluation of live, dead or undifferentiated assemblages. Usually, in ecology-focused studies, the use of "live" foraminifera is advised (e.g., Schönfeld et al., 2012; Jorissen et al., 2018) since the undifferentiated fauna can be altered by many processes, for example winnowing, down slope transport, vertical mixing etc. Nonetheless, many publications state, somewhat assumingly, the similarity of the live assemblage to the undifferentiated. In the SoM, only one of the analyzed studies was done on "live" assemblages (rose Bengal stained individuals), one on dead assemblages (non-stained individuals) and the rest of the studies were done on undifferentiated assemblages. The only two stations in which live foraminiferal assemblage was studied belong to Fontanier et al. (2018, SoM_01), and is drastically different from all other stations (Figure 5.10). The assemblages in both cores are dominated by *Bolivina vadescens*, and only three and ten more taxa were recognized in the two stations, effectively making these

assemblages two of the least diverse in the whole SoM. The only study of dead assemblage is Phipps et al. (2010, SoM_02) who studied a transect from the Erdek Bay to open Southern shelf to slope (stations 1 to 101 from near shore to offshore). The stations belonging to SoM_02 are grouped in five different clusters/subclusters: station 1, the most inner shore station in cluster 2 along with several other near-shore stations (of Kırcı-Elmas, 2013, SoM_07); station 2, by itself makes up the cluster 14; stations 3-8 are grouped in cluster 15 with one other Erdek Bay station (of Kırcı-Elmas, 2013, SoM_07); stations 9-91, outside Erdek Bay, down to 130 m water depth, are grouped in subcluster 13c; and stations on the slope (92-101) are grouped in subcluster 12a with two stations of Kaminski et al. (2002, SoM_11) from the Prince Islands shelf and central Southern slope. Incorporating of other stations from other studies with Phipps et al.'s stations (2010) show that the dead assemblage differs little from the undifferentiated one. Indeed, the relative abundance of rB stained individuals was found to be maximum 8% by Phipps et al. (2002), and 10% by this study in the deep Central basin station (K51.2K09); these numbers would barely affect the assemblage compositions.

What is curious, though, is the absence of other Erdek Bay stations (in Kırcı-Elmas, 2013, stations 11c, 12b and 12c, SoM_07; Avşar et al., 2006, SoM_12) in the clusters/subclusters with Phipps et al.'s stations (2010, SoM_02). Instead, the rest of the SoM_07 stations are found in subcluster 13b with northern shelf stations, and almost all stations of SoM_12 are clustered in subcluster 13a. Even the very geographically close stations (e.g., SoM_07_11c, SoM_02_5, SoM_12_167) are separated in this way into different clusters/subclusters. A similar observation is the grouping of all stations of this study (SoM_TS), which come from various different settings, in one subcluster (12b), and not into the respective geographic/bathymetric groups. These discrepancies imply a significant difference between the studies inherent in the data, i.e., the taxonomic framework.

Many studies analyzed here did not include a complete list of distinguished taxa with references to show the interpretation of the taxa for all identified forms, in addition, the visualization of the distinguished taxa is, too, incomplete (given for only more

common taxa) or completely lacking in many of these publications, creating the above mentioned discrepancies. In the absence of such crucial data, complete homogenization (i.e., sorting the synonymous taxa) of the data is impossible, although an effort was made to homogenize at least the taxa distinguished/researched in this study (Supplementary Table E.2). Still, many unaddressed issues in the data are present; mainly due to lumping of taxa, creating a false dominance of the name the taxa were lumped under (e.g., it is most likely that many studies lumped *B. vadescens* with *Bolivina spathulata*, or *B. spathulata* with *Bolivina dilatata*). These incongruities between the studies are well explained with a co-occurrence table (Table 9.1) which shows how many common taxa occur in pairs of studies (after homogenization). The difference between the number of identified taxa in a study and the number of co-occurring taxa with other studies is higher when comparing studies conducted in areas of different environmental settings; e.g., out of 67 taxa Alavi (1988, SoM_13) identified from the Çınarcık Basin, only 15 occurs in Avşar et al. (2006, SoM_12) from the Erdek Bay. However, the difference does not diminish when studies from similar sites are compared; e.g., out of 191 taxa identified in Kırcı-Elmas (2018, SoM_06) from the northern shelves, only 94 occurs in Avşar (2010, SoM_08) also from the northern shelves, and is one of the better examples. A worse example is from the Erdek Bay where Avşar (2010, SoM_08) and Phipps et al. (2010) have only 52 taxa in common, explaining the separation of the stations of these studies in the cluster analysis (Figure 5.10).

In conclusion, a serious and comprehensive taxonomic review including the establishment of a solid taxonomic framework and encouragement of its widespread usage is necessary for the benthic foraminifera of the Sea of Marmara. Only then the data from different studies can be incorporated for evaluation of distributions of taxa.

Table 9.1. Co-occurrence table (symmetrical) for the taxa identified in the analyzed studies after homogenization of data (437 taxa). Number of identified taxa in the studies (after homogenization) given in the diagonal (purple). Maximum co-occurrence numbers (per column) are highlighted yellow. Study codes same as Table 5.2; 01: Fontanier et al. 2018; 02: Phipps et al. 2010, 03: Kırcı-Elmas, 2006; 06: Kırcı-Elmas, 2018; 07: Kırcı-Elmas, 2013; 08: Avşar, 2010; 09: Kırcı-Elmas et al., 2008; 11: Kaminski et al., 2002; 12: Avşar et al. 2006; 13: Alavi, 1988; TS: this study.

	01	02	03	06	07	08	09	11	12	13	TS
01	13	5	5	5	7	4	4	6	3	3	6
02	5	177	66	98	95	75	50	68	52	41	80
03	5	66	136	91	103	51	95	69	35	40	66
06	5	98	91	191	154	94	64	81	56	39	83
07	7	95	103	154	198	86	76	77	54	41	82
08	4	75	51	94	86	113	36	56	56	28	55
09	4	50	95	64	76	36	96	51	24	36	56
11	6	68	69	81	77	56	51	146	37	32	64
12	3	52	35	56	54	56	24	37	73	15	33
13	3	41	40	39	41	28	36	32	15	67	43
TS	6	80	66	83	82	55	56	64	33	43	152

9.4 Applicability and utility of the quantitative foraminiferal indices

The organic carbon flux to the seafloor is assumed to directly affect the number of benthic foraminifera living on the seafloor (epifaunal forms) while the number of benthic foraminifera living in the sediment (infaunal forms) is assumed to be related

to the buried organic matter (Corliss, 1985; Berger and Diestar-Haas, 1988; Van der Zwaan et al., 1990); while, the organic carbon flux to the seafloor, export productivity, is found to be proportional to the planktonic foraminiferal abundance, and is a function of water depth (Berger and Diestar-Haas, 1988; Van der Zwaan et al., 1990). In addition, bottom water dissolved oxygen, both affecting and being affected by the organic enrichment, is assumed to control the distribution and abundance of benthic foraminifera as well (Kaiho, 1994; Jorissen et al., 1995). These three interconnected parameters, i.e., water depth, organic content, and dissolved oxygen have been a subject of foraminiferal research, and models were developed from data generally collected from open ocean settings. Four of these models, in other words, quantitative indices were evaluated and applied to the studied core-top samples from the Sea of Marmara to assess their applicability in restricted basins.

The planktonic foraminiferal ratio in an assemblage is shown to be increasing with water depth and was modeled to be used in paleobathymetry investigations (Van der Zwaan et al., 1990, De Rijk et al., 1999). The two models were tested with the data produced from 18 core-top samples. De Rijk et al.'s (1999) model, using the planktonic foraminiferal ratio in all foraminifera (P%), although was produced from data from the Mediterranean Sea, greatly underestimates the water depths of studied samples. Therefore, this ratio cannot be used directly for paleodepth estimations, but can be utilized in recognition of depositional and environmental changes along a core (e.g., Hayward et al., 2019; Tapia et al., 2022; see Chapter 4 for changes in P% and its utilization in the studied cores). Van der Zwaan et al.'s (1990) model, using a modified planktonic foraminiferal ratio (%P*, PF ratio calculated by the omission of infaunal taxa) on the other hand, is more promising. 11 of the 18 studied core-top samples fit well to Van der Zwaan et al.'s (1990) model, while the remaining sevenstations deviate from the model greatly. The stations which deviate from the model come from various settings, and regarding other criteria (e.g., absolute abundances, BF assemblage, bottom water conditions) the deviations are mostly probably due to post-mortem alterations in the assemblage, i.e., they do not represent the in-situ configuration. This shows that %P* can be used for paleobathymetry

estimations, even in suboxic basins such as the Sea of Marmara; however, care must be taken to identify samples which may not reflect the in-situ assemblage due to bottom processes (such as winnowing, resedimentation and dissolution). If applied to modern assemblages with known water depths, this index can point out the samples with altered assemblages. However, in older strata, another measure for the detection of such alterations should be employed.

Corliss (1985) proposed a relationship between morphologic characteristics of benthic foraminifera and their microhabitat, i.e., their tolerance to oxygen and food gradients therefore their infaunal or epifaunal preference. Corliss and Chen (1988) then showed a relationship between the infaunal and epifaunal ratio with the organic carbon content in the sediment. Following the proposed classification schemes (Corliss, 1985; Corliss and Chen, 1988; Corliss and Fois, 1990) the taxa identified in this study were distinguished as infaunal and epifaunal (see Section 6.2.2). However, the relative abundances of infaunal or epifaunal groups in the core-top samples show no clear relationship with total organic carbon (TOC), bottom depth or bottom water dissolved oxygen (DO) (Figure 6.7). Although only the taxa with more than 2% abundance in at least one sample (>2% taxa) were classified according to Corliss's scheme, those taxa covered 74% to 92% of the total assemblage, therefore the possible error due to the unassigned taxa are thought to be negligible. The lack of relationship, then, may be attributed i. narrow gradient of TOC studied, ii. suboxic nature of the basin (narrow gradient of DO), iii. to alteration of the benthic assemblages by bottom processes such as winnowing, resedimentation and dissolution, which was not corrected for.

Kaiho's classification of benthic foraminiferal taxa is built on similar assumptions with respect to benthic foraminiferal morphology and microhabitat, and a relationship between an index calculated from relative abundances of different groups of taxa and bottom water dissolved oxygen (DO) was proposed (1994, 1999). Using their classification scheme and proposed model, the estimated bottom water DO values were calculated and compared to measured values. For the suboxic and low oxic stations (>0.3 ml/l, Figure 6.8) the model gives promising results. Under

lower oxygenation conditions, however, estimated values deviate from measured values. This means that the model cannot resolve the lower DO conditions with accuracy. This error may be due to the restricted nature of the basin, or may be due to the alteration of the assemblages by bottom processes, as in the previous index.

The most recent index, Foram-AMBI, was developed for environmental monitoring (Borja et al., 2000; Alve et al., 2016; Jorissen et al., 2018). Foram-AMBI assigns the benthic foraminifera species into five ecological groups according to their abundances across the total organic carbon (TOC) gradient, then uses the relative abundances of the five groups to calculate the index which classifies the samples according to pollution status. Following Jorissen et al.'s (2018) foraminiferal assignments for the Mediterranean Sea, the relative abundances of the five ecological groups (Figure 6.9) and the Foram-AMBI index for the studied sites were calculated (Table 6.16). The index classified all studied stations as slightly polluted with an unbalanced assemblage. However, only a slight relationship between the calculated Foram-AMBI values and the TOC values of the stations was discovered (Figure 6.10). The relationship is less well correlated than expected, considering that the assignment of the taxa was done according to their abundances along the TOC gradient. Assignments of more taxa for a more complete evaluation is necessary, and the present assignments should be reconsidered for the broader applicability of the index.

9.5 Conclusions

Benthic foraminifera (BF) is one of the major elements of meiobenthos, and due to their high abundance, diversity and small size, both in recent sediments and as fossils in older strata, are used for time keeping and as environmental proxies. To assign predictive power to BF assemblages or individual BF taxa, their study in various settings is necessary. The Sea of Marmara (SoM) provides a unique setting for such studies of BF due to its permanently stratified water column and suboxic deep basins, limited circulation, high anthropogenic stress resulting from dense industrial and

residential settlements on its coasts, and its position and importance as a link between the Black Sea and the Mediterranean Sea.

For this purpose, the BF of the SoM were studied from 18 short sediment cores from 15 stations (82 samples in total), mainly from the eastern side of the SoM. Stations span a wide geographic area and water depths, including the Izmit Bay, shelf around Prince Islands, Çınarcık Basin, Imralı Basin, Southern shelf, Southern slope and Central Basin, from 53.5 m to 1214 m water depth.

172 BF taxa were identified, and a comprehensive systematic taxonomy was constructed. Taxa were quantified from the samples, and relative abundances of taxa were used for their relationship with environmental variables such as water depth, dissolved oxygen, and measured concentrations of nitrite, nitrate, ammonium, phosphate in the bottom, interface and pore waters of the stations. Total absolute abundances of benthic and planktonic foraminifera (PF) and distributions of taxa were determined and differences and similarities between stations from the 18 core-top samples were documented.

Along selected 15 sediment cores the total absolute abundances of benthic and planktonic foraminifera (PF), relative abundances of taxa, the ratio of PF (P%) and sand content were analyzed to distinguish changes in the vertical dimension. Most of the studied cores showed no significant changes, however in several of them shifts in foraminiferal assemblages were detected. The shifts in the abundances of *Bulimina inflata*, *Melonis pompilioides* and *Sigmoilopsis* sp. 1 were interpreted in terms of change in the quality and quantity of food reaching the sea floor especially in the deep basins (Central and Çınarcık basins). The shift in the relative abundance of *V. fragilis*, along with a change in P% and total absolute abundance of benthic foraminifera, evaluated with the radiocarbon dating of the core, was linked with the establishment of sulfidic conditions in the Karamürsel Basin, after the 1999 earthquake.

The produced benthic foraminifera dataset was compared to the previous quantitative works, and the data from 10 other studies were incorporated to effectively and

comprehensively evaluate the distribution of taxa in the SoM. Cluster analysis was utilized to assess the differences and similarities of stations, showing that different assemblages prevail in different bathymetric zones and near stream mouths. Adjacent to stream mouths, the assemblage is the poorest in terms of diversity; the shallowest shelf is dominated by *Ammonia* and *Elphidium* genera, below, about 40 m to 150 m the assemblage is dominated by *Cassidulina laevigata*, and below that the dominance of *Bolivina spathulata*, *Bolivina vadescens* and *Paracassidulina minuta* was distinguished. Combining of the data from the literature showed the need to establish a solid taxonomic framework for the benthic foraminifera of the SoM and encourage its wide usage.

The data from the studied core-top samples were used in application of four quantitative foraminiferal biotic indices: %P* (as depth proxy, Van der Zwaan et al. 1990), morphotype classification (as total organic carbon proxy, Corliss, 1985), BFOI and (as bottom water oxygen proxy, Kaiho, 1994) and Foram-AMBI (as ecological quality status proxy, Alve et al., 2016, Jorissen et al., 2018), and assessment of their utility in the Sea of Marmara. It is evident that the omission of infaunal taxa in the calculation of planktonic foraminiferal relative abundance (%P*) results in a better relationship with water depth than using unmodified planktonic foraminiferal ratios (P%). Van der Zwaan et al.'s (1990) model would especially be useful when used in modern assemblages with known water depths: any major deviations from the modeled regression curve would indicate alteration of the foraminiferal assemblages, most probably by bottom processes. Both Corliss's morphotype classification and BFOI showed limitations for use in such restricted environments. Calculated Foram-AMBI values show all stations to be slightly polluted with an unbalanced assemblage. Foram-AMBI is very promising in terms of monitoring applications; however, further research is necessary until it can be widely utilized.

In conclusion, this study presents a comprehensive systematic taxonomy with numerous high-quality illustrations of mainly deep-sea benthic foraminiferal taxa which can be used as a reference material in future studies, forms a basis for future

monitoring studies by supplying quantitative foraminiferal data and calculated biotic indices from various settings in the SoM showing the present configuration.

REFERENCES

Acar, S., Ateş, A. S., Dağlı, E., & Doğan, A., 2023. Relationships between environmental variables and abundance of Cnidaria and Echinodermata in Çardak Lagoon, Çanakkale Strait. Ege Journal of Fisheries and Aquatic Sciences, 40(2), 103-109.

Aiello, G., Amato, V., Barra, D., Caporaso, L., Caruso, T., Giaccio, B., ... and Rossi, A., 2020. Late Quaternary benthic foraminiferal and ostracod response to palaeoenvironmental changes in a Mediterranean coastal area, Port of Salerno, Tyrrhenian Sea. Regional studies in marine science, 40, 101498.

Akcaalan, R., Kaleli, A., & Köker, L., 2022. Distribution of marine benthic diatoms on the coasts of the sea of Marmara and their responses to environmental variables. Journal of Marine Systems, 234, 103780.

Akçay, İ., 2022. Coastal eutrophication and hypoxia under focus: redox dependent benthic nutrient fluxes across sea boundaries in the Northeastern Mediterranean and Marmara Sea. Institute of Marine Sciences, Middle East Technical University, PhD thesis.

Akdemir, T., & Dalgic, G., 2021. The impact of the marine sewage outfalls on the sediment quality: The Black Sea and the Marmara case. Saudi journal of biological sciences, 28(1), 238-246.

Aksu, A. E., Hiscott, R. N., Kaminski, M. A., Mudie, P. J., Gillespie, H., Abrajano, T., & Yaşar, D., 2002. Last glacial–Holocene paleoceanography of the Black Sea and Marmara Sea: stable isotopic, foraminiferal and coccolith evidence. Marine Geology, 190(1-2), 119-149.

Alavi, S. N., 1980. Micropalaeontological studies of recent sediments from the Cilicia Basin (NE Mediterranean). PhD Thesis. Royal School of Mines, Department of Geology, London, 230 pp (Unpublished).

Alavi, S. N., 1988. Late Holocene deep-sea benthic foraminifera from the Sea of Marmara. Marine Micropaleontology, 13(3), 213-237.

Albani, A. D., 1974. New benthonic Foraminiferida from Australian waters. The Journal of Foraminiferal Research. 4(1): 33-39.

Albayrak, S., Balkıs, H., & Balkıs, N., 2004. Bivalvia (Mollusca) fauna of the Sea of Marmara. Acta Adriatica, 45(1), 9-26.

Albayrak, S., & Çağlar, S., 2016. Mollusca fauna of the Sea of Marmara. The Sea of Marmara Marine Biodiversity, Fisheries, Conservation and Governance, (Eds: E. Özsoy, MN Çağatay, N. Balkıs, N. Balkıs, and B. Öztürk), İstanbul, Turkey: Turkish Marine Research Foundation, 503-516.

Algan, O., Altıok, H., and Yüce, H., 1999. Seasonal Variation of Suspended Particulate Matter in Two-layered İzmit Bay, Turkey. Estuarine, Coastal and Shelf Science, 49(2), 235–250. doi:10.1006/ecss.1999.0494

Alımlı, N., 2022. Seafloor iron mobilization across the deep-water redox gradients of the Black Sea and the Sea of Marmara. Institute of Marine Sciences, Middle East Technical University, MSc thesis.

Alve, E., 1994. Opportunistic features of the foraminifer Stainforthia fusiformis (Williamson): evidence from Frierfjord, Norway. Journal of Micropalaeontology, 13(1), 24-24.

Alve, E., 2003. A common opportunistic foraminiferal species as an indicator of rapidly changing conditions in a range of environments. Estuarine, Coastal and Shelf Science, 57(3), 501-514.

Alve, E., and Bernhard, J. M., 1995. Vertical migratory response of benthic foraminifera to controlled oxygen concentrations in an experimental mesocosm. Marine Ecology Progress Series, 137-151.

Alve, E., and Goldstein, S. T., 2010. Dispersal, survival and delayed growth of benthic foraminiferal propagules. Journal of Sea Research, 63(1), 36-51.

Alve, E., and Murray, J. W., 2001. Temporal variability in vertical distributions of live (stained) intertidal foraminifera, southern England. The Journal of Foraminiferal Research, 31(1), 12-24.

Alve, E., Korsun, S., Schönfeld, J., Dijkstra, N., Golikova, E., Hess, S., ... and Panieri, G., 2016. Foram-AMBI: A sensitivity index based on benthic foraminiferal faunas from North-East Atlantic and Arctic fjords, continental shelves and slopes. Marine Micropaleontology, 122, 1-12.

Al-Wosabi M., Mohammed, M., and Basardah, F., 2017. Taxonomy and distribution of recent benthic foraminifera from Bir Ali Beach, Shabwah Governorate, Arabian Sea, Yemen. Türkiye Jeoloji Bülteni, 60(3), 383-432.

Anschutz, P., Jorissen, F. J., Chaillou, G., Abu-Zied, R., & Fontanier, C., 2002. Recent turbidite deposition in the eastern Atlantic: early diagenesis and biotic recovery. Journal of Marine Research, 60(6), 835-854.

Armijo, R., Meyer, B., Navarro, S., King, G., & Barka, A., 2002. Asymmetric slip partitioning in the Sea of Marmara pull-apart: A clue to propagation processes of the North Anatolian fault?. Terra nova, 14(2), 80-86.

Armijo, R., Pondard, N., Meyer, B., Uçarkus, G., de Lépinay, B. M., Malavieille, J., ... & Sarikavak, K., 2005. Submarine fault scarps in the Sea of Marmara pull-apart (North Anatolian Fault): Implications for seismic hazard in Istanbul. Geochemistry, Geophysics, Geosystems, 6(6).

Arslan Kaya, T.N., Sarı, E., & Gül, M., 2023a. Assessment of eco-toxicological and health risks of core sediment from İzmit Gulf, Marmara Sea, Türkiye. Regional Studies in Marine Science, 64, 103059.

Arslan Kaya, T. N., Sarı, E., Çağatay, M. N., Kurt, M. A., Kösesakal, T., Kılıç, Ö., and Acar, D., 2023b. The effects of the 1999 Gölcük earthquake (Mw 7.4) on

trace element contamination of core sediments from İzmit Gulf, Turkey. Natural Hazards, 116(1), 1189-1208.

Artüz, M. L., and Sakınç, M., 2022. Last glaciation to the present: Paleohydrographic reconstruction based on the paleobiofacies distribution in the sediment in the Sea of Marmara. Marine Geology, 453, 106923.

Atkinson, K., 1969. The association of living foraminifera with algae from the littoral zone, south Cardigan Bay, Wales. Journal of Natural History. 3(4): 517-542.

Avşar, N., Aksu, A., and Dinçer, F., 2006. Erdek Körfezi (GB Marmara Denizi) bentik foraminifer toplulukları. Yerbilimleri, 27(3), 125-141.

Avşar, N., 2010. Benthic foraminiferal assemblages in the coastal environment of the northern Marmara Shelf (NW Turkey). Micropaleontology, 56(5).

Baas, J. H., Schönfeld, J., & Zahn, R., 1998. Mid-depth oxygen drawdown during Heinrich events: evidence from benthic foraminiferal community structure, trace-fossil tiering, and benthic δ13C at the Portuguese Margin. Marine Geology, 152(1-3), 25-55.

Balkıs, N., 2003. The effect of Marmara (Izmit) Earthquake on the chemical oceanography of Izmit Bay, Turkey. Marine Pollution Bulletin, 46(7), 865-878.

Balkıs, N., & Tas, S., 2016. Phytoplankton of the Sea of Marmara: A review. In: The Sea of Marmara: Marine Biodiversity, fisheries, conservation and governance, Ozsoy, E., Cagatay, M.N., Balkıs, N., Balkıs, N. and Ozturk, B. Eds. Turkish Marine Research Foundation (TUDAV), Publication No: 42, pp. 326-343.

Balkwill, F. P.; Millett, F. W., 1884. The Foraminifera of Galway. Second part. Journal of Microscopy and Natural Science: Journal of the Postal Microscopical Society. 3: 78-90.,

Balkwill, F. P.; Wright, J. 1885. Report on some Recent foraminifera found off the coast of Dublin and in the Irish Sea. Transactions of the Royal Irish Academy. 28: 317-368.

Banner, F. T.; Culver, S. J., 1978. Quaternary Haynesina n. gen. and Paleogene Protelphidium Haynes; their morphology, affinities and distribution. *The Journal of Foraminiferal Research.* 8(3): 177-207.

Bapst, D.W., 2012. paleotree: Paleontological and Phylogenetic Analyses of Evolution. Methods in Ecology and Evolution, 803-807.

Barmawidjaja, D. M. 1991. Studies in living and fossil foraminifers from seasonally productive regions, Faculteit Aardwetenschappen der Rijksuniversiteit te Utrecht, PhD thesis.

Barmawidjaja, D. M., Jorissen, F. J., Puskaric, S., and van der Zwaan, G. J., 1992. Microhabitat selection by benthic Foraminifera in the northern Adriatic Sea. The Journal of Foraminiferal Research, 22(4), 297–317. doi:10.2113/gsjfr.22.4.297

Barrientos, N., Lear, C. H., Jakobsson, M., Stranne, C., O'Regan, M., Cronin, T. M., ... & Coxall, H. K., 2018. Arctic Ocean benthic foraminifera Mg/Ca ratios and global Mg/Ca-temperature calibrations: New constraints at low temperatures. Geochimica et Cosmochimica Acta, 236, 240-259.

Barut, İ. F., Meriç, E., Nazik, A., Dinçer, F., Kam, E., & Eryılmaz, M., 2024. Evaluation of radioactive properties and microfaunal evidence in the Bosphorus and the Dardanelles straits and Golden Horn sediments. Bulletin of the Mineral Research and Exploration, 173(173), 203-233.

Batsch, A.J.G.C., 1791. Testaceorum arenulae marinae tabulae sex... Sechs Kupfertafeln mit Conchylien des Seesanders. Akademische Buchhandlung, Jena.

Beken, Ç.P., 2018. Marmara Denizi'nin mevcut kirlilik durumunun tarihsel süreci. In In III. Marmara Denizi Sempozyumu Bildirileri ve Çalıştay Raporları,

Kahraman, A.C., and Özkul, M. Eds. Marmara Belediyeler Birliği Kültür Yayınları.

Bektaş, Z., Avşar, U., Ribot, M., Klinger, Y., and Jónsson, S., 2024. Seismo-turbidites reveal locations of major earthquakes during the past millennium in the Gulf of Aqaba, southern Dead Sea Fault. Earth and Planetary Science Letters, 629, 118595.

Belivermiş, M., Kılıç, Ö., Sezer, N., Sıkdokur, E., Güngör, N. D., & Altuğ, G., 2021. Microplastic inventory in sediment profile: A case study of Golden Horn Estuary, Sea of Marmara. Marine pollution bulletin, 173, 113117.

Berg, S., Jivcov, S., Kusch, S., Kuhn, G., Wacker, L., & Rethemeyer, J., 2020. Compound-specific radiocarbon analysis of (sub-) Antarctic coastal marine sediments—Potential and challenges for chronologies. Paleoceanography and Paleoclimatology, 35(10), e2020PA003890.

Berger, W. H., and Parker, F. L., 1970. Diversity of planktonic foraminifera in deep-sea sediments. Science, 168(3937), 1345-1347.

Berger, W. H., and Diester-Haass, L., 1988. Paleoproductivity: the benthic/planktonic ratio in foraminifera as a productivity index. Marine Geology, 81(1-4), 15-25.

Bermúdez, P. J. 1949. Tertiary smaller foraminifera of the Dominican Republic. Cushman laboratory for foraminiferal research special publication. 25: 1-322.

Bermúdez, P. J., 1952. Estudio sistematico de los Foraminiferos rotaliformes. Venezuela Minist. Minas and Hidrocarb. Boletin de geologia. 2(4): 1-230.,

Bernhard, J. M., 1986. Characteristic assemblages and morphologies of benthic foraminifera from anoxic, organic-rich deposits; Jurassic through Holocene. The Journal of Foraminiferal Research, 16(3), 207-215.

Bernhard, J. M., 2003. Potential symbionts in bathyal foraminifera. Science, 299(5608), 861-861.

Bernhard, J. M., & Bowser, S. S., 1999. Benthic foraminifera of dysoxic sediments: chloroplast sequestration and functional morphology. Earth-Science Reviews, 46(1-4), 149-165.

Bernhard, J. M., & Bowser, S. S., 2008. Peroxisome proliferation in foraminifera inhabiting the chemocline: an adaptation to reactive oxygen species exposure? 1. Journal of Eukaryotic Microbiology, 55(3), 135-144.

Bernhard, J. M., Ostermann, D. R., Williams, D. S., & Blanks, J. K., 2006. Comparison of two methods to identify live benthic foraminifera: A test between Rose Bengal and CellTracker Green with implications for stable isotope paleoreconstructions. Paleoceanography, 21(4).

Bernhard, J. M., Tsuchiya, M., & Nomaki, H., 2018. Ultrastructural observations on prokaryotic associates of benthic foraminifera: Food, mutualistic symbionts, or parasites?. Marine Micropaleontology, 138, 33-45.

Berthois, L.; Le Calvez, Y., 1959. Deuxième contribution à l'étude de la sédimentation dans le golfe de Gascogne. Revue des Travaux de l'Institut des Pêches Maritimes. vol. 23 n° 3: 323-375

Beşiktepe, Ş. T., Sur, H. I., Özsoy, E., Latif, M. A., Oğuz, T., & Ünlüata, Ü., 1994. The circulation and hydrography of the Marmara Sea. Progress in Oceanography, 34(4), 285-334.

Blainville, H. M. D. de. 1825-1827. Manuel de malacologie et de conchyliologie. Paris, Levrault 1-647 [1825], 649-664 + 109 pl. [1827].

Bodur, M. N., 1991. Sedimentology and geochemistry of the Late-Holocene sediments from the Sea of Marmara and its straits. Institute of Marine Sciences, Middle East Technical University, PhD thesis.

Boltovskoy, E.; Giussani de Kahn, G., 1983. Evaluation of Benthic Monothalamous Foraminifers as Guide Fossils in Cenozoic Deep-Sea Deposits of the South Atlantic. Micropaleontology. 29(3): 298-308.

Boltovskoy, E., Giussani, G., Watanabe, S., and Wright, R., 1980. Atlas of Benthic Shelf Foraminifera of the Southwest Atlantic. doi:10.1007/978-94-009-9188-0

Borja, A., and Muxika, I. 2005. Guidelines for the use of AMBI (AZTI's Marine Biotic Index) in the assessment of the benthic ecological quality. Marine pollution bulletin, 50(7), 787-789.

Borja, A., Franco, J., and Pérez, V. 2000. A marine biotic index to establish the ecological quality of soft-bottom benthos within European estuarine and coastal environments. Marine pollution bulletin, 40(12), 1100-1114.

Borja, Á., Mader, J., & Muxika, I., 2012. Instructions for the use of the AMBI index software (Version 5.0). Revista de Investigación Marina, AZTI-Tecnalia, 19(3), 71-82.

Bornemann, J. G., 1855. Die mikroskopische Fauna des Septarienthones von Hermsdorf bei Berlin. Zeitschrift der Deutschen Geologischen Gesellschaft. 7: 307-371.

Bostan, Ü., 2018. Izmit Körfezi kirlilik önleme ve atıksu arıtma çalışmaları. In III. Marmara Denizi Sempozyumu Bildirileri ve Çalıştay Raporları, Kahraman, A.C., and Özkul, M. Eds. Marmara Belediyeler Birliği Kültür Yayınları.

Bouchet, V. M., Alve, E., Rygg, B., & Telford, R. J., 2012. Benthic foraminifera provide a promising tool for ecological quality assessment of marine waters. Ecological indicators, 23, 66-75.

Bouchet, V. M., Frontalini, F., Francescangeli, F., Sauriau, P. G., Geslin, E., Martins, M. V. A., ... and Du Châtelet, E. A., 2021. Indicative value of benthic

foraminifera for biomonitoring: Assignment to ecological groups of sensitivity to total organic carbon of species from European intertidal areas and transitional waters. Marine Pollution Bulletin, 164, 112071.

Brady, H. B., 1878. On the reticularian and Radiolarian Rhizopoda (Foraminifera and Polycystina) of the North-Polar Expedition of 1875–76. Annals and magazine of Natural History. (5) 1(6): 425-440.

Brady, H. B., 1879. Notes on some of the Reticularian Rhizopoda of the "Challenger" Expedition. II. Additions to the knowledge of porcellanous and hyaline types. Quarterly Journal of Microscopical Science. 19 (75): 261-299.

Brady, H. B., 1881. Notes on some of the Reticularian Rhizopoda of the "Challenger" Expedition. Part III. Quarterly Journal of Microscopical Science. (2) 21 (81): 31-71.

Brady, H. B. in Tizard; Murray, J. 1882. Exploration of the Faroe Channel, during the Summer of 1880, in H.M.'s hired ship “Knight Errant.”. Proceedings of the Royal Society of Edinburgh. 11: 638-720.

Brady, H. B., 1884. Report on the Foraminifera dredged by H.M.S. Challenger, during the years 1873-1876. In Report on the scientific results of the Voyage of H.M.S. Challenger during the years 1873-1876. Zoology Vol IX.

Brady, G. S. and Robertson, D., 1870. XXVI.—The Ostracoda and Foraminifera of tidal rivers. With an analysis and descriptions of the Foraminifera, by Henry B. Brady, F.L.S. Annals and Magazine of Natural History. 6(34): 273-309.

Brady, H. B.; Parker, W. K. and Jones, T. R., 1888. On some Foraminifera from the Abrohlos Bank. Transactions of the Zoological Society of London. 12 (7): 211-239.

Bronk Ramsey, C. 1995. Radiocarbon calibration and analysis of stratigraphy: the OxCal program. Radiocarbon, 37(2), 425-430.

Bronk Ramsey, C. 2009. Bayesian analysis of radiocarbon dates. Radiocarbon, 51(1), 337-360.

Bronk Ramsey, C. 2021. OxCal v.4.4.4 [software]. URL: https://c14.arch.ox.ac.uk/oxcal.html. Accessed on April 1st, 2024.

Brotzen, F., 1948. The Swedish Paleocene and its Foraminiferal Fauna. Årsbok Sveriges Geologiska Undersökning. n° 493 t. 42(2): 1-140.

Brun, L., Chierici, M. A., and Meijer, M., 1984. Evolution and morphological variations of the principal species of Bolivinitidae in the Tertiary of the Gulf of Guinea. *Géologie Méditerranéenne, 11*(1), 13-57.

Brünnich, M.T., 1771. Zoologiae fundamenta praelectionibus Academicis accomodata. Hafniae et Lipsiae. 253 [+ 1] pp.

Buchner, P., 1940. Die Lagenen des Golfes von Neapel und der marinen Ablagerungen auf Ischia. (Beiträge zur Naturgeschichte der Insel Ischia 1). Kaiserlich-Leopoldinisch-Carolinische Deutsche Akademie der Naturforscher. 9(62): 361-560.

Bugrova, E. M., 1989. Мелкие бентосные фораминиферы зональных комплексов эоцена юга СССР - Small benthic foraminifers from zonal complexes of the Eocene of the south of the USSR. Ежегодник Всесоюзного палеонтологического общества - Yearbook of the All-Union Paleontological Society. 32: 13-29.

Burbach, O., 1886. Beiträge zur Kenntnis der Foraminiferen des mittleren Lias von grossen Seeberg bei Gotha; 1- Die Gattung Frondicularia Defr., 2- Die Milioliden. Zeitschrift für Naturwissenschaften. 59: 30-53, 493-502.

Buzas, M. A., 1990. Another look at confidence limits for species proportions. Journal of Paleontology, 64(5), 842-843.

Buzas, M. A., and T G. Gibson. 1969. Species diversity: benthonic Foraminifera in western north Atlantic. Science 163:72- 75

Caner, H., & Algan, O., 2002. Palynology of sapropelic layers from the Marmara Sea. Marine Geology, 190(1-2), 35-46.

Caralp, M. H., 1988; Late glacial to recent deep-sea benthic foraminifera from the northeastern Atlantic (Cadiz Gulf) and western Mediterranean (Alboran Sea): Paleooceanographic results. Marine Micropaleontology, 13(3), 265–289. doi:10.1016/0377-8398(88)90006-0

Caralp, M. H., 1989a. Size and morphology of the benthic foraminifer Melonis barleeanum; relationships with marine organic matter. The Journal of Foraminiferal Research, 19(3), 235–245.

Caralp, M. H., 1989b. Abundance of Bulimina exilis and Melonis barleeanum: relationship to the quality of marine organic matter. Geo-Marine Letters, 9, 37-43.

Cardich, J., Morales, M., Quipúzcoa, L., Sifeddine, A., & Gutiérrez, D., 2012. Benthic foraminiferal communities and microhabitat selection on the continental shelf off central Peru. In Anoxia: evidence for eukaryote survival and paleontological strategies (pp. 323-340). Dordrecht: Springer Netherlands.

Carpenter, W. B.; Parker, W. K.; Jones, J. R., 1862. Introduction to the study of the foraminifera. The Ray Society, London.

Cavaliere, M., Angeles, I. B., Montresor, M., Bucci, C., Brocani, L., Balassi, E., ... and Frontalini, F., 2021. Assessing the ecological quality status of the highly polluted Bagnoli area (Tyrrhenian Sea, Italy) using foraminiferal eDNA metabarcoding. Science of the Total Environment, 790, 147871.

Chao, A., 1984. Nonparametric estimation of the number of classes in a population. Scandinavian Journal of Statistics 11:265-270

Chapman, F., and Parr, W.J.,1937. Foraminifera. Australian Antarctic Expedition 1911-14 Scientific Reports Series C – Zoology And Botany Vol. I Part 2

Chapman, F.; Parr, W. J.; Collins, A. C., 1934. Tertiary Foraminifera of Victoria, Australia.-The Balcombian Deposits of Port Phillip. Part III. Journal of the Linnean Society of London, Zoology. 38(262): 553-577.

Chaster, G. W., 1892. Report upon the foraminifera of the Southport Society of Natural Science district. First report Southport Society of Natural Science (1890-1891), appendix: 54-72.

Chendeş, C., Kaminski, M. A., Filipescu, S. O. R. I. N., Aksu, A. E., and Yasar, D. 2004. The response of modern benthic foraminiferal assemblages to water mass properties along the southern shelf of the Marmara Sea. Acta palaeontologica romaniae, *4*, 69-80.

Cherif, O.H., 1970. Die Miliolacea der Westküste von Naxos (Griechenland) und ihre Lebensbereiche. Dissertation Facultät Natur- und Geisteswissenschaften Technischen Universität Clausthal, p 176.

Cimerman, F. and Langer, M. 1991. Mediterranean Foraminifera. Academia Scientiarum et Artium Slovenica, Ljubljana. 30.

Corliss, B. H. 1985. Microhabitats of benthic foraminifera within deep-sea sediments. Nature, 314(6010), 435-438.

Corliss, B. H., and Chen, C. 1988. Morphotype patterns of Norwegian Sea deep-sea benthic foraminifera and ecological implications. Geology, 16(8), 716-719.

Corliss, B. H., and Fois, E. 1990. Morphotype analysis of deep-sea benthic foraminifera from the northwest Gulf of Mexico. Palaios, 589-605.

Cormier, M. H., Seeber, L., McHugh, C. M., Polonia, A., Çagatay, N., Emre, Ö., ... and Newman, K. R., 2006. North Anatolian Fault in the Gulf of Izmit (Turkey): Rapid vertical motion in response to minor bends of a nonvertical continental transform. Journal of Geophysical Research: Solid Earth, 111(B4).

Costa, O. G. 1850-1856. Paleontologia del regno di Napoli: contenente la descrizione e figura di tutti gli avanzi organici fossili racchuisi nel suolo di questo regno. Atti dell' Accademia Pontaniana Napoli. 512 p.

Cushman, J. A., 1910. A monograph of the Foraminifera of the North Pacific Ocean. Part I. Astrorhizidae and Lituolidae. Bulletin of the United States National Museum. 71(1): 1-134.

Cushman, J. A., 1911. A monograph of the Foraminifera of the North Pacific Ocean. Part II. Textulariidae. Bulletin of the United States National Museum. 71(2): 1-108.

Cushman, J. A., 1913. A monograph of the Forminifera of the North Pacific Ocean pt. 3: Lagenidae. Bulletin of the United States National Museum.

Cushman, J. A., 1915. A monograph of the Foraminifera of the North Pacific Ocean. Part V. Rotaliidae. Bulletin of the United States National Museum. 71 (5): 1-87.

Cushman, J. A., 1917. A monograph of the Foraminifera of the North Pacific Ocean. Part VI. Miliolidae. Bulletin of the United States National Museum. 71(6): 1-108.

Cushman, J.A. 1921. Foraminifera of the Philippine and adjacent seas. Bull. U.S. Natl. Mus. 100(4).

Cushman, J. A., 1922a. Foraminifera of the Atlantic Ocean. Part III - Textulariidae. United States National Museum Bulletin. 104: 1-149.

Cushman, J. A., 1922b. Shallow-water Foraminifera of the Tortugas region. Publications of the Carnegie Institution of Washington 311. Department of Marine Biology of the Carnegie Institution of Washington. Volume 17: 1-85.

Cushman, J.A., 1923. The foraminifera of the Atlantic Ocean, Part 4: Lagenidae. Bulletin of the United States National Museum, 104(4):1-129

Cushman, J.A., 1925. Recent Foraminifera from British Columbia. Contr. Cushman Lab. Foram. Res. 1 (2): 38-47.

Cushman, J.A., 1926a. Foraminifera of the typical Monterey of California. Contribution from the Cushman Laboratory for foraminiferal Research 2(3): 53-69.

Cushman, J. A., 1926b. The foraminifera of the Velasco Shale of the Tampico Embayment. *Bulletin of the American Association of Petroleum Geologists.* 10: 581-612.

Cushman, J. A., 1927. An outline of a reclassification of the foraminifera. Contributions from the Cushman laboratory for foraminiferal research. 3(1): 1-105.

Cushman, J.A., 1929. The Foraminifera of the Atlantic Ocean. Part 6. Miliolidae, Ophthalmidiidae and Fischerinidae. Bull. U.S. Natl. Mus. 104. p. 28 pl. 3 fig. 3-4

Cushman, J.A., 1930a. The Foraminifera of the Choctawhatchee Formation of Florida. Florida State Geological Survey, Bulletin. 4: 1-89.

Cushman, J.A., 1930b. The Foraminifera of the Atlantic Ocean. Part 7. Nonionidae, Camerinidae, Peneroplidae and Alveolinellidae. Bull. U.S. Natl. Mus. 104.

Cushman, J.A. 1931. The Foraminifera of the Atlantic Ocean. Part 8. Rotaliidae, Amphisteginidae, Calcarinidae, Cymbaloporettidae, Globorotaliidae,

Anomalinidae, Planorbulinidae, Rupertiidae and Homotremidae. Bull. U.S. Natl. Mus. 104.

Cushman, J. A., 1932. Notes on the genus Virgulina. Contributions from the Cushman laboratory for Foraminiferal Research. 8(1): 7-23.

Cushman, J. A., 1933a. Some new Recent foraminifera from the tropical Pacific. Contributions from the Cushman Laboratory for Foraminiferal Research, 9(4), 77-95.

Cushman, J.A., 1933b. The Foraminifera of the tropical Pacific collections of the Albatross , 1899-1900 pt. 2: Lagenidae to Alveolinellidae. Bulletin of the United States National Museum. i–vi, 1-79, 19 pls.

Cushman, J.A., 1933c. Foraminifera their classification and economic use. Cushman Laboratory for Foraminiferal Research, Special Publication 4:1-349.

Cushman, J. A., 1936. New genera and species of the families Verneuilinidae and Valvulinidae and of the subfamily Virgulininae. Cushman Laboratory for Foraminiferal Research, Special Publication, 6, 1-71.

Cushman, J.A., 1937. A monograph of the subfamily Virgulininae of the foraminiferal family Buliminidae. Cushman Foundation for Foraminiferal Research Special Publication. 9: 1-228.

Cushman, J.A., 1942, The Foraminifera of the tropical Pacific collections of the "Albatross", 1899-1900, Pt. 3. Heterohelicidae and Buliminidae. Smithtonian Institution United States National Museum Bulletin 161, United States Government Printing Office, Washington.

Cushman, J.A., 1944. Foraminifera from the shallow water of the New England coast. Special Publ. No. 12, Cushman Lab. Foram. Res. 1-37.

Cushman, J.A., 1945. Foraminifera of the United States Antarctic Service Expedition 1939-1941. Proceedings of the American Philosophical Society, 89(1), 285-288.

Cushman, J.A., 1947. New species and varieties of Foraminifera from off the southeastern coast of the United States. Contr. Cushman Lab. Foram. Res. 23: 86-92.

Cushman, J.A.; Brönnimann, P., 1948. Some new genera and species of foraminifera from brackish water of Trinidad. Contribution to Laboratory for Foraminiferal Research. 24(1): 15-21.

Cushman, J. A.; Edwards, P. G., 1937. Astrononion a new genus of the foraminifera and its species. Contributions from the Cushman laboratory for foraminiferal research. 13(1): 29-36.

Cushman, J.A. and Jarvis, P.W., 1929. New foraminifera from Trinidad. Contributions from the Cushman Laboratory for Foraminiferal Research 5: 6-17.

Cushman, J. A. and Martin, L. T., 1935. A new genus of Foraminifera, Discorbinella, from Monterey Bay, California. Contributions from the Cushman laboratory for foraminiferal research. 11(4): 89-90.

Cushman, J. A., & McCulloch, I. 1942. Some Virgulininae in the collections of the Allan Hancock Foundation: plates 21-28. The University of Southern California Publications Alan Hancock Pacific Expeditions Vol. 6 No 4.

Cushman, J.A. and Moyer, D.A., 1930. Some Recent Foraminifera from off San Pedro. Contributions from the Cushman Laboratory for Foraminiferal Research. 6(3): 49-62.

Cushman, J.A. and Parker, F.L., 1936. Some species of Robertina. Contributions from the Cushman laboratory for foraminiferal research. 12(4): 92-100.,

Cushman, J. A. and Parker, F. L., 1938. Notes on some Pliocene and Pleistocene species of Bulimina and Buliminella. Contributions from the Cushman laboratory for foraminiferal research. 14(3): 53-62.

Cushman, J. A., and Parker, F. L., 1947. Bulimina and related foraminiferal genera. United States Department of the Interior, Geological Survey, Professional Paper No. 210-D, Washington, pp. 55-160.

Cushman, J.A. and Todd, R., 1949. Species of the genus Chilostomella and related genera. Contr. Cushman Lab. Foram. Res. 25: 84-99

Čžjžek, J., 1848. Beitrag zur Kenntniss der fossilen Foraminiferen des Wiener Beckens. Haidinger's Natur-wissenschaftliche Abhandlungen. 2: 137-150.,

Čžjžek, J., 1849. Über zwei neue Arten von Foraminiferen aus dem Tegel von Baden und Möllersdorf. Bericht über die Mitteilungen von Freunden der Naturwissenschaften in Wien. 5: 50-56.

Çağatay, M. N., Algan, O., Sakınç, M., Eastoe, C. J., Egesel, L., Balkis, N., ... & Caner, H., 1999. A mid-late Holocene sapropelic sediment unit from the southern Marmara sea shelf and its palaeoceanographic significance. Quaternary Science Reviews, 18(4-5), 531-540.

Çağatay, M. N., Görür, N., Algan, O., Eastoe, C., Tchapalyga, A., Ongan, D., ... & Kuşcu, I., 2000. Late Glacial–Holocene palaeoceanography of the Sea of Marmara: timing of connections with the Mediterranean and the Black Seas. Marine Geology, 167(3-4), 191-206.

Çağatay, M. N., Erel, L., Bellucci, L. G., Polonia, A., Gasperini, L., Eriş, K. K., ... and Damcı, E., 2012. Sedimentary earthquake records in the İzmit gulf, sea of Marmara, Turkey. Sedimentary Geology, 282, 347-359.

Çağatay, M. N., Eriş, K. K., Makaroğlu, Ö., Yakupoğlu, N., Henry, P., Leroy, S. A., ... & Kende, J., 2019. The sea of Marmara during marine isotope stages 5 and 6. Quaternary Science Reviews, 220, 124-141.

Çinar, M. E., Bakir, K., Öztürk, B., Doğan, A., Açik, Ş., Kirkim, F., ... & Bitlis, B., 2020. Spatial distribution pattern of macroinvertebrates associated with the black mussel Mytilus galloprovincialis (Mollusca: Bivalvia) in the Sea of Marmara. Journal of Marine Systems, 211, 103402.

Çinar, M. E., Bilecenoğlu, M., Yokeş, M. B., & Güçlüsoy, H., 2024. Soft-bottom macrobenthic assemblages around the south Marmara Islands (Sea of Marmara). In: Ecological Changes in the Sea of Marmara; Isinibilir, M., Kıdeys, A.E., Malej, A., Eds. Istanbul Üniversitesi press, pp. 693-719.

Darling, K. F., Thomas, E., Kasemann, S. A., Seears, H. A., Smart, C. W., and Wade, C. M., 2009. Surviving mass extinction by bridging the benthic/planktic divide. Proceedings of the National Academy of Sciences, 106(31), 12629–12633. doi:10.1073/pnas.0902827106 .

Debenay, J. P., 2012. A guide to 1,000 foraminifera from Southwestern Pacific: New Caledonia. IRD Editions. Publications Scientifiques du Muséum, Paris.

Debenay, J. P., Bénéteau, E., Zhang, J., Stouff, V., Geslin, E., Redois, F., and Fernandez-Gonzalez, M., 1998. Ammonia beccarii and Ammonia tepida (Foraminifera): morphofunctional arguments for their distinction. Marine micropaleontology, 34(3-4), 235-244.

Debenay, J. P., Tsakiridis, E., Soulard, R., and Grossel, H., 2001. Factors determining the distribution of foraminiferal assemblages in Port Joinville Harbor (Ile d'Yeu, France): the influence of pollution. Marine Micropaleontology, 43(1-2), 75-118.

Defrance J.L.M., 1824. In: Dictionnaire des Sciences Naturelles, dans lequel on traite méthodiquement des diffrents êtres de la nature […] par plusieurs professeurs du Jardin du Roi, et de principales Écoles de Paris. Tome 32: Mollus - Morf, Levrault, F.G. (ed), Paris.

Delage, Y.; Hérouard, E., 1896. Traité de Zoologie Concrète. Tome I. La Cellule et les Protozoaires. *Schleicher Frères, Paris.* 1-584.

Demir, M., 2003. Shells of Mollusca collected from the seas of Turkey. Turkish Journal of Zoology, 27(2), 101-140.

De Montfort D., 1808. Conchyliologie systématique et classification méthodique des coquilles. Tome 1. Paris: Schoell.

De Rijk, S., Troelstra, S. R., & Rohling, E. J., 1999. Benthic foraminiferal distribution in the Mediterranean Sea. The Journal of Foraminiferal Research, 29(2), 93-103.

Deshayes, G. P. 1832. Encyclopédie méthodique ou par ordre de matières. Histoire naturelle des Vers et Mollusques. Vol. 3: 595-1152 [Livraison 102, 29 Sept. 1832]

Dimiza, M.D.; Triantaphyllou, M.V.; Koukousioura, O.; Hallock, P.; Simboura, N.; Karageorgis, A.P.; Papathanasiou, E. 2016. The Foram Stress Index: A New Tool for Environmental Assessment of Soft-Bottom Environments Using Benthic Foraminifera. A Case Study from the Saronikos Gulf, Greece, Eastern Mediterranean. Ecological Indicators, 60, 611–621.

Dimiza, M. D., Fatourou, M., Arabas, A., Panagiotopoulos, I., Gogou, A., Kouli, K., ... and Triantaphyllou, M. V. 2020. Deep-sea benthic foraminifera record of the last 1500 years in the North Aegean Trough (northeastern Mediterranean): A paleoclimatic reconstruction scenario. Deep Sea Research Part II: Topical Studies in Oceanography, 171, 104705.

Duijnstee, I. A. P., Ernst, S. R., & Van der Zwaan, G. J., 2003. Effect of anoxia on the vertical migration of benthic foraminifera. Marine Ecology Progress Series, 246, 85-94.

Du Châtelet, E. A., Bout-Roumazeilles, V., Coccioni, R., Frontalini, F., Guillot, F., Kaminski, M. A., ... & Ventalon, S., 2013. Environmental control on shell structure and composition of agglutinated foraminifera along a proximal–distal transect in the Marmara Sea. Marine Geology, 335, 114-128.

d’Orbigny, A. D. 1826. Tableau méthodique de la classe des Céphalopodes. Annales des Sciences Naturelles. vol. 7: 96-169, 245-314.

d’Orbigny, A. D. 1839a. Voyage dans l'Amérique Méridionale. Foraminifères. t. 5 pt. 5: 1-86.

d’Orbigny, A. D., 1839b. Foraminifères, in de la Sagra R., Histoire physique, politique et naturelle de l'ile de Cuba. A. Bertrand. 1-224.

d'Orbigny, A. D., 1839c. Foraminifères des îles Canaries. Histoire naturelle des Iles Canaries. 2(2): 120-146.

d’Orbigny, A.D.,1846. Die fossilen Foraminiferen des tertiären Beckens von Wien. Foraminifères fossiles du bassin tertiaire de Vienne. 312 p.

d'Orbigny, A. D., 1850-1852. Prodrome de paléontologie stratigraphique universelle des animaux mollusques et rayonnés, faisant suite au cours élémentaire de paléontologie et de géologie stratigraphiques. Paris: Masson. vol. 1 [January 1850 ("1849")]: lx + 394 pp.; vol. 2 [November 1850]: 427 pp.; vol. 3 [1852]: 196 pp. + Table alphabétique et synonymique des genres et des espèces: 189 pp

d’Orbigny, C., (ed), 1841-1849. Dictionnaire universel d'histoire naturelle. 13 vols [vol. 1 (1841), 2 (1842), 3 (1843), 4 (1844), 5 (1848-1849), 6 (1845)] + 3 vols Atlas [all 1849]. Renard and Martinet, Paris.

Eade, J. V. (1969). Globocassidulina nipponensis, new name for Cassidulina orientale Cushman, 1925 preoccupied. Contributions from the Cushman Foundation for Foraminiferal Research. 20: 65-66.

Earland, A., 1933. Foraminifera, Part II, South Georgia. Discovery Reports. 7: 27-138 + plates.

Ediger, D., Beken, Ç., Yüksek, H., Tugrul, S., 2016. Eutrophication in the Sea of Marmara. In: The Sea of Marmara; Marine Biodiversity, Fisheries,

Conservation and Governance. (Ozsoy, E., Cagatay, M.N., Balkıs, N., Balkıs, N and Ozturk, B). Turkish Marine Research Foundation (TUDAV), Publication No: 42, Istanbul, Turkey, 723-736.

Egger, J. G., 1857. Die Foraminiferen der Miocän-Schichten bei Ortenburg in Nieder-Bayern. Neues Jahrbuch für Mineralogie, Geognosie, Geologie und Petrefakten-Kunde. 266-384.

Egger, J. G. 1893. Foraminiferen aus Meeresgrundproben, gelothet von 1874 bis 1876 von S.M. Sch. "Gazelle". Abhandlungen der Mathematisch-Physikalischen Classe der Königlich Bayerischen Akademie der Wissenschaften. (2) 18[1895]: 193-458.

Ehrenberg, C. G., 1839. Uber die Bildung der Kreidefelsen und des Kreidemergels durch unsichtbare Organismen. physikalische abhandlungen der Koniglichen akademie der wissenschaften zu Berlin, 59-147.

Ehrenberg, C. G., 1840. Eine weitere Erläuterung des Organismus mehrerer in Berlin lebend beobachteter Polythalamien der Nordsee. Bericht über die zur Bekanntmachung geeigneten Verhandlungen der Königlich-Preussischen Akademie der Wissenschaften zu Berlin. 1840: 18-23.

Ehrenberg, C.G., 1843. Verbreitung und Einfluss des mikroskopischen Lebens in Süd-und Nord-Amerika. Abhandlungen der Königlichen Akademie der Wissenschaften zu Berlin. 1841: 291-445, 4 pls.

Ehrenberg, C.G., 1844. Kleinste Lebenformen in Quellenlande des Euprats und Araxes, und formenreiche marine Tripelbildung auf den Bermuda-Inseln. Keis. Preussische Ber., Akad. Wiss., 253-275.

El Kateb, A., Stalder, C., Martínez-Colón, M., Mateu-Vicens, G., Francescangeli, F., Coletti, G., ... and Spezzaferri, S., 2020. Foraminiferal-based biotic indices to assess the ecological quality status of the Gulf of Gabes (Tunisia): Present limitations and future perspectives. Ecological Indicators, 111, 105962.

Erbacher, J., & Nelskamp, S., 2006. Comparison of benthic foraminifera inside and outside a sulphur-oxidizing bacterial mat from the present oxygen-minimum zone off Pakistan (NE Arabian Sea). Deep Sea Research Part I: Oceanographic Research Papers, 53(5), 751-775.

Ergin, M., and Bodur, M. N., 1999. Silt/clay fractionation in surficial Marmara sediments: implication for water movement and sediment transport paths in a semi-enclosed and two-layered flow system (northeastern Mediterranean Sea). Geo-Marine Letters, 18, 225-233.

Ergin, M., and Yörük, R., 1990. Distribution and texture of the bottom sediments in a semi-enclosed coastal inlet, the Izmit Bay from the Eastern Sea of Marmara (Turkey). Estuarine, Coastal and Shelf Science, 30(6), 647-654.

Ergin, M., Bodur, M. N., Ediger, D., Ediger, V., and Yilmaz, A., 1993. Organic carbon distribution in the surface sediments of the Sea of Marmara and its control by the inflows from adjacent water masses. Marine Chemistry, 41(4), 311-326.

Ergin, M., Kazanci, N., Varol, B., Ileri, Ö., & Karadenizli, L., 1997. Sea-level changes and related depositional environments on the southern Marmara shelf. Marine Geology, 140(3-4), 391–403. doi:10.1016/s0025-3227(97)00029-7

Ergin, M., Kapur, S., Karakaş, Z., Akca, E., Kangal, Ö., & Keskin, Ş., 1999. Grain size and clay mineralogy of Late Quaternary sediments on a tectonically active shelf, the southern Sea of Marmara: clues to hydrographic, tectonic and climatic evolution. Geological Journal, 34(1-2), 199-210.

Ergin, M., Bayhan, E., & Temel, A., 2012. Clay mineral distribution in last Glacial-Holocene sediment cores from the eastern Marmara Sea (Çınarcık Basin–İzmit Gulf Transition), NW-Turkey: Multisources and transport paths in a two-way flow system. Quaternary International, 261, 53-74.

Ergün, M., & Özel, E., 1995. Structural relationship between the Sea of Marmara basin and the North Anatolian Fault Zone. Terra Nova, 7(2), 278-288.

Eriş, K. K., Ryan, W. B. F., Çağatay, M. N., Sancar, U., Lericolais, G., Menot, G., & Bard, E., 2007. The timing and evolution of the post-glacial transgression across the Sea of Marmara shelf south of Istanbul. Marine Geology, 243(1-4), 57-76.

Eriş, K. K., Çağatay, N., Beck, C., de Lepinay, B. M., & Corina, C., 2012. Late-Pleistocene to Holocene sedimentary fills of the Çınarcık Basin of the Sea of Marmara. Sedimentary Geology, 281, 151-165.

Ernst, S., Bours, R., Duijnstee, I., and van der Zwaan, B., 2005. Experimental effects of an organic matter pulse and oxygen depletion on a benthic foraminiferal shelf community. The Journal of Foraminiferal Research, 35(3), 177-197.

Ertan, K. T., Hemleben, V., and Hemleben, C. (2004). Molecular evolution of some selected benthic foraminifera as inferred from sequences of the small subunit ribosomal DNA. Marine Micropaleontology, 53(3-4), 367-388.

EU-Hydro River Network Database 2006-2012 (vector), Europe. European Union's Copernicus Land Monitoring Service information, https://doi.org/10.2909/393359a7-7ebd-4a52-80ac-1a18d5f3db9c

Finlay, H. J., 1939. New Zealand Foraminifera: Key Species in Stratigraphy - No. 1. Transactions of the Royal Society of New Zealand. 68: 504-533.

Finlay, H. J., 1947. New Zealand Foraminifera: Key Species in Stratigraphy - No. 5. New Zealand journal of science and technology. B28: 259-292.

Fisher, R.A., Corbet, A.S., Williams, C.B., 1943. The relation between the number of species and the number of individuals in a random sample of an animal population. The Journal of Animal Ecology 12:42-58.

Fleming, J., 1828. A history of British animals, exhibiting the descriptive characters and systematical arrangement of the genera and species of quadrupeds, birds, reptiles, fishes, Mollusca, and Radiata of the United Kingdom; including the indigenous, extirpated, and extinct kinds, together with periodical and

occasional visitants. Edinburgh, Bell and Bradfute / London, James Duncan. Pp. i-xxii, 1-565. corrigenda.

Flint, J. M., 1899. Recent Foraminifera: a descriptive catalogue of specimens dredged by the U.S. Fish Commission steamer Albatross. Report of the United States National Museum. [1897]: 249-349.

Fichtel, L.v.; Moll, J.P.C., 1798. Testacea microscopia, aliaque minuta ex generibus Argonauta et Nautilus, ad naturam delineata et descripta. A. Pichler, Wien. xii + 123 pp., 24 pl.

Finlay, H. J. 1939. New Zealand Foraminifera: Key Species in Stratigraphy - No. 3. Transactions of the Royal Society of New Zealand. 69: 309-329.

Fontanier, C., Jorissen, F. J., Licari, L., Alexandre, A., Anschutz, P., and Carbonel, P. 2002. Live benthic foraminiferal faunas from the Bay of Biscay: faunal density, composition, and microhabitats. Deep Sea Research Part I: Oceanographic Research Papers, 49(4), 751-785.

Fontanier, C., Dissard, D., Ruffine, L., Mamo, B., Ponzevera, E., Pelleter, E., ... and Savignac, F. 2018. Living (stained) deep-sea foraminifera from the Sea of Marmara: A preliminary study. Deep Sea Research Part II: Topical Studies in Oceanography, 153, 61-78.

Fornasini, C., 1888. Tavola paleo-protistografica. Bollettino della Società Geologica Italiana. 7: 44-48.

Fornasini, C., 1898. Intorno a l'Uvigerina bononiensis Forn. Rivista Italiana di Paleontologia. 4 (1): 27-28.

Fornasini, C., 1900. Le polimorfine e le uvigerine fossili d'Italia. Bollettino della Società geologica italiana. 19(1): 132-172.

Fornasini, C., 1904. Illustrazione di specie orbignyane di foraminiferi istituite nel 1826. Memorie della Reale Accademia delle Scienze dell'Istituto di Bologna, Classe di Scienze Fisiche. ser. 6 t. 1: 1-17.,

Fornasini, C., 1905. Illustrazione di specie Orbignyane di Miliolidi istitute nel 1826. Memorie della Reale Accademia delle Scienze dell'Istituto di Bologna,. 6: 59-70.

Fornasini, C., 1908. Illustrazione di specie Orbignyane di Nodosaridi, di Rotalidi e d'altri foraminiferi. Memorie della Reale Accademie della Scienze dell'Istituto di Bologna, Scienze Naturali. 6(5): 41-54.

Fossile, E., Sabbatini, A., Spagnoli, F., Caridi, F., Dell'Anno, A., De Marco, R., ... and Negri, A., 2021. Sensitivity of foraminiferal-based indices to evaluate the ecological quality status of marine coastal benthic systems: A case study of the Gulf of Manfredonia (southern Adriatic Sea). Marine Pollution Bulletin, 163, 111933.

Frezza, V., & Carboni, M. G., 2009. Distribution of recent foraminiferal assemblages near the Ombrone River mouth (Northern Tyrrhenian Sea, Italy). Revue de micropaléontologie, 52(1), 43-66.

Frontalini, F. and Coccioni, R., 2008. Benthic foraminifera for heavy metal pollution monitoring: a case study from the central Adriatic Sea coast of Italy. Estuarine, Coastal and Shelf Science, 76(2), 404-417.

Galloway, J. J., 1933. A manual of Foraminifera. Bloomington, Principia Press.

Gary, A. C., Healey-Williams, N., and Ehrlich, R., 1989. Water-mass relationships and morphologic variability in the benthic foraminifer Bolivina albatrossi Cushman, northern Gulf of Mexico. The Journal of Foraminiferal Research, 19(3), 210-221.

Gasperini, L., Polonia, A., Del Bianco, F., Etiope, G., Marinaro, G., Favali, P., ... & Çağatay, M. N., 2012. Gas seepage and seismogenic structures along the

North Anatolian Fault in the eastern Sea of Marmara. Geochemistry, Geophysics, Geosystems, 13(10).

Gasperini, L., Polonia, A., ad Çağatay, M. N., 2018. Fluid flow, deformation rates and the submarine record of major earthquakes in the Sea of Marmara, along the North-Anatolian Fault system. Deep Sea Research Part II: Topical Studies in Oceanography, 153, 4-16.

Goës, A., 1882. On the reticularian Rhizopoda of the Caribbean Sea. Kongl. Svenka Vetenskaps-Akademiens Handlinger. 19: 1-151.

Goës, A. T. (1894). A synopsis of the Arctic and Scandinavian Recent marine Foraminifera hitherto discovered. Kongl. svenka vetenskaps-Akademiens handlinger. 25: 1-127 + pls.

Goldfinger, C., 2011. Submarine paleoseismology based on turbidite records. Annual Review of Marine Science, 3, 35-66.

Gooday, A. J., and Alve, E., 2001. Morphological and ecological parallels between sublittoral and abyssal foraminiferal species in the NE Atlantic: a comparison of Stainforthia fusiformis and Stainforthia sp. Progress in Oceanography, 50(1-4), 261-283.

Görür, N., Cagatay, M. N., Sakinc, M., Sümengen, M., Sentürk, K., Yaltirak, C., & Tchapalyga, A., 1997. Origin of the Sea of Marmara as deduced from Neogene to Quaternary paleogeographic evolution of its frame. International Geology Review, 39(4), 342-352.

Gözel, F., Belivermiş, M., Sezer, N., Kurt, M. A., Sıkdokur, E., & Kılıç, Ö., 2022. Chronology of trace elements and radionuclides using sediment cores in Golden Horn Estuary, Sea of Marmara. Environmental Pollution, 315, 120359.

Green, K. E., 1959. Ecology of some Arctic foraminifera. In Bushnell, V.: Scientific Studies at Fletcher's Ice Island, T-3, 1952-1955. Vol. 1. Terrestrial Sciences Laboratory, Geophysics Research Directorate, Air Force Cambridge

Research Center, Air Research and Development Command, U.S. Air Force. Geophysical Research Papers no. 63.

Green, K. E. 1960. Ecology of some Arctic foraminifera. Micropaleontology, 6(1), 57-78.

Griffith, J. W., and A. Henfrey, 1875, The Micrographic Dictionary, vol. 1, 3rd ed. London: van Voorst.

Grimm, G. W., Stögerer, K., Ertan, K. T., Kitazato, H., Kučera, M., Hemleben, V., and Hemleben, C. 2007. Diversity of rDNA in Chilostomella: Molecular differentiation patterns and putative hermit types. Marine Micropaleontology, 62(2), 75-90.

Grindell, D. S. and Collen, J. D., 1976. Virgulinella fragilis n. sp. (Foraminiferida) from Wellington Harbour, New Zealand. Revista española de micropaleontología. 8: 273-278.

Guérin-Méneville, F.E., 1832. Iconographie du Règne Animal de G. Cuvier, ou représentation d'après nature de l'une des espèces les plus remarquables, et souvent non encore figurées, de chaque genre d'animaux, avec un texte descriptif mis au courant de la science. Ouvrage pouvant servir d'atlas à tous les traités de zoologie. Tome 2. Planches des animaux invertébrés. Mollusques. J.B. Baillière, Paris and London.

Guy-Haim, T., Hyams-Kaphzan, O., Yeruham, E., Almogi-Labin, A., & Carlton, J. T., 2017. A novel marine bioinvasion vector: Ichthyochory, live passage through fish. Limnology and Oceanography Letters, 2(3), 81-90.

Haake, F.-W. 1977. Living benthic Foraminifera in the Adriatic Sea; influence of water depth and sediment. The Journal of Foraminiferal Research, 7(1): 62-75.

Haeckel, E., 1894, Systematische Phylogenie. Entwurf eines Natürlichen Systems der Organismen auf Grund ihrer Stammesgeschichte. Theil1, Systematische Phylogenie der Protisten und Pflanzen. Berlin.

Haman, D., 1978, Cribrolenticulina, a new genus of the family Nodosariidae Ehrenberg, 1838 (Foraminifera), Tulane Studies in Geology and Paleontology 14:81-103.

Hammer, Ø., & Harper, D. A., 2006. Paleontological data analysis. Blackwell Publishing.

Hammer, Ø., Harper, D.A.T., and P. D. Ryan, 2001. PAST: Paleontological Statistics Software Package for Education and Data Analysis. Palaeontologia Electronica 4(1): 9 pp.

Hansen, H. J., and Revets, S., 1992. A revision and reclassification of the Discorbidae, Rosalinidae, and Rotaliidae. The Journal of Foraminiferal Research, 22(2), 166-180.

Hansen, K. E., Giraudeau, J., Limoges, A., Massé, G., Rudra, A., Wacker, L., ... & Seidenkrantz, M. S., 2022. Characterization of organic matter in marine sediments to estimate age offset of bulk radiocarbon dating. Quaternary Geochronology, 67, 101242.

Hantken, M. Von. 1875. Die fauna der Clavulina Szabói-Schichten. Theil I - Foraminiferen. Kaiserlich Ungarische Anstalt, Mitteilungen, Jahrbuch. 4: 1-93.

Hasegawa, S., Sprovieri, R., and Poluzzi, A., 1990. Quantitative analysis of benthic foraminiferal assemblages from Plio-Pleistocene sequences in the Tyrrhenian Sea, ODP LEG 107, p. 461-478. In Kastens, K.A. and Mascle, J. et al. (eds.), Proceedings of the Ocean Drilling Program, Scientific Results, Vol. 107, College Station, TX (Ocean Drilling Program), Texas.

Haunold, T. G., 1990. The new Neogene genus Pappina in the new family Pappinidae; polymorphine mode of chamber addition in the Buliminacea. The Journal of Foraminiferal Research, 20(1), 56-64.

Haynes, J., 1958. Certain smaller British Paleocene foraminifera. Part III. Polymorphinidae. Contributions from the Cushman Foundation for Foraminiferal Research. 9(1): 4-16.

Haynes, J. R., 1973. Cardigan Bay Recent Foraminifera (Cruises of the R. V. Antur, 1962-1964). Bulletin of the British Museum (Natural History), Zoology. Supplement 4, pp. 1-245.

Haynes, J.R., 1981. Foraminifera. Macmillan, London.

Hayward, B.W., Grenfell, H.R., Reid, C.M., Hayward, K.A., 1999. Recent New Zealand shallow-water benthic Foraminifera: Taxonomy, ecologic distribution, biogeography, and use in paleoenvironmental assessment. Institute of Geological and Nuclear Sciences Monograph 21, 258 p.

Hayward, B. W., Holzmann, M., Grenfell, H. R., Pawlowski, J., and Triggs, C. M., 2004. Morphological distinction of molecular types in Ammonia–towards a taxonomic revision of the world's most commonly misidentified foraminifera. Marine Micropaleontology, 50(3-4), 237-271.

Hayward, B. W., Holzmann, M., and Tsuchiya, M., 2019a. Combined molecular and morphological taxonomy of the beccarii/T3 group of the foraminiferal genus Ammonia. Journal of Foraminiferal Research, 49(4), 367-389.

Hayward, B. W., Sabaa, A. T., and Triggs, C. M., 2019b. Using foraminiferal test-size distribution and other methods to recognise Quaternary bathyal turbidites and taphonomically-modified faunas. Marine Micropaleontology, 148, 65-77.

Hayward, B. W., Holzmann, M., Pawlowski, J., Parker, J. H., Kaushik, T., Toyofuku, M. S., and Tsuchiya, M., 2021. Molecular and morphological taxonomy of living Ammonia and related taxa (Foraminifera) and their biogeography. Micropaleontology, 67.

Heaton, T. J., Köhler, P., Butzin, M., Bard, E., Reimer, R. W., Austin, W. E., ... and Skinner, L. C. 2020. Marine20—the marine radiocarbon age calibration curve (0–55,000 cal BP). Radiocarbon, 62(4), 779-820.

Hieke, W., 1984. A thick Holocene homogenite from the Ionian Abyssal Plain (eastern Mediterranean). Marine Geology, 55(1-2), 63–78. doi:10.1016/0025-3227(84)90133-6

Heinz, P., Kitazato, H., Schmiedl, G., and Hemleben, C., 2001. Response of deep-sea benthic foraminifera from the Mediterranean Sea to simulated phytoplankton pulses under laboratory conditions. The Journal of Foraminiferal Research, 31(3), 210-227.

Hermelin, J.O.R. and Scott, D.B. 1985. Recent benthic foraminifera from the central North Atlantic. Micropaleontology, 31:199-220.

Hermelin, J. O. R., 1991. Hyalinea balthica (Schroeter) in lower Pliocene sediments of the northwest Arabian Sea. *The Journal of Foraminiferal Research*, *21*(3), 244-251.

Heron-Allen, E., and Earland, A., 1913. Clare Island Survey: Part 64. Foraminifera. Proceedings of the Royal Irish Academy. Vol. 31.

Heron-Allen, E. and Earland, E., 1915. XVIII. The Foraminifera of the Kerimba Archipelago (Portuguese East Africa) – Part II. The Transactions of the Zoological Society of London. Vol. 20, Is. 17, pp. 543-794.

Heron-Allen, E.; Earland, A., 1930. The Foraminifera of the Plymouth district. I. Journal of the Royal Microscopical Society. 50(1): 46-84.

Heron-Allen, E.; Earland, A., 1932. Foraminifera: Part I. The ice-free area of the Falkland Islands and adjacent seas. Discovery Reports Vol. IV, Cambridge, University Press. pp. 291-460.

Hofker, J., 1932. Notizen über die Foraminiferen des Golfes von Neapel III, Die Foraminiferenfauna des Ammontatura. Pubblicazioni della Stazione Zoologica di Napoli, 12:61-144.

Hofker, J., 1951a. The Foraminifera of the Siboga Expedition. Part 3. Siboga Expeditie, monograph. 4: 1-513.

Hofker, J., 1951b. The Toothplate-Foraminifera. Archives Néerlandaises de Zoologie. 8(1), 353-373.

Hofker, J., 1956. Tertiary foraminifera of coastal Ecuador- Part II Additional notes on the Eocene species. Journal of palaeontology. 30: 891-958.

Hofker, J., 1960, Foraminiferen aus dem Golf von Neapel. Paldont. Z. 34 (3/4), 233-262, Stuttgart.

Hofker, J., 1968. Foraminifera from the bay of Jakarta, Java. Bijdragen tot de Dierkunde, 37(1), 11-35.

Hohenegger, J.; Piller, W., 1975. Wandstrukturen und Grossgliederung der Foraminiferen. Sitzungberichten der österreichische Akademie der Wissenschaften, mathematisch-naturwissenschaftliche Klasse. Abteilung 1, 184: 67-96.

Holbourn, A., Henderson, A. S., and MacLeod, N., 2013. Atlas of benthic foraminifera. John Wiley and Sons.

Holzmann, M., and Pawlowski, J. 2000. Taxonomic relationships in the genus Ammonia (Foraminifera) based on ribosomal DNA sequences. Journal of Micropalaeontology, 19(1), 85-95.

Holzmann, M., and Pawlowski, J., 2017. An updated classification of rotaliid foraminifera based on ribosomal DNA phylogeny. Marine Micropaleontology.

Hottinger, L., Halicz, E., and Reiss, Z., 1990. Wall texture of Spirorutilus. The Journal of Foraminiferal Research, 20(1), 65–70. doi:10.2113/gsjfr.20.1.65

Howe, H. V.; Wallace, W. E., 1932. Foraminifera of the Jackson Eocene at Danville Landing on the Ouachita, Catahoula Parish, Louisiana. Bulletin of the Geological Survey of Louisiana. 2: 1-118.

Höglund, H., 1947. Foraminifera in the Gullmar Fjord and the Skagerak. Zoologiska bidrag från Uppsala. 26: 1-328.

Imren, C., Le Pichon, X., Rangin, C., Demirbağ, E., Ecevitoğlu, B., & Görür, N., 2001. The North Anatolian Fault within the Sea of Marmara: a new interpretation based on multi-channel seismic and multi-beam bathymetry data. Earth and Planetary Science Letters, 186(2), 143-158.

Ishimura, T., Tsunogai, U., Hasegawa, S., Nakagawa, F., Oi, T., Kitazato, H., ... & Toyofuku, T., 2012. Variation in stable carbon and oxygen isotopes of individual benthic foraminifera: tracers for quantifying the magnitude of isotopic disequilibrium. Biogeosciences, 9(11), 4353-4367.

Jennings, A., Andrews, J., Reilly, B., Walczak, M., Jakobsson, M., Mix, A., ... and Cheseby, M., 2020. Modern foraminiferal assemblages in northern Nares Strait, Petermann Fjord, and beneath Petermann ice tongue, NW Greenland. Arctic, Antarctic, and Alpine Research, 52(1), 491-511.

Jones T.R. 1895. A monograph of the Foraminifera of the Crag. Part II. Monograph of the Palaeontographical Society, London, 49: i-vii, 73-210.

Jones, T.R.; Parker, W.K., 1860. On the rhizopodal fauna of the Mediterranean compared with that of the Italian and some other Tertiary deposits. Quarterly Journal of the Geological Society of London. 16: 292-307.

Jones, R. W., 1984. A revised classification of the unilocular Nodosariida and Buliminida (Foraminifera). Revista española de micropaleontología. 16: 91-160.

Jones, R.W., 1994. The Challenger Foraminifera. Oxford University Press. USA, 149pp.

Jorissen, F. J., 1987. The distribution of benthic foraminifera in the Adriatic Sea. Marine Micropaleontology, 12, 21-48.

Jorissen, F. J., 1988. Benthic foraminifera from the Adriatic Sea; principles of phenotypic variation. Utrecht Micropaleontological Bulletins, (37).

Jorissen, F. J., de Stigter, H. C., and Widmark, J. G., 1995. A conceptual model explaining benthic foraminiferal microhabitats. Marine micropaleontology, 26(1-4), 3-15.

Jorissen, F., Nardelli, M. P., Almogi-Labin, A., Barras, C., Bergamin, L., Bicchi, E., ... and Spezzaferri, S. 2018. Developing Foram-AMBI for biomonitoring in the Mediterranean: species assignments to ecological categories. Marine Micropaleontology, 140, 33-45.

Kaasschieter, J., 1961. Foraminifera of the Eocene of Belgium. Institut Royal des Sciences Naturelles de Belgique, Mémoires. 147: 1-271.

Kaiho, K., 1989. Morphotype changes of deep-sea benthic foraminifera during the Cenozoic Era and their paleoenvironmental implications. Kaseki (Fossils), 47, 1-23. (in Japanese with English abstract).

Kaiho, K., 1991. Global changes of Paleogene aerobic/anaerobic benthic foraminifera and deep-sea circulation. Palaeogeography, Palaeoclimatology, Palaeoecology, 83(1-3), 65-85.

Kaiho, K. 1994. Benthic foraminiferal dissolved-oxygen index and dissolved-oxygen levels in the modern ocean. Geology, 22(8), 719-722.

Kaiho, K. 1999. Effect of organic carbon flux and dissolved oxygen on the benthic foraminiferal oxygen index (BFOI). Marine micropaleontology, 37(1), 67-76.

Kaminski, M.A., 2004. The Year 2000 Classification of the Agglutinated Foraminifera. In: Bubik, M. & Kaminski, M.A. (eds) Proceedings of the Sixth International Workshop on Agglutinated Foraminifera. Grzybowski Foundation Special Publication. 8: 237-255.

Kaminski, M. A., 2012. Calibration of the benthic foraminiferal oxygen index in the Marmara Sea. Geological Quarterly, 56(4), 757-764.

Kaminski, M. A., Aksu, A., Box, M., Hiscott, R. N., Filipescu, S., and Al-Salameen, M. 2002. Late Glacial to Holocene benthic foraminifera in the Marmara Sea: implications for Black Sea–Mediterranean Sea connections following the last deglaciation. Marine Geology, 190(1-2), 165-202.

Kanmacher F., 1798. Essays on the microscope. The Second Edition, with considerable additions and improvements. Dillon and Keating, London. xvii + [7 unnumbered] + 724 pp., 32 pl.

Karrer, F., 1868. Die miocene Foraminiferenfauna von Kostej im Banat. Sitzungsberichte der Kaiserlichen Akademie der Wissenschaften. Mathematisch-Naturwissenschaftliche Classe. Wien. 58: 121-193.

Kassambara A. and Patil I., 2023. ggcorrplot: Visualization of a Correlation Matrix using 'ggplot2', 10.32614/CRAN.package.ggcorrplot.

Kastens, K. A., and Cita, M. B., 1981. Tsunami-induced sediment transport in the abyssal Mediterranean Sea. Geological Society of America Bulletin, 92(11), 845-857.

Kılıç, S., Kılıç, Ö., Belivermiş, M., & Ergül, H. A., 2023. Chronology of PAH and PCB pollution using sediment core in the Golden Horn estuary (Sea of Marmara). Marine Pollution Bulletin, 187, 114570.

Kırcı-Elmas, E. 2006. Marmara Denizi geç kuvaterner foraminifer topluluğu ve paleoşinografik değerlendirmesi. Istanbul Universitesi Deniz Bilimleri ve İşletmeciliği Enstitüsü. PhD Thesis.

Kırcı-Elmas, E. 2013. Benthic foraminiferal distribution (living and dead) from a permanently stratified marginal sea (Marmara Sea, Turkey). The Journal of Foraminiferal Research, 43(4), 340-360.

Kırcı-Elmas, E., 2018. Benthic Foraminiferal Composition from the Brackish-Marine Transition Zone of the Marmara Sea, Turkey (Eastern Mediterranean). Thalassas: An International Journal of Marine Sciences, 34(2), 421-436.

Kırcı-Elmas, E., & Meriç, E., 2016. Benthic foraminiferal fauna of the Sea of Marmara. In: The Sea of Marmara: marine biodiversity, fisheries, conservation and governance, Eds: Özsoy, E., Çağatay, N., Balkıs, N, Balkıs, N., Öztürk, B., Turkish Marine Research Foundation, publication no 42: pp. 401-417.

Kırcı-Elmas, E., Algan, O., Öngen, İ. Ö., Struck, U., Altenbach, A. V., Sagular, E. K., and Nazik, A., 2008. Palaeoenvironmental investigation of sapropelic sediments from the Marmara Sea: A biostratigraphic approach to palaeoceanographic history during the last glacial-Holocene. Turkish Journal of Earth Sciences, 17(1), 129-168.

Kırcı Elmas, E., Nazik, A., Kapan, S., Meriç, E., Şeker Zor, E., Kalkan, B., ... and Güney, A. 2021. Ponto-caspian and mediterranean faunal and floral records of upper pleistocene-holocene sediments from the Izmit Gulf (Marmara Sea, Turkey). Acta Palaeontologica Romaniae v. 17 (2), p. 23-62.

Kisel'man, E. N., 1972, Verkhnemelovye i Paleotsenovye foraminifery novogo roda Spiroplectinella [Upper Cretaceous and Paleocene new foraminiferal genus Spiroplectinella], Trudy Sibirskogo Nauchno Issledovatel'skogo Instituta

Geologii Geofiziki i Mineral'nogo Syr'ya (SNIIGGIMS) Ministerstva Geologii i Okhrany Nedr SSSR, Novosibirsk 146:134-140.

Knight, R., 1986. Apertural characteristics of certain unilocular foraminifera: methods of study, nomenclature and taxonomic significance. Journal of Micropalaeontology, 5(2), 19.

Knudsen, K. L., and Seidenkrantz, M. S., 1994. Stainforthia feylingi new species from arctic to subarctic environments, previously recorded as Stainforthia schreibersiana (Czjzek). Late Cenozoic Benthic Foraminifera. Taxonomy Ecology and Stratigraphy, Cushman Foundation Special Publication No. 32. pp. 5-13.

Koho, K. A., & Piña-Ochoa, E, 2011. Benthic foraminifera: inhabitants of low-oxygen environments. In Anoxia: Evidence for eukaryote survival and paleontological strategies (pp. 249-285). Dordrecht: Springer Netherlands.

Krebs, C.J. 1989. Ecological Methodology. Harper & Row, New York.

Kruit, C., 1955. Sediments of the Rhône delta. I. Grain size and microfauna. Verhandlingen van het Koninklijk Nederlandsch Geologisch-Mijnbouwkundig Genootschap, Geologische Serie. 15: 357-514.

Kubanç, S. N., 2005. Diversity and comparison of Ostracoda of south Marmara Sea. Journal of Black Sea/Mediterranean Environment, 12(1), 17-34.

Kubanç, C., Kubanç, S. N., and Akıncı, H., 2008. Diversity of marine ostracoda (Crustacea) on the northern coasts of sea of Marmara (Turkey). Journal of Black Sea/Mediterranean Environment, 14(3), 167-182.

Kucera, M., Silye, L., Weiner, A. K., Darling, K., Lübben, B., Holzmann, M., ... and Morard, R. 2017. Caught in the act: anatomy of an ongoing benthic–planktonic transition in a marine protist. Journal of Plankton Research, 39(3), 436-449.

Kuşçu, İ., Okamura, M., Matsuoka, H., Gökaşan, E., Awata, Y., Tur, H., ... & Keçer, M., 2005. Seafloor gas seeps and sediment failures triggered by the August 17, 1999 earthquake in the Eastern part of the Gulf of İzmit, Sea of Marmara, NW Turkey. Marine Geology, 215(3-4), 193-214.

Lacroix, E., 1932. Textularidae [sic] du plateau continental Méditerranéen entre Saint-Raphael et Monaco. Bulletin de l'Institut Océanographique, Monaco. 591: 1-28.

Lagoe, M. B., 1979. Recent benthonic foraminiferal biofacies in the Arctic Ocean. Micropaleontology, 214-224.

Lalicker, C. G., 1935. Two new Foraminifera of the genus Textularia. Smithsonian Miscellaneous Collections. 91(22)[1947]: 1-2.

Lamarck, J.B.P.A. de., 1804. Suite des mémoires sur les fossiles des environs de Paris. Annales du Muséum d'Histoire Naturelle. 5: 28-36; 91-98; 179-188; 237-245; 349-367.

Lankester, E.R., 1885. Protozoa. In: Anon (ed.): Encyclopaedia Britannica, 9th ed. 19: 830-866.

Lankford, R. R., 1959. Distribution and ecology of foraminifera from east Mississippi Delta margin. AAPG Bulletin, 43(9), 2068-2099.

Lankford, R. R., and Phleger, F. B., 1973. Foraminifera from the nearshore turbulent zone, western North America. The Journal of Foraminiferal Research, 3(3), 101–132.

Le Calvez, J.; Le Calvez, Y., 1958. Répartition des foraminifères dans la baie de Villefranche. I. "Miliolidae". Annales de l'Institut océanographique. Nouvelle série. T. XXXV. Fasc. 3.

Le Calvez, Y., 1958. Les foraminifères de la Mer Celtique. Revue des travaux de l'Institut des pêches maritimes, 22(2), 148-211.

Lei, Y., and Li, T., 2016. Atlas of benthic foraminifera from China seas: The Bohai Sea and the Yellow Sea. Springer. 399 pp.

Leiter, C. 2008. Benthos-Foraminiferen in Extremhabitaten: Auswertung von METEOR-Expeditionen vor Namibia. Unpublished Ph.D. Thesis, Ludwig-Maximilians-Universität, München, Germany. 151 pp.

Leiter, C., & Altenbach, A. V., 2010. Benthic foraminifera from the diatomaceous mud belt off Namibia: characteristic species for severe anoxia. Palaeontologia Electronica, 13(2), 19.

Le Pichon, X., Chamot-Rooke, N., Rangin, C., & Sengör, A. M. C., 2003. The North Anatolian fault in the sea of marmara. Journal of Geophysical Research: Solid Earth, 108(B4).

Leroy, S. A. G., Henry, P., Peyron, O., Rostek, F., Kende, J., Bard, E., & Tachikawa, K., 2023. Palynology, palaeoclimate and chronology from the Saalian Glacial to Saint-Germain II interstadial from two long cores at the limit between the Mediterranean and Euxinian regions. Quaternary Science Reviews, 311, 108145.

Levin, L. A., Ekau, W., Gooday, A. J., Jorissen, F., Middelburg, J. J., Naqvi, S. W. A., ... and Zhang, J., 2009. Effects of natural and human-induced hypoxia on coastal benthos. Biogeosciences, 6(10), 2063-2098.

Lévy, A.; Mathieu, R.; Poignant, A.; Rosset-Moulinier, M. 1992. The Miliolacea with Quinqueloculina and Triloculina morphology from the Mediterranean. In: Takayanagi, Y.; Saito, T. (Editors), Studies in Benthic Foraminifera, pp 117-126. Tokai University Press.

Linnaeus, C., 1758. Systema Naturae per regna tria naturae, secundum classes, ordines, genera, species, cum characteribus, differentiis, synonymis, locis. Editio decima, reformata [10th revised edition], vol. 1: 824 pp. Laurentius Salvius: Holmiae.

Lipps, J.H., 1965. Revision of the foraminiferal family Pseudoparrellidae Voloshinova. Tulane Studies in Geology and Paleontology 3: 117-147.

Lipps, J. H., and Langer, M. R., 1999. Benthic foraminifera from the meromictic Mecherchar Jellyfish Lake, Palau (western Pacific). Micropaleontology, 45(3), 3430.

Little, S. N., and van Hengstum, P. J., 2019. Intertidal and subtidal benthic foraminifera in flooded caves: Implications for reconstructing coastal karst aquifers and cave paleoenvironments. Marine Micropaleontology, 149, 19-34.

Lobegeier, M. K., and Sen Gupta, B. K., 2008. Foraminifera of hydrocarbon seeps, Gulf of Mexico. The Journal of Foraminiferal Research, 38(2), 93-116.

Loeblich, A.R., and Tappan, H., 1953. Studies of Arctic foraminifera. Smithsonian miscellaneous collections. 121 (7):1–150.

Loeblich, A. R., and Tappan, H., 1961. Suprageneric classification of the Rhizopodea. Journal of Paleontology. 35: 245-330.

Loeblich, A. R., and Tappan, H., 1964. Treatise on Invertebrate Paleontology, Part C: Protista 2, Sarcodina, chiefly "Thecamoebians" and Foraminiferida. Geological Society of America and University of Kansas Press, Lawrence.

Loeblich, A. R.; Tappan, H., 1984. Suprageneric Classification of the Foraminiferida (Protozoa). Micropaleontology. 30(1): 1-70.

Loeblich, A. R., and Tappan, H., 1985. Some new and redefined genera and families of agglutinated foraminifera; II. The Journal of Foraminiferal Research, 15(3), 175–217. doi:10.2113/gsjfr.15.3.175

Loeblich, A. R., and Tappan, H., 1986. Some New and Revised Genera and Families of Hyaline Calcareous Foraminiferida (Protozoa). Transactions of the American Microscopical Society. 105(3): 239-265.

Loeblich, A. R., and Tappan, H., 1988. Foraminiferal genera and their classification. Van Nostrand Reinhold Company, New York.

Loeblich, A. R., and Tappan, H., 1994. Foraminifera of the Sahul shelf and Timor Sea. Cushman Foundation for Foraminiferal Research Special Publication No. 31, pp. 661.

Londeix, L., Herreyre, Y., Turon, J. L., & Fletcher, W., 2009. Last Glacial to Holocene hydrology of the Marmara Sea inferred from a dinoflagellate cyst record. Review of Palaeobotany and Palynology, 158(1-2), 52-71.

Łuczkowska, E., 1972. Miliolidae (Foraminiferida) from Miocene of Poland. Part I. Revision of the classification. Acta Palaeontologica Polonica. 17 (3): 341-377.

Łuczkowska, E., 1974. Miliolidae (Foraminiferida) from the Miocene of Poland Part II. Biostratigraphy, palaeoecology and systematics. Acta Palaeontologica Polonica. 19 (1): 3-176.

Lyu, J., Kouwenhoven, T. J., Calieri, R., and Lourens, L. J. 2022. Foraminifera of the Faneromeni section (Crete, Greece) reflect the palaeoenvironmental development towards the Messinian salinity crisis. Marine Micropaleontology, 172, 102107.

Magurran, A. E., 2004. Measuring biological diversity, 2nd ed. Blackwell Science Ltd, Oxford, U.K.

Margalef, R. 1958. Information theory in ecology. General Systematics, 3: 36–71.

Margerel, J. P., 1970, Aubignyna, nouveau genre de Foraminifères du Pliocène du Bosq d'Aubigny (Manche), Revue de Micropaléontologie 13:58-64.

Margerel, J.-P., 2016. Étude critique des genres Favulina, Homalohedra, Oolina, Entosolenia et Pseudofavulinan. gen. du Pliocène et du Pléistocène inférieur de la France occidentale et du Sud de l'Angleterre. Geodiversitas, 38(4), 559–578. doi:10.5252/g2016n4a6

Margreth, S. 2010. Benthic foraminifera associated to cold-water coral ecosystems. PhD Thesis. Departement für Erdwissenschaften – Geologie und Paläontologie Universität Freiburg (Schweiz). Thèse N° 1686. Freibourg. 248 pp.

Marie, P., 1941. Les Foraminifères de la craie à Belemnitella mucronata du Bassin de Paris. Mémoires du Muséum National d'Histoire Naturelle de Paris, Nouvelle Série. 12: 1-296.

Martins, M. V. A., Helali, M. A., Zaaboub, N., Boukef-BenOmrane, I., Frontalini, F., Reis, D., ... and Aleya, L. 2016. Organic matter quantity and quality, metals availability and foraminiferal assemblages as environmental proxy applied to the Bizerte Lagoon (Tunisia). Marine Pollution Bulletin, 105(1), 161-179.

Mathews, R. D. 1945. Rectuvigerina, a new genus of foraminifera from a restudy of Siphogenerina. Journal of Paleontology. 19: 588-606.

McCulloch, I., 1977. Qualitative observations on Recent foraminiferal tests with emphasis on the eastern Pacific. University of Southern California. Los Angeles.

McHugh, C. M., Seeber, L., Cormier, M. H., Dutton, J., Cagatay, N., Polonia, A., ... and Gorur, N., 2006. Submarine earthquake geology along the North Anatolia Fault in the Marmara Sea, Turkey: a model for transform basin sedimentation. Earth and Planetary Science Letters, 248(3-4), 661-684.

McHugh, C. M., Gurung, D., Giosan, L., Ryan, W. B., Mart, Y., Sancar, U., ... & Cagatay, M. N., 2008. The last reconnection of the Marmara Sea (Turkey) to the World Ocean: A paleoceanographic and paleoclimatic perspective. Marine Geology, 255(1-2), 64-82.

McHugh, C. M., Braudy, N., Çağatay, M. N., Sorlien, C., Cormier, M. H., Seeber, L., and Henry, P., 2014. Seafloor fault ruptures along the North Anatolia Fault in the Marmara Sea, Turkey: Link with the adjacent basin turbidite record. Marine Geology, 353, 65-83.

Menhinick, E.F. 1964. A comparison of some species-individuals diversity indices applied to samples of field insects. Ecology, 45: 859–61.

Meilland, J., Siccha, M., Weinkauf, M. F., Jonkers, L., Morard, R., Baranowski, U., ... & Kucera, M., 2019. Highly replicated sampling reveals no diurnal vertical migration but stable species-specific vertical habitats in planktonic foraminifera. Journal of plankton research, 41(2), 127-141.

Meilland, M., Cornuault, P., Morard, R., Brummer, G. -J. A., and Kucera, M. 2022. Identification guide to extant planktonic foraminifera. Part 1: Family Candeinidae and genera Berggrenia, Bolivina, Dentigloborotalia, and Neogallitellia. ICES Identification Leaflets for Plankton No. 196. 22 pp.

Melis, R., Celio, M., Bouchet, V. M., Varagona, G., Bazzaro, M., Crosera, M., and Pugliese, N. 2019. Seasonal response of benthic foraminifera to anthropogenic pressure in two stations of the Gulf of Trieste (northern Adriatic Sea, Italy): the marine protected area of Miramare versus the Servola water sewage outfall. Mediterranean Marine Science, 20(1), 120-141.

Mendes, I., Dias, J. A., Schönfeld, J., and Ferreira, Ó. 2012. Distribution of living benthic foraminifera on the northern Gulf of Cadiz continental shelf. The Journal of Foraminiferal Research, 42(1), 18-38.

Meriç, E., Avşar, N., Nazik, A., Alpar, B., Yokeş, B., Barut, İ.F., Ünl, S., 2005. Gemlik Körfezi yüzey çökellerinin foraminifer, ostrakod ve mollusk faunası, foraminifer kavkılarında gözlenen morfolojik anomaliler ile bölgenin sedimentolojik, hidrokimyasal ve biokimyasal özellikleri. MTA Dergisi 131, pp. 21-48.

Meric, E., Avşar, N., Yokeş, M.B. And Dincer, F., 2014a. Atlas of recent benthic foraminifera from Turkey. Micropaleontology, vol. 60 no. 3-4, pp. 211-398.

Meriç, E., Avşar, N., Yokeş, M. B., Dinçer, F., and Demir, V., 2014b. Foraminifera Population from South Africa Coast Line (Indian and Atlantic Oceans). International Journal of Environment and Geoinformatics, 1(1), 29-39.

Meriç, E., Yümün, Z. Ü., Nazik, A., Sagular, E. K., Yokeş, M. B., Büyükmeriç, Y., ... & Yavuzlar, G., 2020. Drilling and core data from the Gulf of Gemlik (SE Sea of Marmara): Holocene fauna and flora assemblages. Bulletin of the Mineral Research and Exploration, 161(161), 121-149.

Mikhalevich, V. I., 1980. Систематика и эволюция фораминифер в свете новых данных по их цитологии и ультраструктуре - Sistematika i evolyutsiya foraminifer v svete novykh dannykh po ikh tsitologii i ul'trastrukture - Systematics and evolution of foraminifera in the light of new data on their cytology and ultrastructure. In: Крылов, М. В., Старобогатов, Я. И. (ред.), Принципы построения макросистемы одноклеточных животных. In: Krylov, M. V., Starobogatov, Y. I. (eds.), Printsipy postroyeniya makrosistemy odnokletochnykh zhivotnykh [Principles of the construction of the macrosystem of the unicellular animals]. Труды Зоологического института Академия наук СССР - Trudy Zoologicheskogo Instituta Akademiya Nauk SSSR - Proceedings of the Zoological Institute, Academy of Sciences of the USSR. 94: 42-61.

Mikhalevich, V.I. 1981. Parallelizm i konvergentsiya v evolyutsii skeletov foraminifer [Parallelism and convergence in the skeletal evolution of foraminifera]. Trudy Zoologicheskogo Instituta, Akademiya Nauk SSSR 107: 19-41.

Mikhalevich, V. I., 1983. The bottom foraminifera from the shelves of the tropical Atlantic. USSR Academy of Sciences, Zoological Institute. 1-247.

Mikhalevich, V. I., 1993. New higher taxa of the subclass Nodosariata (Foraminifera). Zoosystematica Rossica. 2(1): 5-8.

Mikhalevich, V. I., 2013. New insight into the systematics and evolution of the foraminifera. Micropaleontology, 493-527.

Milker, Y. and Schmiedl, G., 2012. A taxonomic guide to modern benthic shelf foraminifera of the western Mediterranean Sea. Palaeontologia electronica, 15(2), pp.1-134.

Millett, F. W., 1898. Report on the Recent foraminifera of the Malay Archipelago collected by Mr. A. Durrand, FRMS. Journal of the Royal Microscopical Society, 18(3), 258-269.

Millett, F. W., 1901. Report on the Recent Foraminifera of the Malay Archipelago. Part XI. Journal of the Royal Microscopical Society. 485-497.

Milne-Edwards, A., 1881. Compte rendu sommaire d'une exploration zoologique, faite dans la Méditerranée, à bord du navire de l'Etat ≪le Travailleur≫. Comptes Rendu Hebdomadaires des Séances de l'Académie des Sciences. 93(2): 876-882.

Mischke, S., Schudack, U., Bertrand, S., and Leroy, S. A. 2012. Ostracods from a Marmara Sea lagoon (Turkey) as tsunami indicators. Quaternary International, 261, 156-161.

Montagu, G., 1803. Testacea Britannica or natural history of British shells, marine, land, and fresh-water, including the most minute: Systematically arranged and embellished with figures. J. White, London, Vol. 1, xxxvii + 291 pp;; Vol. 2, pp. 293–606, pl. 1-16.

Mudie, P. J., Aksu, A. E., & Yasar, D., 2001. Late Quaternary dinoflagellate cysts from the Black, Marmara and Aegean seas: variations in assemblages, morphology and paleosalinity. Marine Micropaleontology, 43(1-2), 155-178.

Mudie, P. J., Rochon, A., Aksu, A. E., & Gillespie, H., 2002. Dinoflagellate cysts, freshwater algae and fungal spores as salinity indicators in Late Quaternary cores from Marmara and Black seas. Marine geology, 190(1-2), 203-231.

Mudie, P. J., Rochon, A., Aksu, A. E., & Gillespie, H., 2004. Late glacial, Holocene and modern dinoflagellate cyst assemblages in the Aegean–Marmara–Black Sea corridor: statistical analysis and re-interpretation of the early Holocene

Noah's Flood hypothesis. Review of Palaeobotany and Palynology, 128(1-2), 143-167.

Mudie, P. J., Marret, F., Aksu, A. E., Hiscott, R. N., & Gillespie, H., 2007. Palynological evidence for climatic change, anthropogenic activity and outflow of Black Sea water during the late Pleistocene and Holocene: centennial-to decadal-scale records from the Black and Marmara Seas. Quaternary International, 167, 73-90.

Mudie, P. J., Aksu, A. E., & Hiscott, R. N., 2024. Late Pleistocene–Holocene palynology and paleoceanography of İmralı Basin, Marmara Sea: Pollen-spore, dinoflagellate cyst and other NPP zonations. Review of Palaeobotany and Palynology, 331, 105179.

Mullineaux, L. S., and Lohmann, G. P., 1981. Late Quaternary stagnations and recirculation of the eastern Mediterranean; changes in the deep water recorded by fossil benthic foraminifera. The Journal of Foraminiferal Research, 11(1), 20–39. doi:10.2113/gsjfr.11.1.20

Murray, J.W. 1991. Ecology and Palaeoecology of Benthic Foraminifera. Longman Scientific and Technical, England.

Murray, J. W., 1984. Paleogene and Neogene benthic foraminifers from Rockall Plateau. Init. Rep. DSDP, 81, 503-534.

Murray, J.W. 2003. An illustrated guide to the benthic foraminifera of the Hebridean shelf, west of Scotland, with notes on their mode of life. Paleaeontologia Electronica Vol. 5, Issue 1: 31p.

Murray, J. W., and Alve, E., 2011. The distribution of agglutinated foraminifera in NW European seas: Baseline data for the interpretation of fossil assemblages. Palaeontologia Electronica, 14(2), 1-41.

Murray, J. W., Whittaker, J. E., and Alve, E., 2000. On the type species of Aubignyna and a description of A. hamblensis, a new microforaminifer from temperate shallow waters. Journal of Micropalaeontology, 19(1), 61-67.

Musco, M. 2012. Study of benthic foraminifera in the Sicilian Channel and their applicability as bio-indicators. PhD Thesis. Università Ca' Foscari Venezia, 191 pp (Unpublished).

Mutlu, S., Önol, B., Ilıcak, M., & Altıok, H., 2024. Sensitivity Simulations of Wind-driven Water Circulation in İzmit Bay. Journal of Marine Science and Engineering, 12(5), 824.

Nazik, A., 2001. Ostracode faunas of bottom sediments from the continental shelf, south Marmara Sea, NW Turkey, and their comparison with other shelf environments in the Mediterranean and Aegean regions. Geological Journal, 36(2), 111-123.

Nomura, R. 1983. Cassidulinidae (foraminiferida) from the uppermost Cenozoic of Japan (part 1). Tohoku University Scientific Reports, 2nd Series (Geology), 53, 1-101.

Nørvang, A., 1958. Islandiella n. g. and Cassidulina d'Orbigny. Videnskabelige Meddelelser fra Dansk naturhistorisk Forening. v. 120, p. 25–41, pls, 6–9.

Nunes, M., Martins, M. V. A., Frontalini, F., Bouchet, V. M., Francescangeli, F., Hohenegger, J., ... and Geraldes, M. C., 2023. Inferring the ecological quality status based on living benthic foraminiferal indices in transitional areas of the Guanabara bay (SE Brazil). Environmental Pollution, 320, 121003.

O'Malley, B. J., Schwing, P. T., Martínez-Colón, M., Spezzaferri, S., Machain-Castillo, M. L., Larson, R. A., ... and Hollander, D. J. 2021. Development of a benthic foraminifera based marine biotic index (Foram-AMBI) for the Gulf of Mexico: A decision support tool. Ecological Indicators, 120, 106916.

O'Neill, B. J. 1981. Pliocene and Pleistocene benthic foraminifera from the central Arctic Ocean. Journal of Paleontology, 1141-1170.

Oglesby, D. D., & Mai, P. M., 2012. Fault geometry, rupture dynamics and ground motion from potential earthquakes on the North Anatolian Fault under the Sea of Marmara. Geophysical Journal International, 188(3), 1071-1087.

Olguner, B., Mülayim, A., & Gündüz, S. K., 2023. Microplastic concentration in the sediment of the Istanbul Strait (the Sea of Marmara, Türkiye). Journal of Soils and Sediments, 23(7), 2892-2904.

Okay, A. İ., Kaşlılar-Özcan, A., İmren, C., Boztepe-Güney, A., Demirbağ, E., & Kuşçu, İ., 2000. Active faults and evolving strike-slip basins in the Marmara Sea, northwest Turkey: a multichannel seismic reflection study. Tectonophysics, 321(2), 189-218.

Okyar, M., Pinar, A., Tezcan, D., and Kamaci, Z., 2008. Late quaternary seismic stratigraphy and active faults of the Gulf of Izmit (NE Marmara Sea). Marine Geophysical Researches, 29, 89-107.

Otansev, P., Taşkın, H., Başsarı, A., & Varinlioğlu, A., 2016. Distribution and environmental impacts of heavy metals and radioactivity in sediment and seawater samples of the Marmara Sea. Chemosphere, 154, 266-275.

Ovsepyan, Y. S., and Taldenkova, E. E. 2019. Distribution Patterns and Morphology of Islandiella norcrossi (Cushman) in the Upper Quaternary Deposits of the Laptev Sea. Paleontological Journal, 53(1), 10-19

Özgür Özbek, E., 2016. Echinoderm fauna of the Sea of Marmara, Turkey. In: The Sea of Marmara: Marine biodiversity, fisheries, conservation and governance, Eds: Özsoy, E., Çağatay, M.N., Balkıs, N., Balkıs, N., Öztürk, B., Turkish Marine Research Foundation Publication No: 42, pp. 517-532.

Öztoprak, B., Doğan, A., & Dağli, E., 2014. Checklist of Echinodermata from the coasts of Turkey. Turkish Journal of Zoology, 38(6), 892-900.

Panieri, G., Gamberi, F., Marani, M., and Barbieri, R., 2005. Benthic foraminifera from a recent, shallow-water hydrothermal environment in the Aeolian Arc (Tyrrhenian Sea). Marine Geology, 218(1-4), 207-229.

Papp, A., and Schmid, M. E., 1985. Die fossilen Foraminiferen des tertiären Beckens von Wien. Revision der Monographie von ALCIDE d'ORBIGNY (1846). The fossil foraminifera of the Tertiary Basin of Vienna. Revision of the monograph by ALCIDE d'ORBIGNY (1846). Abhandlungen Der Geologischen Bundesanstalt. Band 37, Wien. 311 pp.

Parr, W. J., 1932. Victorian and South Australian shallow-water foraminifera. Part II. *Proceedings of the Royal Society of Victoria.* 44: 218-234.

Parker, F. L., 1952. Foraminiferal distribution in the Long Island Sound - Buzzards Bay area. Bulletin of the Museum of Comparative Zoology. 106: 428-473.

Parker, F. L. 1954. Distribution of the foraminifera in the northeastern Gulf of Mexico. Bulletin of the Museum of Comparative Zoology at Harvard College. 111(10):453-588.

Parker, F.L. 1958. Eastern Mediterranean Foraminifera. Reports of the Swedish Deep-Sea Expedition, Sediment Cores from the Mediterranean Sea and the Red Sea, 8:217-285.

Parker, F.L., Pheleger, F.B., Peirson, J.F., 1953. Ecology of foraminifera from San Antonio Bay and environs, Southwest Texas. Cushman Foundation for Foraminiferal Research, Special Publication, No. 2.

Parker, W. K. and Jones, T. R., 1865. On some Foraminifera from the North Atlantic and Arctic Oceans, including Davis Straits and Baffin's Bay. Philosophical transactions of the Royal Society of London. vol. 155: 325-441.

Parker W. K., Jones T. R. and Brady H. B. 1865. On the nomenclature of the Foraminifera. Part X. (continued). The species enumerated by D'Orbigny in the 'Annales des Sciences Naturelles,' 1826, vol. vii. - III. The species illustrated by models. Annals and Magazine of Natural History. (3) 16 (91): 15-41.

Parker W. K., Jones T. R. and Brady H. B., 1871. On the nomenclature of the Foraminifera. Part XIV. The species enumerated by D'Orbigny in the 'Annales des Sciences Naturelles,' 1826, vol. vii. - IV. The species founded upon the figures in Soldani's 'Testaceographia ac Zoophytogeographia'. [Continued from vol. iv. p. 392.]. *Annals and Magazine of Natural History.* (4) 8 (45): 145-179.

Parr, W. J., 1932. Victorian and South Australian shallow-water foraminifera. Part II. Proceedings of the Royal Society of Victoria. 44: 218-234.

Parr, W. J., 1942. New genera of Foraminifera from the Tertiary of Victoria. Mining and Geological Journal. 2(6): 361-363.

Parr, W. J., 1945. Recent Foraminifera from Barwon Heads, Victoria. Proceedings of the Royal Society of Victoria, new series. 56: 189-228.

Parr, W. J., 1947. The Lagenid Foraminifera and their Relationships. Proceedings of the Royal Society of Victoria. 58: 116-133.

Parr, W. J. 1950. Foraminifera. B.A.N.Z. Antarctic Research Expedition 1929-1931. Report. Series B 5 (6): 232-392.

Patterson, R. T.; Richardson, R. H. (1987). A taxonomic revision of the unilocular foraminifera. The Journal of Foraminiferal Research. 17(3): 212-226.

Patterson, R. T.; Richardson, R. H. 1988. Eight New Genera of Unilocular Foraminifera. Transactions of the American Microscopical Society. 107: 240-258.

Pawlowski, J., Bolivar, I., Farhni, J., and Zaninetti, L., 1995. DNA analysis of “Ammonia beccarii” morphotypes: One or more species?. Marine micropaleontology, 26(1-4), 171-178.

Pawlowski, J.; Holzmann, M.; Tyszka, J., 2013. New supraordinal classification of Foraminifera: Molecules meet morphology. Marine Micropaleontology. 100: 1-10.

Pekey, H., Karakaş, D., Ayberk, S., Tolun, L., & Bakoğlu, M., 2004. Ecological risk assessment using trace elements from surface sediments of Izmit Bay (Northeastern Marmara Sea) Turkey. Marine pollution bulletin, 48(9-10), 946-953.

Pellegrino, L., Abe, K., Gennari, R., Lozar, F., Pierre, F. D., Natalicchio, M., ... and Carnevale, G. 2020. Integrated micropaleontological study of the Messinian diatomaceous deposits of the Monferrato Arc (Piedmont basin, NW Italy): New insights into the paleoceanographic evolution of the northernmost Mediterranean region. Marine Micropaleontology, 160, 101910.

Perçin-Paçal, F., and Balkıs, H., 2012. Seasonal distribution of Ostracoda in Bandirma Bay and Erdek Bay, Sea of Marmara, Turkey. Crustaceana, 847-875.

Perçn-Paçal, F., and Balkıs, H., 2015. The Ecology of The Ostracoda (Crustacea) Species Obtained From Erdek Bay (The Marmara Sea, Turkey). International Journal of Environmental Research, 9(4), 1245-1258.

Perçin-Paçal, F., Altınsaçlı, S., and Balkıs, H., 2016. Recent Ostracoda Species of the Sea of Marmara with Çanakkale (Dardanelles) and İstanbul Strait (Bosphorus): A Review. In: The Sea of Marmara: Marine biodiversity, fisheries, conservation and governance, Eds: Özsoy, E., Çağatay, M.N., Balkıs, N., Balkıs, N., Öztürk, B., Turkish Marine Research Foundation Publication No: 42, pp. 454-467.

Perçin-Paçal, F., Altınsaçlı, S., Arısal, S. B., and Balkıs, H., 2019. Assessment of the spatio-temporal distribution and habitat preferences of Ostracoda (Crustacea) related to certain environmental factors in Kapıdağ Peninsula (the Sea of Marmara, Turkey). Hacettepe Journal of Biology and Chemistry, 47(4), 347-365.

Phipps, M.D., Kaminski, M.A. and Aksu, A.E., 2010. Calcareous benthic foraminiferal biofacies along a depth transect on the southwestern Marmara shelf (Turkey). Micropaleontology, vol 56 nos 3-4 pp.377-392.

Phleger, F.B. 1965. Living benthic foraminifera from coastal marsh, southwestern Florida. Boletín de la Sociedad Geológica Mexicana, 28:45-60.

Phleger, F. B., and Parker, F. L. 1951. Part II. Foraminifera Species. Ecology of Foraminifera, Northwest Gulf of Mexico, 1–80.

Pielou, E. C., 1966. The measurement of diversity in different types of biological collections. Journal of Theoretical Biology, 13, 131-144. doi:10.1016/0022-5193(66)90013-0.

Poignant, A., 2019. The" avatars" of Triloculina laevigata Orbigny, 1826, generic and specific attribution. Carnets Geol., 19(03), 35.

Pokorný, V. 1956. New Discorbidae (Foraminifera) from the Upper Eocene brown Pouzdrany Marl, Czechoslovakia. Universitas Carolina, Geologica. 2/3: 257–278.

Polonia, A., Gasperini, L., Amorosi, A., Bonatti, E., Bortoluzzi, G., Cagatay, N., ... & Seeber, L., 2004. Holocene slip rate of the North Anatolian Fault beneath the Sea of Marmara. Earth and Planetary Science Letters, 227(3-4), 411-426.

Popescu, G., and Crihan, I. M., 2004. Contributions to the knowledge of the Miocene foraminifera from Romania: superfamily Nodosariacea (fam. Nodosariidae and Vaginulinidae). Acta Paleontologica Romaniae, 4, 385-402.

Pracht, H., Metcalfe, B., & Peeters, F. J., 2019. Oxygen isotope composition of the final chamber of planktic foraminifera provides evidence of vertical migration and depth-integrated growth. Biogeosciences, 16(2), 643-661.

Rana, S. S., 2009. Study of foraminiferal distribution in surface and subsurface sediments off central east coast of India and their paleoecological significance (Doctoral dissertation, Goa University).

Rasmussen, T. L., 1991. Benthonic and planktonic foraminifera in relation to the Early Holocene stagnation in the Ionian Basin, Central Mediterranean. Boreas, 20(4), 357-376.

Rasmussen, T.L., 2005. Systematic paleontology and ecology of benthic foraminifera from the Plio-Pleistocene Kallithea Bay section, Rhodes, Greece. Cushman Foundation Special Publication, 39:53-157.

Resig, J. M., 1958. Ecology of foraminifera of the Santa Cruz. Basin, California. Micropaleontology. 4(3): 287-308.

Reimer PJ, Reimer RW, 2001. A marine reservoir correction database and on-line interface. Radiocarbon 43:461-3.

Reiss, Z., 1963. Reclassification of perforate foraminifera. Bull. Geol Surv. Israel. 35: 1-111.

Reuss, A. E., 1850. Neue Foraminiferen aus den Schichten des österreichischen Tertiärbeckens. Denkschriften der Kaiserlichen Akademie der Wissenschaften. 1: 365-390.

Reuss, A. E., 1851. Ueber die fossilen Foraminiferen und Entomostraceen der Septarienthone der Umgegend von Berlin. Zeitschrift der Deutschen Geologischen Gesellschaft. 3 (1): 49-92

Reuss, A.E., 1858. Über die Foraminiferen von Pietzbühl. Zeitschrift der Deutschen geologischen Gesellschaft, 10:433-438.

Reuss, A. E., 1860. Die Foraminiferen der westphälischen Kreideformation. Sitzungsberichte der mathematisch-naturwissenschaflichen Classe der kaiserlichen Akademie der Wissenschaften. 40 (8): 147-238.

Reuss, A. E., 1861. Beiträge zur Kenntniss der tertiären Foraminiferen-Fauna. I. Die Foraminiferen des Crag's von Antwerpen. II. Die Foraminiferen von Dingden in Westphalen. Sitzungsberichte der Kaiserlichen Akademie der Wissenschaften. Mathematisch-Naturwissenschaftliche Classe. 42 (24): 355-370.

Reuss, A. E., 1862a. Paläontologische Beiträge. Sitzungsberichte der Kaiserlichen Akademie der Wissenschaften. Mathematisch-Naturwissenschaftliche Classe. Abt. 1, Mineralogie, Botanik, Zoologie, Anatomie, Geologie und Paläontologie. 44[1861]: 301-342.

Reuss, A. E., 1862b. Entwurf einer systematischen Zusammenstellung der Foraminiferen. Sitzungsberichte der Kaiserlichen Akademie der Wissenschaften. Mathematisch-Naturwissenschaftliche Classe. Abt. 1, Mineralogie, Botanik, Zoologie, Anatomie, Geologie und Paläontologie. (1861) 44(1).355-396.

Reuss, A. E., 1863. Die Foraminiferen - Familie der Lagenideen. Sitzungsberichte der Akademie der Wissenschaften. Mathematisch-naturwissenschaftliche Klasse, Wien. 46: 308-342.

Reuss, A. E., 1870. Die Foraminiferen des Septarienthones von Pietzpuhl. Sitzungsberichte der mathematisch-naturwissenschaflichen Classe der kaiserlichen Akademie der Wissenschaften. 62 (9): 455-493.

Revets, S. A., 1993a. The revision of the genus Elongobula Finlay, 1939. The Journal of Foraminiferal Research. 23(4): 254-266.

Revets, S. A., 1993b. The revision of the genus Buliminellita Cushman and Stainforth, 1947, and Eubuliminella gen. nov. The Journal of Foraminiferal Research, 23(2), 141-151.

Revets, S. A., 1996. The Generic Revision of Five Families of Rotaliine Foraminifera. Part 1--The Bolivinitidae. Part 2--The Anomalinidae, Alabaminidae, Cancrisidae and Gavelinellidae. Cushman Foundation for Foraminiferal Research Special Publication No. 34, 113 pp.

Revets, S. A., 2005. A key to the unilocular hyaline Foraminifera. Journal of Micropalaeontology, 24(2), 145-158.

Reyment, R.A. 1983. Internal Structure of Bolivina and Afrobolivina. Micropaleontology, Vol. 29, No. 1.

Rhumbler, L., 1906. Die Foraminiferen von Laysan und den Chatham-Inseln. Zoologische Jahrbücher. 24(1): 21-80.

Rigaud, S., and Martini, R., 2016. Agglutinated or porcelaneous tests: where to draw the line?. The Journal of Foraminiferal Research, 46(3), 333-344.

Rigaud, S.; Vachard, D.; Schlagintweit, F.; Martini, R., 2015. New lineage of Triassic aragonitic Foraminifera and reassessment of the class Nodosariata. Journal of Systematic Palaeontology. 14(11): 919-938.

Risso, A., 1826. Aperçu sur l'histoire naturelle de mollusques qui vivent sur les Bords de la Méditerranée Boréale et des coquilles terrestres, fluviatiles et marines, subfossiles, fossils et pétrifiée, […]. In Histoire naturelle des principales productions de l'Europe Méridionale. Tome 4. Paris.

Ritt, B., Duperron, S., Lorion, J., Lazar, C. S., & Sarrazin, J., 2012. Integrative study of a new cold-seep mussel (Mollusca: Bivalvia) associated with chemosynthetic symbionts in the Marmara Sea. Deep Sea Research Part I: Oceanographic Research Papers, 67, 121-132.

Romano, E., Bergamin, L., Pierfranceschi, G., Provenzani, C., and Marassich, A., 2018. The distribution of benthic foraminifera in Bel Torrente submarine cave (Sardinia, Italy) and their environmental significance. Marine environmental research, 133, 114-127.

Ross, C. R., and Kennett, J. P., 1984. Late Quaternary paleoceanography as recorded by benthonic foraminifera in Strait of Sicily sediment sequences. Marine Micropaleontology, 8(4), 315–336. doi:10.1016/0377-8398(84)90019-7

Rögl, F., and Hansen, H. J., 1984. Foraminifera described by Fitchel and Moll in 1798. A revision of Testacea Microscopica. Neue Denkschriften des Naturhistorischen Museum in Wien. 3: 1-143.

Ruffine, L., Ondreas, H., Blanc-Valleron, M. M., Teichert, B. M., Scalabrin, C., Rinnert, E., ... & Géli, L., 2018. Multidisciplinary investigation on cold seeps with vigorous gas emissions in the Sea of Marmara (MarsiteCruise): Strategy for site detection and sampling and first scientific outcome. Deep Sea Research Part II: Topical Studies in Oceanography, 153, 36-47.

Ryan, W. B., Carbotte, S. M., Coplan, J. O., O'Hara, S., Melkonian, A., Arko, R., ... & Zemsky, R., 2009, Global Multi-Resolution Topography (GMRT) synthesis data set, Geochemistry, Geophysics, Geosystems, 10, Q03014, doi:10.1029/2008GC002332.

Rzehak, A., 1885, Bemerkungen über einige Foraminiferen der Oligocän Formation, Verhandlungen des Naturforschenden Vereins in Brünn (1884) 23:123-129.

Rzehak, A., 1888, Die Foraminiferen der Nummuliten-schichten des Waschberges und Michelsberges bei Stockerau in Nieder-Osterreich, Verhandlungen der Geologischen Bundesanstalt 1888:226-229.

Sakınç, M. 2008. Marmara Denizi Bentik Foraminiferleri: Sistematik ve Otoekoloji. İstanbul Teknik Üniveristesi, Maslak, İstanbul.

Sakınç, M., & Artüz, M. L., 2019. New records of Foraminifera: The Sea of Marmara (Turkey). Revue de Micropaleontologie, 64, 100359.

Sarı, E., & Çağatay, M. N., 2006. Turbidites and their association with past earthquakes in the deep Çınarcık Basin of the Marmara Sea. Geo-Marine Letters, 26, 69-76.

Saidova, K. M., 1975. Бентосине фораминиферий Тихого океана-Bentosniye foraminifery Tikhogo Okeana-Benthonic Foraminifera of the Pacific Ocean.

Институт океанологии им. П. П. Шершова Академии наук СССР-P.P. Shirshov Institute of Oceanology, Academy of Sciences of the USSR, Moscow. 3: parts.

Saidova, K. M., 1981. О современном состоянии системы надвидовых таксонов кайнозойских бентосных фораминифер - [On an up-to-date system of supraspecific taxonomy of Cenozoic benthonic foraminifera]. *Akademiya Nauk SSSR.* 1-73.

Saunders, J. B., and Mueller-Merz, E., 1982. The genus Pseudononion in relationship with Nonion, Nionella, and Nionellina. The Journal of Foraminiferal Research, 12(3), 261-275.

Schiebel, R. 1992. Rezente benthische Foraminiferen in Sedimenten des Schelfes und oberen Kontinentalhanges im Golf von Guinea (Westafrika). BerichteReports, Geol. Paläont. Inst., Universität Kiel, 51:1-126

Schlumberger, C., 1887. Note sur le genre Planispirina. Bulletin de la Société Zoologique de France. 12:475-488

Schlumberger, C., 1891. Révision des Biloculines des grands fonds. Mémoires de la Société zoologique de France. 4: 542-579.

Schlumberger, C., 1893. Monographie des Miliolidées du Golfe de Marseille. Mémoires de la Société zoologique de France. 6: 57-80

Schönfeld, J., 1997. The impact of the Mediterranean Outflow Water (MOW) on benthic foraminiferal assemblages and surface sediments at the southern Portuguese continental margin. Marine Micropaleontology, 29(3-4), 211-236.

Schönfeld, J. 2006. Taxonomy and distribution of the Uvigerina peregrina plexus in the tropical to northeastern Atlantic. The Journal of Foraminiferal Research, 36(4), 355-367.

Schönfeld, J., Alve, E., Geslin, E., Jorissen, F., Korsun, S., and Spezzaferri, S., 2012. The FOBIMO (FOraminiferal BIo-MOnitoring) initiative—Towards a standardised protocol for soft-bottom benthic foraminiferal monitoring studies. Marine Micropaleontology, 94-95, 1–13. doi:10.1016/j.marmicro.2012.06.001

Schönfeld, J., Golikova, E., Korsun, S., & Spezzaferri, S., 2013. The Helgoland Experiment–assessing the influence of methodologies on Recent benthic foraminiferal assemblage composition. Journal of Micropalaeontology, 32(2), 161-182.

Schröter, J. S., 1783. Einleitung in die Conchylienkenntniß nach Linné. Erster Band, von den Schnecken. pp. i-xxxii, 1-860, [1-2], pls 1-3. Johan Jacob Gebauer, Halle.

Schubert, R. J., 1904. Die Ergebnisse der mikroskopischen Untersuchung der bei der ärarischen Tiefbohrung zu Wels durchteuften Schichten. Jahrbuch der kaiserlich-königlichen geologischen Reichsanstalt. 53(3): 385-422.

Schultze, M. J. S., 1854. Über den Organismus der Polythalamien (Foraminiferen), nebst Bemerkungen über die Rhizopoden im allgemeinen. Ingelmann, Leipzig. 1-68.

Schwager, C. 1866. Fossile Foraminiferen von Kar Nikobar. Reise der Österreichischen Fregatte Novara um die Erde in den Jahren 1857, 1858, 1859 unter den Befehlen des Commodore B. von Wüllerstorf-Urbair. Geologischer Theil (Zweite Abtheilung, Paläontologische Mittheilungen) 2(2): 187-268.

Schwager, C., 1876, Saggio di una classificazione dei foraminiferi avuto riguardo alle loro famiglie naturali, Bolletino R. Comitato Geologico d'Italia 7:475-485.

Schwager, C., 1877. Quadro del proposto sistema di classificazione dei foraminiferi con guscio. Bolletino R. Comitato Geologico d'Italia. 8: 18-27.

Schweizer, M., Pawlowski, J., Duijnstee, I. A., Kouwenhoven, T. J., and Van der Zwaan, G. J. 2005. Molecular phylogeny of the foraminiferal genus Uvigerina based on ribosomal DNA sequences. Marine Micropaleontology, 57(3-4), 51-67.

Schweizer, M., Pawlowski, J., Kouwenhoven, T., and Van Der Zwaan, B., 2009. Molecular phylogeny of common cibicidids and related Rotaliida (Foraminifera) based on small subunit rDNA sequences. The Journal of Foraminiferal Research, 39(4), 300-315.

Scott, D. B., and Vilks, G. 1991. Benthic foraminifera in the surface sediments of the deep-sea Arctic Ocean. The Journal of Foraminiferal Research, 21(1), 20-38.

Seeber, L., Cormier, M. H., McHugh, C., Emre, O., Polonia, A., & Sorlien, C., 2006. Rapid subsidence and sedimentation from oblique slip near a bend on the North Anatolian transform fault in the Marmara Sea, Turkey. Geology, 34(11), 933-936.

Seiglie, G. A., 1965, Some observations on Recent foraminifers from Venezuela, Part I, Contributions from the Cushman Foundation for Foraminiferal Research 16:70-73.

Seguenza, G. 1862a. Prime ricerche intorno ai rizopodi fossili delle argille pleistoceniche dei dintorni di Catania. *Atti della Accademia gioenia di scienze naturali in Catania.* ser. 2 vol. 18: 85-125.

Seguenza, G. 1862b. Dei Terreni Terziarii del Distretto di Messina. Parte II - Descrizione dei Foraminiferi Monotalamici delle Marne Mioceniche del Distretto di Messina. Capra, Messina. 1-84.

Sejrup, H. P., and Guilbault, J. P. (1980). Cassidulina reniforme and C. obtusa (Foraminifera), taxonomy, distribution, and ecology. Sarsia, 65(2), 79-85.

Sen Gupta, B. K., Eugene Turner, R., & Rabalais, N. N., 1996. Seasonal oxygen depletion in continental-shelf waters of Louisiana: Historical record of benthic foraminifers. Geology, 24(3), 227-230.

Sgarrella, F., and Moncharmont Zei, M. 1993. Benthic foraminifera of the Gulf of Naples (Italy): systematics and autoecology. Bollettino della Società Paleontologica Italiana, (2).

Shannon, C.E. & W. Weaver. 1949. The Mathematical Theory of Communication. University of Illinois Press, Urbana, IL.

Siani, G., Paterne, M., Arnold, M., Bard, E., Métivier, B., Tisnerat, N., and Bassinot, F. 2000. Radiocarbon reservoir ages in the Mediterranean Sea and Black Sea. Radiocarbon, 42(2), 271-280.

Sidebottom, H., 1912. Lagenae of the South-West Pacific Ocean. From soundings taken by H.M.S. Waterwitch, 1895. Journal of the Quekett Microscopical Club. 2(11): 375-434 + pls.

Sigal, J., 1952. Aperçu stratigraphique sur la micropaléontologie du Crétacé. Monographies Régionales, Algérie. 1(26): 3-43.

Silvestri, A., 1896. Foraminiferi pliocenici della provincia di Siena. Part I. Memorie dell'Accademia Pontificia dei Nuovi Lincei 12: 1-224.

Silvestri, A., 1898. Foraminiferi Pliocenici della Provincia di Siena. Parte II. Memorie dell'Accademia Pontificia dei Nuovi Lincei, Roma. 15: 155-381.

Silvestri, A., 1903. Dimorfismo e nomenclatura d'una Spiroplecta. Altre notizie sulla struttura della Siphogenerina columellaris. Atti della Pontificia Accademia Romana dei Nuovi Lincei, Roma. 56: 59-66.

Silvestri, A., 1904. Ricerche strutturali su alcune forme dei Trubi dei Bonfornello (Palermo). Memorie dell'Accademia Pontificia dei Nuovi Lincei. 22: 235-276.

Silvestri, A., 1923. Lo stipite della Elissoforme e le sue affinità. Memorie della Pontificia Accademia della Scienze, Nuovi Lincei, ser. 2. 6: 231-270.

Silvestri, O., 1872. Saggio di studj sulla fauna microscopica fossile appartenente al terreno subapennino italiano. Memoria Prima - Monografia delle Nodosarie. Atti dell'Accademia Gioenia di Scienze Naturali di Catania. (3), 7: 1-108.

Simpson, E.H., 1949. Measurement of diversity. Nature, 163: 688.

Skinner, H. C., 1961. Revision of 'Proteonina difflugiformis'. Journal of palaeontology. 35: 1238-1240.

Sliter, W. V., 1968. Upper Cretaceous Foraminifera from southern California and northwestern Baja California, Mexico. University of Kansas Paleontological Contributions. 49(7): 1-141.

Sliter, W. V., 1970. Inner-neritic Bolivinitidae from the eastern Pacific margin. Micropaleontology, 155-174.

Soldani, A., 1780. Saggio Orittografico Ovvero Osservazioni Sopra Le Terre Nautilitiche Ed Ammonitiche Della Toscana. Sienna.

Soldani, A., 1798. Minutas testas maris fossils, item lacustres, earumque varietates. In Testaceographiae ac Zoophytographiae parvae et microscopicae Tomus Secundus.

Sorichetta, A., Seeber, L., Taramelli, A., McHugh, C., & Cormier, M., 2010. Geomorphic evidence for tilting at a continental transform: The Karamursel Basin along the North Anatolian Fault, Turkey. Geomorphology, 119(3-4), 221-231.

Sperling, M., Schmiedl, G., Hemleben, C., Emeis, K. C., Erlenkeuser, H., & Grootes, P. M., 2003. Black Sea impact on the formation of eastern Mediterranean

sapropel S1? Evidence from the Marmara Sea. Palaeogeography, Palaeoclimatology, Palaeoecology, 190, 9-21.

Spezzaferri, S., Rüggeberg, A., Stalder, C., and Margreth, S., 2015. Taxonomic notes and illustrations of benthic foraminifera from cold-water coral ecosystems. Cushman Foundation Special Publication No. 44, p. 49–140.

Spezzaferri, S., and Yanko-Hombach, V., 2007. Hyalinea marmarica, a new species of benthic foraminifera from the Sea of Marmara (Turkey). The Journal of Foraminiferal Research, 37(4), 309-317.

Strunk, A., Olsen, J., Sanei, H., Rudra, A., & Larsen, N. K., 2020. Improving the reliability of bulk sediment radiocarbon dating. Quaternary Science Reviews, 242, 106442.

Stuiver, M., and Reimer, P. J., 1993. Extended 14C data base and revised CALIB 3.0 14C age calibration program. Radiocarbon, 35(1), 215-230.

Stuiver, M., and Reimer, P. J., 2020. CALIB REV8.2 [software]. URL: http://calib.org/calib/. Accessed on April 3rd, 2024.

Suess, E., 1980. Particulate organic carbon flux in the oceans—surface productivity and oxygen utilization. Nature, 288(5788), 260-263.

Şengör, A. M. C., Tüysüz, O., Imren, C., Sakınç, M., Eyidoğan, H., Görür, N., ... & Rangin, C., 2005. The North Anatolian fault: A new look. Annu. Rev. Earth Planet. Sci., 33(1), 37-112.

Şengör, A. C., Grall, C., Imren, C., Le Pichon, X., Görür, N., Henry, P., ... & Siyako, M., 2014. The geometry of the North Anatolian transform fault in the Sea of Marmara and its temporal evolution: implications for the development of intracontinental transform faults. Canadian Journal of Earth Sciences, 51(3), 222-242.

Takata, H., Murakami, S., Seto, K., Sakai, S., Tanaka, S., & Takayasu, K., 2003. Foraminiferal assemblages in Aso-kai Lagoon, central Japan. Laguna, 10 [Japanese].

Takata, H., Seto, K., Sakai, S., Tanaka, S., and Takayasu, K., 2005a. Correlation of Virgulinella fragilis Grindell and Collen (benthic foraminiferid) with near-anoxia in Aso-kai Lagoon, central Japan. Journal of Micropalaeontology, 24(2), 159-167.

Takata, H., Tanaka, S., Murakami, S. S., Seto, K., and Takayasu, K., 2005b. Fossil benthic foraminifera from Aso-kai Lagoon, central Japan. LAGUNA, 12, 45-52.

Takata, H., Seto, K., Sakai, S., Tanaka, S., & Takayasu, K., 2006. Hypolimnetic Transitions and Sand-bar Development in Aso-kai Lagoon (Central Japan) during the Past 1,200 Years, Inferred from Benthic Foraminifera. The Quaternary Research (Daiyonki-Kenkyu), 45(5), 361-373.

Takata, H., Tanaka, S., Seto, K., Sakai, S., Takayasu, K., & Khim, B. K., 2014. Biotic response of benthic foraminifera in Aso-kai lagoon, central Japan, to changes in terrestrial climate and ocean conditions (~ AD 700–1600). Journal of paleolimnology, 51(3), 421-435.

Tapia, R., Le, S., Ho, S. L., Bassetti, M. A., Lin, I. T., Lin, H. L., ... and Su, C. C., 2022. Planktic-benthic foraminifera ratio (% P) as a tool for the reconstruction of paleobathymetry and geohazard: A case study from Taiwan. Marine Geology, 453, 106922.

Taş, S., 2017. Planktonic diatom composition and environmental conditions in the Golden Horn Estuary (Sea of Marmara, Turkey). Fundamental and Applied Limnology, 189(2), 153-166.

Taş, S., & Hernández-Becerril, D. U., 2017. Diversity and distribution of the planktonic diatom genus Chaetoceros (Bacillariophyceae) in the Golden Horn Estuary (Sea of Marmara). Diatom research, 32(3), 309-323.

Tekdal, D., Demet, A. E., Eker-Develi, E., & Yıldız, H. B., 2024. Diatoms isolated from the marine mucilage in the Sea of Marmara in 2021. Journal of the Black Sea/Mediterranean Environment, 30(2).

Ter Braak, C. J., 1986. Canonical correspondence analysis: a new eigenvector technique for multivariate direct gradient analysis. Ecology, 67(5), 1167-1179.

Terquem, M. O. 1876. Essai sur le classement des animaux qui vivent sur la plage et dans les environs de Dunkerque. Mémoires de la Société dunkerquoise pour l'encouragement des sciences, des lettres et des arts , vol. 20. 146-191.

Terquem, O., 1878. Les Foraminifères et les Entomostracés Ostracodes du Pliocene Supérieur de l'île de Rhodes. Mémoires de la Société Géologique de France. (3) 1: 1-135.

Terquem, M. O., 1882. Les Foraminifères de l'Éocène des environs de Paris. Mémoires de la Société géologique de France, troisième séries. 2(mém. 3): 1-193.,

Thalmann, H. E., 1950. New names and homonyms in Foraminifera. Contribution from the Cushman Foundation for foraminiferal research. 1(3/4): 41-45.

Timm, S., 1992. Rezente Tiefsee Benthosforaminiferen aus Oberflächensedimenten des Golfes von Guinea (Westafrika) Taxonomie, Verbreitung, Ökologie und Korngrößenfraktionen. - Dissertationsschrift, Berichte Geologisch-Paläontologisches Institut der Universität Kiel 59.

Troelsen, J. C., 1954. Studies on Ceratobuliminidae (Foraminifera). Medd. fra Dansk Geol. Forening København. Bd. 12: 448-478.

Tsuchiya, M., Tazume, M., and Kitazato, H., 2008. Molecular characterization of the non-costate morphotypes of buliminid foraminifers based on internal transcribed region of ribosomal DNA (ITS rDNA) sequence data. Marine Micropaleontology, 69(2), 212-224.

Tsuchiya, M., Grimm, G. W., Heinz, P., Stögerer, K., Ertan, K. T., Collen, J., ... and Kitazato, H., 2009. Ribosomal DNA shows extremely low genetic divergence in a world-wide distributed, but disjunct and highly adapted marine protozoan (Virgulinella fragilis, Foraminiferida). Marine Micropaleontology, 70(1-2), 8-19.

Tsuchiya, M., Toyofuku, T., Uematsu, K., Brüchert, V., Collen, J., Yamamoto, H., & Kitazato, H., 2015. Cytologic and genetic characteristics of endobiotic bacteria and kleptoplasts of Virgulinella fragilis (Foraminifera). Journal of Eukaryotic Microbiology, 62(4), 454-469.

Tuğrul, S., Morkoç, E., 1989. Oceanographic Characteristics of İzmit Bay. NATO TU-WATERS Project, Technical Report. TÜBİTAK, MRC Publ, Kocaeli, Turkey.

Tunoğlu, C., 1996a. Larger ostracoda in the sea of marmara: general distribution of bosquetina dentata (GW Muller, 1894). *Journal of Black Sea/Mediterranean Environment*, *2*(2).

Tunoğlu, C., 1996b. General Distribution of Pterigocythereis jonesii (Baird, 1850) and Pterigocythereis ceratoptera (Bosquet, 1852)(Ostracoda) in the sea of Marmara. Journal of Black Sea/Mediterranean Environment, 2(2).

Tüfekçi, V., Balkis, N., Beken, C. P., Ediger, D., & Mantikci, M., 2010. Phytoplankton composition and environmental conditions of the mucilage event in the Sea of Marmara. Turkish Journal of Biology, 34(2), 199-210.

T.C. Çevre, Şehircilik ve İklim Değişikliği Bakanlığı, 2022. Deniz Kalitesi Bülteni: Marmara Denizi, https://webdosya.csb.gov.tr/db/ced/icerikler/den-z-kal-tes--bulten--2022_marmara_den-z--20230720163728.pdf.

Uçarkuş, G., 2010. Active Faulting And Earthquake Scarps A Long The North Anatolian Fault In The Sea Of Marmara. Eurasia Institute of Earth Sciences, Istanbul Technical University, PhD Thesis.

Uysal, Z., 1996. A net-plankton study in the Bosphorus junction of the Sea of Marmara. Turkish Journal of Botany, 20(4), 321-329.

Ünlüata, Ü., Oğuz, T., Latif, M. A., Özsoy, E., 1990. On the Physical Oceanography of the Turkish Straits, in: The Physical Oceanography of Sea Straits, L. J. Pratt (editor), NATO/ASI Series, Kluwer, Dordrecht, 25-60.

Van der Zwaan, G. J., Jorissen, F. J., & De Stigter, H. C., 1990. The depth dependency of planktonic/benthic foraminiferal ratios: constraints and applications. Marine geology, 95(1), 1-16.

Van Morkhoven, F. P. C. M., Berggren, W. A., Edwards, A. S., and Oertli, H. J., 1986. Cenozoic cosmopolitan deep-water benthic Foraminifera. Elf Aquitaine.

van Voorthuysen, J. H. 1973. Foraminiferal ecology in the Ria de Arosa, Galicia, Spain. Zoologische Verhandelingen, 123(1), 1-68.

Vella, P., 1957. Studies in New Zealand Foraminifera; Part I- Foraminifera from Cook Strait. Part II- Upper Miocene to Recent Species of the Genus Notorotalia. New Zealand Geological Survey Paleontological Bulletin. 28: 1-64.

Verhallen, P. J. 1991. Late Pliocene to Early Pleistocene Mediterranean mud-dwelling foraminifera: influence of a changing environment on community structure and evolution PhD Thesis, Utrecht University.

Voloshinova, N. A.; Dain, L. G., 1952. Нониониды, Кассидулиниды и хилостомеллиды-Nonionidae, Cassidulinidae and Chilostomellidae. Ископаемые фораминиферы CCCP-Fossil foraminifera of the USSR, Proceedings of the Oil Research Geological Institute (ВНИГРИ-VNIGRI). new ser. 63: 1-114.

Voloshinova, N.A., 1958, On new systematics of the Nonionidae. Trudy Vsesoyuznogo Neftyanogo Nauchno - Issledovatel' skogo, Geologo - razvedochnogo Instituta (VNIGRI) (New Series), vol. 115 , pp. 117 – 223.

Voloshinova, N. A., 1960. Uspekhi mikropaleontologii v dele izucheniya vnutrennego stroeniya foraminifer [Progress in micropaleontology in the work of studying the inner structure of Foraminifera], in Trudy Pervogo Seminara po Mikrofaune. Leningrad: Vsesoyuznyy Neftyanoy Nauchno-issledovatel'skii Geologo-razvedochnyy Institut (VNIGRI), pp. 48-87.

Vyalov, O. S., 1968. Certain considerations on classification of siliceous foraminifera. Доповіді Академії наук української РСР - Reports of the Academy of Sciences of the Ukrainian SSR. 1: 3-6.

Walker, G. and Boys, W., 1784. Testacea minuta rariora, nuperrime detecta in arena littoris Sandvicensis / A collection of the minute and rare shells, lately discovered in the sand of the sea shore near Sandwich / by William Boys ... ; considerably augmented, and all their figures accurately drawn, as magnified with the microscopy, by Geo. Walker, bookseller, at Faversham. [Booklet]. 25 pp, published by George Walker.

Wedekind, R., 1937. Einführung in die Grundlagen der historischen Geologie.II. Mikrobiostratigraphie. Die Korallen- und Foraminiferenzeit. Ferdinand Enke Verlag. 8: 1-136.

Wickham H., 2016. ggplot2: Elegant Graphics for Data Analysis. Springer-Verlag New York. ISBN 978-3-319-24277-4, https://ggplot2.tidyverse.org.

Wiesner, H., 1912 Zur Systematik adriatischer Nubecularien, Spiroloculinen. Miliolinen und Biloculinen. Archiv für Protistenkunde, 25: 201-239.

Wiesner, H., 1920. Zur Systematik der Miliolideen. Zoologischer Anzeiger. 51 (1/2): 13-20.

Wiesner, H., 1923. Die Miliolideen der östlichen Adria. Prag-Bubenec. 1-113.

Wiesner, H., 1931. Die Foraminiferen der deutschen Südpolar Expedition 1901-1903. Deutsche Südpolar-Expedition, Berlin (Zoology). 20: 53-165.

Williamson, W. C., 1848. On the Recent British species of the genus *Lagena*. Annals and Magazine of Natural History. (2) 1 (1): 1-20.

Williamson, W.C. 1858. On the recent Foraminifera of Great Britain. The Ray Society, London. 1-107.

Wollenburg, J. E., and Mackensen, A., 1998. Living benthic foraminifers from the central Arctic Ocean: faunal composition, standing stock and diversity. Marine Micropaleontology, 34(3-4), 153-185.

Wollenburg, J. E., and Mackensen, A., 2009. The ecology and distribution of benthic foraminifera at the Håkon Mosby mud volcano (SW Barents Sea slope). Deep Sea Research Part I: Oceanographic Research Papers, 56(8), 1336-1370.

WoRMS Editorial Board (2025). World Register of Marine Species. Available from https://www.marinespecies.org at VLIZ. Accessed 2025-01-27. doi:10.14284/170

Wright, R. 1978. 31. Neogene benthic foraminifers from DSDP Leg 42A, Mediterranean Sea. Deep Sea Drilling Project Initial Reports Volume XLII Part 1 doi:10.2973/dsdp.proc.42-1.131.1978.

Wright, J., 1891. Report on the foraminifera obtained off the south-west of Ireland during the cruise of the" Flying Falcon," 1888. Proceedings of the Royal Irish Academy ser. 3, vol. 1, 460-502.

Yakupoğlu, N., Uçarkuş, G., Eriş, K. K., Henry, P., & Çağatay, M. N., 2019. Sedimentological and geochemical evidence for seismoturbidite generation in the Kumburgaz Basin, Sea of Marmara: Implications for earthquake recurrence along the Central High Segment of the North Anatolian Fault. Sedimentary Geology, 380, 31-44.

Yalçın, B., Artüz, M.L., Pavlidou, A., Çubuk, S., Dassenakis, M., 2017. Nutrient dynamics and eutrophication in the Sea of Marmara: Data from recent oceanographic research. Science of the Total Environment, 601, 405-424.

Yaltırak, C., 2002. Tectonic evolution of the Marmara Sea and its surroundings. Marine Geology, 190(1-2), 493-529.

Yaltırak, C., & Alpar, B., 2002. Kinematics and evolution of the northern branch of the North Anatolian Fault (Ganos Fault) between the Sea of Marmara and the Gulf of Saros. Marine Geology, 190(1-2), 351-366.

Yaltırak, C., Sakınç, M., Aksu, A. E., Hiscott, R. N., Galleb, B., & Ulgen, U. B., 2002. Late Pleistocene uplift history along the southwestern Marmara Sea determined from raised coastal deposits and global sea-level variations. Marine Geology, 190(1-2), 283-305.

Yassini, I.; Jones, B. G., 1995. Recent Foraminifera and Ostracoda from estuarine and shelf environments on the southeastern coast of Australia. University of Wollongong Press, Wollongong, NSW. 1-484.

Yıldız, A., and Toker, V., 2006. Pleistocene–Holocene calcareous nannofossil biostratigraphy of core samples from The Northeastern Sea of Marmara, Fenerbahçe–Pendik, NW Turkey. Journal of Asian Earth Sciences, 27(6), 835-846.

Yılmaz, A., Tolun, L. G., & Okay, O. S., 2019. Pollution and toxicity of sediment in potential dredging sites of the Marmara Sea, Turkey. Journal of Environmental Science and Health, Part A, 54(12), 1206-1218.

Yümün, Z. Ü., & Önce-Nişancioğlu, M., 2023. THE ROLE OF ORGANIC AND INORGANIC SUBSTANCES IN SEDIMENT POLLUTION IN THE MARMARA SEA BETWEEN GEMLIK (BURSA) AND BANDİRMA (BALİKESIR) AND THEIR EFFECT ON FORAMINIFERA. Applied Ecology & Environmental Research, 21(4).

Zachariasse, W. J., and Lourens, L. J. 2022. About the age and depositional depth of the sediments with reported bipedal footprints at Trachilos (NW Crete, Greece). Scientific reports, 12(1), 18471.

Zheng, S.-Y., 1979. The Recent foraminifera of the Xisha Islands, Guangdong Province, China. II. Studia marina sinica. 15: 101-232.

Zheng, S. and Fu, Z., 2008. Class Foraminifera. *In: Liu, J.Y. (ed) Checklist of Marine Biota of China Seas. China Science Press.* 108-174.

Zitter, T. A., Henry, P., Aloisi, G., Delaygue, G., Çagatay, M. N., De Lepinay, B. M., ... & Lericolais, G., 2008. Cold seeps along the main Marmara Fault in the Sea of Marmara (Turkey). Deep Sea Research Part I: Oceanographic Research Papers, 55(4), 552-570.

Zitter, T. A. C., Grall, C., Henry, P., Özeren, M. S., Çağatay, M. N., Şengör, A. M. C., ... & Géli, L., 2012. Distribution, morphology and triggers of submarine mass wasting in the Sea of Marmara. Marine Geology, 329, 58-74.

APPENDICES

A. Taxa names and abbreviations

Supplementary Table A.1. Full names of taxa and shortened versions used in various tables and figures in the text, listed alphabetically.

Taxa	Abbreviation
Adelosina spp.	Adelosi
Ammonia spp.	Amm_spp
Ammoscalaria pseudospiralis (Williamson)	A_pspir
Amphicoryna scalaris (Batsch	Amphi_s
Amphicoryna sp. 1	Amphi_1
Amphicoryna sp. 2	Amphi_2
Articulina tubulosa (Seguenza)	A_tubul
Astacolus crepidula (Fichtel and Moll)	Astac_c
Astacolus sp. 1	Astac_1
Asterigerinata adriatica Haake	Aster_a
Asterigerinata mamilla (Williamson)	Aster_m
Astrononion stelligerum (d'Orbigny)	Astro_s
Aubignyna perlucida (Heron-Allen and Earland)	A_perlu
Bigenerina nodosaria d'Orbigny	B_nodos
Biloculinella globula (Bornemann)	B_globu
Biloculinella labiata (Schlumberger)	B_labia
Bolivina alata (Seguenza)	B_alata
Bolivina albatrossi Cushman	B_albat
Bolivina cf. *vadescens* Cushman	B_vades
Bolivina dilatata Reuss	B_dilat
Bolivina pseudoplicata Heron-Allen and Earland	B_pspli
Bolivina spathulata (Williamson)	B_spath
Bolivina spp.	Bol_spp
Bolivina striatula (Cushman)	B_stria
Bolivina subspinescens Cushman	B_sspin
Bolivina variabilis Williamson	B_varia
Bolivinellina sp.	Bolnell
Bulimina aculeata d'Orbigny	B_acule
Bulimina costata d'Orbigny	B_costa
Bulimina elongata d'Orbigny	B_elong
Bulimina inflata Seguenza	B_infla
Bulimina marginata d'Orbigny	B_margi
Bulimina spp.	Bul_spp
Buliminella elegantissima (d'Orbigny)	B_elega
Cancris auricula (Fichtel and Moll)	C_auric
Cassidulina laevigata d'Orbigny	C_laevi

Supplementary Table A.1. Continued.

Taxa	Abbreviation
Ceratolamarckina arctica (Green)	C_arc
Chilostomella sp. 1	Chilost
Cibicides refulgens de Montfort	C_refulg
Cibicides spp.	Cib_spp
Cornuspira involvens (Reuss)	C_invol
Cribroelphidium poeyanum (d'Orbigny	Celp_po
Cycloforina rugosa (d'Orbigny)	C_rugos
Cycloforina tenuicollis (Wiesner)	C_tenui
Dentalina spp.	Dentali
Discorbinella bertheloti (d'Orbigny)	D_berthe
Eilohedra vitrea (Parker)	E_vitre
Ellipsolagenidae	Elagen
Elphidium spp.	Elphidi
Eubuliminella sp.	Eubulim
Favulina hexagona (Williamson)	F_hexag
Fursenkoina schreibersiana (Cžjžek)	F_schrei
Gavelinopsis praegeri (Heron-Allen and Earland)	G_praeg
Glabratellidae	Glabra
Globobulimina spp.	Gbulimi
Globocassidulina cf. *obtusa* Sejrup and Guilbault	G_obtus
Globocassidulina oblonga (Reuss)	Gcassid
Globocassidulina subglobosa Brady	G_sglob
Glomospira charoides (Jones and Parker)	G_charo
Glomospira gordialis (Jones and Parker)	G_gordi
Grigelis spp.	Grigeli
Gyroidina umbonata (Silvestri)	G_umbon
Haynesina depressula (Walker and Jacob)	H_depre
Hopkinsina pacifica Cushman	H_pacif
Hyalinea balthica (Shröter)	H_balth
Hyalinea marmarica Spezzaferri and Yanko-Hombach	H_marma
Hyalinonetrion gracilimum Seguenza	H_graci
Indeterminate 1	Indet_1
Indeterminate 2	Indet_2
Labrospira kosterensis Höglund	L_koster
Laevidentalina spp.	Laevide
Lagena cf. *laevis* Montagu	L_laevi
Lagena hispidula Cushman	L_hispi
Lagena interrupta Williamson	L_inter
Lagena perlucida (Montagu)	L_perlu
Lagena sp. 1	Lagen_1
Lagena sp. 2	Lagen_2
Lagena strumosa Reuss	L_strum
Lagenammina arenulata (Skinner)	L_arenu

Supplementary Table A.1. Continued.

Taxa	Abbreviation
Lenticulina cf. *nitida* (Brady)	L_nitid
Lenticulina cultrata (de Monfort)	L_cultr
Lenticulina gibba (d'Orbigny)	L_gibba
Lenticulina sp. 1	Lenti_1
Lenticulina spp.	Lenti_2
Lobatula lobatula (Walker and Jackob)	L_lobat
Melonis pompilioides (Fichtel and Moll)	M_pompi
Miliolida unidentified	M_unid
Miliolinella elongata Kruit	Milioli
Miliolinella subrotunda (Montagu)	M_subro
Morulaeplecta bulbosa Höglund	M_bulbo
Neoconorbina terquemi (Rhezak)	N_terqu
Neolenticulina variabilis (Reuss)	Nlent_v
Nodosariata unidentified	N_unid
Nonionella iridea Heron-Allen and Earland	N_iride
Nonionella opima Cushman	N_opima
Nonionella stella Cushman and Moyer	N_stell
Nonionoides grateloupii (d'Orbigny)	N_grate
Nonionoides minuta (Parker)	N_minut
Paracassidulina minuta (Cushman)	Pcas_mi
Patellina corrugata Williamson	P_corru
Planodiscorbis rarescens (Brady)	Pdisc_r
Planorbulina mediterranensis d'Orbigny	Plor_me
Polymorphinoidae	Polymor
Porosononion granosum (d'Orbigny)	Poros_g
Porosononion simplex (Cushman)	Poros_s
Pseudoclavulina crustata Cushman	P_crust
Pseudotriloculina laevigata (d'Orbigny)	P_laevi
Pullenia spp.	Pulleni
Pyrgo anomala (Schlumberger)	P_anoma
Pyrgo elongata (d'Orbigny)	P_elong
Pyrgo spp.	Pyrgo
Quinqueloculina bosciana d'Orbigny	Q_bosci
Quinqueloculina pygmaea Reuss	Q_pygma
Quinqueloculina schlumbergeri (Wiesner)	Q_schlu
Quinqueloculina seminulum ? (Linnaeus)	Q_semin
Quinqueloculina sp. 1	Quinq_1
Quinqueloculina sp. 2	Quinq_2
Quinqueloculina sp. 3	Quinq_3
Quinqueloculina stalkeri Loeblich and Tappan	Q_stalk
Quinqueloculina vandiemeniensis Loeblich and Tappan	Q_vandi
Quinqueloculina viennensis Le Calvez and Le Calvez	Q_vienn
Rectuvigerina phlegeri Le Calvez	R_phleg

Supplementary Table A.1. Continued.

Taxa	Abbreviation
Reussella spinulosa (Reuss)	R_spinu
Robertinoides bradyi (Cushman and Parker)	Rober_b
Robertinoides pumilum Höglund	Rober_p
Rosalina bradyi (Cushman)	R_brady
Rosalina globularis d'Orbigny	R_globu
Rosalina macropora (Hofker)	R_mpora
Rosalina spp.	Ros_spp
Rosalina williamsoni (Chapman and Parr)	R_willi
Rotaliana unidentified	R_unid
Sigmoilina sigmoidea Brady	S_sigmo
Sigmoilinita costata (Schlumberger)	S_costa
Sigmoilinita distorta (Phleger and Parker)	S_disto
Sigmoilinita grata (Terquem)	S_grata
Sigmoilinita tenuis (Czjzek)	S_tenui
Sigmoilopsis sp. 1	Sigmoi_1
Siphonaperta horrida (Cushman)	S_horri
Siphonaperta spp.	Siphona
Siphonina reticulata (Czjzek)	S_retic
Siphoscutula ? sp. 1	Sscut_1
Siphotextularia concava (Karrer)	S_concav
Sphaeroidina bulloides d'Orbigny	S_bullo
Spirillina spp.	Spirill
Spiroloculina cymbium d'Orbigny	S_cymb
Spiroloculina excavata d'Orbigny	S_excav
Spiroloculina sp. 1	Spirol_1
Spiroloculina tenuiseptata Brady	S_tsept
Spiroplectinella wrighti (Silvestri)	S_wrigh
Spirorbina? sp.	Spirorb
Stainforthia ? sp.	Stai_sp
Stainforthia fusiformis (Williamson)	Stai_fu
Svratkina tuberculata (Balkwill and Wright)	S_tuber
Textularia agglutinans d'Orbigny	T_agglu
Textularia gramen d'Orbigny	T_grame
Textularia pala Czjzek	T_pala
Textularia sp. 1	Textu_1
Textulariana unidentiified	T_unid
Trifarina angulosa (Williamson)	T_angul
Triloculina tricarinata (d'Orbigny)	T_trica
Triloculina trigonula (Lamarck)	T_trigo
Uvigerina mediterranea Hofker	U_medit
Valvulineria bradyana (Fornasini)	V_brady
Virgulinella fragilis Grindell and Collen	V_frag

B. Raw count data

CD

Supplementary Table B.1. The raw count data for core-top samples of Station 1 (19), Station 3 (19) and 45C-1.

Supplementary Table B.2. The raw count data for Station 2.

Supplementary Table B.3. The raw count data for Station 4.

Supplementary Table B.4. The raw count data for Station 5.

Supplementary Table B.5. The raw count data for Station 6.

Supplementary Table B.6. The raw count data for Station 7-2.

Supplementary Table B.7. The raw count data for Station 8.

Supplementary Table B.8. The raw count data for Station 1 (21).

Supplementary Table B.9. The raw count data for Station 3 (21).

Supplementary Table B.10. The raw count data for Station 45C-2.

Supplementary Table B.11. The raw count data for Station Izmit-deep.

Supplementary Table B.12. The raw count data for Station K40K46.

Supplementary Table B.13. The raw count data for Station K42K20.

Supplementary Table B.14. The raw count data for Station K49.5L04.

Supplementary Table B.15. The raw count data for Station K51.2K09.

Supplementary Table B.16. The raw count data for Station MM50.

C. Relative abundances in the core-top samples

CD

Supplementary Table C.1. Classification of taxa according to their distribution and relative abundance; shadings as used in Supplementary Table C.2.

Supplementary Table C.2. Quantitative details of taxa identified in core-top samples. Count: number of core-top samples the taxon is present in; Min, Max and Ave: minimum, maximum and average relative abundances of the taxon among the samples it was found in. Shadings as in Supplementary Table C.1. Taxa name abbreviations as in Supplementary Table A.1. Arranged alphabetically.

Supplementary Table C.3. Relative abundances of taxa in the core-top samples. Shadings as in Supplementary Table C.1. Taxa name abbreviations as in Supplementary Table A.1. Arranged alphabetically.

D. Numerical results for CCA

CD

Supplementary Table D.1. Eigenvalues of the canonical correspondence analysis axes and the percent variation they explain. Analysis for all surface samples and >2% taxa (same data set used in Cluster analysis, Section 3.4), and seven environmental variables (Table 3.7).

Supplementary Table D.2. Variable (taxa, environmental variables) and site (stations) scores of canonical correspondence analysis, values rounded to four digits after decimal. Analysis for all surface samples and >2% taxa (same data set used in Cluster analysis, Section 3.4), and seven environmental variables (Table 3.7). Taxa abbreviations as in Supplementary Table A.1.

Supplementary Table D.3. Eigenvalues of the canonical correspondence analysis axes and the percent variation they explain. Analysis for Cluster I and II samples and >2% taxa (see Figure 3.9), and seven environmental variables (Table 3.7).

Supplementary Table D.4. Variable (taxa, environmental variables) and site (stations) scores of canonical correspondence analysis. Analysis for Cluster I and II samples and >2% taxa (see Figure 3.9), and seven environmental variables (Table 3.7). Taxa abbreviations as in Supplementary Table A.1.

E. Data for Chapter 5

CD

Supplementary Table E.1. Coordinates, locations and water depths for every station included in the analyses. Coordinates for Phipps et al. (2010, SoM_2) were produced by georeferencing the given map (Text-figure 1 therein). For Stations 97 and 99 no map icons were present; due to similarity in depth, the coordinates for 96 and 100 were copied for them. Coordinates in Kırcı-Elmas (2006, SoM_3) were incorrectly formatted like decimal degrees (aa.bbccc, Table 5 therein), but in fact were degrees (aa) and decimal minutes (bb.ccc), corrected here. Station 7 in Kırcı-Elmas (2013, SoM_7) had incorrect coordinates in the original publication (Table 2 therein), therefore the coordinates for Station 7 was extracted by georeferencing the map (Figure 1 therein).

Supplementary Table E.2. Synonyms and presence table for taxa identified in the analyzed studies. Y stands for presence of taxon, under the name given in "Taxon name". Other names explained in the same row. For references see Table 5.2.

Supplementary Table E.3. Diversity indices in the surface samples of included publications. cmbs: centimeters below sediment-water interface; S: species richness, N: number of individuals, D: dominance, H': Shannon's diversity, E: evenness. See Table 5.2 for references. Note the missing N values in SoM_7 (only relative abundances were published) and the summation of first three samples (0.5, 1, 1.5 cm) in SoM_01 MRS-DV05-PC-06.

F. Data for Chapter 6

CD

Supplementary Table F.1. Master table for the ecological group assignments (given in Arabic numerals) of the four studies. [1]: Alve et al., 2016 (Shelf to upper slope; below halocline), [2]: Jorissen et al., 2018, Mediterranean, [3]: O'Malley et al., 2021, [4-1]: Bouchet et al., 2021: English Channel/European Atlantic intertidal and Transitional Waters (TWs), [4-2]: Bouchet et al., 2021: Mediterranean Sea intertidal and TWs. #: number of datasets the taxon occurs in. EG_A: aggreed ecological group assignment for taxa present in more than one dataset with the same assignment in all. Assignments color coded.

Supplementary Table F.2. Synonyms table used for homogenization of data. (2) for the opinion of Jorissen et al. (2018), (TS) for the opinion of the author.

G. Systematic taxonomy: summary and plates

Supplementary Table G.1. Summary table for the systematic taxonomy of the identified benthic foraminifera taxa.

Class Globothalamea		
Subclass Robertinida		
Suborder Robertinina		
Superfamily Ceratobuliminoidea		
Family Creatobuliminidae		
Subfamily Ceratobulimininae		
	Ceratolamarckina	*arctica*
Superfamily Robertinoidea		
Family Robertinidae		
Subfamily Robertininae		
	Robertinoides	*bradyi*
	Robertinoides	*pumilum*
Subclass Rotaliana		
Order Rotaliida		
Superfamily Asterigerinoidea		
Family Asterigerinatidae		
	Asterigerina	*adriatica*
	Asterigerina	*mamilla*
Superfamily Bolivinitoidea		
Family Bolivinitidae		
Subfamily Bolivinitinae		
	Bolivina	*alata*
	Bolivina	*albatrossi*
	Bolivina	*pseudoplicata*
	Bolivina	*striatula*
	Bolivina	*subspinescens*
	Bolivina	cf. *vadescens*
	Bolivina	*variabilis*
	Bolivina	*spathulata*
	Bolivina	*dilatata*
Family Bolivinitidae		
	Bolivinellina	sp.
Subfamily Fursenkoininae		
	Fursenkoina	*schreibersiana*

Supplementary Table G.1. Continued.

Class Globothalamea		
Subclass Rotaliana		
Order Rotaliida		
Superfamily Buliminoidea		
Family Buliminidae		
	Bulimina	*aculeata*
	Bulimina	*costata*
	Bulimina	*inflata*
	Bulimina	*elongata*
	Bulimina	*marginata*
Family Buliminellidae		
	Buliminella	*elegantissima*
Family Reussellidae		
	Reussella	*spinulosa*
Family Siphogenerinoididae		
Subfamily Tubulogenerininae		
	Rectuvigerina	*phlegeri*
Superfamily Cassidulinoidea		
Family Cassidulinidae		
Subfamily Cassidulininae		
	Cassidulina	*laevigata*
	Globocassidulina	*oblonga*
	Globocassidulina	*obtusa*
	Globocassidulina	*subglobosa*
	Paracassidulina	*minuta*
Family Globobuliminidae		
	Globobulimina	spp.
Family Sphaeroidinidae		
	Sphaeroidina	*bulloides*
Family Uvigerinidae		
Subfamily Angulogerininae		
	Trifarina	*angulosa*
Subfamily Uvigerininae		
	Uvigerina	*mediterranea*
Superfamily Chilostomelloidea		
Family Chilostomellidae		
Subfamily Chilostomellinae		
	Chilostomella	sp. 1

Supplementary Table G.1. Continued.

Class Globothalamea		
Subclass Rotaliana		
Order Rotaliida		
Superfamily Chilostomelloidea		
Family Gavelinellidae		
Subfamily Gavelinellinae		
	Gyroidina	*umbonata*
Family Svratkinidae		
	Svratkina	*tuberculata*
Superfamily Discorbinelloidea		
Family Discorbinellidae		
Subfamily Discorbinellinae		
	Discorbinella	*bertheloti*
Family Pseudoparrellidae		
Subfamily Pseudoparellinae		
	Eilohedra	*vitrea*
Family Bagginidae		
Subfamily Serovaininae		
	Rotamorphina?	*involuta*
Family Cancrisidae		
	Cancris	*auricula*
	Valvulineria	*bradyana*
Family Rosalinidae		
	Gavelinopsis	*praegeri*
	Neoconorbina	*terquemi*
	Planodiscorbis	*rarescens*
	Rosalina	*bradyi*
	Rosalina	*globularis*
	Rosalina	*macropora*
	Rosalina	*williamsoni*
	Spirorbina?	sp.
Superfamily Glabratelloidea		
Family Glabratellidae		
Superfamily Nonionoidea		
Family Astrononionidae		
Subfamily Astrononioninae		
	Astrononion	*stelligerum*
Family Melonidae		
	Melonis	*pompilioides*

Supplementary Table G.1. Continued

Class Globothalamea		
Subclass Rotaliana		
Order Rotaliida		
Superfamily Nonionoidea		
Family Nonionidae		
Subfamily Nonioninae		
	Nonionella	*iridea*
	Nonionella	*opima*
	Nonionella	*stella*
	Nonionoides	*grateloupi*
	Nonionoides	*minuta*
Family Pulleniidae		
Subfamily Pulleniinae		
	Pullenia	spp.
Superfamily Planorbulinoidea		
Family Cibicididae		
Subfamily Cibicidinae		
	Cibicides	*refulgens*
	Lobatula	*lobatula*
Family Planorbulinidae		
Subfamily Planorbulininae		
	Planorbulina	*mediterranensis*
Family Planulinidae		
	Hyalinea	*balthica*
	Hyalinea	*marmarica*
Superfamily Rotalioidea		
Family Ammoniidae		
Subfamily Ammoniinae		
	Ammonia	spp.
Family Elphidiidae		
Subfamily Elphidiinae		
	Elphidium	spp.
	Cribroelphidium	*poeyanum*
	Porosononion	*granosum*
	Porosononion	*simplex*
Family Haynesinidae		
	Aubignyna	*perlucida*
	Haynesina	*depressula*

Supplementary Table G.1. Continued

- Class Globothalamea
  - Subclass Rotaliana
    - Order Rotaliida
      - Superfamily Siphoninoidea
        - Family Siphoninidae
          - Subfamily Siphonininae
            - *Siphonina* *reticulata*
      - Superfamily Turrilinoidea
        - Family Stainforthiidae
          - *Stainforthia* *fusiformis*
          - *Stainforthia* sp.
          - *Hopkinsina* *pacifica*
        - Family Turrilinidae
          - *Eubuliminella* sp.
      - Superfamily Virgulinelloidea
        - Family Virgulinellidae
          - *Virgulinella* *fragilis*
  - Subclass Textulariana
    - Order Lituolida
      - Suborder Lituolina
        - Superfamily Lituoloidea
          - Family Discamminidae
            - *Ammoscalaria* *pseudospiralis*
          - Family Haplophragmoididae
            - *Labrospira* *kosterensis*
      - Suborder Spiroplectamminina
        - Superfamily Spiroplectamminoidea
          - Family Spiroplectamminidae
            - Subfamily Spiroplectammininae
              - *Spiroplectinella* *wrighti*
            - Subfamily Morulaeplectinae
              - *Morulaeplecta* *bulbosa*
      - Suborder Verneuilinina
        - Superfamily Verneuilinoidea
          - Family Prolixoplectidae
            - *Eggerelloides* *scabrus*

Supplementary Table G.1. Continued

Class Globothalamea		
Subclass Textulariana		
Order Textulariida		
Suborder Textulariina		
Superfamily Eggerelloidea		
Family Pseudogaudrynidae		
Subfamily Pseudogaudryninae		
	Pseudoclavulina	*crustata*
Superfamily Textularioidea		
Family Textulariidae		
Subfamily Siphotextulariinae		
	Siphoscutula ?	sp. 1
	Siphotextularia	*concava*
Subfamily Textulariinae		
	Bigenerina	*nodosaria*
	Textularia	*agglutinans*
	Textularia	*gramen*
	Textularia	*pala*
	Textularia	sp. 1
Class Monothalamea		
Order Astrorhizida		
Suborder Saccamminina		
Superfamily Saccamminoidea		
Family Saccamminidae		
Subfamily Saccammininae		
	Lagenammina	*arenulata*
Class Nodosariata		
Subclass Nodosariana		
Order Nodosariida		
Suborder Nodosariina		
Superfamily Nodosarioidea		
Family Lagenidae		
	Hyalinonetrion	*gracillimum*
	Lagena	cf. *annellatrachia*
	Lagena	cf. *laevis*
	Lagena	*hispidula*
	Lagena	*perlucida*
	Lagena	*strumosa*

Supplementary Table G.1. Continued

Class Nodosariata		
Subclass Nodosariana		
Order Nodosariida		
Suborder Nodosariina		
Superfamily Nodosarioidea		
Family Lagenidae		
	Lagena	*interrupta*
	Lagena	sp. 1
	Lagena	sp. 2
Family Nodosariidae		
Subfamily Nodosariinae		
	Dentalina	spp.
	Enantiodentalina	*timorensis*
	Grigelis	*orectus*
	Laevidentalina	spp.
Order Polymorphinida		
Suborder Polymorphinina		
Superfamily Polymorphinoidea		
Family Ellipsolagenidae		
Subfamily Ellipsolageninae		
	Fissurina	*annectens*
	Fissurina	*castanea*
	Fissurina	*laevigata*
	Fissurina	*neptuni*
	Fissurina	*robusta*
	Fissurina	*variocarinata*
	Fissurina	sp. 1
	Fissurina	sp. 2
	Fissurina	sp. 3
	Fissurina	sp. 4
	Lagenosolenia	*strigimarginata*
	Palliolatella	sp.
Subfamily Oolininae		
	Favulina	*hexagona*
	Anturina	*haynesi*
Subfamily Parafissurininae		
	Parafissurina	*lata*
	Parafissurina	*basispinata*

Supplementary Table G.1. Continued

Class Nodosariata		
Subclass Nodosariana		
Order Vaginulinida		
Family Vaginulinidae		
Subfamily Lenticulininae		
	Lenticulina	*cultrata*
	Lenticulina	*gibba*
	Lenticulina	cf. *nitida*
	Lenticulina	sp. 1
	Neolenticulina	*variabilis*
	Saracenaria	sp.
Subfamily Marginulininae		
	Amphicoryna	*scalaris*
	Amphicoryna	sp. 1
	Amphicoryna	sp. 2
	Astacolus	*crepidulus*
	Astacolus	? Sp. 1
Class Tubulothalamea		
Order Miliolida		
Suborder Miliolina		
Superfamily Cornuspiroidea		
Family Cornuspiridae		
	Cornuspira	*involvens*
Superfamily Miliolidea		
Family Cribrolinoididae		
	Adelosina	spp.
Family Hauerinidae		
Subfamily Hauerininae		
	Cycloforina	*rugosa*
	Cycloforina	*tenuicollis*
	Quinqueloculina	*bosciana*
	Quinqueloculina	*pygmaea*
	Quinqueloculina	*schlumbergeri*
	Quinqueloculina	*stalkeri*
	Quinqueloculina	*seminulum*
	Quinqueloculina	*vandiemeniensis*
	Quinqueloculina	*viennensis*
	Quinqueloculina	sp. 1
	Quinqueloculina	sp. 2
	Quinqueloculina	sp. 3

Supplementary Table G.1. Continued

Class Tubulothalamea		
Order Miliolida		
Suborder Miliolina		
Superfamily Miliolidea		
Family Hauerinidae		
Subfamily Miliolinellinae		
	Biloculinella	*subsphaerica*
	Biloculinella	*labiata*
	Miliolinella	*subrotunda*
	Miliolinella	*elongata*
	Pseudotriloculina	*laevigata*
	Pyrgo	*anomala*
	Pyrgo	*elongata*
	Triloculina	*tricarinata*
	Triloculina	*trigonula*
Subfamily Sigmoilinitinae		
	Sigmoilina	*sigmoidea*
	Sigmoilinita	*costata*
	Sigmoilinita	*distorta*
	Sigmoilinita	*grata*
	Sigmoilinita	*tenuis*
Subfamily Sigmoilopsinae		
	Sigmoilopsis	sp. 1
Subfamily Siphonapertinae		
	Siphonaperta	*horrida*
Subfamily Tubinellinae		
	Articulina	*tubulosa*
Family Spiroloculinidae		
	Spiroloculina	*cymbium*
	Spiroloculina	*excavata*
	Spiroloculina	*tenuiseptata*
	Spiroloculina	sp. 1
Suborder Nubeculariina		
Superfamily Nubecularioidea		
Family Ophtalmidiidae		
	Cornuloculina	*incostans*

Supplementary Table G.1. Continued

Class Tubulothalamea		
Order Spirillinida		
Suborder Ammodiscina		
Superfamily Ammodiscoidea		
Family Ammodiscidae		
Subfamily Usbekistaniinae		
	Glomospira	*charoides*
	Glomospira	*gordialis*
Suborder Spirillinina		
Family Patellinidae		
Subfamily Patellininae		
	Patellina	*corrugata*
Family Spirillinidae		
	Spirillina	*vivipara*
	Spirillina	sp. 1

PLATES

PLATE 1: Robertinida, Asterigerinatidae; SEM images; scale bar: 100 μm.

1-3: *Ceratolamarckina arctica* (Green) 1. spiral, Station 5 sample 8 cm, IS_25_D_001; 2. umbilical, Station 5 sample 8 cm, IS_25_D_002; 3. umbilical oblique, Station 2 sample 15 cm, IS_8_Q_001; **4-6**: *Robertinoides pumilum* Höglund 4. lateral - apertural side, Station 5 sample 8 cm, IS_25_H_003; 5. lateral - apertural side, Station 5 sample 8 cm, IS_25_H_002; 6. lateral - adapertural side, Station 5 sample 8 cm, IS_25_H_001; **7-10**: *Asterigerinata adriatica* Haake 7. spiral, Station 5 sample 8 cm, IS_17_B_001; 8. spiral, Station 5 sample 8 cm, IS_17_B_004; 9. umbilical, Station 5 sample 8 cm, IS_17_B_007; 10. spiral-oblique, Station 5 sample 8 cm, IS_17_B_005; **11-15**: *Asterigerinata mamilla* (Williamson) 11. spiral, Station 5 sample 8 cm, IS_17_A_003; 12. umbilical, Station 5 sample 8 cm, IS_17_A_002; 13. umbilical-oblique, Station 5 sample 8 cm, IS_17_A_001; 14. umbilical, Station 5 sample 8 cm, IS_17_A_004; 15. spiral, Station 5 sample 8 cm, IS_17_A_005.

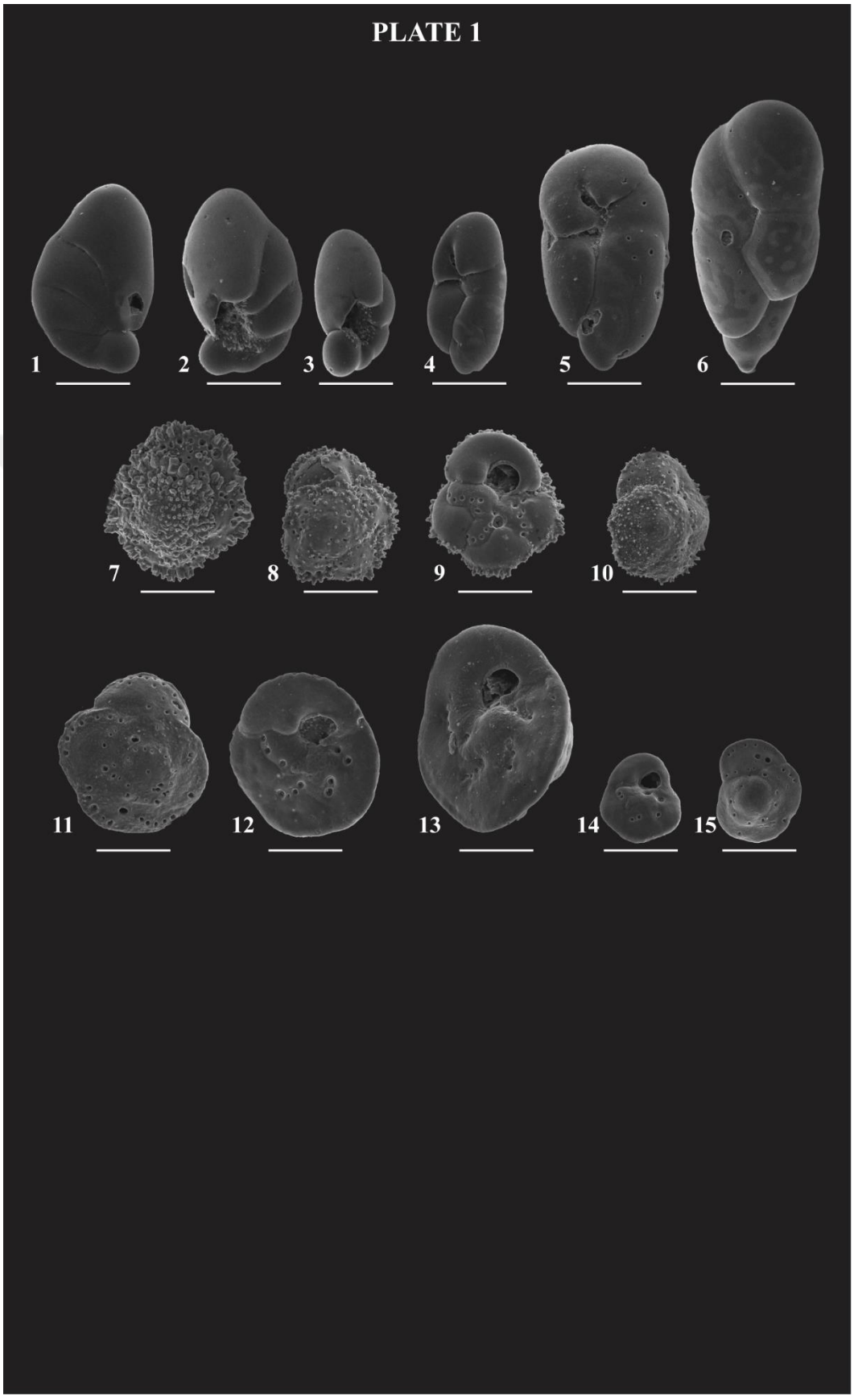

PLATE 1
1
2
3
4
5
6
7
8
9
10
11
12
13
14
15

PLATE 2: Robertinida, Asterigerinatidae, stereomicrographs; scale bar: 100 μm.

1-8: *Ceratolamarckina arctica* (Green) 1. Umbilical, Station 5 sample 8 cm, IS_25_D_001; 2. Umbilical, Station 5 sample 8 cm, IS_25_D_002; 3. Umbilical, Station 5 sample 8 cm, IS_25_D_003; 4. (a. edge, b. umbilical) Station 5 sample 8 cm, IS_25_D_005; 5. (a. edge, b. umbilical) Station 5 sample 8 cm, IS_25_D_006; 6. (a. edge, b. umbilical) Station 5 sample 8 cm, IS_25_D_004; 7. (a. spiral, b. umbilical) Station 2 sample 5 cm, IS_07_L_001; 8. (a. spiral, b. edge, c. umbilical) Station 1 (19) sample 4 cm, IS_01_I_001; **9**. *Robertinoides bradyi* (Cushman and Parker), lateral - adapertural side, Station 5 sample 8 cm, IS_25_H_004, 10-15; **10-15**: *Robertinoides pumilum* Höglund 10. lateral - apertural side, Station 5 sample 8 cm, IS_25_H_003; 11. lateral - apertural side, Station 5 sample 8 cm, IS_25_H_002; 12a. lateral - apertural side, 12b. lateral - adapertural side, Station 1 (19) sample 4 cm, IS_01_R_002; 13. lateral - adapertural side, Station 5 sample 8 cm, IS_25_H_005; 14. lateral - apertural side, Station 5 sample 8 cm, IS_25_H_001; 15a. lateral - adapertural side, 15b. lateral - apertural side, Station 1 (19) sample 4 cm, IS_01_R_001; **16-21**: *Asterigerinata adriatica* Haake 16a. umbilical, 16b. spiral, Station 5 sample 8 cm, IS_17_B_001; 17a. umbilical, 17b. spiral, Station 5 sample 8 cm, IS_17_B_006; 18a. umbilical, 18b. spiral Station 5 sample 8 cm, IS_17_B_004; 19a. umbilical, 19b. spiral, Station 5 sample 8 cm, IS_17_B_007; 20a. umbilical, 20b. spiral, Station 5 sample 8 cm, IS_17_B_005, 21a. umbilical, 21b. spiral, Station 5 sample 8 cm, IS_17_B_002; **22-28**: *Asterigerinata mamilla* (Williamson) 22. spiral, Station 5 sample 8 cm, IS_17_A_003; 23. umbilical, Station 5 sample 8 cm, IS_17_A_002; 24. umbilical-oblique, Station 5 sample 8 cm, IS_17_A_001; 25. spiral, Station 5 sample 8 cm, IS_17_A_004; 26. spiral, Station 5 sample 8 cm, IS_17_A_005; 27a. spiral, 27b. umbilical, Station 5 sample 8 cm, IS_12_I_001; 28a. spiral, b. umbilical, Station 5 sample 8 cm, IS_05_T_001.

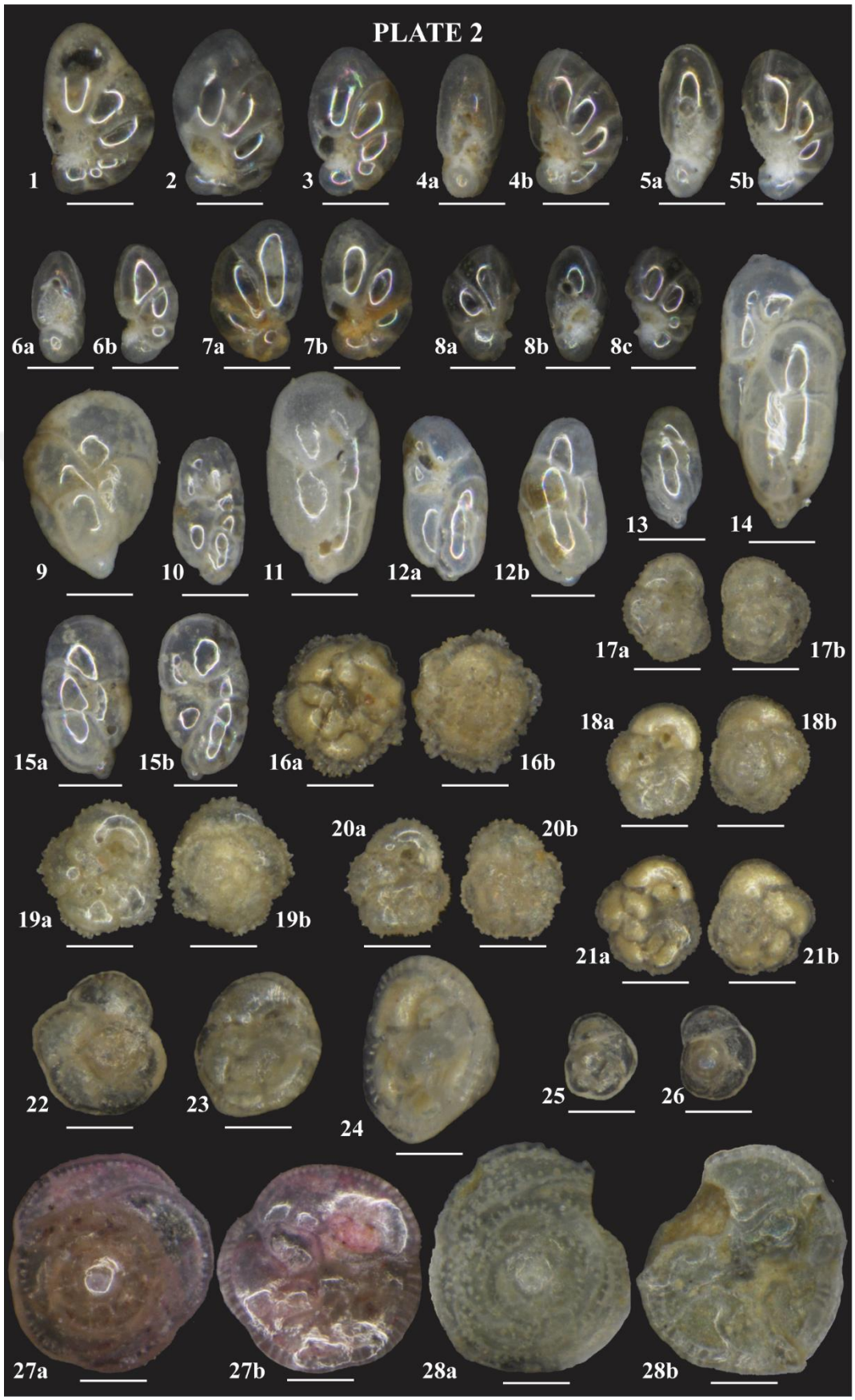

PLATE 2
1
2
3
4a
4b
5a
5b
6a
6b
7a
7b
8a
8b
8c
9
10
11
12a
12b
13
14
15a
15b
16a
16b
17a
17b
18a
18b
19a
19b
20a
20b
21a
21b
22
23
24
25
26
27a
27b
28a
28b

PLATE 3: Bolivinitidae, SEM images; scale bar: 100 μm.

1-5: *Bolivina alata* (Seguenza) 1. lateral, Station 5 sample 8 cm, IS_25_M_002, last chamber tending uniserial; 2. lateral, Station 5 sample 8 cm, IS_25_M_001; 3. lateral, Station 4 sample 15 cm, IS_14_2A_002; 4. lateral, Station 2 sample 2 cm, IS_06_K_001; 5. lateral, Station 4 sample 15 cm, IS_14_2A_001; **6-9**: *Bolivina albatrossi* Cushman 6. lateral, K51.2K09 sample 8 cm, IS_30_H_002, broken; 7. lateral, Station 5 sample 8 cm, IS_25_O_002, juvenile; 8. lateral, Station 5 sample 8 cm, IS_25_O_001; 9. lateral, K51.2K09 sample 8 cm, IS_30_H_001; **10-12**: *Bolivina pseudoplicata* Heron-Allen and Earland 10. lateral, Station 5 sample 8 cm, IS_25_N_001; 11. lateral, Station 5 sample 8 cm, IS_25_N_002, juvenile; 12. lateral, Station 5 sample 8 cm, IS_25_N_003, juvenile; **13-16**: *Bolivina variabilis* Williamson, 13. lateral, Station 5 sample 8 cm, IS_25_P_001; 14. lateral, Station 5 sample 8 cm, IS_25_P_002; 15. lateral, Station 5 sample 8 cm, IS_25_P_003; 16. lateral, 45C-2 sample 35 cm, IS_15_D_001; **17-24**: *Bolivina striatula* (Cushman), 17. lateral, Station 1 (21) sample 4 cm, IS_03_G_001, weak striations; 18. Station 1 (21) sample 8 cm, IS_04_X_001, weak striations; 19. Station 4 sample 15 cm, IS_14_2B_001, weak striations; 20. lateral, MM50 sample 15 cm, IS_21_C_001b, strong striations; 21. lateral, MM50 sample 15 cm, IS_21_C_001a, strong striations; 22. lateral, MM50 sample 15 cm, IS_21_C_001c, strong striations; 23. lateral, Station 5 sample 8 cm, IS_25_U_001a, weak striations; 24. lateral, Station 5 sample 8 cm, IS_25_U_001b, weak striations; **25-28**: *Bolivina subspinescens* Cushman 25. lateral, Station 2 sample 2 cm, IS_06_L_001; 26. lateral, Station 3 (21) sample 15 cm, IS_13_M_002; 27. apertural-oblique, Station 3 (21) sample 15 cm, IS_13_M_001, broken, juvenile; 28. apertural-edge, Station 2 sample 25 cm, IS_09_T_001; **29-34**: *Bolivina* cf. *vadescens* Cushman, 29. lateral, Station 5 sample 8 cm, IS_25_S_001; 30. lateral, MM50 sample 30 cm, IS_20_E_001a; 31. lateral, Station 1 (21) sample 4 cm, IS_03_D_001; 32. lateral, MM50 sample 30 cm, IS_20_E_002a; 33. lateral, MM50 sample 30 cm, IS_20_E_002b, juvenile; 34. lateral, Station 1 (21) sample 8 cm, IS_04_Z_001, juvenile.

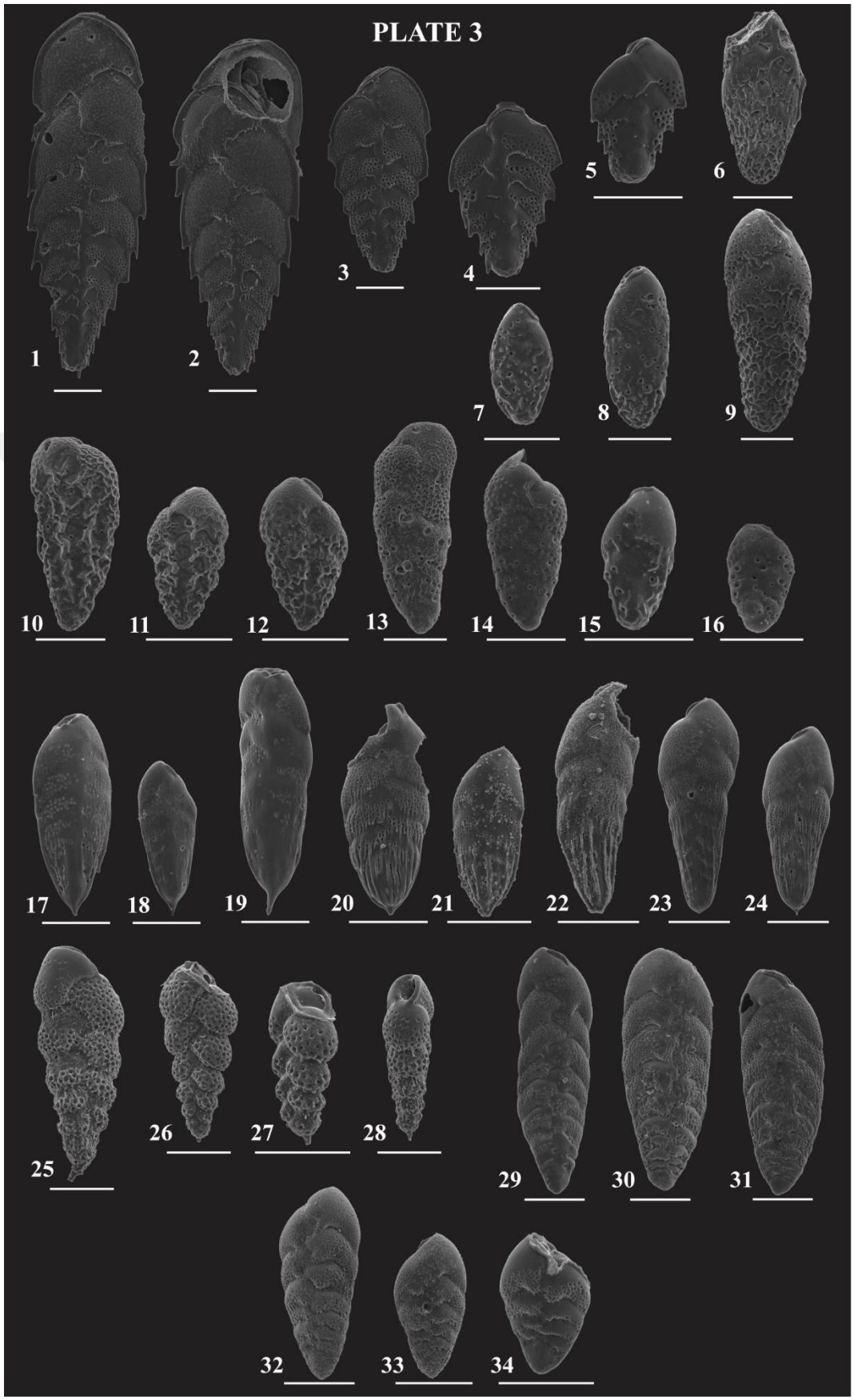

PLATE 3
1
2
3
4
5
6
7
8
9
10
11
12
13
14
15
16
17
18
19
20
21
22
23
24
25
26
27
28
29
30
31
32
33
34

PLATE 4: Bolivinitidae, stereomicrographs; scale bar: 100 μm.

1-5: *Bolivina alata* (Seguenza) 1. lateral, Station 5 sample 8 cm, IS_25_M_002, last chamber tending uniserial; 2. lateral, Station 5 sample 8 cm, IS_25_M_001; 3. lateral, Station 4 sample 15 cm, IS_14_2A_002; 4. lateral, Station 2 sample 2 cm, IS_06_K_001; 5. lateral, Station 4 sample 15 cm, IS_14_2A_001; **6-9**: *Bolivina albatrossi* Cushman 6. lateral, K51.2K09 sample 8 cm, IS_30_H_002, broken; 7. lateral, Station 5 sample 8 cm, IS_25_O_002, juvenile; 8. lateral, Station 5 sample 8 cm, IS_25_O_001; 9. lateral, K51.2K09 sample 8 cm, IS_30_H_001; **10-12**:, *Bolivina pseudoplicata* Heron-Allen and Earland 10. lateral, Station 5 sample 8 cm, IS_25_N_001; 11. lateral, Station 5 sample 8 cm, IS_25_N_002, juvenile; 12. lateral, Station 5 sample 8 cm, IS_25_N_003, juvenile; **13-16**: *Bolivina variabilis* Williamson 13. lateral, Station 5 sample 8 cm, IS_25_P_001; 14. lateral, Station 5 sample 8 cm, IS_25_P_002; 15. lateral, Station 5 sample 8 cm, IS_25_P_003; 16. lateral, 45C-2 sample 35 cm, IS_15_D_001; **17-24**: *Bolivina striatula* (Cushman) 17. lateral, Station 1 (21) sample 4 cm, IS_03_G_001, weak striations; 18. lateral, Station 1 (21) sample 8 cm, IS_04_X_001, weak striations; 19. lateral, Station 4 sample 15 cm, IS_14_2B_001, weak striations; 20. lateral, MM50 sample 15 cm, IS_21_C_001b, strong striations; 21. lateral, MM50 sample 15 cm, IS_21_C_001a, strong striations; 22. lateral, MM50 sample 15 cm, IS_21_C_001c, strong striations; 23. lateral, Station 5 sample 8 cm, IS_25_U_001a, weak striations; 24. lateral, Station 5 sample 8 cm, IS_25_U_001b, weak striations; **25-29**: *Bolivina subspinescens* Cushman 25. lateral, Station 2 sample 2 cm, IS_06_L_001; 26. lateral, Station 3 (21) sample 15 cm, IS_13_M_002; 27. apertural-oblique, Station 3 (21) sample 15 cm, IS_13_M_001, broken, juvenile; 28. apertural-edge, Station 2 sample 25 cm, IS_09_T_001; 29. lateral, Station 1 (19) sample 4 cm, IS_01_P_001, broken; **30-35**: *Bolivina* cf. *vadescens* Cushman 30. lateral, Station 5 sample 8 cm, IS_25_S_001; 31. lateral, MM50 sample 30 cm, IS_20_E_001a; 32a. lateral, 32b. apertural-edge, Station 1 (21) sample 4 cm, IS_03_D_001; 33. lateral, MM50 sample 30 cm, IS_20_E_002a; 34. lateral, MM50 sample 30 cm, IS_20_E_002b, juvenile; 35. lateral, Station 1 (21) sample 8 cm, IS_04_Z_001, juvenile.

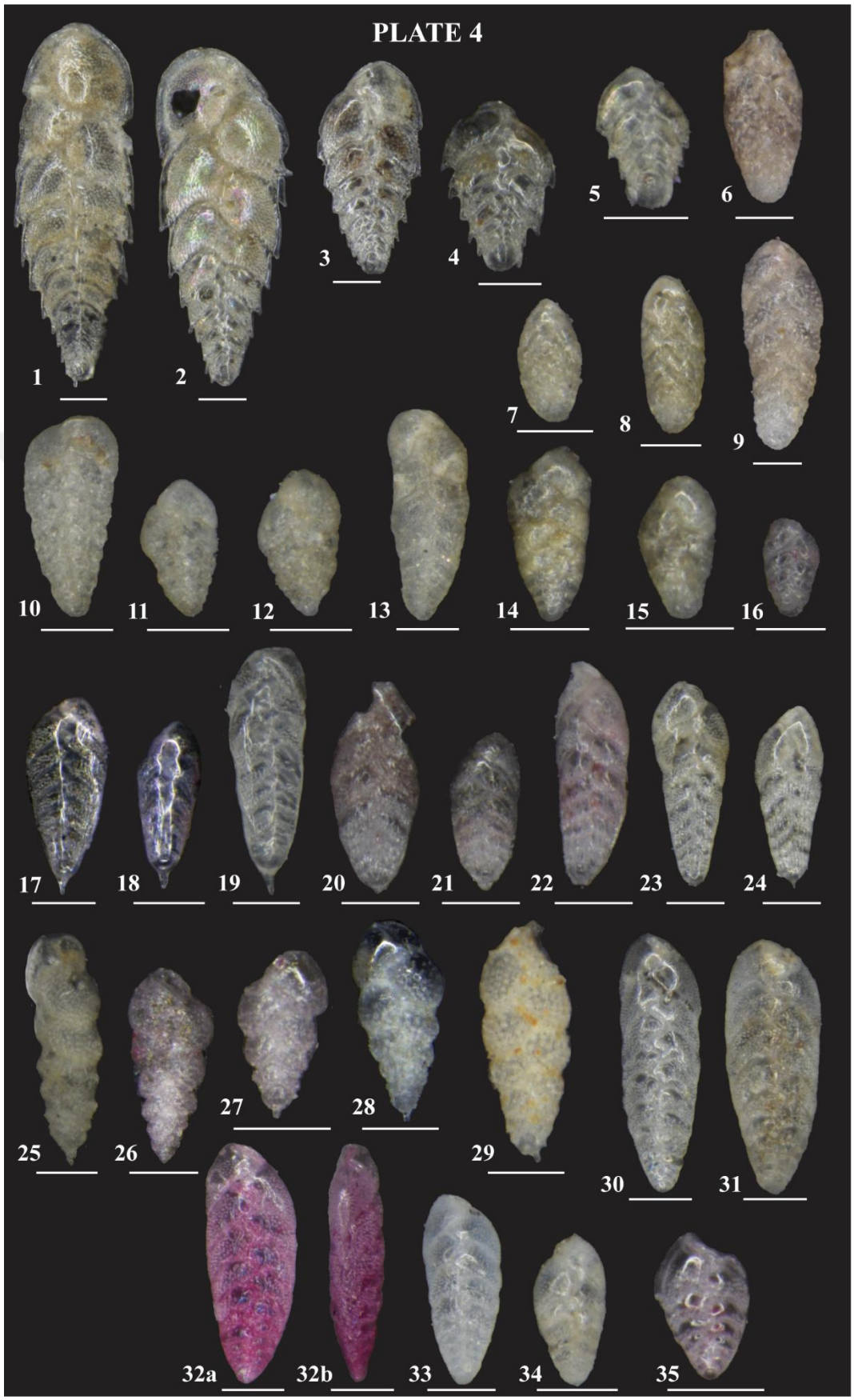

PLATE 4
1
2
3
4
5
6
7
8
9
10
11
12
13
14
15
16
17
18
19
20
21
22
23
24
25
26
27
28
29
30
31
32a
32b
33
34
35

PLATE 5: Bolivinitidae, SEM images; scale bar: 100 µm.

1-7: *Bolivina dilatata* Reuss 1. lateral, Station 1 (2021) sample 4 cm, IS_03_A_001; 2. lateral, Station 5 sample 8 cm, IS_25_Q_001; 3. lateral, Station 5 sample 8 cm, IS_25_Q_002; 4. lateral, Station 3 (21) sample 15 cm, IS_13_N2_001; 5. lateral, Station 3 (21) sample 15 cm, IS_13_N2_002a; 6. lateral, Station 3 (21) sample 15 cm, IS_13_N2_002b, juvenile; 7. lateral, Station 1 (21) 4 cm, IS_03_A_003, juvenile; **8-18**: *Bolivina spathulata* (Williamson) 8. lateral, Station 3 (21) sample 15 cm, IS_13_N3_001, edges broken; 9. lateral, Station 1 (21) 4 cm, IS_03_B_001; 10. lateral, Station 5 sample 8 cm, IS_25_R_001; 11. lateral, Station 3 (21) sample 15 cm, IS_13_N1_001; 12. lateral, Station 3 (21) sample 15 cm, IS_13_N1_002; 13. lateral, Station 3 (21) sample 15 cm, IS_13_N1_003; 14. lateral, MM50 sample 15 cm, IS_21_A_001, serrated carina; 15. lateral, MM50 sample 15 cm, IS_21_A_002, serrated carina; 16. lateral, Station 1 (21) 4 cm, IS_03_B_006, lobulate; 17. lateral, Station 5 sample 8 cm, IS_25_R_002, lobulate; **18-21**: *Bolivinellina* sp. 18. lateral, Station 1 (21) 4 cm, IS_03_E_001, terminal aperture; 19. edge, Station 2 sample 2 cm, IS_03_E_001, broken; 20. lateral, Station 5 sample 8 cm, IS_25_T_001, juvenile and broken; 21. lateral, Station 5 sample 8 cm, IS_25_T_002, juvenile; **22-24**: *Fursenkoina schreibersiana* (Cžjžek), 22. lateral, Station 1 (19) 4 cm, IS_01_M_002; 23, lateral, Station 2 sample 5 cm, IS_07_W_001; 24. lateral-oblique, Station 1 (19) 4 cm, IS_01_M_001.

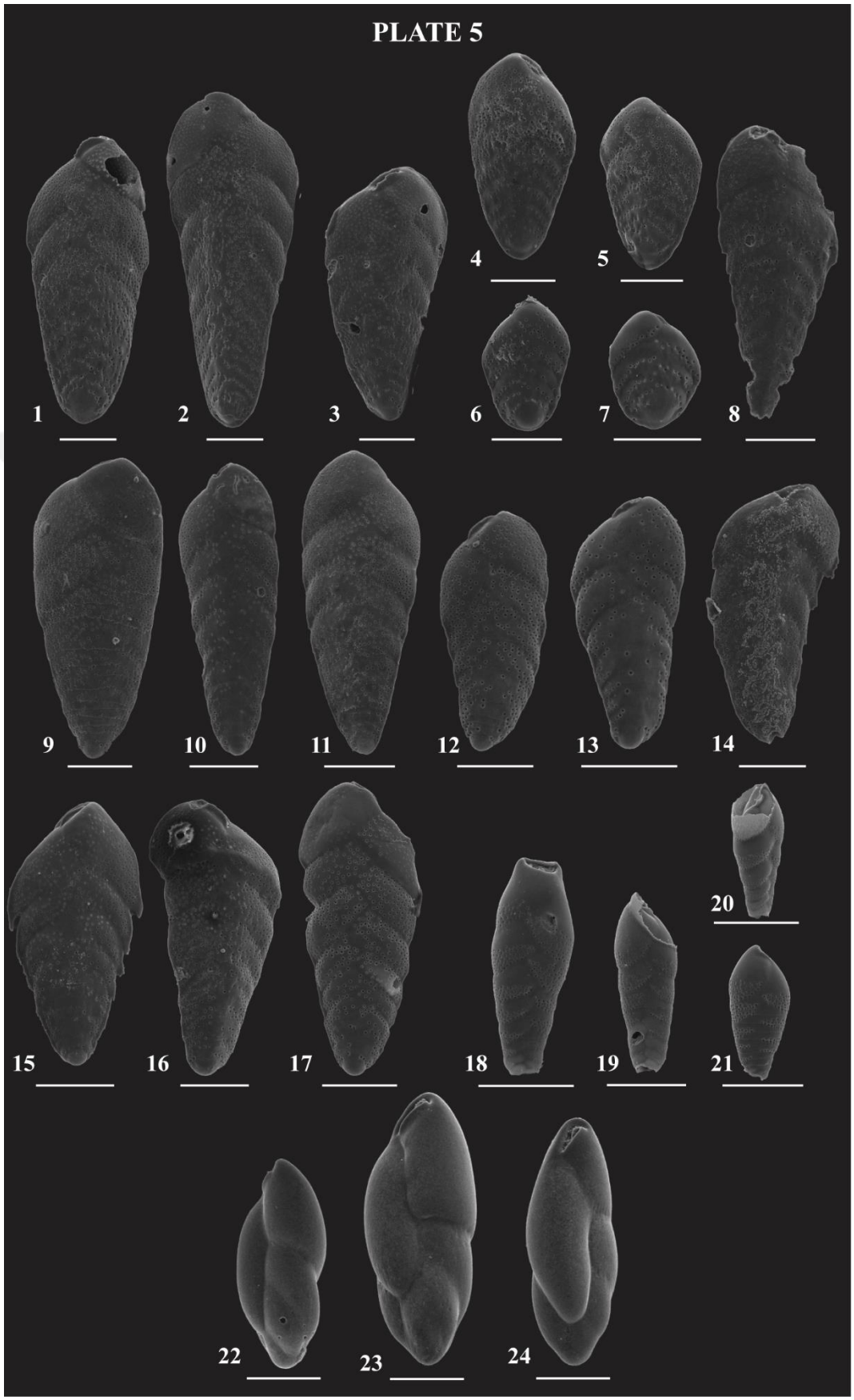

PLATE 5
1
2
3
4
5
6
7
8
9
10
11
12
13
14
15
16
17
18
19
20
21
22
23
24

PLATE 6: Bolivinitidae, stereomicrographs; scale bar: 100 μm.

1-9: *Bolivina dilatata* Reuss 1. lateral, Station 1 (2021) sample 4 cm, IS_03_A_001; 2. lateral, other side, Station 1 (2021) sample 4 cm, IS_03_A_001; 3. edge-apertural, Station 1 (2021) sample 4 cm, IS_03_A_001; 4. lateral, Station 5 sample 8 cm, IS_25_Q_001; 5. lateral, Station 5 sample 8 cm, IS_25_Q_002; 6. lateral, Station 3 (21) sample 15 cm, IS_13_N2_003; 7. lateral, Station 3 (21) sample 15 cm, IS_13_N2_002a; 8. lateral, Station 3 (21) sample 15 cm, IS_13_N2_002b, juvenile; 9. lateral, Station 1 (21) 4 cm, IS_03_A_003, juvenile; **10-21**: *Bolivina spathulata* (Williamson) 10. lateral, Station 1 (21) 4 cm, IS_03_B_001; 11. edge-apertural, Station 1 (21) 4 cm, IS_03_B_002; 12. edge-apertural, Station 1 (21) 4 cm, IS_03_B_004a; 13. lateral, Station 1 (21) 4 cm, IS_03_B_004b; 14. lateral, Station 5 sample 8 cm, IS_25_R_001; 15. lateral, Station 3 (21) sample 15 cm, IS_13_N1_001; 16. lateral, Station 3 (21) sample 15 cm, IS_13_N1_002; 17. lateral, Station 3 (21) sample 15 cm, IS_13_N1_003; 18. lateral, MM50 sample 15 cm, IS_21_A_001, serrated carina; 19. lateral, MM50 sample 15 cm, IS_21_A_002, serrated carina; 20. lateral, Station 1 (21) 4 cm, IS_03_B_006, lobulate; 21. lateral, Station 5 sample 8 cm, IS_25_R_002, lobulate; **22-25**: *Bolivinellina* sp. 22. lateral, Station 1 (21) 4 cm, IS_03_E_001, terminal aperture; 23. edge, Station 1 (21) 4 cm, IS_03_E_001, terminal aperture; 24. lateral, Station 2 sample 2 cm, IS_03_E_001, broken; 25. lateral, Station 5 sample 8 cm, IS_25_T_002, juvenile; **26-29**: *Fursenkoina schreibersiana* (Cžjžek) 26a. lateral, 26b. lateral, Station 1 (19) 4 cm, IS_01_M_002; 27a. lateral, 27b. lateral, Station 1 (19) 4 cm, IS_01_M_001; 28a. lateral, 28b. edge, Station 2 sample 5 cm, IS_07_W_001; 29a. lateral, 29b. lateral, Station 1 (19) 4 cm, IS_01_M_003.

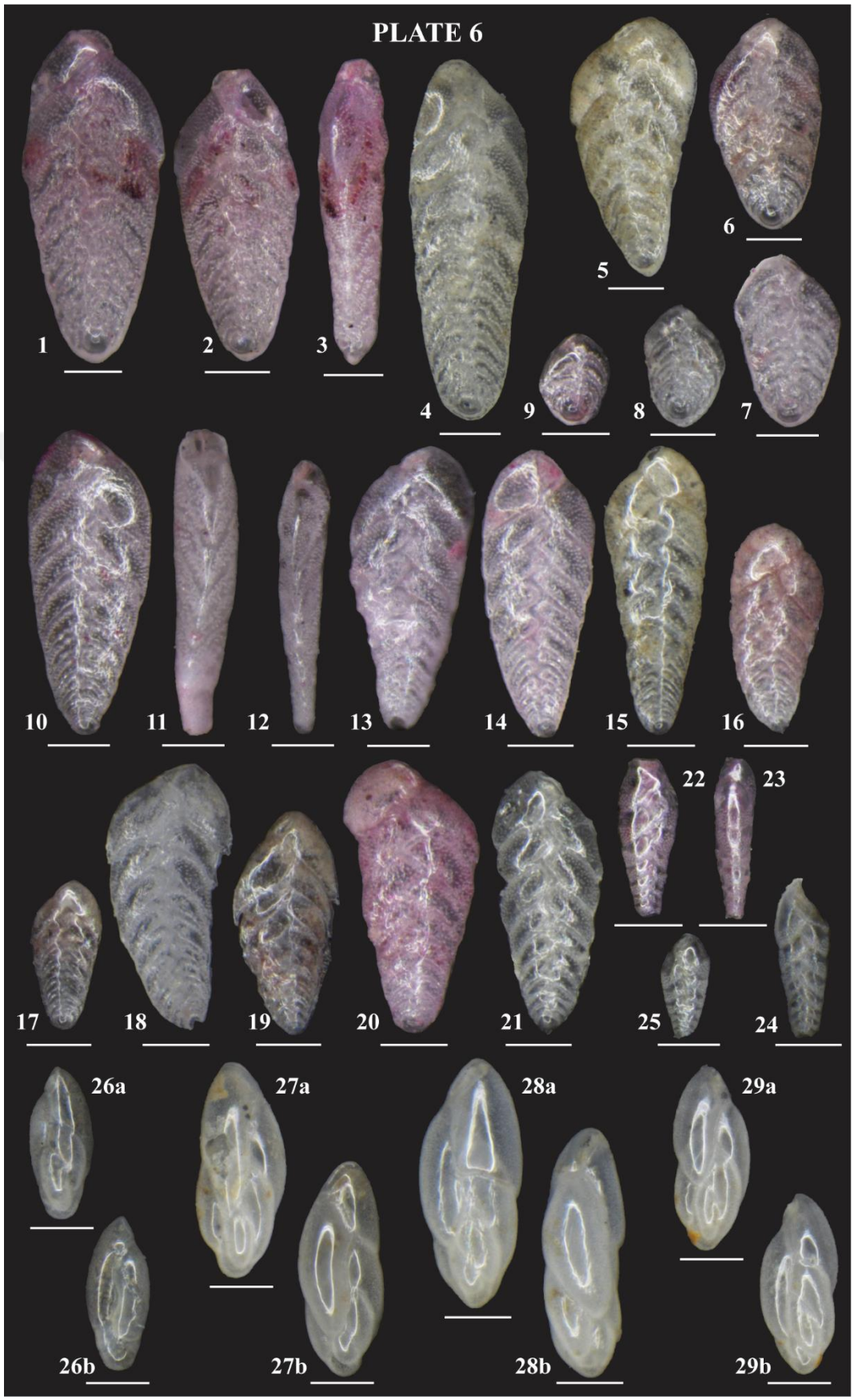

PLATE 6
1
2
3
4
9
8
7
5
6
10
11
12
13
14
15
16
17
18
19
20
21
22
23
25
24
26a
27a
28a
29a
26b
27b
28b
29b

PLATE 7: Buliminidae, SEM images; scale bar: 100 μm.

1-7: *Bulimina aculeata* d'Orbigny 1. lateral-apertural, Station 2 sample 2 cm, IS_06_G_001; 2. lateral-apertural, Station 1 (21) sample 8 cm, IS_04_F_001; 3. lateral-apertural, Station 2 sample 2 cm, IS_06_G_003; 4. lateral-adapertural, MM50 sample 15 cm, IS_28_H_001, broken; 5. lateral-adapertural, MM50 sample 15 cm, IS_28_H_002, broken; 6. lateral-adapertural, MM50 sample 15 cm, IS_28_H_003; 7. lateral, MM50 sample 15 cm, IS_28_H_004; **8-10**: *Bulimina elongata* d'Orbigny, lateral, Station 2 sample 2 cm, IS_06_I_002; 9. lateral, Station 1 (21) sample 8 cm, IS_04_G_001; 10. lateral, Station 1 (21) sample 8 cm, IS_04_G_002; **11-17**: *Bulimina marginata* d'Orbigny 11. lateral, MM50 sample 15 cm, IS_28_F_001; 12. lateral, MM50 sample 15 cm, IS_28_F_002; 13. lateral, K51.2K09 sample 8 cm, IS_31_C1_001, juvenile; 14. lateral, K51.2K09 sample 8 cm, IS_31_C3_001; 15. lateral, K51.2K09 sample 8 cm, IS_31_C3_002; 16. lateral, K51.2K09 sample 8 cm, IS_31_C2_001; 17. lateral, K51.2K09 sample 8 cm, IS_31_C2_002; **18-21**: *Bulimina costata* d'Orbigny 18. lateral, Station 1 (19) sample 4 cm, IS_01_Z_001; 19. lateral, Station 3 (21) 1 cm, IS_11_2A_001; 20. lateral, Station 3 (21) 1 cm, IS_11_2A_002; 21. lateral, Station 3 (21) 1 cm, IS_11_2A_003, juvenile; **22-25**: *Bulimina inflata* Seguenza 22. lateral, K51.2K09 sample 8 cm, IS_31_A_001a, juvenile; 23. lateral, K51.2K09 sample 8 cm, IS_31_A_001b, juvenile; 24. lateral, K51.2K09 sample 8 cm, IS_31_A_002a; 25. lateral, K51.2K09 sample 8 cm, IS_31_A_002b.

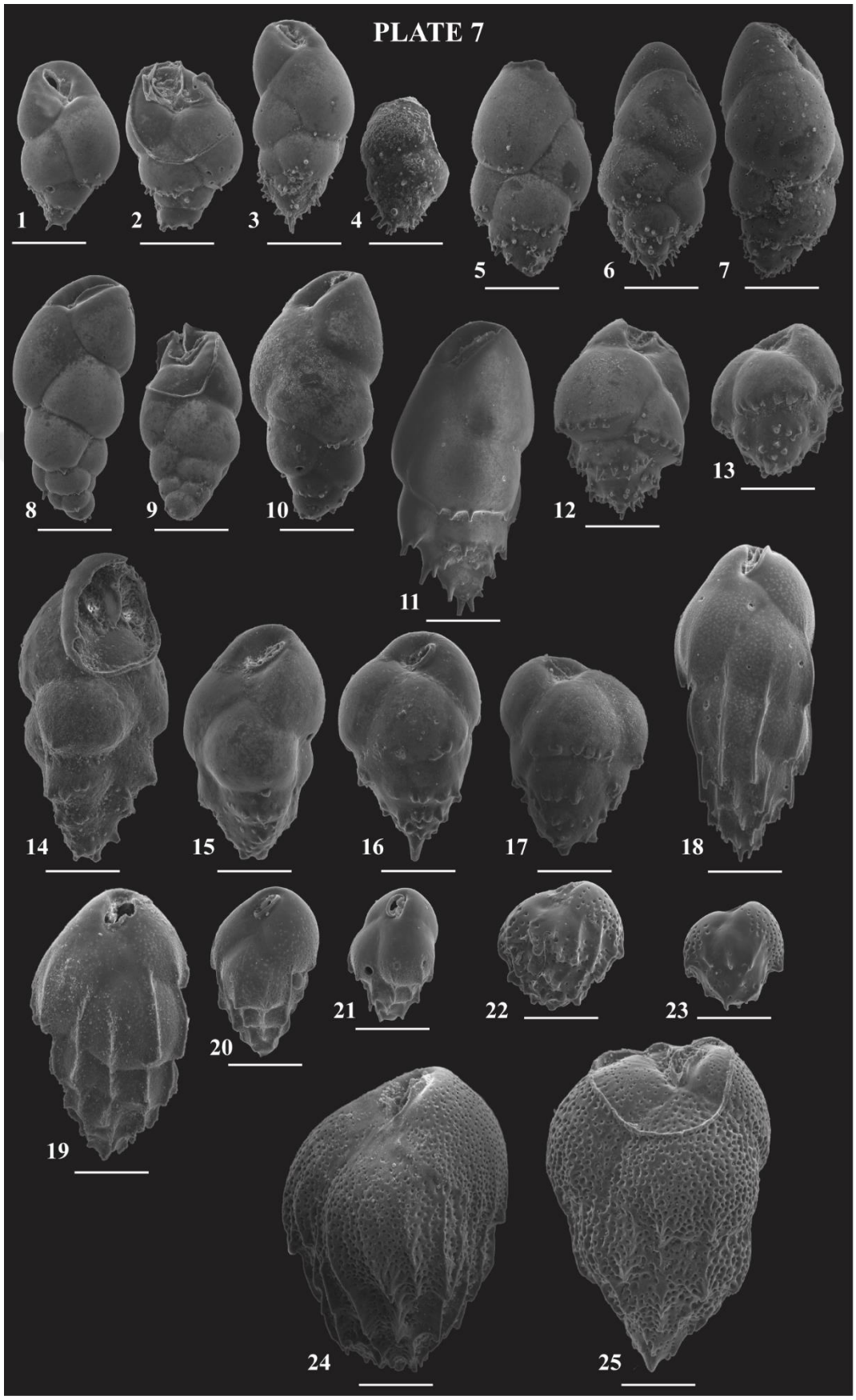

PLATE 7
1
2
3
4
5
6
7
8
9
10
11
12
13
14
15
16
17
18
19
20
21
22
23
24
25

PLATE 8: Buliminidae, stereomicrographs; scale bar: 100 μm.

1-8: *Bulimina aculeata* d'Orbigny 1a. lateral-apertural, 1b. lateral-adapertural, Station 2 sample 2 cm, IS_06_G_001; 2a. lateral-apertural, 2b. lateral-adapertural, Station 1 (21) sample 8 cm, IS_04_F_001; 3a. lateral-apertural, 3b. lateral-adapertural, Station 1 (21) sample 8 cm, IS_04_F_002; 4. lateral-adapertural, Station 2 sample 2 cm, IS_06_G_003; 5. lateral, MM50 sample 15 cm, IS_28_H_001, broken; 6. lateral-adapertural, MM50 sample 15 cm, IS_28_H_002, broken; 7. lateral-adapertural, MM50 sample 15 cm, IS_28_H_003; 8. lateral-apertural, MM50 sample 15 cm, IS_28_H_004; **9-13**: *Bulimina elongata* d'Orbigny, 9. lateral, Station 2 sample 2 cm, IS_06_I_002; 10. lateral, Station 2 sample 2 cm, IS_06_I_001; 11. lateral, Station 1 (21) sample 8 cm, IS_04_G_001; 12. lateral, Station 1 (21) sample 8 cm, IS_04_G_002; 13. lateral, Station 1 (21) sample 8 cm, IS_04_H_001; **14-23**: *Bulimina marginata* d'Orbigny 14. lateral, MM50 sample 15 cm, IS_28_F_001, elongate; 15. lateral, Station 3 (21) 1 cm, IS_11_2B_001, juvenile; 16. oblique, K51.2K09 sample 8 cm, IS_31_C1_001, juvenile classic; 17. lateral, Station 1 (19) sample 4 cm, IS_01_Y_001, classic; 18. lateral, MM50 sample 15 cm, IS_28_F_002, classic; 19. lateral, Station 3 (21) 1 cm, IS_11_2B_002, classic; 20. lateral, K51.2K09 sample 8 cm, IS_31_C3_001, pyramidal; 21. lateral, K51.2K09 sample 8 cm, IS_31_C3_002, pyramidal; 22. lateral, K51.2K09 sample 8 cm, IS_31_C2_001, pyramidal; 23. lateral, K51.2K09 sample 8 cm, IS_31_C2_002, pyramidal; **24-28**. *Bulimina costata* d'Orbigny 24. lateral, Station 1 (19) sample 4 cm, IS_01_Z_001; 25. lateral, Station 3 (21) 1 cm, IS_11_2A_001; 26. lateral, Station 3 (21) 1 cm, IS_11_2A_002; 27. lateral, Station 3 (21) 1 cm, IS_11_2A_003; 28. lateral, Station 3 (21) 1 cm, IS_11_2A_004; **29-36**: *Bulimina inflata* Seguenza 29. lateral, K51.2K09 sample 8 cm, IS_31_A_002a; 30. lateral, K51.2K09 sample 8 cm, IS_31_A_002b; 31. lateral, K51.2K09 sample 8 cm, IS_31_A_002e; 32. lateral, K51.2K09 sample 8 cm, IS_31_A_002f; 33. lateral, K51.2K09 sample 8 cm, IS_31_A_001a, juvenile; 34. lateral, K51.2K09 sample 8 cm, IS_31_A_001b, juvenile; 35. lateral, K51.2K09 sample 8 cm, IS_31_A_002c, juvenile; 36. lateral, K51.2K09 sample 8 cm, IS_31_A_002d, juvenile.

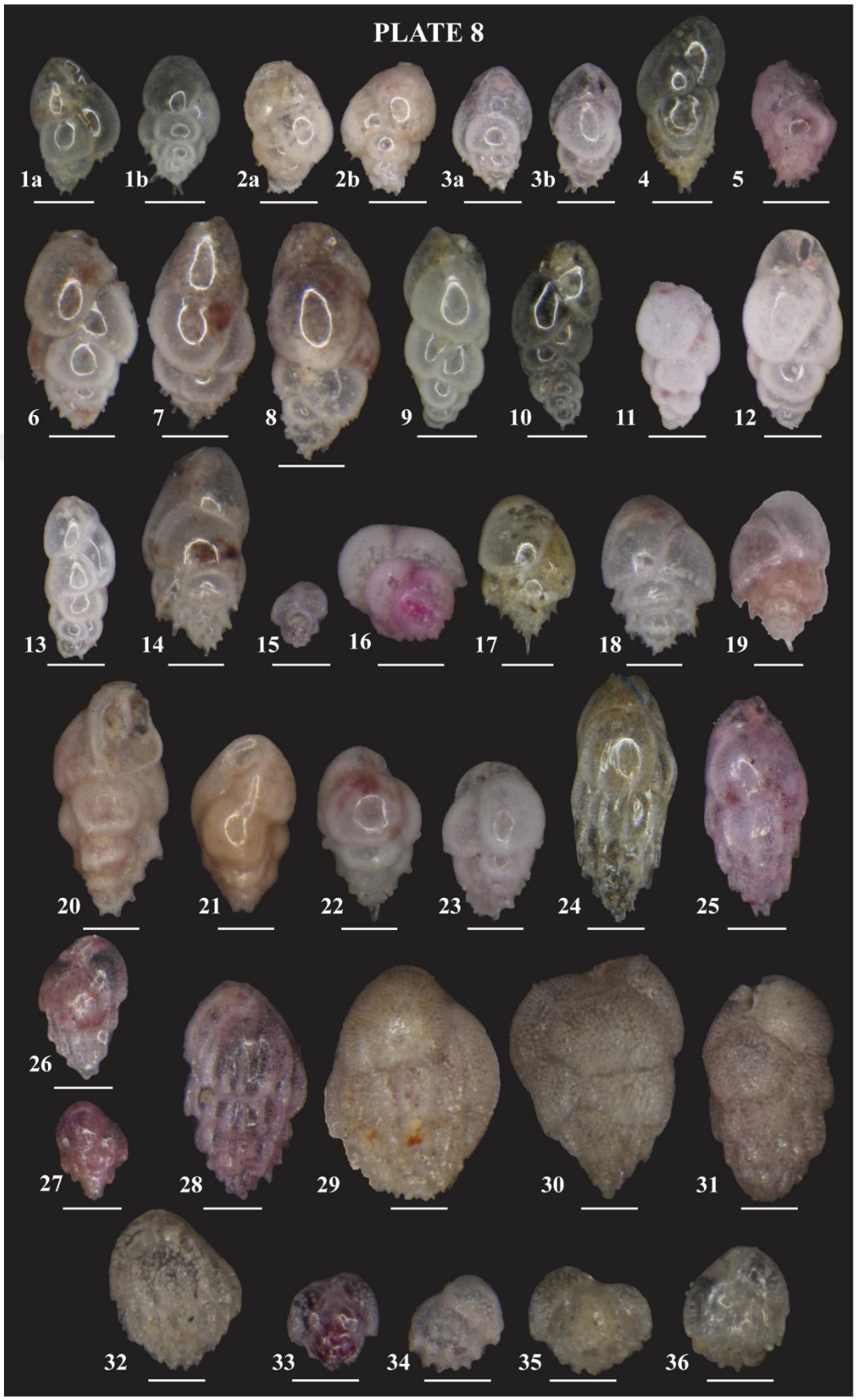

PLATE 8
1a
1b
2a
2b
3a
3b
4
5
6
7
8
9
10
11
12
13
14
15
16
17
18
19
20
21
22
23
24
25
26
27
28
29
30
31
32
33
34
35
36

PLATE 9: Buliminoidea, Cassidulinoidea, SEM images; scale bar: 100 μm.

1-6: *Rectuvigerina phlegeri* Le Calvez, lateral view, 1. MM50 sample 15 cm, IS_28_J_004; 2. MM50 sample 15 cm, IS_28_J_002; 3. MM50 sample 15 cm, IS_28_J_001; 4. MM50 sample 15 cm, IS_28_J_003; 5. Station 2 sample 25 cm, IS_10_K_001, juvenile specimen; 6. Station 2 sample 25 cm, IS_10_K_002, juvenile specimen; **7**: *Reussella spinulosa* (Reuss) lateral view, MM50 sample 15 cm, IS_28_G_001, broken specimen; **8-12**: *Trifarina angulosa* (Williamson), lateral view 8. Station 3 (2021) sample 1 cm, IS_11_H_001; 9. Station 2 sample 5 cm, IS_07_U_001; 10. MM50 sample 15 cm, IS_28_K_001; 11. MM50 sample 15 cm, IS_28_K_002; 12: Station 1 (2021) sample 8 cm, IS_04_J_001, juvenile specimen; **13-15**: *Sphaeroidina bulloides* d'Orbigny, apertural view, 13. Station 3 (2021) sample 15 cm, IS_12_A_001; 14. K51.2K09 sample 8 cm, IS_32_H_001; 15. K51.2K09 sample 8 cm, IS_32_H_002, juvenile specimen; **16-22**: *Globobulimina* spp., lateral 16. K51.2K09 sample 8 cm, IS_32_I_001; 17. Station 2 sample 2 cm, IS_05_E_001; 18. Station 2 sample 2 cm, IS_06_B_003; 19. Station 2 sample 2 cm, IS_05_E_002; 20. Station 5 sample 8 cm, IS_18_A_003, juvenile; 21. Station 5 sample 8 cm, IS_18_A_001, juvenile; 22. Station 5 sample 8 cm, IS_18_A_002, juvenile; **23-26**: *Uvigerina mediterranea* Hofker, lateral, 23. K51.2K09 sample 8 cm, IS_30_A_005, juvenile; 24. K51.2K09 sample 8 cm, IS_30_A_004, juvenile; 25. K51.2K09 sample 8 cm, IS_30_A_002; 26. K51.2K09 sample 8 cm, IS_30_A_001.

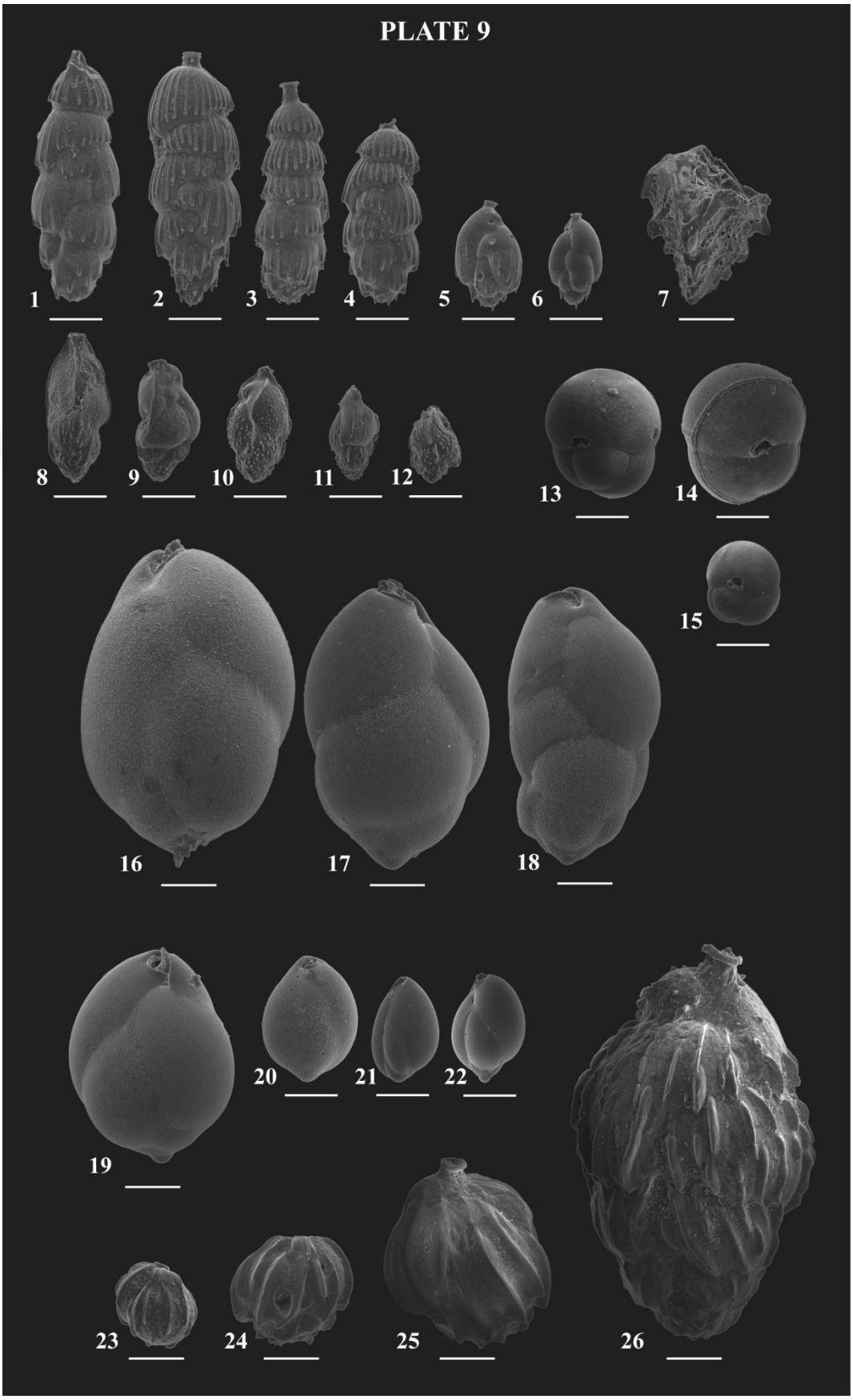

PLATE 9
1
2
3
4
5
6
7
8
9
10
11
12
13
14
15
16
17
18
19
20
21
22
23
24
25
26

PLATE 10: Buliminoidea, Cassidulinoidea, stereomicrographs; scale bar: 100 μm.

1-7: *Rectuvigerina phlegeri* Le Calvez, lateral view, 1. MM50 sample 15 cm, IS_J_004; 2. MM50 sample 15 cm, IS_J_002; 3. MM50 sample 15 cm, IS_J_001; 4. MM50 sample 15 cm, IS_J_003; 5. Station 2 sample 25 cm, IS_10_K_001, juvenile specimen; 6. Station 2 sample 25 cm, IS_10_K_002, juvenile specimen; 7. Station 2 sample 25 cm, IS_10_K_003, juvenile specimen; **8-9**: *Reussella spinulosa* (Reuss) lateral views, MM50 sample 15 cm, IS_28_G_001, broken specimen; **10-14**: *Trifarina angulosa* (Williamson), lateral view 10. Station 3 (2021) sample 1 cm, IS_11_H_001; 11. Station 2 sample 5 cm, IS_07_U_001; 12. MM50 sample 15 cm, IS_28_K_001; 13. MM50 sample 15 cm, IS_28_K_002; 14: Station 1 (2021) sample 8 cm, IS_04_J_001, juvenile specimen; **15-17**: *Sphaeroidina bulloides* d'Orbigny 15a. adapertural view, 15b. apertural view, Station 3 (2021) sample 15 cm, IS_12_A_001; 16. K51.2K09 sample 8 cm, IS_32_H_001; 17. K51.2K09 sample 8 cm, IS_32_H_002, juvenile specimen; **18-26**: *Globobulimina* spp., lateral 18. K51.2K09 sample 8 cm, IS_32_I_001; 19. Station 2 sample 2 cm, IS_05_E_001; 20. Station 2 sample 2 cm, IS_06_B_003; 21. Station 2 sample 2 cm, IS_06_B_002; 22. Station 2 sample 2 cm, IS_05_E_002; 23. K51.2K09 sample 8 cm, IS_32_I_002; 24. Station 5 sample 8 cm, IS_18_A_003, juvenile; 25. Station 5 sample 8 cm, IS_18_A_001, juvenile; 26. Station 5 sample 8 cm, IS_18_A_002, juvenile; **27-31**: *Uvigerina mediterranea* Hofker, lateral, 27. K51.2K09 sample 8 cm, IS_30_A_002; 28. K51.2K09 sample 8 cm, IS_30_A_003; 29. K51.2K09 sample 8 cm, IS_30_A_004, juvenile; 30. K51.2K09 sample 8 cm, IS_30_A_005, juvenile; 31. K51.2K09 sample 8 cm, IS_30_A_001.

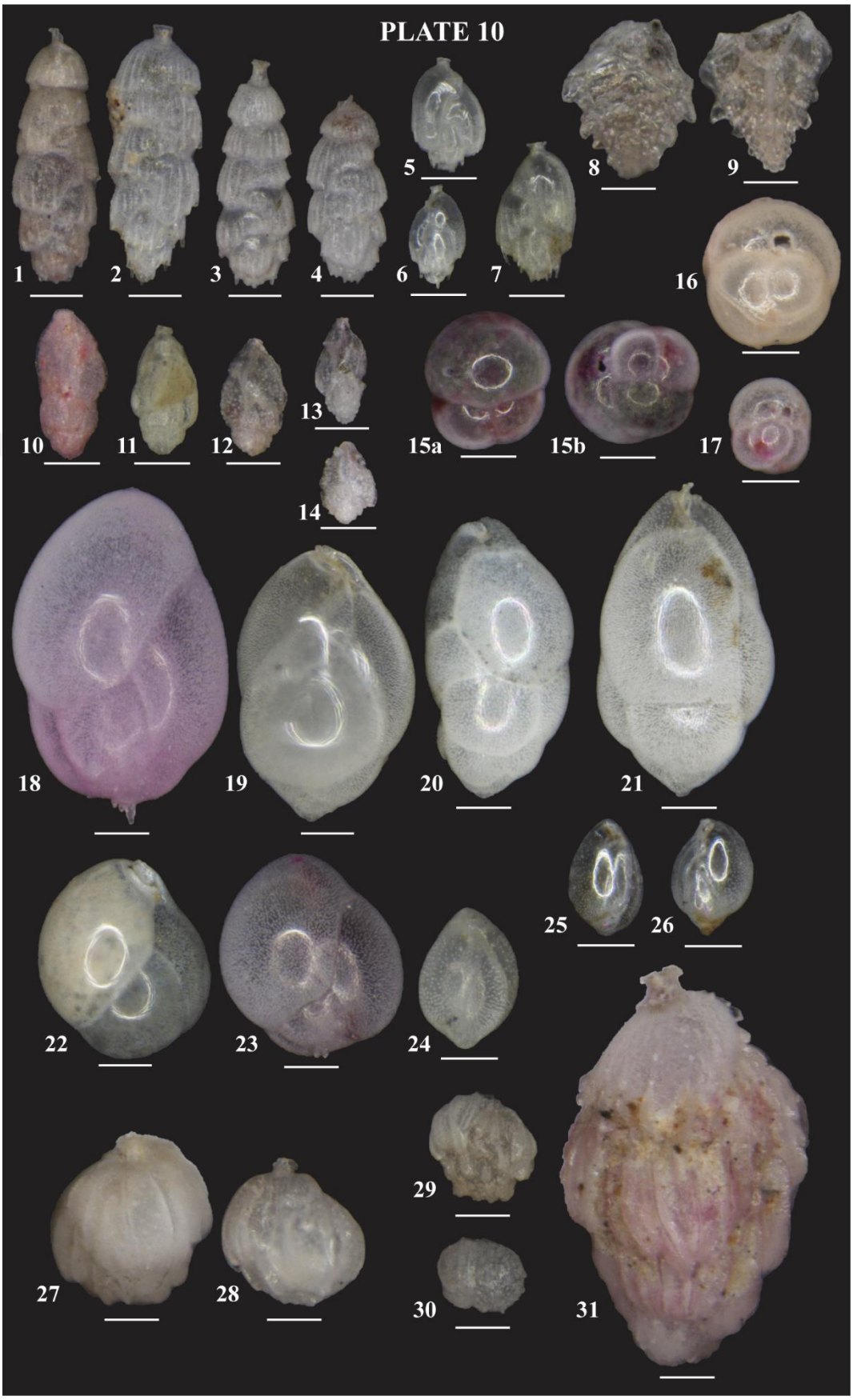

PLATE 10
1
2
3
4
5
6
7
8
9
10
11
12
13
14
15a
15b
16
17
18
19
20
21
22
23
24
25
26
27
28
29
30
31

PLATE 11: Cassidulinidae, SEM images; scale bar: 100 μm.

1-12: *Cassidulina laevigata* d'Orbigny 1. MM50 sample 15 cm, IS_29_A_006a; 2. MM50 sample 15 cm, IS_29_A_007a; 3. MM50 sample 15 cm, IS_29_A_006b; 4. MM50 sample 15 cm, IS_29_A_007b_01; 5. frontal, apertural side, MM50 sample 30 cm, IS_20_A_002, broken specimen; 6. oblique-edge, adapertural side, MM50 sample 30 cm, IS_20_A_003; 7. oblique, apertural side, MM50 sample 15 cm, IS_29_B_002a; 8. oblique, apertural side, MM50 sample 15 cm, IS_29_B_004; 9. edge, MM50 sample 15 cm, IS_29_B_005; 10. edge, MM50 sample 15 cm, IS_29_B_006; 11. frontal, apertural side, MM50 sample 15 cm, IS_29_B_007; 12. edge, MM50 sample 15 cm, IS_29_B_008; **13-21**: *Paracassidulina minuta* (Cushman) 13. frontal, apertural side, Station 4 sample 15 cm, IS_14_2H_002a; 14. frontal, adapertural side, Station 4 sample 15 cm, IS_14_2H_002b; 15. oblique, edge, 45C-2 sample 35 cm, IS_15_2B_001; 16. frontal, apertural side, Station 5 sample 8 cm, IS_17_E_002; 17. frontal, adapertural side, Station 5 sample 8 cm, IS_17_E_008; 18. edge, Station 5 sample 8 cm, IS_17_E_009; 19. frontal, apertural side, Station 5 sample 8 cm, IS_17_E_007; 20. frontal, adapertural side, Station 5 sample 8 cm, IS_17_E_010; 21. edge, Station 5 sample 8 cm, IS_17_E_011; **22-25**: *Globocassidulina subglobosa* Brady 22. oblique, Station 5 sample 8 cm, IS_17_G_001; 23. frontal, apertural side, Station 5 sample 8 cm, IS_17_G_002; 24. frontal, adapertural side, Station 5 sample 8 cm, IS_17_G_003; 25. frontal, apertural side, MM50 sample 15 cm, IS_29_E_001; **26-29**: *Globocassidulina* cf. *obtusa* sensu Sejrup and Guilbault 26. frontal, apertural side, Station 5 sample 8 cm, IS_17_F_001; 27. oblique, edge, Station 4 sample 15 cm, IS_14_2I_001; 28. edge, Station 5 sample 8 cm, IS_17_F_002; 29. frontal, apertural side, Station 5 sample 8 cm, IS_17_H_004; **30-32**: *Globocassidulina oblonga* (Reuss) 30. oblique, edge, Station 5 sample 8 cm, IS_17_H_001; 31. frontal, apertural side, Station 5 sample 8 cm, IS_17_H_002; 32. edge, Station 5 sample 8 cm, IS_17_H_003.

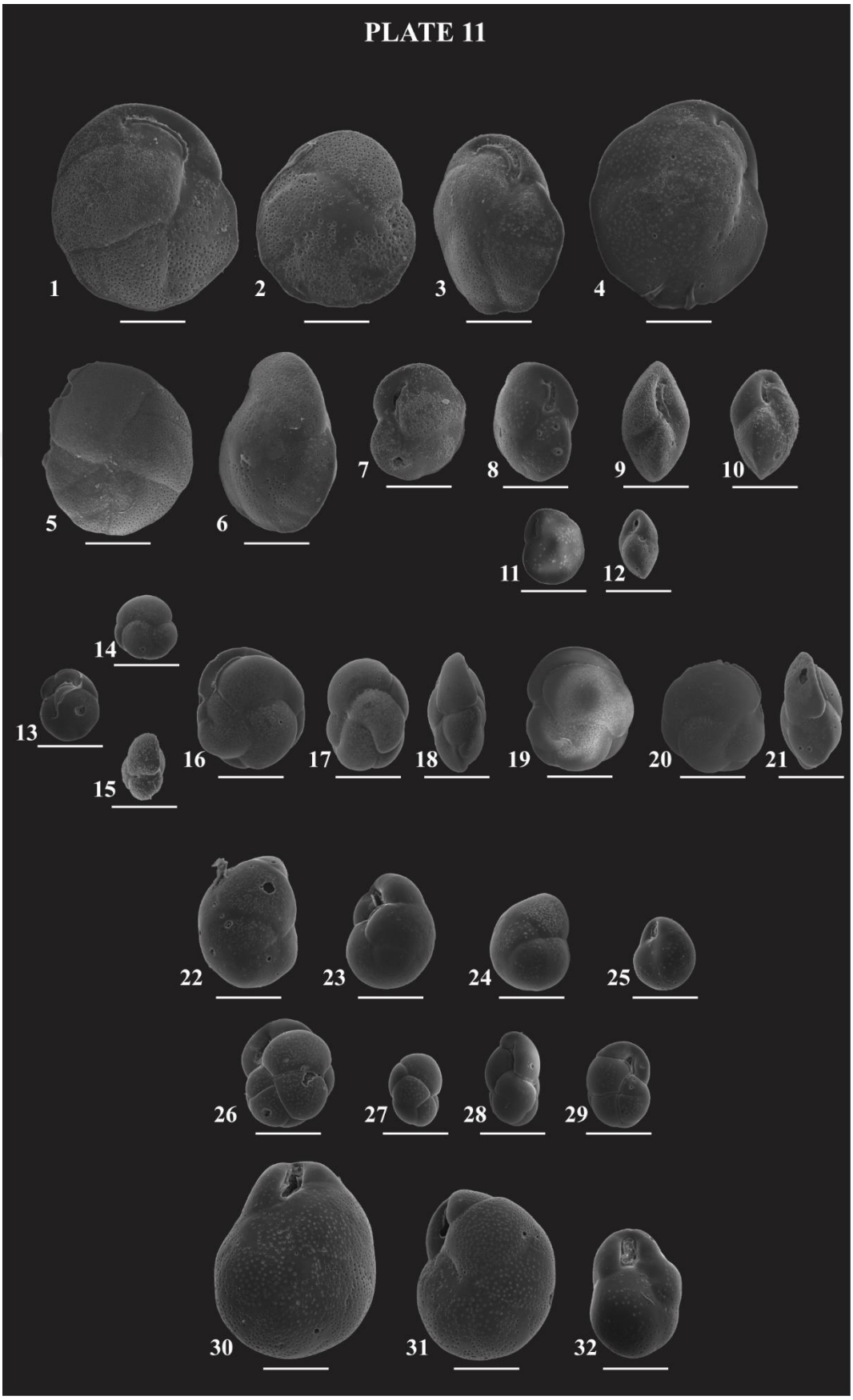

PLATE 11
1
2
3
4
5
6
7
8
9
10
11
12
13
14
15
16
17
18
19
20
21
22
23
24
25
26
27
28
29
30
31
32

PLATE 12: Cassidulinidae, stereomicrographs; scale bar: 100 μm.

1-7: *Cassidulina laevigata* d'Orbigny 1a. frontal, apertural side, 1b. edge, 1c. frontal, adapertural side, MM50 sample 15 cm, IS_29_A_006a; 2a. frontal, apertural side, 2b. edge, 2c. frontal, adapertural side, MM50 sample 15 cm, IS_29_A_007a; 3a frontal, adapertural side, 3b. edge, 3c. frontal, apertural side, MM50 sample 15 cm, IS_29_A_006b; 4a. frontal, apertural side, 4b. edge, 4c. frontal, apertural side, MM50 sample 15 cm, IS_29_A_007b_01; 5. frontal, apertural side, MM50 sample 30 cm, IS_20_A_001; 6a. frontal, apertural side, 6b. edge, 6c. frontal, apertural side, MM50 sample 15 cm, IS_29_B_002a; 7a. frontal, apertural side, 1b. edge, MM50 sample 15 cm, IS_29_B_003a; **8-14**: *Paracassidulina minuta* (Cushman) 8a. frontal, apertural side, 8b. frontal, adapertural side, Station 4 sample 15 cm, IS_14_2H_002a; 9a. frontal, apertural side, 9b. frontal, adapertural side, Station 4 sample 15 cm, IS_14_2H_002b; 10a. frontal, apertural side, 10b. edge, Station 5 sample 8 cm, IS_17_E_002; 11a. frontal, apertural side, 11b. edge, Station 5 sample 8 cm, IS_17_E_007; 12. frontal, apertural side, Station 5 sample 8 cm, IS_17_E_001; 13. frontal, apertural side, Station 5 sample 8 cm, IS_17_E_004; 14. frontal, apertural side, Station 5 sample 8 cm, IS_17_E_005; **15-20**: *Globocassidulina subglobosa* Brady 15. frontal, apertural side, Station 5 sample 8 cm, IS_17_G_001; 16. frontal, apertural side, Station 5 sample 8 cm, IS_17_G_002; 17. frontal, apertural side, Station 5 sample 8 cm, IS_17_G_003; 18. frontal, adapertural side, Station 5 sample 8 cm, IS_17_G_004; 19. frontal, adapertural side, Station 5 sample 8 cm, IS_17_G_005; 20. frontal, apertural side, Station 5 sample 8 cm, IS_17_G_006; **21-26**: *Globocassidulina* cf. *obtusa* sensu Sejrup and Guilbault 21. frontal, apertural side, Station 5 sample 8 cm, IS_17_F_001; 22a. frontal, adapertural side, 22b. oblique, apertural side, Station 4 sample 15 cm, IS_14_2I_001; 23a. frontal, adapertural side, 23b. oblique, apertural side, 23c. frontal, apertural side, Station 4 sample 15 cm, IS_14_2I_002; 24. frontal, apertural side, Station 5 sample 8 cm, IS_17_F_002; 25. frontal, apertural side, Station 5 sample 8 cm, IS_17_F_004; 26. frontal, apertural side, Station 5 sample 8 cm, IS_17_F_003; **27-31**: *Globocassidulina oblonga* (Reuss) 27. oblique, edge, Station 5 sample 8 cm, IS_17_H_001; 28. edge, Station 5 sample 8 cm, IS_17_H_002; 29. oblique edge, Station 5 sample 8 cm, IS_17_H_003; 30. frontal, apertural side, Station 5 sample 8 cm, IS_17_H_004; 31. edge, Station 5 sample 8 cm, IS_17_H_005.


PLATE 12
1a
1b
1c
2a
2b
2c
3a
3b
3c
4a
4b
4c
5
6a
6b
6c
7a
7b
8a
8b
9a
9b
10a
10b
11a
11b
12
13
14
15
16
17
18
19
20
21
22a
22b
23a
23b
23c
24
25
26
27
28
29
30
31

PLATE 13: Chilostomelloidea SEM images; scale bar: 100 μm.

1-6: *Chilostomella* sp. 1 1. frontal, apertural side, Station 1 (2021) sample 4 cm, IS_02_J_001; 2. frontal, adapertural side, Station 2 sample 25 cm, IS_05_C_001; 3. apertural pole, Station 2 sample 2 cm, IS_06_C_001; 4. side, Station 2 sample 25 cm, IS_10_H_001; 5. side, Station 4 sample 15 cm, IS_14_S_002; 6. broken, Station 4 sample 15 cm, IS_14_S_001; **7-11**: *Gyroidina umbonata* (Silvestri) 7. umbilical, Station 5 sample 8 cm, IS_26_I_001; 8. spiral, Station 5 sample 8 cm, IS_26_I_002; 9. umbilical-oblique, Station 5 sample 8 cm, IS_26_I_003; 10. spiral-oblique, Station 5 sample 8 cm, IS_26_I_004; 11. spiral, 45C-2 sample 35 cm, IS_15_V_001, juvenile; **12:17**: *Svratkina tuberculata* (Balkwill and Wright) 12. spiral, Station 4 sample 15 cm, IS_14_O_001; 13. edge, Station 4 sample 15 cm, IS_14_O_002; 14. umbilical, MM50 sample 15 cm, IS_29_K_001; 15. edge, MM50 sample 15 cm, IS_29_K_002; 16. spiral, Station 5 sample 8 cm, IS_27_R_001; 17. umbilical-oblique, IS_27_R_002; **18-22**: *Eilohedra vitrea* (Parker), Station 5 sample 8 cm, 18. spiral, IS_27_S_003; 19. edge, IS_27_S_002; 20. umbilical, IS_27_S_001; 21. umbilical, IS_27_S_004; 22. spiral, IS_27_S_005, juvenile; **23-25**: *Rotamorphina*? *involuta* Parker 23. spiral, K51.2K09 sample 8 cm, IS_32_C_001; 24. umbilical, K51.2K09 sample 8 cm, IS_32_C_002; 25. spiral, Station 5 sample 8 cm, IS_27_C_001.

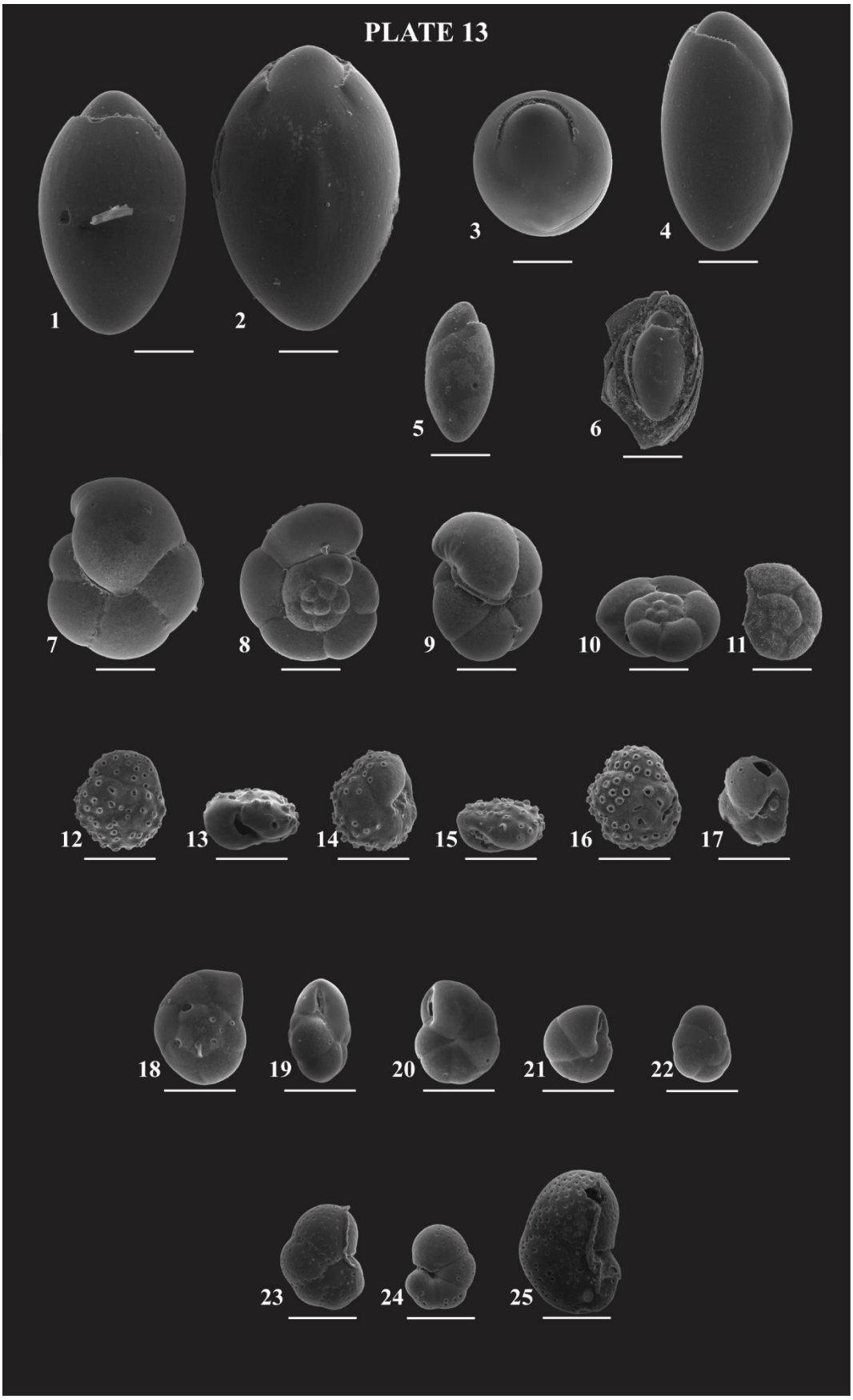

PLATE 13
1
2
3
4
5
6
7
8
9
10
11
12
13
14
15
16
17
18
19
20
21
22
23
24
25

PLATE 14: Chilostomelloidea stereomicrographs; scale bar: 100 μm.

1-5: *Chilostomella* sp. 1 1a. frontal, apertural side, 1b. frontal, spiral side, 1c. apertural pole, Station 1 (2021) sample 4 cm, IS_02_J_001; 2. frontal, adapertural side, Station 2 sample 25 cm, IS_05_C_001; 3a. frontal, spiral side, 3b. frontal, apertural side, Station 2 sample 2 cm, IS_06_C_001; 5. broken, Station 4 sample 15 cm, IS_14_S_001; 6a. side, 6b. frontal, spiral side, Station 2 sample 2 cm, IS_06_C_002; **6-10**: *Gyroidina umbonata* (Silvestri) 6a. spiral, 6b. umbilical, Station 5 sample 8 cm, IS_26_I_001; 7a. spiral, 7b. umbilical, Station 5 sample 8 cm, IS_26_I_002; 8a. spiral, 8b. umbilical, Station 5 sample 8 cm, IS_26_I_003; 9a. spiral-oblique, 9b. umbilical, Station 5 sample 8 cm, IS_26_I_004; 10a. umbilical, 10b. edge, 10c. spiral, Station 2 sample 2 cm, IS_05_X_001; **11-12**: *Svratkina tuberculata* (Balkwill and Wright) 11a. spiral, 11b. edge, 11c. umbilical, Station 4 sample 15 cm, IS_14_O_002; 13a. umbilical, 13b. edge, 13c. spiral, Station 4 sample 15 cm, IS_14_O_001; **13-20**: *Eilohedra vitrea* (Parker) 13. spiral, Station 5 sample 8 cm, IS_27_S_003; 14. edge, Station 5 sample 8 cm, IS_27_S_002; 15. umbilical, Station 5 sample 8 cm, IS_27_S_001; 16. umbilical, Station 5 sample 8 cm, IS_27_S_004; 17. spiral, Station 5 sample 8 cm, IS_27_S_005, juvenile; 18a. umbilical, 18b. spiral, Station 3 (2021) sample 1 cm, IS_11_N_001; 19a. umbilical, 19b. edge, 19c. spiral, MM50 sample 15 cm, IS_29_J_002; 20a. umbilical, 20b. edge, 20c. spiral, MM50 sample 15 cm, IS_29_J_001; **21-23**: *Rotamorphina*? *involuta* Parker 21a. spiral, 21b. edge, 21c. umbilical, K51.2K09 sample 8 cm, IS_32_C_001; 22a. spiral, 22b. edge, 22c. umbilical, K51.2K09 sample 8 cm, IS_32_C_002; 23a. spiral, 23b. edge, 23c. umbilical, Station 5 sample 8 cm, IS_27_C_001.

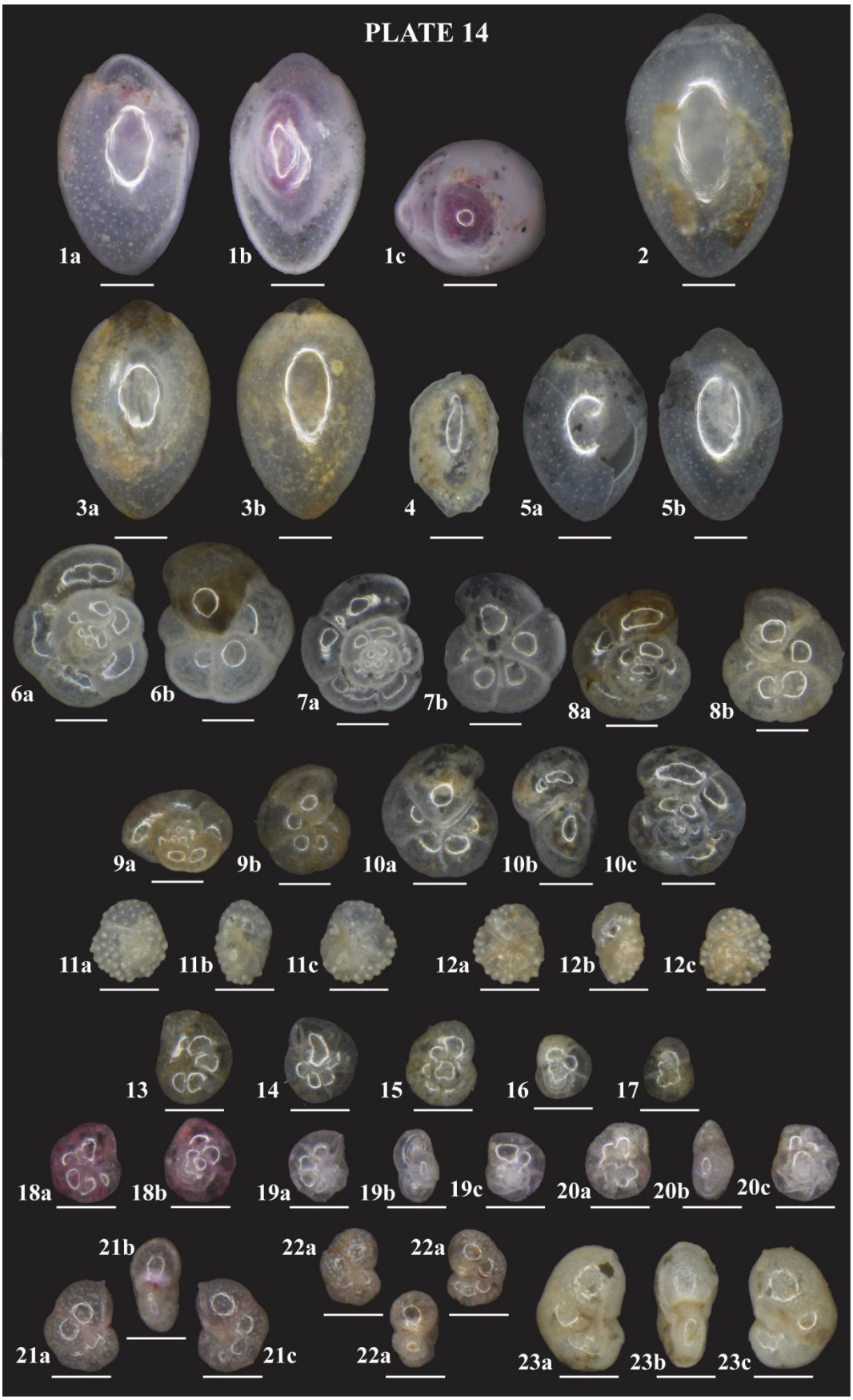

PLATE 14
1a
1b
1c
2
3a
3b
4
5a
5b
6a
6b
7a
7b
8a
8b
9a
9b
10a
10b
10c
11a
11b
11c
12a
12b
12c
13
14
15
16
17
18a
18b
19a
19b
19c
20a
20b
20c
21a
21b
21c
22a
22a
22a
23a
23b
23c

PLATE 15: Chilostomelloidea, Discorboidea SEM images; scale bar: 100 μm.

1-6: *Gavelinopsis praegeri* (Heron-Allen and Earland) 1. umbilical, Station 2 sample 5 cm, IS_07_G_001, juvenile; 2. spiral, Station 2 sample 5 cm, IS_07_G_002, juvenile; 3. spiral, Station 3 (2021) sample 1 cm, IS_11_K_001, juvenile; 4. spiral, Station 2 sample 25 cm, IS_10_E_001; 5. umbilical, Station 3 (2021) sample 15 cm, IS_12_D_001; 6. edge-oblique, Station 4 sample 15 cm, IS_14_I_001; **7-14**: *Valvulineria bradyana* (Fornasini) 7. umbilical, MM50 sample 15 cm, IS_28_A_001; 8. spiral, MM50 sample 15 cm, IS_28_A_002; 9. edge, 45C-2 sample 35 cm, IS_15_M_001; 10. umbilical, 45C-2 sample 35 cm, IS_15_M_002, juvenile; 11.spiral-oblique, Station 1 (2021) sample 8 cm, IS_04_A_004, juvenile; 12. edge, Station 1 (2021) sample 8 cm, IS_04_A_005, juvenile; 13. umbilical, 45C-2 sample 35 cm, IS_15_M_003, juvenile; 14. edge, 45C-2 sample 35 cm, IS_15_M_004, juvenile; **15-18**: *Discorbinella bertheloti* (d'Orbigny) 15. spiral, Station 5 sample 8 cm, IS_26_B_001; 16. spiral, Station 5 sample 8 cm, IS_26_B_003; 17. umbilcial, Station 5 sample 8 cm, IS_26_B_002; 18. edge-oblique, Station 5 sample 8 cm, IS_26_B_004; **19-21**: *Neoconorbina terquemi* (Rzehak) 19. umbilical, Station 2 sample 2 cm, IS_05_V_001; 20. spiral, Station 3 (2021) sample 15 cm, IS_12_J_001; 21. edge, Station 5 sample 8 cm, IS_26_J_004; **22-23**: *Spirorbina*? sp., Station 5 sample 8 cm, 22. umbilical, IS_26_J_002; 23. spiral, IS_26_J_001.

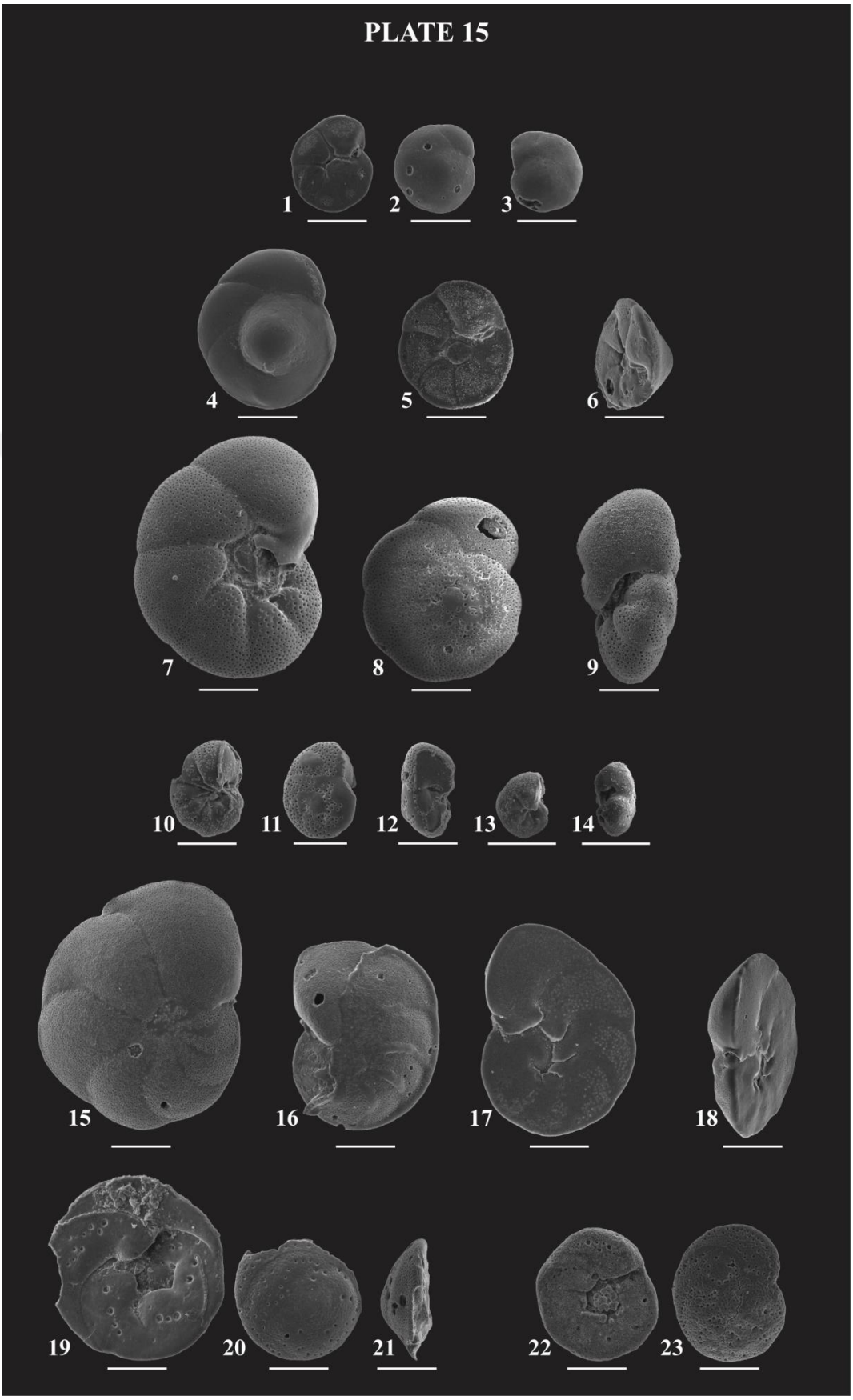

PLATE 15
1
2
3
4
5
6
7
8
9
10
11
12
13
14
15
16
17
18
19
20
21
22
23

PLATE 16: Chilostomelloidea, Discorboidea stereomicrographs; scale bar: 100 μm.

1-5: *Gavelinopsis praegeri* (Heron-Allen and Earland) 1a. umbilical, 1b. edge, 1c. spiral, Station 2 sample 5 cm, IS_07_G_001, juvenile; 2a. spiral, 2b. edge, 2c. umbilical, Station 2 sample 5 cm, IS_07_G_002, juvenile; 3a. spiral, 3b. umbilical, spiral, Station 2 sample 25 cm, IS_10_E_001; 4a. umbilical, 4b. spiral, Station 3 (2021) sample 15 cm, IS_12_D_001; 5. spiral, Station 4 sample 15 cm, IS_14_I_001; **6-12**: *Valvulineria bradyana* (Fornasini) 6. umbilical, 45C-2 sample 35 cm, IS_15_M_002, juvenile; 7. umbilical, MM50 sample 15 cm, IS_28_A_001; 8. umbil,cal, MM50 sample 15 cm, IS_28_A_002; 9. umbilical, 45C-2 sample 35 cm, IS_15_M_001; 10a. spiral, 10b. edge, 10c. umbilical, Station 1 (2021) sample 8 cm, IS_04_A_003; 11a. umbilical, 11b. edge, 11c. spiral, Station 1 (2021) sample 8 cm, IS_04_A_002; 12a. umbilical, 12b. edge, 12c. spiral, Station 1 (2021) sample 8 cm, IS_04_A_001; **13-18**: *Discorbinella bertheloti* (d'Orbigny) 13a. spiral, 13b. umbilical, Station 5 sample 8 cm, IS_26_B_001; 14a. spiral, 14b. umbilical, Station 5 sample 8 cm, IS_26_B_002; 15a. umbilical, 15b. spiral, Station 5 sample 8 cm, IS_26_B_003; 16a. spiral, 16b. umbilical, Station 5 sample 8 cm, IS_26_B_004; 17a. umbilical, 17b. spiral, Station 5 sample 8 cm, IS_26_B_006; 18a. spiral, 18b. umbilical, Station 5 sample 8 cm, IS_26_B_005; **19-23**: *Neoconorbina terquemi* (Rzehak) 19a. spiral, 19b. umbilical, Station 2 sample 2 cm, IS_05_V_001; 20. umbilical, Station 3 (2021) sample 15 cm, IS_12_J_001; 21. spiral, Station 5 sample 8 cm, IS_26_J_004; 22. spiral, Station 5 sample 8 cm, IS_26_J_005; 23. umbilical, Station 5 sample 8 cm, IS_26_J_006; **24-25**: *Spirorbina*? sp. Station 5 sample 8 cm, 22. umbilical, IS_26_J_002; 23. umbilical, IS_26_J_001.

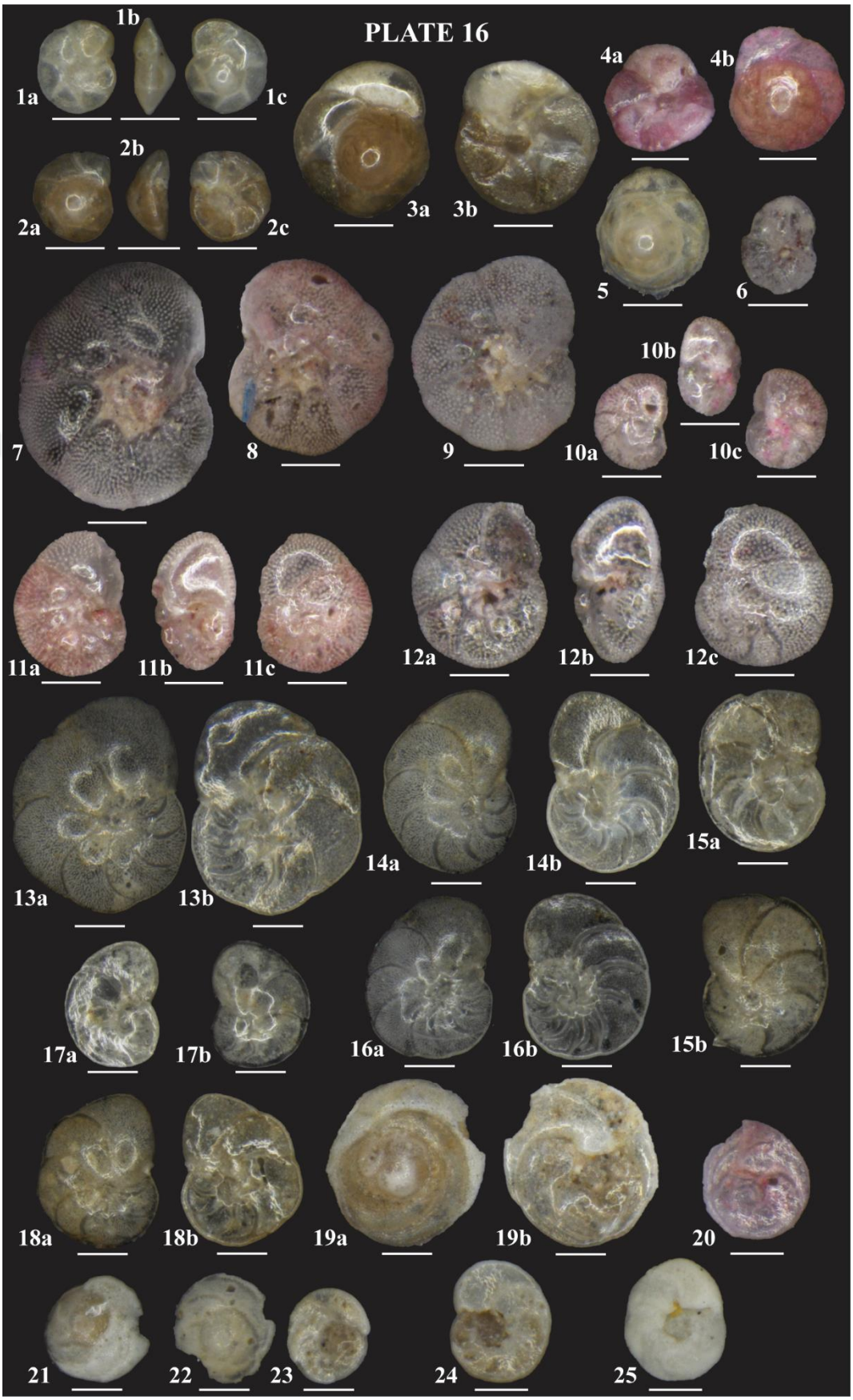

PLATE 16
1a
1b
1c
2a
2b
2c
3a
3b
4a
4b
5
6
7
8
9
10a
10b
10c
11a
11b
11c
12a
12b
12c
13a
13b
14a
14b
15a
15b
16a
16b
17a
17b
18a
18b
19a
19b
20
21
22
23
24
25

PLATE 17: Discorboidea SEM images; scale bar: 100 μm.

1-4: *Planodiscorbis rarescens* (Brady) 1. umbilical, Station 5 sample 8 cm, IS_26_A_001; 2. umbilical, Station 5 sample 8 cm, IS_26_A_003; 3. umbilical, Station 2 sample 25 cm, IS_10_C_001; 4. spiral, Station 5 sample 8 cm, IS_26_A_001; **5-10**: *Rosalina globularis* d'Orbigny 5. edge-oblique, Station 2 sample 5 cm, IS_07_D_001; 6. spiral, MM50 sample 15 cm, IS_28_B_001; 7. umbilical, MM50 sample 30 cm, IS_20_F_001; 8. umbilical-oblique, Station 2 sample 5 cm, IS_07_D_002, juvenile; 9. spiral, Station 5 sample 8 cm, IS_26_E_001, juvenile; 10. umbilical-oblique, Station 3 (2021) sample 15 cm, IS_12_F_001, juvenile; **11**: *Rosalina macropora* (Hofker), spiral, Station 3 (2021) sample 15 cm, IS_12_G_001; **12-16**: *Rosalina bradyi* (Cushman) 12. umbilical, Station 5 sample 8 cm, IS_26_F_001; 13. spiral, Station 5 sample 8 cm, IS_26_F_002; 14. edge, Station 5 sample 8 cm, IS_26_F_003; 15. edge, 45C-2 sample 35 cm, IS_15_Y_001; 16. umbilical, Station 5 sample 8 cm, IS_26_F_004, juvenile; **17-22**: *Rosalina williamsoni* (Chapman and Parr) 17. umbilical, Station 4 sample 15 cm, IS_14_H_001; 18. spiral, Station 5 sample 8 cm, IS_27_T_001; 19. umbilical, Station 4 sample 15 cm, IS_14_H_002, juvenile; 20. spiral, Station 5 sample 8 cm, IS_27_T_002, juvenile; 21. edge, Station 5 sample 8 cm, IS_27_T_005, juvenile; 22. umbilical-oblique, Station 5 sample 8 cm, IS_27_T_006, juvenile.

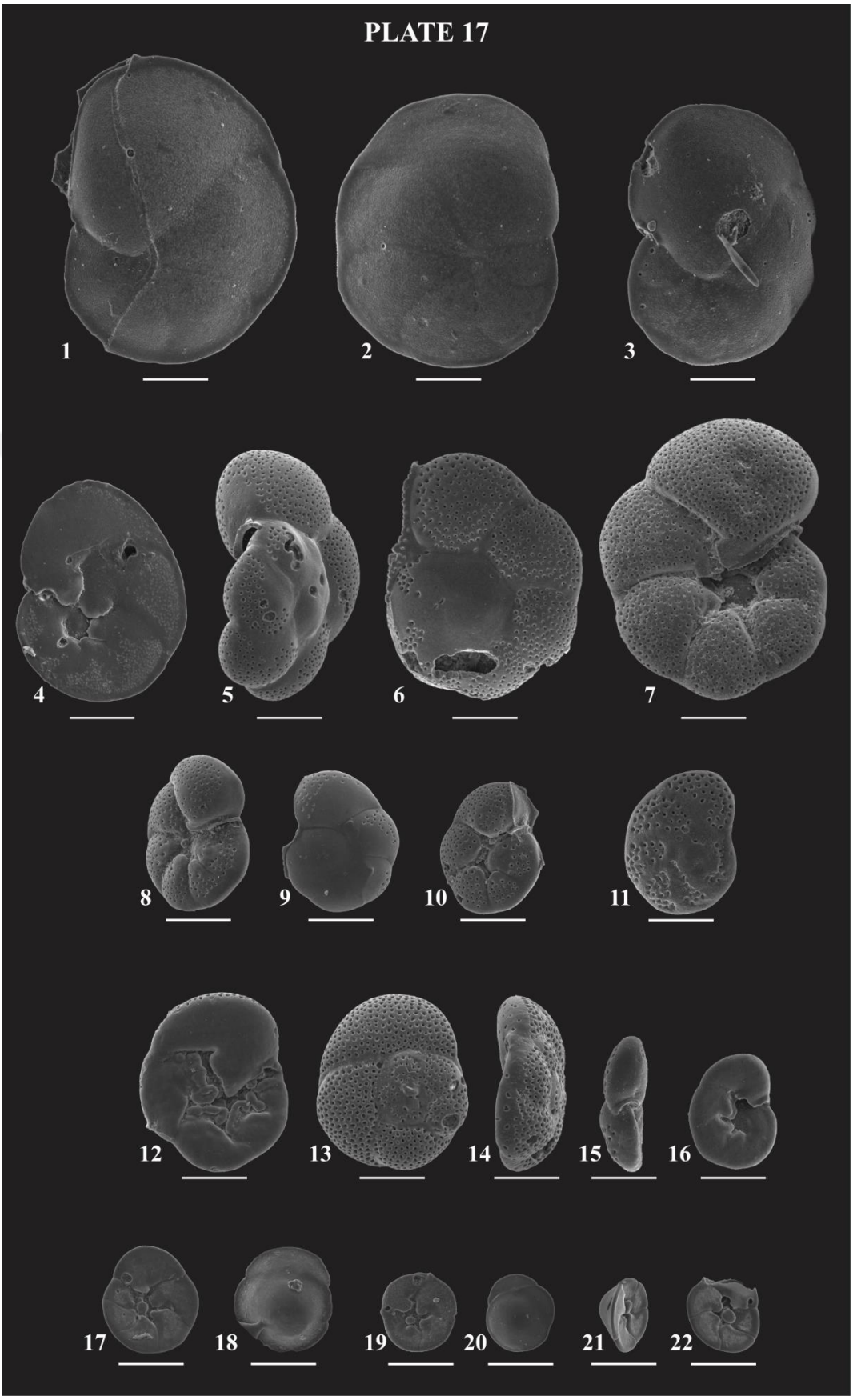

PLATE 17
1
2
3
4
5
6
7
8
9
10
11
12
13
14
15
16
17
18
19
20
21
22

PLATE 18: Discorboidea stereomicrographs; scale bar: 100 μm.

1-6: *Planodiscorbis rarescens* (Brady) 1a. spiral, 1b. umbilical, Station 5 sample 8 cm, IS_26_A_001; 2a. spiral, 2b. umbilical, Station 5 sample 8 cm, IS_26_A_003; 3a. spiral, 3b. umbilical, Station 2 sample 25 cm, IS_10_C_001; 4a. umbilical, 4b. spiral, Station 5 sample 8 cm, IS_26_A_001; 5a. umbilical, 5b. spiral, Station 5 sample 8 cm, IS_26_A_005; 6a. umbilical, 6b. spiral, Station 5 sample 8 cm, IS_26_A_002; **7-12**: *Rosalina globularis* d'Orbigny 7a. umbilical, 7b. edge, 7c. spiral, Station 2 sample 5 cm, IS_07_D_001; 8a. umbilical, 8b. spiral, MM50 sample 15 cm, IS_28_B_001; 9a. umbilical, 9b. spiral, MM50 sample 30 cm, IS_20_F_001; 10a. umbilical, 10b. edge, 10c. spiral, Station 2 sample 5 cm, IS_07_D_002, juvenile; 11. spiral, Station 5 sample 8 cm, IS_26_E_001, juvenile; 12a. umbilical, 12b. spiral, Station 3 (2021) sample 15 cm, IS_12_F_001, juvenile; **13**: *Rosalina macropora* (Hofker) Station 3 (2021) sample 15 cm, IS_12_G_001, 13a. spiral, 13b. umbilical; **14-18**: *Rosalina bradyi* (Cushman) 14. umbilical, Station 5 sample 8 cm, IS_26_F_001; 15. spiral, Station 5 sample 8 cm, IS_26_F_002; 16. umbilical, Station 5 sample 8 cm, IS_26_F_003; 17a. spiral, 17b. umbilical, 45C-2 sample 35 cm, IS_15_Y_001; 18. umbilical, Station 5 sample 8 cm, IS_26_F_004, juvenile; **19-24**: *Rosalina williamsoni* (Chapman and Parr) 19a. spiral, 19b. umbilical, Station 4 sample 15 cm, IS_14_H_001; 20. umbilical-oblique, Station 5 sample 8 cm, IS_27_T_001; 21a. spiral, 21b. edge, 21c. umbilical, Station 4 sample 15 cm, IS_14_H_002, juvenile; 22. spiral, Station 5 sample 8 cm, IS_27_T_002, juvenile; 23a. spiral, 23b. umbilical-oblique, Station 5 sample 8 cm, IS_27_T_005, juvenile; 24. umbilical-oblique, Station 5 sample 8 cm, IS_27_T_006, juvenile.

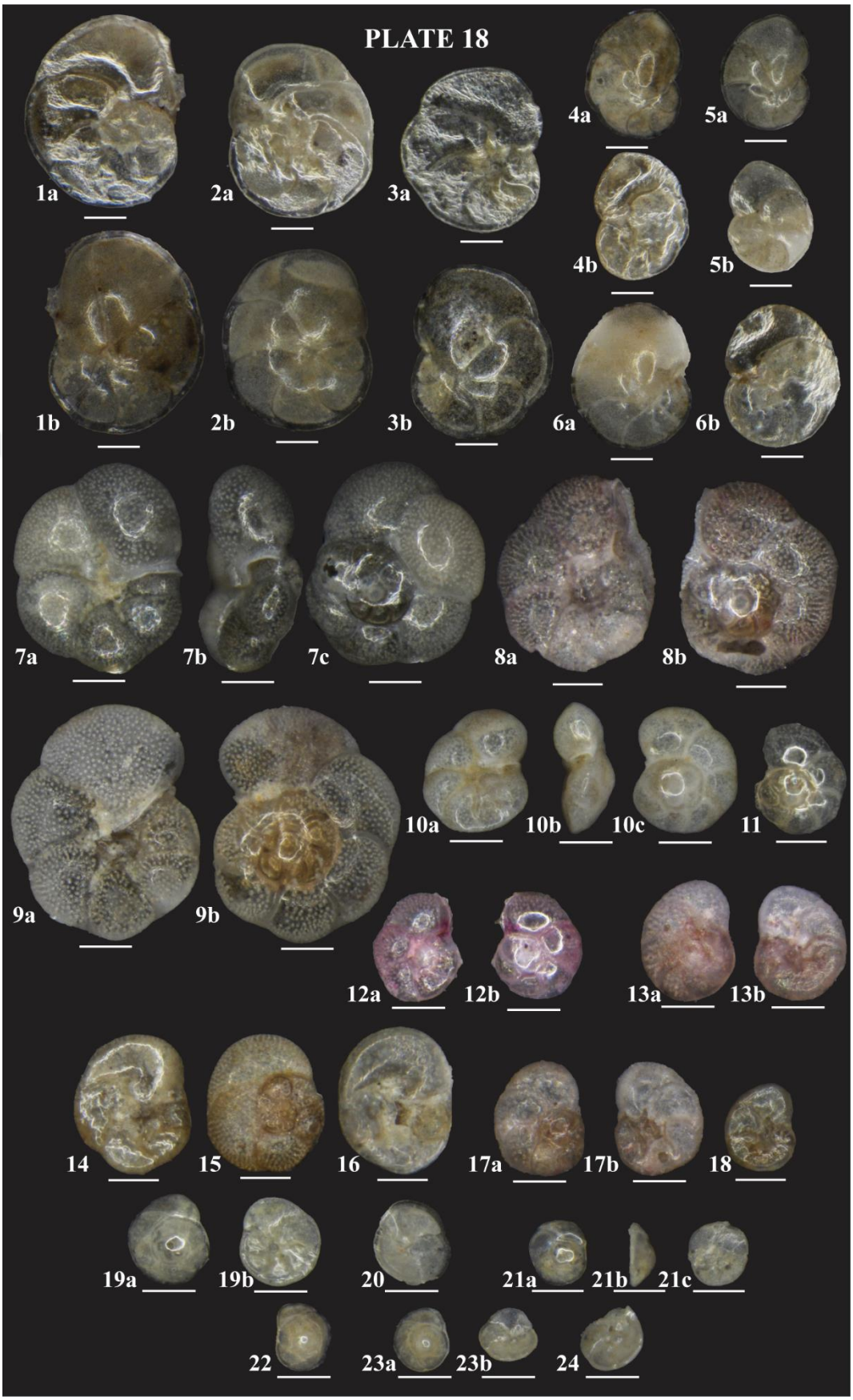

PLATE 18
1a
2a
3a
4a
5a
4b
5b
1b
2b
3b
6a
6b
7a
7b
7c
8a
8b
10a
10b
10c
11
9a
9b
12a
12b
13a
13b
14
15
16
17a
17b
18
19a
19b
20
21a
21b
21c
22
23a
23b
24

PLATE 19: Glabratelloidea, Nonionoidea SEM images; scale bar: 100 μm.

1-12: Glabratellidae 1. spiral, Station 3 (2021) sample 15 cm, IS_12_E_001; 2. umbilical, MM50 sample 15 cm, IS_29_N_001; 3. umbilical-oblique, IS_26_K_001; 4. spiral, Station 5 sample 8 cm, IS_26_K_002; 5. spiral, IS_26_K_003; 6. spiral, Station 5 sample 8 cm, IS_26_K_006; 7. spiral, Station 5 sample 8 cm, IS_26_K_004; 8. spiral, Station 5 sample 8 cm, IS_26_K_005; 9. umbilical, Station 5 sample 8 cm, IS_26_K_007; 10. umbilical, 45C-2 sample 35 cm, IS_15_2A_001; 11. edge, 45C-2 sample 35 cm, IS_15_2A_003; 12. umbilical, 45C-2 sample 35 cm, IS_15_2A_002_01; **13-20**: *Melonis pompilioides* (Fitchel and Moll) K51.2K09 sample 8 cm, 13. edge, IS_32_A_002; 14. frontal, IS_32_A_003; 15. edge, IS_32_A_016; 16. frontal, IS_32_A_001; 17. edge, IS_32_A_010; 18. frontal, IS_32_A_022; 19. frontal, IS_32_A_013, juvenile; 20. edge, IS_32_A_012, juvenile; **21-24**: *Astrononion stelligerum* (d'Orbigny) Station 5 sample 8 cm, 21. frontal, IS_27_A_001; 22. frontal, IS_27_A_002; 23. edge, IS_27_A_003; 24. frontal, IS_27_A_005; **25-27**: *Pullenia* spp. 25. edge, K51.2K09 sample 8 cm, IS_32_B_002; 26. frontal, Station 5 sample 8 cm, IS_27_B_001, juvenile; 27. frontal, K51.2K09 sample 8 cm, IS_32_B_001.

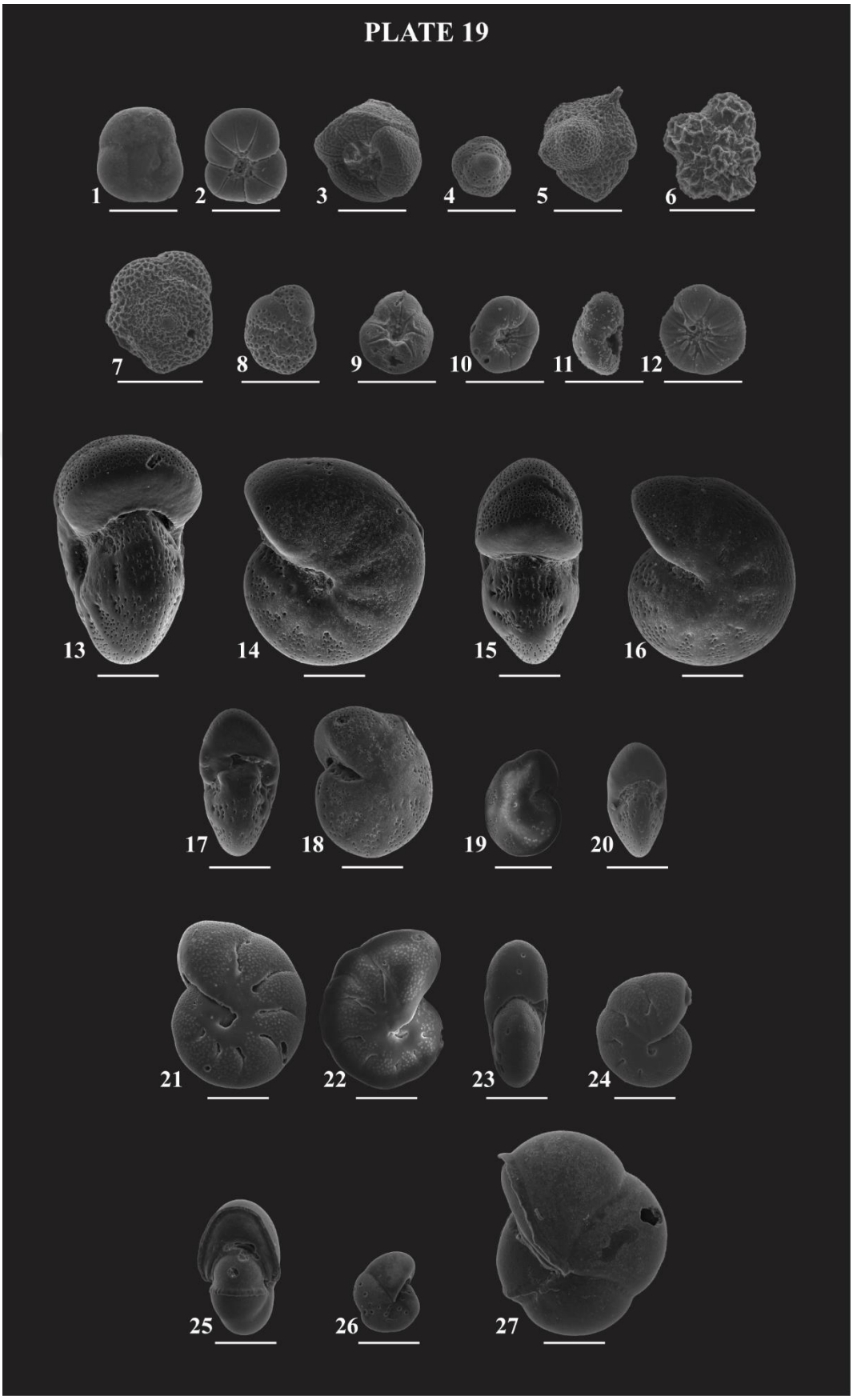

PLATE 19
1
2
3
4
5
6
7
8
9
10
11
12
13
14
15
16
17
18
19
20
21
22
23
24
25
26
27

PLATE 20: Glabratelloidea, Nonionoidea stereomicrographs; scale bar: 100 μm.

1-12: Glabratellidae 1a. umbilical, 1b. spiral, Station 3 (2021) sample 15 cm, IS_12_E_001; 2a. spiral, 2b. umbilical, MM50 sample 15 cm, IS_29_N_001; 3a. spiral, 3b. umbilical-oblique, IS_26_K_001; 4a. umbilical-oblique, 4b. spiral, Station 5 sample 8 cm, IS_26_K_002; 5a. umbilical, 5b. spiral, IS_26_K_003; 6a. umbilical, 6b. spiral, Station 5 sample 8 cm, IS_26_K_006; 7a. spiral, 7b. umbilical, Station 5 sample 8 cm, IS_26_K_004; 8a. umbilical, 8b. spiral, Station 5 sample 8 cm, IS_26_K_005; 9a. umbilical, 9b. spiral, Station 5 sample 8 cm, IS_26_K_007; 10a. spiral, 10b. umbilical, 45C-2 sample 35 cm, IS_15_2A_001; 11a. spiral, 11b. umbilical, 45C-2 sample 35 cm, IS_15_2A_003; 12a. spiral, 12b. umbilical, 45C-2 sample 35 cm, IS_15_2A_002_01; **13-22**: *Melonis pompilioides* (Fitchel and Moll) 13. frontal, K51.2K09 sample 8 cm, IS_32_A_002; 14. frontal, K51.2K09 sample 8 cm, IS_32_A_003; 15. frontal, K51.2K09 sample 8 cm, IS_32_A_016; 16. frontal, K51.2K09 sample 8 cm, IS_32_A_001; 17. frontal, K51.2K09 sample 8 cm, IS_32_A_010; 18. frontal, K51.2K09 sample 8 cm, IS_32_A_022; 19. frontal, K51.2K09 sample 8 cm, IS_32_A_013, juvenile; 20. frontal, K51.2K09 sample 8 cm, IS_32_A_012, juvenile; 21a. edge, 21b. frontal, Station 1 (2021) sample 4 cm, IS_02_P_001; 22a. edge, 22b. frontal, 45C-2 sample 35 cm, IS_15_L_001; **23-27**: *Astrononion stelligerum* (d'Orbigny) Station 5 sample 8 cm, 23a. frontal, 23b. edge, IS_27_A_001; 24a. frontal, 24b. edge, IS_27_A_002; 25a. edge, 25b. frontal, IS_27_A_003; 26a. frontal, 26b. edge, IS_27_A_005; 27a. edge, 27b. frontal, IS_27_A_004; **28-30**: *Pullenia* spp. 28a. edge, 28b. frontal, K51.2K09 sample 8 cm, IS_32_B_002; 29a. frontal, 29b. edge, 29c. frontal, Station 5 sample 8 cm, IS_27_B_001, juvenile; 30a. frontal, 30b. edge, K51.2K09 sample 8 cm, IS_32_B_001.

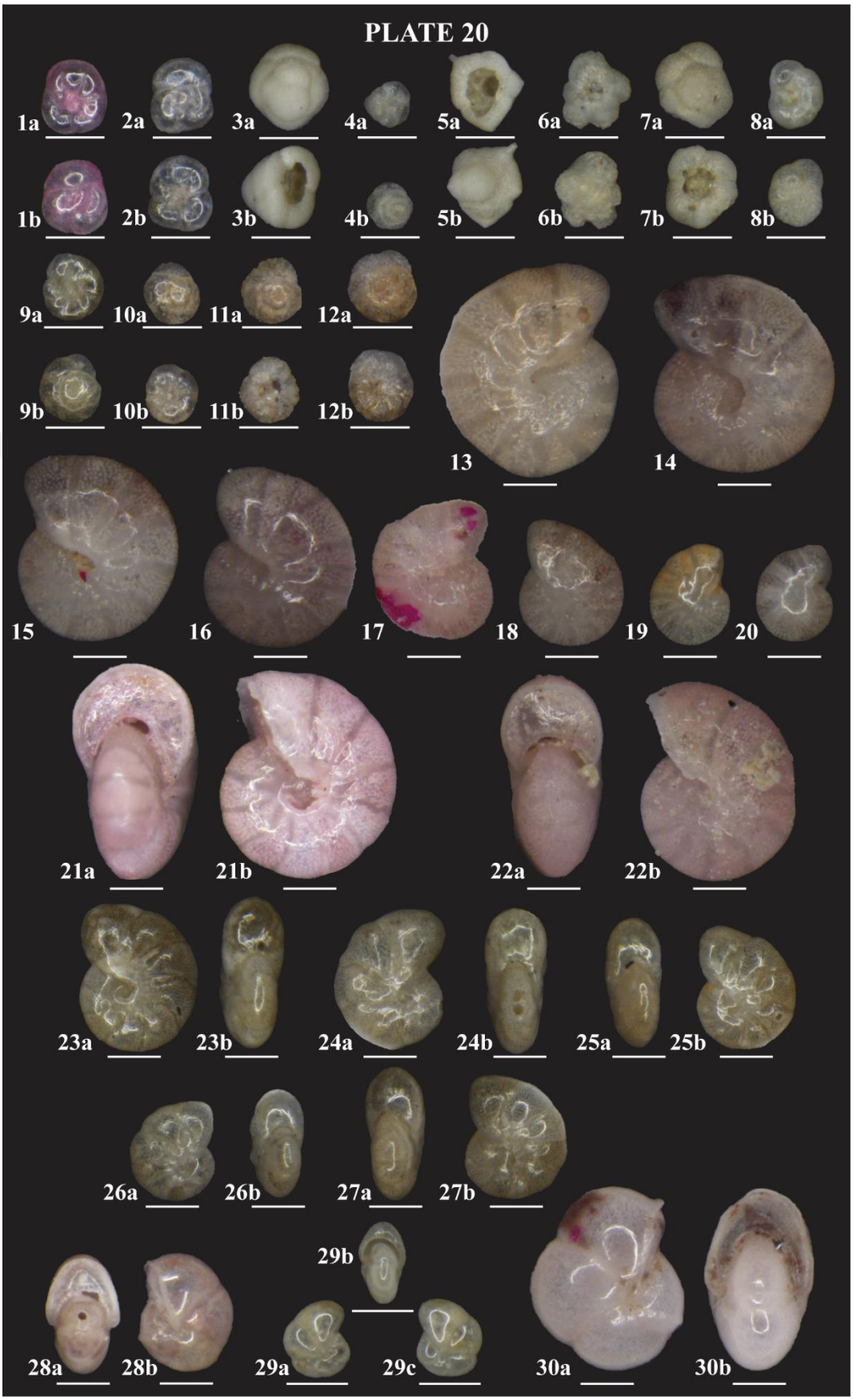

PLATE 20
1a
2a
3a
4a
5a
6a
7a
8a
1b
2b
3b
4b
5b
6b
7b
8b
9a
10a
11a
12a
9b
10b
11b
12b
13
14
15
16
17
18
19
20
21a
21b
22a
22b
23a
23b
24a
24b
25a
25b
26a
26b
27a
27b
29b
28a
28b
29a
29c
30a
30b

PLATE 21: Nonionoidea SEM images; scale bar: 100 μm.

1-5: *Nonionella opima* Cushman, Station 5 sample 8 cm, 1. spiral, IS_27_M_001; 2. umbilical, IS_27_M_002; 3. spiral-oblique, IS_27_M_005; 4. spiral-oblique, IS_27_M_004; 5. umbilical, IS_27_M_003; **6-10**: *Nonionella stella* Cushman and Moyer, Station 5 sample 8 cm, 6. umbilical, IS_27_N_001; 7. spiral, IS_27_N_002; 8. spiral, IS_27_N_005; 9. umbilical, IS_27_N_004; 10. edge, IS_27_N_009; **11-17**: *Nonionella iridea* Heron-Allen and Earland 11. spiral, Station 5 sample 8 cm, IS_27_O_007; 12. umbilical, Station 5 sample 8 cm, IS_27_O_001; 13. edge, Station 5 sample 8 cm, IS_27_O_008; 14. spiral, 45C-2 sample 35 cm, IS_15_W_001, juvenile; 15. spiral, MM50 sample 15 cm, IS_29_L_001; 16. umbilical, MM50 sample 15 cm, IS_29_L_002; 17. edge, MM50 sample 15 cm, IS_29_L_001; **18-23**: *Nonionoides grateloupii* (d'Orbigny) Station 5 sample 8 cm, 18. spiral, IS_27_L_001; 19. umbilical, IS_27_L_002; 20. edge, IS_27_L_003; 21. umbilical, IS_27_L_004; 22. spiral, IS_27_L_005; 23. edge, IS_27_L_006; **24-28**: *Nonionoides minuta* (Parker), Station 5 sample 8 cm, 24. umbilical, IS_27_J_001; 25. spiral, IS_27_J_002; 26. spiral-oblique, IS_27_J_003; 27. umbilical, IS_27_J_004; 28. spiral, IS_27_J_005, juvenile.

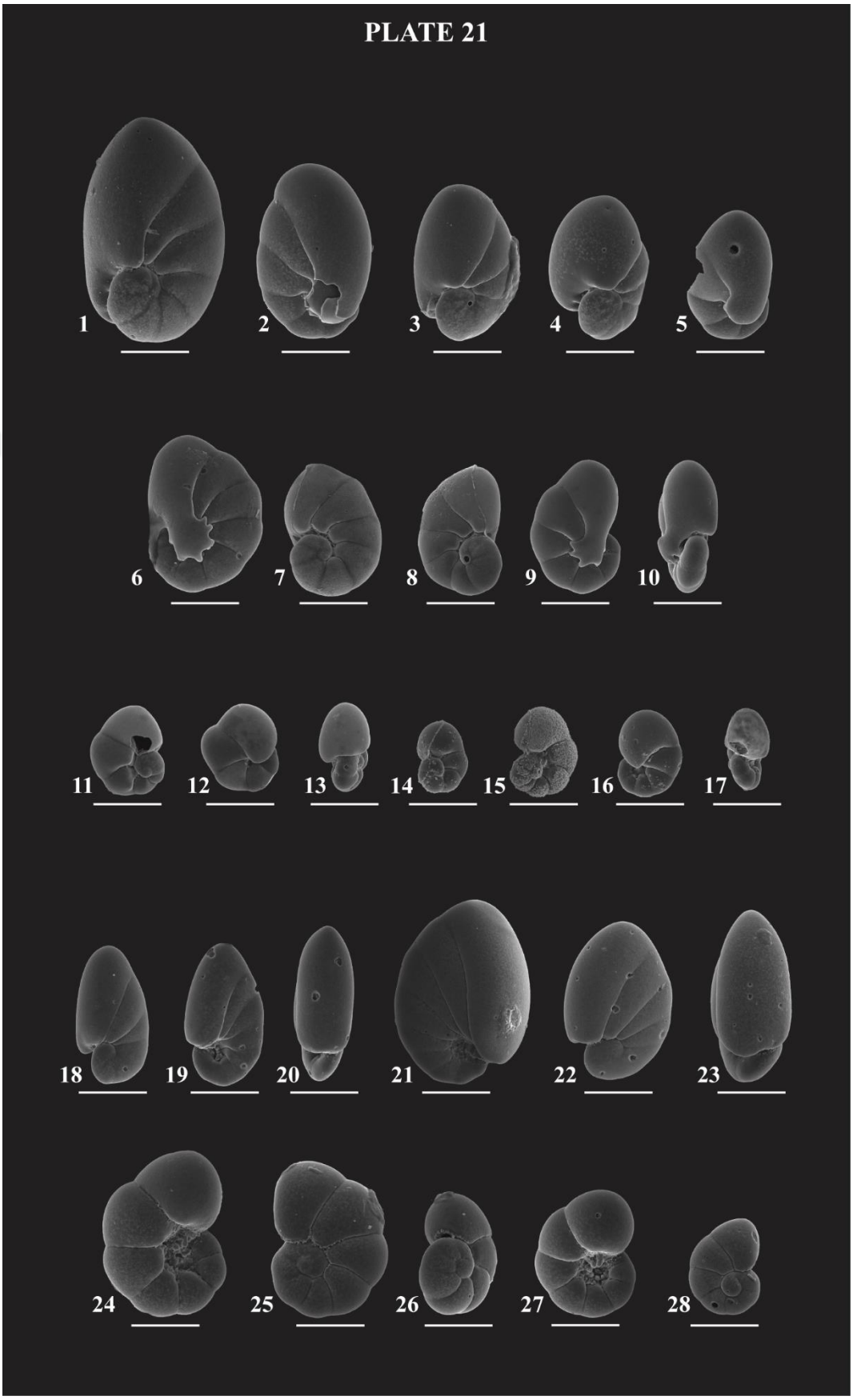

PLATE 21
1
2
3
4
5
6
7
8
9
10
11
12
13
14
15
16
17
18
19
20
21
22
23
24
25
26
27
28

PLATE 22: Nonionoidea stereomicrographs; scale bar: 100 μm.

1-10: *Nonionella opima* Cushman 1. spiral, Station 5 sample 8 cm, IS_27_M_001; 2. umbilical, Station 5 sample 8 cm, IS_27_M_002; 3. umbilical, Station 5 sample 8 cm, IS_27_M_005; 4. umbilical, Station 5 sample 8 cm, IS_27_M_004; 5. umbilical, Station 5 sample 8 cm, IS_27_M_003; 6a. spiral, 6b. umbilical, Station 2 sample 2 cm, IS_05_D_001; 7. spiral, Station 2 sample 2 cm, IS_06_D_004; 8. spiral-oblique, Station 2 sample 2 cm, IS_06_D_003; 9. spiral, Station 2 sample 2 cm, IS_06_D_002; 10. spiral, Station 2 sample 2 cm, IS_06_D_001; **11-21**: *Nonionella stella* Cushman and Moyer, 11. spiral, Station 5 sample 8 cm, IS_27_N_001; 12. spiral, Station 5 sample 8 cm, IS_27_N_002; 13. spiral-oblique, Station 5 sample 8 cm, IS_27_N_005; 14. umbilical, Station 5 sample 8 cm, IS_27_N_004; 15. spiral, Station 5 sample 8 cm, IS_27_N_009; 16a. umbilical, 16b. spiral, Station 2 sample 5 cm, IS_07_I_002b; 17a. spiral, 17b. umbilical, Station 4 sample 15 cm, IS_14_M_001; 18. umbilical, Station 5 sample 8 cm, IS_27_N_003; 19. spiral, Station 5 sample 8 cm, IS_27_N_008; 20. spiral, Station 5 sample 8 cm, IS_27_N_006; 21. spiral, Station 5 sample 8 cm, IS_27_N_007; **22-32**: *Nonionella iridea* Heron-Allen and Earland 22. spiral, Station 5 sample 8 cm, IS_27_O_007; 23. umbilical, Station 5 sample 8 cm, IS_27_O_001; 24. edge, Station 5 sample 8 cm, IS_27_O_008; 25. umbilical, Station 5 sample 8 cm, IS_27_O_002; 26. spiral, Station 5 sample 8 cm, IS_27_O_003, juvenile; 27. umbilical, Station 5 sample 8 cm, IS_27_O_004; 28. spiral, Station 5 sample 8 cm, IS_27_O_005; 29. umbilical, Station 5 sample 8 cm, IS_27_O_006; 30. spiral, Station 5 sample 8 cm, IS_27_O_009, juvenile; 31a. umbilical, 31b. edge, 31c. spiral, Station 4 sample 15 cm, IS_14_N_001, juvenile; 32a. umbilical, 32b. spiral, 45C-2 sample 35 cm, IS_15_W_001, juvenile; **33-40**: *Nonionoides grateloupii* (d'Orbigny) 33. spiral, Station 5 sample 8 cm, IS_27_L_001; 34. umbilical, Station 5 sample 8 cm, IS_27_L_002; 35. spiral, Station 5 sample 8 cm, IS_27_L_003; 36. umbilical, Station 5 sample 8 cm, IS_27_L_004; 37. spiral, Station 5 sample 8 cm, IS_27_L_005; 38. umbilical, Station 5 sample 8 cm, IS_27_L_006; 39. spiral-oblique, Station 5 sample 8 cm, IS_27_L_007; 40a. spiral, 40b. umbilical, Station 2 sample 5 cm, IS_07_I_002a; **41-45**: *Nonionoides minuta* (Parker), Station 5 sample 8 cm, 41a. umbilical, 41b. spiral, IS_27_J_001; 42a. umbilical, 42b. spiral, IS_27_J_002; 43a. umbilical, 43b. spiral, IS_27_J_003; 44a. umbilical, 44b. spiral, IS_27_J_004; 45a. spiral, 45b. umbilical, IS_27_J_005, juvenile.

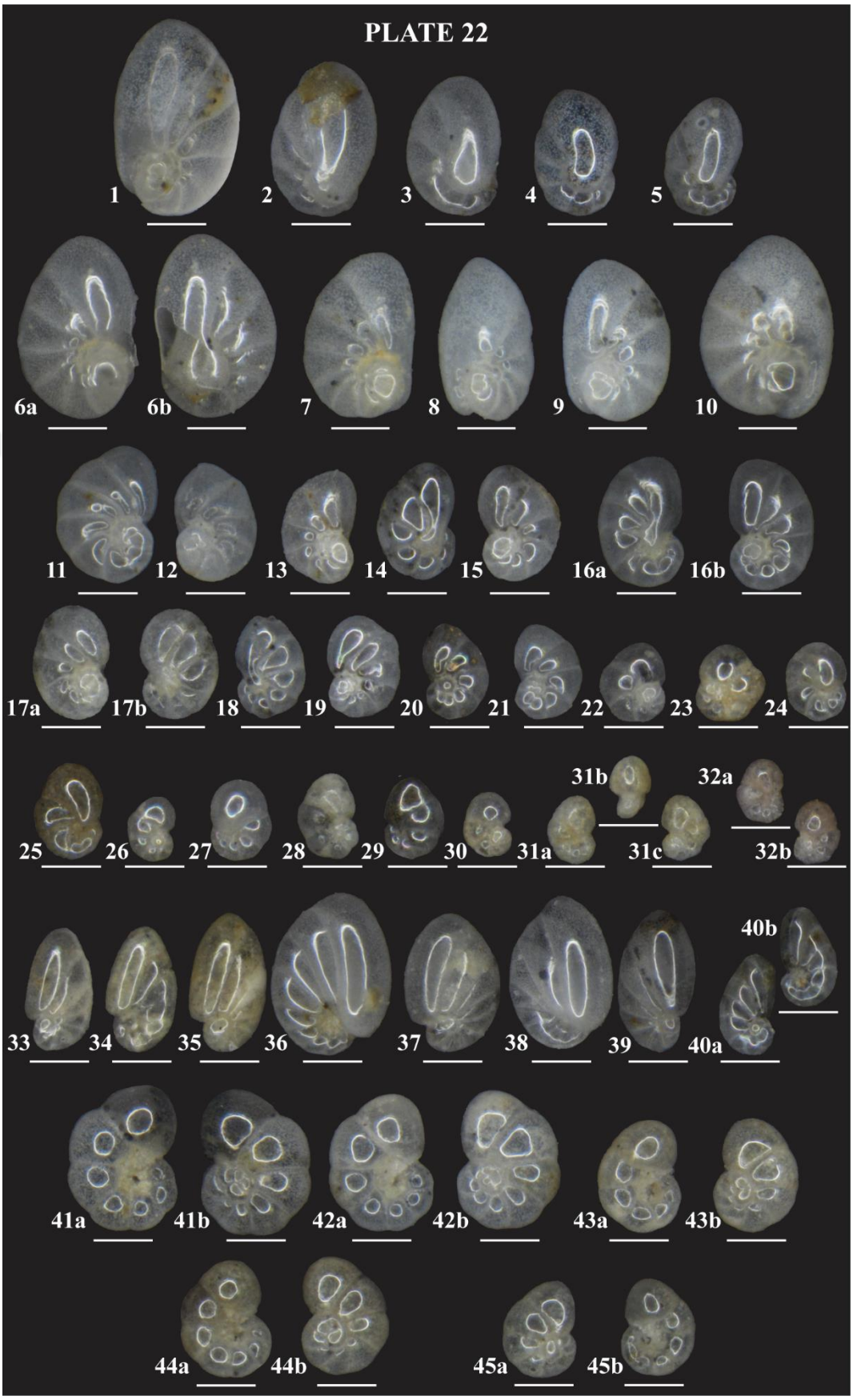

PLATE 22
1
2
3
4
5
6a
6b
7
8
9
10
11
12
13
14
15
16a
16b
17a
17b
18
19
20
21
22
23
24
25
26
27
28
29
30
31a
31b
31c
32a
32b
33
34
35
36
37
38
39
40a
40b
41a
41b
42a
42b
43a
43b
44a
44b
45a
45b

Plate 23: Planorbulinoidea SEM images; scale bar: 100 μm.

1-7: *Lobatula lobatula* (Walker and Jackob) 1. spiral, Station 2 sample 15 cm, IS_08_L_001; 2. spiral, Station 1 (2021) sample 4 cm, IS_02_K_001; 3. Spiral, Station 2 sample 15 cm, IS_08_L_002; 4. spiral-oblique, Station 2 sample 2 cm, IS_05_Q_003; 5. umbilical, Station 2 sample 2 cm, IS_05_Q_001; 6. umbilical, Station 2 sample 2 cm, IS_05_Q_002; 7. spiral, Station 5 sample 8 cm, IS_26_C_001, juvenile; **8-10**: *Cibicides refulgens* de Montfort 8. spiral-oblique, Station 5 sample 8 cm, IS_26_D_003; 9. umbilical, Station 5 sample 8 cm, IS_26_D_002; 10. spiral, Station 2 sample 25 cm, IS_10_B_002; **11-15**: *Planorbulina mediterranensis* d'Orbigny 11. umbilical, Station 2 sample 2 cm, IS_05_P_001; 12. spiral, Station 2 sample 5 cm, IS_07_V_001; 13. umbilical, Station 2 sample 5 cm, IS_07_V_002; 14. umbilical, Station 2 sample 5 cm, IS_07_V_003; 15. umbilical, Station 1 (2019) 4 cm, IS_01_L_001; **16-17**: *Hyalinea* spp. juveniles 16. frontal, Station 3 (2021) sample 1 cm, IS_11_R_002; 17. frontal, Station 3 (2021) sample 1 cm, IS_11_R_001; **18-20**: *Hyalinea marmarica* Spezzaferri and Yanko-Hombach 18. frontal, Station 3 (2021) sample 15 cm, IS_12_C_002; 19. edge-oblique, Station 3 (2021) sample 15 cm, IS_12_C_003; 20. frontal, Station 5 sample 8 cm, IS_27_P_001; **21-23**: *Hyalinea balthica* (Shröter) 21. frontal, Station 4 sample 15 cm, IS_14_L_001; 22. frontal, Station 5 sample 8 cm, IS_27_P_003; 23. edge, Station 5 sample 8 cm, IS_27_P_005;

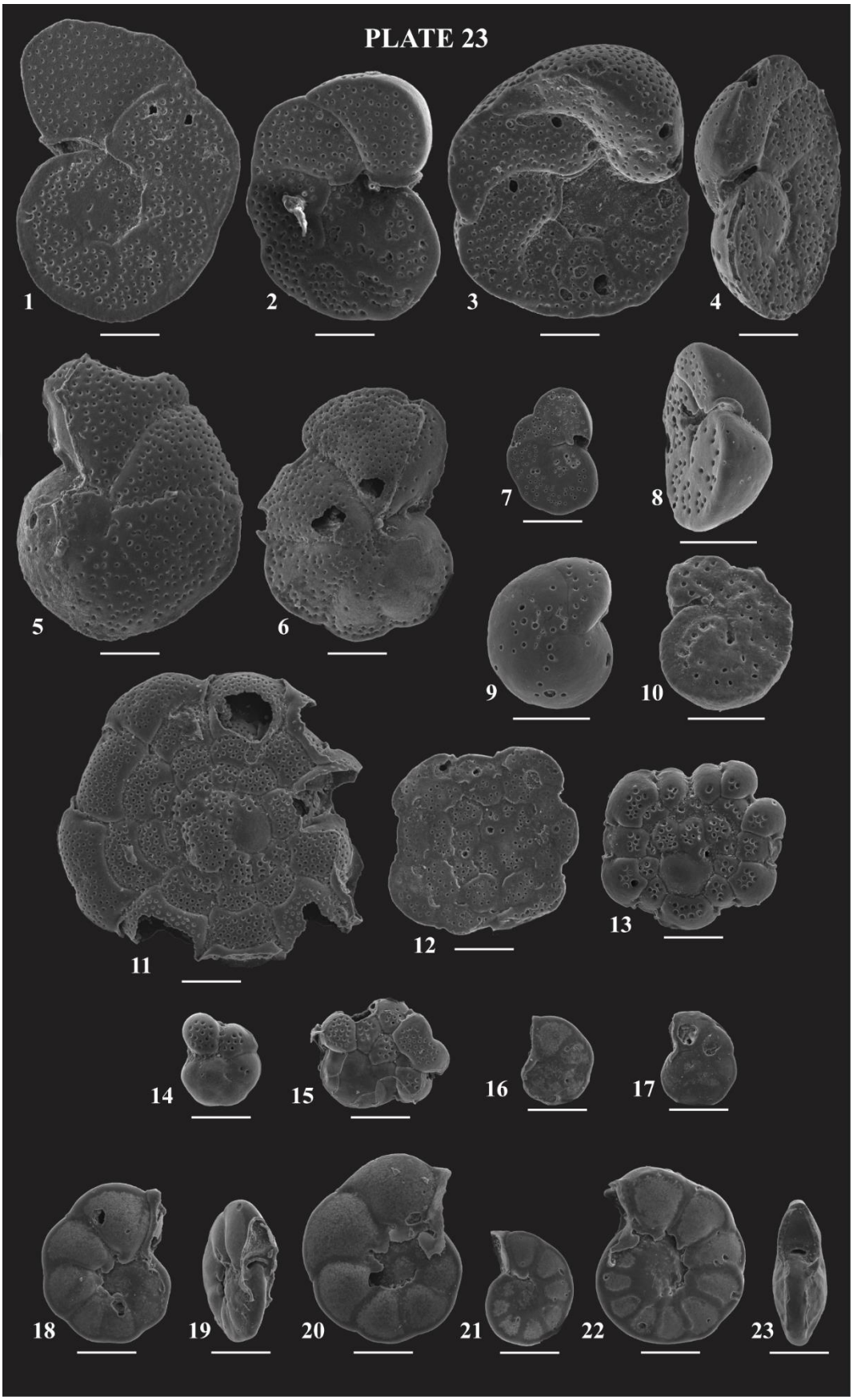

PLATE 23
1
2
3
4
5
6
7
8
9
10
11
12
13
14
15
16
17
18
19
20
21
22
23

PLATE 24: Planorbulinoidea stereomicrographs; scale bar: 100 μm.

1-6: *Lobatula lobatula* (Walker and Jackob) 1a. umbilical, 1b. edge, 1c. spiral, Station 2 sample 15 cm, IS_08_L_001; 2a. spiral, 2b. umbilical, Station 1 (2021) sample 4 cm, IS_02_K_001; 3a. spiral, 3b. edge, 3c. umbilical, Station 2 sample 15 cm, IS_08_L_002; 4a. spiral, 4b. edge, 4c. umbilical, Station 2 sample 2 cm, IS_05_Q_003; 5a. spiral, 5b. umbilical, Station 2 sample 2 cm, IS_05_Q_001; 6a. umbilical, 6b. edge, 6c. spiral, Station 2 sample 2 cm, IS_05_Q_002; **7-11**: *Cibicides refulgens* de Montfort 7a. umbilical, 7b. spiral, Station 2 sample 25 cm, IS_10_B_002; 8a. umbilical, 8b. spiral, Station 2 sample 25 cm, IS_10_B_001; 9. spiral, Station 5 sample 8 cm, IS_26_D_002; 10. umbilical, Station 5 sample 8 cm, IS_26_D_001; 11. umbilical, Station 5 sample 8 cm, IS_26_D_003; **12-16**: *Planorbulina mediterranensis* d'Orbigny 12a. umbilical, 12b. spiral, Station 2 sample 2 cm, IS_05_P_001; 13a. umbilical, 13b. spiral, Station 2 sample 5 cm, IS_07_V_001; 14a. spiral, 41b. umbilical, Station 2 sample 5 cm, IS_07_V_002; 15. umbilical, Station 1 (2019) 4 cm, IS_01_L_001; 16a. spiral, 16b. umbilical, Station 2 sample 5 cm, IS_07_V_003; **17-19**: *Hyalinea* spp. juveniles 17. frontal, Station 3 (2021) sample 1 cm, IS_11_R_002; 18. frontal, Station 3 (2021) sample 1 cm, IS_11_R_001; 19. frontal, Station 3 (2021) sample 1 cm, IS_11_R_003; **20-26**: *Hyalinea marmarica* Spezzaferri and Yanko-Hombach, frontal views 20. Station 3 (2021) sample 15 cm, IS_12_C_004; 21. Station 3 (2021) sample 15 cm, IS_12_C_001; 22. Station 3 (2021) sample 15 cm, IS_12_C_002; 23. Station 3 (2021) sample 15 cm, IS_12_C_003; 24. Station 5 sample 8 cm, IS_27_P_006; 25. Station 5 sample 8 cm, IS_27_P_001; 26. Station 5 sample 8 cm, IS_27_P_002; **27-34**: *Hyalinea balthica* (Shröter), frontal views 27. Station 5 sample 8 cm, IS_27_P_003; 28. Station 5 sample 8 cm, IS_27_P_004; 29. Station 5 sample 8 cm, IS_27_P_008; 30. Station 5 sample 8 cm, IS_27_P_007; 31. Station 4 sample 15 cm, IS_14_L_001; 32. Station 4 sample 15 cm, IS_14_L_002; Station 4 sample 15 cm, IS_14_L_003; 34. Station 5 sample 8 cm, IS_27_P_005.

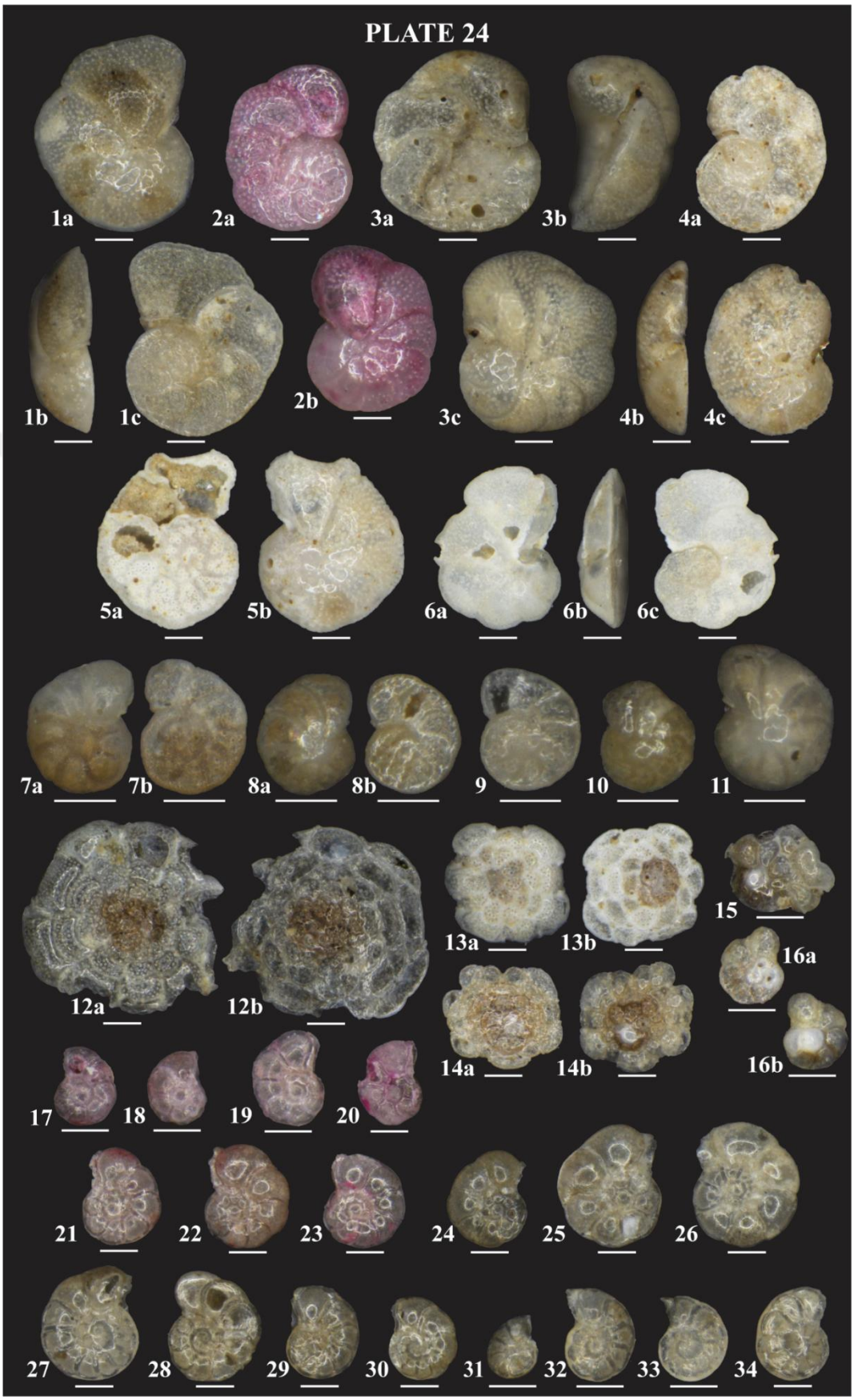

PLATE 24
1a
2a
3a
3b
4a
1b
1c
2b
3c
4b
4c
5a
5b
6a
6b
6c
7a
7b
8a
8b
9
10
11
12a
12b
13a
13b
15
16a
14a
14b
16b
17
18
19
20
21
22
23
24
25
26
27
28
29
30
31
32
33
34

PLATE 25: Rotaloidea SEM images; scale bar: 100 μm.

1-18: *Elphidium* spp. 1. frontal, Station 2 sample 5 cm, IS_07_A_001; 2. frontal, Station 2 sample 5 cm, IS_07_A_002; 3. frontal, Station 2 sample 5 cm, IS_07_A_003; 4. frontal, Station 2 sample 25 cm, IS_10_I_002; 5. frontal, Station 2 sample 25 cm, IS_10_I_001; 6. frontal, Station 3 (2021) sample 1 cm, IS_11_I_001; 7. frontal, Station 3 (2021) sample 1 cm, IS_11_I_002, juvenile; 8. edge, Station 4 sample 15 cm, IS_14_D_002; 9. frontal, Station 4 sample 15 cm, IS_14_D_003; 10. frontal, Station 5 sample 8 cm, IS_27_D_005; 11. edge, Station 5 sample 8 cm, IS_27_D_002; 12. frontal, Station 5 sample 8 cm, IS_27_D_001; 13. frontal, Station 5 sample 8 cm, IS_27_D_011; 14. edge-oblique, Station 5 sample 8 cm, IS_27_D_010; 15. frontal, Station 1 (2021) sample 8 cm, IS_04_V_001; 16. frontal, 45C-2 sample 35 cm, IS_15_J_001; 17. edge, MM50 sample 15 cm, IS_29_H_001; 18. edge, Station 5 sample 8 cm, IS_27_D_013; **19-22**: *Cribroelphidium poeyanum* (d'Orbigny) 19. frontal, MM50 sample 15 cm, IS_28_C_001; 20. edge-oblique, Station 5 sample 8 cm, IS_27_E_001; 21. edge, Station 4 sample 15 cm, IS_14_D_001, juvenile; 22. frontal, Station 5 sample 8 cm, IS_27_E_003; **23-27**: *Porosononion granosum* (d'Orbigny), Station 5 sample 8 cm, 23. frontal, IS_27_F_001; 24. edge, IS_27_F_002; 25. frontal, IS_27_F_003, juvenile; 26. edge, IS_27_H_003; 27. edge, IS_27_H_002.

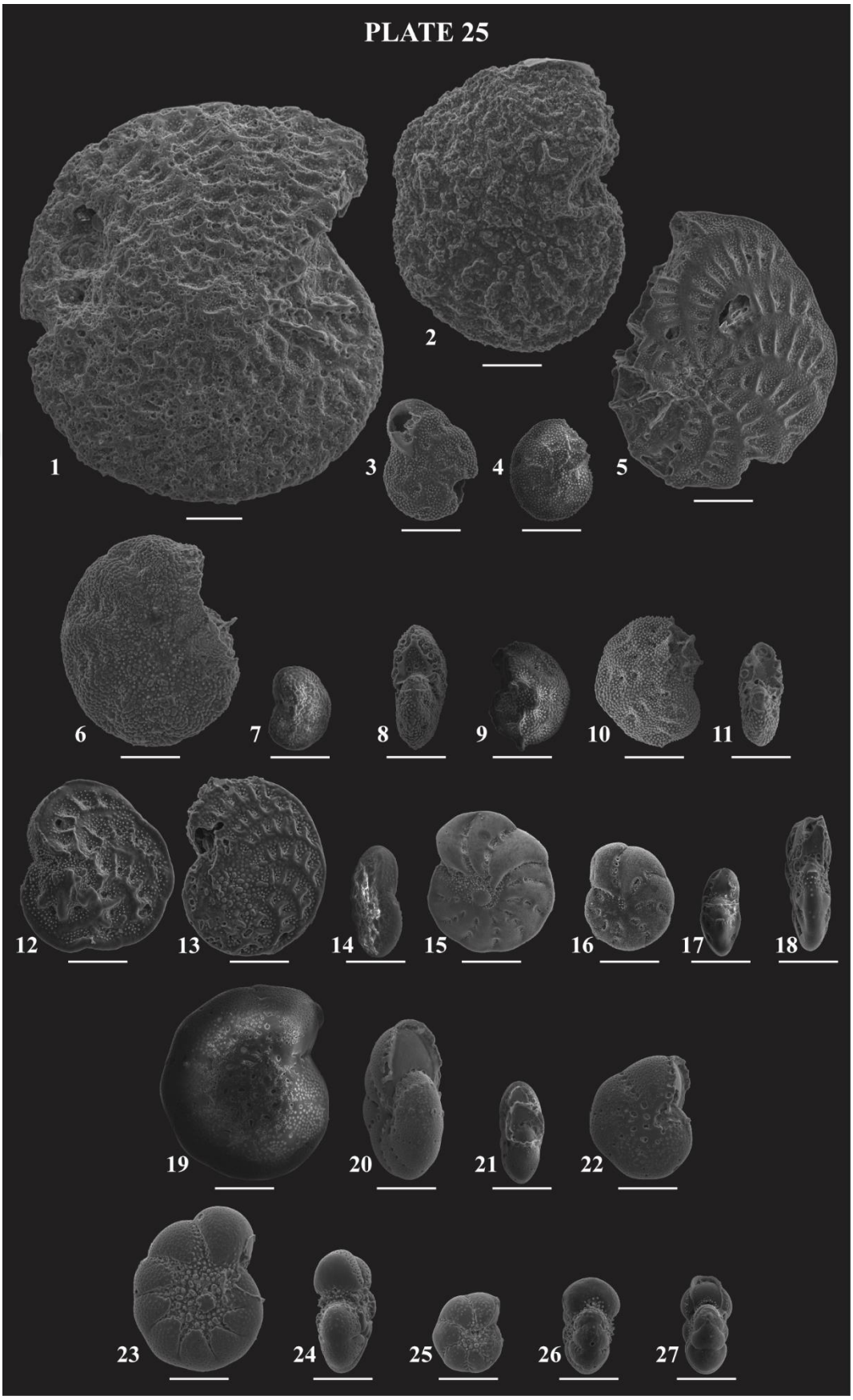

PLATE 25
1
2
3
4
5
6
7
8
9
10
11
12
13
14
15
16
17
18
19
20
21
22
23
24
25
26
27

PLATE 26: Rotaloidea stereomicrographs; scale bar: 100 µm.

1-17: *Elphidium* spp. 1. frontal, Station 2 sample 5 cm, IS_07_A_001; 2. frontal, Station 2 sample 5 cm, IS_07_A_002; 3. frontal, Station 2 sample 5 cm, IS_07_A_003; 4a and b. frontal, Station 2 sample 25 cm, IS_10_I_002; 5. frontal, Station 2 sample 25 cm, IS_10_I_001; 6. frontal, Station 3 (2021) sample 1 cm, IS_11_I_001; 7. frontal, Station 3 (2021) sample 1 cm, IS_11_I_002, juvenile; 8a. edge, 8b. frontal, Station 4 sample 15 cm, IS_14_D_002; 9. frontal, Station 4 sample 15 cm, IS_14_D_003; 10. frontal, Station 5 sample 8 cm, IS_27_D_005; 11. frontal, Station 5 sample 8 cm, IS_27_D_002; 12. frontal, Station 5 sample 8 cm, IS_27_D_001; 13. frontal, Station 5 sample 8 cm, IS_27_D_011; 14. frontal, Station 5 sample 8 cm, IS_27_D_010; 15. frontal, 45C-2 sample 35 cm, IS_15_J_001; 16. frontal, Station 5 sample 8 cm, IS_27_D_013; 17. frontal, Station 5 sample 8 cm, IS_27_D_006; **18-22**: *Cribroelphidium poeyanum* (d'Orbigny) 18. frontal, MM50 sample 15 cm, IS_28_C_001; 19. edge-oblique, Station 5 sample 8 cm, IS_27_E_001; 20. frontal, Station 5 sample 8 cm, IS_27_E_002; 21a. frontal, 21b. edge, Station 4 sample 15 cm, IS_14_D_001, juvenile; 22. frontal, Station 5 sample 8 cm, IS_27_E_003; **23-27**: *Porosononion granosum* (d'Orbigny), Station 5 sample 8 cm, 23. frontal, IS_27_F_001; 24. frontal, IS_27_F_002; 25. frontal, IS_27_F_003, juvenile; 26. frontal, IS_27_H_003; 27. frontal, IS_27_H_002.


PLATE 26
1
2
3
4a
4a
5
6
7
8a
8a
9
10
11
12
13
14
15
16
17
18
19
20
21a
21b
22
23
24
25
26
27

PLATE 27: Rotaloidea, Siphoninoidea SEM images; scale bar: 100 μm.

1-15: *Ammonia* spp. 1. spiral, Station 2 sample 2 cm, IS_06_A_001; 2. spiral, Station 2 sample 2 cm, IS_06_A_002; 3. edge, Station 2 sample 2 cm, IS_06_A_003; 4. umbilical, Station 2 sample 2 cm, IS_06_A_004; 5. umbilical, Station 2 sample 2 cm, IS_06_A_005; 6. umbilical, Station 1 (2021) sample 8 cm, IS_04_B_007; 7. edge, Station 1 (2021) sample 8 cm, IS_04_B_004; 8. spiral, Station 1 (2021) sample 4 cm, IS_02_N_003; 9. spiral, Station 2 sample 5 cm, IS_07_C_001; 10. spiral-oblique, Station 2 sample 2 cm, IS_06_A_006; 11. edge, Station 1 (2021) sample 4 cm, IS_02_N_001; 12. umbilical, Station 1 (2021) sample 8 cm, IS_04_B_001; 13. umbilical, Station 2 sample 15 cm, IS_08_K_001; 14. edge, Station 2 sample 5 cm, IS_07_C_001; 15. spiral, Station 1 (2021) sample 4 cm, IS_02_N_004; **16-18**: *Haynesina depressula* (Walker and Jacob), Station 5 sample 8 cm, 16. frontal, IS_27_H_001; 17. edge, IS_27_G_002; 18. frontal, IS_27_G_001; **19-20**: *Porosononion simplex* (Cushman) 19. frontal, K51.2K09 sample 8 cm, IS_32_D_001; 20. frontal, Station 2 sample 25 cm, IS_10_J_001; **21-22**: *Aubignyna perlucida* (Heron-Allen and Earland); 21. umbilical, Station 5 sample 8 cm, IS_27_I_001_01; 22. spiral-oblique, MM50 sample 30 cm, IS_20_J_001, juvenile; **23-25**: *Siphonina reticulata* (Czjzek) 23. umbilical, Station 3 (2021) sample 15 cm, IS_12_B_001; 24. umbilical, Station 3 (2021) sample 15 cm, IS_12_B_002; 25. spiral, Station 2 sample 5 cm, IS_07_F_001.

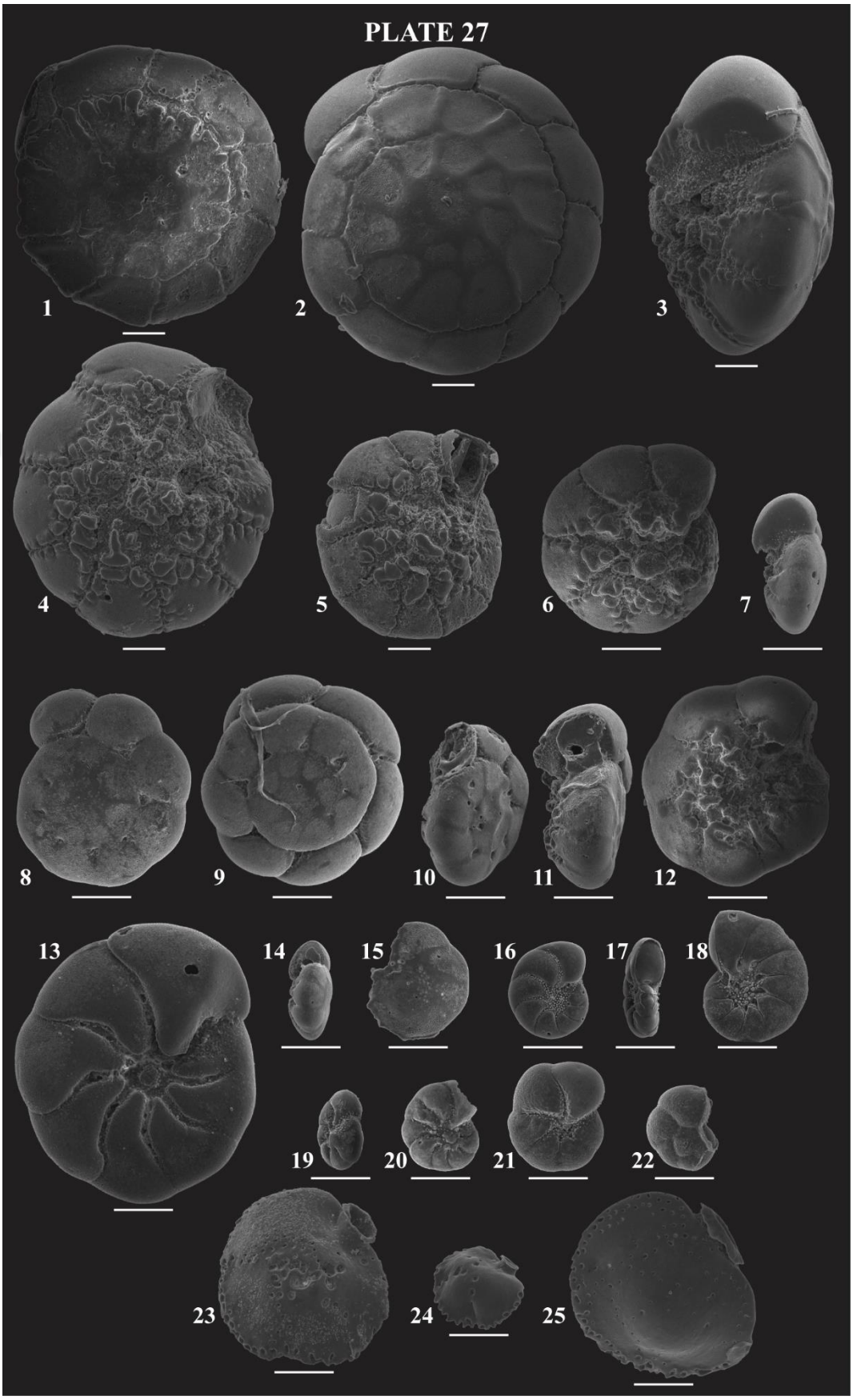

PLATE 27
1
2
3
4
5
6
7
8
9
10
11
12
13
14
15
16
17
18
19
20
21
22
23
24
25

PLATE 28-A: Rotaloidea, Siphoninoidea stereomicrographs; scale bar: 100 μm.

1-10: *Ammonia* spp. 1a. umbilical, 1b. edge, 1c. spiral, Station 2 sample 2 cm, IS_06_A_001; 2a. umbilical, 2b. spiral Station 2 sample 2 cm, IS_06_A_005; 3a. umbilical, 3b. edge, 3c. spiral, Station 2 sample 2 cm, IS_06_A_002; 4a. spiral, 4b. umbilical, Station 2 sample 2 cm, IS_06_A_004; 5a. umbilical, 5b. spiral, Station 2 sample 2 cm, IS_06_A_003; 6a. umbilical, 6b. edge, 6c. spiral, Station 1 (2021) sample 8 cm, IS_04_B_004; 7a. umbilical, 7b. edge, 7c. spiral, Station 1 (2021) sample 4 cm, IS_02_N_003; 8a. spiral, 8b. edge, 8c. umbilical, Station 2 sample 5 cm, IS_07_C_001; 9a. umbilical, 9b. edge, 9c. spiral, Station 1 (2021) sample 4 cm, IS_02_N_001; 10a. umbilical, 10b. spiral, Station 2 sample 2 cm, IS_06_A_006.

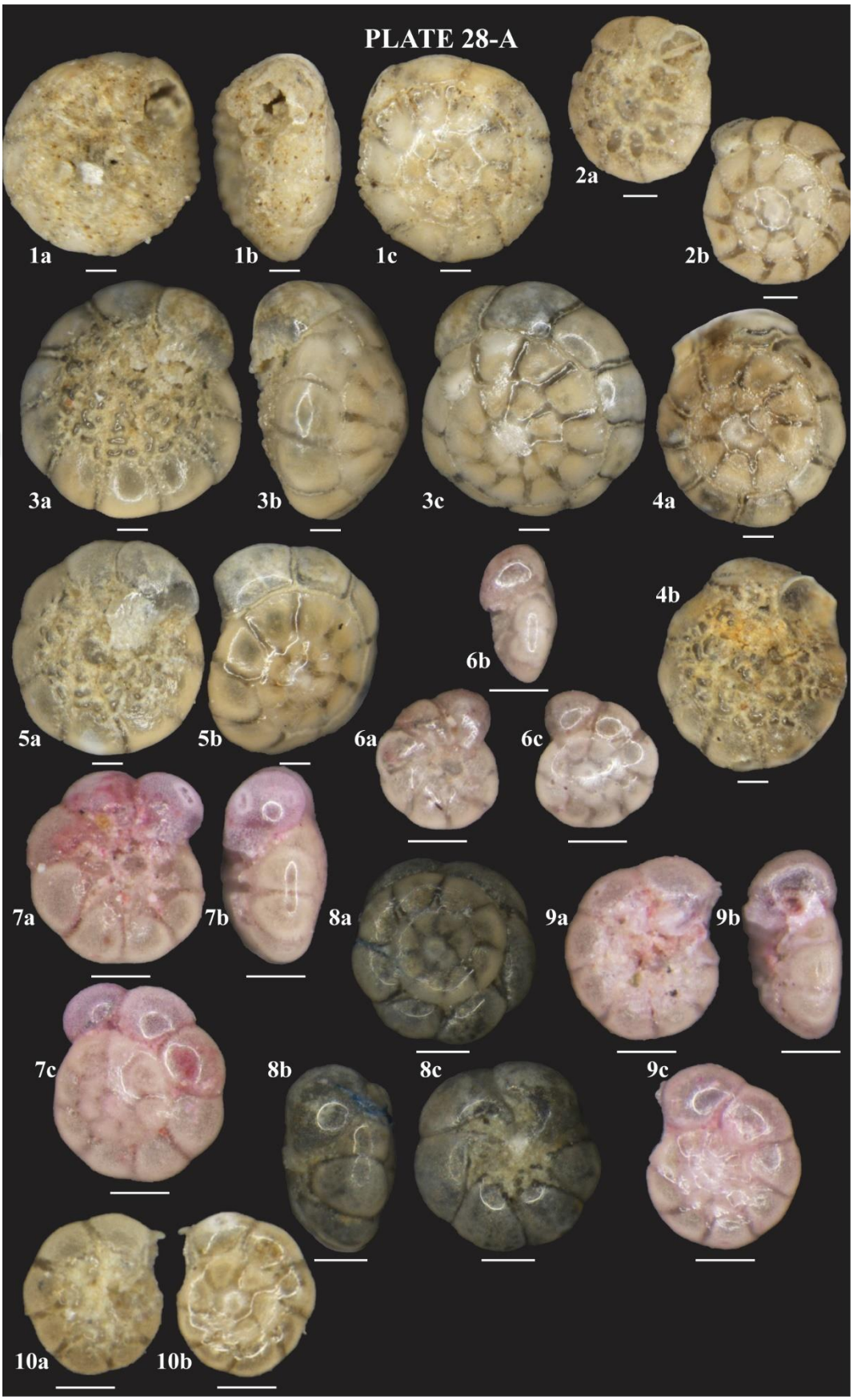

PLATE 28-A
1a
1b
1c
2a
2b
3a
3b
3c
4a
4b
5a
5b
6a
6b
6c
7a
7b
7c
8a
8b
8c
9a
9b
9c
10a
10b

PLATE 28-B: Rotaloidea, Siphoninoidea stereomicrographs; scale bar: 100 μm.

1-6: *Ammonia* spp. 1a. umbilical, 1b. edge, 1c. spiral, Station 1 (2021) sample 8 cm, IS_04_B_001; 2a. edge, 2b. spiral, 2c. umbilical, Station 1 (2021) sample 8 cm, IS_04_B_003; 3a. umbilical, 3b. edge, 3c. spiral,Station 1 (2021) sample 8 cm, IS_04_B_002; 4a. umbilical, 4b. edge, 4c. spiral, Station 2 sample 15 cm, IS_08_K_001; 5a. spiral, 5b. umbilical, Station 2 sample 5 cm, IS_07_C_001; 6a. umbilical, 6b. edge, 6c. spiral,Station 1 (2021) sample 4 cm, IS_02_N_004; **7-9**: *Haynesina depressula* (Walker and Jacob), Station 5 sample 8 cm, 7. frontal, IS_27_H_001; 8a. frontal, 8b. edge, IS_27_G_002; 9a. edge, 9b. frontal, IS_27_G_001; **10**: *Aubignyna perlucida* (Heron-Allen and Earland); 10a. umbilical, 10b. edge, 10c. spiral, Station 5 sample 8 cm, IS_27_I_001_01; **11-13**: *Siphonina reticulata* (Czjzek) 11. umbilical, Station 3 (2021) sample 15 cm, IS_12_B_001; 12. umbilical, Station 3 (2021) sample 15 cm, IS_12_B_002; 13a. spiral, 13b, edge-apertural, 13c. umbilical, Station 2 sample 5 cm, IS_07_F_001;

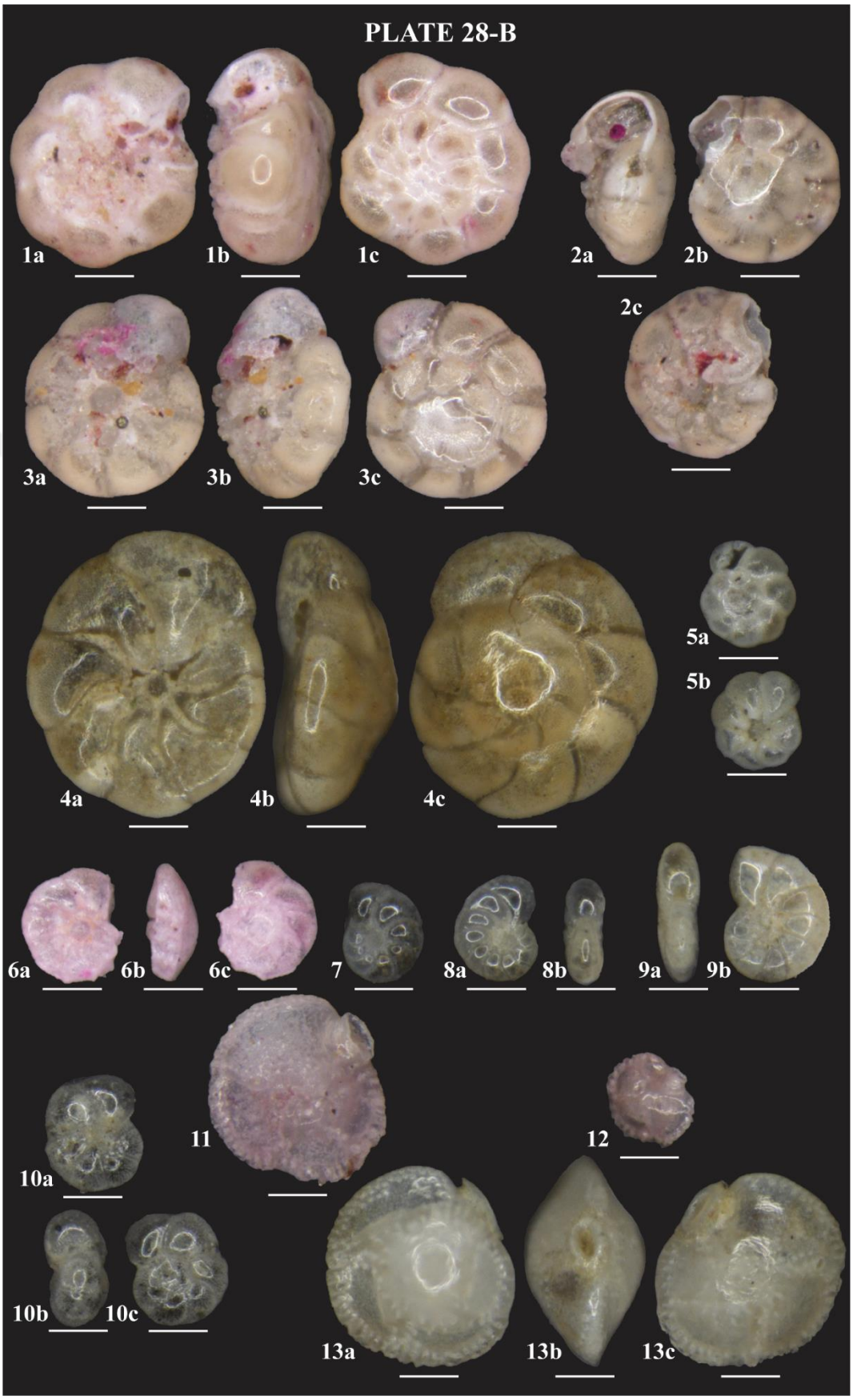

PLATE 28-B
1a
1b
1c
2a
2b
2c
3a
3b
3c
4a
4b
4c
5a
5b
6a
6b
6c
7
8a
8b
9a
9b
10a
10b
10c
11
12
13a
13b
13c

PLATE 29: Turrilinoidea, Virgulinelloidea SEM images; scale bar: 100 μm.

1-7: *Stainforthia*? sp. frontal views, 1. Station 1 (2019) sample 4 cm, IS_01_N_001_01; 2. Station 1 (2021) sample 8 cm, IS_04_E_001; 3. Station 3 (2021) sample 15 cm, IS_12_T_001; 4. Station 1 (2019) sample 4 cm, IS_01_N_004; 5. Station 3 (2021) sample 1 cm, IS_11_2F_001; 6. MM50 sample 30 cm, IS_20_L_001; 7. Station 5 sample 8 cm, IS_25_B_002; **8-11**: *Stainforthia fusiformis* (Williamson) frontal views, 8. Station 1 (2019) sample 4 cm, IS_01_O_001; 9. Station 1 (2021) sample 4 cm, IS_02_R_001; 10. Station 3 (2021) sample 1 cm, IS_11_2G_001; 11. Station 5 sample 8 cm, IS_25_C_001, terminal aperture; **12-13**: *Hopkinsina pacifica* Cushman frontal views, 12. Station 3 (2021) sample 15 cm, IS_12_ST_001; 13. Station 1 (2021) sample 4 cm, IS_02_T_001; **14-17**: *Eubuliminella* sp. frontal views, Station 1 (2021) sample 4 cm, 14. IS_02_Q_002; 15. IS_02_Q_001; 16. IS_02_Q_003; 17. IS_02_Q_004; **18-19**: *Virgulinella fragilis* Grindell and Collen frontal views, 18. Station 5 sample 8 cm, IS_25_G_001; 19. Station 2 sample 2 cm, IS_06_N_001.

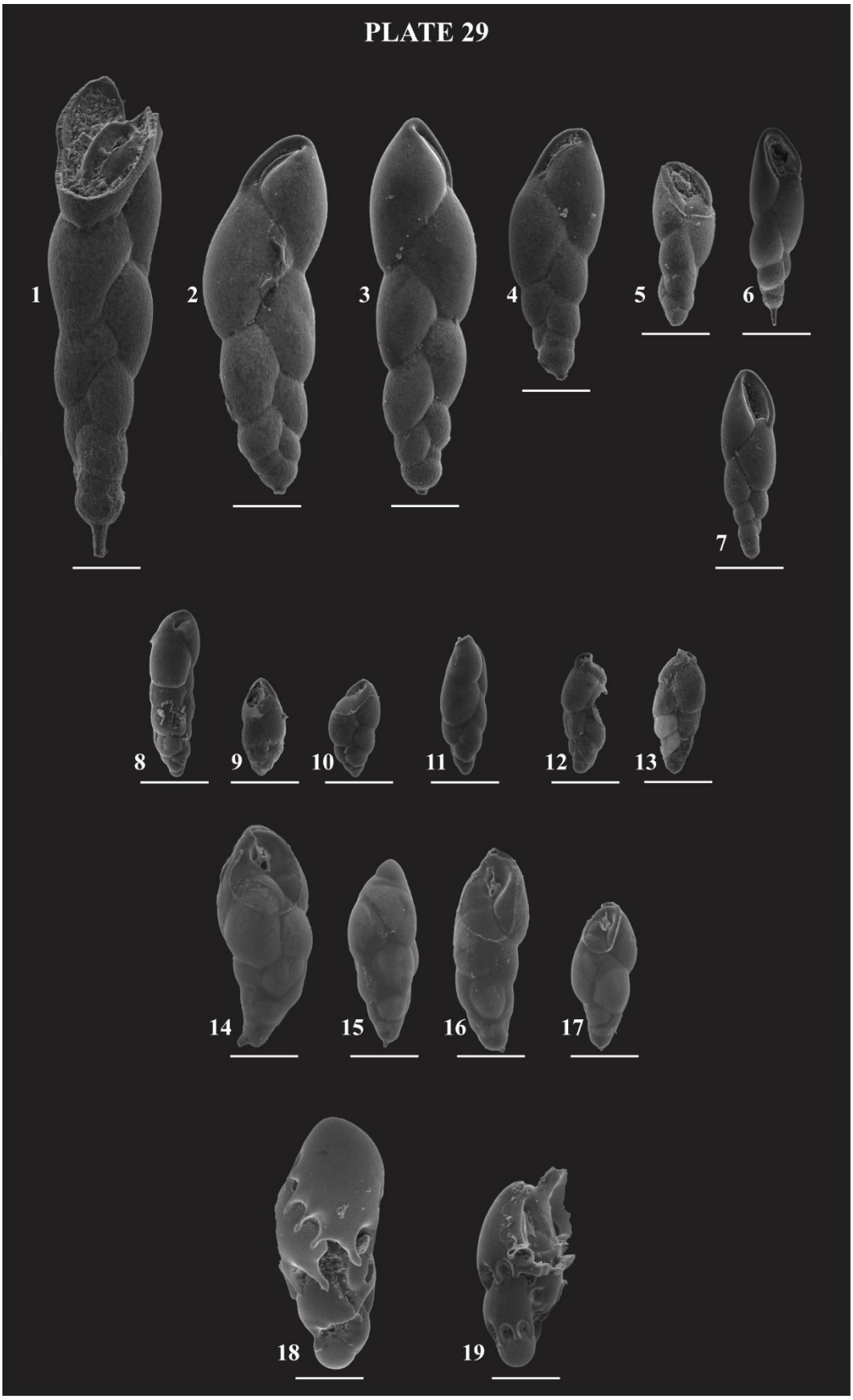

PLATE 29
1
2
3
4
5
6
7
8
9
10
11
12
13
14
15
16
17
18
19

PLATE 30: Turrilinoidea, Virgulinelloidea stereomicrographs; scale bar: 100 μm.

1-11: *Stainforthia*? sp. frontal views, 1. Station 1 (2019) sample 4 cm, IS_01_N_001_01; 2. Station 1 (2021) sample 8 cm, IS_04_E_001; 3. Station 3 (2021) sample 15 cm, IS_12_T_001; 4. Station 3 (2021) sample 1 cm, IS_11_2F_001; 5. Station 1 (2021) sample 4 cm, IS_02_S_001; 6. Station 1 (2021) sample 4 cm, IS_02_S_002; 7. Station 3 (2021) sample 15 cm, IS_12_T_002; 8. Station 1 (2019) sample 4 cm, IS_01_N_002; 9. Station 1 (2019) sample 4 cm, IS_01_N_004; 10. Station 5 sample 8 cm, IS_25_B_001; 11. Station 1 (2019) sample 4 cm, IS_01_N_003; **12-21**: *Stainforthia fusiformis* (Williamson) frontal views, 12. Station 1 (2019) sample 4 cm, IS_01_O_001; 13. Station 1 (2019) sample 4 cm, IS_01_O_002; 14. Station 1 (2021) sample 4 cm, IS_02_R_001; 15. Station 1 (2021) sample 4 cm, IS_02_R_002; 16. Station 3 (2021) sample 1 cm, IS_11_2G_001; 17. Station 3 (2021) sample 1 cm, IS_11_2G_003; 18. Station 3 (2021) sample 1 cm, IS_11_2G_002, rB stained; 19. Station 5 sample 8 cm, IS_25_C_001, terminal aperture; 20. Station 5 sample 8 cm, IS_25_C_003; 21. Station 5 sample 8 cm, IS_25_C_002; **22-23**: *Hopkinsina pacifica* Cushman frontal views, 22. Station 3 (2021) sample 15 cm, IS_12_ST_001; 23. Station 1 (2021) sample 4 cm, IS_02_T_001; **24-27**: *Eubuliminella* sp. frontal views, Station 1 (2021) sample 4 cm, 14. IS_02_Q_002; 15. IS_02_Q_001; 16. IS_02_Q_003; 17. IS_02_Q_004; **28-31**: *Virgulinella fragilis* Grindell and Collen frontal views, 28. Station 5 sample 8 cm, IS_25_G_001; 29. Station 2 sample 2 cm, IS_06_N_001; 30. Station 5 sample 8 cm, IS_25_G_002; 31. Izmit-deep sample 4 cm, No. 01.

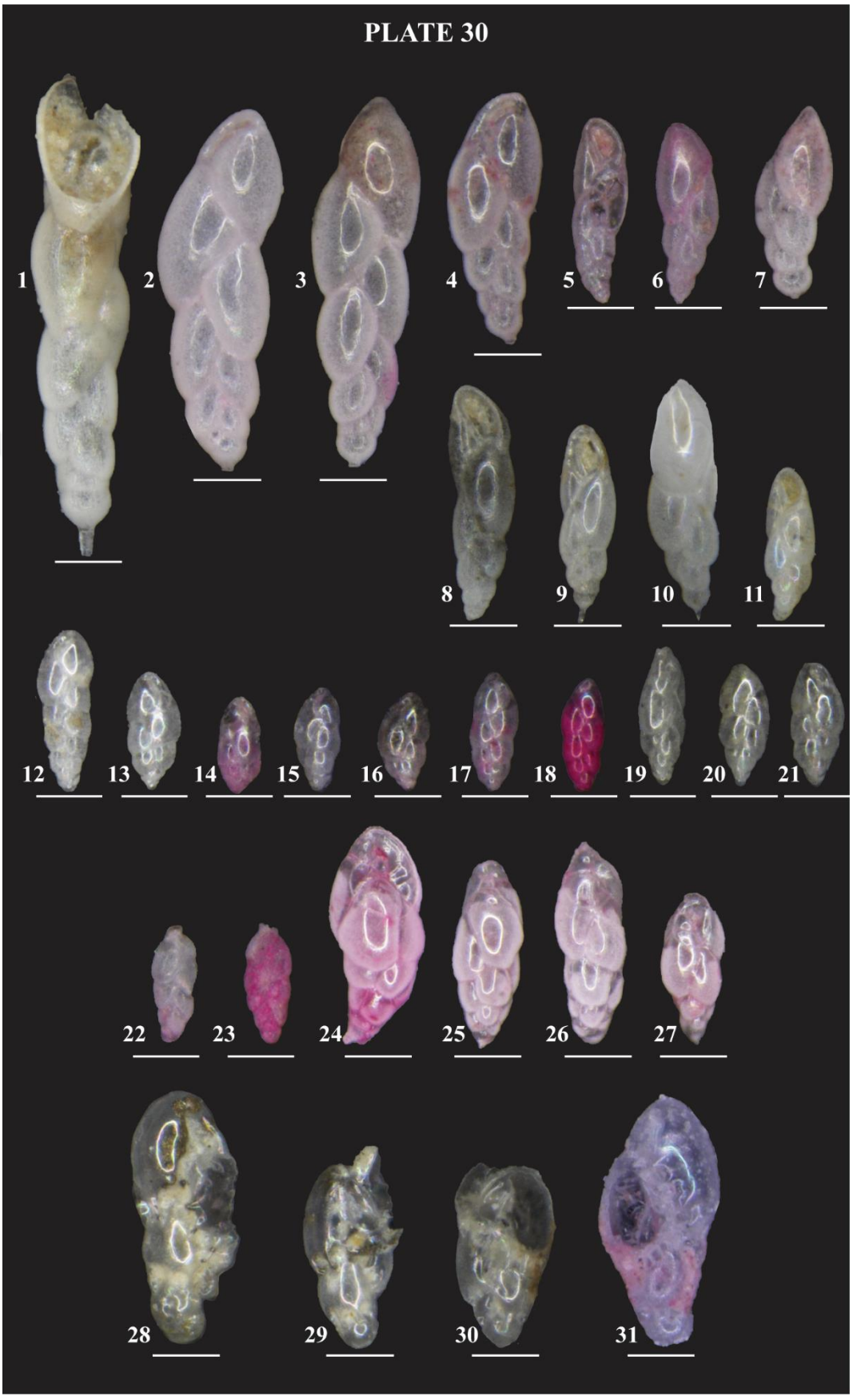

PLATE 30
1
2
3
4
5
6
7
8
9
10
11
12
13
14
15
16
17
18
19
20
21
22
23
24
25
26
27
28
29
30
31

PLATE 31: Textulariana SEM images; scale bar: 100 μm.

1: *Morulaeplecta bulbosa* Höglund, frontal view, Station 1 (2019) sample 4 cm, IS_01_A_001, after top two chambers were broken off; **2-7**: *Spiroplectinella wrighti* (Silvestri) 2. frontal, Station 2 sample 5 cm, IS_07_Q_002; 3. oblique, Station 2 sample 25 cm, IS_09_S_002; 4. frontal, microspheric, Station 1 (2019) sample 4 cm, IS_01_C_001; 5. frontal, megalospheric, Station 2 sample 5 cm, IS_07_Q_001, juvenile; 6. frontal, megalospheric, Station 1 (2019) sample 4 cm, IS_01_C_002 juvenile; 7. frontal, Station 2 sample 5 cm, IS_07_Q_003; **8-11**: *Siphotextularia concava* (Karrer) 8. edge, Station 2 sample 25 cm, IS_09_R_002; 9. frontal, Station 2 sample 25 cm, IS_09_R_001; 10. edge, Station 5 sample 8 cm, IS_25_K_002; 11. frontal, Station 5 sample 8 cm, IS_25_K_001; **12**: *Textularia agglutinans* d'Orbigny, frontal, last chamber broken, Station 2 sample 25 cm, IS_09_O_001; **13-18**: *Textularia gramen* d'Orbigny 13. edge, Station 2 sample 25 cm, IS_09_P_001; 14. frontal, Station 2 sample 2 cm, IS_05_N_001; 15. frontal, Station 1 (2021) sample 8 cm, IS_04_AB_001, juvenile; 16. frontal, Station 1 (2021) sample 4 cm, IS_01_E_001, juvenile; 17. frontal, Station 1 (2021) sample 4 cm, IS_05_O_001; 18. frontal, Station 2 sample 25 cm, IS_09_P_002; **19-20**: *Textularia* sp. 1, Station 2 sample 25 cm, 19. edge, IS_09_Q_002; 20. frontal, IS_09_Q_001.

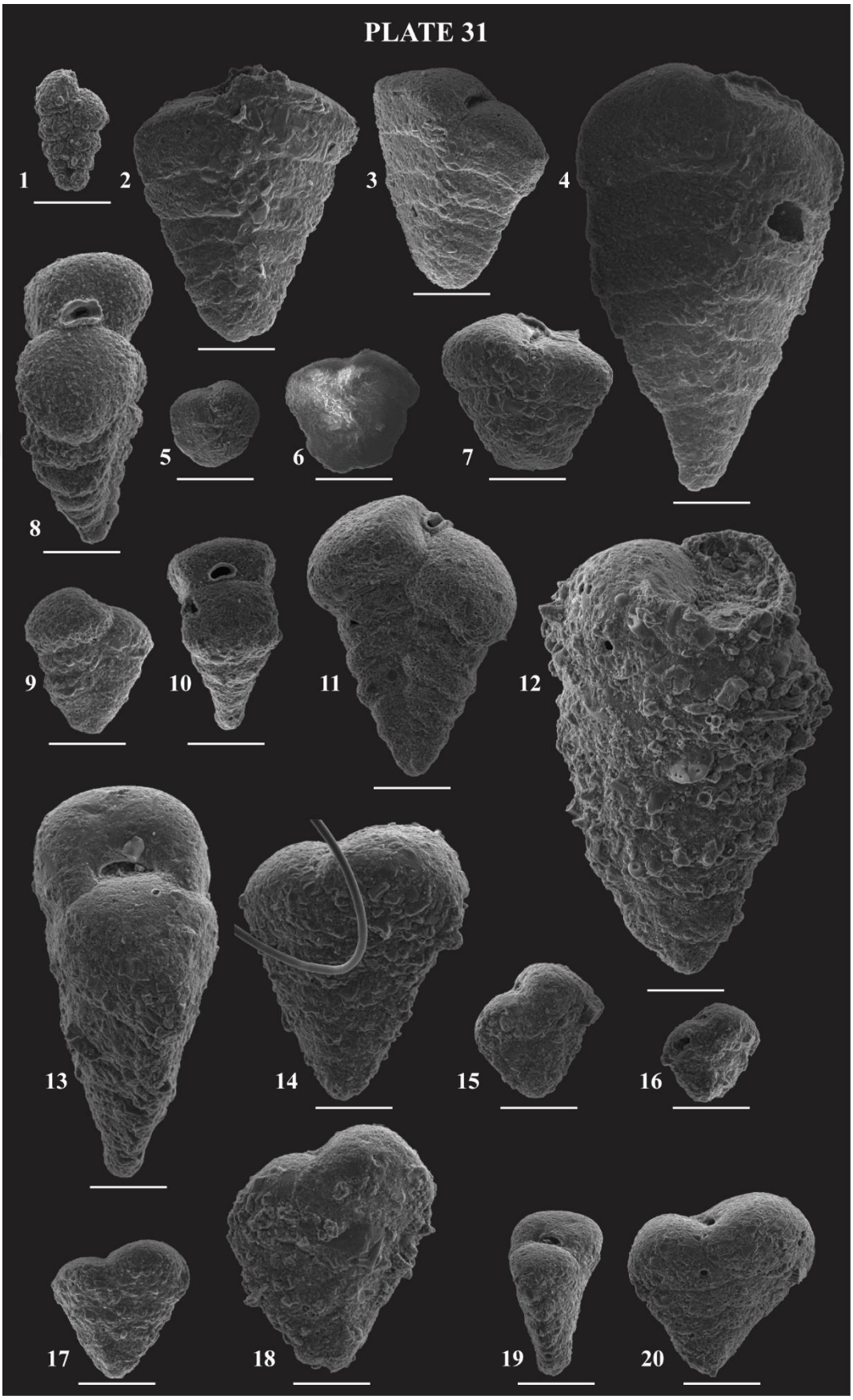

PLATE 31
1
2
3
4
5
6
7
8
9
10
11
12
13
14
15
16
17
18
19
20

PLATE 32: Textulariana stereomicrographs; scale bar: 100 μm.

1: *Morulaeplecta bulbosa* Höglund, Station 1 (2019) sample 4 cm, IS_01_A_001, 1a. frontal, 1b. frontal, after top two chambers were broken off, 1c. edge, after top two chambers were broken off; **2-8**: *Spiroplectinella wrighti* (Silvestri) 2. frontal, Station 2 sample 5 cm, IS_07_Q_002; 3. oblique, Station 2 sample 25 cm, IS_09_S_002; 4. frontal, Station 1 (2019) sample 4 cm, IS_01_C_001; 5a. edge, 5b. frontal, Station 2 sample 5 cm, IS_07_Q_004; 6. frontal, megalospheric, Station 2 sample 5 cm, IS_07_Q_001, juvenile; 7a. frontal, 7b. edge, megalospheric, Station 1 (2019) sample 4 cm, IS_01_C_002, juvenile; 8. frontal, Station 2 sample 5 cm, IS_07_Q_003; **9-12**: *Siphotextularia concava* (Karrer) 9. frontal, Station 2 sample 25 cm, IS_09_R_002; 10. frontal, Station 2 sample 25 cm, IS_09_R_001; 11. frontal, Station 5 sample 8 cm, IS_25_K_002; 12. frontal, Station 5 sample 8 cm, IS_25_K_001; **13**: *Textularia agglutinans* d'Orbigny, frontal, last chamber broken, Station 2 sample 25 cm, IS_09_O_001; **14-19**: *Textularia gramen* d'Orbigny 14. frontal, Station 2 sample 25 cm, IS_09_P_001; 15a. frontal, 15b. edge, Station 2 sample 2 cm, IS_05_N_001; 16. frontal,Station 1 (2021) sample 8 cm, IS_04_AB_001, juvenile; 17. frontal, Station 1 (2021) sample 4 cm, IS_01_E_001, juvenile; 18a. frontal, 18b. edge, Station 1 (2021) sample 4 cm, IS_05_O_001; 19. frontal, Station 2 sample 25 cm, IS_09_P_002; **20-21**: *Textularia* sp. 1, frontal views, Station 2 sample 25 cm, 20. IS_09_Q_001; 21. IS_09_Q_002.

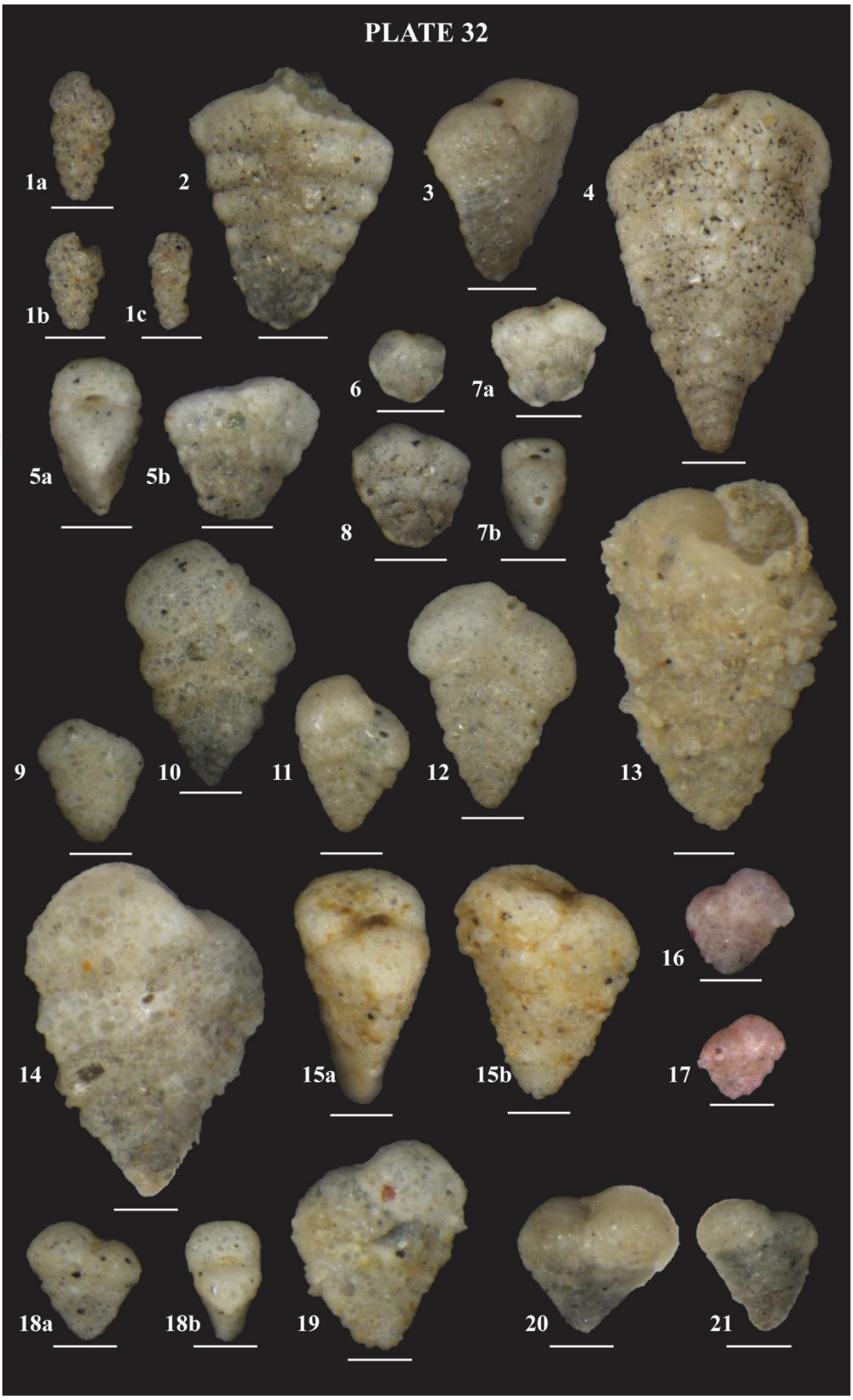

PLATE 32
1a
2
3
4
1b
1c
6
7a
5a
5b
8
7b
9
10
11
12
13
16
14
15a
15b
17
18a
18b
19
20
21

PLATE 33: Textulariana SEM images; scale bar: 100 μm.

1-7: *Ammoscalaria pseudospiralis* (Williamson) 1. frontal, planispiral part, Station 5 sample 8 cm, IS_25_I_001; 2. frontal, planispiral part, Station 2 sample 2 cm, IS_05_G_001c; 3. frontal, planispiral part, Station 2 sample 2 cm, IS_05_B_001b; 4. frontal, planispiral part, Station 2 sample 2 cm, IS_05_G_001b; 5. frontal, Station 2 sample 5 cm, IS_07_N_001a; 6. frontal, Station 2 sample 5 cm, IS_07_N_006; 7. frontal, Station 2 sample 5 cm, IS_07_N_004; **8-12**: *Bigenerina nodosaria* d'Orbigny 8. frontal, broken uniserial part, Station 1 (2021) sample 4 cm, IS_02_A_001; 9. frontal, K51.2K09 sample 8 cm, IS_31_D_002; 10. frontal, broken single rectilinear chamber, Station 2 sample 2 cm, IS_05_J_001; 11. frontal, Station 2 sample 5 cm, IS_07_O_001; 12. frontal, K51.2K09 sample 5 cm, IS_31_D_001; **13-14**: *Pseudoclavulina crustata* Cushman 13. frontal-oblique, broken initial triserial part, Station 5 sample 8 cm, IS_18_F_002; 14. frontal, brokan initial triserial part, Station 5 sample 8 cm, IS_18_F_001; **15**: *Siphoscutula* ? sp. 1, oblique, K51.2K09 sample 5 cm, IS_31_D_003; **16**: *Eggerelloides scabrus* (Williamson), frontal, Station 2 sample 2 cm, IS_05_K_001.

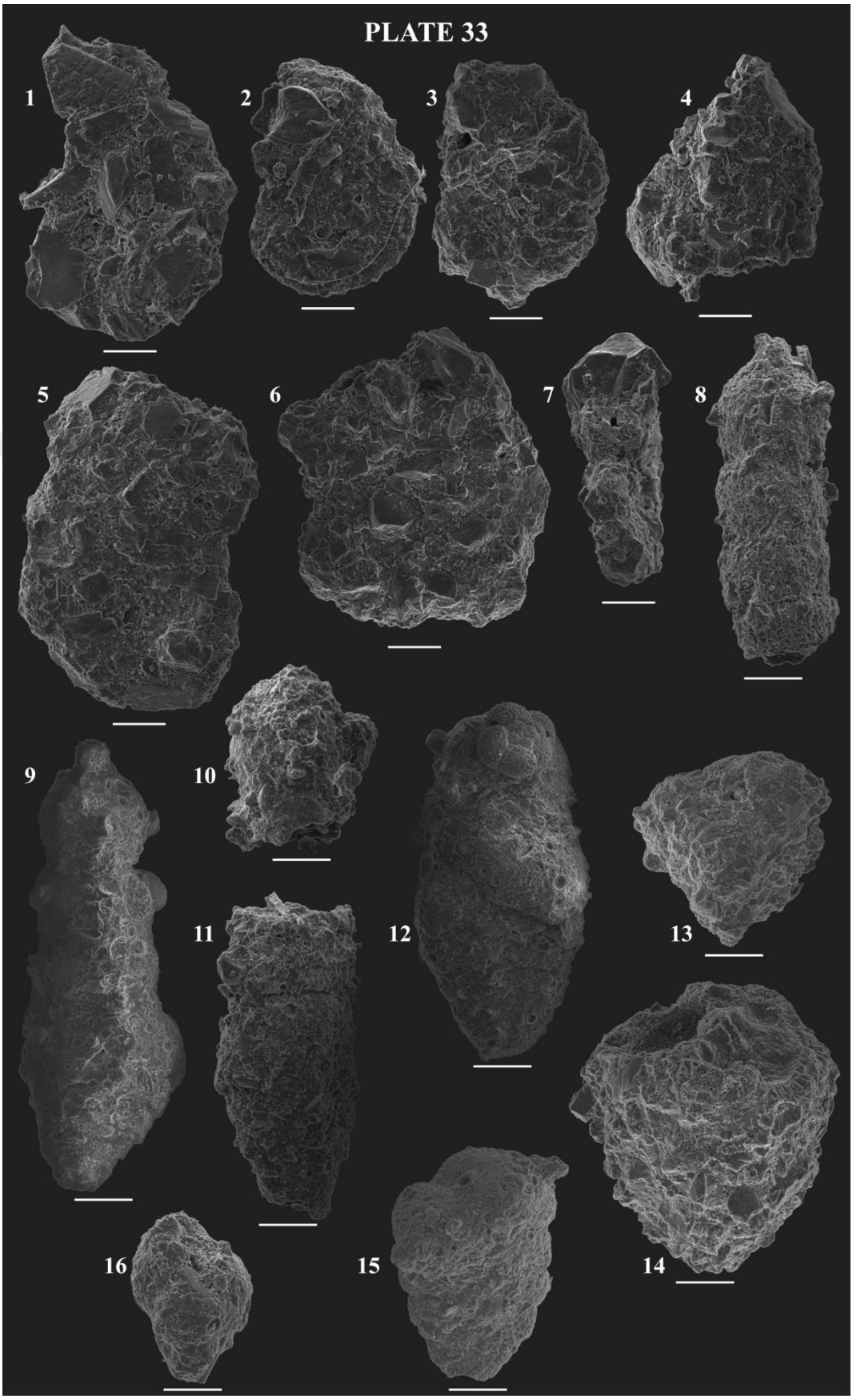

PLATE 33
1
2
3
4
5
6
7
8
9
10
11
12
13
14
15
16

PLATE 34: Textulariana stereomicrographs; scale bar: 100 μm.

1-6: *Ammoscalaria pseudospiralis* (Williamson) 1a. frontal, 1b. edge, planispiral part, Station 5 sample 8 cm, IS_25_I_001; 2. frontal, planispiral part, Station 2 sample 2 cm, IS_05_B_001c; 3. frontal, planispiral part, Station 2 sample 2 cm, IS_05_B_001b; 4. frontal, planispiral part, Station 2 sample 2 cm, IS_05_G_001b; 5. frontal, Station 2 sample 5 cm, IS_07_N_006; 6. frontal, Station 2 sample 5 cm, IS_07_N_001a; **7-15**: *Bigenerina nodosaria* d'Orbigny 7. frontal, broken uniserial part, Station 1 (2021) sample 4 cm, IS_02_A_001; 8. frontal, K51.2K09 sample 8 cm, IS_31_D_002; 9. frontal, broken single rectilinear chamber, Station 2 sample 2 cm, IS_05_J_001; 10. frontal, Station 2 sample 5 cm, IS_07_O_001; 11. frontal, K51.2K09 sample 5 cm, IS_31_D_005; 12. frontal, K51.2K09 sample 5 cm, IS_31_D_001; 13. frontal, broken single rectilinear chamber septal face, K51.2K09 sample 5 cm, IS_31_D_006; 14. frontal, broken single rectilinear chamber, K51.2K09 sample 5 cm, IS_31_D_008; 15. frontal, broken single rectilinear chamber septal face, K51.2K09 sample 5 cm, IS_31_D_007; **16-17**: *Siphoscutula* ? sp. 1, 16a. frontal, 16b. oblique, K51.2K09 sample 5 cm, IS_31_D_003; 17. edge, K51.2K09 sample 5 cm, IS_31_D_004; **18**: *Pseudoclavulina crustata* Cushman, frontal, broken initial triserial part, Station 5 sample 8 cm, IS_18_F_001; **19**: *Eggerelloides scabrus* (Williamson), a and b. frontal views, Station 2 sample 2 cm, IS_05_K_001.

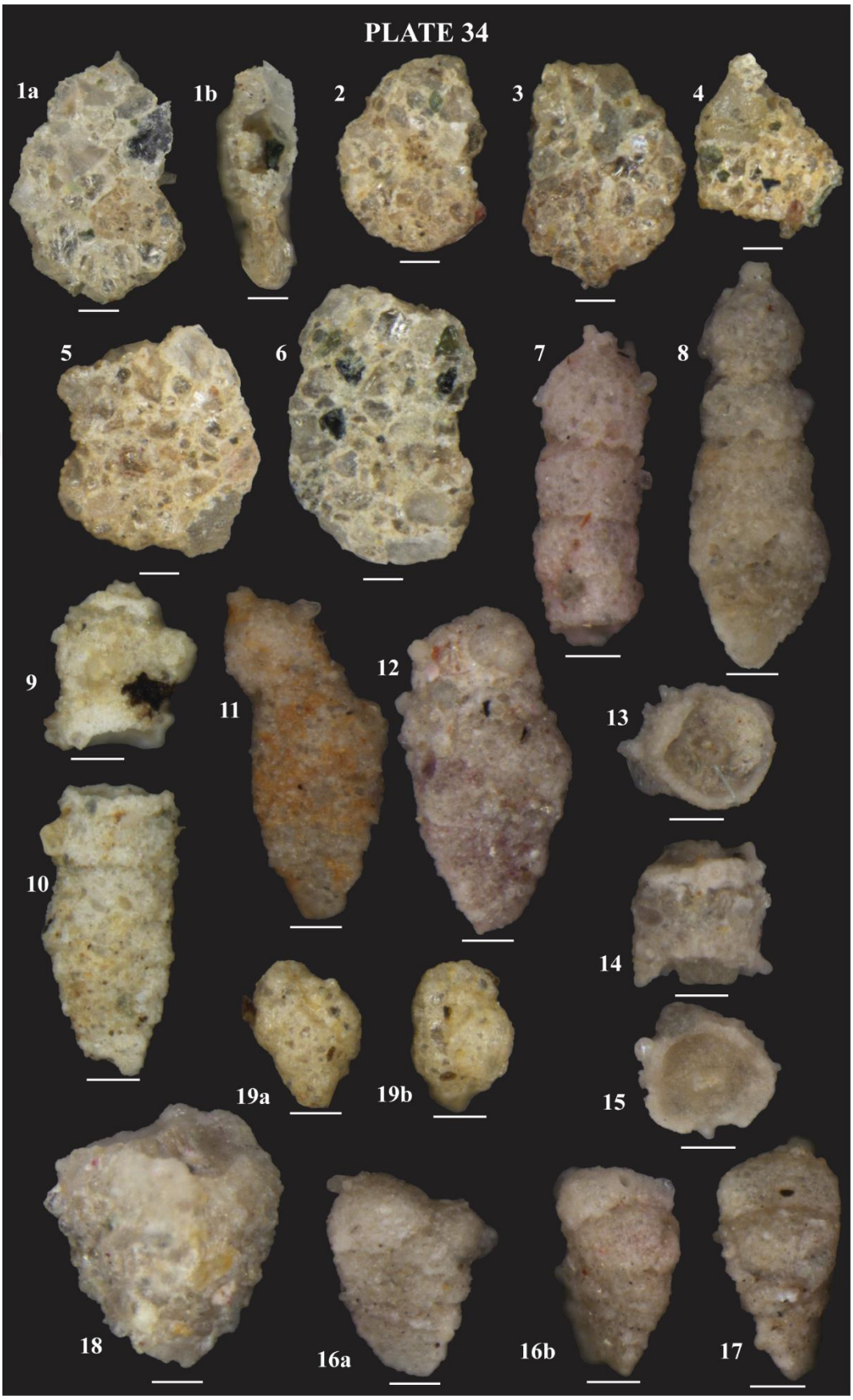

PLATE 34
1a
1b
2
3
4
5
6
7
8
9
11
12
13
10
14
19a
19b
15
18
16a
16b
17

PLATE 35: Nodosariata SEM images; scale bar: 100 μm.

1: *Hyalinonetrion gracilimum* (Seguenza), frontal, both poles broken, MM50 sample 15 cm, IS_28_M_001; **2**: *Lagena interrupta* Williamson, frontal, Station 1 (2021) sample 4 cm, IS_03_J_004; **3**: *Lagena hispidula* Cushman, frontal, Station 4 sample 15 cm, IS_14_U_001; **4**: *Lagena perlucida* (Montagu), frontal, Station 1 (2021) sample 4 cm, IS_03_J_002; **5**: *Lagena strumosa* Reuss, frontal, Station 1 (2021) sample 4 cm, IS_03_J_003; **6**: *Lagena* cf. *annellatrachia* Loeblich and Tappan, frontal, K51.2K09 sample 8 cm, IS_30_F_001; **7**: *Lagena* cf. *laevis* Montagu, frontal, Station 5 sample 8 cm, IS_18_C_001; **8**: *Lagena* sp. 1, frontal, Station 2 sample 25 cm, IS_09_X_001; **9**: *Lagena* sp. 2, frontal, Station 2 sample 25 cm, IS_09_X_003; **10-12**: *Favulina hexagona* (Williamson), Station 5 sample 8 cm, 10. frontal, IS_18_D_001; 11. frontal, IS_18_D_003; 12. oblique-apertural, IS_18_D_002;**13-16**: *Amphicoryna scalaris* (Batsch), 13. frontal, K51.2K09 sample 8 cm, IS_30_B_001; 14. frontal, K51.2K09 sample 8 cm, IS_30_B_002; 15. frontal, Station 1 (2019) sample 4 cm, IS_01_F_001; 16. frontal, Station 3 (2021) sample 15 cm, IS_12_P_002; **17**: *Amphicoryna* sp. 1, frontal, Station 2 sample 2 cm, IS_06_O_001; **18**: *Amphicoryna* sp. 2, frontal, last chamber offset, Station 2 sample 2 cm, IS_06_O_002; **19**: *Astacolus credipula* (Fichtel and Moll), frontal, Station 1 (2021) sample 4 cm, IS_03_L_001; **20**: *Astacolus* ? sp. 1, frontal, Station 3 (2021) sample 15 cm, IS_12_N_001; **21-22**: *Grigelis orectus* Loeblich and Tappan, 21. frontal, broken specimen, Station 1 (2021) sample 4 cm, IS_03_J_001; 22. frontal, broken specimen, Station 3 (2021) sample 15 cm, IS_12_M_002; **23**. *Enantiodentalina timorensis* Loeblich and Tappan, frontal, Station 1 (2019) sample 4 cm, IS_01_E_001; **24**: *Dentalina* spp., frontal, broken specimen, Station 3 (2021) sample 15 cm, IS_12_M_001;**25-26**: *Laevidentalina* spp., K51.2K09 sample 8 cm, 25. frontal, broken specimen, IS_30_D_002; 26. frontal, broken specimen, IS_30_D_001; **27**: *Saracenaria* sp., oblique-frontal, broken specimen, K51.2K09 sample 8 cm, IS_30_C_001.

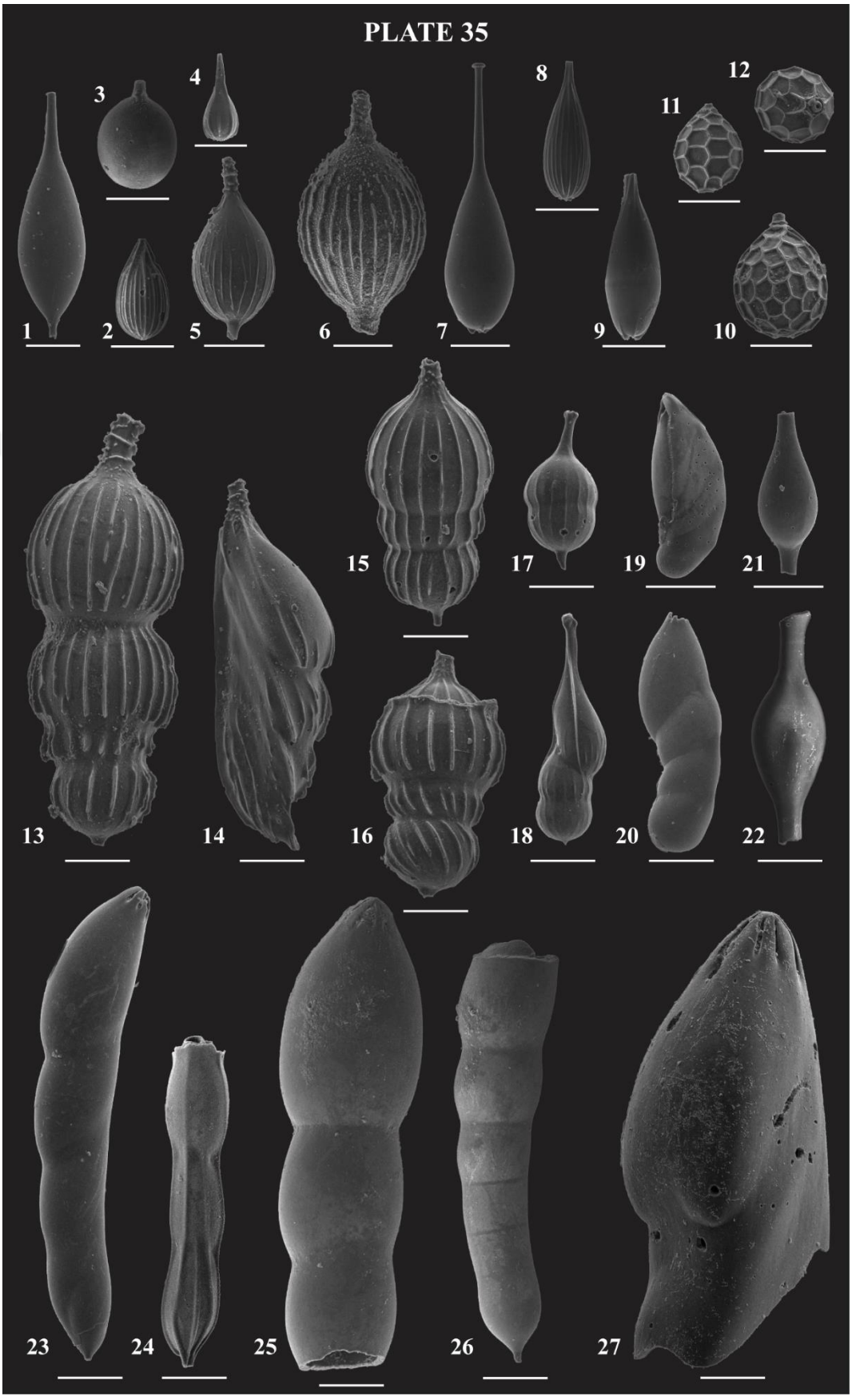

PLATE 35
1
2
3
4
5
6
7
8
9
10
11
12
13
14
15
16
17
18
19
20
21
22
23
24
25
26
27

PLATE 36: Nodosariata stereomicrographs; scale bar: 100 μm.

1: *Hyalinonetrion gracilimum* (Seguenza), frontal, both poles brokens, MM50 sample 15 cm, IS_28_M_001; **2-3**: *Lagena interrupta* Williamson, 2. frontal, Station 1 (2021) sample 4 cm, IS_03_J_004; 3. frontal, K51.2K09 sample 8 cm, IS_30_K_002; **4-5**: *Lagena hispidula* Cushman, 4. frontal, Station 4 sample 15 cm, IS_14_U_001; 5. frontal, Station 5 sample 8 cm, IS_18_C_003; **6-7**: *Lagena perlucida* (Montagu), 6. frontal, Station 1 (2021) sample 4 cm, IS_03_J_002; 7. frontal, Station 2 sample 25 cm, IS_09_K_002; **8-9**: *Lagena strumosa* Reuss, 8. frontal, Station 1 (2021) sample 4 cm, IS_03_J_003; 9. frontal, Station 5 sample 8 cm, IS_18_C_002; **10**: *Lagena* cf. *annellatrachia* Loeblich and Tappan, frontal, K51.2K09 sample 8 cm, IS_30_F_001; **11**: *Lagena* cf. *laevis* Montagu, frontal, Station 5 sample 8 cm, IS_18_C_001; **12**: *Lagena* sp. 1, frontal, Station 2 sample 25 cm, IS_09_X_001; **13-14**: *Lagena* sp. 2, 13. frontal, Station 2 sample 25 cm, IS_09_X_003; 14. frontal, Station 2 sample 15 cm, IS_08_R_001; **15-18**: *Favulina hexagona* (Williamson), 15-17:. Station 5 sample 8 cm, 15. frontal, IS_18_D_001; 16. frontal-oblique, IS_18_D_003; 17. frontal, IS_18_D_002; 18a. apertural, 18b. frontal, Station 4 sample 15 cm, IS_14_T_001; **19-24**: *Amphicoryna scalaris* (Batsch), 19. frontal, K51.2K09 sample 8 cm, IS_30_B_001; 20. frontal, K51.2K09 sample 8 cm, IS_30_B_002; 21. frontal, Station 1 (2019) sample 4 cm, IS_01_F_001; 22. frontal, Station 3 (2021) sample 15 cm, IS_12_P_002; 23. frontal, broken specimen, MM50 sample 15 cm, IS_28_L_001; 24. frontal, Station 5 sample 8 cm, IS_18_E_001; **25-27**: *Amphicoryna* sp. 1, 25. frontal, Station 2 sample 2 cm, IS_06_O_001; 26. frontal, Station 1 (2019) sample 4 cm, IS_01_G_001; 27. frontal, Station 3 (2021) sample 15 cm, IS_12_P_003; **28-29**: *Amphicoryna* sp. 2, 28. frontal, last chamber offset, Station 2 sample 2 cm, IS_06_O_002; 29. frontal, last chamber offset, Station 2 sample 15 cm, IS_08_S_001; **30-31**: *Astacolus credipula* (Fichtel and Moll), 30a. oblique-dorsal, 30b. oblique-frontal, Station 1 (2021) sample 4 cm, IS_03_L_001; 31. frontal view, Station 5 sample 8 cm, IS_18_E_002; **32-33**: *Grigelis orectus* Loeblich and Tappan, 32. frontal, broken, Station 3 (2021) sample 15 cm, IS_12_M_002; 33. frontal, broken, Station 1 (2021) sample 4 cm, IS_03_J_001; **34-35**: *Laevidentalina* spp., 34. frontal, broken, K51.2K09 sample 8 cm, IS_30_D_001; 35. frontal, broken, K51.2K09 sample 8 cm, IS_30_D_002; **36**: *Astacolus* ? sp. 1, frontal, Station 3 (2021) sample 15 cm, IS_12_N_001; **37**: *Dentalina* spp., frontal, broken, Station 3 (2021) sample 15 cm, IS_12_M_001; **38-41**: *Enantiodentalina timorensis* Loeblich and Tappan, 38a. frontal, 38b. dorsal, Station 1 (2019) sample 4 cm, IS_01_E_001; 39. frontal, broken, Station 1 (2019) sample 4 cm, IS_01_E_002; 40. frontal, MM50 sample 15 cm, IS_21_J_001; 41. frontal, broken specimen, Station 4 sample 15 cm, IS_14_Y_001; **42**: *Saracenaria* sp., oblique frontal, broken specimen, K51.2K09 sample 8 cm, IS_30_C_001.

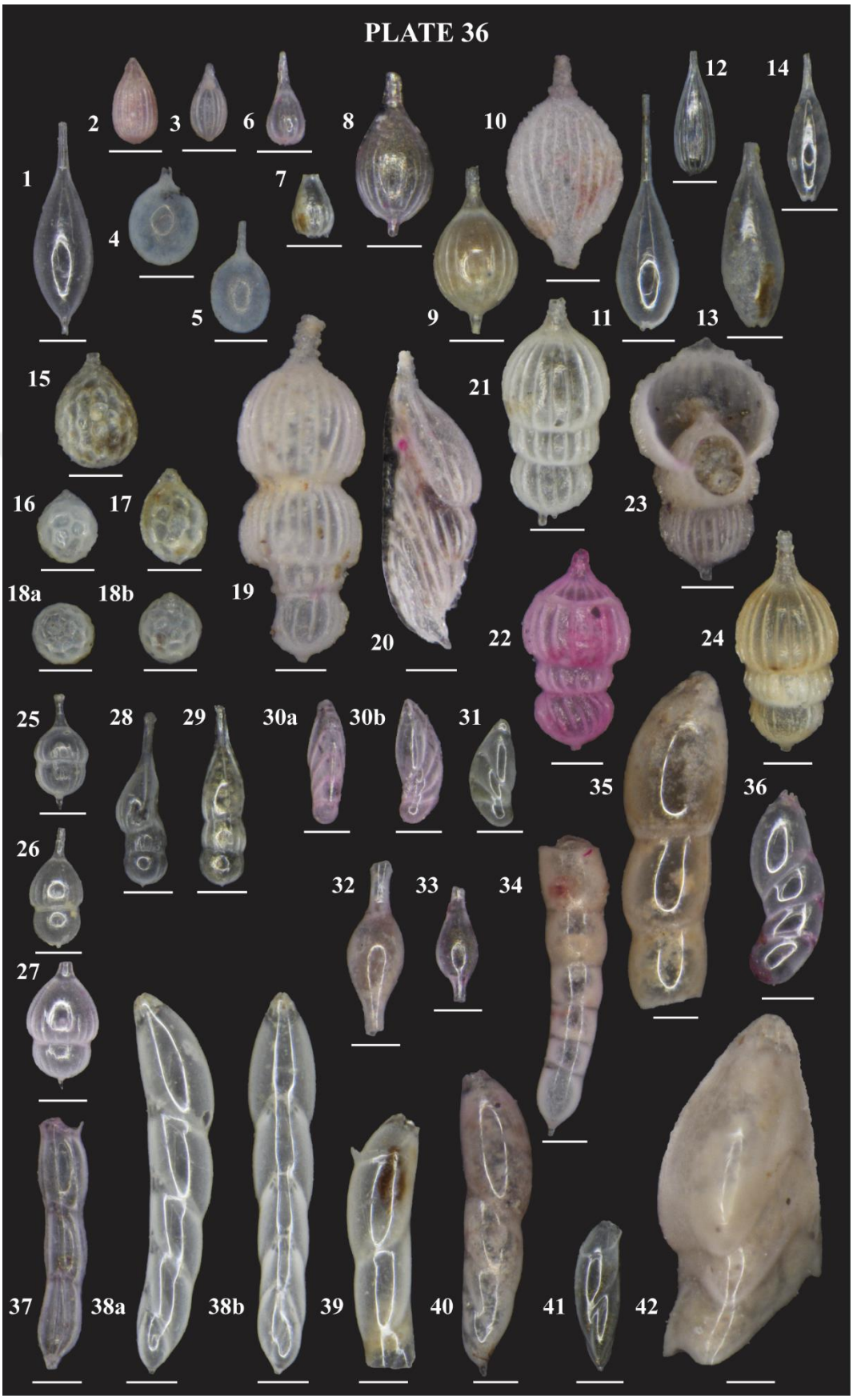

PLATE 36
1
2
3
4
5
6
7
8
9
10
11
12
13
14
15
16
17
18a
18b
19
20
21
22
23
24
25
26
27
28
29
30a
30b
31
32
33
34
35
36
37
38a
38b
39
40
41
42

PLATE 37: Nodosariata SEM images; scale bar: 100 μm for all but 7* and 8* which are 50 μm.

1-4: *Fissurina annectens* (Burrows and Holland), 1. edge, Station 1 (2019) sample 4 cm, IS_01_K_003a; 2. oblique-frontal, Station 1 (2019) sample 4 cm, IS_01_K_003b; 3. oblique-edge, Station 2 sample 5 cm, IS_07_AA_002; 4. frontal, Station 2 sample 5 cm, IS_07_AA_003; **5-6**: *Fissurina castanea* (Flint), 5. frontal, flange broken, Station 1 (2019) sample 4 cm, IS_01_K_007; 6. oblique-edge, flange broken, Station 2 sample 25 cm, IS_09_Y_001; **7-8**: *Fissurina laevigata* Reuss, 7. frontal, 7*. close up of apertural part, scale 50 mm,Station 5 sample 8 cm, IS_18_B2_001; 8. edge, 8*. close up of apertural part, scale 50 mm, Station 5 sample 8 cm, IS_18_B2_002; **9-10**: *Fissurina neptuni* (Buchner), 9. frontal, K51.2K09 sample 8cm, IS_30_E_001; 10. oblique-edge, K51.2K09 sample 8cm, IS_30_E_002; **11-12**: *Fissurina robusta* Zheng, 11. frontal, Station 4 sample 15 cm, IS_14_V_002; 12. frontal, Station 1 (2019) sample 4 cm, IS_01_K_005; **13-14**: *Fissurina variocarinata* (Buchner), 13. oblique-edge, Station 5 sample 8 cm, IS_18_B7_002; 14. frontal, Station 5 sample 8 cm, IS_18_B7_001; **15-17**: *Fissurina* sp. 1, 15. oblique-frontal, apertural part tilted up, Station 5 sample 8 cm, IS_18_B4_001; 16. frontal, adapertural part tilted up, faintly costate, Station 4 sample 15 cm, IS_14_V_003; 17. oblique-edge, adapertural part tilted up, Station 5 sample 8 cm, IS_18_B4_002; **18-19**: *Fissurina* sp. 2, Station 5 sample 8 cm, 18. oblique-frontal, IS_18_B6_001; 19. oblique-edge, IS_18_B6_002; **20**: *Fissurina* sp. 3, frontal, Station 3 (2021) sample 15 cm_ IS_12_R_002; **21**: *Fissurina* sp. 4, frontal, Station 4 sample 15 cm, IS_14_V_001; **22**: *Lagenosolenia strigimarginata* Loeblich and Tappan, frontal, Station 5 sample 8 cm, IS_18_B1_001; **23**: *Palliolatella* sp., frontal, Station 5 sample 8 cm, IS_18_B1_002; **24-26**: *Parafissurina lata* (Wiesner), 24. frontal, one apertural lip broken, Station 5 sample 8 cm, IS_18_B8_002; 25. oblique-frontal, adapertural side, Station 5 sample 8 cm, IS_18_B8_001; 26. oblique-frontal, one apertural lip broken, Station 1 (2021) sample 4 cm, IS_03_M_003; **27-30**: *Parafissurina basispinata* McCulloch, 27. frontal, Station 1 (2019) sample 4 cm, IS_01_K_001; 28. oblique-frontal, Station 1 (2021) sample 4 cm, IS_03_M_002; 29. frontal, K51.2K09 sample 8 cm, IS_30_E_003; 30. frontal, Station 3 (2021) sample 15 cm, IS_12_R_001.

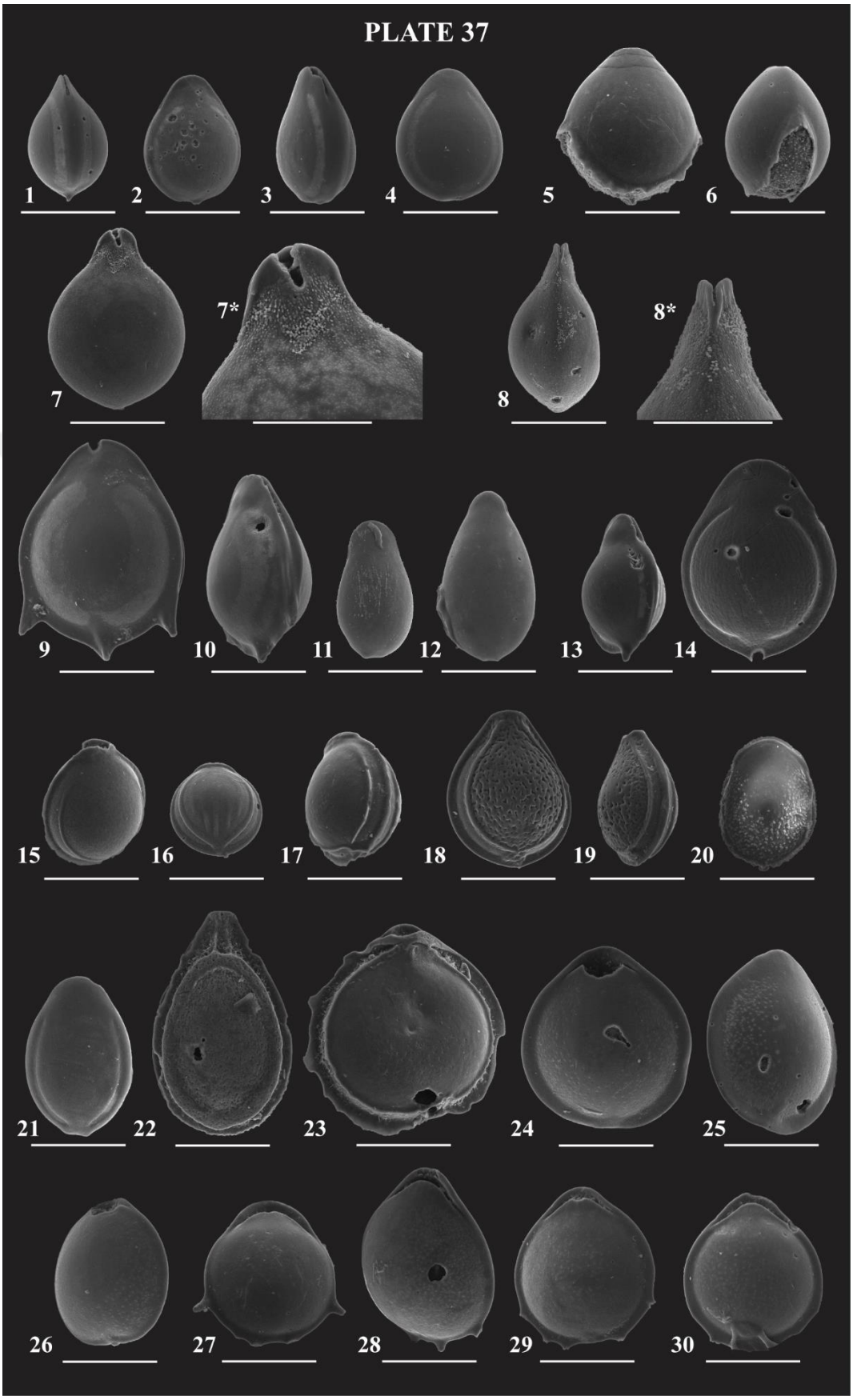

PLATE 37
1
2
3
4
5
6
7
7*
8
8*
9
10
11
12
13
14
15
16
17
18
19
20
21
22
23
24
25
26
27
28
29
30

PLATE 38: Nodosariata stereomicrographs; scale bar: 100 μm.

1-4: *Fissurina annectens* (Burrows and Holland), 1. frontal, Station 1 (2019) sample 4 cm, IS_01_K_003a; 2a. frontal, 2b. apertural, Station 1 (2019) sample 4 cm, IS_01_K_003b; 3a. frontal, 3b. edge, Station 2 sample 5 cm, IS_07_AA_002; 4. frontal, Station 2 sample 5 cm, IS_07_AA_003; **5-6**: *Fissurina castanea* (Flint), 5a. frontal, 5b. oblique-apertural, 5c. edge, flange broken, Station 1 (2019) sample 4 cm, IS_01_K_007; 6. apertural, Station 2 sample 25 cm, IS_09_Y_001; **7-8**: *Fissurina laevigata* Reuss, Station 5 sample 8 cm, 7. frontal, IS_18_B2_001; 8a. edge, 8b. frontal, IS_18_B2_002; **9-11**: *Fissurina neptuni* (Buchner), 9. frontal, K51.2K09 sample 8cm, IS_30_E_001; 10. frontal, K51.2K09 sample 8cm, IS_30_E_002; 11. frontal, Station 2 sample 5 cm, IS_07_AA_001; **12-13**: *Fissurina robusta* Zheng, 12. frontal, Station 4 sample 15 cm, IS_14_V_002; 13a. frontal, 13b. edge, Station 1 (2019) sample 4 cm, IS_01_K_005; **14-15**: *Fissurina variocarinata* (Buchner), Station 5 sample 8 cm, 14. frontal, IS_18_B7_002; 15a. frontal, 15b. edge, IS_18_B7_001; **16-18**: *Fissurina* sp. 1, 16. frontal, Station 5 sample 8 cm, IS_18_B4_001; 17. frontal view, Station 4 sample 15 cm, IS_14_V_003; 18a. frontal, 18b. edge, Station 5 sample 8 cm, IS_18_B4_002; **19-20**: *Fissurina* sp. 2, Station 5 sample 8 cm, 19a. frontal, 19b. edge, IS_18_B6_001; 20. frontal, IS_18_B6_002; **21**: *Fissurina* sp. 3, frontal, Station 3 (2021) sample 15 cm_ IS_12_R_002; **22**: *Fissurina* sp. 4, frontal, Station 4 sample 15 cm, IS_14_V_001; **23**: *Lagenosolenia strigimarginata* Loeblich and Tappan, 23a. frontal, 23b. edge Station 5 sample 8 cm, IS_18_B1_001; **24**: *Palliolatella* sp., 24a. frontal, 24b. edge, Station 5 sample 8 cm, IS_18_B1_002; **25-27**: *Parafissurina lata* (Wiesner), 25. frontal, one apertural lip broken, Station 5 sample 8 cm, IS_18_B8_002; 26a. frontal, 26b. edge, Station 5 sample 8 cm, IS_18_B8_001; 27. frontal, one apertural lip broken, Station 1 (2021) sample 4 cm, IS_03_M_003; **28-31**: *Parafissurina basispinata* McCulloch, 28. frontal, Station 1 (2019) sample 4 cm, IS_01_K_001; 29. frontal, Station 1 (2021) sample 4 cm, IS_03_M_002; 30. frontal, K51.2K09 sample 8 cm, IS_30_E_003; 31. frontal, Station 3 (2021) sample 15 cm, IS_12_R_001.

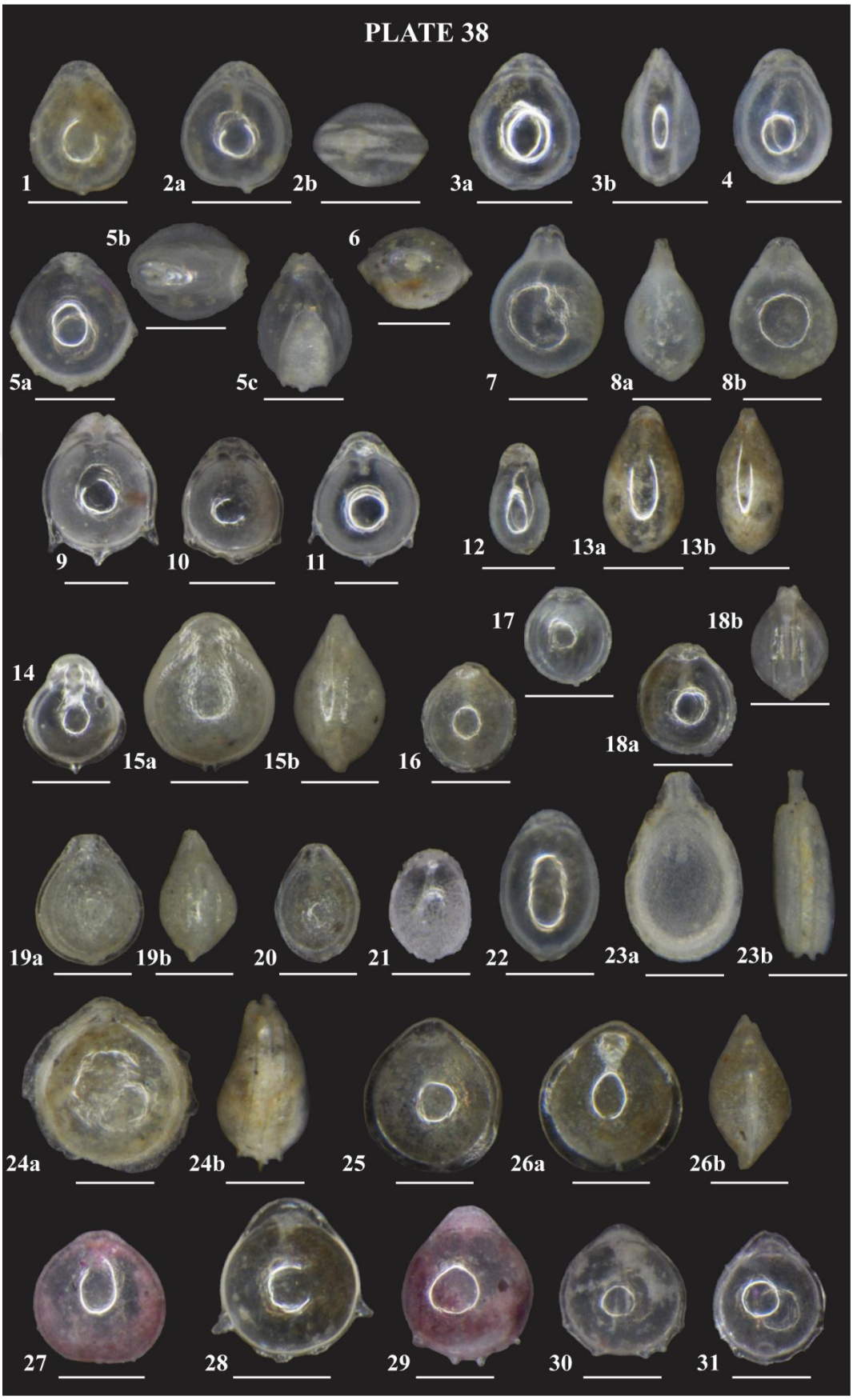

PLATE 38
1
2a
2b
3a
3b
4
5b
6
5a
5c
7
8a
8b
9
10
11
12
13a
13b
17
18b
14
15a
15b
16
18a
19a
19b
20
21
22
23a
23b
24a
24b
25
26a
26b
27
28
29
30
31

PLATE 39: Nodosariata, Monothalamea, Spirillinida SEM images; scale bar: 100 μm.

1: *Anturina haynesi* Jones, frontal, Station 3 (2021) sample 15 cm, IS_12_Q_001; **2-5**: Polymorphinoidea (indeterminate), 2. frontal, Station 3 (2021) sample 15 cm, IS_12_O_001a; 3. frontal, broken specimen, Station 3 (2021) sample 15 cm, IS_12_O_001b; 4. frontal, Station 4 sample 15 cm, IS_14_X_001; 5. frontal, Station 5 sample 8 cm, IS_26_N_001; **6**: *Lenticulina gibba* (d'Orbigny), oblique-frontal, Station 2 sample 2 cm, IS_06_F_002; **7-9**: *Lenticulina cultrata* (de Monfort), 7. frontal, K51.2K09 sample 8 cm, IS_32_G_001; 8. frontal, K51.2K09 sample 8 cm, IS_32_G_002, juvenile; 9. oblique-frontal, K51.2K09 sample 8 cm, IS_32_G_003, juvenile ; **10**: *Lenticulina* cf. *nitida* (Brady), frontal, Station 1 (2021) sample 8 cm, IS_04_M_001a; **11**: *Lenticulina* sp. 1, frontal, Station 1 (2021) sample 8 cm, IS_04_M_001b; **12-13**: *Neolenticulina variabilis* (Reuss, 1850), 12. frontal, K51.2K09 sample 8 cm, IS_32_F_002, juvenile; 13. frontal, K51.2K09 sample 8 cm, IS_32_F_001; **14-15**: *Spirillina* sp. 1, 14. spiral, Station 5 sample 8 cm, IS_25_E_004; 15. umbilical, Station 5 sample 8 cm, IS_25_E_003; **16-17**: *Spirillina vivipara* Ehrenberg, Station 5 sample 8 cm, 16. spiral, IS_25_E_002; 17. umbilical, IS_25_E_001; **18**: *Lagenammina arenulata* (Skinner), frontal, Station 5 sample 8 cm, IS_25_L_001; **19-21**: *Patellina corrugata* Williamson, 19. edge, Station 4 sample 15 cm, IS_14_R_001; 20. spiral, Station 5 sample 8 cm, IS_25_F_002; 21. umbilical, Station 5 sample 8 cm, IS_25_F_001; **22-25**: *Glomospira charoides* (Jones and Parker), K51.2K09 sample 8 cm, 22. IS_30_G_004; 23. IS_30_G_001; 24. IS_30_G_003; 25. IS_30_G_002.

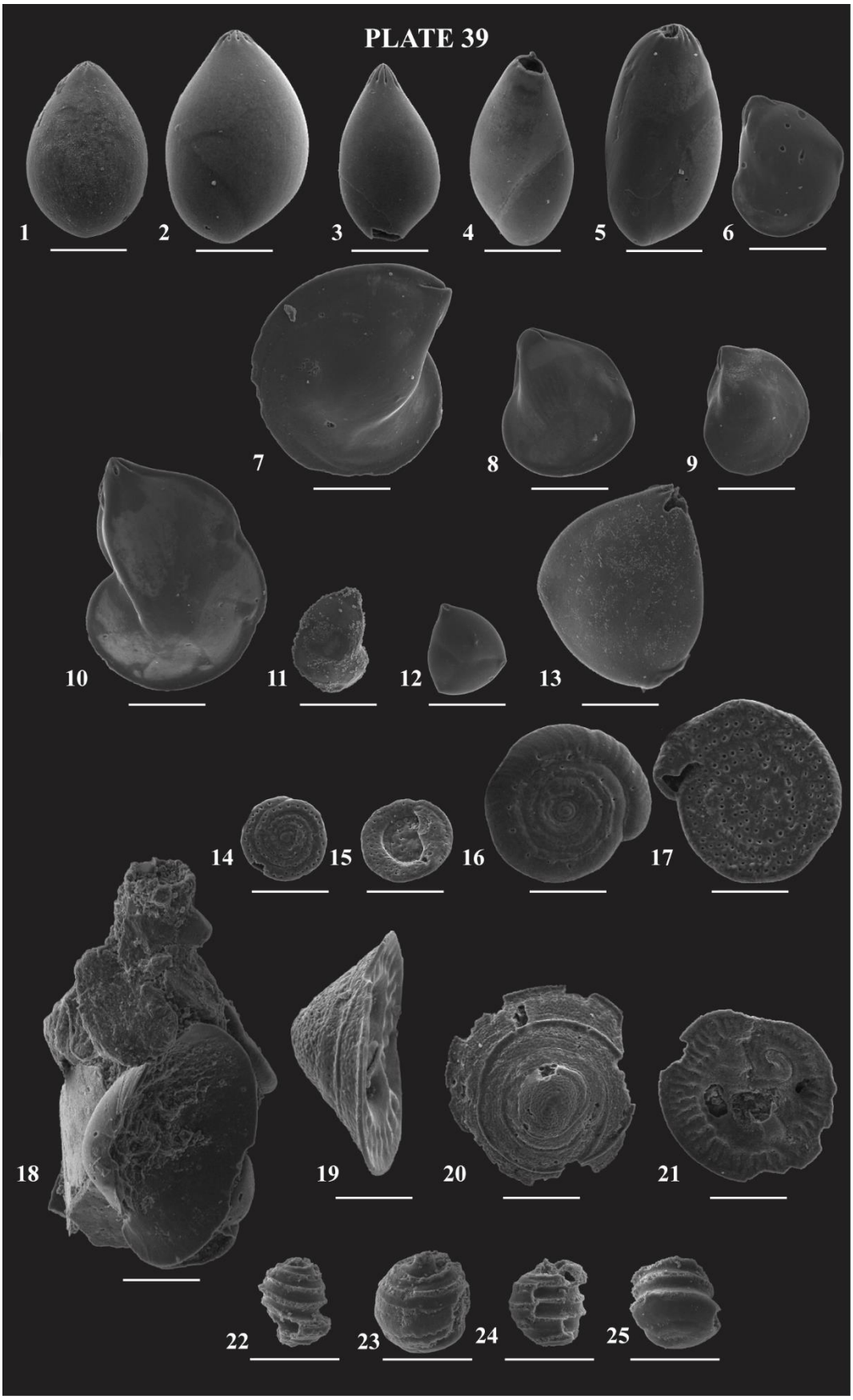

PLATE 39
1
2
3
4
5
6
7
8
9
10
11
12
13
14
15
16
17
18
19
20
21
22
23
24
25

PLATE 40: Nodosariata, Monothalamea, Spirillinida stereomicrographs; scale bar: 100 μm.

1: *Anturina haynesi* Jones, frontal, Station 3 (2021) sample 15 cm, IS_12_Q_001; **2-5**: Polymorphinoidea (indeterminate), 2. frontal, Station 3 (2021) sample 15 cm, IS_12_O_001a; 3. frontal, broken specimen, Station 3 (2021) sample 15 cm, IS_12_O_001b; 4. frontal, Station 4 sample 15 cm, IS_14_X_001; 5. frontal, Station 5 sample 8 cm, IS_26_N_001; **6-8**: *Lenticulina gibba* (d'Orbigny), 6. oblique-frontal, Station 2 sample 2 cm, IS_06_F_002; 7. oblique-frontal, Station 2 sample 2 cm, IS_06_F_001; 8. oblique-frontal, Station 2 sample 2 cm, IS_06_F_003, juvenile; **9-14**: *Lenticulina cultrata* (de Monfort), 9a. frontal, 9b. edge, K51.2K09 sample 8 cm, IS_32_G_001; 10a. frontal, 10b. edge, K51.2K09 sample 8 cm, IS_32_G_005; 11a. frontal, 11b. edge, K51.2K09 sample 8 cm, IS_32_G_005; 12. frontal, inner whorl observable through clear umbonal boss, Station 2 sample 5 cm, IS_07_K_001a; 13. frontal, K51.2K09 sample 8 cm, IS_32_G_002, juvenile; 14. frontal, K51.2K09 sample 8 cm, IS_32_G_003, juvenile; **15-16**: *Neolenticulina variabilis* (Reuss), 15a. frontal, 15b. edge, K51.2K09 sample 8 cm, IS_32_F_001, juvenile; 16. frontal, K51.2K09 sample 8 cm, IS_32_F_002; **17**: *Lenticulina* cf. *nitida* (Brady), a. edge-dorsal, b. frontal, c. frontal, d. edge-apertural , Station 1 (2021) sample 8 cm, IS_04_M_001a; **18-19**: *Lenticulina* sp. 1, Station 1 (2021) sample 8 cm, 18a. and b. oblique-edge views, IS_04_M_001b; 19a. oblique-edge views, IS_04_M_001c; **20**: *Lagenammina arenulata* (Skinner), a. and b. frontal views, Station 5 sample 8 cm, IS_25_L_001; **21-22**: *Spirillina vivipara* Ehrenberg, Station 5 sample 8 cm, 21a. umbilical, 21b. spiral, IS_25_E_001; 22a. umbilical, 22b. spiral, IS_25_E_002; **23-24**: *Spirillina* sp. 1, Station 5 sample 8 cm, 23a. umbilical, 23b. spiral, IS_25_E_003; 24a. umbilical, 24b. spiral, IS_25_E_004; **25-27**: *Patellina corrugata* Williamson, 25a. spiral, 25b. umbilical, Station 5 sample 8 cm, IS_25_F_001; 26a. spiral, 26b. umbilical, Station 5 sample 8 cm, IS_25_F_002; 27. spiral, Station 4 sample 15 cm, IS_14_R_001; **28-31**: *Glomospira charoides* (Jones and Parker), K51.2K09 sample 8 cm, 28. IS_30_G_004; 29. IS_30_G_001; 30. IS_30_G_003; 31. IS_30_G_002.

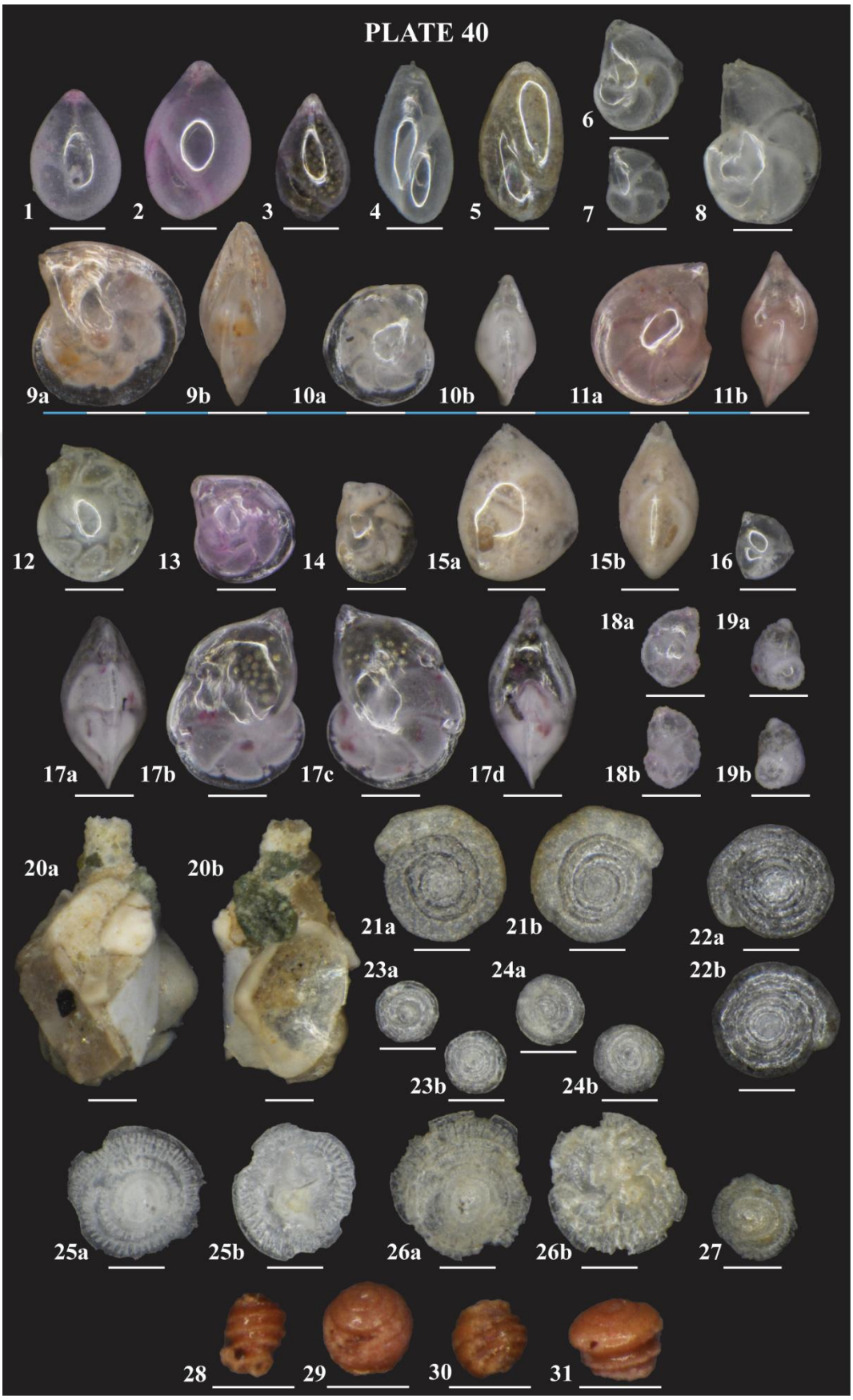

PLATE 40
1
2
3
4
5
6
7
8
9a
9b
10a
10b
11a
11b
12
13
14
15a
15b
16
17a
17b
17c
17d
18a
18b
19a
19b
20a
20b
21a
21b
22a
22b
23a
23b
24a
24b
25a
25b
26a
26b
27
28
29
30
31

PLATE 41: Cornuspiroidea, Miliolidea SEM images; scale bar: 100 μm.

1-7: *Adelosina* spp. 1. frontal, Station 5 sample 8 cm, IS_17_J_001; 2. frontali IS_17_J_002; 3. frontal, Station 3 (2021) sample 1 cm, IS_11_A_001; 4. frontal, Station 4 sample 15 cm, IS_14_2E_001; 5. frontal, Station 2 sample 25 cm, IS_09_I_001; 6. frontal, Station 2 sample 15 cm, IS_08_I_001; 7. frontal, Station 3 (2021) sample 15 cm, IS_13_B_001; **8-9**: *Cycloforina tenuicollis* (Wiesner), Station 5 sample 8 cm, 8. frontal, IS_17_Q_001; 9. frontal, IS_17_Q_002; **10-12**: *Cycloforina rugosa* (d'Orbigny), Station 5 sample 8 cm, 10. frontal, IS_17_P_001; 11. frontal, IS_17_P_002; 12. apertural, IS_17_P_003; **13-14**: *Quinqueloculina bosciana* d'Orbigny, Station 3 (2021) sample 15 cm, 13. frontal, IS_13_E_001; 14. frontal, IS_13_E_002; **15-17**: *Quinqueloculina schlumbergeri* (Wiesner), Station 5 sample 8 cm, 15. frontal, IS_17_K_002; 16. apertural-oblique, IS_17_K_003; 17. frontal, IS_17_K_001; **18-21**: *Quinqueloculina stalkeri* Loeblich and Tappan, 18. frontal, Station 2 sample 25 cm, IS_09_K_001; 19. frontal, MM50 sample 15 cm, IS_21_E_001; 20. frontal, MM50 sample 15 cm, IS_21_E_002; 21. frontal, Station 4 sample 15 cm, IS_14_2D_001; **22-25**: *Quinqueloculina pygmaea* Reuss, Station 5 sample 8 cm, 22. frontal, IS_17_N_001; 23. frontal, IS_17_N_002; 24. apertural oblique, IS_17_N_003; 25. frontal, IS_17_N_004.

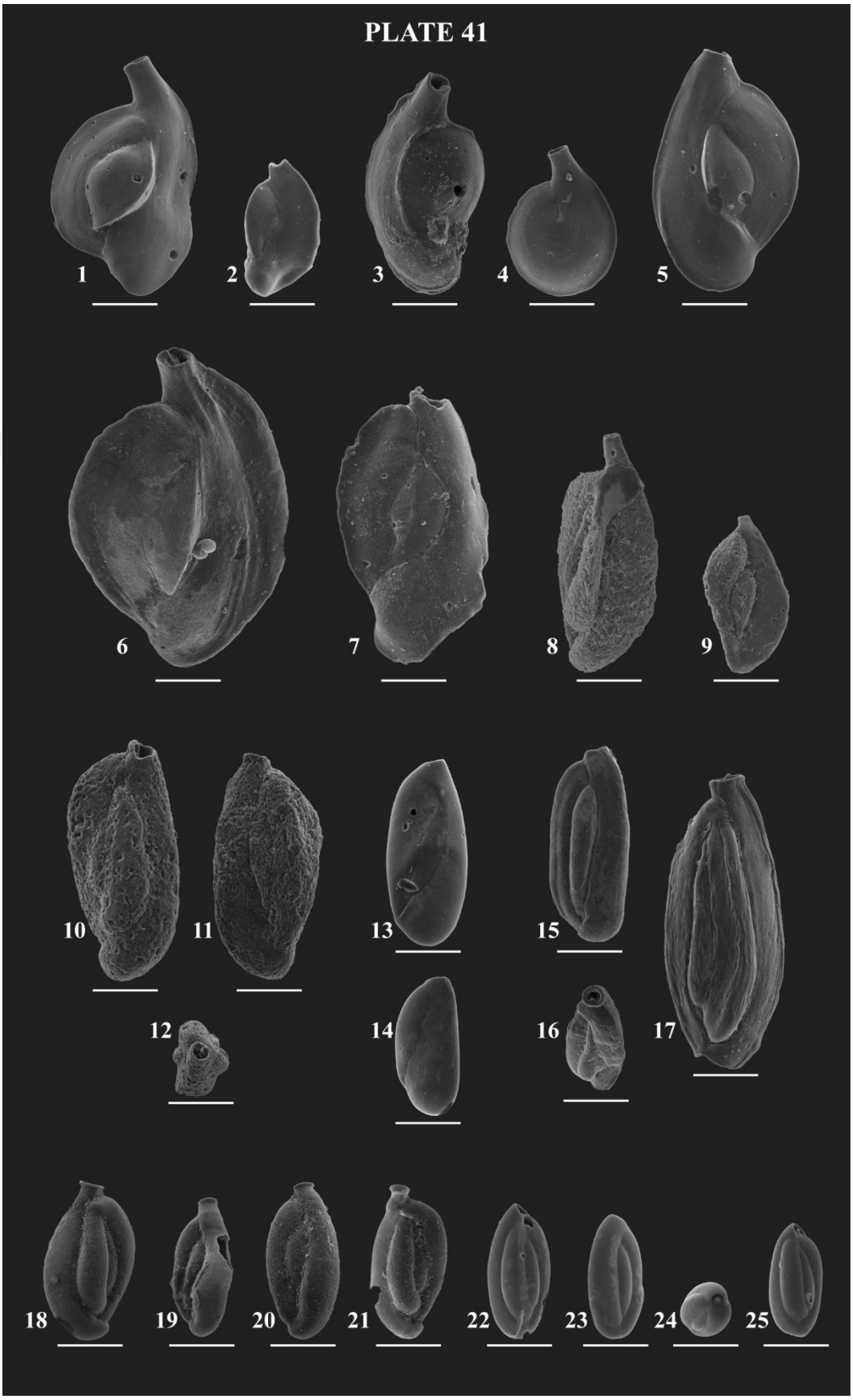

PLATE 41
1
2
3
4
5
6
7
8
9
10
11
13
15
12
14
16
17
18
19
20
21
22
23
24
25

PLATE 42: Cornuspiroidea, Miliolidea stereomicrographs; scale bar: 100 μm.

1-8: *Adelosina* spp. 1. frontal, Station 5 sample 8 cm, IS_17_J_001; 2. frontali IS_17_J_002; 3. frontal, Station 3 (2021) sample 1 cm, IS_11_A_001; 4. frontal, Station 3 (2021) sample 15 cm, IS_13_B_002; 5a. and b. frontal, Station 4 sample 15 cm, IS_14_2E_001; 6. frontal, Station 2 sample 25 cm, IS_09_I_001; 7a. frontal, 7b. apertural, 7c. frontal, Station 2 sample 15 cm, IS_08_I_001; 8. frontal, Station 3 (2021) sample 15 cm, IS_13_B_001; **9-11**: *Cycloforina tenuicollis* (Wiesner), 9a. frontal, 9b. apertural-oblique, 9c. frontal, Station 2 sample 15 cm, IS_08_J_002; 10. frontal, Station 5 sample 8 cm, IS_17_Q_001; 11. frontal, Station 5 sample 8 cm, IS_17_Q_002; **12-14**: *Cycloforina rugosa* (d'Orbigny), Station 5 sample 8 cm, 12. frontal, IS_17_P_001; 13. frontal, IS_17_P_002; 14. apertural, IS_17_P_003; **15-16**: *Quinqueloculina bosciana* d'Orbigny, Station 3 (2021) sample 15 cm, 15a. frontal, 15b. apertural-oblique, 15c. frontal, IS_13_E_001; 16a. frontal, 16b. apertural-oblique, 16c. frontal, IS_13_E_002; **17-19**: *Quinqueloculina schlumbergeri* (Wiesner), Station 5 sample 8 cm, 17. frontal, IS_17_K_002; 18a. apertural-oblique, 18b. frontal, IS_17_K_001; 19. frontal, IS_17_K_003; **20-15**: *Quinqueloculina stalkeri* Loeblich and Tappan, 20. frontal, Station 2 sample 25 cm, IS_09_K_001; 21. frontal, MM50 sample 15 cm, IS_21_E_001; 22. frontal, MM50 sample 15 cm, IS_21_E_002; 23. frontal, Station 4 sample 15 cm, IS_14_2D_001; 24a. frontal, 24b. apertural-oblique, 24c. frontal, Station 2 sample 15 cm, IS_08_G_002; 25. frontal, Station 4 sample 15 cm, IS_14_2D_002; **26-30**: *Quinqueloculina pygmaea* Reuss, 26. frontal, Station 5 sample 8 cm, IS_17_N_001; 27. frontal, Station 5 sample 8 cm, IS_17_N_002; 28. frontal, Station 5 sample 8 cm, IS_17_N_003; 29. frontal, Station 5 sample 8 cm, IS_17_N_004; 30a. frontal, 30b. apertural-oblique, 30c. frontal, Station 2 sample 25 cm, IS_09_M_001; **31**: *Cornuspira involvens* (Reuss), Station 4 sample 15 cm, IS_14_Q_001, 31a. spiral, 31b. umbilical.

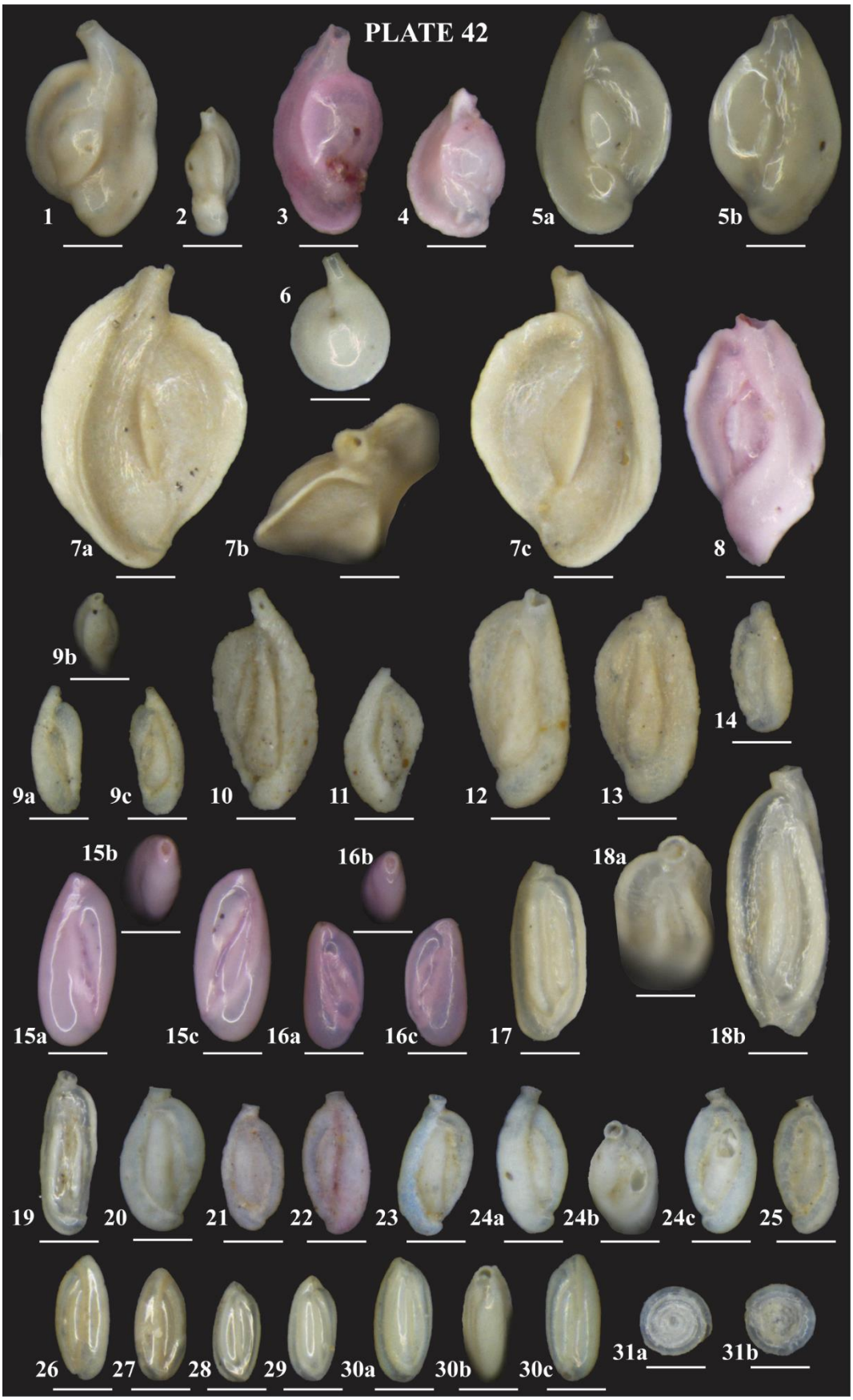

PLATE 42
1
2
3
4
5a
5b
6
7a
7b
7c
8
9b
9a
9c
10
11
12
13
14
15b
15a
15c
16b
16a
16c
17
18a
18b
19
20
21
22
23
24a
24b
24c
25
26
27
28
29
30a
30b
30c
31a
31b

PLATE 43: Miliolidea SEM images; scale bar: 100 μm.

1: *Quinqueloculina seminulum ?* (Linnaeus), Station 3 (2021) sample 15 cm, apertural, IS_13_F_001; **2-6**: *Quinqueloculina viennensis* Le Calvez and Le Calvez, 2. four chambered face, MM50 sample 15 cm, IS_21_H_001; 3. four chambered face, frontal, MM50 sample 30 cm, IS_20_M_001; 4. three chambered face, MM50 sample 30 cm, IS_20_M_002; 5. apertural, Station 2 sample 15 cm, IS_08_B_001; 6. three chambered face, MM50 sample 15 cm, IS_21_H_002; **7-8**: *Quinqueloculina vandiemeniensis* Loeblich and Tappan 7. four chambered face, Station 2 sample 15 cm, IS_08_J_004a; 8. three chambered face, Station 5 sample 8 cm, IS_17_U_002; **9**: *Quinqueloculina* sp. 1, four chambered face, Station 5 sample 8 cm, IS_17_U_003; **10**: *Pseudotriloculina laevigata* (d'Orbigny), frontal, Station 5 sample 8 cm, IS_17_U_001; **11-12**: *Quinqueloculina* sp. 2, 11. three chambered face, Station 5 sample 8 cm, IS_17_T_001; 12. four chambered face, Station 2 sample 15 cm, IS_08_J_004b; **13-15**: *Quinqueloculina*? sp. 3, K51.2K09 sample 8 cm, 13. four chambered face, IS_24_J_001; 14. three chambered face, IS_24_J_002; 15. oblique-apertural, IS_24_J_003; **16-18**: *Miliolinella subrotunda* (Montagu), K51.2K09 sample 8 cm, 16. frontal, IS_24_G_001; 17. oblique, adapertural edge, IS_24_G_002; 18. edge, IS_24_G_003; **19-21**: *Biloculinella globula* (Bornemann), K51.2K09 sample 8 cm, 19. frontal, IS_24_H_001; 20. frontal, IS_24_H_002; 21. edge, IS_24_H_001; **22-23**: *Pyrgo elongata* (d'Orbigny), 22. oblique, Station 2 sample 25 cm, IS_09_F_001; 23. oblique, K51.2K09 sample 8 cm, IS_24_I_002; **24-26**: *Pyrgo anomala* (Schlumberger), 24. frontal, Station 2 sample 15 cm, IS_08_E_001; 25. frontal, Station 5 sample 8 cm, IS_17_O_001; 26. frontal, K51.2K09 sample 8 cm, IS_24_I_001.

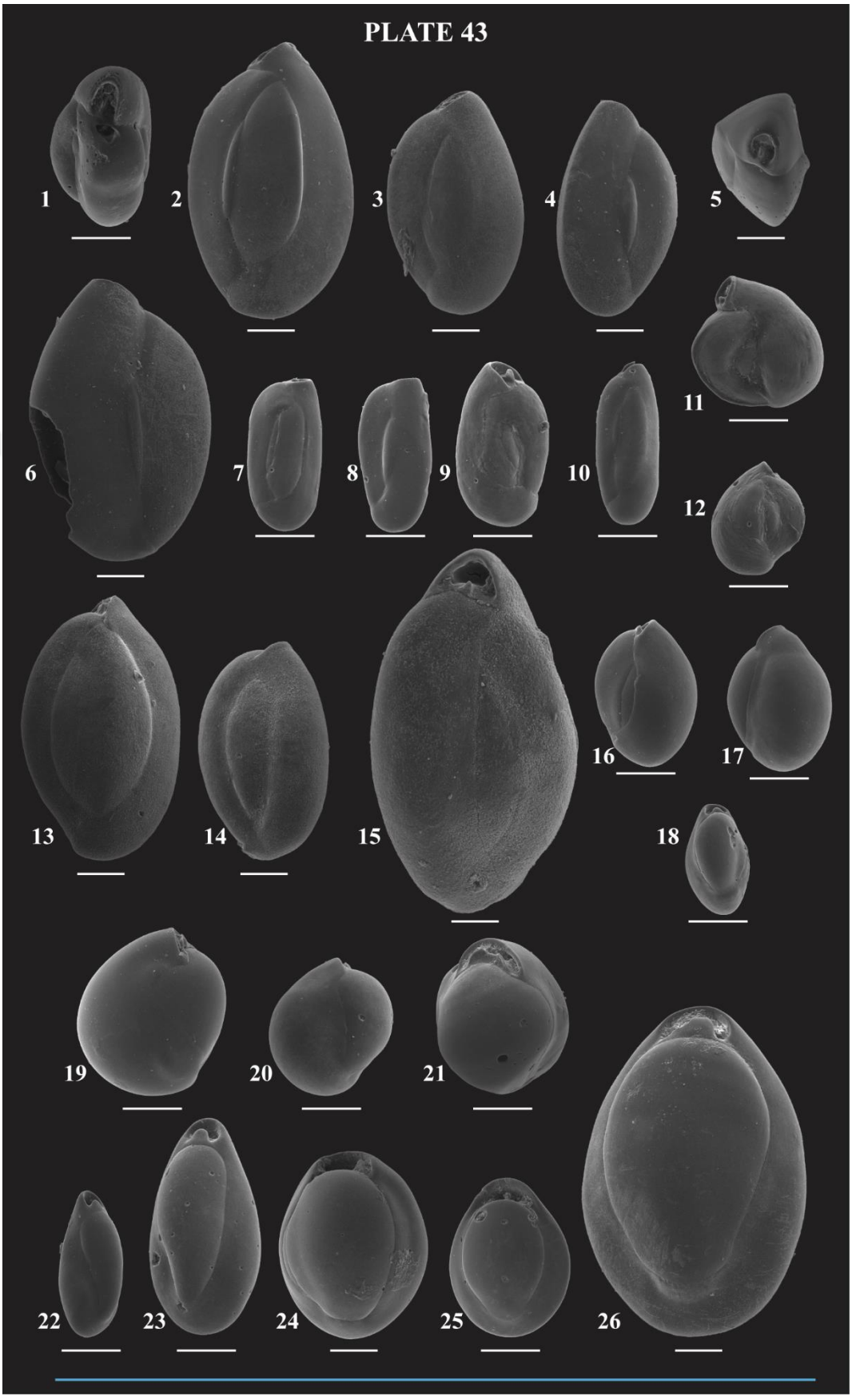

PLATE 43
1
2
3
4
5
6
7
8
9
10
11
12
13
14
15
16
17
18
19
20
21
22
23
24
25
26

PLATE 44-A: Miliolidea stereomicrographs; scale bar: 100 µm.

1: *Quinqueloculina seminulum ?* (Linnaeus), Station 3 (2021) sample 15 cm, apertural, IS_13_F_001; **2-7**: *Quinqueloculina viennensis* Le Calvez and Le Calvez, 2. MM50 sample 15 cm, IS_21_H_001; 3. MM50 sample 15 cm, IS_21_H_002; 4a. four chambered face, 4b. edge, Station 2 sample 15 cm, IS_08_B_001; 5a. three chambered face, 5b. apertural, 5c. four chambered face, Station 2 sample 15 cm, IS_08_B_002; 6a. three chambered face, 6b. apertural, 6c. four chambered face, 6d. edge, Station 2 sample 2 cm, IS_05_A_001; 7a. four chambered face, 7b. apertural, 7c. three chambered face, Station 1 (2021) sample 4 cm, IS_02_B_001; **8-9**: *Quinqueloculina vandiemeniensis* Loeblich and Tappan 8a. three chambered face, 8b. aperural-oblique, 8c. four chambered face, Station 2 sample 15 cm, IS_08_J_004a; 9. four chambered face, Station 5 sample 8 cm, IS_17_U_002.

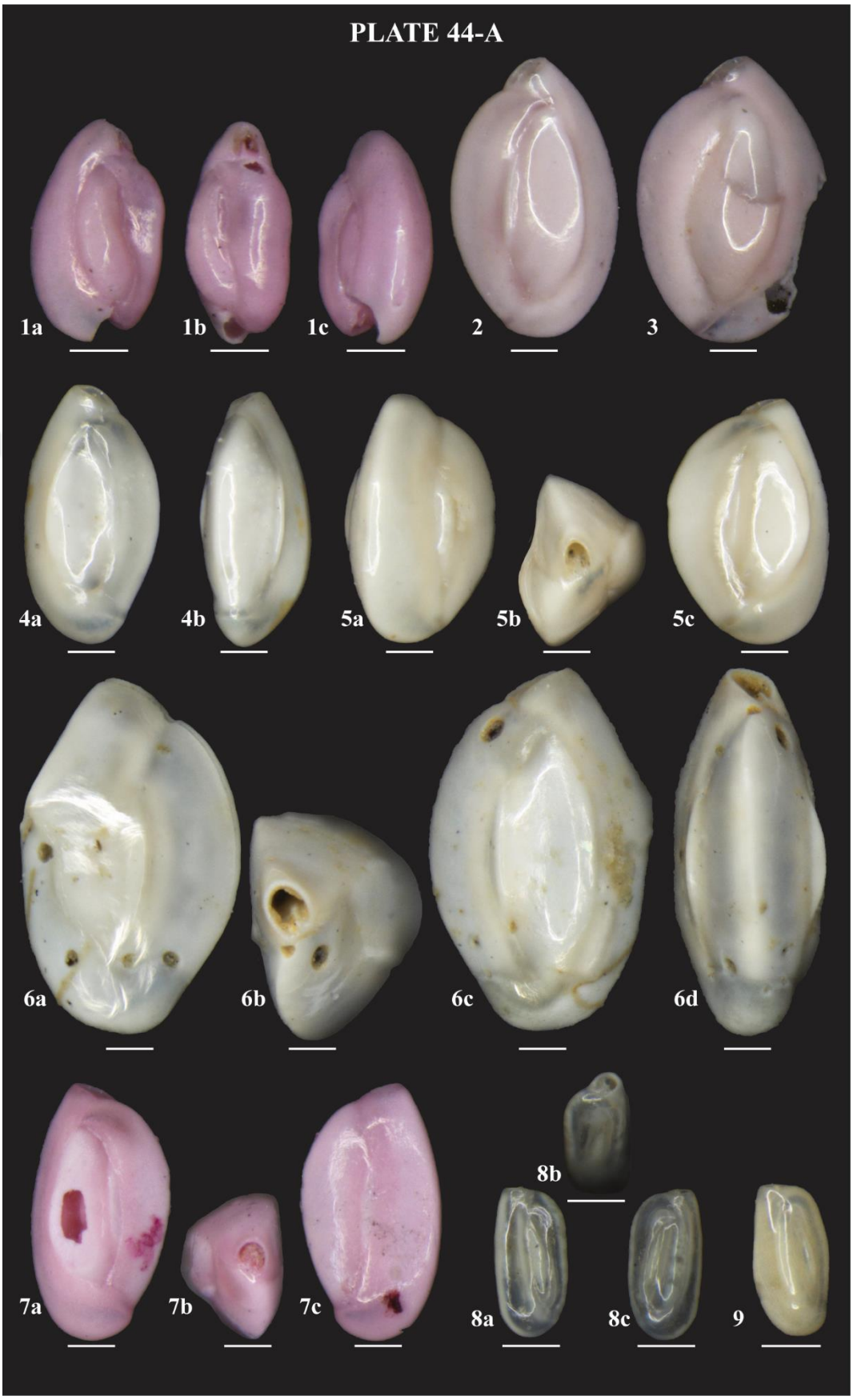

PLATE 44-A
1a
1b
1c
2
3
4a
4b
5a
5b
5c
6a
6b
6c
6d
7a
7b
7c
8a
8b
8c
9

PLATE 44-B: Miliolidea stereomicrographs; scale bar: 100 μm.

1: *Quinqueloculina* sp. 1, three chambered face, Station 5 sample 8 cm, IS_17_U_003; **2-3**: *Pseudotriloculina laevigata* (d'Orbigny), frontal views, Station 5 sample 8 cm, 2. IS_17_U_001; 3. IS_17_U_005; **4-5**: *Quinqueloculina* sp. 2, 4a. four chambered face, 4b. apertural, 4c. three chambered face, Station 2 sample 15 cm, IS_08_J_004b; 5. three chambered face, Station 5 sample 8 cm, IS_17_T_001; **6-8**: *Quinqueloculina*? sp. 3, K51.2K09 sample 8 cm, 6a. three chambered face, 6b. edge, 6c. four chambered face, IS_24_J_001; 7a. four chambered face, 7b. apertural, 7c. three chambered face, IS_24_J_002; 8a. three chambered face, 8b oblique, 8c. four chambered face, IS_24_J_003; **9-13**: *Miliolinella subrotunda* (Montagu), K51.2K09 sample 8 cm, 9. frontal, K51.2K09 sample 8 cm, IS_24_G_001; 10. oblique, adapertural edge, K51.2K09 sample 8 cm, IS_24_G_002; 11. frontal, K51.2K09 sample 8 cm, IS_24_G_003; 12. frontal, Station 2 sample 25 cm, IS_09_E_001, juvenile; 13. frontal, Station 4 sample 15 cm, IS_14_2F_001, juvenile; **14-16**: *Biloculinella globula* (Bornemann), K51.2K09 sample 8 cm, 19. apertural, IS_24_H_003; 20. frontal, IS_24_H_001; 21. frontal, IS_24_H_002; **17-18**: *Pyrgo elongata* (d'Orbigny), 17a. edge, 17b. frontal, K51.2K09 sample 8 cm, IS_24_I_002; 18a. edge, 18b. frontal, Station 2 sample 25 cm, IS_09_F_001; **19-20**: *Pyrgo anomala* (Schlumberger), 19a. frontal, 19b. edge, K51.2K09 sample 8 cm, IS_24_I_001; 20. frontal, Station 5 sample 8 cm, IS_17_O_001.

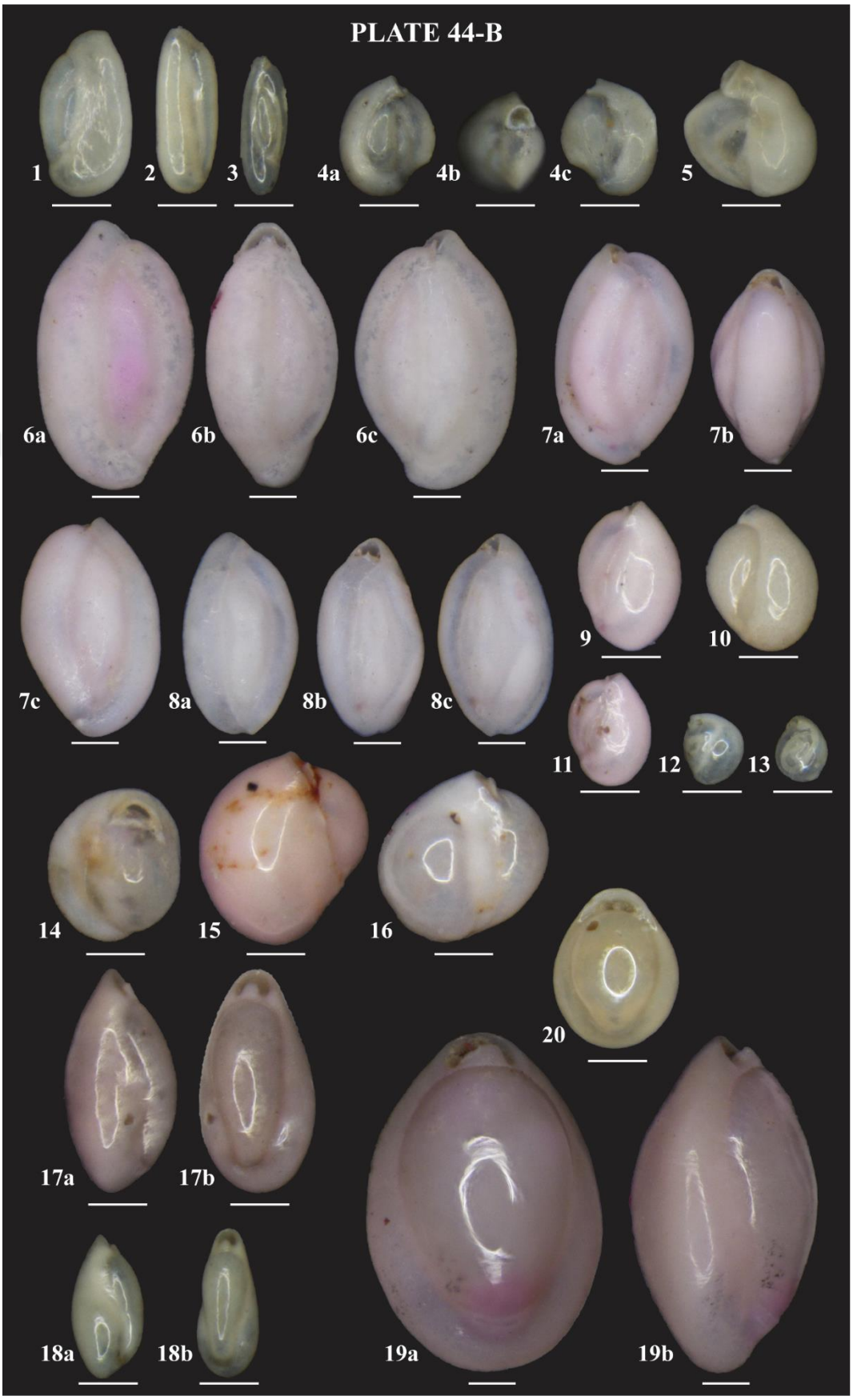

PLATE 44-B
1
2
3
4a
4b
4c
5
6a
6b
6c
7a
7b
7c
8a
8b
8c
9
10
11
12
13
14
15
16
20
17a
17b
18a
18b
19a
19b

PLATE 45: Miliolidea SEM images; scale bar: 100 μm.

1: *Triloculina tricarinata* (d'Orbigny), frontal, Station 5 sample 8 cm, IS_17_I_001; **2**: *Triloculina trigonula* (Lamarck), frontal, Station 5 sample 8 cm, IS_17_I_002; **3**: *Sigmoilinita grata* (Terquem), frontal, Station 2 sample 25 cm, IS_09_H_001; **4**: *Sigmoilinita costata* (Schlumberger), edge, Station 5 sample 8 cm, IS_17_M_004; **5-9**: *Sigmoilinita distorta* (Phleger and Parker), 5. frontal, MM50 sample 15 cm, IS_21_F_001; 6. frontal, MM50 sample 15 cm, IS_21_F_002; 7. frontal, K51.2K09 sample 8 cm, IS_24_C_001; 8. frontal, K51.2K09 sample 8 cm, IS_24_C_004; 9. apertural, K51.2K09 sample 8 cm, IS_24_C_003; **10-14**: *Sigmoilinita tenuis* (Czjzek), 10. frontal, K51.2K09 sample 8 cm, IS_24_B_001; 11. frontal, Station 3 (2021) sample 15 cm, IS_13_H_001; 12. frontal, Station 3 (2021) sample 15 cm, IS_13_H_002; 13. frontal, Station 4 sample 15 cm, IS_14_2G_001, juvenile; 14. oblique, Station 3 (2021) sample 4 cm, IS_02_C_001; **15**: *Sigmoilina sigmoidea* Brady, frontal, Station 2 sample 25 cm, IS_09_D_001; **16-18**: *Siphonaperta horrida* (Cushman), Station 2 sample 25 cm, 16. frontal, IS_09_A_002a; 17. frontal, IS_09_A_002b; 18. apertural, IS_09_A_003; **19-21**: *Sigmoilopsis* sp. 1, frontal views, K51.2K09 sample 8 cm, 19. IS_24_D_001; 20. IS_24_D_002; 21. IS_24_D_003, broken.

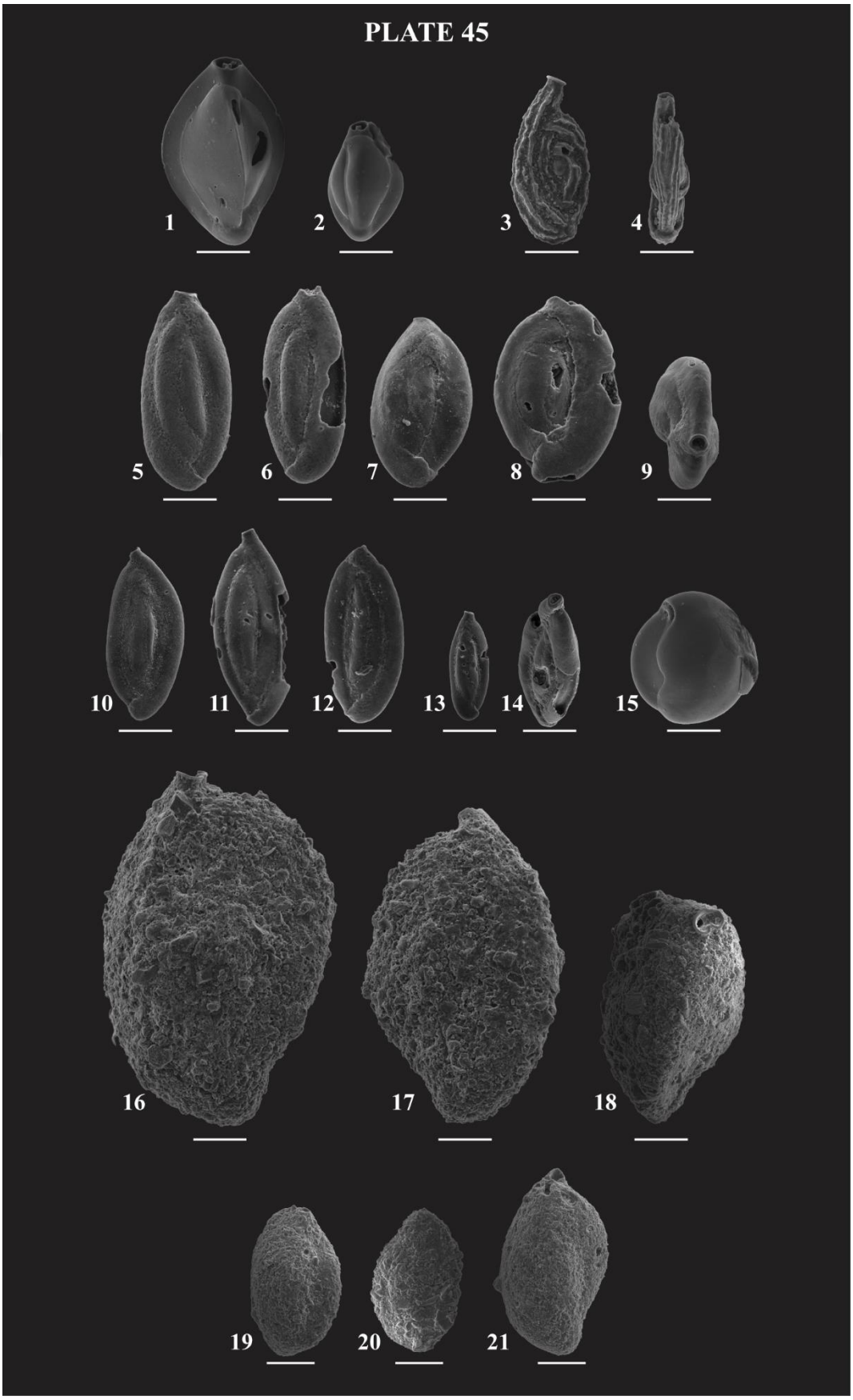

PLATE 45
1
2
3
4
5
6
7
8
9
10
11
12
13
14
15
16
17
18
19
20
21

PLATE 46: Miliolidea stereomicrographs; scale bar: 100 μm.

1: *Triloculina tricarinata* (d'Orbigny), 1a. frontal, 1b. apertural, Station 5 sample 8 cm, IS_17_I_001; **2**: *Triloculina trigonula* (Lamarck), frontal, Station 5 sample 8 cm, IS_17_I_002; **3**: *Sigmoilinita grata* (Terquem), frontal, Station 2 sample 25 cm, IS_09_H_001; **4**: *Sigmoilinita costata* (Schlumberger), 4a. frontal, 4b. edge, Station 5 sample 8 cm, IS_17_M_004; **5-11**: *Sigmoilinita distorta* (Phleger and Parker), 5. frontal, MM50 sample 15 cm, IS_21_F_001; 6. frontal, MM50 sample 15 cm, IS_21_F_002; 7. frontal, K51.2K09 sample 8 cm, IS_24_C_001; 8. frontal, K51.2K09 sample 8 cm, IS_24_C_002; 9. frontal, K51.2K09 sample 8 cm, IS_24_C_003; 10a. frontal, 10b. apertural, 10c. frontal, Station 2 sample 15 cm, IS_08_H_001; 11a. and 11b. frontal views, 2 sample 25 cm,IS_09_C_001; **12-19**: *Sigmoilinita tenuis* (Czjzek), 12. frontal, K51.2K09 sample 8 cm, IS_24_B_001; 13. frontal, Station 3 (2021) sample 15 cm, IS_13_H_001; 14. frontal, Station 3 (2021) sample 15 cm, IS_13_H_002; 15. frontal, Station 4 sample 15 cm, IS_14_2G_001, juvenile; 16. frontal, Station 3 (2021) sample 4 cm, IS_02_C_001; 17. frontal, K51.2K09 sample 8 cm, IS_24_B_002; 18. frontal, Station 3 (2021) sample 15 cm, IS_13_H_003; 19. frontal, MM50 sample 15 cm, IS_21_I_001; **20**: *Sigmoilina sigmoidea* Brady, 20a. edge, 20b. frontal, Station 2 sample 25 cm, IS_09_D_001; **21-25**: *Siphonaperta horrida* (Cushman), frontal views, Station 2 sample 25 cm, 21. IS_09_A_002a; 22. IS_09_A_001a, juvenile; 23. IS_09_A_002b; 24. IS_09_A_001a, juvenile; 25. IS_09_A_003; **26-31**: *Sigmoilopsis* sp. 1, frontal views, K51.2K09 sample 8 cm, 26. IS_24_D_001; 27. IS_24_D_002; 28. IS_24_D_003, broken; 29. IS_24_D_004; 30. IS_24_D_005; 31. IS_24_D_006.

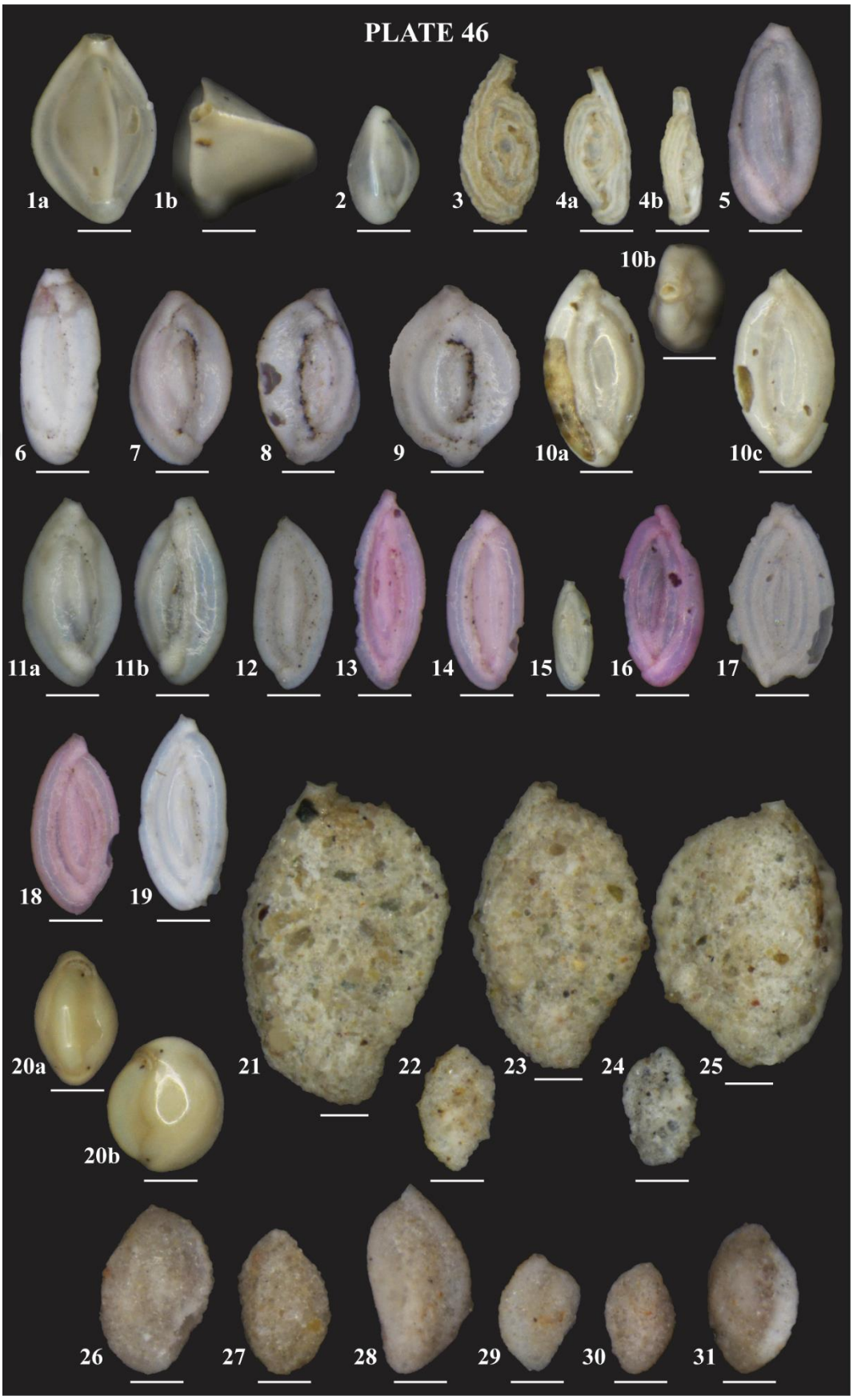

PLATE 46
1a
1b
2
3
4a
4b
5
10b
6
7
8
9
10a
10c
11a
11b
12
13
14
15
16
17
18
19
20a
20b
21
22
23
24
25
26
27
28
29
30
31

PLATE 47: Miliolidea SEM images; scale bar: 100 μm.

1-5: *Articulina tubulosa* (Seguenza), 1. frontal, initial coiled portion, K51.2K09 sample 8 cm, IS_24_F; 2. frontal, initial coiled portion, 45C-2 sample 35 cm, IS_15_A_001; 3. frontal, 45C-2 sample 35 cm, IS_15_A_002; 4. one chamber from rectilinear portion, 45C-2 sample 35 cm, IS_15_A_003; 5. one chamber from rectilinear portion, 45C-2 sample 35 cm, IS_15_A_004; **6**: *Cornuloculina inconstans* (Brady), frontal, Station 2 sample 15 cm, IS_08_J_001; **7**: *Spiroloculina cymbium* d'Orbigny, frontal, Station 5 sample 8 cm, IS_17_M_001; **8-10**: *Spiroloculina excavata* d'Orbigny, K51.2K09 sample 8 cm, 8. frontal, IS_24_A_001a; 9. edge, IS_24_A_001b; 10. frontal, IS_24_A_002a, juvenile; **11-12**: *Spiroloculina tenuiseptata* Brady, 11. frontal, Station 2 sample 25 cm, IS_09_G_001; 12. edge, Station 2 sample 15 cm, IS_08_C_001; **13-14**: *Spiroloculina* sp. 1, Station 5 sample 8 cm, 13. frontal, IS_17_M_002; 14. edge, IS_17_M_003.

PLATE 47

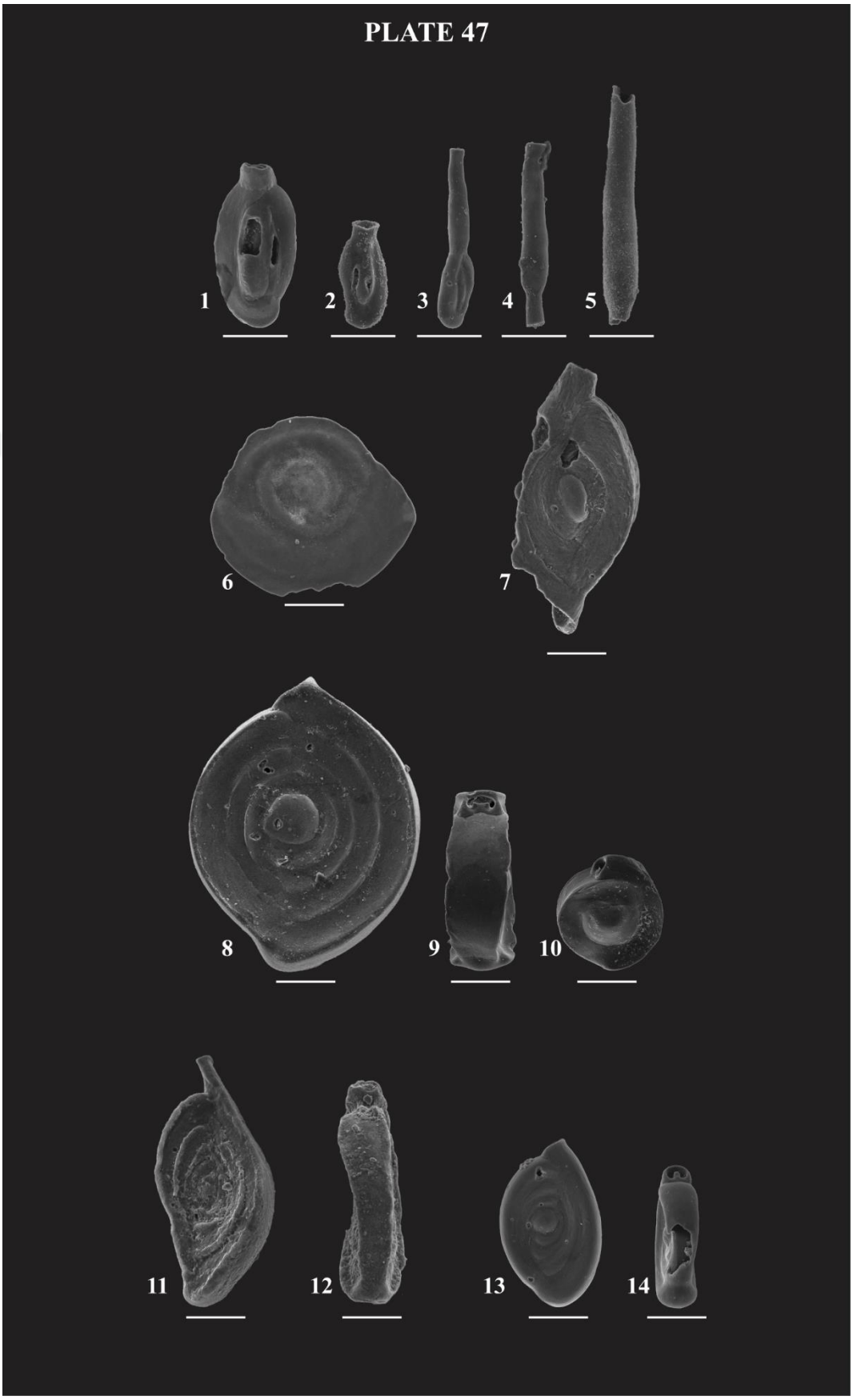
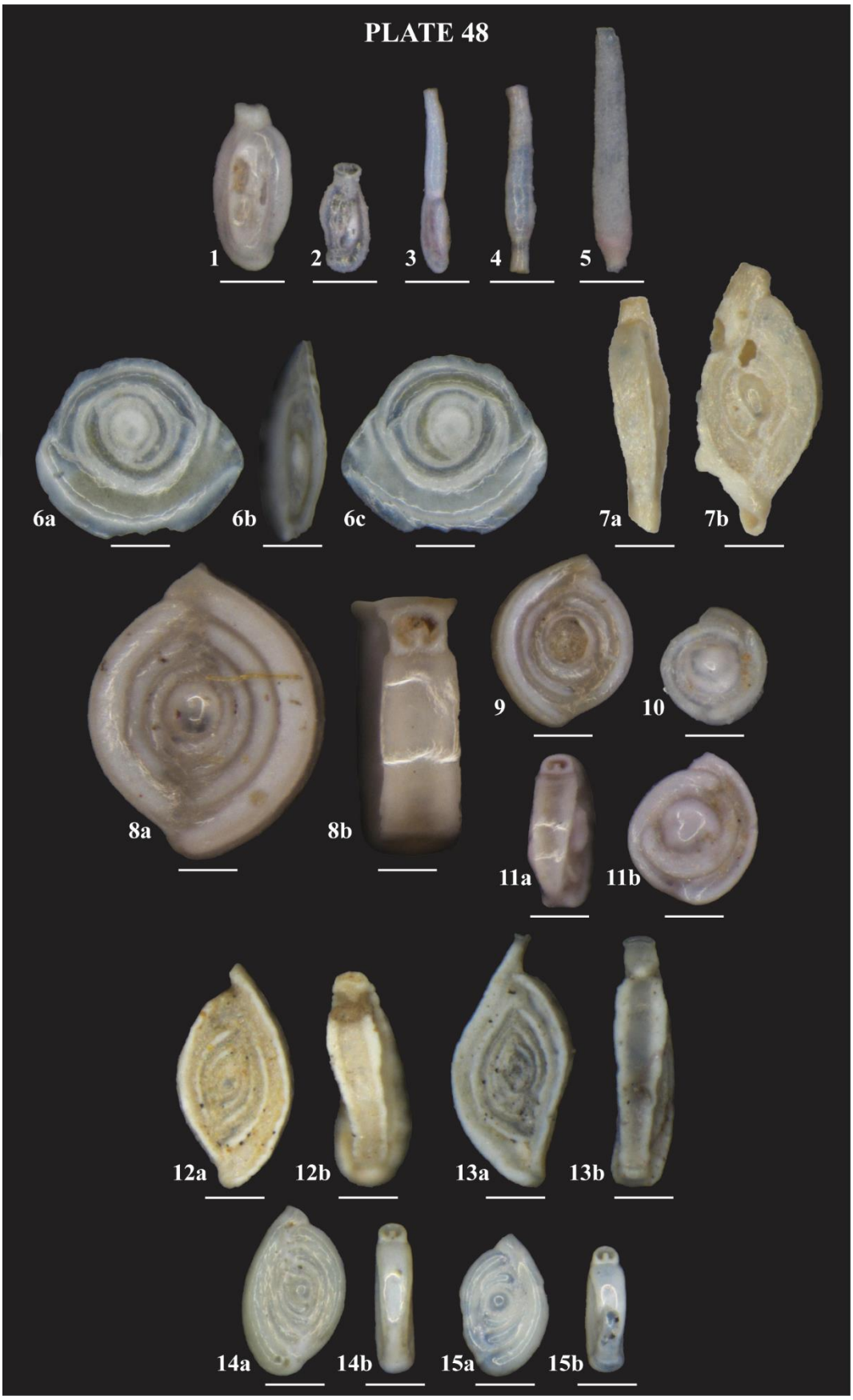


PLATE 48: Miliolidea stereomicrographs; scale bar: 100 μm.

1-5: *Articulina tubulosa* (Seguenza), 1. frontal, initial coiled portion, K51.2K09 sample 8 cm, IS_24_F; 2. frontal, initial coiled portion, 45C-2 sample 35 cm, IS_15_A_001; 3. frontal, 45C-2 sample 35 cm, IS_15_A_002; 4. one chamber from rectilinear portion, 45C-2 sample 35 cm, IS_15_A_003; 5. one chamber from rectilinear portion, 45C-2 sample 35 cm, IS_15_A_004; **6**: *Cornuloculina inconstans* (Brady), 6a. frontal, 6b. edge-oblique, 6c. frontal, Station 2 sample 15 cm, IS_08_J_001; **7**: *Spiroloculina cymbium* d'Orbigny, 7a. edge, 7b. frontal, Station 5 sample 8 cm, IS_17_M_001; **8-11**: *Spiroloculina excavata* d'Orbigny, K51.2K09 sample 8 cm, 8. frontal, IS_24_A_001a; 9. edge, IS_24_A_001b; 10. frontal, IS_24_A_002a, juvenile; 11a. edge, 11b. frontal, IS_24_A_002b; **12-13**: *Spiroloculina tenuiseptata* Brady, 12a. frontal, 12b. edge, Station 2 sample 25 cm, IS_09_G_001; 13a. frontal, 13b. edge, Station 2 sample 15 cm, IS_08_C_001; **14-15**: *Spiroloculina* sp. 1, Station 5 sample 8 cm, 14a. frontal, 14b. edge, IS_17_M_002; 15a. frontal, 15b. edge, IS_17_M_003.


PLATE 48
1
2
3
4
5
6a
6b
6c
7a
7b
8a
8b
9
10
11a
11b
12a
12b
13a
13b
14a
14b
15a
15b

CURRICULUM VITAE

PERSONAL INFORMATION

Surname, Name: Tanık, Gamze

EDUCATION

Degree	Institution	Year of Graduation
MS	METU Geological Engineering	2017
BS	METU Geological Engineering	2014
High School	Mamak Anadolu High School, Ankara	2006

WORK EXPERIENCE

Year	Place	Enrollment
2015 - ongoing	METU Geological Engineering	Research assistant
2013-2014	METU Geological Engineering	Part-time working student
2013	Demir Export	Intern
2012	Anagold Mining	Intern

FOREIGN LANGUAGES

Advanced English

PUBLICATIONS

1. Tanık G. & Özkan-Altıner S., Initial Findings on Planktonic Foraminiferal Biostratigraphy of an Upper Paleocene – Lower Eocene Succession in Northern

Haymana (Ankara, Turkey). Oral presentation in 70th Geological Congress of Turkey; April 2017; Ankara, Turkey.

2. Tanık G. & Özkan-Altıner S., Upper Paleocene-Lowermost Eocene Planktonic Foraminiferal Biostratigraphy and Record of the Paleocene-Eocene Thermal Maximum in the Haymana Basin (Ankara, Turkey). Oral presentation in EGU2018; April 2018; Vienna, Austria.
3. Tanık G. & Özkan-Altıner S., Late Paleocene-early Eocene pteropods (Gastropoda: Euthecosomata) from the Haymana Basin (Central Anatolia, Turkey). Oral presentation in 73rd Geological Congress of Turkey; 24-28 May 2021; Online.
4. Yücel, M., Akçay, İ., Sevgen, S., Alımlı, N., Ermiş, E., Tanık, G., Esti, M., 2021. Türkiye Derin Denizlerinde Anaerobik ve Kemosentetik Ekosistemler, in Öztürk, H., Alkan, G. (Eds.), Türkiye'nin Ekstrem Deniz Ortamları, Türk Deniz Araştırmaları Vakfı (TÜDAV), publication no: 61, pp. 1-27, İstanbul.
5. Tanık G., Özkan-Altıner S., Yücel, M., Alımlı, N., Akçay, İ., An Opportunistic Foraminifera Virgulinella fragilis Grindel and Collen in the Anoxic/Sulphidic Izmit Bay. Oral presentation in 75th Geological Congress of Turkey; 10-14 April 2023.

HOBBIES

Sourdough bread baking, cooking, home brewing, yoga, ukulele